Impact of body weight and antibiotic disturbance on canine gut microbiota : in vitro simulation and restoration strategies

Charlotte Deschamps

PHD THESIS

IMPACT OF BODY WEIGHT AND ANTIBIOTIC DISTURBANCE ON CANINE GUT MICROBIOTA

In vitro simulation and restoration strategies

CHARLOTTE DESCHAMPS

Defended the 30th of June 2023

École Doctorale des Sciences de la Vie, Santé, Agronomie et Environnement

Charlotte Deschamps

Impact of body weight and antibiotic disturbance on canine gut microbiota: *in vitro* simulation and restoration strategies

Defended on June 30th, 2023

Referees
Dr **Marianne DIEZ**, Department of Animal Productions, Liege University, Liege, Belgium
Dr **Etienne GIRAUD**, UMR INTHERES, Université de Toulouse, INRAE, ENVT, Toulouse, France

Examiners
Pr **Monique ALRIC**, UMR MEDIS, Université Clermont Auvergne, INRAE, Clermont-Ferrand, France
Dr **Pieter VAN DEN ABBEELE**, Cryptobiotix, Gent, Belgium
Dr **Nicolas LAPAQUE**, INRAE MICALIS, France

Promotors
Pr **Stéphanie BLANQUET-DIOT**, UMR MEDIS, Université Clermont Auvergne, INRAE, Clermont-Ferrand, France
Dr **Emmanuelle APPER**, Lallemand Animal Nutrition, Blagnac, France
Mrs **Delphine HUMBERT**, Dômes Pharma, Pont-du-Château, France

UMR MEDIS 454, Microbiologie Environnement Digestif et Santé
Université Clermont Auvergne et INRAE, Lallemand Animal Nutrition & Dômes Pharma

Cover illustration
Charlotte Deschamps

Please refer to this work as:
DESCHAMPS, C. (2023). Impact of body weight and antibiotic disturbance on canine gut microbiota: *in vitro* simulation and restoration strategies.
PhD thesis, Université Clermont Auvergne

À ma grand-mère Marie-Jeanne,
Ma Bonne Maman,

À ma famille,

ABSTRACT

Different dog sizes are associated with variations in digestive physiology, mainly related to the large intestine and its resident microorganisms. This gut microbiota plays a key role in animal health, supporting nutritional, immunological and physiological processes. Nevertheless, diseases or antibiotherapy can disturb microbial equilibrium and induce a perturbated state called dysbiosis. To restore microbiota eubiosis, new restorations strategies have been developed such as pre-, pro- or postbiotics. However, very few studies have evaluated their effects on gut microbiota in the context of antibiotherapy. This joint PhD between the Microbiology, Digestive Environment and Health unit from Université Clermont Auvergne and the two compagnies Lallemand Animal Nutrition and Dômes Pharma, aimed to investigate the impact of body weight and antibiotic disturbance on canine colonic microbiota, as well as the potential of microbial restoration strategies, using *in vitro* gut models.

This thesis started by evaluating the impact of different methods for faecal sample storage (48-h freezing -80°C, 48-h -80°C with glycerol or lyophilization with maltodextrin/trehalose) on the kinetics of microbiota colonization and metabolic activities in the Mucosal Artificial Colon (M-ARCOL). Compared to fresh stools, inoculating with raw frozen stool without cryoprotectant was the best option among those tested. Second, thanks to a large literature review, the M-ARCOL model was adapted to reproduce the main nutritional, physicochemical and microbial parameters specific from small, medium and large size conditions in a new model called Canine M-ARCOL (CANIM-ARCOL), further validated through *in vitro-in vivo* comparisons. This adaptation allowed to reproduce in vitro the increase in *Bacteroidota* and *Firmicutes* abundances and higher main short-chain fatty acid (SCFA) concentrations observed *in vivo*. Then, we used the CANIM-ARCOL to perform a mechanistic study, which revealed that nutritional and physicochemical parameters are enough to shape microbiota activity according to dog size, but faecal inoculum was necessary to reproduce size-related microbiota composition. The next step was to adapt the CANIM-ARCOL to diseased situation, focusing on antibiotic-induced dysbiosis. In accordance with *in vivo* data, antibiotherapy induced an increase in *Enterobacteriaceae*, *Streptococcaceae* and *Lactobacillaceae* relative abundances while alpha-diversity and SCFA production decreased. Similar but lower effects were observed in mucus-associated microbiota. Lastly, we evaluated the effect of the live probiotic yeast *Saccharomyces boulardii* CNCM I-1079 and the heat-inactivated bacteria *Lactobacillus helveticus* HA-122 on microbiota resistance during antibiotic treatment and resilience afterwards. Of interest, both microbial strategies decreased the *Enterobacteriaceae* bloom during antibiotherapy and allowed, in the first two days, a quicker recovery of microbiota composition and activity, in both the luminal and mucosal compartments.

This PhD work provided pioneering and significant insights into the impact of dog size and antibiotherapy on canine colonic luminal and mucus-associated microbiota composition and activity, filling gaps in knowledge in these fields. This work also contributed to a better understanding of microbiota resilience in response to antibiotic disturbance. In a near future, in accordance with the European 3R's rules aiming to reduce at a maximum animal experiments, our *in vitro* approaches could be used for mechanistic studies on the interactions between nutrients, feed additives or veterinary products and canine colonic microbiota. Such experiments could be performed under healthy but also disturbed gut microbial situations (including obesity, inflammatory bowel diseases or chronic enteropathies), always considering interindividual variabilities to move towards personalized nutrition and medicine.

RESUME

Différentes tailles de chiens sont associées à des variations de la physiologie digestive, principalement liées au colon et à ses microorganismes résidents. Ce microbiote intestinal joue un rôle clé en santé, soutenant les processus nutritionnels, immunologiques et physiologiques. Néanmoins, les maladies ou l'antibiothérapie peuvent altérer l'équilibre microbien et induire un état perturbé appelé dysbiose. Pour restaurer l'eubiose du microbiote, de nouvelles stratégies de restauration ont été développées telles que les pré, pro ou postbiotiques. Cependant, peu d'études ont évalué leurs effets sur le microbiote dans le cadre de l'antibiothérapie. Cette thèse entre l'unité Microbiologie, Environnement digestif et Santé de l'Université Clermont Auvergne et les deux sociétés Lallemand Animal Nutrition et Dômes Pharma, visait à étudier l'impact du poids corporel et des antibiotiques sur le microbiote colique canin, ainsi que le potentiel de stratégies de restauration microbienne, à l'aide de modèles intestinaux *in vitro*.

Cette thèse a commencé par évaluer l'impact de différentes méthodes de stockage des échantillons fécaux (congélation 48 h à -80°C, 48 h à -80°C avec du glycérol ou lyophilisation avec maltodextrine/tréhalose) sur la cinétique de colonisation du microbiote et ses activités métaboliques dans Mucosal Artificial Colon (M-ARCOL). Par rapport aux selles fraîches, l'inoculation avec des selles congelées brutes est apparue comme la meilleure option. Grâce à une revue de la littérature, le modèle a été adapté pour reproduire les paramètres nutritionnels, physicochimiques et microbiens spécifiques des conditions du petit, moyen et grand chien dans un nouveau modèle appelé Canine M-ARCOL (CANIM-ARCOL), validé avec des comparaisons *in vitro-in vivo*. Ceci a permis de reproduire *in vitro* l'augmentation de la production des principaux acides gras à chaîne courte (AGCC), et la prolifération des *Bacteroidota* et *Firmicutes* observées *in vivo*. Puis, le modèle a permis de réaliser une étude mécanistique, révélant que les paramètres nutritionnels et physicochimiques façonnent l'activité du microbiote associé à la taille du chien, mais que l'inoculum fécal est nécessaire pour reproduire sa composition. Enfin, notre modèle a été adapté pour reproduire la dysbiose induite par les antibiotiques. Conformément aux données *in vivo*, l'antibiothérapie a induit la prolifération des *Enterobacteriaceae*, *Streptococcaceae* et *Lactobacillaceae*, tandis que la diversité et la production d'AGCC diminuaient. Des effets similaires mais moindres ont été observés dans le microbiote mucosal. Enfin, nous avons évalué l'effet de *Saccharomyces boulardii* CNCM I-1079 et de *Lactobacillus helveticus* HA-122 tyndallisée sur la résistance du microbiote pendant le traitement antibiotique et la résilience après celui-ci. Les deux stratégies ont réduit la prolifération des *Enterobacteriaceae* pendant l'antibiothérapie et permis au cours des deux premiers jours, une résilience plus rapide de la composition et l'activité du microbiote, dans le lumen et le mucus.

Ce travail a fourni des informations pionnières et significatives sur l'impact de la taille du chien et de l'antibiothérapie sur la composition et l'activité du microbiote luminal et mucosal du colon canin, comblant les lacunes dans ces domaines. Ces travaux améliorent la compréhension de la résilience du microbiote en réponse aux perturbations antibiotiques. Dans un futur proche, en accord avec les règles européennes 3R visant à réduire les expérimentations animales, nos approches *in vitro* pourraient être utilisées pour des études mécanistiques des interactions entre nutriments, additifs alimentaires ou produits vétérinaires et microbiote. De telles expériences pourraient être réalisées en situations saines ou perturbées (obésité, maladies inflammatoires de l'intestin ou entéropathies chroniques), en tenant compte des variabilités interindividuelles pour progresser vers une nutrition et une médecine personnalisées.

ACKNOWLEDGMENTS - REMERCIEMENTS

Mes premières pensées vont vers **Stéphanie Blanquet-Diot**, après ces 4 ans à travailler ensemble. Cela va peut-être te sembler bizarre mais je voudrais te remercier de m'avoir demandé toujours **plus**. **Plus** de manips (juste sur les 3 ans de ma thèse : 38 fermenteurs et 168 jours de fermentations), **plus** d'analyses (je ne parlerai même pas de Tax4Fun ou des acides biliaires), **plus** de publications (2 revues et 6 articles en premier auteur), **plus** de stagiaires (6 au total), **plus** d'enseignement, **plus** de vulgarisation, **plus** de déplacements en congrès ou ailleurs. Alors vraiment du fond du cœur merci, parce que tu m'as demandé tellement **plus** que j'ai donné des choses dont je ne me pensais même pas capable. Pour être un peu plus précise, tu m'as fait venir à 23h faire des prélèvements, maniper jusqu'à 26 jours de suite, rédiger des demandes de financement un vendredi soir à 21h alors que tu avais le COVID et que j'étais en weekend chez mes parents, tu m'as fait soumettre une revue un 23 décembre à 20h, tu m'as fait courir après des chiens pour récupérer leurs crottes, tu m'as même fait contacter des inconnus pour leur demander la crotte de leur chien (rien que ça, ceux qui me connaissent depuis longtemps savent que c'est un exploit). Tu m'as fait parler en public, en français et en anglais, à Toulouse, à Paris, en Slovaquie, en Belgique, et bientôt en Ecosse, tu m'as fait dire le mot « crotte » devant une caméra, tu m'as aussi fait parler de crotte devant 40 lycéens, tu m'as même fait parler de crotte devant des doctorants et des chercheurs, en anglais, et j'ai obtenu un premier prix pour ça. Alors voilà, pour tout ce qu'on a fait ensemble et ce qu'on fera je l'espère, MERCI. Merci d'avoir cru en moi dès le départ, lorsque je n'étais qu'un petit canard de la Duck Family, puis chaque jour de cette thèse. Merci de m'avoir poussée dans mes retranchements, merci de m'avoir bousculée parfois. Enfin, merci d'avoir alimenté ce *toujours plus* qui m'anime aussi chaque jour pour en arriver aujourd'hui, à clôturer mes 9 années postbac avec le grade de docteur (et là ce sont mes proches qui se disent toujours plus !). C'est dans la difficulté qu'on apprend à se connaitre soi-même et à connaitre les autres. Et quelle guide j'ai eu !

Je souhaiterai ensuite remercier mes deux autres encadrantes de thèse, **Delphine Humbert** et **Emmanuelle Apper**. Pour commencer, merci de m'avoir accordé la possibilité de réaliser cette thèse autour des mots clés microbiote et chien qui rassemblent deux thématiques auxquelles je m'intéresse depuis longtemps. Merci pour votre confiance tout au long de cette thèse, vos encouragements et votre soutien dans les périodes plus difficiles. J'ai beaucoup apprécié nos échanges, qu'ils soient scientifiques ou parfois plus personnels.

Je souhaite également remercier chaleureusement **Mathieu Castex** et **Etienne Saunier** pour la confiance qu'ils m'ont accordé et nos échanges toujours très enrichissants. Un grand merci également à **Frédérique Chaucheyras-Durand**, **Lysiane Dunière** et **Caroline Achard** pour leurs conseils et la bienveillance dont elles ont fait preuve à chaque fois que nous nous sommes croisées.

Enfin, je remercie **Sylvain Denis**, le 4ème encadrant de cette thèse. Mon premier souvenir de toi remonte au début de mon stage de Master 2, un jour de lancement de fermenteur où je t'avais assistée (enfin disons plutôt que j'étais là) pour la calibration des sondes, nous étions encore au 4ème dans les anciens locaux. J'avais noté tellement d'informations que mon cerveau allait exploser mais j'étais fière, et déjà visiblement dans mon élément entre informatique, pratique et… microbiote. Merci d'avoir essayé (et réussi un peu je l'espère, mais j'y travaille toujours) à me transmettre ta rigueur et ta patience. Je ne sais plus combien de fois je t'ai demandé si tu avais '*5 minutes'* à m'accorder. Merci pour tes conseils, que ce soit pour la thèse mais aussi sur le plan personnel et professionnel, je n'oublierai pas tes mots lorsque nous avions discuté d'un éventuel nouveau job. J'espère que nous aurons encore l'occasion de travailler ensemble et pourquoi pas un jour lancer le premier TOU-TIM (c'est le TIM toutou) au labo !

Merci également aux membres du jury, **Monique Alric**, **Marianne Diez**, **Etienne Giraud**, **Nicolas Lapaque** et **Pieter Van den Abbeele**, qui ont accepté de faire partie de mon jury de thèse et examiner ce travail.

Plus généralement, travailler chez **MEDIS** a été un peu comme trouver au travail un seconde famille... Mais une famille avec qui on peut discuter travail et qui trouve ça cool. Une famille à qui je peux dire « ma qPCR bac-tot

n'a pas marché pourtant j'ai fait un lavage au citrate et utilisé le kit zymo pour extraire mes billes, et les rapports 240/260 du Nanodrop étaient bons » … et qui comprend *vraiment* ce que je dis. C'était vraiment de très belles années passées entre le 4ème et le 5ème étage du CBRV, à manger tantôt au milieu des paillasses, tantôt devant les toilettes. Parfois dans un joyeux brouhaha et toujours dans la bonne humeur, entre deux blagues de Éric ou Claude ! Je souhaite remercier plus particulièrement :

Lucie Etienne-Mesmin. Un immense merci pour TOUT (et la liste est bien longue !). Merci d'avoir lu en moi dès le début de mon stage de master, merci pour tes conseils que j'ai gardés précieusement pour affronter les trois années qui viennent de s'écouler. Quelle chance d'avoir eu quelqu'un comme toi, toujours disponible pour m'écouter, me conseiller, me soutenir quand j'en ai eu besoin, me calmer aussi parfois. Je n'oublierai pas cette réunion dans la salle des étuves de l'IUT, ni cette discussion dans le couloir caché du P3 un après-midi où c'était pour moi un peu la fin du monde. Merci pour ces discussions parfois quasi-nocturnes (et parfois même presque matinales à Bratislava) à discuter de tout et de rien, à refaire le monde de la recherche. J'ai vu les choses sous un autre angle grâce à toi. Merci d'avoir bataillé pour que je puisse enseigner à l'IUT pour un moment. Merci pour les blagues et les rires, pour les sms tardifs pour savoir si j'allais bien. Enfin et surtout, merci pour ta confiance, c'est pour moi l'une des plus belles choses que l'on puisse donner. Et merci pour toutes les choses que tu as faites pour moi, qui peuvent sembler insignifiantes mais qui sont importantes à mes yeux. Et bien que j'ai reçu une certaine pression pour que ce texte fasse une demi-page, ma position ne me permet pas d'en dire plus ;)

Sandrine Chalancon. Ma Sandrine, comme elles étaient chouettes ces semaines de fermentation avec toi à mes côtés ! On aura bien fait les 400 coups, ou presque. Je nous revois pendant les semaines de préparation, à courir partout comme des piles électriques (seulement jusqu'à midi parce que l'aprèm c'est tisane), enchainer 3 séries de sucres dans la journée, parfois dans un nuage de pro… enfin non de *fumées toxiques* ☺ Je t'ai parfois détestée, surtout à 7h35 quand tu m'appelais en disant « oulala il faut que tu viennes ***vite*** ça a débordé !!! », mais qu'est-ce que j'ai apprécié travailler avec toi. Merci pour ton soutien infaillible (sauf le mercredi). Qu'est-ce qu'on a pu rire… et pleurer quelques fois aussi. Merci ma Sandrine, sans le moindre doute tu as vraiment contribué à faire de ces manips interminables des moments de bonheur et de partage. Finalement 3 ans ça passe presque un peu trop vite quand on est bien entouré ! Merci pour tous tes conseils et pour ta bonne humeur légendaire qui ferai même sourire un clown triste. Ce n'est pas pour rien si t'es la meilleure assistante ingénieure du monde.

Morgane Brun. Ma Morgane, quelle rencontre ! et quel binôme de choc ! D'abord stagiaire tu es devenue une collègue, puis une amie. Merci pour ton aide sur les dernières manips de ma thèse, on n'était pas trop de deux et il y a bien eu des jours où tu comptais pour un et demi à toi toute seule ! Tu as été d'un soutien infaillible. Merci de m'avoir aidée tant que tu as pu, sans jamais rechigner à la tache malgré la fatigue et les centaines de tubes qu'il a fallu fermer, annoter, puis extraire, les centaines de boite à couler puis ensemencer. Merci d'avoir rattrapé mes bêtises (quand il a fallu refaire des solutions au dernier moment, couler des boites en urgence, ou encore pour avoir essuyé de *minuscules* quantités de harvest qui avaient à peine un tout petit peu débordé…). Heureusement que tu étais là. Merci pour tout ! <3

Claude Durif. Cher Claude, je ne saurai te remercier pour toute l'aide apportée pendant cette thèse, pendant les manips, pour les analyses, mais aussi sur le plan personnel. Je n'oublierai pas de sitôt ces après-midis passées à gratter un fichu script R qui ne fonctionne pas comme prévu. Merci pour nos pauses café/tisane à refaire le monde, merci pour ta patience, ta bienveillance, ton calme et tes conseils. Je ne sais pas trop si je dois te remercier pour tes blagues de mauvais goût mais pour les autres c'était chouette ☺ Merci pour ta bonne humeur, ta disponibilité, ton soutien et aussi pour le reste. Que de bons moments passés qui ont contribués à faire de cette thèse ce qu'elle a été ! Et quelle chance d'avoir passé ces années avec le meilleur joueur de flute de MEDIS !

Merci également à **mes autres collègues, d'hier et d'aujourd'hui, de l'UCA et de l'INRAe**, merci pour vos conseils, votre soutien et nos échanges autour d'un repas ou d'un café. Plus particulièrement, je souhaite remercier :

Monique Alric, merci pour tes conseils toujours avisés et bienveillants, c'est un vrai plaisir que tu aies accepté de présider ce jury de thèse ; **Éric Beyssac**, **Imen Dhifallah**, **Khaled Fadhlaoui**, **Ghislain Garrait**, **Emmanuelle Lainé**, merci pour vos conseils sur l'HPLC ou la pharma. Merci à tous pour votre bonne humeur. J'aurai aimé qu'on puisse collaborer un peu plus ensemble, un jour peut-être ! **Laetitia Coudert**, merci pour ton aide tout au long de ma thèse ! Merci pour ta réactivité et ta bonne humeur, toujours là pour nous sortir des méandres de l'administration de

l'université. **Cathy Dhainaut**, tu es un vrai rayon de soleil, merci pour nos discussions c'est toujours un plaisir ! **Sophie Marre**, **Carine Mazal**, merci pour votre soutien tout au long de ma thèse, et merci d'avoir été toujours présentes quand j'en ai eu besoin, que ce soit pour parler boulot, travaux ou jardinage ☺ **Philippe Ruiz**, merci pour tes conseils en bioinfo qui m'ont été bien utiles, et merci de t'être toujours rendu dispo quand j'en ai eu besoin ; **Ophélie Uriot**, elle est déjà bien loin la duck family… comme le temps passe vite ! Merci pour tes conseils et ta bienveillance. **Cécile Verdier**, merci de t'être occupé de la cagnotte café c'était sympa (la suite au prochain épisode). Merci également aux stagiaires et doctorants, de MEDIS et d'ailleurs, qui ont connu la galère, l'ont parfois partagée avec moi, et l'on rendue plus douce : **Elora Fournier**, **Frédérique Lajoie**, **Thomas Sauvaitre**, **Thomas Merciecca**, **Ines Gouveia**, **Marion Garofalo**, **Pauline Descôtes-Genon**, **Oshma Shakoory**, **Deborah O'Sullivan**, et ceux que j'oublie peut-être…

Plus particulièrement, **Elora**, mon acolyte de stage, ma copine de galère, ma voisine de bureau. Merci pour ces belles années partagées. Elles sont passées en un claquement de doigts… Merci d'avoir été un soutien de tous les jours, dans les bons et les mauvais moments que nous avons partagé dans la thèse ou dans la vie. Merci pour ta bonne humeur, ton sourire. Tu trouvais toujours les mots justes quand j'en ai eu besoin. Merci <3

Enfin, je voudrais remercier ma collègue devenue une amie très proche, **Cécile** alias Céc' Verdi. Au moment où je relis ces mots je suis devenue Tatie Saint Nec. Tu as énormément contribué à cette thèse. D'abord, tu m'as formée au labo sur une bonne partie des techniques que j'ai utilisé au cours de ces 4 dernières années, les fermenteurs, la microGC, la qPCR ou encore l'HPLC. Merci de m'avoir transmis ta rigueur et d'avoir toujours été là quand j'en ai eu besoin. Merci pour ces après-midi passées (ou perdues) à calculer, recalculer et recalculer encore les concentrations d'acides biliaires dans mes fermenteurs (sans *trop* te plaindre). Quand je regarde en arrière je me dis qu'on a bien changé depuis mon arrivée au labo il y a 4 ans. Aujourd'hui les mots sont durs à trouver pour décrire à quel point tu es devenue importante à mes yeux. Merci d'être toujours là pour moi et de l'avoir été tout au long de cette thèse, merci de m'écouter me plaindre souvent et me réjouir quelques fois. Merci de me supporter dans la vie, au sens propre comme au sens figuré ☺

Je souhaite également remercier l'ensemble des chercheurs, vétérinaires, techniciens, avec qui nous avons collaboré tout au long de cette thèse et qui ont largement contribué à la réussite de ce projet : **Nathalie Priymenko**, **Jurgen Zentek**, **Tom Van de Wiele**, **Ignacio Ipharraguerre**, **Valérie Marquegnies**. Merci également aux propriétaires de ***Gipsy, Leo, Loki, Onyx, Joy, Django, Pashka, Loov, Largo, Oura, Nala, Lou, Indy, Ines, Maya et Princesse*** qui ont accepté de récupérer les selles de leur chien et d'en faire dons pour la science. Sans vous, nous n'aurions pas réussi !

Merci aux membres de mon comité de thèse pour leurs conseils et leur bienveillance : **Frédérique Chaucheyras-Durand**, **Nathalie Priymenko**, **Etienne Saunier**, **Jurgen Zentek** et **Laure Ginger**.

Pour finir, je voudrai adresser mes derniers remerciements à **ma famille et à mon fiancé**.

À **Benjamin**, mon soutien de tous les jours, merci de me supporter depuis tant d'années. Merci d'avoir supporté mes histoires de fermenteurs, d'administration, ma fatigue et mes plaintes tout au long de cette thèse. Merci de croire en moi en toutes circonstances et d'accepter mes choix même s'ils impliquent parfois des sacrifices pour nous deux (vous avez dit des vacances improvisées ?). Heureusement pour moi tu manies l'art de dédramatiser une situation comme personne, ce qui m'aura été bien utile au cours de ce thèse. Merci pour tout, merci de faire mon bonheur chaque jour, je t'aime (même si 3 ans plus tard mon travail se résume toujours par « caca de chien, bactoss', qPCR et bec-bunzen » <3).

Chez les Deschamps, on n'a jamais été très doués pour parler de ce qui compte vraiment (ou alors jamais sans pleurer, Maman, Papa je vous vois), je vais donc essayer de vous l'écrire. À mes **parents**, à mes **grands-parents**, merci d'y avoir cru aussi fort que moi, quand je vous ai dit que je serai '*mécaniqueuse' comme mon papa*, que je serai *vétérinaire*, que je serai *assistante sociale*, que je serai *chirurgien*, ou que je serai *chercheur dans la police scientifique*. Finalement j'ai mixé un peu tout ça et bientôt je serai docteur, et si je le dois à quelqu'un c'est bien grâce à vous.

À mes **parents**, **Jean-Marc** et **Aline**, merci de m'avoir tant transmis. Quelle chance ! Ma curiosité et mes connaissances sur les animaux, les arbres, le jardinage, la pêche, les champignons, la cuisine ou encore le bricolage, tout est grâce à vous. Vous m'avez tout appris. Merci de m'avoir transmis cette capacité à apprécier les petites choses du quotidien, à m'émerveiller de tout, dans le monde d'aujourd'hui je savoure tous les jours cette chance. Merci de m'avoir toujours encouragée à faire ce qui me plaisait dans la vie, merci pour toutes les opportunités que vous m'avez offertes, merci d'avoir soutenu mes échecs et applaudi mes réussites, merci de m'avoir toujours laissé la liberté de faire mes propres choix, qu'importe ce qu'il vous en a coûté. À mes **grands-parents**, **Xavier** et **Marie-Jeanne**, merci de m'avoir toujours encouragée et soutenue de tous les moyens qu'il existe. Merci pour les vacances, pour la brioche au petit déjeuner, merci pour les meilleures pommes de terres/carottes du monde, merci pour les 'bolettes', pour les 'chic dit la mouche', pour les 'essaye ça -je n'aime pas -oui mais c'est la mode à Paris', merci pour les musées et pour les tours du lac de Saint Evroult. Merci pour les rires jusqu'aux larmes, pour ces étés inoubliables et pour vos conseils qui raisonnent toujours en moi. Merci de m'avoir poussée à faire des études, merci de m'avoir tant appris et également transmis le goût d'apprendre et de faire apprendre aux autres. C'est pour moi un cadeau et une richesse inestimables, je ne l'oublierai jamais. Et bien que Bonne-Maman n'aimait pas les chiens, je pense qu'aujourd'hui elle serait très fière. Il n'y a pas une seule fois où je n'ai pas pensé à elle avant une présentation importante, où qu'elle soit elle est toujours avec moi.

À **Benjamin**, ma **famille**, mes **amis**, je ne sais comment vous remercier. Depuis toutes ces années vous m'avez soutenu dans chaque moment de doute, vous avez contribué pierre à pierre à construire la personne que je suis aujourd'hui. Merci d'avoir compris et accepté les sacrifices que j'ai eu à faire ces trois dernières années… Merci de m'avoir appris que *chaque instant compte*, et merci de faire de chaque instant un *souvenir qui compte vraiment*.

À vous tous qui comptez pour moi,
À mon fiancé **Benjamin**,
À mes parents **Aline** et **Jean-Marc**,
À mon petit frère **Lucas**,
À mes grands-parents **Marie-Jeanne**, **Marcel**, **Suzanne** et **Xavier**,
À mon oncle et ma tante **Franck** et **Joëlle**,
À ceux qui me regardent de là-haut,

Merci de n'avoir jamais brisé mes rêves d'ambition, merci d'avoir toujours cru que j'en serais capable -même si souvent je n'y croyais pas moi-même- merci d'avoir toujours pensé, ou du moins m'avoir laissé penser que je pouvais *tout réaliser à moins de le vouloir*, merci d'avoir cru que je pourrais rénover une maison et préparer une thèse en même temps, vous en avez la preuve aujourd'hui.

Merci d'avoir cru avec moi que l'ambition, le travail, l'acharnement et l'impatience payent un jour.

Au bon moment, au bon endroit.
Quand on veut, on peut.

Résumé de la thèse

A. Contexte scientifique et réglementaire de la thèse

Canis lupus familiaris, ou chien domestique, appartient à la famille des canidés. Descendant du loup gris, le chien pourrait avoir été le premier animal domestiqué par l'homme il y a environ 20 000 à 40 000 ans. Les chiens étaient initialement des carnivores stricts, mais au cours de la révolution agricole ils ont probablement acquis la capacité de digérer l'amidon et sont devenus des carnivores facultatifs. En fonction de leur utilité pour l'Homme, les sous-espèces de *Canis lupus familiaris* se sont lentement différenciées, avec l'apparition de nouvelles espèces sélectionnées pour des tâches spécifiques, comme la protection des troupeaux ou la chasse. Aujourd'hui, l'espèce comprend environ 400 races avec des variations morphologiques, métaboliques et de taille et un poids allant de 1 kg pour un Chihuahua à 100 kg pour un Saint-Bernard.

Les chiens occupent une place à part entière dans la famille et leur santé et leur bien-être sont d'une importance capitale pour leurs propriétaires, à tel point que 7 % des chiens français ont leur propre assurance maladie, contre 30 % au Royaume-Uni et 80 % en Suède. En 2023, on estime que les chiens seront plus de 900 millions dans le monde, ce qui représente un énorme marché pour l'industrie du petfood et de la santé animale. En 2018, le marché mondial de l'alimentation pour animaux de compagnie a atteint 91,1 milliards de dollars, représentant une augmentation de 31 % en 5 ans, avec la nécessité constante d'innover (par exemple en matière d'alimentation, de probiotiques et de prébiotiques). Une vaste gamme d'aliments, de snacks et de suppléments nutritionnels a été récemment mise au point pour favoriser le bien-être et la santé des chiens. Les aliments pour animaux de compagnie ont ainsi été adaptés au mode de vie de chaque chien, par exemple pour les chiots ou les chiennes gestantes, les chiens adultes sédentaires ou actifs, pour un régime d'entretien ou un régime hypocalorique. À l'interface entre les aliments pour animaux de compagnie et les composés vétérinaires, les compléments alimentaires pour animaux de compagnie représentent un marché spécifique en expansion avec une large gamme de produits. Par exemple, des micronutriments tels que le sélénium, la taurine ou les polyphénols peuvent être ajoutés pour les chiens âgés, le calcium, le phosphore, les acides gras oméga-3 et la vitamine E pour les chiennes en lactation, ou la L-carnitine pour les chiens sportifs.

En 2019, la médecine des animaux de compagnie représentait un marché de 17,5 milliards de dollars, incluant les ventes de composés vétérinaires tels que les vaccins, les traitements antiparasitaires ou les antibiotiques. Comme pour l'homme, une large gamme de produits a été développée pour améliorer la santé et l'hygiène des chiens. Des traitements spécifiques ont également été mis au point pour soigner des maladies, par exemple pour éviter l'absorption de lipides en cas d'obésité ou pour réduire la douleur en cas de maladie inflammatoire de l'intestin. Il convient de noter que certaines races ou tailles de chiens sont plus sensibles aux maladies. Par exemple, le surpoids et les problèmes dentaires sont plus fréquents chez les petits chiens, tandis que les grands chiens présentent souvent une sensibilité digestive accrue.

La forte expansion de la médecine vétérinaire, des aliments pour animaux de compagnie et des compléments oraux avec des allégations de santé est associée à un contexte réglementaire de plus en plus spécifique. En Europe, la fédération européenne de l'industrie des aliments pour animaux de compagnie (Fediaf)

a pour objectif d'encadrer la production d'aliments pour animaux de compagnie sûrs, nutritifs et appétissants. Les responsables des agences du médicament ou des agences nationales doivent accorder une autorisation de mise sur le marché des médicaments vétérinaires, après avoir évalué la qualité et la sécurité du médicament pour les animaux, les consommateurs, les utilisateurs et l'environnement, ainsi que bien sur son efficacité. En outre, l'absence de toxicité et la stabilité des compléments oraux (y compris les probiotiques) doivent être démontrées. Pour l'évaluation de ces produits, généralement liée à la digestibilité des aliments ou à la bioaccessibilité des composés actifs (y compris des médicaments) dans le tractus gastro-intestinal canin, les études *in vivo* restent plébiscitées. De plus, les expériences *in vivo* sur les chiens peuvent également servir de modèle pour l'Homme en raison de similitudes importantes dans la physiologie digestive. Dans le monde en 2015, encore 207 724 chiens étaient impliqués dans des expérimentations scientifiques. Cependant, les essais *in vivo* sont de plus en plus limités par des contraintes réglementaires, éthiques et sociétales, associées à des coûts élevés. La mise sur le marché d'un nouvel additif ou d'un nouveau médicament est de plus en plus réglementée, avec un niveau de justification scientifique croissant, dans un contexte où il est de plus en plus difficile de mener des essais sur les animaux. Ces dernières décennies, les règles européennes et nord-américaines des "3R" ont largement encouragé une forte réduction du nombre d'animaux utilisés dans la recherche et favorisé le développement d'approches alternatives *in vitro.* Tous ces éléments limitent la capacité à prouver l'efficacité et à comprendre le mode d'action de nouvelles molécules sélectionnées dans des études *in vivo* chez le chien.

Parmi les alternatives *in vitro*, les modèles simulant l'environnement digestif du chien (culture de cellules intestinales, organoïdes ou modèles digestifs artificiels) peuvent aider à répondre à de nombreuses questions scientifiques associées au devenir des aliments et des médicaments au cours de la digestion canine. Une approche alternative aux essais sur les animaux est l'utilisation de systèmes digestifs artificiels permettant d'étudier le devenir des composés d'intérêt ingérés par voie orale, de réaliser des études mécanistiques, et/ou d'évaluer les interactions avec le microbiote du chien. Il existe actuellement très peu de modèles *in vitro* reproduisant l'environnement gastro-intestinal ou colique du chien et la majorité des travaux publiés concerne des modèles *in vitro* statiques, très simplifiés et ne reproduisant pas le dynamisme et la complexité du processus de digestion *in vivo.* Enfin, la plupart des modèles développés à ce jour ne reproduisent pas le microbiote intestinal, qui fait pourtant l'objet d'un nombre croissant d'études chez le chien mettant en évidence son rôle essentiel dans l'homéostasie de l'hôte, et son implication dans diverses pathologies digestives ou extra-digestives lorsqu'il est perturbé (on parle alors d'un état de dysbiose). Ainsi, disposer d'un modèle *in vitro*, simulant au plus près les paramètres physico-chimiques, nutritionnels, mécaniques et/ou microbiens propres à l'environnement digestif du chien, constituerait une avancée technologique et scientifique majeure, permettant d'acquérir de multiples connaissances, de comprendre les modes d'action de nouveaux produits, de développer des biomarqueurs microbiens ou encore d'affiner un protocole lors d'une étude clinique pilote (choix de la dose, fréquence d'administration des composés d'intérêt...). Cependant, la mise au point de tels modèles nécessite une compréhension complète et précise des processus digestifs chez le chien.

Ainsi, la digestion est un processus essentiel au centre des études sur la santé des chiens et d'un grand intérêt pour les industries vétérinaires et de l'alimentation des animaux de compagnie. La digestion du chien est un processus complexe et régionalisé impliquant des paramètres physicochimiques (pH, sécrétions digestives, temps de transit), mécaniques (péristaltisme) et microbiens (microbiote intestinal) variant tout au long du tractus gastro-intestinal. Chaque compartiment est colonisé par un microbiote résident, la diversité et l'abondance des microorganismes étant plus élevées dans le compartiment colique. Tous ces paramètres digestifs affectent la digestibilité des aliments, l'absorption des nutriments et la libération d'énergie, mais aussi la libération, l'absorption et le métabolisme des médicaments, ainsi que la survie des microorganismes probiotiques. De ce fait, le développement de nouveaux produits alimentaires ou vétérinaires doit prendre en compte tous ces aspects pour répondre à des questions importantes, telles que : comment les paramètres physicochimiques modulent la digestibilité des aliments ; quelle est l'importance du microbiote intestinal dans la digestion canine et le métabolisme des médicaments ; où les médicaments sont-ils libérés et absorbés ; comment la bioaccessibilité des médicaments est-elle influencée par la matrice alimentaire, la forme galénique, les paramètres physicochimiques du tractus digestif ou le microbiote ; comment les souches probiotiques survivent-elles le long du tractus gastro-intestinal ? Pourtant, à ce jour, les recommandations relatives à l'alimentation des animaux de compagnie et à l'ingestion de médicaments ne sont basées que sur le poids corporel ou le poids métabolique du chien. Les fabricants d'aliments pour animaux de compagnie et les sociétés vétérinaires cherchent à développer des gammes de produits adaptés à la taille (par exemple, croissance à long terme des chiots de grandes races, mauvaise tolérance digestive et torsion d'estomac pour les grands chiens) ou à répondre à certaines prédispositions raciales telles que l'obésité chez les Labradors ou les entéropathies chez les Terriers. Néanmoins, les impacts de la taille ou de la race du chien sur les paramètres digestifs restent très peu décrits alors qu'ils intéressent pleinement les acteurs de la nutrition et la santé canines. Le développement de futurs produits devrait donc considérer non seulement le poids du chien, mais aussi toutes les variations du processus de digestion associées aux différentes tailles et races, avec l'objectif de s'orienter vers une nutrition et une médecine vétérinaire plus personnalisées.

B. Financement et partenariat

Cette thèse a été réalisée dans le cadre d'un projet collaboratif entre l'UMR MEDIS (Microbiologie, Environnement Digestif et Santé, Université Clermont Auvergne-INRAE, Clermont-Ferrand) et deux entreprises, Lallemand Animal Nutrition (Blagnac) et Dômes Pharma (Pont-du-Château). Ce travail de thèse a été financé par une bourse CIFRE (Convention Industrielle de Formation par la REcherche) attribuée à Lallemand et par des financements industriels des deux entreprises pour le fonctionnement.

Le laboratoire **MEDIS** vise à mieux comprendre le rôle du microbiote intestinal humain et animal dans la santé et les maladies et ses recherches sont structurées en quatre axes thématiques. Mon travail de thèse s'inscrit dans les axes INNOVITRO (INNOvation et développement de modèles *in VITRO*) et FM2D (Fonctions métaboliques du Microbiote Digestif et Dysbiose). L'équipe bénéficie de plus de 25 ans d'expertise et de savoir-

faire internationalement reconnus dans le domaine de la simulation *in vitro* de l'environnement digestif humain et animal, avec une plateforme technologique associant des modèles *in vitro* du tractus supérieur, comme TIM (TNO gastroIntestinal Model), et du tractus inférieur, tels que le M-ARCOL (Mucosal ARtificial COLon). **Lallemand**, et plus particulièrement l'unité d'affaires **Animal Nutrition** (**LAN**), développe, produit et commercialise des solutions à base de microorganismes (levures vivantes, bactéries et leurs dérivés) pour la santé et la nutrition animales. Ces solutions ont notamment pour effet de stabiliser les écosystèmes microbiens digestifs. Ainsi, la société LAN cherche à comprendre les modes d'action des solutions sur les communautés microbiennes du tractus gastro-intestinal afin de mieux expliquer leurs effets sur l'efficacité digestive des produits et la santé de l'hôte. La société possède également de solides connaissances dans le domaine des pré-, pro- et postbiotiques et du microbiote, de la physiologie digestive canine, de la nutrition, des ingrédients fonctionnels, mais travaille également en étroite collaboration avec des vétérinaires. **Dômes Pharma** est une société pharmaceutique avec une forte expertise en santé animale, en particulier pour les animaux de compagnie. La société souhaite développer ses connaissances sur la sphère digestive du chien afin de mieux répondre aux besoins des vétérinaires et des propriétaires. L'expertise principale du groupe concerne la santé vétérinaire, en particulier l'utilisation des antibiotiques et le développement de formes pharmaceutiques. Ensemble, les trois partenaires possèdent donc une expertise complémentaire en physiologie digestive canine, en simulation *in vitro* de l'environnement digestif et en développement d'aliments et de produits pharmaceutiques, nécessaire à la réalisation de ce projet de thèse.

C. Questions de recherche et développements technologiques associés

Dans ce contexte, ce travail de doctorat a d'abord été consacré à une meilleure compréhension de l'impact des différentes tailles de chiens sur sa physiologie digestive, incluant aussi et surtout le microbiote intestinal. Pour ce travail, les chiens ont été répartis en trois groupes en fonction de leur poids corporel : "**petit**" inférieur à 10 kg, "**moyen**" entre 10 et 30 kg et "**grand**" jusqu'à 30 kg. Conformément aux règles des 3R et pour répondre à l'absence de modèle *in vitro* canin complexe incluant le microbiote intestinal, les vastes connaissances acquises après une revue extensive de la littérature ont été utilisées pour mettre en place un nouveau système colique *in vitro* adapté aux différentes tailles de chiens, basé sur le modèle M-ARCOL précédemment développé pour simuler le système gastro-intestinal humain. Puis, une situation perturbée a été reproduite dans le modèle *in vitro* par l'ajout d'antibiotiques et des stratégies de restauration du microbiote basées sur l'utilisation d'un probiotique et d'un postbiotique ont été évaluées. De manière plus détaillée, les principaux objectifs scientifiques et les développements technologiques associés de cette thèse de doctorat sont :

1) **Impact de différentes méthodes de conservation des échantillons fécaux sur la composition du microbiote intestinal et l'activité métabolique dans le modèle *in vitro* M-ARCOL.** Ces expériences ont été réalisées en collaboration avec une autre doctorante de MEDIS sur des échantillons de matières fécales humaines, afin de sélectionner la méthode la plus appropriée de conservation des selles pour les expériences suivantes avec des matières fécales canines.

2) **Compréhension approfondie de l'impact du poids corporel sur les paramètres nutritionnels, physicochimiques et microbiens du gros intestin du chien et développement d'un nouveau modèle colique *in vitro* adapté à la taille et basé sur la technologie M-ARCOL**
   - Revues bibliographiques sur l'effet du poids corporel du chien sur la physiologie digestive et sur les modèles digestifs *in vitro* canins actuellement disponibles
   - Développement d'un nouveau modèle colique adapté à la taille du chien appelé CANIM-ARCOL (CANIne Mucosal ARtificial COLon) et validation par comparaison avec des données *in vivo*
   - Étude mécanistique utilisant le nouveau modèle de côlon *in vitro*, visant à étudier la capacité des paramètres physico-chimiques et nutritionnels associés aux chiens de petites et grandes tailles à remodeler la structure et la fonction du microbiote colique obtenu à partir de selles de chiens de taille moyenne
3) **Étude de l'impact de l'antibiothérapie sur la structure et les fonctions du microbiote canin et développement d'un modèle colique dysbiotique basé sur le nouveau modèle CANIM-ARCOL**
   - Revue bibliographique sur l'impact des antibiotiques sur le microbiote du chien
   - Expériences de criblage d'antibiotiques afin de sélectionner le cocktail le plus approprié pour le développement du modèle colique dysbiotique
   - Développement d'un modèle dysbiotique *in vitro* pour les chiens de taille moyenne et validation basée sur des données canines *in vivo* de la littérature
4) **Évaluation d'une nouvelle stratégie postbiotique basée sur des cellules de *Lactobacillus helveticus* HA-122 tyndallisées (inactivées par la chaleur) pour restaurer l'équilibre microbien après un traitement antibiotique et comparaison avec une stratégie probiotique basée sur la levure vivante *Saccharomyces boulardii* CNCM I-1079**
   - Revue bibliographique sur l'impact des pré, pro, post (y compris para) -biotiques sur le microbiote canin
   - Effet du probiotique et du postbiotique sur la structure et les fonctions du microbiote du chien dans le modèle dysbiotique *in vitro* (chien de taille moyenne)

D. Organisation du manuscrit

La **première section** du manuscrit est une revue de la littérature, divisée en quatre parties et fournissant une vue d'ensemble complète des connaissances actuelles sur l'impact de la taille du chien sur les paramètres digestifs physicochimiques et microbiens. Dans la **première partie**, qui reprend notre revue publiée dans *International Journal of Biological Sciences*, l'impact du poids corporel du chien sur les paramètres physicochimiques du côlon est décrit. La **partie 2** est plutôt axée sur l'impact du poids du chien sur les paramètres microbiens, à savoir la composition du microbiote colique et son activité métabolique, après avoir présenté les rôles clés du microbiote intestinal dans la santé canine. Dans la **partie 3**, les facteurs connus pour façonner le microbiote intestinal canin sont détaillés, classés par facteurs survenant dans un état sain (par exemple, paramètres morphologiques et environnementaux) ou dans des conditions dysbiotiques associées à

l'antibiothérapie, à des pathologies digestives ou extra-digestives, ainsi que les stratégies de restauration actuellement disponibles comme les pré-, pro- ou postbiotiques et la transplantation de microbiote fécal. Enfin, la **partie 4**, retravaillée à partir de notre revue publiée dans le journal *ALTEX*, fournit une description détaillée des modèles *in vitro* du tractus digestif du chien actuellement disponibles, avant de discuter leur potentiel dans les domaines alimentaires et vétérinaires, mais aussi leurs limites et les défis auxquels les scientifiques doivent faire face dans ce domaine.

La **deuxième section** présente les résultats de chaque étape du travail expérimental. Tout d'abord, le **chapitre 1** présente une étude comparative portant sur différentes méthodes de stockage des échantillons de matières fécales, afin de préserver la structure et les fonctions du microbiote après ensemencement de selles humaines dans le modèle M-ARCOL. Ensuite, le **chapitre 2** dévoile le développement et la validation comparativement à des données *in vivo* du CANIM-ARCOL qui simule les paramètres nutritionnels, physico-chimiques et microbiens du côlon, en fonction de la taille du chien. Le **chapitre 3** décrit l'importance relative de l'inoculum fécal et des paramètres physicochimiques et nutritionnels du côlon associés à différentes tailles de chien sur l'activité et la structure du microbiote canin *in vitro.* Dans le **chapitre 4,** l'impact de l'antibiothérapie sur la structure et les fonctions du microbiote colique canin a été évalué afin de développer un nouveau modèle colique dysbiotique chez le chien de taille moyenne. Enfin, le **chapitre 5** examine deux nouvelles stratégies basées sur l'administration de levures *Saccharomyces boulardii* CNCM I-1079 et *Lactobacillus helveticus* HA-122 tyndallisées visant à limiter les perturbations ou à restaurer l'équilibre microbien après un traitement antibiotique *in vitro* en utilisant le modèle dysbiotique précédemment développé.

Enfin, la **troisième section** discute les résultats obtenus au cours de cette thèse par rapport à la littérature disponible et développe quelques perspectives à ce travail.

E. Modèle de colon artificiel utilisé dans le travail de thèse

Le modèle digestif *in vitro* utilisé au cours de l'ensemble de ce travail de thèse a été adapté à la digestion du chien à partir du modèle de fermentation continue précédemment développé pour reproduire les conditions coliques humaines : le Mucosal ARtificial COLon (M-ARCOL). Ce modèle *in vitro* permet de reproduire les phases luminale et mucosale du côlon à l'aide respectivement d'un bioréacteur et un module de verre étanche relié à ce bioréacteur et contenant des billes de mucine. Tous les deux jours, les billes de mucine/alginate restant dans le compartiment mucosal sont renouvelées et remplacées par de nouvelles billes sous un flux constant de CO_2 pour éviter l'entrée d'oxygène. Le bioréacteur est maintenu à la température corporelle. Le pH colique et le potentiel d'oxydoréduction sont enregistrés en permanence et le pH est ajusté si nécessaire avec de la soude. Après flushage initial avec du gaz N_2 exempt d'O_2, l'anaérobiose est maintenue pendant toute la durée de la fermentation dans le système *in vitro* par la seule activité du microbiote résident. Un milieu nutritif, simulant la composition des effluents iléaux et contenant diverses sources de carbohydrates, de protéines, de lipides, de minéraux et de vitamines est introduit en continu dans le bioréacteur, tandis que du milieu de fermentation est

soutiré, maintenant un volume colique constant et assurant le temps de rétention moyen souhaité (assimilable au temps de transit colique).

F. Principaux résultats et discussion

Chapitre 1 - Méthodes comparatives de conservation des échantillons de matières fécales pour préserver la structure et la fonction du microbiote colique dans un modèle *in vitro* du côlon humain

La plupart du temps, les modèles de côlon artificiels, que ce soit chez l'animal ou chez l'Homme, sont inoculés avec des échantillons de selles pour reproduire la composante microbienne de l'écosystème intestinal. L'utilisation de selles fraîches (dans les 6 h suivant leur collecte) semble être la stratégie idéale, mais cela n'est pas toujours possible et des méthodes de stockage telles que la congélation ou la lyophilisation sont souvent utilisées en pratique. Jusqu'à présent, un nombre restreint d'études a évalué l'impact des méthodes de conservation sur le microbiote fécal canin. *A fortiori*, l'impact de ces méthodes sur l'établissement du microbiote dans des modèles coliques *in vitro* n'a pas encore été étudié, en particulier dans des conditions canines. Par conséquent, cette étude visait à évaluer l'effet du stockage à court terme (congélation et lyophilisation) sur la cinétique de colonisation du microbiote luminal et associé au mucus, ainsi que sur les activités métaboliques associées, dans le modèle M-ARCOL (reproduisant les conditions coliques humaines). Les expérimentations associées à cette étude ont été réalisées en 2019 lors de mon stage de Master 2 à MEDIS sur des échantillons fécaux humains, dans le cadre d'un travail collaboratif avec le Dr Marion Leclerc de l'unité INRAE MICALIS (Jouy-en-Josas). L'article correspondant a été rédigé au début de ma thèse et les résultats ont été utilisés pour sélectionner l'option la plus appropriée pour les expériences menées lors de ce travail de doctorat sur des échantillons fécaux canins.

Dans cette étude, des échantillons fécaux provenant de deux volontaires sains ont été soumis à différents protocoles de conservation : congélation 48 h à -80°C, congélation 48 h à -80°C avec du glycérol comme agent conservateur ou lyophilisation avec de la maltodextrine/tréhalose suivant le protocole développé par l'équipe MICALIS, et les résultats obtenus ont été comparés à ceux des mêmes échantillons fécaux frais. La composition et la diversité du microbiote ainsi que l'activité métabolique (gaz et acides gras à chaîne courte) ont été suivis tout au long du processus de fermentation dans le M-ARCOL (9 jours). L'ensemble des traitements testés a permis de maintenir à l'intérieur du modèle colique *in vitro* un microbiote complexe et fonctionnel. Cependant, si l'on considère le temps de stabilisation des profils et des activités microbiennes, nos résultats ont montré que la congélation pendant 48 heures à -80 °C sans cryoprotecteur était la méthode la plus efficace parmi celles testées.

Comme le montrent nos résultats, la préparation de l'inoculum fécal est une étape critique à prendre en compte, mais il n'existe pas encore de consensus dans la littérature concernant la collecte, le stockage et la préparation des échantillons des selles canines. Très récemment, l'impact de la méthode d'échantillonnage des matières fécales a été étudié et n'a montré aucun effet du site d'échantillonnage dans les selles sur les populations microbiennes ciblées, mais des variations des concentrations d'acides gras saturés et d'ammoniac, ainsi que des

variations de pH. Les auteurs ont conclu sur la nécessité d'homogénéiser l'ensemble des selles avant échantillonnage. En ce qui concerne le stockage des échantillons de selles canines, aucun impact de la température (température ambiante, 37°C ou 50°C et cycles de congélation-décongélation) sur les diversités bactériennes alpha et bêta n'a été mis en évidence sur les échantillons stabilisés dans les dispositifs de collecte PERFORMAbiome-GUT, alors que la diversité alpha a augmenté dans les échantillons non stabilisés stockés à température ambiante pendant 14 jours, démontrant une croissance des microorganismes et une altération de 24 genres bactériens. De plus, cette étude a révélé une modification de l'abondance relative de 9 genres en fonction des sites de collecte dans un échantillon de matières fécales canines, comme cela a été observé précédemment avec des matières fécales humaines. L'effet de la réfrigération ou de la congélation des fèces canines pendant 24 h a également été évalué à travers son impact sur la production de gaz et les produits finaux de fermentation en modèle statique pendant 72 h. La congélation a réduit la production de gaz tout en augmentant les concentrations d'indoles et de phénols produits.

En prenant en compte les résultats de notre étude, mais aussi les données extraites de la littérature, des matières fécales canines fraîches ont été utilisées pour la suite des expériences de cette thèse, ou lorsque ce n'était pas possible des matières fécales brutes congelées à -80°C pendant 12h sans cryoprotecteur et en condition anaérobie. De plus, tout au long de ce travail de thèse, nous avons travaillé avec des échantillons fécaux non mélangés, puisque des études antérieures ont montré d'importantes variations interindividuelles dans la composition du microbiote fécal entre les chiens. Les expériences réalisées par la suite sur les microbiotes de chiens de petite, moyenne et grande tailles ont confirmé ces variations importantes dans la composition du microbiote entre donneurs et l'importance d'utiliser des selles non poolées pour les études de fermentation chez le chien.

Chapitre 2 – Canine Mucosal Artificial Colon : simulation *in vitro* des paramètres nutritionnels, physicochimiques et microbiens de l'écosystème colique adaptés à différentes tailles de chiens

Après une revue approfondie de la littérature disponible pour définir les paramètres microbiens, nutritionnels et physico-chimiques de la digestion du chien, nous avons observé que des modifications importantes existent entre les chiens de petite, moyenne et grande taille, en particulier au niveau du gros intestin. De façon notable, le temps de transit colique, le pH colique, mais aussi les profils d'acides biliaires et la composition des aliments industriels étaient différents (par exemple, le type de fibres utilisé ou le ratio fibres solubles/insolubles) entre les trois tailles. Nous avons également référencé tous les modèles digestifs artificiels canin disponibles et souligné que la plupart d'entre eux reproduisent le tractus gastro-intestinal inférieur (et non supérieur) du chien, mais en utilisant de simples modèles de fermentation en batch. Seul un modèle dynamique *in vitro* (M-SCIME) reproduisait efficacement le côlon des chiens de taille moyenne avant ce travail de thèse.

Dans ce contexte et pour pallier à ce manque de modèles, l'étape suivante de ce travail de thèse a été de développer un nouveau modèle *in vitro* de côlon canin, le CANIM-ARCOL, simulant les principaux paramètres physicochimiques (pH, temps de transit, anaérobiose), nutritionnels (composition des effluents iléaux) et

microbiens (microbiote présent dans la lumière digestive et associé au mucus) de cet écosystème, et adapté à trois tailles de chiens (petit c'est-à-dire moins de 10 kg, moyen de 10 à 30 kg et grand de plus de 30 kg). Pour valider le nouveau modèle en termes de composition et d'activités métaboliques du microbiote, des fermentations *in vitro* ont été réalisées dans des bioréacteurs inoculés avec les selles de 13 chiens (4 petits, 5 moyens et 4 grands). Après une période de stabilisation, les profils du microbiote colique sont clairement regroupés en fonction de la taille du chien. Les abondances relatives des *Bacteroidota* et des *Firmicutes* sont positivement corrélées à la taille du chien à la fois *in vitro* et *in vivo*, tandis que des tendances opposées sont observées pour les *Actinobacteria* et les *Proteobacteria*. Comparativement à des données coliques *in vivo* chez le chien de taille moyenne obtenues à partir de biopsies ou de digesta coliques, notre modèle permet de maintenir 27 des 31 familles bactériennes détectées (excepté les *Prevotellaceae*, *Streptococcaceae*, *Turicibacteraceae* et *Veillonellaceae*). Notre étude suggère également que la diversité microbienne diminue avec la taille du chien, contrairement aux données issues de la littérature montrant la plus forte diversité microbienne dans les selles de chiens de taille moyenne. Cependant, les résultats *in vitro* comme *in vivo* suggèrent une plus faible diversité observée dans les selles des grands chiens. De manière intéressante, les archées méthanogènes *Methanobrevibacter smithii* ont été détectées pour la première fois dans notre modèle colique, et ce, uniquement dans les fermenteurs reproduisant la digestion des petits chiens. À ce jour, *in vivo* cette population n'a été décrite que dans les selles de chien moyens ce qui ne permet pas de conclure sur un éventuel effet taille sur leur abondance. De plus, en accord avec les observations *in vivo*, l'intensité des processus de fermentations augmente avec la taille du chien *in vitro,* comme le montrent la production de gaz, d'acides gras à chaîne courte et branchés, d'ammoniac et la déhydroxylation des acides biliaires. Il est cependant à noter que certaines des tendances observées dans nos fermenteurs peuvent être en désaccord avec la littérature, par exemple l'association positive entre taille de chien et concentrations en isovalérate, isobutyrate ou valérate. Ces différences pourraient s'expliquer par le faible nombre d'études impliquant des chiens de petites et grandes tailles pouvant biaiser les conclusions sur l'effet taille.

Depuis des décennies, les recommandations des industriels et des vétérinaires en matière d'aliments et de médicaments pour animaux de compagnie sont uniquement basées sur le poids corporel ou le poids métabolique du chien. Cependant, comme l'a montré ce projet de thèse, la littérature disponible a également mis en évidence de nombreuses spécificités associées à chaque taille de chien concernant la physiologie digestive, en particulier liées au gros intestin et au microbiote associé. Par exemple, ces travaux ont mis en évidence des différences de perméabilité intestinale et colique et de capacités d'absorption en fonction de la taille des chiens, ce qui peut avoir un impact évident sur la bioaccessibilité des nutriments ou des médicaments. De plus, le temps de transit et le pH varient en fonction de la taille des chiens, ce qui doit être pris en compte car ces paramètres impactent non seulement la cinétique de libération des médicaments et la digestibilité des aliments mais aussi la composition du microbiote intestinal et les activités métaboliques associées. À la lumière de ces connaissances, le développement de nouveaux compléments alimentaires ou produits vétérinaires devrait prendre en compte toutes les facettes associées aux effets de la taille du chien, afin de tendre vers une nutrition et une médecine

vétérinaire plus personnalisées. Cette compréhension approfondie de l'impact de la taille corporelle sur les paramètres nutritionnels, physico-chimiques et microbiens du gros intestin du chien a été associée au développement du nouveau modèle colique canin, le CANIM-ARCOL. Ce modèle est le deuxième modèle dynamique *in vitro* (avec le M-SCIME) reproduisant le gros intestin du chien et distinguant le microbiote associé à la lumière de celui associé au mucus. Le CANIM-ARCOL est néanmoins le premier à avoir été adapté aux spécificités digestives associées aux petites, moyennes et grandes tailles de chiens. Il est intéressant de noter que ce travail fournit également une description détaillée des échantillons de selle de 13 chiens sains appartenant aux trois tailles, ce qui a rarement été fait auparavant dans une seule étude. Cela inclut la composition du microbiote, avec l'analyse de la charge bactérienne totale et des profils de séquençage, mais aussi les activités métaboliques *via* le dosage des principaux produits finaux de fermentation tels que les gaz, les acides gras à chaine courte, les acides gras branchés, l'ammoniac et la description des profils d'acides biliaires. Nous avons ainsi fourni au cours de ce travail de thèse les premières données sur les profils de gaz produits dans les conditions coliques du chien, grâce à l'absence de flushage des bioréacteurs avec du N_2 ou du CO_2. Le suivi de la production de gaz est d'un grand intérêt parce que leur volume et leur composition peuvent être liés à l'état de santé des chiens. En effet, une production excessive de gaz est associée à des flatulences et une gêne intestinale et reflète généralement un régime alimentaire peu digeste. Suivre les gaz *in vitro* pourrait ainsi être un paramètre intéressant permettant d'évaluer la digestibilité de différents régimes ou l'impact de certaines modifications alimentaires. Cette étude fournit également, pour la première fois, des données précises sur l'impact de la taille du chien sur la composition en bactéries et archées du microbiote. L'étude de la fraction archéale est intéressante, car même si les archées représentent environ 1,1 % du microbiote fécal du chien, elles n'ont été, jusqu'à présent, que très peu étudiées *in vivo* et encore jamais décrites dans des modèles coliques *in vitro.* Basé sur les données disponibles chez d'autres mammifères, y compris l'Homme, nous pouvons émettre l'hypothèse que les archées peuvent être impliquées dans des interactions mutualistes avec les bactéries dans l'intestin du chien. En modèle souris, il a été suggéré que le transfert d'hydrogène entre espèces bactériennes et archées était impliqué dans l'augmentation de l'absorption d'énergie provenant des aliments. Dans les selles humaines, une relation inverse entre l'abondance des archées et l'indice de masse corporelle a été mise en évidence, en accord avec nos résultats montrant une corrélation négative entre abondances des archées et taille des chiens. De plus, il serait également intéressant d'explorer à la fois le mycobiome et le virome du microbiote colique, représentant chacun 0,4 % du microbiote fécal et encore peu décrits chez le chien. Il est intéressant de noter qu'une étude très récente a mis en évidence une altération de la composition et de la diversité du virome associée à la diarrhée chez le chien. Chez l'Homme, le mycobiome a récemment été décrit comme un composant indispensable du microbiome, perturbé dans certaines maladies gastro-intestinales ou cancers, suggérant une fois de plus l'intérêt de leur suivi dans de prochaines études *in vitro* chez le chien. Cependant, les expériences précédentes dans le M-ARCOL en situation humaine ont mis en évidence des difficultés à maintenir *in vitro* la fraction eucaryote du microbiote fécal. Enfin, au cours de ces travaux nous avons évalué pour la première fois l'effet de la taille du chien sur le microbiote de la lumière digestive et celui associé au mucus. En condition canine, le microbiote mucosal a été précédemment étudié dans un seul modèle *in vitro*, le M-SCIME simulant

la digestion de chiens de taille moyenne. Des familles bactériennes similaires ont été observées entre les fractions mucosales du M-SCIME et du CANIM-ARCOL, même si aucun *Verrucomicrobia* n'a été détecté dans notre étude, ni dans l'inoculum fécal, ni dans les bioréacteurs. À ce jour, le microbiote associé au mucus dans le côlon du chien n'a été étudié que par des approches ciblées telles que l'hybridation *in situ*, principalement pour suivre des bactéries pathogènes telles que les *Escherichia coli* adhérentes et invasives. Il serait très intéressant de mieux décrire chez le chien ce microbiote, car il existe de plus en plus de preuves de leur importance en santé. Notre étude *in vitro* suggère que chez le chien, les *Bacteroidaceae* (toutes tailles confondues), les *Fusobacteriaceae* et les *Lachnospiraceae* (petites et moyennes tailles) ainsi que les *Clostridiaceae* et les *Sporanaerobacteraceae* (grandes tailles) semblent être des familles importantes associées au mucus, en accord avec les observations réalisées sur d'autres espèces (pour les *Bacteroidaceae* et les *Lachnospiraceae*). Ces résultats renforcent également l'idée d'un rôle fonctionnel des *Fusobacteriaceae* chez le chien sain, probablement très typique de l'espèce canine. Chez l'Homme, chez la souris, mais aussi chez le chien, l'invasion de la couche externe du mucus a déjà été associée à des maladies telles que la colite granulomateuse. Des modifications de l'épaisseur ou de la composition du mucus ont également été associées à différentes pathologies chez l'Homme. Le mucus colique présente des caractéristiques similaires chez le chien et l'Homme -mais aussi chez le porc- avec une majorité de protéines MUC2, appuyant l'hypothèse d'un rôle probable de la couche de mucus dans la santé du chien.

Une fois développé, le modèle CANIM-ARCOL a été validé par des comparaisons *in vivo-in vitro* basées sur des données coliques chez le chien (taille moyenne uniquement) et fécales, extraites de notre revue de la littérature. Il est surprenant de constater que jusqu'à présent, seules deux études ont déterminé la composition du microbiote colique, uniquement chez des chiens de taille moyenne, certainement en raison de la nécessité d'utiliser des méthodes invasives pour l'échantillonnage. Le développement récent de nouvelles technologies d'échantillonnage (i.e. capsules intelligentes comme les SmartPills) pourrait contribuer à combler ce manque de données, en permettant un accès facile à l'ensemble du tractus gastro-intestinal. Malgré cette validation *in vitro-in vivo*, au vu des résultats obtenus dans notre étude, quelques améliorations supplémentaires pourraient être apportées au modèle CANIM-ARCOL afin de mieux discriminer le microbiote des chiens de petite et moyenne taille *in vitro*. En parallèle, il faudrait également essayer de mieux expliquer la faible diversité bactérienne et la perte des *Fusobacteriaceae* associée à l'explosion de l'abondance relative des *Sporanaerobacteraceae,* chez le chien de grande taille *in vitro.* Une première réponse pourrait être apportée grâce à une analyse métabolomique du contenu des bioréacteurs. Nous espérons également que grâce à ce travail, les chercheurs pourront commencer à prendre en compte l'effet de la taille des chiens dans les études sur le microbiome canin, voire pourront même rendre accessibles les données de séquençage obtenues lors d'études précédentes permettant ainsi de réanalyser ces résultats en tenant compte de cet effet. Cela permettrait d'affiner la validation du CANIM-ARCOL et d'avoir plus de données *in vivo* pour le développement de nouveaux modèles digestifs *in vitro* et accroître leur pertinence. Enfin, cette étude s'est focalisée sur la partie inférieure du tractus gastrointestinal du chien, mais le devenir des produits alimentaires ou vétérinaires dans le tractus digestif supérieur du chien est également un point clé pour les industriels et les académiques des domaines de l'alimentation et de la pharmacie.

Jusqu'à présent, seul un modèle dynamique de l'estomac et de l'intestin grêle du chien a été développé : le modèle FIDO, basé sur la technologie du TIM-1 disponible au laboratoire MEDIS. Ce modèle simule les conditions rencontrées dans l'estomac et l'intestin grêle du chien de taille moyenne uniquement. Malheureusement, le manque de données *in vivo* relatives au tractus digestif supérieur (c'est-à-dire la cinétique du pH, les concentrations d'enzymes et de bile, l'épaisseur du mucus et la composition du microbiote dans les différents compartiments) nous a empêchés d'adapter le modèle FIDO aux conditions digestives des chiens de petite et de grande taille au cours de ce travail de doctorat. Disposer d'un tel outil *in vitro* constituerait néanmoins une valeur ajoutée importante, notamment pour étudier la survie des probiotiques ou le devenir et la bioaccessibilité de composés d'intérêts tels que les nutriments ou les médicaments dans le tractus digestif supérieur du chien.

Chapitre 3 - Étude mécanistique : vers une meilleure compréhension de l'importance relative de l'inoculum fécal et des paramètres environnementaux pour remodeler le microbiote canin en fonction de la taille du chien *in vitro*

Une fois le CANIM-ARCOL développé et validé pour chaque taille de chien, nous avons choisi d'approfondir nos études avec une approche plus mécanistique. Dans notre revue de la littérature et avec le CANIM-ARCOL également, comme précédemment décrit nous avons mis en évidence des différences nutritionnelles, physicochimiques et microbiennes dans le compartiment colique des trois tailles de chiens, telles que le pH et le temps de transit, les profils d'acides biliaires et les teneurs en macronutriments dans les effluents iléaux. Dans ce troisième chapitre, profitant de la flexibilité de notre approche *in vitro*, nous avons cherché à évaluer l'importance relative du microbiote (inoculum fécal) et des conditions environnementales du côlon (paramètres nutritionnels et physico-chimiques) sur la structure et les fonctions du microbiote colique du chien. À cet effet, nous avons réalisé de nouvelles fermentations lorsque le CANIM-ARCOL était configuré pour reproduire les paramètres coliques de petits, moyens ou grands chiens, mais avec des bioréacteurs inoculés seulement avec des échantillons fécaux de chiens de taille moyenne (2 donneurs, un mâle et une femelle). Cette étude visait également à vérifier si les paramètres nutritionnels et physicochimiques seuls, sans tenir compte des conditions de l'hôte (c'est-à-dire de l'interaction avec les cellules de l'hôte, les hormones, la perméabilité intestinale ou le système immunitaire) étaient suffisants ou non pour orienter le microbiote d'un profil de chien de taille moyenne vers des profils plus spécifiques des chiens de petite et de grande taille.

L'application de différents paramètres associés aux trois tailles de chiens sur des bioréacteurs inoculés avec des selles de chien de taille moyenne a permis de retrouver une association positive entre la taille des chiens et la production de gaz ou d'acides gras à chaine courte, ainsi que des profils de microbiote distincts en fonction des trois tailles, tels que révélés par un séquençage 16S du contenu des bioréacteurs. Des comparaisons ont également été effectuées avec les résultats *in vitro* obtenus précédemment lorsque le CANIM-ARCOL a été inoculé avec des échantillons fécaux provenant des chiens de trois tailles différentes, et des données fécales *in vivo*. En effectuant de telles comparaisons il est toutefois important de garder en tête que les résultats peuvent différer entre les deux études *in vitro* en raison de différences au niveau des durées de fermentations (9 jours

dans cette étude *versus* 21 jours dans la précédente) et le nombre de réplicats biologiques (2 selles ici *versus* 13 dans l'étude précédente). L'impact de la taille du chien sur la diversité bactérienne était similaire dans les deux études. Cependant, l'effet taille observé ici au niveau des phyla n'est pas en accord avec la précédente étude, avec des tendances opposées pour 3 des 5 phyla majoritaires et pas d'effet taille observé pour les deux autres. Au niveau des familles, les variations observées pour respectivement 7 et 5 familles sur 12 dans le milieu luminal et les billes de mucine étaient en accord avec l'étude *in vitro* précédente. Concernant l'activité du microbiote, 10 sur 11 des indicateurs mesurés (dont la production de gaz, d'acides gras à chaine courte et d'ammoniac) présentaient des tendances identiques avec la précédente étude. La comparaison avec les données fécales *in vivo* a également permis d'observer que la plupart des familles retrouvées dans les échantillons de selle sont maintenus *in vitro*. Un effet taille similaire a également été démontré *in vitro* et *in vivo* dans les selles pour 6 des 12 familles bactériennes. Ainsi, ces résultats démontrent que les paramètres coliques environnementaux sont suffisants pour orienter les fonctions du microbiote *in vitro*. L'étude révèle également que les microbes fécaux associés à la taille sont nécessaires pour reproduire fidèlement *in vitro* l'écosystème colique des chiens de petite, moyenne et grande tailles. Pour la première fois, cette étude apporte des informations sur les principaux paramètres de l'écosystème colique qui orientent le microbiote en fonction de la taille du chien.

Ce travail a bénéficié d'une approche mécanistique *in vitro* jamais décrite dans la littérature, mais déjà employée avec succès dans l'étude réalisée pendant mon stage de Master 2, qui visait à étudier l'impact des paramètres physicochimiques et nutritionnels de l'environnement colique humain sur la dysbiose du microbiote intestinal associée à l'obésité. Nos données suggèrent que les activités métaboliques du microbiote s'adaptent plus rapidement aux changements que sa composition. Ces observations sont en accord avec des travaux précédents menés avec le modèle M-ARCOL en conditions humaines, qui ont mis en évidence une restauration plus rapide de l'activité du microbiote par rapport aux profils bactériennes après antibiothérapie et un traitement par transplantation de microbiote fécal. Des résultats similaires ont également été obtenus en conditions porcines dans le M-ARCOL après simulation *in vitro* du stress nutritionnel associé au sevrage. Cette forte résilience des fonctions métaboliques est certainement permise par la redondance fonctionnelle observée au sein du microbiote. Pour compléter ces travaux, d'autres fermentations impliquant un plus grand nombre de donneurs (seuls deux chiens ont participé à notre étude) seraient un plus. Il serait également très intéressant de voir l'impact de chacun des facteurs qui ont été modifiés, de façon indépendante, afin de confirmer leur importance relative dans la structuration du microbiote intestinal et de ses fonctions. À titre d'exemple, nous pourrions évaluer de façon indépendante l'impact du pH ou du temps de transit, sans changer aucun autre des paramètres de fermentation, afin évaluer l'effet de ces paramètres sur la composition et les activités métaboliques du microbiote.

Chapitre 4 - Développement d'un nouveau modèle dysbiotique du microbiote du colon chez le chien associé à l'antibiothérapie

Après avoir évalué l'impact de la taille du chien et l'importance relative de l'inoculum fécal par rapport aux paramètres environnementaux colique sur le microbiote dans le CANIM-ARCOL en conditions saines, nous avons souhaité reproduire *in vitro* une situation perturbée. Nous nous sommes d'abord intéressés à la reproduction de l'état de dysbiose du microbiote associé à des maladies telles que l'obésité ou les maladies inflammatoires chroniques de l'intestin, comme nous avions déjà développé avec succès chez l'Homme ce type de modèle. Reproduire l'obésité a été parmi les situations perturbées l'option que nous avions privilégiée au début car j'avais participé au développement du modèle obèse dans le M-ARCOL au cours de mon stage de Master 2. Cependant, le manque de données *in vivo* pertinentes chez le chien (notamment en ce qui concerne les paramètres physico-chimiques du côlon) nous a dissuadés d'adapter le CANIM-ARCOL à cette pathologie pour l'instant. Nous nous sommes donc tournés vers une autre pathologie chez le chien, l'entéropathie chronique. Dans l'urgence, cette maladie est souvent traitée par antibiothérapie par les vétérinaires avant même de chercher des stratégies alternatives. Néanmoins, des études récentes ont mis en évidence l'émergence de résistances aux antibiotiques chez les chiens, en réponse à une utilisation inappropriée des antibiotiques. Il s'agit d'un sujet de préoccupation mondiale, du fait du lien croissant entre les animaux de compagnie et de leurs propriétaires. En effet, des transferts horizontaux de microorganismes entre les deux espèces peuvent avoir lieu et entraîner la transmission de résistances aux antibiotiques. Cependant, jusqu'à présent, l'impact de l'antibiothérapie sur le microbiote est mal décrit chez les chiens, avec seulement 10 études *in vivo* basées sur l'analyse des selles. À noter aussi que, jusqu'à présent, l'impact de l'antibiothérapie sur la composition et les fonctions du microbiote colique canin n'a jamais été décrit, et qu'aucune étude n'a été menée pour évaluer l'impact des antibiotiques en modèles coliques canins. Dans 8 de ces 10 études *in vivo*, les auteurs ont observé des perturbations du microbiote, notamment caractérisé par une diminution de la diversité bactérienne et une modification de l'abondance relative de certains phyla. Ainsi, dans cette nouvelle partie de la thèse nous avons décidé d'utiliser les antibiotiques comme inducteurs de dysbiose. L'objectif était de développer le premier modèle colique *in vitro* permettant d'étudier l'impact de l'antibiothérapie sur la structure et les fonctions métaboliques du microbiote associé à la lumière et au mucus chez les chiens, en se focalisant sur ceux de taille moyenne.

Pour cela, une étape de pré-screening a été réalisée sur cinq cocktails d'antibiotiques différents (i.e. métronidazole seul, métronidazole/enrofloxacine, métronidazole/enrofloxacine/ciprofloxacine, amoxicilline et tylosine) utilisés à des doses physiologiques. Ces pré-études ont conduit à sélectionner pour la suite des travaux un traitement de 5 jours au métronidazole/enrofloxacine. Ainsi, deux bioréacteurs du CANIM-ARCOL ont été inoculés avec un échantillon de matières fécales (n=2 donneurs de taille moyenne) et ont fonctionné en parallèle pendant 26 jours dans des conditions contrôle (sans antibiotique) ou traité avec les antibiotiques. Le traitement antibiotique a réduit la diversité microbienne et induit des changements majeurs dans les populations bactériennes, conduisant à un état de dysbiose caractérisé par une augmentation des abondances relatives des *Streptococcaceae*, *Lactobacillaceae* et *Enterobacteriaceae* et une diminution des *Bacteroidaceae*, *Fusobacteriota* et *Clostridiaceae*. Comme décrit *in vivo*, une diminution significative de la diversité bactérienne

a également été induite par le traitement antibiotique. Toutefois, dans l'ensemble, le microbiote associé au mucus a été moins impacté par les antibiotiques que celui de la lumière digestive. Les altérations microbiennes ont été associées à des perturbations drastiques de l'activité du microbiote. Pendant le traitement antibiotique nous avons observé une réduction sévère de la production de gaz et des concentrations en acides gras à chaine courte. De manière intéressante, après l'arrêt du traitement, les niveaux initiaux de gaz et d'acides gras à chaine courte ont été rapidement retrouvés (en 24-48 h), tandis que le retour à un état stable des profils bactériens (mais différent de l'état initial) a été atteint après un temps plus long (supérieur à 7 jours).

Même si l'étape de pré-screening réalisée dans cette partie des travaux a été utilisée comme un criblage préliminaire d'antibiotiques, il pourrait être intéressant d'augmenter le nombre de réplicats biologiques pour évaluer si des réponses dépendantes du donneur peuvent être observées. Il est intéressant de noter que l'amoxicilline et le métronidazole seuls ont eu un impact limité sur le microbiote colique *in vitro*, tandis que la tylosine a entraîné une situation très perturbée. L'absence d'impact de l'amoxicilline et du métronidazole est quelque peu surprenante étant donné les altérations du microbiote précédemment décrites *in vivo* dans des échantillons fécaux de chiens. Néanmoins, ces données ont été obtenues après des traitements plus longs (14 jours pour le métronidazole et 7 jours pour l'amoxicilline -contre 7 jours pour le métronidazole et 5 pour l'amoxicilline dans nos expériences-, plus long que les recommandations des vétérinaires) et des méthodes de séquençage différentes qui peuvent impacter les résultats. Les résultats obtenus avec la tylosine sont généralement en accord avec la littérature rapportant une augmentation des *Enterobacteriaceae* alors que l'alpha-diversité et l'abondance relative des *Fusobacteriaceae* diminuent. *In fine*, le cocktail métronidazole/enrofloxacine a été choisi pour le développement du modèle dysbiotique. Le métronidazole est largement utilisé chez les chiens souffrant d'entéropathies ou de diarrhées chroniques, tandis que l'enrofloxacine est principalement employée pour traiter les infections gastro-intestinales qui n'ont pas répondu à une antibiothérapie antérieure. Il convient de noter que le cocktail métronidazole/enrofloxacine n'est pas largement prescrit par les vétérinaires, mais cette association a été décrite comme augmentant considérablement le spectre d'activité des antibiotiques, ce qui augmente le risque de signes gastro-intestinaux associés chez les chiens et induit des altérations sévères du microbiote fécal et du métabolome associé.

L'état de dysbiose du microbiote intestinal est défini par une altération à la fois de sa composition et de ses fonctionnalités. Ainsi, au cours du développement du modèle dysbiotique, nous avons réalisé une analyse de séquençage du microbiote associé à la lumière et au mucus et une mesure des gaz et des acides gras à chaine courte en tant que principaux produits finaux de la fermentation microbienne. Nous avons également calculé, pour la première fois dans un modèle colique *in vitro*, un indice de dysbiose. Cet indice a été initialement décrit dans le cadre d'entéropathies chroniques, et est basé sur des quantifications par qPCR de 7 populations bactériennes considérées comme des marqueurs de dysbiose. Dans la présente étude, les scores de dysbiose ont été calculés en utilisant la même méthode mais d'une manière originale, à partir des données de séquençage 16S au lieu de celles obtenues par qPCR. Cela a été possible grâce au développement récent du package R 'dysbiosisR'. Dans nos travaux, le calcul d'indices de dysbiose associés à l'antibiothérapie indiquent que ces 7

populations spécifiques peuvent être utilisées non seulement pour prédire la dysbiose associée aux entéropathies chroniques mais aussi celle liée à l'antibiothérapie. Comme prévu, le cocktail métronidazole/enrofloxacine a induit *in vitro* une altération importante du microbiote colique, en particulier dans le compartiment luminal du CANIM-ARCOL. Le microbiote associé au mucus a été moins impacté, en accord avec de précédentes observations *in vitro* réalisées dans le dispositif M-SHIME en conditions humaines et après ajout d'acides gras polyinsaturés. Les auteurs ont décrit les billes de mucine comme un microenvironnement robuste permettant l'attachement physique des bactéries, leur conférant un avantage compétitif. Une formation importante de biofilm a été observée dans un précédent travail de thèse à la surface de billes de mucine prélevées dans le modèle M-ARCOL en conditions porcelet, grâce à une analyse par microscopie électronique à balayage. Les biofilms sont connus pour protéger les bactéries des antibiotiques en agissant comme un milieu protecteur. Nous pouvons ainsi formuler l'hypothèse que ce microenvironnement préservé peut agir comme un réservoir bactérien réinoculant continuellement le milieu luminal. Dans le milieu luminal du CANIM-ARCOL, une réduction de la charge bactérienne totale, de la production de gaz et des concentrations en acides gras à chaine courte, associés à une augmentation de l'indice de dysbiose, ont été observés pendant le traitement antibiotique et maintenus par la suite. En outre, une prolifération des *Enterobacteriaceae* a été observée pendant l'antibiothérapie, associée à une augmentation des abondances relatives de pathogènes opportunistes tels que *Enterococcus*, *Escherichia* et *Proteus*, tandis que celles des *Fusobacterium*, *Faecalibacterium* et *Clostridium* ont diminué. Ces résultats étaient attendus car la prolifération des *Enterobacteriaceae* a été précédemment décrite comme un marqueur commun de dysbiose chez l'Homme et le chien.

Il est également intéressant de noter que ces modifications de la composition et de l'activité du microbiote sont en parfaite adéquation avec les résultats de la seule étude *in vivo* qui a évalué dans les selles de chien l'effet du même cocktail d'antibiotiques sur le microbiome, validant ainsi notre modèle dysbiotique. Cependant, il est à noter que la production et les profils de gaz n'ont jamais été suivis *in vivo* chez le chien dans un contexte d'antibiothérapie, ce qui n'a pas permis d'établir les comparaisons *in vitro-in vivo* sur ces paramètres. De manière surprenante, la présente étude a également démontré qu'un traitement de 5 jours avec le cocktail métronidazole/enrofloxacine (ce qui est 4 fois plus court que le traitement de 21 jours appliqué dans l'étude *in vivo*, et plus en adéquation avec les prescriptions vétérinaires) est capable d'induire des changements critiques dans le microbiote colique du chien et ce, indépendamment de l'hôte. De plus, la plupart des populations bactériennes affectées étaient encore perturbées après l'antibiothérapie, comme cela a été précédemment observé *in vivo*. Cependant, dans notre étude *in vitro*, les altérations du microbiote ont persisté pendant quelques jours, alors que jusqu'à 4 semaines ont été nécessaires pour restaurer la composition du microbiote *in vivo*. Ceci est surprenant car il existe chez le chien de nombreuses sources de ré-inoculation bactérienne, comme l'alimentation ou l'environnement, qui n'existent pas *in vitro,* les bioréacteurs étant des systèmes clos. Une telle différence pourrait s'expliquer principalement par une période d'antibiothérapie plus longue *in vivo* que *in vitro*. Une autre explication est que dans le CANIM-ARCOL, la phase muqueuse est plus efficace que *in vivo* pour réinoculer le compartiment luminal, peut-être en raison d'un ratio de surface mucosale plus élevé *in vitro* comparativement à la situation *in vivo*. Cette quantité de mucus a été précédemment définie au laboratoire sur la base de données

humaines et il n'existe malheureusement pas de données publiées sur l'épaisseur du mucus colique du chien pour les ajuster à la situation canine. Dans l'ensemble, les données recueillies ont confirmé les effets négatifs que l'antibiothérapie peut avoir sur le microbiote colique des chiens. Ainsi, nos résultats encouragent encore d'avantage les vétérinaires à effectuer des prélèvements fécaux pour des tests de résistance aux antibiotiques avant toute antibiothérapie chez le chien (sauf en cas d'urgence), afin de limiter autant que possible une utilisation inappropriée.

Ce travail de thèse s'est focalisé sur un état dysbiotique associé à un traitement antibiotique chez des chiens de taille moyenne. Dans un avenir proche, nous pourrions également envisager d'adapter le modèle de dysbiose induit par les antibiotiques à d'autres tailles de chiens (c'est-à-dire aux chiens de petite et de grande taille). Toutefois, de tels développements seraient limités par le manque de données *in vivo*, étant donné que jusqu'à présent toutes les études sur les antibiotiques ont été réalisées sur des chiens de taille moyenne. Le potentiel du CANIM-ARCOL pourrait également être étendu à d'autres situations pathologiques dans lesquelles une dysbiose du microbiote intestinal a été mise en évidence, telles que l'obésité, les maladies inflammatoires de l'intestin ou les entéropathies chroniques. La simulation d'une situation dysbiotique dans des modèles coliques *in vitro* nécessitera l'utilisation d'échantillons fécaux provenant de donneurs malades, mais aussi l'adaptation de tous les paramètres physico-chimiques et nutritionnels associés pour reproduire les conditions environnementales coliques spécifiques de la maladie. Ces adaptations sont cruciales en raison de l'importante capacité de résilience du microbiote intestinal, qui retournera rapidement à un état d'eubiose si le maximum de paramètres associés à la maladie n'est pas reproduit. Par exemple, simuler l'obésité canine *in vitro* impliquerait d'adapter la quantité de nourriture (la suralimentation étant le principal facteur d'obésité canine), mais aussi la composition des effluents iléaux car des profils lipidiques et biliaires altérés ont été rapportés chez les chiens obèses. Ce type d'adaptation a déjà été réalisé avec succès avec le modèle M-ARCOL pour reproduire les conditions d'obésité humaine.

Chapitre 5 - Efficacité du postbiotique dérivé de *Lactobacillus helveticus* et de *Saccharomyces boulardii* pour préserver ou restaurer le microbiote colique après une perturbation induite par les antibiotiques dans un modèle *in vitro* du chien de moyenne taille

Le modèle CANIM-ARCOL a été adapté et validé avec succès pour reproduire une dysbiose induite par un antibiotique avec des corrélations *in vivo-in vitro* pertinentes. La dernière étape de cette thèse de doctorat a donc été consacrée aux tests *in vitro* de stratégies de restauration microbienne. Une recherche bibliographique a mis en évidence un manque de connaissance manifeste concernant les stratégies de restauration associées à l'antibiothérapie chez le chien. Basé sur les connaissances acquises chez l'Homme, différentes stratégies peuvent être utiles dans ce contexte, notamment les stratégies prébiotiques, probiotiques et postbiotiques. Une seule étude *in vivo* chez le chien a évalué l'effet d'*Enterococcus faecium* administré avec du métronidazole à des animaux atteints de diarrhées, montrant un impact positif de la bactérie sur les paramètres cliniques et les fréquences des diarrhées. Le probiotique bien connu *S. boulardii* pourrait également être un candidat probiotique

intéressant pour les chiens, compte tenu des effets positifs déjà observés chez l'Homme sur la diminution des diarrhées associées aux antibiotiques. À ce jour, la levure *S. boulardii* n'a été testée que chez des chiens en bonne santé, des femelles allaitantes ou des animaux souffrant de maladies inflammatoires chroniques de l'intestin, mais n'a jamais été testée dans le cadre d'antibiothérapie chez le chien. Par ailleurs, les postbiotiques constituent une autre stratégie alternative prometteuse, encore peu documentée chez le chien.

Dans ce contexte, nous avons décidé, comme dernière étape de ce travail de thèse, d'évaluer l'impact d'une levure probiotique vivante (*S. boulardii* CNCM I-1079) et d'une bactérie tyndallisée (*L. helveticus* HA-122 inactivée par la chaleur) sur la composition et l'activité du microbiote colique du chien dans un contexte d'antibiothérapie dans le modèle CANIM-ARCOL. Les stratégies de restauration ont été administrées deux fois par jour à des doses physiologiques afin d'évaluer leur capacité à augmenter la résistance pendant la perturbation antibiotique et à améliorer la restauration de l'équilibre du microbiote présent dans la lumière digestive et associé au mucus après antibiothérapie. Pendant le traitement antibiotique, les deux stratégies ont permis de réduire la perturbation du microbiote. En particulier, *L. helveticus* tyndallisé tend à préserver la production d'acétate alors que la levure *S. boulardii* permet de limiter l'augmentation du potentiel d'oxydoréduction au cours du traitement antibiotique. Les effets les plus notables ont été observés dans les deux jours suivant le traitement antibiotique, où *S. boulardii* et *L. helveticus* ont atténué la prolifération des *Enterobacteriaceae* et favorisé une résilience plus rapide du microbiote, en particulier en termes de population bactérienne totale, de diversité bactérienne et de production d'acides gras à chaîne courte. Les deux microorganismes ont permis d'inhiber les voies métaboliques activées par l'antibiothérapie et potentiellement impliquées dans le métabolisme de souches pathobiontes.

De nos jours, il existe un nombre croissant de stratégies de restauration du microbiote intestinal commercialisées pour les chiens mais jusqu'à présent, seule la bactérie *E. faecium* a été testée *in vivo* dans un contexte d'antibiothérapie. Par conséquent, pour combler ce manque de connaissances, deux candidats potentiels ont été sélectionnés parmi les souches produites par l'un des partenaires de cette thèse, Lallemand, à savoir la levure probiotique vivante *S. boulardii* CNCM I-1079 (déjà commercialisée sous le nom de LevucellSB pour les porcs et les volailles) et la bactérie inactivée par la chaleur *L. helveticus* HA-122 (récemment commercialisé pour les chiens et les chats et nécessitant de recueillir d'avantage d'éléments mécanistiques en relation avec son mode d'action). *S. boulardii* a été choisie ici comme "contrôle positif" en raison de ses effets bénéfiques reconnus chez l'Homme dans le contexte de l'antibiothérapie. Chez l'Homme, *S. boulardii* a démontré des effets très intéressants sur les diarrhées associées à l'antibiothérapie en réduisant leur fréquence grâce à une augmentation de la production d'acides gras à chaine courte et en particulier de butyrate. La levure probiotique est aussi connue pour sécréter des polyamines, considérées comme bénéfiques pour la santé de la muqueuse colique. Une capacité d'exclusion des agents pathogènes a également été démontrée par liaison des agents pathogènes (par exemple *E. coli* ou *Salmonella*) aux cellules de la levure ou par la sécrétion de composés antimicrobiens. Par ailleurs, des effets anti-toxiniques ont été décrits contre *Clostridium difficile* et la toxine cholérique. Enfin, *S. boulardii* aurait des effets immunomodulateurs et anti-inflammatoires, principalement en

réprimant la voie NF-κB et la production d'IL-8 tout en induisant la production d'IL-10 anti-inflammatoires. Des effets probiotiques intéressants de *S. boulardii* CNCM I-1079 ont également été démontrés chez les chiens, induisant une amélioration de la résilience du microbiote chez les chiennes en gestation et en lactation au moment de la mise bas et une modulation du microbiote des chiots. Des diminutions significatives des marqueurs inflammatoires et de stress dans les selles, sans impact sur la composition du microbiote ont également été observées chez des chiens sains et atteints d'entéropathies chroniques. Jusqu'à cette étude, les effets de *S. boulardii* ont été très peu décrits dans un contexte d'antibiothérapie chez le chien mais la levure a déjà montré des effets prometteurs chez des animaux sains recevant un antibiotique de type lincomycine. Ainsi, dans cette étude nous avons montré une diminution de l'abondance d'*Escherichia* dans le CANIM-ARCOL en présence de la levure probiotique. Cet effet inhibiteur peut être lié à la production d'acide acétique par la levure, qui est connu pour exercer un effet inhibiteur sur *E. coli*. Il convient de noter que, contrairement à nos résultats, des études canines antérieures faisant état d'une supplémentation en *S. boulardii* pendant 10 à 35 jours chez des chiens en bonne santé et des chiens souffrant d'entéropathies chroniques n'ont pas rapporté d'impact sur le microbiote fécal et le mycobiote. De plus, une étude *in vitro* simulant les conditions du rumen a montré que *S. boulardii,* à la fois sous forme vivante et autoclavée, stimulait de manière significative la production d'acides gras à chaine courte (i.e. acétate et butyrate) et d'acides gras branchés (i.e. isovalérate et valérate), sans différence majeure entre les deux conditions. Les auteurs ont conclu à un effet prébiotique potentiel de la levure, mais les populations microbiennes n'ont pas été suivies pour confirmer cette hypothèse. Cet effet prébiotique était supposé être associé à l'utilisation des composants de la paroi cellulaire de la levure (tels que les glucanes, les mannoprotéines et la chitine) comme substrats pour la fermentation microbienne par diverses bactéries productrices d'acides gras à chaine courte. Nous pouvons donc supposer que les effets observés dans le CANIM-ARCOL lors de l'ajout de *S. boulardii* seraient liés à l'effet antimicrobien des levures ou à leur effet prébiotique, indépendamment de toute implication de la levure dans la réponse immunitaire ou les interactions cellulaires. Cela est également confirmé par le fait que le traitement par *S. boulardii* a augmenté l'abondance relative de la famille des *Lactobacillaceae* dans notre étude *in vitro*, population considérée comme bénéfique, tandis que celle des *Enterobacteriaceae* a diminué. D'autres investigations pourraient être menées pour vérifier cette hypothèse, comme la répétition de la même étude avec des *S. boulardii* non viables et/ou avec des glucanes, des mannoprotéines et de la chitine, purifiés ou en cocktail, afin d'évaluer l'importance relative de chaque composant de la paroi cellulaire dans les effets observés.

Néanmoins, une telle stratégie probiotique requiert par définition la viabilité de la souche dans le tractus gastro-intestinal, ce qui peut s'avérer difficile en raison de contraintes industrielles (extrusion pour les croquettes) et de problèmes de conservation (grande sensibilité à l'eau et à la chaleur). De plus, les levures vivantes sont considérées comme des additifs alimentaires et nécessitent une autorisation européenne de l'EFSA pour être mises sur le marché. Une solution alternative consiste à utiliser des souches inactivées par la chaleur, appelées "paraprobiotiques" ou "postbiotiques". Ces produits sont moins sensibles aux conditions industrielles et de stockage et sont considérés comme des matières premières dans la réglementation européenne, ce qui

facilite leur utilisation dans l'industrie des aliments pour animaux de compagnie. Ces approches ont été développées récemment et, à ce jour, très peu d'études *in vivo* ont été réalisées. Néanmoins, ces produits ont déjà démontré des effets bénéfiques potentiels sur le microbiote et la santé des chiens. Il est intéressant de noter que des *Lactobacillus* inactivés par la chaleur ont permis d'améliorer le score fécal de chiots en bonne santé et montré un effet protecteur contre la diarrhée virale chez des chiens adultes, en augmentant la diversité des *Firmicutes* et la consistance des selles après une supplémentation à long terme (10 mois). Cependant, le potentiel de modulation du microbiote de *L. helveticus* inactivés par la chaleur dans un contexte d'antibiothérapie n'a jamais été étudié chez les chiens. Bien qu'un effet direct des bactéries tyndallisées sur le microbiote a été observé dans le CANIM-ARCOL, le principal mode d'action envisagé pour les bactéries inactivées par la chaleur est lié aux interactions avec les cellules épithéliales de l'hôte ou le système immunitaire. De plus, les propriétés de *L. helveticus* HA-122 inactivés étaient supposées être principalement basées sur leurs parois cellulaires. Le processus d'inactivation par la chaleur a été mis au point par Lallemand pour conserver les cellules bactériennes intactes, et la caractérisation des parois cellulaires est en cours (données non publiées). Sur la base des données de la littérature, nous pouvons néanmoins émettre quelques hypothèses. En particulier, une étude a montré que les acides lipoteichoïques purifiés à partir de *Lactobacillus* inhibaient la formation de biofilms par *S. mutans*, *S. aureus* ou *Enterococcus faecalis in vitro.* Une autre possibilité impliquerait la lectine présente à la surface des bactéries, qui a montré des effets anti-biofilm pour *E. coli* et *Salmonella*. Enfin, certains mécanismes de co-agrégation peuvent avoir lieu entre *L. helveticus* inactivés par la chaleur et les bactéries vivantes. D'autres caractérisations des cellules tyndallisées de *L. helveticus* sont nécessaires pour vérifier si le site d'adhésion ou les récepteurs sont conservés intacts pendant le traitement thermique et s'ils sont toujours actifs. Dans l'ensemble, ces résultats suggèrent que le probiotique *S. boulardii* et le postbiotique *L. helveticus* peuvent être des stratégies de restauration prometteuses pour restaurer l'équilibre du microbiote après une antibiothérapie chez le chien.

Le traitement antibiotique chez le chien est généralement associé au traitement de la diarrhée aiguë, induite dans la plupart des cas par des pathogènes entériques tels que les bactéries entéro-invasives (c'est-à-dire *E. coli*, *Salmonella*, *Shigella*, *Campylobacter*) ou entérotoxinogènes (*Clostridium*, *S. aureus* et *Klebsiella*). Dans cette étude, la perturbation du microbiote a été induite par la seule supplémentation en antibiotiques et nous n'avons pas reproduit d'infection entérique. Une avancée dans le développement du modèle dysbiotique serait d'introduire un pathogène entérique avant le traitement antibiotique pour se rapprocher de la situation *in vivo.* Nous pourrions donc étudier le potentiel de la levure vivante *S. boulardii* CNCM I-1079 ou du postbiotique *L. helveticus* HA-122 inactivé par la chaleur à atténuer l'impact des pathogènes entériques dans un contexte d'antibiothérapie. Par exemple, nous pourrions suivre la colonisation des pathogènes dans les bioréacteurs et dans les billes de mucine, mais aussi la synthèse des toxines et l'expression des gènes de virulence, comme cela a été fait précédemment chez l'Homme ou le porc dans le modèle *in vitro* M-ARCOL. Cependant, d'autres études seront nécessaires pour déterminer la dose de pathogènes à administrer, étant donné que la plupart du temps ils ne sont pas quantifiés avant antibiothérapie dans les échantillons de fèces des chiens. Notre modèle dysbiotique *in vitro* (complexifié ou non par l'ajout d'un pathogène entérique) peut être un outil performant et utile pour

évaluer l'impact de nouvelles stratégies de restauration, comme des pré, pro- ou postbiotiques. De manière originale, l'efficacité de la transplantation de microbiote fécal, qui est à ce jour plus destinée à la recherche qu'à des applications pratiques chez le chien, peut également être évaluée dans le CANIM-ARCOL. Grâce à notre outil *in vitro*, nous pourrons apporter des informations pertinentes sur la cinétique de restauration du microbiote intestinal après transplantation de microbiote fécal, telle qu'elle a été précédemment évaluée en conditions humaines. Enfin, le modèle peut également être facilement adapté pour reproduire la dysbiose associée à d'autres cocktails d'antibiotiques ou d'autres posologies, ouvrant ainsi de multiples possibilités pour l'évaluation des stratégies de restauration.

G. Perspectives : de la simulation in vitro à la commercialisation de produits microbiens protecteurs

Ce projet de doctorat a été divisé en quatre parties, toutes basées sur des approches *in vitro* utilisant le modèle M-ARCOL. La première partie visait à définir les meilleures conditions de conservation des échantillons fécaux, la seconde à décrypter l'impact de la taille du chien sur la fermentation colique, la troisième à étudier l'impact de l'antibiothérapie sur le microbiote colique du chien, et la dernière à étudier des stratégies de restauration basées sur l'administration d'un probiotique et d'un postbiotique. Concernant cette dernière partie, ce projet de thèse ouvre de nouvelles voies dans le développement de produits microbiens protecteurs, mais des étapes supplémentaires seront évidemment nécessaires avant toute commercialisation chez le chien.

Collecter des données supplémentaires grâce au potentiel d'autres modèles digestifs artificiels

Les résultats obtenus au cours de ce travail de doctorat peuvent être complétés par l'utilisation d'autres systèmes digestifs artificiels. Tout d'abord, le développement de bioréacteurs miniaturisés simulant le côlon du chien, plus simples et moins coûteux que le CANIM-ARCOL, permettrait de cribler un plus grand nombre de nouveaux additifs ou ingrédients alimentaires. Ce type d'approche permettrait de sélectionner efficacement les produits les plus pertinents avant une étude *in vitro* plus approfondie dans des modèles plus complexes comme CANIM-ARCOL ou M-SCIME, ce qui devrait accélérer la recherche dans ce domaine. Ces mini bioréacteurs permettraient également d'augmenter le nombre de donneurs testés et ainsi mieux prendre en compte les variabilités interindividuelles pour évoluer vers des approches plus personnalisées. Un autre modèle *in vitro* complémentaire au CANIM-ARCCOL est le système FIDO qui pourrait être utilisé pour évaluer le devenir de tout composé d'intérêt dans le tractus digestif supérieur des chiens avant d'entrer dans le côlon. Ce modèle *in vitro* peut fournir des informations précieuses sur l'impact des paramètres de l'estomac et de l'intestin grêle, tels que le pH acide, les enzymes digestives ou la bile, sur la digestibilité de macronutriments ou la bioaccessibilité de micronutriments, la survie de souches probiotiques ainsi que leurs effets sur la survie et la virulence de pathogènes entériques, comme cela a été fait précédemment en conditions humaines. Jusqu'à présent, ce modèle n'a été mis en place que dans des conditions de chien sain de taille moyenne, mais comme pour le CANIM-ARCOL, si des données *in vivo* sont disponibles à l'avenir nous pourrons envisager pleinement son adaptation à d'autres tailles ou même à des situations pathologiques. Enfin, la dernière approche complémentaire, mais non la moindre, serait l'adaptation du modèle gastro-intestinal Engineered Stomach and Small Intestine (ESIN) pour

simuler la digestion canine. À ce jour, ESIN est le modèle *in vitro* le plus complexe du tractus digestif supérieur, intégrant tous les paramètres du modèle TIM-1, plus la possibilité de digérer des particules alimentaires de taille réelle et la simulation d'une vidange gastrique différentielle. À titre d'exemple, l'ESIN adapté au chien pourrait fournir de premières informations sur l'importance de la taille des particules alimentaires sur la digestibilité des nutriments, ce qui pourrait être intéressant puisque les chiens avalent de plus gros morceaux de nourriture que les humains. Le modèle ESIN sera également bientôt amélioré pour reproduire le microbiote iléal, qui suscite un intérêt croissant dans le domaine de la santé humaine. Cependant, plusieurs années seront nécessaires pour franchir cette étape chez le chien, la recherche sur le microbiote canin n'étant pas assez avancée par rapport au microbiote humain.

Intégrer la réponse de l'hôte en couplant les modèles *in vitro* à des modèles de culture cellulaire

Tous les modèles digestifs artificiels mentionnés ci-dessus ne permettent pas de reproduire les interactions avec l'hôte, ne simulent pas les fonctions de la barrière intestinale et du système immunitaire, ainsi que toutes les contrôles de l'hôte, qu'ils soient nerveux ou hormonaux. Pour améliorer la pertinence des modèles CANIM-ARCOL sains et dysbiotiques, nous pouvons envisager d'intégrer une partie des composantes de l'hôte en couplant le modèle avec des cellules intestinales épithéliales ou immunitaires canines. Cela serait particulièrement pertinent pour la présente étude sur les stratégies de restauration, étant donné que *S. boulardii* et *L. helveticus* sont censés agir par le biais d'interactions avec ces cellules. Jusqu'à présent, une telle adaptation a déjà été réalisée avec succès avec des modèles *in vitro* en conditions humaines ou porcines, permettant de suivre par exemple le niveau d'expression des gènes codant pour des mucines, des protéines des jonctions serrées ou des voies impliquées dans les réponses inflammatoires. De plus, les dispositifs *gut-on-a-chip* pourraient également être couplés à des modèles de fermentation. Une adaptation récente de cette approche a permis de réaliser des analyses pharmacologiques et toxicologiques en couplant les processus de digestion dans la bouche, l'estomac et l'intestin (y compris les sécrétions digestives) aux cellules intestinales. Cependant, ces adaptations n'ont jamais été réalisées avec des modèles digestifs *in vitro* canins. Différentes lignées cellulaires canines sont disponibles, telles que les monocouches de cellules du jéjunum ou les cellules épithéliales iléales canines (cIEC). Les différences observées entre Caco-2 humaines et les cellules intestinales épithéliales canines suggèrent que des modèles spécifiques à l'espèce doivent être utilisés lors de l'étude de la fonction de barrière. De plus, la co-culture de cellules intestinales et de cellules productrices de mucus (comme cela a été réalisé précédemment avec les lignées de cellules humaines Caco2 et HT29 MTX) ou des cellules immunitaires (macrophages ou cellules dendritiques) peuvent également être très instructives pour étudier les interactions entre composés d'intérêt et hôte. Cependant, à nouveau, une telle co-culture n'a jamais été mise en place chez le chien. Enfin, pour augmenter encore la complexité cellulaire, il pourrait également être envisagé d'associer les modèles digestifs artificiels à des organoïdes tridimensionnels canins. À ce jour, les approches organoïdes canine les plus complexe sont l'entéroïde et le colonoïde dérivés de tissus prélevé sur plus de 40 chiens sains et atteints de maladies gastro-intestinales (maladies inflammatoires chroniques de l'intestin et carcinomes intestinaux). Ces couplages permettraient d'évaluer l'impact de nutriments, de médicaments ou d'agents pathogènes sur la

fonction de barrière intestinale, l'inflammation ou toutes voies métaboliques d'intérêt. Les modèles organoïdes peuvent constituer une approche complémentaire pertinente, permettant d'étudier à la fois l'état sain ou malade chez le chien et fournissant une meilleure simulation des caractéristiques physiologiques et moléculaires trouvées dans l'environnement tissulaire par rapport aux cultures cellulaires bidimensionnelles.

Prochaines étapes jusqu'à l'autorisation de mise sur le marché des produits microbiens

L'étape finale du développement des produits sera leur commercialisation en tant qu'additifs pour l'alimentation animale ou médicaments vétérinaires (seule façon d'utiliser la qualification "probiotique" ou "postbiotique"). En France, l'EFSA réglemente l'utilisation des additifs pour l'alimentation animale et délivre une autorisation après évaluation de la qualité et de la sécurité des additifs aussi bien pour les animaux, les consommateurs, les utilisateurs et l'environnement, ainsi que leur efficacité. Pour ce faire, des études *in vivo* chez le chien doivent être réalisées avec une période minimale de 28 jours d'administration du produit. L'Agence Nationale du Médicament Vétérinaire (ANMV) est l'autorité française compétente pour l'évaluation et la gestion des risques liés aux médicaments vétérinaires. L'ANMV délivre l'autorisation de mise sur le marché à l'issue d'une procédure qui nécessite de fournir des informations sur la qualité pharmaceutique du produit (y compris les composants qualitatifs et quantitatifs, le procédé de fabrication, les méthodes d'analyse et les études de stabilité), sur la sécurité (données toxicologiques, pharmacocinétique et étude de la sécurité de l'utilisateur) et sur l'efficacité démontrée par des études pré-cliniques et cliniques.

De manière intéressante, les résultats d'efficacité fournis par notre étude *in vitro* sur *S. boulardii* CNCM I-1079 et *L. helveticus* HA-122 inactivé par la chaleur nous permettent de spéculer sur une future commercialisation de *S. boulardii* CNCM I-1079 en tant que "stabilisateur de la flore intestinale" (dans la catégorie des additifs alimentaires), recommandé en tant que stratégie de restauration après une perturbation induite par un antibiotique. *L. helveticus* HA-122 inactivé par la chaleur est actuellement commercialisé en tant que matière première et nos résultats *in vitro* ont démontré l'efficacité du produit comme stratégie de restauration après une perturbation antibiotique. Cependant, d'autres études doivent être menées pour augmenter la puissance statistique, fournir des informations supplémentaires sur les modes d'action de *L. helveticus* HA-122 et accroître les connaissances concernant les interactions potentielles avec l'hôte. Il est à noter que seules les études cliniques *in vivo* sont approuvées par l'EFSA pour les études de toxicité, de tolérance et d'efficacité, ce qui signifie évidemment qu'une étude clinique devra être réalisée avant la commercialisation de *S. boulardii* CNCM I-1079 pour les chiens. Cependant, ce travail de thèse a mis en évidence le potentiel du modèle *in vitro* CANIM-ARCOL pour fournir des données pertinentes sur l'efficacité des produits, conformément à la confiance accordée par l'EFSA elle-même lorsqu'elle a sollicité MEDIS pour évaluer l'impact de nanocelluloses (utilisées comme additifs dans l'alimentation humaine) sur le microbiote colique à l'aide du modèle M-ARCOL. Ainsi, nous avons l'espoir que les systèmes digestifs artificiels dynamiques et multi-compartimentés puissent être, dans un avenir proche, des outils alternatifs permettant de remplacer les études cliniques *in vivo* dans les processus de réglementation et de commercialisation de produits alimentaires et vétérinaires destinés aux animaux.

TABLE OF CONTENT

Abstract ..... *- 1 -*

Résumé ..... *- 2 -*

Acknowledgments - Remerciements ..... *- 4 -*

Résumé de la thèse ..... *I-XXIII*

List of figures and tables ..... *- 11 -*

Abbreviations ..... *- 17 -*

Foreword ..... *- 20 -*

A. Scientific and regulatory context of the PhD thesis ..... - 20 -
B. Funding and partnership ..... - 23 -
C. Research questions and technical outcomes ..... - 24 -
D. Manuscript organization ..... - 25 -

Section I - Literature review ..... *- 27 -*

Part 1 - Impact of canine body weight on gut physiology and physicochemical parameters ..... **- 28 -**

1.1. Canine digestive anatomy and associated digestive processes ..... - 28 -
1.2. Gastrointestinal pH ..... - 31 -
1.3. Digestive secretions ..... - 32 -
1.3.1. Enzymes ..... - 32 -
1.3.2. Bile salts ..... - 32 -
1.3.3. Mucus and mucins ..... - 33 -
1.4. Nutrient digestibility ..... - 35 -
1.5. Intestinal absorption ..... - 36 -
1.5.1. Permeability ..... - 36 -
1.5.2. Passive absorption ..... - 37 -
1.5.3. Active absorption ..... - 37 -
1.6. Mechanical digestion and gastrointestinal transit time ..... - 38 -
1.6.1. Motility ..... - 38 -
1.6.2. Transit time ..... - 38 -

Part 2 - Impact of canine body weight on microbial parameters ..... **- 41 -**

2.1. Gut microbiota composition ..... - 41 -
2.1.1. Longitudinal variations ..... - 41 -
2.1.2. Radial variations ..... - 44 -
2.2. Microbiota's functions in the gastrointestinal tract ..... - 45 -
2.2.1. Key roles of the canine gut microbiota ..... - 45 -
2.2.2. Carbohydrates metabolism ..... - 46 -
2.2.3. Protein metabolism ..... - 47 -
2.2.4. Vitamin synthesis ..... - 53 -
2.2.5. Bile acid metabolism ..... - 53 -

Part 3 - Factors shaping canine gut microbiota ..... **- 57 -**

3.1. Factors driving microbiota in healthy dogs ..... - 57 -
3.2. Factors driving microbiota under diseased situations ..... - 61 -
3.2.1. Antibiotic treatment ..... - 62 -
3.2.2. Obesity ..... - 65 -
3.2.3. Inflammatory bowel disease ..... - 66 -
3.2.4. Restoration strategies of the canine microbiota ..... - 68 -
3.2.4.1. Prebiotics ..... - 68 -
3.2.4.2. Probiotics ..... - 69 -
3.2.4.3. Postbiotics and paraprobiotics ..... - 74 -

3.2.4.4. Faecal microbial transplantation ..... - 77 -

Part 4 - In vitro canine models as an alternative to *in vivo* assays in dogs ..... - 79 -

4.1. Generalities on *in vitro* gut models: static versus dynamic and comparison with *in vivo* ..... - 79 -

4.2. Currently available canine *in vitro* gut models ..... - 81 -

4.2.1. *In vitro* models of the upper gut ..... - 81 -

4.2.2. *In vitro* models of the lower gut: batch and continuous models ..... - 82 -

4.3. *In vitro* gut models as powerful tools to study canine digestion ..... - 85 -

4.3.1. Scientific and technical challenges to be addressed ..... - 85 -

4.3.2. Future developments and quality requirements ..... - 89 -

4.3.3. Potential applications of canine gut models in food and pharma ..... - 90 -

Section II - Experimental work ..... - 94 -

Chapter 1 – Comparative methods for faecal sample storage to preserve gut microbial structure and function in an *in vitro* model of the human colon ..... - 95 -

Abstract ..... - 96 -

1.1. Introduction ..... - 97 -

1.2. Materials and methods ..... - 98 -

1.3. Results ..... - 102 -

1.4. Discussion ..... - 109 -

1.5. Supplementary figures ..... - 116 -

1.6. Conclusion on canine faecal sample preparation and storage ..... - 118 -

Chapter 2 – Canine Mucosal Artificial Colon: *in vitro* simulation of physicochemical and microbial colonic ecosystem adapted to different dog sizes ..... - 119 -

Abstract ..... - 120 -

2.1. Introduction ..... - 120 -

2.2. Materials and methods ..... - 122 -

2.3. Results ..... - 128 -

2.4. Discussion ..... - 139 -

2.5. Supplementary figures ..... - 146 -

2.6. Additional results ..... - 150 -

2.7. Conclusion ..... - 154 -

Chapter 3 – Mechanistic study: towards a better understanding of the relative importance of gut microbes and environmental parameters to reshape canine microbiota *in vitro* in relation to dog sizes- 155 -

Abstract ..... - 156 -

3.1. Introduction ..... - 156 -

3.2. Materials and methods ..... - 157 -

3.1. Results ..... - 162 -

3.2. Discussion ..... - 171 -

3.3. Additional results ..... - 176 -

3.4. Conclusion ..... - 178 -

Chapter 4 – Development of a new dysbiotic model of the canine large intestine microbiome associated to antibiotherapy ..... - 180 -

Abstract ..... - 181 -

Importance ..... - 182 -

4.1. Introduction ..... - 183 -

4.2. Results ..... - 184 -

4.3. Discussion ..... - 197 -

4.4. Material and methods ..... - 203 -

4.5. Additional figures ..... - 209 -

4.6. Additional discussion ..... - 209 -

4.7. Conclusion ..... - 211 -

Chapter 5 – Dysbiosis-protective or microbiota restoration strategies: *Lactobacillus helveticus*-derived parabiotic and *Saccharomyces boulardii* are efficient to restore gut microbiota after antibiotic disturbance in an *in vitro* canine gut model ..... - 212 -
Abstract..... - 213 -
5.1. Introduction ..... - 213 -
5.2. Material and methods ..... - 215 -
5.3. Results ..... - 221 -
5.4. Discussion..... - 232 -
5.5. Supplementary figures and tables..... - 236 -
5.6. Additional results..... - 238 -
5.7. Conclusion..... - 241 -

Section III – General discussion ……..……..……..- 242 -
A. Repositioning the global context of the research ……...…….- 243 -
B. Interest and originality of the PhD work ……...……..…….- 244 -
a. Impact of conservative methods on faecal inoculum used in the ARCOL model…... - 244 -
b. Impact of dog size on canine colonic physicochemical parameters & gut microbiota - 245 -
c. Impact of antibiotherapy on microbiota structure and functions……..…….....….. - 248 -
d. Evaluation of restoration strategies based on probiotics and postbiotics ..……...….. - 252 -
C. From *in vitro* simulation to marketing of protective microbial products …….- 255 -

References..... - 260 -

Appendix ……...……... - 294 -
Appendix 1 - Scientific *curriculum vitae* ……..……..…… - 295 -
Appendix 2 - Review in ALTEX ……..……..…. - 298 -
Appendix 3 - Review in International Journal of Biological Sciences ……..…… - 299 -
Appendix 4 - Original article in Microbiology Spectrum ……..…… - 300 -
Appendix 5 - Original article in Microbiome ……..…… - 301 -
Appendix 6 - Poster presentation……..……...…….…….. - 339 -
Appendix 7 - Poster presentation……..……..…….. - 341 -

LIST OF FIGURES AND TABLES

Foreword

Figure 0.1: Popular canine breeds or breeds involved in this PhD work, classified per size ..... - 20 -
Figure 0.2: Outline of the experimental work of the PhD thesis ..... - 26 -

Section I - Literature review

Part I - Impact of canine body weight on gut physiology and physicochemical parameters

Figure 1.1: Canine digestive system ..... - 29 -
Figure 1.2: Impact of dog sizes on pH values in all digestive compartments ..... - 31 -
Figure 1.3: Impact of dog sizes on faecal bile acids ..... - 33 -
Figure 1.4: Physiological properties of mucus layer and associated mucins from seven segments of the large canine gastrointestinal tract ..... - 34 -
Figure 1.5: Diet composition and impact of dog sizes on total apparent digestibility ..... - 35 -
Figure 1.6: Impact of dog sizes on gastrointestinal transit time ..... - 39 -

Part 2 - Impact of canine body weight on microbial parameters

Figure 2.1: Variations in gut microbiota composition along the canine digestive tract ..... - 42 -
Figure 2.2: Variations in gut microbiota composition along the canine digestive tract and impact of body size ..... - 43 -
Figure 2.3: Schematic representation of the key functions of canine gut microbiota ..... - 45 -
Figure 2.4: Carbohydrates metabolism pathways involved in short-chain fatty acids biosynthesis and gas production, and associated bacteria ..... - 47 -
Figure 2.5: Pathways of gut microbial protein metabolism ..... - 48 -
Figure 2.6: Pathways responsible for the biosynthesis of the major microbial metabolites from carbohydrates and proteins metabolisms and impact on gut mucosa ..... - 49 -
Figure 2.7: Effects of microbial tryptophan catabolites on host physiology ..... - 51 -
Figure 2.8: Impact of dog sizes on faecal microbial products production ..... - 52 -
Figure 2.9: Overview of canine bile acid metabolism and enterohepatic recirculation ..... - 54 -
Figure 2.10: Impact of dog sizes on faecal bile acids composition ..... - 55 -
Figure 2.11: Overview of the impact of dog sizes on digestive physiology and faecal microbiota composition and activity ..... - 56 -

Part 3 - Factors shaping canine gut microbiota

Figure 3.1: Overview of the main factors influencing canine gut microbiota ..... - 57 -
Figure 3.2: Major factors shaping the development of growing puppies' gut microbiota from birth to adulthood ..... - 58 -

Figure 3.3: Evolution of the relative abundance of main bacterial phyla in puppies' faecal microbiota with age .....- 59 -
Figure 3.4: Impact of different types of diet on canine faecal gut microbiota .....- 60 -
Figure 3.5: Role of domestication in evolution of the canine gut microbiota.....- 61 -
Figure 3.6: Impact of obesity on dog digestive physiology .....- 65 -
Figure 3.7: Impact of inflammatory bowel disease on dog digestive physiology.....- 67 -
Figure 3.8: Proposed mechanisms of action of probiotics .....- 74 -
Figure 3.9: Technological processes for paraprobiotics production, associated impacts on bacterial cells, and potentially involved cell structures in beneficial health effects in the host .....- 77 -

Table 3.1: Effect of orally administered antibiotics commonly used in veterinary clinics to treat gastrointestinal diseases in canine gut microbiota.....- 64 -
Table 3.2: Main results obtained for probiotics receiving a positive opinion by EFSA for canine use.....- 71 -
Table 3.3: List of bacterial strains used as probiotic properties in canines .....- 72 -
Table 3.4: Example of postbiotics that may impact pet health based on human data .....- 76 -
Table 3.5: Overview of studies evaluating the impact of FMT on canine health and microbiota .....- 78 -

Part 4 - In vitro canine models as an alternative to in vivo assays in dogs

Figure 4.1: Schematic representation of currently available canine *in vitro* models .....- 81 -
Figure 4.2: Main challenges in the development of *in vitro* gut models of the canine digestive tract and their applications in nutritional and veterinary fields.....- 86 -
Figure 4.3: Picture of the ARCOL model with its mucin-alginate beads module, resulting in the M-ARCOL configuration .....- 88 -

Table 4.1: Main *in vitro* models developed to simulate the gastrointestinal tract of dogs and their characteristics .....- 83 -
Table 4.2: Application studies of the currently available canine *in vitro* gut models in food and pharma fields ..... - 92 -

Section II – Experimental work

Chapter I – Comparative methods for faecal sample storage to preserve gut microbial structure and function in an in vitro model of the human colon

Figure I.1: Experimental design of the *in vitro* fermentation experiments in the M-ARCOL.....- 100 -
Figure I.2: Experimental set-up and sampling procedure during M-ARCOL experiments.....- 100 -
Figure I.3: Relative abundance of bacterial families retrieved in the initial stools and in the luminal medium and mucin beads from M-ARCOL.....- 104 -
Figure I.4: Effect of different stool storage conditions on the Shannon diversity index values .....- 105 -
Figure I.5: Effect of different stool storage conditions on qPCR enumeration of main bacterial groups ..- 107 -
Figure I.6: Gas composition and production in M-ARCOL according to stool storage conditions .....- 108 -
Figure I.7: SCFA composition and production in M-ARCOL according to stool storage conditions.....- 110 -

Table I.1: Primers used for qPCR and 16S metabarcoding.....- 101 -
Table I.2: Scientific and technical comparative data on preservative methods applied to fecal samples...- 114 -

Supplementary figure I.1: Effect of different stool storage conditions on community structure at the phylum level. .....- 116 -
Supplementary figure I.2: Redox potential values measured in the M-ARCOL. .....- 117 -

Chapter II – Canine Mucosal Artificial Colon: in vitro simulation of physicochemical and microbial colonic ecosystem adapted to different dog sizes

Figure II.1: Overview of experimental design in the CANIM-ARCOL model.....- 123 -
Figure II.2: Impact of dog sizes on α and β-diversity of microbial populations in the CANIM-ARCOL model .....- 132 -
Figure II.3: Impact of colonic microenvironment and dog size on microbiota composition in the CANIM-ARCOL .....- 133 -
Figure II.4: Microbiota composition of luminal medium and mucin beads at the family level .....- 135 -
Figure II.5: Impact of three dog sizes on microbiota composition at the phylum and family levels .....- 136 -
Figure II.6: Impact of dog sizes on microbiota activity in the CANIM-ARCOL.....- 138 -
Figure II.7: Impact of dog size on redox potential and pH in the CANIM-ARCOL.....- 151 -
Figure II.8: Impact of dog size on faecal bile acids profiles.....- 152 -
Figure II.9: Impact of dog size on faecal bile acids.....- 152 -
Figure II.10: Impact on colonic microenvironment and dog size on microbiota metabolic pathways predictions .....- 153 -

Table II.1: Characteristics of healthy adult dogs included in the study and ranked by small, medium and large dog sizes .....- 122 -
Table II.2: Adaptation of physicochemical and nutritional parameters of CANIM-ARCOL to three dog sizes .....- 125 -
Table II.3: Primers used for qPCR and 16S Metabarcoding analysis.....- 126 -
Table II.4: Comparison of the CANIM-ARCOL model and other currently available models of the dog large intestine .....- 140 -
Table II.5: Comparison of main bacterial populations found in the CANIM-ARCOL model under medium size conditions and *in vivo* in the large intestine of medium size dogs.....- 141 -
Table II.6: *In vitro-in vivo* comparisons of dog size impact on gut microbial composition and activity based on fecal data .....- 144 -

Supplementary figure II.1: Stool characterization for each canine donor .....- 148 -
Supplementary figure II.2: Impact of three dog sizes on gas composition in the CANIM-ARCOL at the individual level.....- 147 -
Supplementary figure II.3: Impact of three dog sizes on SCFA composition in the CANIM-ARCOL at the individual level.....- 148 -

Supplementary figure II.4: Impact of three dog sizes on microbiota composition in the CANIM-ARCOL at the individual level ..... - 149 -
Supplementary figure II.5: Detection of archaea methanogens in the CANIM-ARCOL ..... - 150 -

Chapter III – Mechanistic study: towards a better understanding of the relative importance of gut microbes and environmental parameters to reshape canine microbiota in vitro in relation to dog sizes

Figure III.1: Experimental design in the CANIM-ARCOL ..... - 159 -
Figure III.2: Stool characterization for each canine donor. Stool samples were collected from two healthy medium dogs ..... - 163 -
Figure III.3: Impact of dog size on bacterial load and microbial diversity in the CANIM-ARCOL ..... - 164 -
Figure III.4: Impact of dog size on microbial composition in the CANIM-ARCOL ..... - 167 -
Figure III.5: Differential analysis on dog size impact on microbiota composition at the genus level ..... - 167 -
Figure III.6: Impact of dog size on gas production in the CANIM-ARCOL ..... - 168 -
Figure III.7: Impact of dog size on short-chain fatty acids and ammonia production ..... - 169 -
Figure III.8: Correlations between explainable variables and microbial family abundances ..... - 171 -
Figure III.9: Preliminary results of metabolomic analyses ..... - 179 -

Table III.1: Characteristics of healthy adult dogs from medium size used as fecal donors for *in vitro* experiments ..... - 157 -
Table III.2: Nutritional and physicochemical parameters used to set-up the CANIM-ARCOL under three dog sizes conditions ..... - 159 -
Table III.3: Primers used for qPCR and 16S Metabarcoding analysis ..... - 160 -
Table III.4: *In vitro* - *in vitro* correlations related to dog size effect on colonic microbial populations and metabolic activities between previous results in the CANIM-ARCOL and those obtained in the present study ..... - 173 -
Table III.5: *In vivo* - *in vitro* correlations related to dog size effect on gut microbial populations (a) and metabolic activities (b) between our *in vitro* results in the CANIM-ARCOL and data from fecal samples *in vivo* ..... - 174 -
Table III.6: Putative annotations of metabolites identified by metabolomic analysis on small dog size samples ..... - 178 -

Chapter IV – Development of a new dysbiotic model of the canine large intestine microbiome associated to antibiotherapy

Figure IV.0: Graphical abstract ..... - 181 -
Figure IV.1: Experimental design of antibiotics pre-screening experiment in the CANIM-ARCOL ..... - 185 -
Figure IV.2: Effect of five different antibiotic treatments on canine microbiota activity and composition - 187 -
Figure IV.3: Experimental design used for the set-up of the antibiotic-induced dysbiosis model in the CANIM-ARCOL ..... - 188 -

Figure IV.4: Impact of metronidazole/enrofloxacin treatment on gas production and bile acid profiles ...- 189 -
Figure IV.5: Impact of metronidazole/enrofloxacin treatment on short-chain fatty acids production .....- 192 -
Figure IV.6: Impact of metronidazole/enrofloxacin treatment on canine microbial diversity .....- 192 -
Figure IV.7: Impact of metronidazole/enrofloxacin treatment on canine bacterial populations .....- 194 -
Figure IV.8: Discriminant analysis of antibiotic effect on canine bacterial population at the ASV level..- 195 -
Figure IV.9: Impact of antibiotherapy on dysbiosis index in the CANIM-ARCOL .....- 197 -
Figure IV.10: Impact of antibiotherapy on metabolic pathway predictions in the CANIM-ARCOL .....- 200 -
Figure IV.11: Impact of antibiotherapy on dysbiosis index in the CANIM-ARCOL, calculated for all bacteria populations .....- 210 -

Table IV.1: *In vivo-in vitro* comparisons regarding the effects of metronidazole/enrofloxacin treatment on gut microbial populations and metabolic activities.....- 202 -
Table IV.2: Characteristics of healthy adult dogs from medium size used as fecal donors for *in vitro* experiments .....- 204 -
Table IV.3: Nutritional and physicochemical parameters used to set-up the CANIM-ARCOL under medium size canine colonic conditions.....- 205 -
Table IV.4: Primers used for qPCR and 16S Metabarcoding analyses.....- 206 -

Supplementary figure IV.1: Impact of metronidazole/enrofloxacin treatment on bacterial populations at the phylum level.....- 209 -

Chapter V – Dysbiosis-protective or microbiota restoration strategies: Lactobacillus helveticus-derived parabiotic and Saccharomyces boulardii are efficient to restore gut microbiota after antibiotic disturbance in an in vitro canine gut model

Figure V.1: Experimental design to evaluate the impact of tested restoration strategies on antibiotic-induced dysbiosis in the CANIM-ARCOL model.....- 216 -
Figure V.2: Impact of *S. boulardii* and tyndallized *L. helveticus* on gas production during and after antibiotherapy.....- 222 -
Figure V.3: Impact of *S. boulardii* and tyndallized *L. helveticus* on short-chain fatty acids production during and after antibiotherapy.....- 224 -
Figure V.4: Impact of S. boulardii and tyndallized L. helveticus on canine microbial diversity during and after antibiotherapy.....- 225 -
Figure V.5: Impact of *S. boulardii* and tyndallized *L. helveticus* on canine bacterial microbiota at the family level during and after antibiotherapy .....- 228 -
Figure V.6: Impact of antibiotherapy and *S. boulardii* or tyndallized *L. helveticus* on dysbiosis index in the CANIM-ARCOL.....- 230 -
Figure V.7: Impact of antibiotics and pro- or postbiotic supplementation on functional pathway predictions during and after antibiotherapy .....- 232 -
Figure V.8: Monitoring of *S. boulardii* and *L. helveticus* in the CANIM-ARCOL model.....- 240 -
Figure V.9: Impact of restoration strategies on microbiota composition at the ASV level .....- 240 -

Table V.1: Characteristics of healthy adult dogs from medium size used as fecal donors for *in vitro* experiments .....- 215 -
Table V.2: Nutritional and physicochemical parameters used to set-up the CANIM-ARCOL under medium size canine colonic conditions .....- 217 -

Supplementary figure V.1: Impact of antibiotics and restoration strategies on redox potential in the CANIM-ARCOL model .....- 236 -
Supplementary figure V.2: Impact of *S. boulardii* and tyndallized *L. helveticus* on canine bacterial microbiota at the phylum and genus levels during and after antibiotherapy.....- 237 -
Supplementary figure V.3: Functional pathway predictions before and after antibiotherapy for each condition .....- 238 -

Supplementary table V.1: Primers used for qPCR and 16S Metabarcoding analyses .....- 238 -

Section III – Discussion & Perspectives

Figure III.1: Positioning of CANIM-ARCOL from compound selection to product commercialization.. - 258 -
Figure III.2: Main results of the PhD work on the impact of body weight and antibiotic disturbance on canine gut microbiota……..……..- 259 -

ABBREVIATIONS

A

AAFCO: Association of American Feed Control Officials

AHR: aryl hydrogen receptor

AM: amoxicillin

AMP: antimicrobial peptides

ANSES: Agence Nationale de Sécurité Sanitaire de l'alimentation, de l'environnement et du travail

ARCOL: artificial colon

ARE: antibiotic responsible enteropathy

ASD: Artificial Stomach Duodenum

ASV: amplicon sequence variant

ATB: antibiotic

B

BA I: primary bile acid

BA II: secondary bile acid

BARF: Biologically Appropriate Raw Food

BCFA: branched-chain fatty acids

BCS: body condition score

BSH: bile salt hydrolase

BW: body weight

C

CA: cholic acid

CANIM-ARCOL: CANIne Mucosal ARtificial COLon

CCECAI: Canine Chronic Enteropathy Clinical Activity Index

CDCA: chenodeoxycholic acid

CFU: colony forming units

CH_4: methane

CIBDAI: Canine Inflammatory Bowel Disease Activity Index

CIFRE: Convention Industrielle de Formation par la REcherche

CMET: Center for Microbial Ecology and Technology

CO_2: carbon dioxide

D

DAD: diode-array detection

DCA: deoxycholic acid

DNA: deoxyribonucleic acid

E

EFSA: European Food Safety Authority

ENVT: Ecole Nationale Vétérinaire de Toulouse

ESIN: Engineered Stomach and small INtestine

EU: European Union

F

F/B: *Firmicutes*/*Bacteroidetes*

FEDIAF: Fédération Européenne De l'Industrie des aliments pour Animaux Familiers

FIDO: Functional gastroIntestinal Dog Model

FISH: fluorescent *in situ* hybridization

FM2D: Fonctions Métaboliques du Microbiote digestif et dysbioses

FMT: faecal microbiota transplantation

FOS: fructooligosaccharide

FS: fresh stool

G

GC-MS: gas chromatography-mass spectrometry

GET: gastric emptying time

GFS: glycerol frozen stool

GIT: gastrointestinal tract

GIVIMP: Good *In vitro* Method Practices

GLP-1: glucagon-like peptide-1

GOS: galactooligosaccharides

H

H_2: dihydrogen

H_2S: dihydrogen sulfide

HCl: hydrogen chloride

HDL: high-density lipoprotein

HPLC: High Performance Liquid Chromatography

5-HT: 5-hydrotryptamine

I

I-LCA: Isoallo-3-ketocholate

IBD: inflammatory bowel disease

IF: impact factor

IgA: immunoglobulin A

IgG: immunoglobulin G

IL-22: interleukin 22

IL: interleukine

INFOGEST: Improving health properties of Food by sharing our knowledge on the digestive process

INNOVITRO: Innovation et développement de modèles *in vitro*

INRAE: Institut National de Recherche pour l'Agriculture, l'alimentation et l'Environnement

ISAPP: International Scientific Association of Probiotics and Prebiotics

K

KEGG: Kyoto Encyclopedia of Genes and Genomes

L

LCA: lithocholic acid

LH: *Lactobacillus helveticus* HA-122

LDL: low-density lipoprotein

LITT: large intestine transit time

LS: lyophilized stool

M

M-ARCOL: Mucosal ARtificial COLon

M-SCIME: Mucosal Simulator of the Canine Intestine Microbial Ecosystem

M-SHIME: Mucosal Simulator of the Human Intestinal Microbial Ecosystem

ME: metronidazole/enrofloxacin

MEC: metronidazole/enrofloxacin/ciprofloxacin

MEDIS: Microbiologie Environnement Digestif et Santé

MOS: mannan-oligosaccharide

N

N_2: dinitrogen

N_2: nitrogen

NA: not applicable

ND: not determined or not detected

NF-κB: nuclear factor-kappa B

NMDS: non-metric multidimensional scaling

O

O-LCA: 3-oxolithocholic/dehydrolithocholic acid

O_2: dioxygen

OCTT: orocaecal transit time

OECD: Organization for Economic Co-operation and Development

OTU: operational taxonomic unit

P

PARNUTS: formerly foods for Particular Nutritional Uses

PBS: phosphate-buffered saline

PCoA: principal coordinate analysis

PICRUST: Phylogenetic Investigation of Communities by Reconstruction of Unobserved States

PLS-DA: partial least-squares discriminant analysis

PUFA: poly-unsaturated fatty acid

PXR: pregnane X receptor

Q

QPCR: quantitative polymerase chain reaction

R

RDA: distance-based redundancy analysis

RFS: raw frozen stool

RNA: ribonucleic acid

S

SB: *Saccharomyces boulardii* CNCM I-1079

SCFA: short-chain fatty acids

SCIME: Simulator of the Canine Intestine Microbial Ecosystem

SCUSI: Soutien aux Coopérations Universitaires et Scientifiques Internationales

SD: standard deviation

SHIME: Simulator of the Human Intestine Microbial Ecosystem

SIMGI: multicompartmental dynamic model of the gastrointestinal system

SITT: small intestinal transit time

T

TCA: taurocholic acid

TIM-1: TNO gastroIntestinal Model-1

TTT: total transit time

TY: tylosin

U

UDCA: ursodeoxycholic acid

UMR: unité mixte de Recherche

USA: United States of America

X

XOS: mannanoligosaccharides

FOREWORD

A. *Scientific and regulatory context of the PhD thesis*

Canis lupus familiaris, also known as domesticated dogs, belongs to *Canidae* family. Descending from the grey wolf, dog might have been the first animal domesticated by humans around 20.000 to 40.000 years ago (Botigué *et al.*, 2017). Dogs were initially strict carnivores, but during the agricultural revolution, they have probably acquired the ability to digest starch and became facultative carnivores (Axelsson *et al.*, 2013). Depending on their usefulness for humans, the *Canis lupus familiaris* subspecies have differentiated slowly, with the development of new species selected for specific tasks, such as herd protection (Mastiff), hunting (Pointer), cold hardiness (Siberian husky) or companion (Pekinese). Nowadays, canine species include approximatively 400 breeds with morphological, metabolic and size variabilities and weight ranging from 1 kg for a Chihuahua to 100 kg for a Saint-Bernard (Grandjean & Haymann, 2010; Middleton *et al.*, 2017) (**Figure 0.1**).

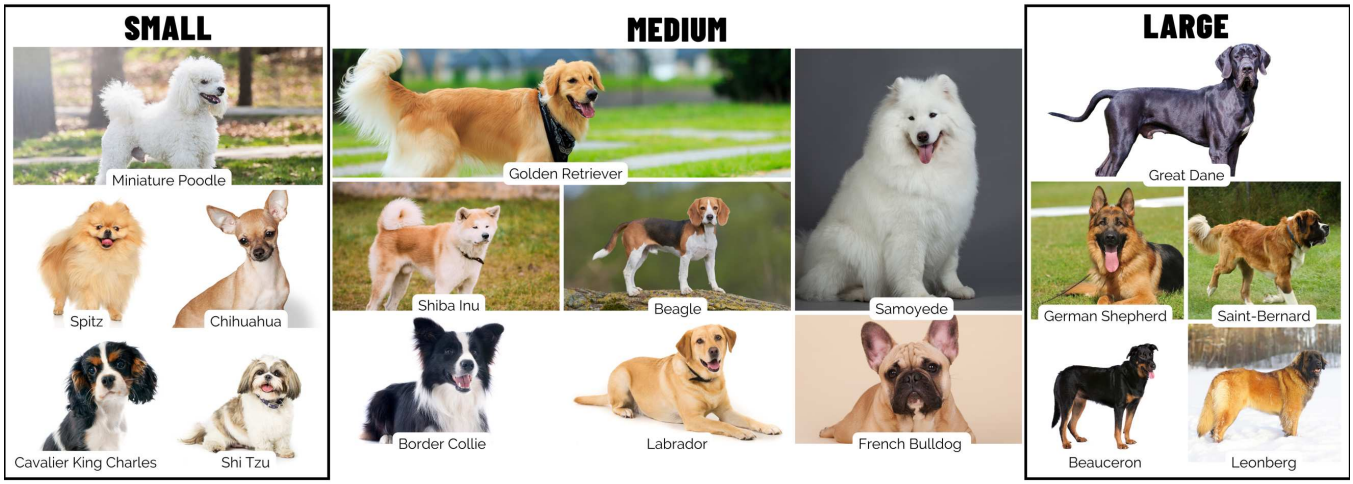

Figure 0.1: Popular canine breeds or breeds involved in this PhD work, classified per size. Dogs are considered in the "small" category under 10 kg, "medium" from 10 to 30 kg and "large" over 30 kg.

Pets, especially dogs, occupy a full place in the family and their health and well-being are therefore of paramount importance to their owners, to the extent that 7 % of French dogs have their own health insurance comparatively to 30 % of dogs homed in the United Kingdom and 80 % in Sweden (SantéVet/Ipsos, 2018). In 2023, dogs are estimated to be more than 900 million worldwide (World Animal Foundation), which represents a huge market for petfood and animal health industry. In 2018, global petfood market size reached $91.1 billion, representing 31 % increase within 5 years, with the need of constantly innovate (e.g. food, probiotics and prebiotics) (Phillips-Donaldson, 2019). A vast array of foods, snacks and nutritional supplements have been recently developed to support well-being, health, improve the health of aging dog or prevent diseases. According to increased interest of owners to maintain dog's health, petfood is adapted to fit each dog's lifestyle, for example for puppies or bitches, sedentary or active, maintenance diet or hypocaloric diet. Different types of

canine food are available and can be classified in three categories: dry food (kibbles), canned food, and alternative food (biologically appropriate raw food, namely BARF, homemade food, and feedstuffs). At the interface between petfood and veterinary compounds, pets' nutritional supplements represent a specific expanding market with large range of products. As an example, micronutrients like selenium, taurine or polyphenols could be added for old dogs, calcium, phosphorus, omega-3 fatty-acids and vitamin E for lactating bitches, or L-carnitine for athletic dogs can be found. Particular nutritional purposes (known as PARNUTS or dietetic feed; EU regulation 2020/354) have to meet the specific nutritional needs of animals whose bodily functions are, or could be, temporarily or irreversibly impaired. In 2019, pet medicine represents a $17.5 billion market including the sales of veterinary compounds such as vaccines, antiparasitic treatments or antibiotics (The Business Research Company, 2020). As for human, a large range of products has been developed to improve dog's health and hygiene. Specific treatments have been also developed to cure diseases, for example to avoid lipid absorption in obesity or decrease pain in inflammatory bowel disease (IBD). Of note, some canine breeds or sizes are more sensitive to diseases. For example, overweight and dental trouble are more prevalent in small dogs whereas large dogs frequently present an increased digestive sensitivity.

Strong expansion of veterinary medicine, petfood and oral supplements with health claims is associated with an increasing specific regulatory context. In Europe, the European Petfood Industry Federation (Fediaf) aims at proposing a framework for production of safe, nutritious, and palatable petfood. Heads of Medicine Agencies or National Agency must grant an authorization for veterinary drug marketing, after evaluating quality and safety of medicinal product for animals, consumers, users, and environment as well as effectiveness of medicinal product. In addition, toxicity, efficiency and stability of oral supplements (including probiotics) have to be demonstrated (EU regulation 1831/2003). For the evaluation of these products, generally related to digestibility of petfood or bioaccessibility of active compounds (including drugs) in the canine gastrointestinal tract, *in vivo* studies remain the golden standard. Actually, *in vivo* experiments in dogs can also be performed as a model of human gut due to important similarities in digestive physiology (Lui *et al.*, 1986; Akimoto *et al.*, 2000). Worldwide, experimentations are still conducted on 192.1 million animals with 207 724 experimentations involving dogs in 2015 as reported in the European Commission (2017). However, *in vivo* assays are more and more restricted by regulation, ethical and societal constraints, coupled to high associated costs. In addition, the marketing of a new additive or drug is becoming increasingly regulated, with an increasing level of scientific justification, in a context of expanding difficulties in conducting animal trials. This last decades, the European and North America "3Rs" rules (adapted from Russel and Burch, 1959) widely encourage a strong reduction in the number of animals used in research and prone the development of alternative *in vitro* approaches. All these elements limit the ability to prove the effectiveness and understand the mode of action of new selected molecules in canine *in vivo* studies.

Among *in vitro* alternatives, models simulating the canine digestive environment (intestinal cell culture, organoids, or *in vitro* gut models) can help to answer many scientific questions associated to food and drug behavior during canine digestion. An alternative approach to animal trials is the use of artificial digestive systems, allowing to study the fate of orally ingested compounds of interest, to perform mechanistic studies,

and/or to evaluate the interactions with the canine microbiota. There are currently very few canine *in vitro* models reproducing the gastrointestinal or colonic environment of the animal and the majority of published work concerns static *in vitro* models, very simplified and therefore not reproducing the dynamism and complexity of the *in vivo* digestion process. Finally, most of the models developed to date pass over the intestinal microbiota component, which is the subject of a growing number of studies in dogs, highlighting the essential role of the intestinal microbiota in host homeostasis, and when perturbated (namely called a dysbiosis state), its involvement in various digestive or extra-digestive pathologies (Suchodolski *et al.*, 2012b; Honneffer, Minamoto & Suchodolski, 2014; Redfern, Suchodolski & Jergens, 2017). Thus, having an *in vitro* model, mimicking as closely as possible the physico-chemical and microbial parameters specific to the dog's digestive environment, would constitute a major technological and scientific advance, making it possible to acquire multiple knowledge, to understand modes of action of new products, to develop microbial biomarkers and even to refine a protocol during a clinical pilot study (choice of dose, frequency of administration…). However, this requires a comprehensive and precise understanding of dog digestive processes.

Digestion is an essential process at the center of dog health study and of high interest for petfood and veterinary industries. Canine digestion is a complex process involving physicochemical (e.g. pH, digestive secretions, transit time), mechanical and microbial parameters varying all along the gastro-intestinal tract (GIT). Each compartment is colonized by a resident microbiota, with the higher diversity and abundance of microorganisms found in the colonic compartment. The gut microbiota and its involvement in dog nutrition and health is becoming a more and more important topic. All these digestive components affect food digestibility, nutrient absorption, and energy release, but also drug metabolism and absorption, and survival of probiotic microorganisms. Thus, developing new food or veterinary products needs to consider all these multi-faceted aspects of canine digestion in order to answer important questions, such as: how physicochemical parameters modulate food digestibility?; what is the importance of gut microbiota in canine digestion and drug metabolism?; where drugs are released and absorbed?; how drug bioaccessibility is impacted by food matrix, galenic form, physicochemical parameters or microbiota?; how probiotic strains survive along the GIT? Yet, recommendations for petfood and drug intakes are only based on dog body weight or metabolic weight. Future development of new products needs therefore to consider not only dog’s weight but also all the variations in digestion process associated to different canine sizes and breeds to move towards personalized nutrition and veterinary medicine. Petfood manufacturers and veterinary companies aim to develop personalized products ranges, adapted to size (e.g. long-term growth of large breeds puppies, poor digestive tolerance and gastric dilatation volvulus for large dogs) or to address certain breed predispositions such as obesity in Labrador Retrievers or enteropathies in Terriers (German *et al.*, 2000; Boillat, Gaschen & Hosgood, 2010; Osto & Lutz, 2015; Raffan *et al.*, 2016). Nevertheless, the impact of dog size or breed on digestive parameters remains poorly described despite its full interest in canine nutrition and health.

B. *Funding and partnership*

This PhD thesis was performed in the frame of a collaborative project between the UMR MEDIS (Microbiology, Digestive Environment and Health, Université Clermont Auvergne-INRAE, Clermont-Ferrand) and two companies, Lallemand Animal Nutrition (Animal Nutrition Center of Excellence, Lallemand SAS, Blagnac) and Dômes Pharma (Pont-du-Château). This PhD work was supported by a CIFRE grant (industrial agreement on training through research) from the French 'Agence Nationale de la Recherche et de la Technologie' attributed to Lallemand and industrial funding from both companies.

MEDIS laboratory aims to better understand the role of human and animal gut microbiota in health and diseases and is structured into four thematic axes. My PhD work takes parts of the INNOVITRO (innovation and *in vitro* model development) and FM2D (Metabolic Functions of Digestive Microbiota and Dysbiosis) axes. The team benefits from more than 25 years of internationally recognized expertise and knowledge in the field of human and animal *in vitro* gut simulation, with a technological platform associating *in vitro* models of the upper tract, namely the TIM model (TNO gastroIntestinal Model), and lower tract with the M-ARCOL model (Mucosal Artificial Colon). **Lallemand** and specifically the **Animal Nutrition** business unit (**LAN**) develops, produces and commercializes microbial-based solutions (alive yeasts, bacteria and their derivatives) for animal health and nutrition. Those solutions result, among other effects, in stabilizing the digestive microbial ecosystems. Thus, the LAN company aims to understand the solutions' modes of action on microbial communities in the gastrointestinal tract in order to better explain the effects on digestive efficiency and host health. The LAN company has strong knowledges in the field of pre-, pro-, postbiotics and microbiota, canine digestive physiology, nutrition, functional ingredients but also had many interactions with veterinarians. Dômes pharma is a pharmaceutic company with a strong expertise in Animal health, especially for the companion animals. The company wants to develop its level of knowledge on the digestive sphere in dogs to better meet the needs of veterinarians and pet owners. The main expertise of the group concerns veterinary health, especially related to the antibiotic use and pharmaceutic form development. Together, the three partners show therefore complementarity expertise in canine digestive physiology, *in vitro* gut simulation and feed and pharma product development, necessary to fulfil this thesis project.

C. *Research questions and technical outcomes*

In this context, this PhD work was first dedicated to a better understanding of how different dog sizes can impact canine digestive physiology including gut microbiota. For this entire work, dogs were stratified into three groups depending on their body weight: "**small**" under 10 kg, "**medium**" between 10-30 kg and "**large**" up to 30 kg. In accordance with the 3Rs rules and to answer the lack of complex canine *in vitro* model including gut microbiota, the broad knowledge acquired after an intensive literature review was used to set-up a new *in vitro* colonic system adapted to different dog sizes, based on the M-ARCOL model previously developed to simulate human GIT. Then, a disturbed situation was reproduced in the *in vitro* model by adding antibiotics, and microbiota restauration strategies based on the use of a probiotic and a postbiotic were evaluated.

Thus, the main scientific objectives and associated technological developments of this PhD thesis are:

1) **Impact of different methods for faecal sample storage on gut microbiota composition and metabolic activity in the M-ARCOL *in vitro* model.** These experiments were performed in collaboration with another PhD student on human faecal samples, in order to select the most suitable method for the following experiments with canine feces (Section II Chapter 1, *published into Applied Microbiology and Biotechnology journal in 2020)*
2) **In-depth understanding of the impact of body weight on physicochemical and microbial parameters of the canine large intestine and development of a new size-related colonic *in vitro* model based on the M-ARCOL technology**
    - Bibliographic reviews on the effect of dog body weight on digestive physiology and on currently available *in vitro* gut canine models (Section I, parts 1, 2 and 4, *published in ALTEX -2022- and International Journal of Biological Science -2022*)
    - Development of a new size-related model of the canine colon named CANIM-ARCOL and validation compared to canine *in vivo* data (Section II, Chapter 2, *submitted in ALTEX -2023*)
    - Mechanistic study using the newly developed *in vitro* colon model, aiming to investigate the ability of physicochemical and nutritional parameters related to small and large dogs to reshape microbiota structure and function from medium dogs (Section II, Chapter 3*, in preparation for Applied Microbiology and Biotechnology -2023*)
3) **Investigating the impact of antibiotherapy on canine microbiota structure and functions and development of a dysbiotic colonic model based on the new CANIM-ARCOL model**
    - Bibliographic review on the impact of antibiotics on canine microbiota (Section I, part 3)
    - Antibiotic screening experiments aiming to select the most appropriated antibiotic for the dysbiotic colonic model development (Section II, Chapter 4, *in preparation for Microbial Spectrum -2023*)
    - Dysbiotic *in vitro* model development for medium dog size and validation based on *in vivo* canine data (Section II, Chapter 4, *in preparation for Microbial Spectrum -2023*)

4) **Evaluation of a novel postbiotic strategy based on tyndallized (heat inactivated) *Lactobacillus helveticus* HA-122 cells to restore microbial balance after antibiotic treatment and comparison with a probiotic strategy using live yeast *Saccharomyces boulardii* CNCM I-1079**

- Bibliographic review on the impact of pre, pro, post (including para) -biotics on canine microbiota (Section I part 3)
- Effect of the probiotic and postbiotic on canine microbiota structure and functions in the antibiotic dysbiotic *in vitro* model (medium dog size) (Section II, Chapter 5, *in preparation for Food International Research journal -2023*)

D. Manuscript organization

The **first section** of the manuscript is a literature review, divided into four parts and providing a complete overview of the current knowledge on the impact of dog size on physicochemical and microbial digestive parameters. In **Part 1**, redrafted from our published review in *International Journal of Biological Science*, the impact of canine body weight on large intestine physicochemical parameters was described. **Part 2** is rather focused on the impact of dog weight on microbial parameters, namely colonic microbiota composition and metabolic activity, after introducing the key roles of gut microbiota role in canine health. In **Part 3**, factors known to shape canine gut microbiota are detailed, classified by factors occurring under a healthy state (e.g. morphological and environmental parameters) or dysbiotic conditions associated to antibiotherapy, digestive (IBD) or extra-digestive (obesity) pathologies, as well as currently available restoration strategies such a pre-, pro-, post- or parabiotics and faecal microbiota transplantation. Lastly, the **Part 4**, redrafted from our published review in *ALTEX Journal*, provides an in-depth description of currently available *in vitro* models of the canine digestive tract before discussing their potentials in the food and veterinary fields, but also their limitations and challenges that scientists have to face.

The **second section** presents the results of each step of the experimental work (**Figure 0.2**). First, **Chapter 1** presents a comparative study for faecal sample storage to preserve gut microbial structure and function. Then, based on the literature work, **Chapter 2** presents the development and validation of the CANIM-ARCOL simulating physicochemical and microbial parameters of the canine colon, related to different dog sizes. **Chapter 3** describes how large intestinal physicochemical and nutritional settings from different dog sizes shape *in vitro* canine microbiota activity and structure from medium dogs. In **Chapter 4**, the impact of antibiotherapy on canine colonic microbiota structure and functions was evaluated using a newly developed canine dysbiotic colonic model of the medium dog. Finally, **Chapter 5** examines two novel strategies based on *Saccharomyces boulardii* CNCM I-1079 and tyndallized *Lactobacillus helveticus* HA-122 cells to restore microbial balance after antibiotic treatment in *in vitro* colonic medium dog size conditions.

The **third section** discusses the results obtained during this PhD thesis compared to the available literature and gives some perspectives to this work.

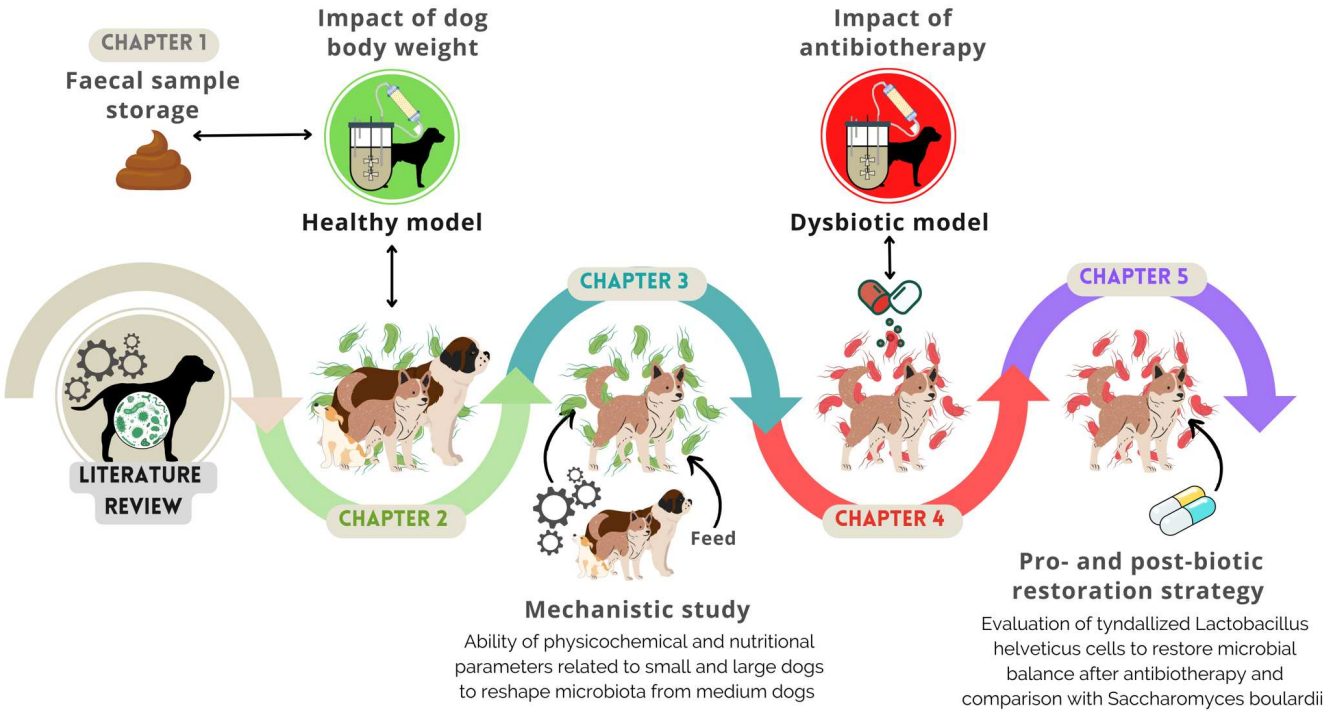

Figure 0.2: Outline of the experimental work of the PhD thesis. The main stages of the experimental work are summarized in this figure. The different chapters correspond to chapters of the results section.

SECTION I

LITERATURE REVIEW

Part 1 - Impact of canine body weight on gut physiology and physicochemical parameters

The following sections are dedicated to the presentation of the impact of canine body weight on the canine gut physiology and associated physicochemical parameters. Focus will be successively brought on the different digestive compartments of the canine GIT, especially considering the impact of dog size on anatomy and associated digestive processes. A specific attention on associated physicochemical parameters (i.e. pH, digestive secretions, nutrient digestibility, intestinal absorption and mechanical digestion including transit time) is made throughout this part. Tables including *in vivo* data from literature review are included in **Annexes** section. Some segments of this state of the art have been published in a review article in the journal *International Journal of Biological Sciences*, redrafted and updated for the present section.

REVIEW ARTICLE **DESCHAMPS, C.**, HUMBERT, D., ZENTEK, J., DENIS, S., PRIYMENKO, N., APPER, E. & BLANQUET-DIOT, S. (2022) From Chihuahua to Saint-Bernard: how did digestion and microbiota evolve with dog sizes. *International Journal of Biological Sciences* **18**, 5086–5102. Ivyspring International Publisher. doi: 10.7150/ijbs.72770 **(IF 10.75)**

1.1. Canine digestive anatomy and associated digestive processes

External morphological differences observed between extreme dog sizes such as Chihuahua and Saint-Bernard obviously reveal internal anatomical modifications. The canine mature digestive tract length can represent 2.8 % to 7 % of the total body weight, in a 60 kg and a 5 kg dog, respectively (Weber, 2006). Since GIT absolute length (in centimeters) is a reflect of dog height at the shoulder with a 6:1 ratio (Morris & Rogers, 1989), it leads to the question: how does the size of dog impact digestive anatomy? Canine digestive anatomy is adapted to their facultative carnivorous diet (i.e. high-protein and high-fat diet) with a short and simple digestive tract (**Figure 1.1**). Digestion starts in the **mouth** with mastication process, helped by saliva. After swallowing, food boluses are transported through the esophagus into the **stomach** which is a J-shaped organ of glandular type, characterized by three anatomical compartments (i.e. *fundus*, corps and *antrum*) leading to the pylorus sphincter (Kararli, 1995). Canine gastric mucosal cells secrete hydrochloric acid (HCl), pepsin and lipase, which makes stomach essential in protein and lipid digestion. Canine stomach has a high dilatation capacity, varying from a maximal volume of 0.5 L for small dogs to 8 L in large dogs, which corresponds to the extreme quantity of food that a dog can ingest (Kararli, 1995). Digestion continues along the **small intestine** which is distributed as 10 % length for duodenum, 85 % for jejunum and 5 % for ileum (Kararli, 1995; López Albors *et al.*, 2011).

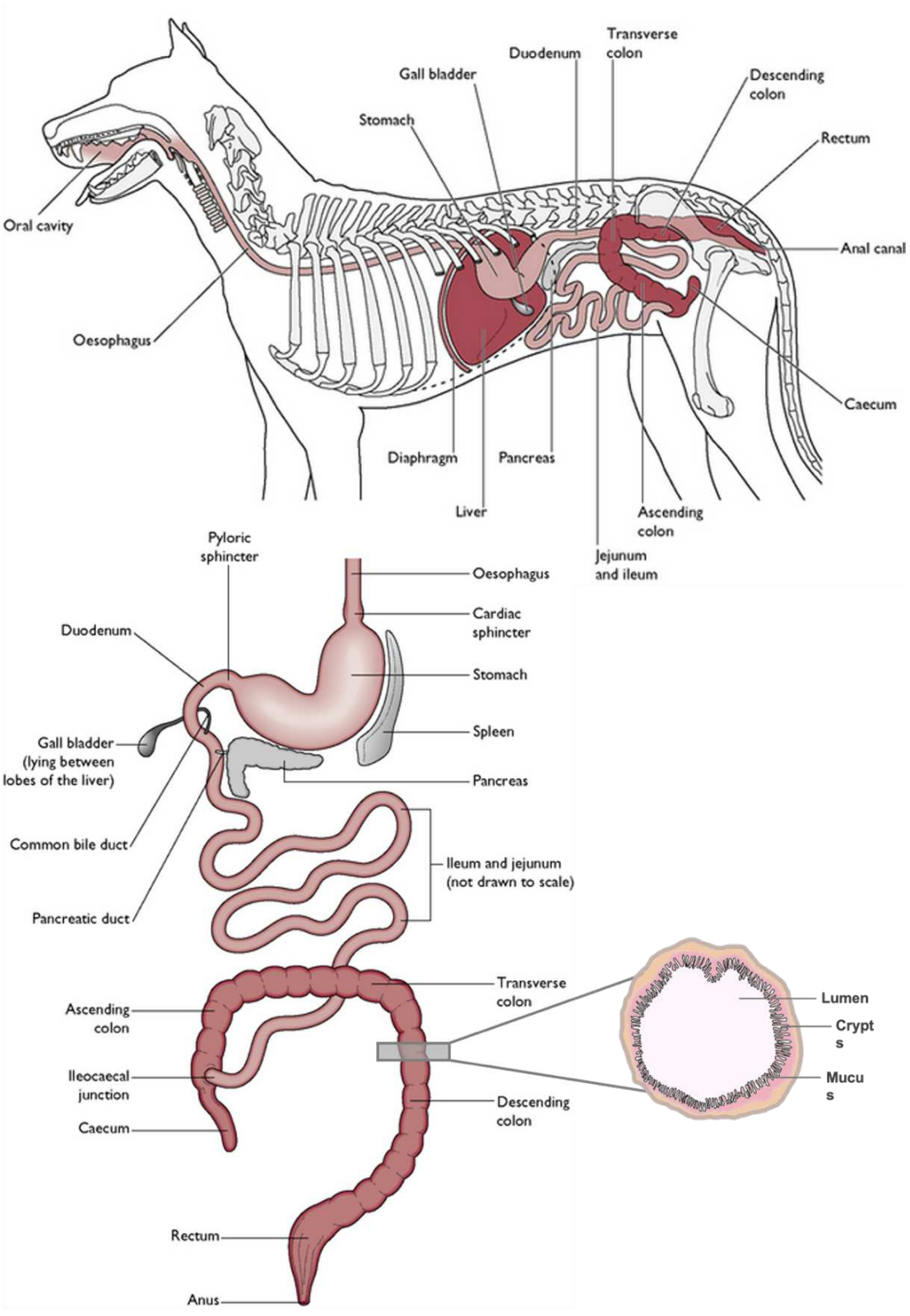

Figure 1.1: Canine digestive system. At the top, organs of the digestive system of the dog are presented in left lateral view. At the bottom, the externalized digestive tract is presented with a transversal cut of the colon. *Modified from http://veteriankey.com.*

Small intestine length measured *post mortem* is positively correlated (Pearson correlation of 0.672) to canine body weight (from 240 cm for a 5 kg to 640 cm for a 33 kg dog), as well as small intestine width (weaker correlation, $R^2 = 0.36$) (López Albors *et al.*, 2011). Canine small intestine, together with peripheral organs such as pancreas and liver, have a key role in canine digestion process. **Pancreas** produces pancreatic juice delivered into duodenum and associated with protein, carbohydrate and lipid digestion. **Liver**, coupled with gallbladder, has a central role in lipid digestion through bile acid production and induction of increased intestinal peristalsis (Robin, 2007). Small intestine is also a central player in nutrient absorption, allowed by the presence of microvilli at the surface of enterocytes. When measuring intestinal wall thickness at different levels of the GIT (descending duodenum, proximal and distal jejunum, proximal and distal ileum), higher values were observed for male dogs compared to female (except for distal ileum) but no correlation was found with dog sizes whatever the intestinal compartment (Sarriá *et al.*, 2012). Regarding small intestinal villus length, an old study from 1978 showed no correlation between dog weight and mucosal dimensions (Hart & Kidder, 1978). In adult dogs from various sizes, duodenal villus length was 722 ± 170 µm (Washabau *et al.*, 2010). Jejunal villi were longer in small dogs like Pomeranian and Fox Terrier (900 µm) than in medium ones such as Newfoundland (500 µm) (Baum *et al.*, 2007). Lastly, ileal villus length was measured in medium size Greyhound female and values around 796-823 µm were found (Feldman *et al.*, 1976). Canine **large intestine** measures around 20-80 cm with 2-3 cm diameter in medium dogs (Kararli, 1995). The three parts of the canine colon (i.e. ascending, transverse and descending) are not so well defined when compared to humans, with the particularity to be non-sacculated and devoid of sigmoid colon (Kararli, 1995). Ascending colon represents in medium size dog 20 % of the colon length, while transverse and descending correspond to 30 % and 50 %, respectively. The two first parts are used for transport, electrolyte and water modification as well as for bacterial fermentation and storage areas, while descending colon mainly functions as conduit ending with rectum. Canine large intestine is involved in water and electrolyte absorption but also degradation of residual nutrients thanks to the fermentation activity of resident microorganisms called gut microbiota. Large intestine total length appears to vary according to dog's body weight, from 32 cm for Miniature Poodles to 99 cm for Great Danes (Weber, Biourge & Nguyen, 2017). Volume and surface are also increased from Miniature Poodle to Great Dane (volume of 92 *versus* 2106 cm^3, surface of 191 *versus* 1612 cm^2). As the large intestine length increases with body weight, the same positive relation is observed for absorption surface with a higher number of villi in large compared to small dogs (Weber *et al.*, 2017). Colonic crypts length was around 500-600 µm but without correlation with dog size (Baum *et al.*, 2007). To conclude, scarce anatomy data (only five publications) evidenced morphological differences depending on dog's body weight (mainly related to the colonic compartment), even if important parameters have not been evaluated such as gastric wall thickness, intestinal microvilli characteristics (i.e. length or number) or peripheral organs anatomy and functions. Variations in digestive anatomy can obviously affect physicochemical parameters such as pH, digestive secretions and transit time, and consequently the gut microbiota.

1.2. Gastrointestinal pH

Gastrointestinal pH changes along the dog digestive tract (**Figure 1.2**). Mean salivary pH of medium dogs is around 7.3-7.8 and quickly decreases by 0.5 point with a stimulation using a piece of solid sugar on the tongue (Larmas & Scheinin, 1971; Smeets-Peeters *et al.*, 1998; Durand, 2010). In the stomach, the arrival of food bolus stimulates HCl production. This compartment shows the lowest pH value along the GIT, allowing dogs to partially digest bones (de Godoy *et al.*, 2014) and putrescent meat and this pH largely depends on feed status. However, due to the paucity of data, it remains difficult to know how body weight affects gastric, small intestinal and colonic pH (**Figure 1.2**).

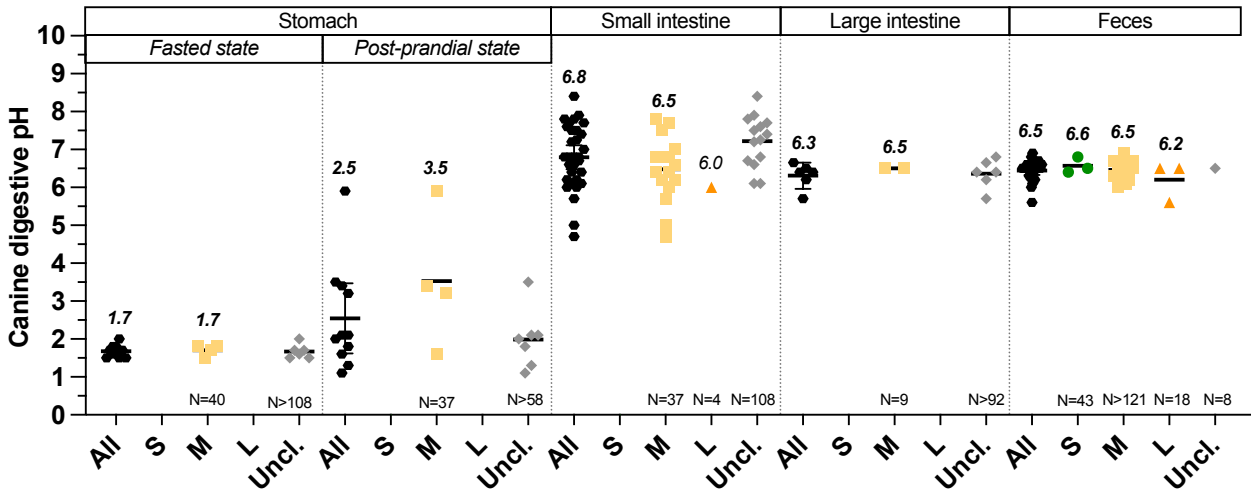

Figure 1.2. Impact of dog sizes on pH values in all digestive compartments. Results from studies measuring in dog's pH values in the stomach (under fasted or fed conditions), small intestine, large intestine and faeces are presented. Small dogs are plotted in green, medium dogs in yellow, large dogs in orange and unclassified dogs in grey. Raw data were pooled in "all" group (in black). Calculated median values are in italic bold, values for a single point in italic. Black bars represent 95 % confidence intervals. The number of dogs involved in studies is indicated as "N=".

To date, gastric pH has not been assessed in small and large dogs. Regarding medium dogs under fasted conditions, mean gastric pH of Beagles is around 1.5 (range 0.9-2.5), punctuated by occasional pH spikes with high frequency changes due to inter-individual variability (Mahar *et al.*, 2012). Those values measured in laboratory animals are in accordance with pH found in mixed-breed owner dogs (Garcia-Mazcorro *et al.*, 2012a). Small intestinal pH increases to value close to the neutrality because of the buffering capacity of pancreatic juice enriched in bicarbonate ions and bile (Kararli, 1995). It also increases from the proximal to the distal parts, from 6.5 to 8 in medium size dogs (Koziolek *et al.*, 2019). To date, there is no available study that investigates the influence of the dog size on duodenal and ileal pH (Martinez, 2002). The few studies investigating the canine jejunal pH measured a mean pH of 6.8 and 6.0 for medium and large dogs, respectively (Mentula *et al.*, 2005; Kalantzi *et al.*, 2006). Only few studies investigated colonic pH using colonic cannula or wireless capsules, and once new, most of them do not discriminate dogs in terms of body weight. Colonic pH is more acidic than the small intestine one, with mean values of 5-6.5 and 6.2, respectively for medium and large dogs, whereas there

is no data concerning small dogs (Smith, 1965; Lidbury *et al.*, 2012; Warrit *et al.*, 2017a; Koziolek *et al.*, 2019). Most of the time, colonic pH is estimated using faeces and there is no information on how pH varies depending on colonic sections. The average canine faecal pH values are in accordance with colonic pH, mainly around 6.4-6.6, as observed in **Figure 1.2**. For small dog group, three studies used faeces of 43 dogs and pH values vary weakly from 6.4 to 6.8 (Weber *et al.*, 2004; Beloshapka *et al.*, 2016; Igarashi *et al.*, 2017). There are also plenty of data on the faecal pH of medium (more than 121 dogs) and large (18 dogs) size dogs, with a pH range of 6-6.9 and 5.6-6.5, respectively (Cutrignelli *et al.*, 2009; Sandri *et al.*, 2016; Eisenhauer *et al.*, 2019; Nogueira *et al.*, 2019). This is an accordance with some studies reporting that colonic and faecal pH of large dogs are more acidic than that of other size dogs fed with the same diet (Oswald *et al.*, 2015; Weber *et al.*, 2017).

1.3. Digestive secretions

1.3.1. Enzymes

First digestion step occurs in the oral cavity with **salivary enzymes**. Numerous recent studies measured amylase activity in saliva of healthy dogs (Contreras-Aguilar *et al.*, 2017; Iacopetti *et al.*, 2017; Sanguansermsri *et al.*, 2018; Tecles *et al.*, 2018; Ricci *et al.*, 2018; Hong *et al.*, 2019). Mean amylase activity varies from 26.5 to 37.3 UI/L of saliva in medium dogs according to literature. One study involved 75 dogs from 8 to 42 kg (52 mixed breeds and 23 pure breeds) and measured 35.9 ± 41 UI/L amylase in saliva but results weren't discussed regarding dog sizes (Ricci *et al.*, 2018). Lactate dehydrogenase and adenosine deaminase activities were also quantified in saliva, without classification with canine body weight (Lavy *et al.*, 2012; Iacopetti *et al.*, 2017; Ricci *et al.*, 2018). Gastric mucosa secretes **gastric juice** containing proteolytic (pepsin, chymosin) and lipolytic (lipase) enzymes (Aspinall, 2004; Durand, 2010). In laboratory Beagles, gastric juice volume output increases with meal viscosity, from a total of 37.2 mL secreted for a low viscosity to 190 mL for a high viscosity meal (Ehrlein & Pröve, 1982). **Pancreatic juice**, discharged in canine duodenum, has an alkaline pH (7.4-8.3). It contains amylase (2013 U/kg body weight), lipase (9.8-33.3 mL 0.05 N NaOH/mL -no longer used unit of measure), phospholipases, cholesterases, proteases (old value of 407.5-2440 mg tyrosin/mL -no longer used unit of measure) and nucleases, without further detailed information (Kienzle, 1988; Robin, 2007). Digestive secretions were mainly studied before 2000s, but values were not discriminated depending on dog sizes, and no study focused on small and large dogs. However, enzymatic activities may vary according to the different diet compositions (i.e. protein, lipid, fiber contents) adapted to each dog size.

1.3.2. Bile salts

Bile is produced by liver, partially stored in gallbladder then discharged to duodenum during postprandial phase, allowing stimulation of intestinal motility, intestinal lipids saponification and vitamins A, D, E and K absorption. In liver, **primary bile acids** such as cholic acid (CA) and chenodeoxycholic acid (CDCA) are synthesized from cholesterol and conjugated to taurine or glycine (Kakimoto *et al.*, 2017). Studies evaluating bile production in healthy dogs never discriminate dog sizes. Bile production was only evaluated in medium dogs and was found to be 29 mL/kg/24 h (Madrid *et al.*, 1983). Once reached gallbladder, bile is up to 10 fold

more concentrated than in liver with a total concentration around 50 (40-90) mmol/L (Kararli, 1995; Kakimoto *et al.*, 2017; Nagahara *et al.*, 2018; Larcheveque, 2019). Here, it contains up to 15 different bile acids but the three majors count for 99 % of total pool, with 72.8 % taurocholic acid, 20.3 % taurodeoxycholic acid and 6.2 % taurochenodeoxycholic acid (Washizu *et al.*, 1994). In the small intestine, bile acids are deconjugated by gut microbiota (see part 2.2.3 for more details) and converted into **secondary bile acids**. Faecal bile acids concentrations were measured in three recent studies involving all dog sizes but without body weight distinction (**Figure 1.3A**). Authors found coherent results with concentrations ranged from 5.8 to 7.5 µg of total bile acids per mg of dry faeces (Schmidt *et al.*, 2018; Blake *et al.*, 2019; Manchester *et al.*, 2019). Another recent study evaluated faecal bile acids concentrations in 24 healthy dogs (Guard *et al.*, 2019). After data retreatment (classification in size groups), small, medium and large dogs present respectively 5.1, 4.7 and 3.4 µg of total bile acids per mg of dry faeces. This suggests a decrease in faecal bile acids concentrations with body weight increase. Further analysis from 8 studies (**Figure 1.3B**) indicates that relative percentages of faecal secondary bile acids (BA II: 84.9 %) are higher than primary bile acids (BA I: 15.5 %). These results suggest that the microbiota activity, and notably the bile acids recycling, differs from small to large breed sizes.

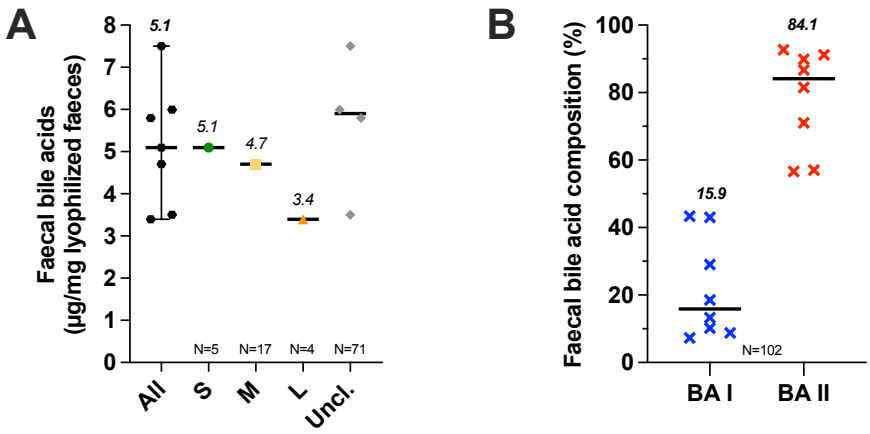

Figure 1.3. Impact of dog sizes on faecal bile acids. Results from studies in dog faeces quantifying total bile acids are represented in (A), further separated into primary (blue crosses) and secondary bile acids (red crosses) in (B). The same caption as used in Figure 1.2 was applied.

1.3.3. Mucus and mucins

Gastrointestinal mucus is secreted by goblet cells and covers the entire length of the GIT (Kararli, 1995). Mucus has an essential role in health by keeping away the luminal content from epithelium. Mucus is a viscous sieve composed by extracellular proteins, glycosylated and gel-forming proteins (namely **mucins**), lipids and extracellular DNA (Meldrum *et al.*, 2018; Macierzanka, Mackie & Krupa, 2019). In the stomach, this mucus layer allows protection of the epithelium against gastric acidic pH and withstands bone fragments (Moon *et al.*, 2018). Mucus thickness has been evaluated only in the canine gastric compartment, with a width of 576 and 425 µm, in the antrum and fundus, respectively (Bickel & Kauffman, 1981; Kararli, 1995). Influence of dog size on mucin secretion and mucus layer thickness has never been assessed whatever the digestive compartment.

Nevertheless, a very recent study has characterized mucus in laboratory large dogs in all digestive compartments, i.e. stomach, duodenum, cecum, jejunum, ileum, proximal and distal colon (Dubbelboer *et al.*, 2022) (**Figure 1.4**). For the first time, this study evidenced variations of mucus pH, from 4.8 in the stomach compartment to an average of 6.5-7 from duodenum to distal colon. Despite its viscosity was similar between each compartment, water content varied with a minimal content of 74 % founded in the ileum, to a maximum of 95 % in the stomach and large intestine. In addition, proteomic analysis using mass spectrometry highlighted different mucin compositions between the various compartments, especially between the stomach which is mainly composed of MUC5AC and the rest of the GIT where MUC2 is the main mucin. Authors described for the first time the form and size of canine mucus pores which vary from circular to elongated forms depending on localization, and perhaps on mucin content (**Figure 1.4**). Finally, this study evidenced similar characteristics between canine digestive mucus (in large dog), human (Linden *et al.*, 2008) and pig (Barmpatsalou *et al.*, 2021).

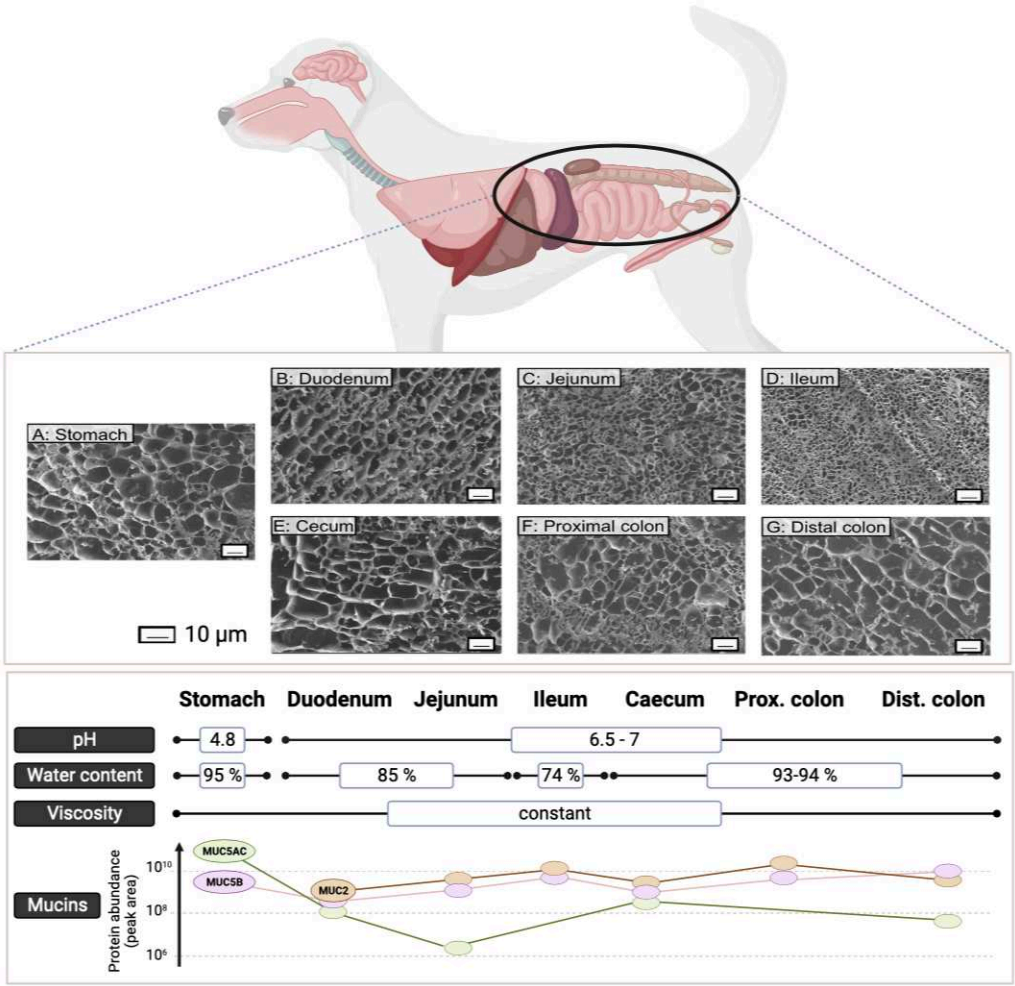

Figure 1.4: Physiological properties of mucus layer and associated mucins from seven segments of the large canine gastrointestinal tract. At the top, microscopic characterization of canine mucus using cryo-scanning electron micrographs of mucus layer collected from the gastrointestinal segments at 2K magnification. At the bottom, physiological properties are presented. Values and microscopic observations were extracted from *(Dubbelboer et al., 2022).*

1.4. Nutrient digestibility

Digestibility defines the degree to which organic matter is digested by an animal. Its measure provides a qualitative and quantitative indicator of food's quality, i.e. the more digestible a food is, the higher the proportion of absorbed nutrients will be. **Figure 1.5A** gives an overview of canine dry food composition in dogs according to body weight. Digestibility performances can be evaluated in dogs by measuring ileal or total (in faeces) apparent digestibility of a tested diet, and standardized digestibility could be obtained by deducing endogen products such as enzymes or metabolites delivered from intestinal cell desquamation.

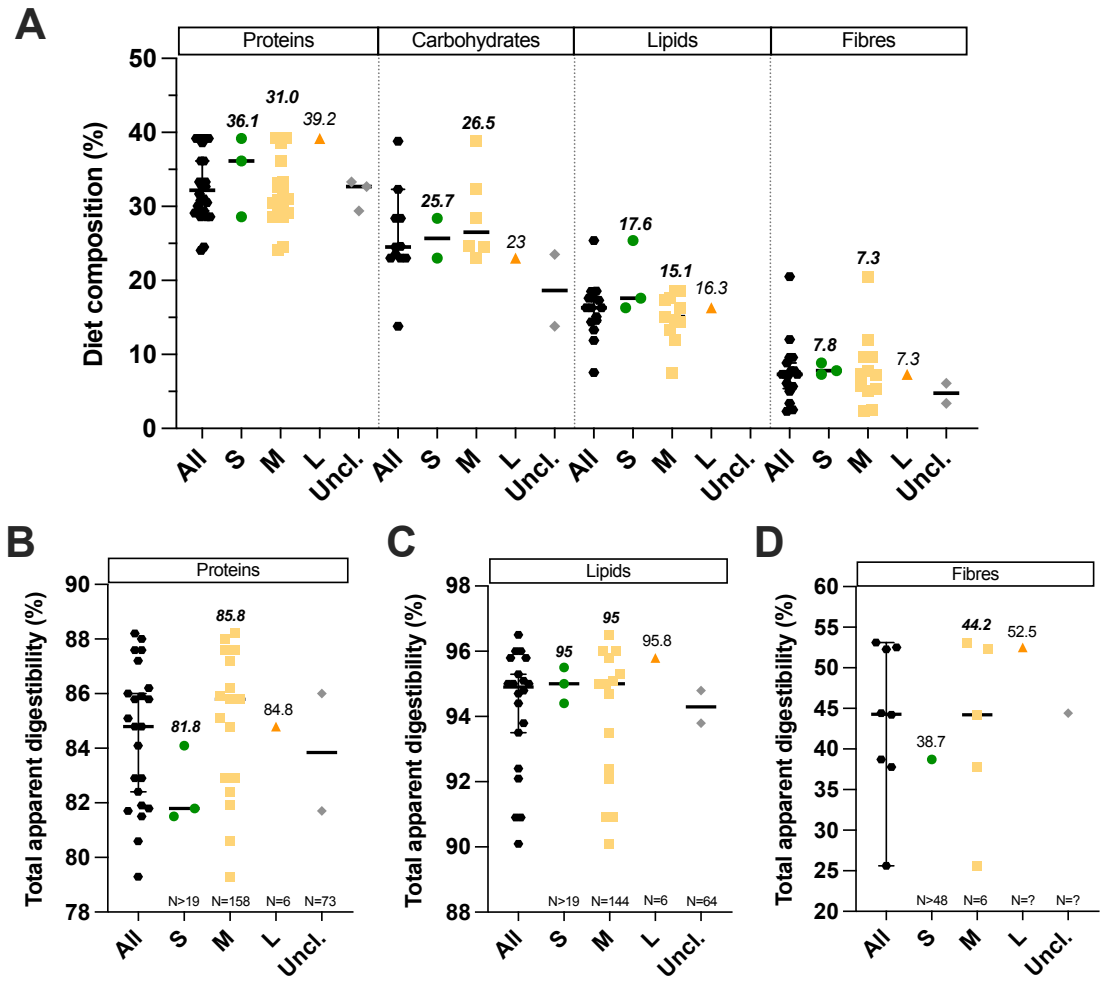

Figure 1.5. Diet composition and impact of dog sizes on total apparent digestibility. Nutritional composition of dry food diet used in canine studies is represented in (A). Results from studies investigating in dogs' total digestibility of proteins, lipids and fibre are presented in (B), (C) and (D), respectively. The same caption as used in Figure 1.2 was applied.

As previously observed for physicochemical parameters, digestibility studies are mainly focused on medium dogs and there are only two publications on small (Weber *et al.*, 2003; Nery *et al.*, 2010) and one on large dogs (Weber *et al.*, 2003). Due to their invasive nature, only 4 studies have been performed with ileal cannula (to measure ileal digestibility), including 3 on medium dogs (Bednar *et al.*, 2000; Flickinger *et al.*, 2003; Propst *et al.*, 2003; Hendriks *et al.*, 2013). **Lipid** digestibility seems to be almost complete at the ileum

level (i.e. 89.3-96.5 %), with only around 3-5 % increased digestibility when evaluating total digestibility in faecal samples. Ileal **protein** digestibility appears to be lower (51.3-76.2 %), with higher variations certainly related to protein quality which largely influences this parameter (Carrière *et al.*, 1993; Zentek *et al.*, 2004; Nery *et al.*, 2010; Pinna *et al.*, 2018). Surprisingly, the only study investigating total **dietary fibre** digestibility found an ileal digestibility of 17.8 %, while according to their definition fibre are only degraded in the large intestine (Bednar *et al.*, 2000). Given the lack of data, it is impossible to conclude on a possible effect of dog body weight on **ileal nutrient digestibility**. **Total apparent** protein (82-88 %) and lipid (95-95.8 %) digestibilities appear to be equal between different dog sizes, whatever the initial proportion of dietary proteins or lipids (**Figure 1.5B-C**). In contrast, total apparent dietary fibre digestibility (**Figure 1.5D**) appears to be higher in large than in small and medium dogs (52.5 ± 4 % for Great Dane *versus* 39 ± 7.4 % for Miniature poodle, and 26-38 % for medium dogs) (Weber *et al.*, 2002b; Detweiler *et al.*, 2019; Nogueira *et al.*, 2019). Indeed, it seems that fibre digestibility would be quite similar between small and medium dogs, while it would be improved in large dogs. In addition, faecal apparent digestibility of dry matter, organic matter and gross energy appears to be significantly higher for large compared to small dogs (Weber *et al.*, 2003). All in all, those results mean that the colonic fermentation seem to be more important in large than in medium and small size dogs.

1.5. Intestinal absorption

1.5.1. Permeability

During digestion process, food is broken down into small soluble compounds (amino acids, fatty acids, monosaccharides, minerals and vitamins), able to be absorbed mainly through the villi-covered wall of the small intestine. Nutrient passage through the epithelial wall is modulated by intestinal permeability, which is the property of epithelium to allow some molecules to be absorbed passively or actively through mucosa while avoiding the passage of microorganisms and macromolecules. Lactulose to L-rhamnose or lactulose to sucralose urinary ratios could be used to monitor changes in canine small and large intestine permeability, respectively (Hernot *et al.*, 2009). A higher lactulose to L-rhamnose ratio is associated with a leakier small intestine, while a lower lactulose to L-rhamnose ratio indicates a higher colonic permeability. Using these methods, Weber *et al.* (Weber *et al.*, 2002a) observed an increased intestinal permeability in Giant Schnauzer and Great Danes (large dogs; lactulose to L-rhamnose ratio: 0.31) compared to small dogs (0.16), and Hernot *et al.* (Hernot *et al.*, 2009) found a higher colonic permeability in large dogs (lactulose to sucralose ratio: 0.35) than in small ones (0.51). Those differences could be related to modifications associated with dog size in intestinal area, pore size, frequency of tight junctions, differences in tightness of tight junctions or accessibility of luminal content to intestinal crypts (Bjarnason, MacPherson & Hollander, 1995). Of note, breed differences were particularly noticed with a higher colonic permeability in Great Danes, as previously described (Zentek & Meyer, 1995; Meyer *et al.*, 1999). An increased permeability could affect both nutrient, metabolite and electrolyte absorption but also microorganism's translocation. This may explain the weaker digestive tolerance of resistant-starch and higher digestive sensibility of large dogs compared to small ones, as discussed by Goudez *et al.*, (2011).

1.5.2. Passive absorption

Water, electrolytes and vitamins are absorbed through passive mechanisms in the small and large intestinal lumen. In healthy dogs, around 90 % fluids crossing the colon are reabsorbed by mucosa (Rolfe, 1999; Durand, 2010). Meyer *et al.* (Meyer *et al.*, 1999) demonstrated that total faecal water increases with dog body weight, but the percentage of free faecal water decreases. This is of high interest because an increase in free faecal water content is associated with a higher colonic water content that can in turn influence *in vivo* drug dissolution, in the case of poorly soluble drugs for which dissolution continues in the large intestine (Oswald *et al.*, 2015). Whereas small dogs tend to have drier stools, a tendency of poorer faecal consistency and higher water content is observed in larger dogs. Potassium and bicarbonate ions are secreted into the colonic lumen, whereas sodium and chloride ions are passively absorbed from luminal contents (Rolfe, 1999). Uptake of sodium ions creates an hypertonic environment next to crypts, generating an electrochemical gradient across colonic mucosa which drives water uptake from luminal contents by osmosis (Rolfe, 1999). Based on observation that large digestibility variations are observed within the same breed and between different breeds, Zentek and Meyer (Zentek & Meyer, 1995) compared mineral digestibility of four food types in Great Danes and Beagles. There was no breed difference for calcium, magnesium and phosphorous absorption, while net colonic sodium absorption tended to be 9-23 % lower in Great Danes compared to Beagles. These data were further supported by Weber *et al.* (Weber *et al.*, 2004) describing an increase in sodium faecal content with an increase in body weight (2.1 ± 0.7 g/kg DM in Miniature Poodle *versus* 6.1 ± 1.3 g/kg DM in Great Dane), traducing a lower sodium absorption by large dogs. Moreover, a reduction of colonic absorption of sodium has been particularly observed in Beagle, Labrador Retriever, Springer Spaniel and Münsterländer, suggesting a breed sensitivity (Weber *et al.*, 2017). Besides, Neri *et al.* (Neri *et al.*, 1991) reported a significantly greater faecal potassium concentration in large compared to smaller dogs. Independently of dog sizes, 9 0% vitamin D, 80-90 % vitamin A, 40-90 % vitamin K and 35-50 % vitamin E are absorbed by passive absorption in the proximal small intestine (Durand, 2010).

1.5.3. Active absorption

Active absorption processes in the small intestine implicate co-transporters (e.g. glucose or sodium-dependent transports) and concerns monosaccharides from carbohydrate degradation and peptides from protein degradation. Thus, 95 % of monosaccharides are absorbed in the duodenum and proximal jejunum (Durand, 2010), and 30 % of amino acids and 70 % of tripeptides are absorbed and assimilated in the proximal jejunum (Robin, 2007). Regarding lipids, 80 % of fatty acids and monoglycerides are absorbed in form of micelles in the small intestine and resulting in chylomicrons that passed into the intestinal lymphatic capillary of villus by endocytosis. There is no available information on the influence of dog size on nutrient absorption. Moreover, the overall active transport capacity of small intestine has been assessed by examining urinary excretion ratio of D-xylose to 3-O-methyl-D-glucose (Weber *et al.*, 2002a). Non-significantly different ratios of 0.57, 0.58 and 0.59 for small, medium and large dogs respectively have been reported, suggesting that small intestinal active transport is relatively consistent between sizes.

1.6. Mechanical digestion and gastrointestinal transit time

1.6.1. Motility

Canine gut motility was firstly evaluated using radiopaque markers, plastic beads or breath test. Recently, wireless motility capsule was developed to measure pressure, forces and gut contractions frequency. Using this method, Boscan *et al.* (Boscan *et al.*, 2013) observed in fed medium dogs a lower maximal amplitude contraction in the stomach compared to small intestine (52 mmHg *versus* 75 mmHg, respectively), coupled with higher gastric contraction frequency, with 3.7 contractions/min in the stomach *versus* 0.5 contraction/min in the small intestine. Another study involving dogs from different sizes observed similar tendency on maximal amplitude contraction (lower in stomach than in small intestine, with 0.2 *versus* 4.1 mmHg), but opposite results on frequency (0.8 in stomach *versus* 10.9 contractions/min in small intestine) (Warrit *et al.*, 2017b). Moreover, in this study, large intestinal contraction frequency seems to be similar to the gastric ones (0.6 contraction/min). Authors also calculated a motility index defined as the area under the pressure curve and the higher motility index was observed in small intestine (306.2 compared to 20 in stomach and 76.1 in colon). Using wireless motility capsule, Farmer *et al.* (Farmer *et al.*, 2018) found that motility indexes were higher in large intestine (199 mmHg*second/min) compared to small intestine (134 mmHg*second/min) and stomach (55 mmHg*second/min) with a similar maximum of 3.7 contractions/min in gastric compartment (Farmer, Ruffle & Hobson, 2019). Lastly, no study has investigated how dog body weight or size influences gut peristalsis.

1.6.2. Transit time

There is no available data on the duration of oral phase in dogs, but they are well known to quickly swallow their whole food. Data on gastric emptying time (GET), small intestinal transit time (SITT), orocaecal transit time (OCTT), large intestinal transit time (LITT) and total transit time (TTT) can be found in the literature with homogeneous definition between studies (**Figure 1.6**). Three different studies evaluate the impact of dog size on **GET** fed animals. Weber *et al.* (Weber *et al.*, 2002b) showed no significant difference in half-gastric emptying time between four breeds dogs (i.e. Miniature Poodle, Standard Schnauzer, Giant Schnauzer and Great Danes) using radiopaque markers ingested with food (T_{50} = 6.4-7.8 h). Without specifying any values, Bourreau *et al.* (Bourreau *et al.*, 2004) concluded on a longer GET in large compared to small breeds after ingestion of a dry food meal using breath test method. Contrarily, Boillat *et al.* (Boillat *et al.*, 2010) described a shorter GET in large compared to medium breeds (range 6.8-15 h), using wireless motility capsule immediately administered after a dry food meal. Thus, there is apparently no relationship between body weight and GET not only in fed, but also in fasted animals (**Figure 1.6**). Besides, a liquid meal conduced to a shorter GET compared to meat, with 90 % emptying in 0.4 h and 50 % in 1-3 h, respectively (unknown dog size and method) (Dressman, 1986). This suggest that canine gastric emptying is influenced by food consistency (Ménard *et al.*, 2018). There is also no consensus on the effect of dog size on **SITT**. in largest dogs, ranging 1.6-3.7 h without linking transit time and dog size(Weber, 2006; Boillat *et al.*, 2010; Oswald *et al.*, 2015).

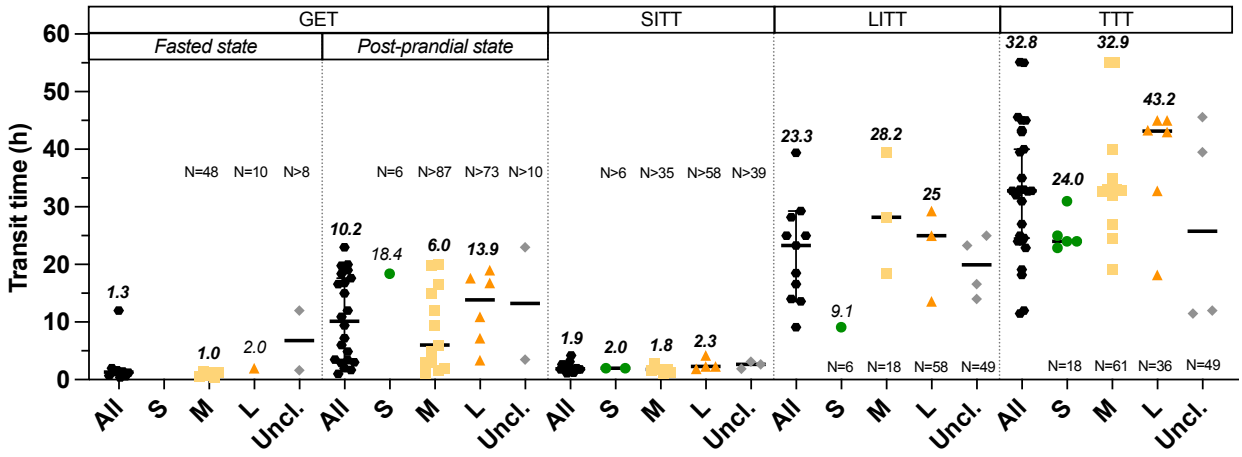

Figure 1.6. Impact of dog sizes on gastrointestinal transit time. Results from studies in dogs evaluating gastric emptying time (GET) under fasted or fed status, small intestinal transit time (SITT), large intestinal transit time (LITT) and total transit time (TTT) are represented. The same caption as used in Figure 1.2 was applied.

Oswald *et al.* (Oswald *et al.*, 2015) and Weber (Weber, 2006) found no influence of breed or body weight, while Boillat *et al.* (Boillat *et al.*, 2010) measured a shorter SITT OCTT was evaluated in dogs using very different methods. Some studies used sulfasalazine (converted into sulfapyridine in plasma) but did not employ the same threshold to define **OCTT**, i.e. either 50 % conversion or first appearance in plasma (Weber *et al.*, 2002b; Hernot *et al.*, 2006), whereas more recent studies used wireless motility capsule. As a consequence, extremely variable results of OCTT are provided, from 2.2-2.8 h with sulfapyridine (Weber *et al.*, 2002b; Hernot *et al.*, 2006) to 20.7 h with capsule (Balsa *et al.*, 2017). Whatever the method used, these authors conclude to an absence of correlation between OCTT and body weight. Studies of Boillat *et al.* (Boillat *et al.*, 2010) and Warrit *et al.* (Warrit *et al.*, 2017a) assessed **LITT** in dogs from several breeds and various body weight using wireless motility capsule. Both works conclude on the absence of correlation between LITT and body weight (**Figure 1.6**), with $T_{1/2}$ ranged 7.1-42.9 h (Boillat *et al.*, 2010) and 25.0 h (1.1-49.1 h) (Warrit *et al.*, 2017b). However, using plastic beads, researches revealed a longer LITT in large dogs (29.3 h for great Dane) than in small dogs (9.1 h for Miniature Poodle) and a significant positive correlation between LITT and body weight, but also between LITT and shoulder height was demonstrated (Hernot *et al.*, 2006). In this study, LITT accounts for 39 % of mean TTT for small breed dogs and 70 % for large ones, which means that longer transit time observed in large dogs could be related to a longer LITT. Lastly, **TTT** showed a clear positive correlation with body weight, as highlighted in **Figure 1.6** (Weber *et al.*, 2017). When gathering the data obtained in all the available studies, TTT ranged from 22.9-31 h (calculated median 24 h) in small dogs, 19.1-55 h (median 32.9 h) in medium dogs and 18.2-45 h (median 43.2 h) in large dogs. Especially, using plastic beads in small and large breeds, TTT observed was 22.9 h in Miniature Poodle and 43.3 h in Great Dane, whilst giant Schnauzer showed an even higher TTT of 55 h (Hernot *et al.*, 2005). This result was explained by the authors through a high stress sensitivity of giant Schnauzer that could influence their transit time in refraining their defecation, emphasizing a breed effect in addition to body size influence.

It should be underlined that data on transit time in the different digestive compartments of dogs (**Figure 1.6**) wary widely depending on the method used (*e.g.* radiopaque markers, plastic beads, ^{13}C-octanic acid breath test, sulfasalazine-sulfapyridine method or wireless motility capsule), breed, age, feed (composition, energy density or viscosity) and environment (laboratory or owners' home, stress context or sedation).

Bullet points - ***Impact of canine body weight on gut physiology and physicochemical parameters***

- Canine physicochemical digestion is a complex and regionalized process
- Clear effects of dog's body weight on gastrointestinal physiology, mainly related to the colonic compartment, have been evidenced
- Large intestine length, area and volume increase with dog size, associated to a higher colonic transit time which can affect nutrient and water absorption, as well as faecal moisture
- Sodium and potassium absorption is lower in large dogs resulting in higher concentrations in faecal samples
- Large dogs are characterized by a higher intestinal permeability inducing an electrolyte backflow into the colonic lumen, translated into a luminal retention of electrolytes and water

Part 2 - Impact of canine body weight on microbial parameters

Many physicochemical parameters of the digestion are impacted by canine body weight, mainly related to the large intestine compartment. All these parameters are continually shaping the microbiota's environment drafting some ecological niches for microorganisms. Consequently, microbiota should be also impacted by changes in physicochemical conditions related to dog sizes. Noteworthy, some parts of this state of the art on impact of canine body size on microbiota have been published in the same review article in *International Journal of Biological Sciences* mentioned in Part 1, and redrafted/updated for the present section.

REVIEW ARTICLE **DESCHAMPS, C.**, HUMBERT, D., ZENTEK, J., DENIS, S., PRIYMENKO, N., APPER, E. & BLANQUET-DIOT, S. (2022) From Chihuahua to Saint-Bernard: how did digestion and microbiota evolve with dog sizes. *International Journal of Biological Sciences* **18**, 5086–5102. Ivyspring International Publisher. doi: 10.7150/ijbs.72770 **(IF 10.75)**

2.1. Gut microbiota composition

2.1.1. Longitudinal variations

In dogs like in other mammals, microorganisms colonize the entire GIT from mouth to rectum. All along GIT, there are longitudinal variations in gut microbiota composition due to changes in pH, substrate concentrations (including oxygen and nutrient availability) and transit time (Hooda *et al.*, 2012; Friedman *et al.*, 2018; Etienne-Mesmin *et al.*, 2019). Gut microbiota has been weakly described in dogs (compared to humans) and most of available studies have been performed since 2003. **Figure 2.1** gives an overview of available data regarding gut bacteria composition depending on gastrointestinal regions in dogs.

Canine **oral** microbiota present similar number (around 350 bacterial taxa from 148 genera) but significantly different populations compared to the human ones (Dewhirst *et al.*, 2012) and is mainly colonized by *Proteobacteria* (45 %), *Bacteroidetes* (25 %) and *Firmicutes* (19 %). Most abundant species are *Porphyromonas cangingivalis* and *Porphyromonas gulae* (Bell *et al.*, 2008; Niemiec *et al.*, 2021). Regarding the other digestive compartments, studies have been mostly performed on faeces to avoid invasive procedures. **Stomach** is the less colonized compartment with 10^4 to 10^5 colony forming units (CFU) per gram of content in medium dogs, mainly composed by *Proteobacteria* (**Figure 2.2A**) including *Helicobacter spp.* that are potential pathogenic strains (Benno *et al.*, 1992; Mentula *et al.*, 2005; Hooda *et al.*, 2012).

Small intestine contains 10^5 to 10^7 CFU/g of content (Benno *et al.*, 1992; Mentula *et al.*, 2005). **Duodenum** (**Figure 2.2A**) is colonized by *Firmicutes* (calculated median 47 %), *Proteobacteria* (30 %), *Bacteroidetes* (7 %), *Fusobacteria* (3 %) and *Actinobacteria* (1 %), whereas **jejunum** is characterized by a higher abundance in *Proteobacteria* (37 %), *Actinobacteria* (11 %) and *Fusobacteria* (10 %), together with lower percentages of *Firmicutes* (33 %) and *Bacteroidetes* (7 %) (Xenoulis *et al.*, 2008; Suchodolski *et al.*, 2009; Garcia-Mazcorro *et al.*, 2012a; Honneffer *et al.*, 2017).

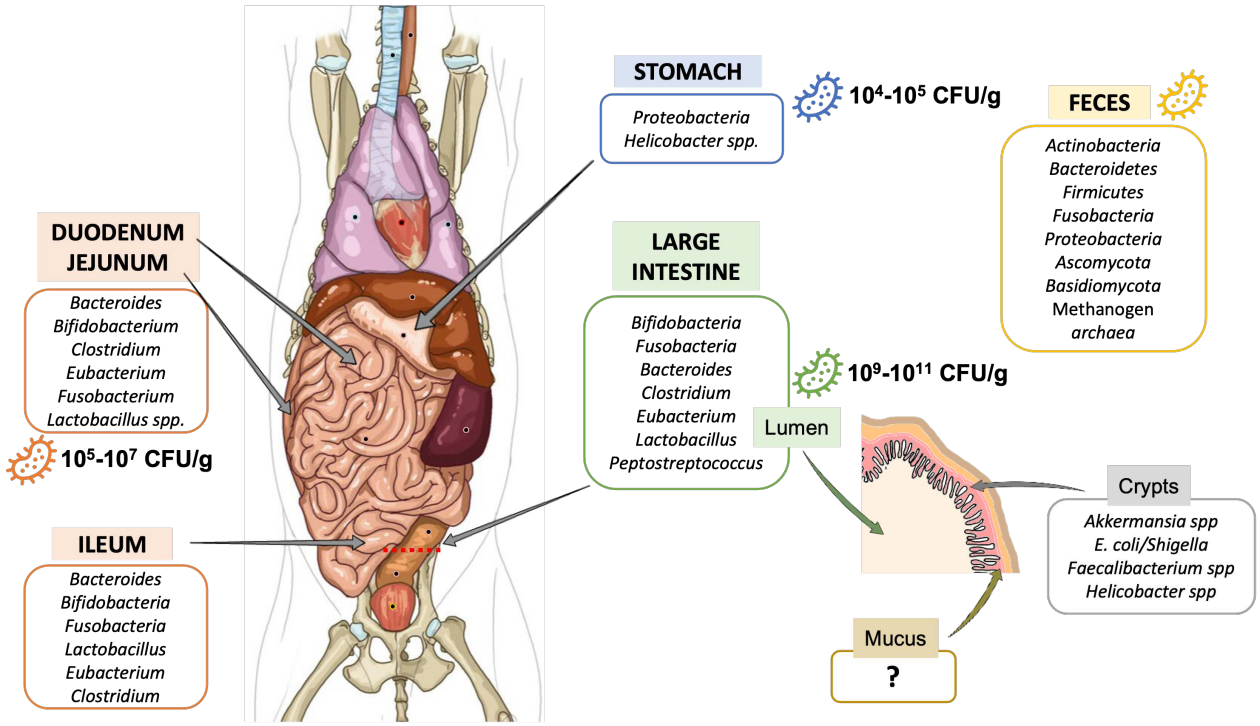

Figure 2.1: Variations in gut microbiota composition along the canine digestive tract. Main bacterial populations found in the different compartments of the gastrointestinal tract of the medium-sized dog are represented. *CFU: colony-forming unit.*

Ileum (**Figure 2.2A**) is dominated by 37 % *Fusobacteria*, 27 % *Firmicutes*, 12 % *Bacteroidetes* and 37 % *Proteobacteria* (Suchodolski, Camacho & Steiner, 2008; Honneffer *et al.*, 2017). These abundances should be considered with caution as they have been found in a single study performed in 6 medium dogs. As for other mammals, **large intestine** is the most colonized part of the GIT, with up to 10^9 to 10^{11} CFU/g of content (Hooda *et al.*, 2012). Only two studies have evaluated the colonic microbiota composition and used 16S gene Illumina sequencing. First, microbiota composition analysis from 6 healthy Hound dogs (Suchodolski *et al.*, 2008) demonstrated that colonic digesta is dominated by 37 % *Firmicutes*, 33 % *Bacteroidetes*, 29 % *Fusobacteria* and 1 % *Proteobacteria* including *E. coli*-like organisms (**Figure 2.2A**). In comparison, Honneffer and colleagues studied colonic microbiota from biopsies and described median relative abundances of 66 % *Firmicutes*, 13 % *Fusobacteria*, 6 % *Proteobacteria*, 5 % *Bacteroidetes* and 1 % *Actinobacteria* (Honneffer *et al.*, 2017) but without distinction between mucosal and luminal sampling. In the same study, authors showed similar bacterial profiles between colonic and **rectal** biopsies (not significant differences). Interestingly, majority of taxa colonizing the colon are also found in canine faeces (Pilla & Suchodolski, 2020) which seems to be rather different from the human situation where a significant number of mucus-adherent bacteria from the colon are not found in faeces (Pilla & Suchodolski, 2020). No study has investigated dog size effect on gut microbiota composition elsewhere than in **stools**, and the main variations in faeces are presented in **Figure 2.2B** and **2.2C**. Whatever dog sizes, faecal microbiota of healthy dogs is dominated by three main bacterial phyla: *Firmicutes*, *Bacteroidetes* and *Fusobacteria* (Pilla & Suchodolski, 2020).

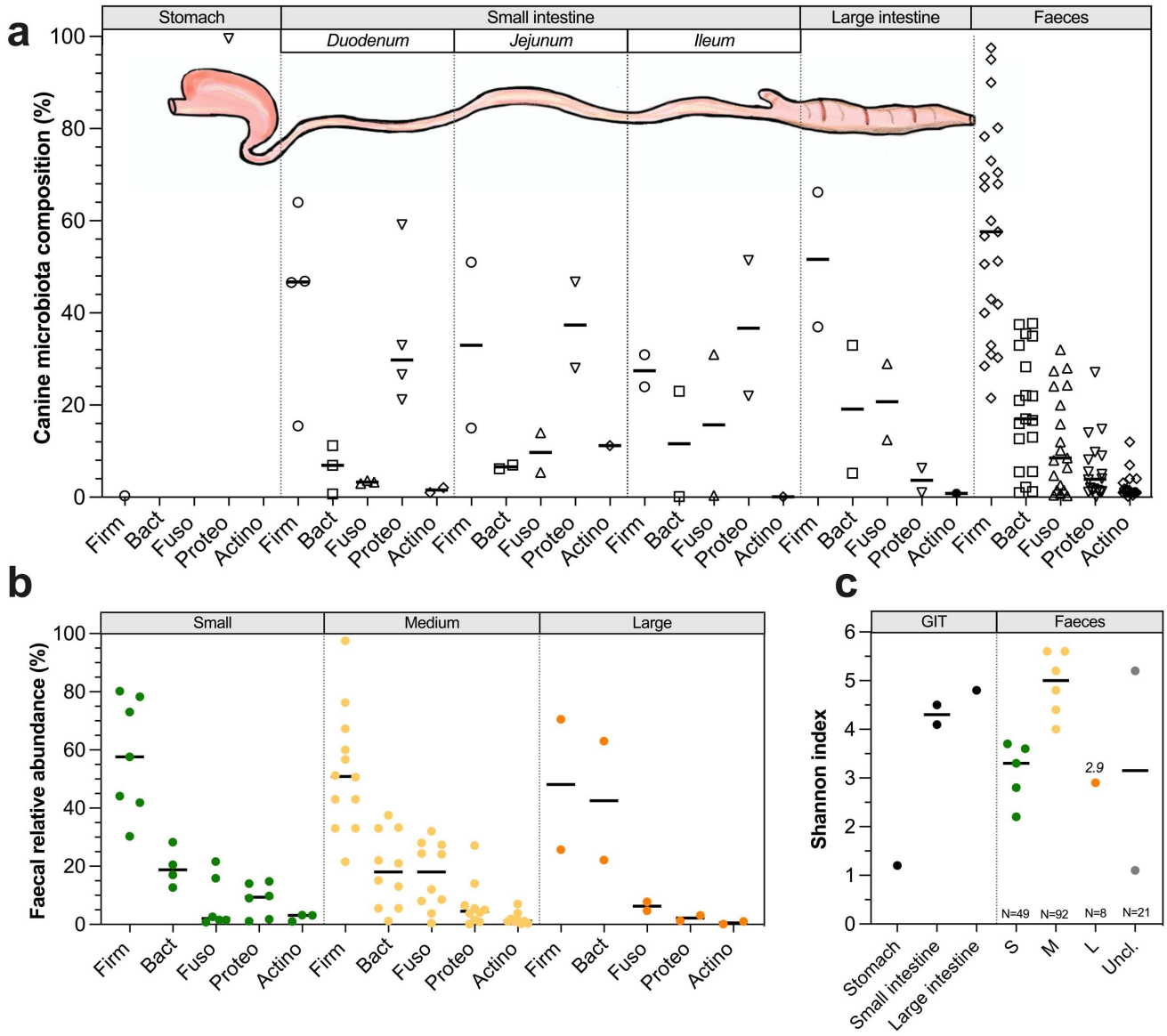

Figure 2.2: Variations in gut microbiota composition along the canine digestive tract and impact of body size. Main bacteria populations found in the different compartments of the dog gastrointestinal tract are represented in (A). Influence of dog sizes on faecal microbiota composition at the phylum level is shown in (B) and corresponding Shannon index are in (C). Only results from 16S rRNA Illumina sequencing were presented. Main phyla represented in dogs are *Firmicutes* (Firm), *Bacteroidetes* (Bact), *Fusobacteria* (Fuso), *Proteobacteria* (Proteo) and *Actinobacteria* (Actino). The same caption as used in Figure 1.2 was applied.

Bacteria from *Actinobacteria* and *Proteobacteria* phyla are also found in canine faeces but in a lesser proportion. Of interest, a variable relative abundance of *Bacteroidetes* was reported and was inversely correlated to *Fusobacteria* relative abundance indicating they might occupy the same ecological niches (Vázquez-Baeza *et al.*, 2016). *Fusobacteria* and *Proteobacteria* seem to be more abundant in dogs than in other omnivorous, probably related to diet changes (Simon, 2019). Unlike in human where *Fusobacterium* is frequently associated with diseases, in dogs this genus is related to non-stressful conditions and is therefore probably a marker of an healthy state, especially because its abundance increases when dogs have access to the outside (Oswald *et al.*, 2015). In small dogs faeces (**Figure 2.2B**), average *Firmicutes* proportions vary widely from 30 to 80 %,

followed by 13-28 % *Bacteroidetes*, while a lower abundance of *Fusobacteria* (1-22 %), *Proteobacteria* (1-15 %) and *Actinobacteria* (1-3 %) was detected (Kim *et al.*, 2015; Omatsu *et al.*, 2018; Reddy *et al.*, 2019; Doulidis *et al.*, 2023). Medium dogs display similar value ranges of *Firmicutes* (15-98%), *Bacteroidetes* (0.1-34 %), *Proteobacteria* (0.1-27 %) and *Actinobacteria* (1 %), but a larger proportion of *Fusobacteria* (0.1-40 %) compared to small dogs (Kim *et al.*, 2015; Algya *et al.*, 2018). Only one study investigated faecal microbiota composition in 8 large dogs and quantified 71 % *Firmicutes*, 22 % *Bacteroidetes*, 5 % *Fusobacteria,* and 1 % *Actinobacteria*, with interestingly a much lower abundance of *Proteobacteria* (1 %) than in small and medium dogs (Sandri *et al.*, 2016). In few studies, canine faecal diversity was followed with Shannon index and calculated medians seem to be higher in medium dogs (5.0, six studies) compared to small (3.3, five studies) and large dogs (2.9, a single study) (**Figure 2.2C**). In addition to Bacteria (representing 98 %), canine faecal microbiota also contains 1.1 % Archaea, 0.4 % Fungi and 0.4 % viruses, mainly bacteriophages (Swanson *et al.*, 2011; Suchodolski, 2011b). The fungal part -namely the **mycobiome**- of the faecal microbiota was composed by 97.9 % *Ascomycota* and 1 % *Basidiomycota* (Foster *et al.*, 2013). However, the role of fungi in the gastrointestinal tract remains mostly unknown. ***Archaea*** from 10 orders have been identified in canine feces among them the *Methanobacteriales* order -including *Methanobrevibacter spp*- was one of the predominant *Archaea* (Swanson *et al.*, 2011). Very recently, canine **virome** was also investigated in 45 healthy adult dogs using 18S gene Illumina sequencing (Shi *et al.*, 2021). Phages were identified as 18 % of the total amount of viral sequences. In addition, 31 DNA and 32 RNA virus families were characterized with homologous sequences to *Astroviridae* (71 %), *Coronaviridae* (17.6 %) and *Circoviridae* (7.3 %).

2.1.2. Radial variations

In addition to longitudinal variations, there are also radial changes in gut microbial composition that starts to be described in human (Albenberg *et al.*, 2014) but are still in infancy in dogs. As mentioned earlier, the entire gut epithelium is covered by a mucus layer that offers an alternative source of host-derived nutrients. This mucus is colonized by a specific mucus-adherent microbiota (namely mucosal microbiota) and seems to play a key role in host homeostasis (Etienne-Mesmin *et al.*, 2019). Of note, there is a lack of studies on the canine mucosal microbiota. Only two studies investigated the mucosa-associated bacteria on the outer mucus layer in the colon of healthy dogs, using targeted FISH (Fluorescent *in situ* hybridization) approach (Simpson *et al.*, 2006; Cassmann *et al.*, 2016). Analysis of colonic biopsy samples from healthy Boxers revealed that bacteria appear to be restricted to the outer mucus layer, as no bacteria was detected within the mucosa (Simpson *et al.*, 2006). In addition, Cassmann *et al.* (Cassmann *et al.*, 2016) demonstrated that free ileal and colonic mucus of healthy young dogs (< 2 years old) was mainly colonized by *Bacteroidetes spp*. and *Eubacteria,* while *Eubacteria* represented the major bacteria attached to adherent mucus. Authors reported that there were almost no bacteria attached to surface epithelium or contained within mucosa. Of interest, *Akkermansia muciniphila*, a well-known mucin-degrading bacteria in humans, inversely correlated to obesity, was not yet identified in canine faeces (Garcia-Mazcorro *et al.*, 2020).

2.2. Microbiota's functions in the gastrointestinal tract

2.2.1. Key roles of the canine gut microbiota

Commensal microorganisms colonize the entire gut of their host and live in a symbiotic relationship with it. Like in human, gut microbiota is known to play several key roles in dog health by maintaining host homeostasis, since it is implicated in many nutritional (e.g. vitamin synthesis, fiber degradation and lipid digestion through the metabolism of primary bile acids into secondary bile acids), immunological (immune system maturation) and physiological processes, such as vascularization, epithelium integrity and "barrier" effect against pathogens (Durand, 2010; Andoh, 2016a) (**Figure 2.3**).

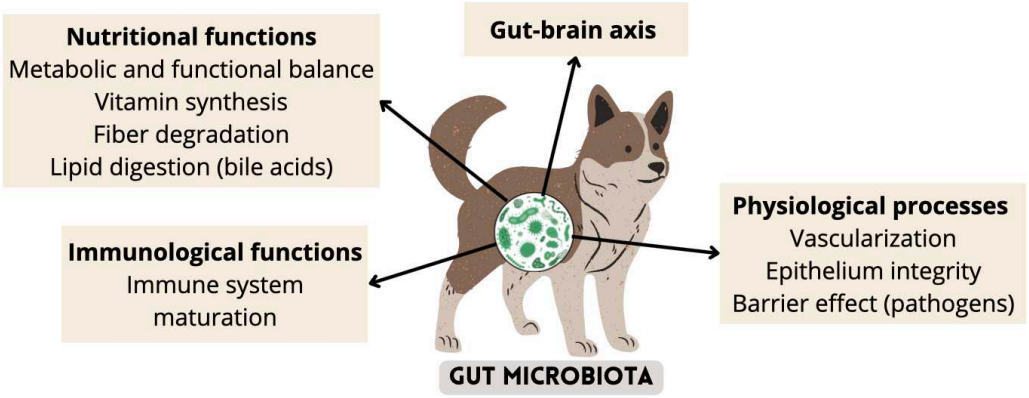

Figure 2.3: Schematic representation of the key functions of canine gut microbiota.

The gut microbiota is involved in the maintenance of structural components of the gut mucosal barrier (i.e. tight junctions, adherent junctions and desmosomes) (Saitoh *et al.*, 2015). In addition, colonic mucus production by goblet cells is stimulated by commensal bacteria (Etienne-Mesmin *et al.*, 2019). Mucin secretion and production of antimicrobial peptides by colonocytes is also favored by short-chain fatty acids (SCFA) produced by microbiota (especially butyrate), which participate to the barrier effect of the mucosa (**Figures 2.4 and 2.6**). In addition, preferential consumption of nutrients by commensal bacteria instead of pathogens is a way of outcompeting the pathogenic bacteria. This phenomenon is called competition, and by consuming the same nutrients, well-established commensal bacteria cause starvation of the competing pathogenic bacteria fighting to find an uncontested niche. Growth of bacterial pathogens can be also inhibited by commensal bacteria producing antimicrobial peptides (AMP) such as bacteriocins (O'Shea *et al.*, 2012). Among all these functions, the next section will focus on the metabolic activities of the canine gut microbiota.

Metabolic activity of the gut microbiota is essential for host health. Regarding functional level, identified microbiome gene content obtained from metagenomic analysis on 6 medium dogs was not impacted by body weight (17.9 to 25.3 kg) and was associated with the metabolism of carbohydrates (12.5-13 %), proteins (8.1-9.1 %), DNA (7.1-7.4 %), cell wall and capsule (7-7.6 %), amino acids and derivatives (6.8-6.9 %), cofactors, vitamins, prosthetic groups and pigments (5.7-6 %) and bacterial virulence (6.2-7.2 %) (Swanson *et al.*, 2011). Besides, Guard and Suchodolski (2016) have studied faeces from 8 healthy dogs (2.7 to 31.8 kg) and observed high inter-variability microbiota composition between animals, while bacteria's functions stay very consistent

(based on PICRUST functional predictions from 16S rRNA gene 454-pyrosequencing data). Thus, despite gut microbiota composition varies a lot between dogs, its functional potential seems to be unchanged whatever dog sizes (Durand, 2010). However, to the best of our knowledge, gut microbiota gene expression has never been investigated between dogs from various breeds or sizes, meaning that expression profiles can differ even if a same functional potential was observed.

2.2.2. Carbohydrates metabolism

Carbohydrates that are not degraded in the small intestine (namely fibers) passed through the large intestine where they are fermented by the resident microbiota. After cleaving, complex polysaccharides are degraded into monosaccharides, mainly by bacteria from the genera *Bacteroides*, *Bifidobacterium*, *Ruminococcus* and *Roseburia*, leading to gases (such as dihydrogen -H_2-, carbon dioxide -CO_2- and methane -CH_4) and SCFA production (**Figure 2.4**). To our knowledge, there is no *in vivo* data related to total gas production associated to carbohydrate metabolism in dogs. However, we can assume that, as for human, SCFA production is associated to H_2 and CO_2 production which can be reused by methanogenic bacteria to produce CH_4 (Swanson *et al.*, 2011). Regarding SCFA, the three main produced are acetate, propionate and butyrate. SCFAs are markers of gut health, involving in stimulation of the intestinal motility and can be further used as an energy source for colonocytes, liver and brain. Acetate is predominantly produced by genera *Bacteroides*, *Clostridium*, *Eubacterium, Phascolarctobacterium and Ruminococcus*. Propionate is mainly produced by genera *Bacteroides*, *Phascolarctobacterium, Propionibacterium* and *Veillonella* (Bernalier-Donadille, 2010). Finally, butyrate-producing species are mainly encountered among *Firmicutes* in the *Ruminococcaceae* and *Lachnospiraceae* families as well as in *Erysipelotrichaceae* and *Clostridiaceae* (Louis & Flint, 2017). Canine SCFA production was only evaluated in **faecal samples**. Values were mainly obtained in medium dogs (especially Beagles) and vary widely due to many differences in design studies (e.g. type of food, composition in carbohydrates, methods, units). However, in a study performed by Weber *et al.*, (2004), the authors compared SCFA production between small, medium and large dogs and demonstrated that total SCFA concentration in stool significantly increased with body weight, with 448 ± 67, 894 ± 80 and 1184 ± 259 mmol/kg of lyophilized faeces for small, medium and large dogs, respectively. This is consistent with a longer LITT in large breed dogs that may promote microbial fermentation. Large quantity of organic acids produced could thus exceeds colonic mucosa absorption capacity, thereby leading to an accumulation in lumen, a decrease in colonic pH and an increased faecal excretion (Weber *et al.*, 2017). Lastly, regarding SCFA ratio, Mondo *et al.*, (2019) reported average percentages of 60:25:15 for acetate, propionate and butyrate in dog feces, respectively, with an obvious effect of sizes according to our literature review (**Figure 2.8B**). Different faecal ratios of around 58:33:10, 57:28:11 and 49:44:8 were calculated in small (a single study), medium and large dogs, respectively, which certainly reflects variations in faecal microbiota profiles between canine sizes.

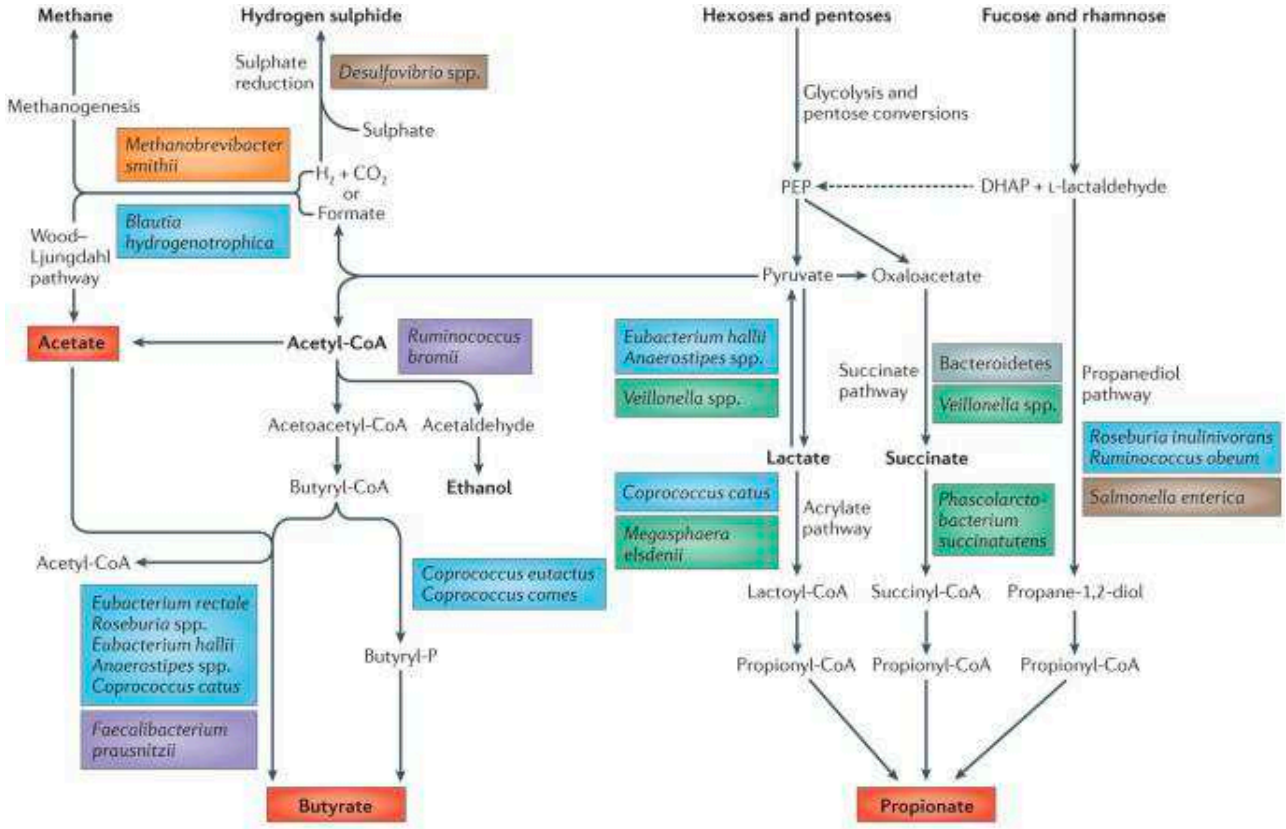

Figure 2.4: Carbohydrates metabolism pathways involved in short-chain fatty acids biosynthesis and gas production, and associated bacteria. Extracted from Louis, Hold & Flint, (2014).

2.2.3. Protein metabolism

Dietary proteins are mainly absorbed in the small intestine in dogs. However, undigested proteins from diet and endogenous proteins (i.e. pancreatic secretory products, desquamated enterocytes, mucins and enzymes) enter the colon where they can be metabolized by microbiota (**Figures 2.5 and 2.6**). Canine faecal relative abundance of *Peptostreptococcaceae*, *Paraprevotellaceae* and *Clostridiaceae* were positively associated to high-protein diet, suggesting their involvement in canine protein metabolism. Protein degradation starts by hydrolyzation of polypeptides by bacterial proteases and peptidase, leading to the production of amino acids, reused to form phenols and indoles, ammonia, biogenic, hydrogen sulfide and BCFA, as detailed below (Weber *et al.*, 2017). To the best of our knowledge, the impact of dog size on the production of total BCFA or BCFA composition has never been directly evaluated within a same study (**Figure 2.8C-D**). In addition, phenols, indoles and ammonia concentrations

were never quantified in the dog large intestine, poorly investigated in faeces of small and medium dogs and never quantified in large dogs (**Figure 2.8E-F**).

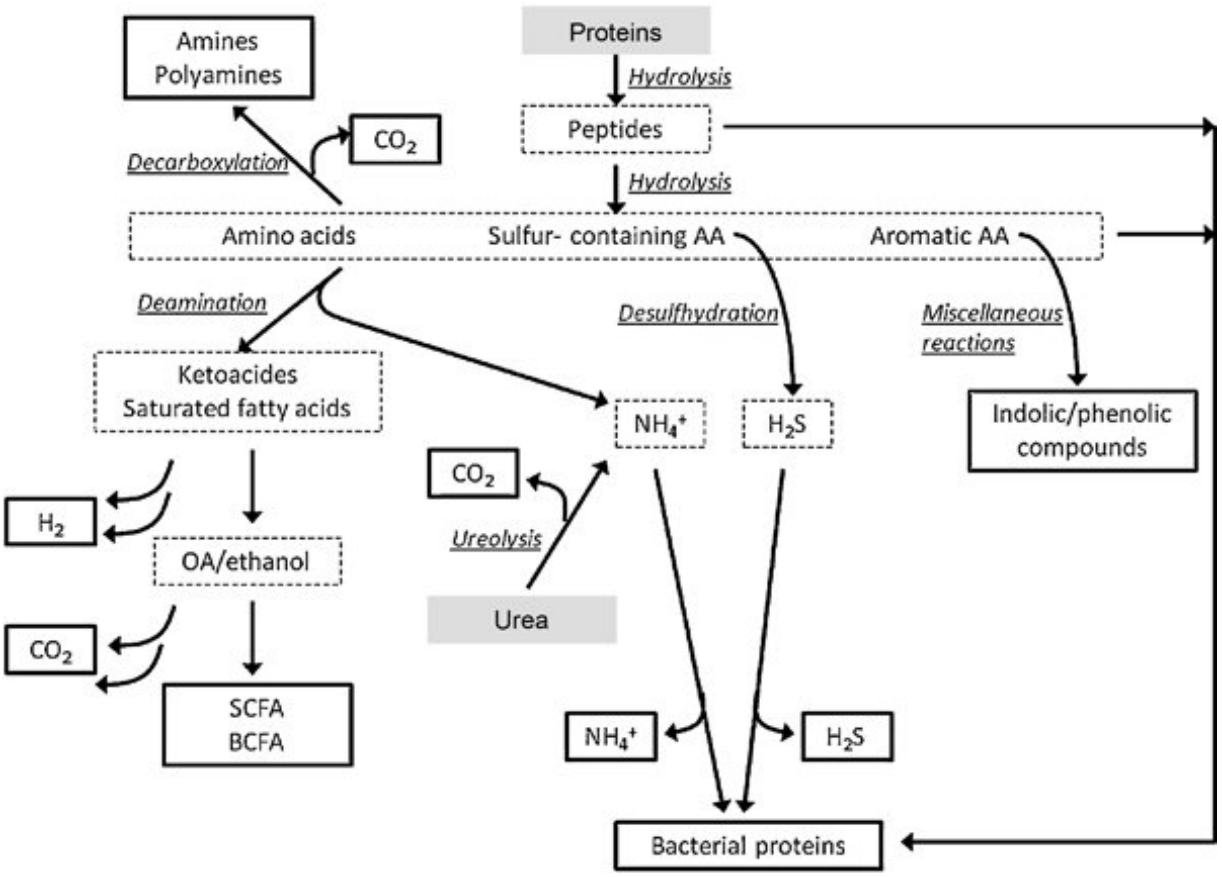

Figure 2.5: Pathways of gut microbial protein metabolism. Extracted from Davila *et al.*, (2013).

: substrate; : intermediary metabolite; : end product.

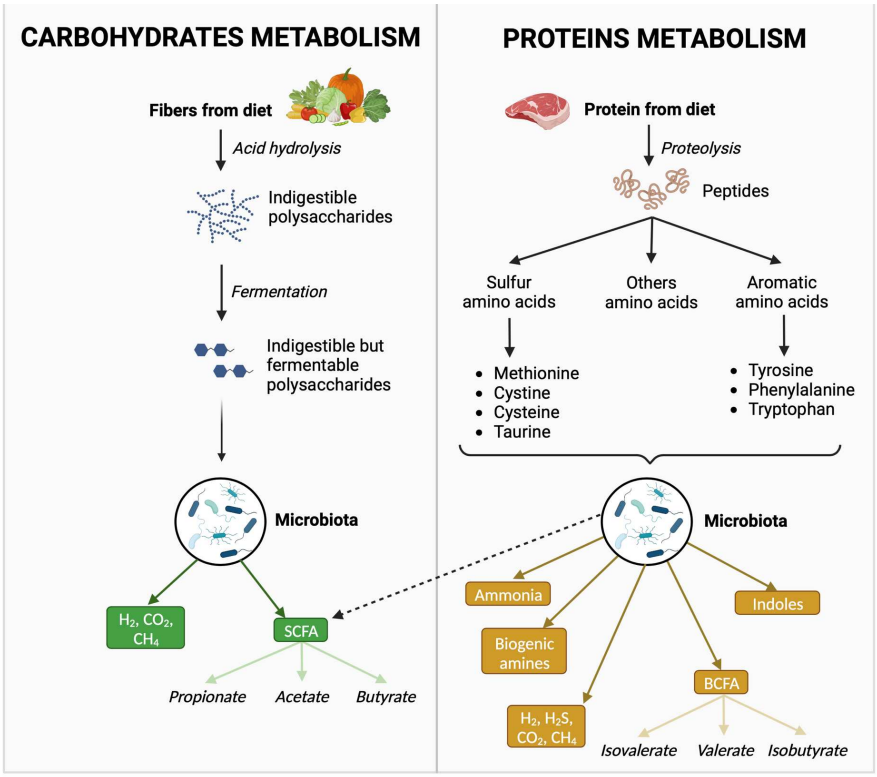

Figure 2.6: Pathways responsible for the biosynthesis of the major microbial metabolites from carbohydrates and proteins metabolisms and impact on gut mucosa. Built with Biorender from personal source, based on Blachier *et al.*, (2007) for human data and Blake & Suchodolski, (2016) for canine data (highlighted in green associated to a dog symbol). *AMP: antimicrobial peptides; BCFA: branched-chain fatty acids; CH_4: methane; CO_2: carbon dioxide; H_2: dihydrogen; H_2S: hydrogen sulfur; IL-22: interleukin-22; SCFA: short-chain fatty acid.*

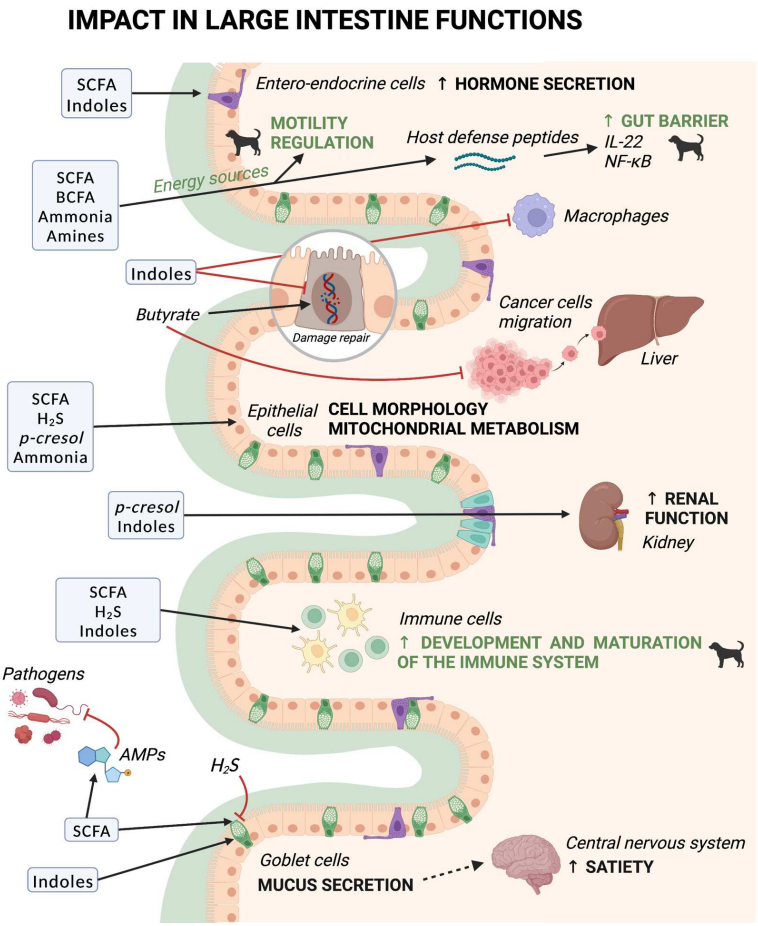

Phenols and **indoles** are produced from the degradation of aromatic amino acids in the large intestine lumen by microbiota (Blachier *et al.*, 2007). In dogs, indoles and phenols levels were increased by consumption of high protein or meat diets (Xu *et al.*, 2017), whereas phenol and 4-ethylphenol faecal concentrations significantly decreased with cellobiose supplementation of 1 g/kg bodyweight/day (Paßlack *et al.*, 2021). **Phenols** (p-cresol and phenol) are the major products from tyrosine degradation, most probably performed by *Clostridia*, as suggested based on human data (Daisley *et al.*, 2021). Contrarily to the human situation (Macfarlane & Macfarlane, 2012), in dogs, no study has correlated colonic phenol concentrations with digestive or extra-digestive diseases. Phenols median concentrations of 0 and 1.1 µmol/g of lyophilized feces were quantified for small and medium dogs respectively (**Figure 2.8C**).

Indoles are derived from tryptophan bacterial metabolism, generating indole, tryptamine, indole-ethanol, indole-propionic acid, indole-lactic acid, indole-acetic acid, skatole, indole-aldehyde and indole-acrylic acid, as shown in human (Daisley *et al.*, 2021) (**Figure 2.6 and 2.7**). These compounds are absorbed through the epithelium and are involved in several pathways in the large intestine. Some catabolites like indole-lactate, indole-acetate, indole-propionate and 2-oxindole-3-acetate are considered as **beneficial** in dogs, as they can modulate innate and adaptive immune system through aryl hydrocarbon receptor (AHR) activation or because of their anti-oxidative and anti-inflammatory effects. Median indoles concentrations of 1.6 and 2.2 µmol/g of lyophilized feces for small and medium dogs respectively were quantified (**Figure 2.8C**). An increase in indole sulfate was associated to kidney diseases and inflammation in dogs (Cheng *et al.*, 2015).

Ammonia levels were always quantified in canine feces and studies showed a median concentration of 39.1 and 54.1 µmol/g of lyophilized feces for small (a single study) and medium dogs, respectively (**Figure 2.8D**). Ammonia can be produced in the human and canine gut from *Bacteroides fragilis*, *B. ovatus* and *B. vulgatus* but also from *E. coli* or *Streptococcus faecalis* (Vince & Burridge, 1980). Impact of high levels of ammonia were tested in human adenocarcinoma HT-29 colonocytes cells and showed an important repression of cell proliferation without affecting cell viability (Mouillé *et al.*, 2003). In addition, ammonia is also able to interfere with the oxidative metabolism of colonocytes by inhibiting butyrate activation or butyrate ß-oxidation in mitochondria (Darcy-Vrillon *et al.*, 1996). Ammonia represents a toxic and potentially carcinogenic compound and high ammonia concentrations in the gut lumen have the ability to damage human mucosa (Blachier *et al.*, 2007) (**Figure 2.6**).

Biogenic amines have been detected in the colonic luminal content of both human and animals. Amines have been identified as key factors for cell growth and can interfere with many cellular processes including stimulation of DNA, RNA and protein synthesis (Blachier *et al.*, 2007). Commensal bacteria of the colon (mainly *Lactobacillus*) are thus able to produce putrescine, agmatine, cadaverine, tyramine and histamine that are known to be involved in large intestine physiology and postprandial colonic motility in human. In dogs, biogenic amines were exclusively quantified in faecal samples of medium dogs (Flickinger *et al.*, 2003; Propst *et al.*, 2003; Faber *et al.*, 2011). Faber' study reported that polyamines (i.e. putrescine, spermine and spermidine) are considered as beneficial metabolites for colonic health thanks to their requirement for cellular metabolic activity (**Figure 2.6**). However, another study reported a deleterious effects of biogenic amines associated to

protein putrefaction, correlated to odor production and an increased incidence of colon cancer in dogs (Propst *et al.*, 2003).

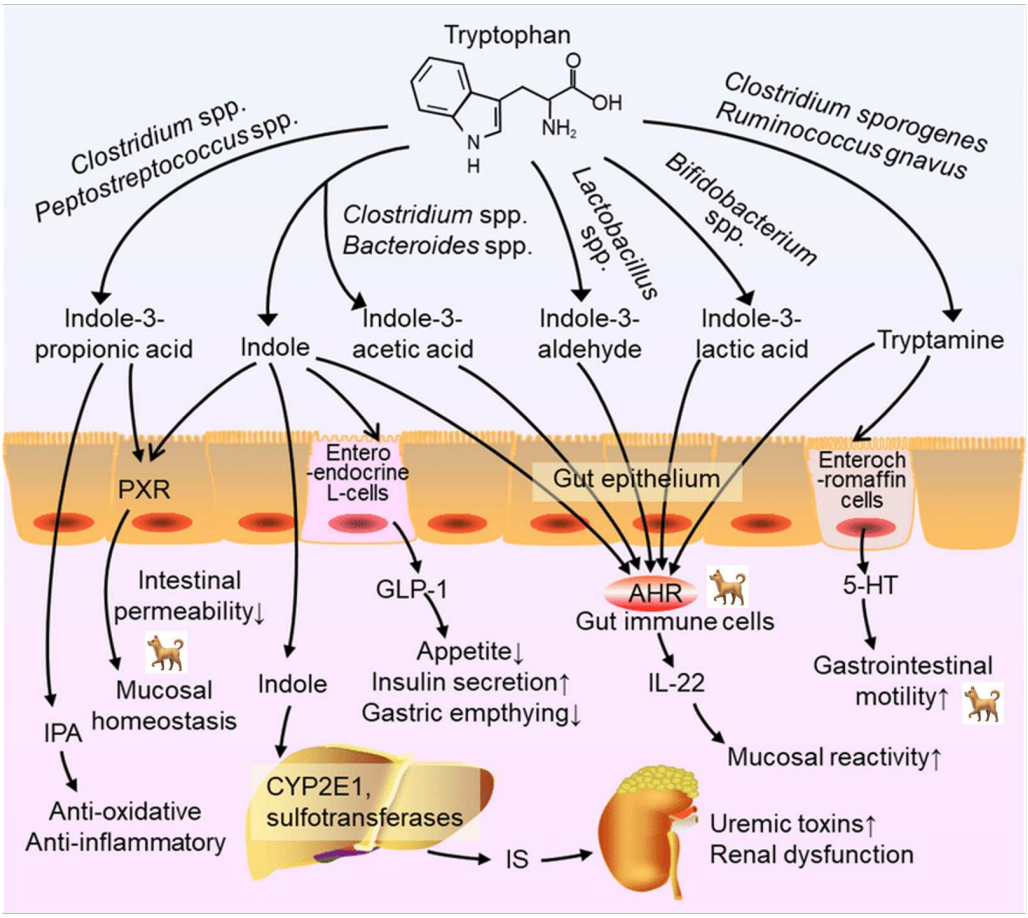

Figure 2.7: Effects of microbial tryptophan catabolites on host physiology. Degradation of dietary proteins leads to the release of tryptophan, which is converted into various catabolites by the gut microbiota. Tryptophan catabolites include indole, tryptamine, indoleethanol, indolepropionic acid, indolelactic acid, indoleacetic acid, skatole, indolealdehyde and indoleacrylic acid. Those compounds can affect host physiology through numerous ways. The effects demonstrated not only in human but also in dogs are symbolized by an icon (🐕). Extracted and modified from Liu *et al.*, (2021). *AHR: aryl hydrocarbon receptor; GLP-1: glucagon-like peptide 1; IL-22: interleukin 22; IS: indoxyl sulfate; PXR: pregnane X receptor; 5-HT: 5-hydroxytryptamine (serotonin).*

Hydrogen sulfide -H_2S- is produced through fermentation of sulfur-containing amino acids. Faecal sulfide excretion was roughly proportional to dietary protein intake in human and especially increased with high meat diet consumption (Magee 2000). Hydrogen sulfide can be produced through different bacterial metabolic pathway such as acetogenesis involving sulfate-reducing bacteria such as *Desulfovibrio*, *Desulfomonas* or *Bilophila wadsworthia* in human (Nava *et al.*, 2012). H_2S is a toxic compound known to disturb lung and brain functions and implicated in the etiology of ulcerative colitis in dogs, maybe because of its capacity to modulate immune response (Honneffer *et al.*, 2014) (**Figure 2.6**). In dogs, H_2S is responsible of malodorous flatus, a canine common problem (Giffard *et al.*, 2001; Collins *et al.*, 2001). Nevertheless, H_2S metabolic pathway remains undescribed in dog's gut.

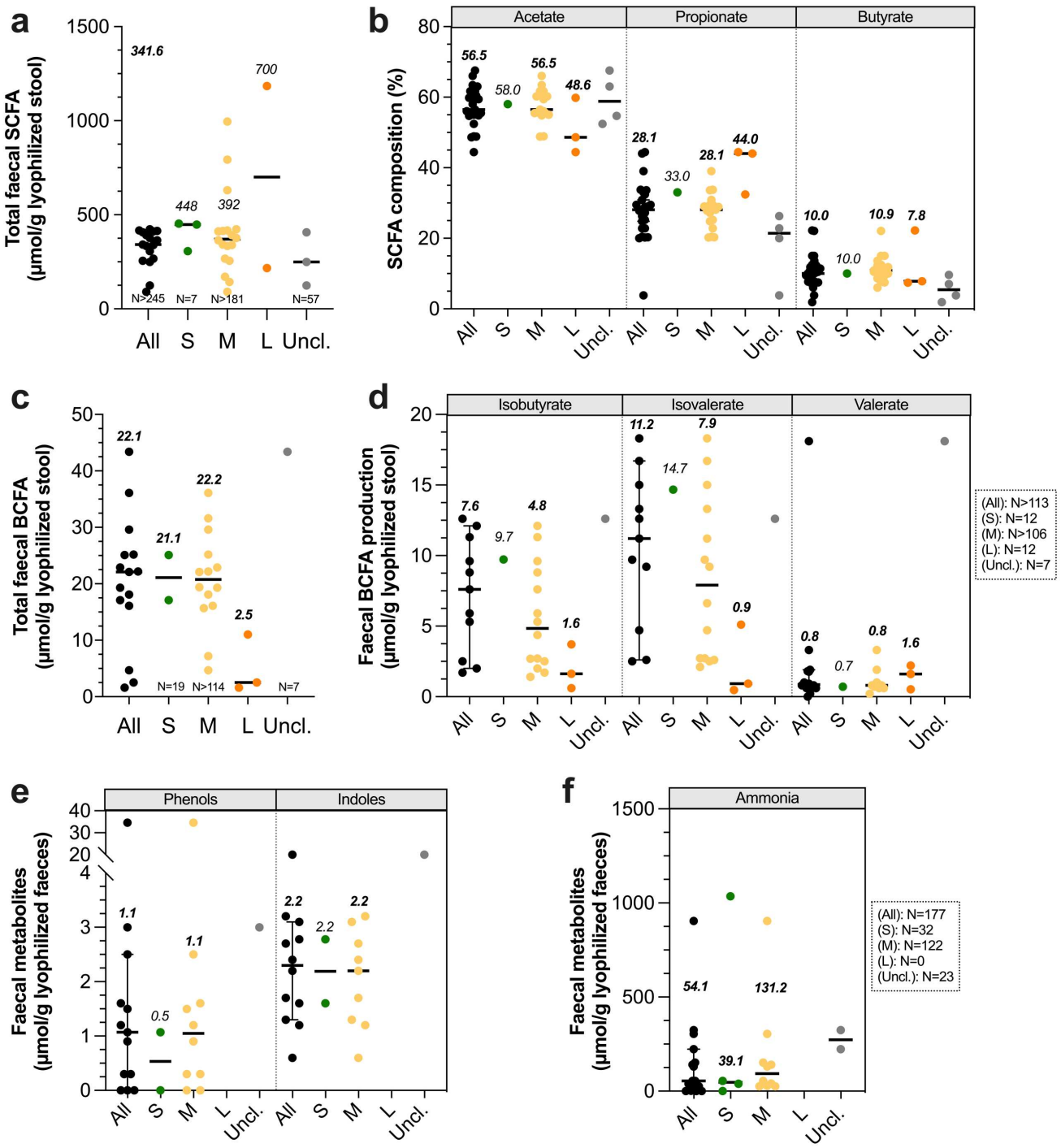

Figure 2.8: Impact of dog sizes on faecal microbial products production. Results from studies in dogs measuring total faecal major short-chain fatty acids (SCFA, i.e. acetate, propionate and butyrate) are presented in (**A**) and detailed in (**B**). Similarly, influence of dog size on major branched-chain fatty acids production (BCFA, i.e. isobutyrate, isovalerate and valerate) is shown in (**C**) and detailed in (**D**). Effect of dog size on other microbial metabolites are presented in (**E**) for phenols and indoles and (**F**) for ammonia. The same caption as used in Figure 1.2 was applied.

Finally, **branched-chain fatty acids** (BCFA) (mainly isovaleric, isobutyric and valeric acids) are produced during fermentation of branched-chain amino acids (valine, leucine, and isoleucine) by *Bacteroides* and *Clostridium* in the human intestinal microbiota (Smith and Macfarlane, 1998; Aguirre *et al.*, 2016). Total

BCFAs were only measured in faecal samples, and mainly in medium dogs (**Figure 2.8C)**. BCFA concentrations seem to be lower in small dogs (a unique value of 17.1 µmol/g) compared to medium ones (calculated median of 22.2 µmol/g). Moreover, BCFA composition was only studied in medium dogs, with a calculated median concentration of 4.8 µmol/g isobutyrate, 7.9 µmol/g isovalerate and 0.8 µmol/g valerate (**Figure 2.8D**). Whether it be in dog or in human, BCFA have attracted considerably less attention than major SCFA, despite they might play important roles in the gut environment and may constitute potential markers of the microbial metabolism taking place in the gut. BCFA are indicators of colonic protein fermentation (Macfarlane *et al.*, 1992), as the process is associated to the production of ammonia, phenol, p-cresol or biogenic amines (**Figure 2.5**). In dogs, increased levels of all these faecal protein degradation products were associated with deleterious effects, like poor faecal quality, inflammation and kidney diseases (Hughes, Magee & Bingham, 2000; Ephraim, Cochrane & Jewell, 2020). Recently, the role of BCFA on the regulation of glucose and lipid metabolism has been also suggested (Heimann *et al.*, 2016).

To conclude, protein degradation metabolites seem to be positively correlated to protein content in the diet and canine body weight, even if those observations should be considered with caution as very few data are available from small and large dogs. Abundance of *Fusobacteria* in dog feces was positively correlated with body weight gain (Chun *et al.*, 2020), strengthening their possible involvement in protein degradation. It is also important to underline that most of data related to protein metabolism are based on human and not canine studies, even if it would be certainly of high interest to have an in-depth understanding on such metabolism in dogs due to their carnivorous status.

2.2.4. Vitamin synthesis

Vitamins are essential components for host health, involving coenzymes or antioxidants. Canine gut microbiota also participate in vitamin synthesis in the large intestine such as vitamin K, vitamin from the B group (e.g. folic acid, niacin, biotin, pantothenic acid, cobalamin or thiamine) (Belzer *et al.*, 2017; Kim *et al.*, 2022). Bacteria from the *Lachnospiraceae* family were identified as vitamin producer in human (Soto-Martin *et al.*, 2020).

2.2.5. Bile acid metabolism

Gut microbiota is also involved in bile acids metabolism (**Figure 2.9**). In the canine liver (as for other mammals), primary bile acids (CA and CDCA mainly) are synthetized from cholesterol and conjugated to taurine or glycine, then stored in gall bladder (Kakimoto *et al.*, 2017). After a meal, bile is excreted in the small intestine where bile acids are involved in lipid digestion by helping to form micelles. About 95 to 97 % of total bile acids produced are reabsorbed in the terminal ileum then recycled in the liver . The remaining 5 % cross the large intestine where canine commensal bacteria like *Peptacetobacter hiranonis* (ex-*Clostridium hiranonis*) and *Lactobacillus spp.* (Suchodolski, 2011b) can deconjugate bile acids (using bile salt hydrolase -BSH) or dehydroxylate (using different bile acid inducible -*bai*- proteins) primary into secondary bile acids, resulting in deoxycholic acid (DCA), lithocholic acid (LCA) and ursodeoxycholic acid (UDCA) (Ridlon *et al.*, 2016). Bile acids play a role in mucosal defense thanks to their antimicrobial properties and have well-known anti-

inflammatory properties through inhibition of NF-κB pathway (demonstrated in human and dogs) (Duboc *et al.*, 2013; Blake & Suchodolski, 2016). Bile acid dysmetabolism was evidenced in human obese patients (Jones *et al.*, 2014), but also in dogs in intestinal inflammation, as well as in antibiotic-induced dysbiosis (Whittemore *et al.*, 2021), diabetes mellitus (Jergens *et al.*, 2019) or chronic inflammatory enteropathies (Guard *et al.*, 2019). Interestingly, relative percentages of primary bile acids such as CA and CDCA seem to be inversely correlated to canine body weight, while the opposite is observed for secondary bile acids (only one study) (**Figure 2.10**). This can be correlated to the longer colonic transit time observed in large dogs, increasing contact time between microbiota and bile acids and therefore favoring bacterial dihydroxylation.

Figure 2.9: Overview of canine bile acid metabolism and enterohepatic recirculation. Primary bile acids (CA and CDCA) are synthesized from cholesterol conjugated to glycine and taurine in the liver. Then, primary bile acids are secreted into the bile and stored in the gallbladder until their secretion into the duodenum. Whereas some passive absorption (dashed arrows) of bile acids can occur in the duodenum and jejunum, about 95 % of the total pool of bile acids (including conjugated and free primary and secondary bile acids) are actively

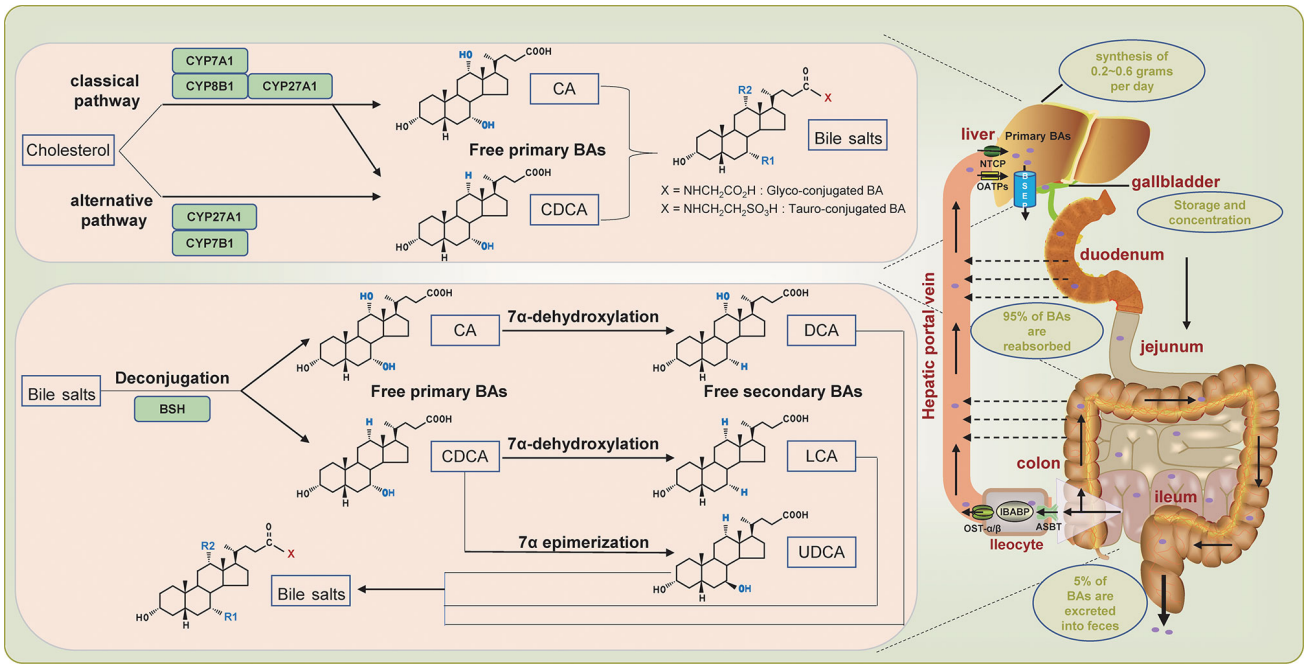

reabsorbed in the ileum and return to the liver where they will be newly conjugated. The remaining 5 % cross the large intestine where resident microbiota can deconjugate conjugated primary bile acids into free primary bile acids. Then, free primary bile acids can be dehydroxylated by bacteria into DCA and LCA. UDCA is also produced by epimerization of CDCA. Extracted and modified from Fu *et al.*, (2021). *CA: cholic acid; CDCA: chenodeoxycholic acid; DCA: deoxycholic acid; LCA: lithocholic acid; UDCA: ursodeoxycholic acid.*

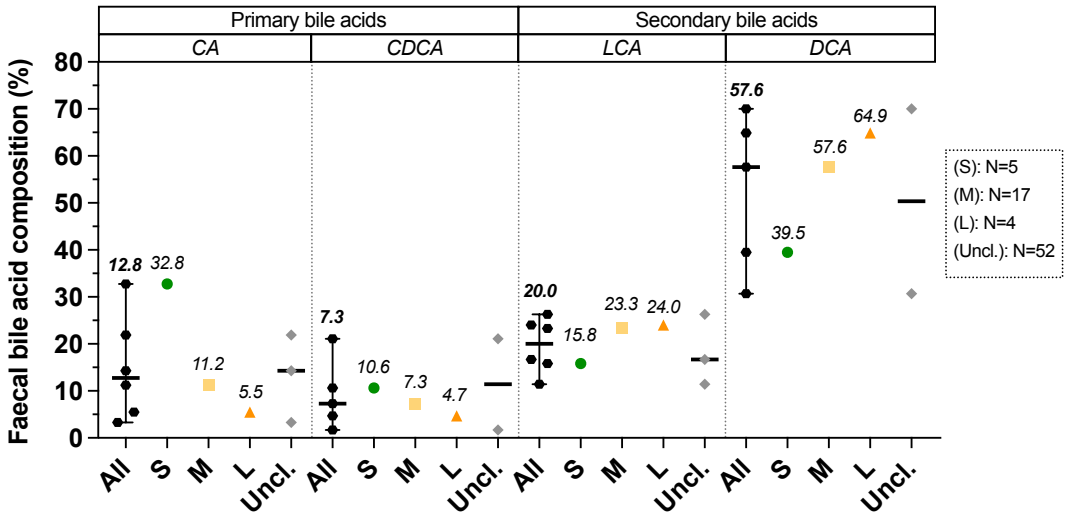

Figure 2.10: Impact of dog sizes on faecal bile acids composition. Results from studies in dog faeces describing bile acid composition in cholic acid (CA), chenodeoxycholic acid (CDCA), lithocholic acid (LCA) and deoxycholic acid (DCA) is shown. The same caption as used in Figure 1.2 was applied.

Bullet points - ***Impact of canine body size on microbial parameters***

- Longer colonic transit time observed in large dogs may promote microbial fermentations, especially carbohydrates degradation by resident bacteria resulting in an increased production of SCFA and bile acid dehydroxylation
- Differences in bile acids concentrations and profiles are observed for each dog size, in accordance with different microbiota profiles between small, medium and large dogs
- Faecal concentrations of microbial degradation products from proteins seem to be positively correlated with dog body weight
- *Fusobacteria* relative abundance seems to increase with body weight in association with an increase in protein-degradation metabolites

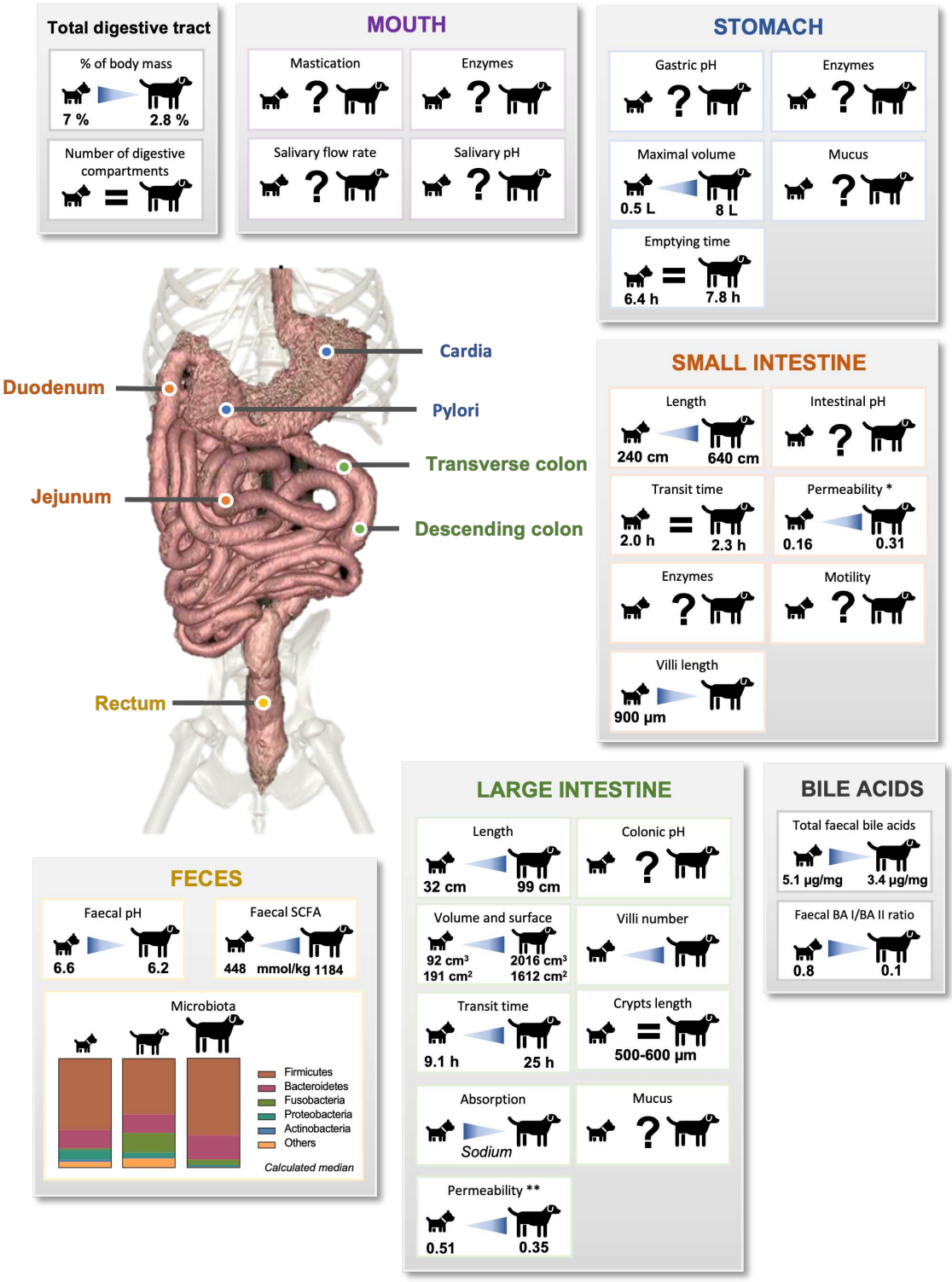

Figure 2.11: Overview of the impact of dog sizes on digestive physiology and faecal microbiota composition and activity. Key parameters of the oral, gastric, intestinal and colonic compartments from the canine digestive tract are summarized. Specified values were obtained from reports comparing within a same study the results obtained for small and large dogs. Lack of data are represented by "?", *BA: bile acid, SCFA: short chain fatty acids. *: Lactulose/L-rhamnose ratio, **: Lactulose/sucralose ratio*

Part 3 - Factors shaping canine gut microbiota

In the previous parts of the literature review, we detailed how dog size can impact physicochemical and microbial parameters of digestion. Beyond weight, several other factors discussed in this part are also able to shape canine gut microbiota under healthy or diseased situations, including morphological and environmental factors, antibiotherapy, digestive or extra-intestinal pathologies such as IBD and obesity. Restoration strategies of the gut microbiota such as prebiotics, probiotics, postbiotics (including paraprobiotics), and faecal microbiota transplantation are then introduced in the next sections, with more emphasis on the factors directly related to this PhD work. Main factors driving gut microbiota composition and/or diversity as well as restauration strategies are summarized in **Figure 3.1**.

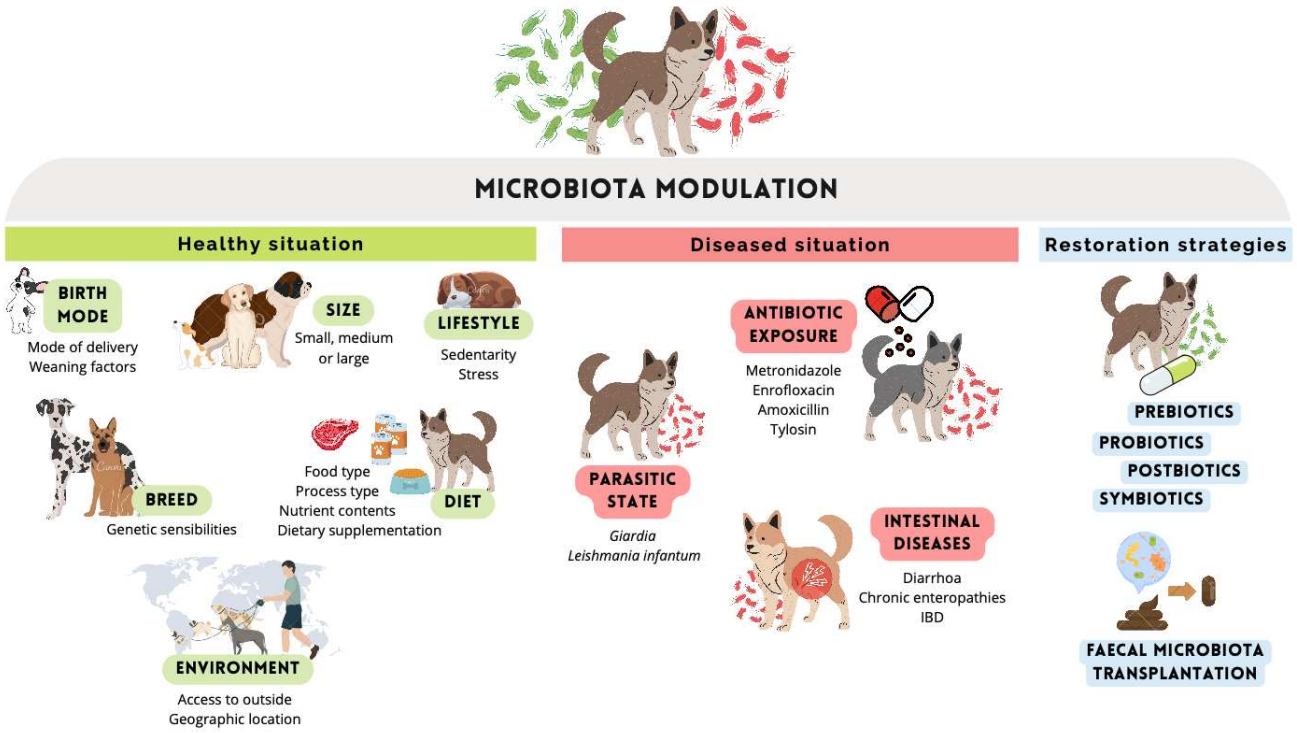

Figure 3.1. Overview of the main factors influencing canine gut microbiota. Influencing factors can be stratified into "normal" factors (in green), occurring under healthy state of dogs and "pathological"-associated factors (in red). Restauration strategies of gut microbiota are indicated in blue. *Build from personal source.*

3.1. Factors driving microbiota in healthy dogs

Birth mode. Depending on birth mode, different microbiota colonization and diversity were observed in puppies. Especially, puppies from different sizes (2.4 to 65 kg) born by vaginal delivery have a faecal microbiota similar to their mother's vagina microbiota (e.g. *Staphylococcus*), whereas puppies born by cesarean section present more *Acinetobacter spp.*, *Staphylococcus* and *Bacillus spp.* (Rota *et al.*, 2021). The meconium microbiota composition of the puppies is similar to the colostrum microbiota of their mothers (Kajdič *et al.*, 2021), suggesting an important vertical transmission between mother and puppy. Of interest, this seems to give

an advantage to puppies born by vaginal birth who gain weight significantly faster than the ones born by cesarean section (Kajdič *et al.*, 2021).

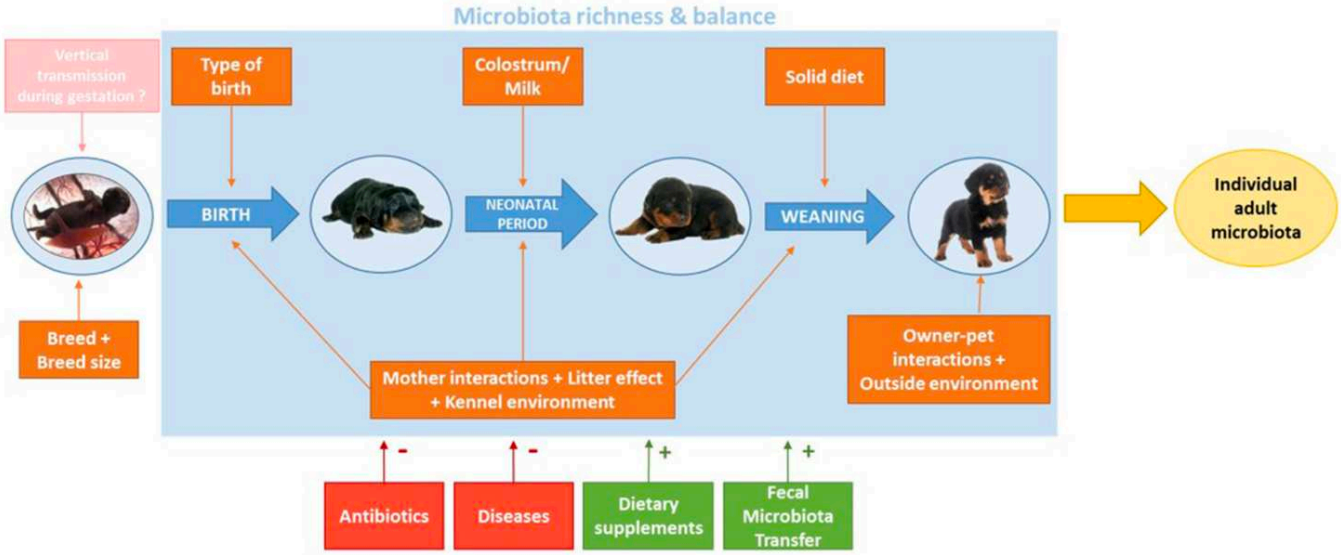

Figure 3.2: Major factors shaping the development of growing puppies' gut microbiota from birth to adulthood. Orange boxes show obligate factors, while the pink box illustrate a hypothetical impact. Factors in red boxes are facultative factors that can be associated with dysbiosis, while green boxes are facultative factors with beneficial effects on microbiota balance. *Extracted from Garrigues et al. 2022.*

Individual characteristics. Some factors shaping the gut microbiota are inherent to dogs such as morphological and genetic traits linked to breed and size (as described in the previous section). Significant differences in *Fusobacteriota* abundance between breeds were also described, as well as variations in *F. perfoetens*, *Romboutsia timonensis* and *Sutterella stercoricanis* abundances at a lower taxonomic level (You & Kim, 2021). In the same study, Bulldog presented a significantly higher microbial richness compared to 8 other breeds. Some metabolic differences were also highlighted between dogs of different breeds. For example, Great Danes have energetical needs above average (AAFCO, 2019). Of note, canine gut microbiota presents an important interindividual variability. In addition, important changes are observed with extreme body condition score (BCS) (i.e. extremely lean and severe obesity, as described in section 3.2.2.). However, some variations can be even observed in overweighed dogs compared to normal ones with an increase of *Actinobacteriota* and *Deferribacteres*, relative abundance associated to increases of the relative abundance of species like *Enterococcus cecorum*, *Peptostreptococcus russellii* or *Bacteroidetes thetaiotaomicron* (You & Kim, 2021).

Age. As in humans (Kim & Jazwinski, 2018), age is also an important factor shaping microbiota in dogs (Guard *et al.*, 2017; Pereira *et al.*, 2020) with important variations occurring during the earlier stage of puppies, as recently reviewed by (Garrigues *et al.*, 2022a) and summarized in **Figure 3.2**.

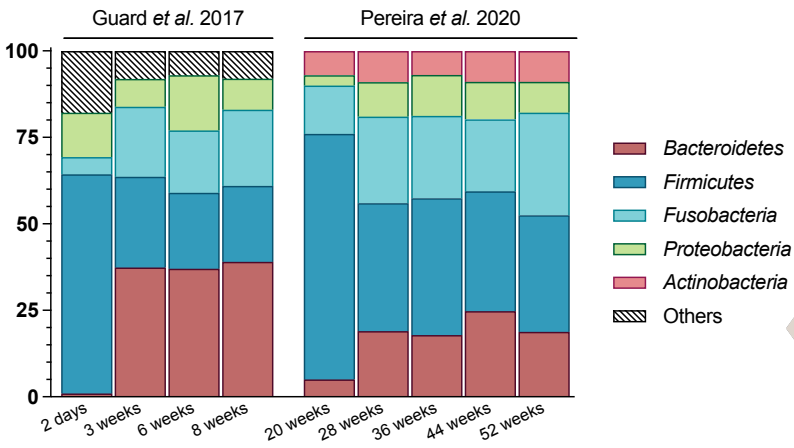

Figure 3.3: Evolution of the relative abundance of main bacterial phyla in puppies' faecal microbiota with age. *Made from data extracted in Guard et al. 2017 and Pereira et al. 2020.*

Following **birth**, the canine GIT is quickly colonized by microorganisms from the environment. After **two days**, faecal microbiota of puppies is mainly represented by *Firmicutes* (around 60 %) (**Figure 3.3**) (Guard *et al.*, 2017). As observed in other mammal species and in human, the important levels of oxygen present in the GIT of newborns promote the colonization of obligate and facultative anaerobes such as *Proteobacteria* and *Bacteroides*. Then, between day 2 and day 21, the part of aerotolerant bacteria decreases, replaced by strict anaerobes such as *Firmicutes* (**Figure 3.3**), coupled with an increase in bacterial richness. During the **neonatal period**, an impressive increase of relative abundance of *Lactobacillaceae* about 100-fold was observed (Buddington, 2003), associated to the ingestion of milk by puppies. From **3 weeks to around 8 weeks-old dogs,** weaning occurs progressively by the introduction of solid diet instead of milk. Abundance and activities of certain bacterial groups are promoting after weaning such as degradation of complex polysaccharides by *Bacteroides* or protein fermentation by *Fusobacteriota* (Pilla & Suchodolski, 2020). At **9 weeks**, the relative abundance of *Proteobacteria* significantly decreased whereas the one of *Faecalibacterium spp. and Peptacetobacter hiranonis* (ex-*Clostridium hiranonis*), two bacteria highly oxygen-sensitive, significantly increased (Pilla & Suchodolski, 2020). While microbial species richness of puppies' feces increases significantly from **2 days up to 52 weeks** (Guard *et al.*, 2017; Pereira *et al.*, 2020; Boucard *et al.*, 2021), few changes of microbial diversity have been observed in dogs between **3 months to 12 years old** (Omatsu *et al.*, 2018; Mizukami *et al.*, 2019; You & Kim, 2021), suggesting a stabilization of the gut microbiota until adulthood. Especially, the abundance of *Fusobacterium perfoetens* is positively correlated with dog age and *Lactobacillus acidophilus* and *L. johnsonii* decrease from **0.5-1 years to 6-10 year groups** (You & Kim, 2021). However, to the best of our knowledge, the impact of age on Archaea or fungi populations has been never investigated, as well as the impact of age on microbiota functions (SCFA production for example).

Diet. In human and animals, diet has been identified as one of the main factors driving microbiota composition, with different modifications depending on the tested diets (**Figure 3.4**). Many studies have investigated the impact of commercial extruded dried food (Weber *et al.*, 2003; Hervera *et al.*, 2007; Hendriks *et al.*, 2013; Bresciani *et al.*, 2018; Detweiler *et al.*, 2019; Nogueira *et al.*, 2019; Penazzi *et al.*, 2021) or raw meat-based diet (Sandri *et al.*, 2016; Herstad *et al.*, 2017, 2018; Schmidt *et al.*, 2018; Algya *et al.*, 2018; Kim *et al.*, 2021) on canine gut microbiota. In a recent study, changing canine diet from dry food to beef induced

variations in microbiota composition within less than one week, which confirms that canine microbiota is very sensitive to diet changes (Herstad *et al.*, 2017). A recent study has compared the effect of different processing methods such as raw, pasteurized and high temperature sterilization made with the same ingredients and nutrients on faecal microbiota from 18 Beagles (Cai *et al.*, 2022). In fact, dogs fed with raw-meet food showed a significantly decreased production of BCFA and SCFA, associated to a variation in the relative abundance of 14 genera in comparison to the two other diets. In addition, protein levels can also impact both faecal metabolome and microbiome (Ephraim *et al.*, 2020). Regarding the impact of three canine diets with various protein percentages from 19 to 46 % on medium dogs, indole and indoli-2-one significantly increased with protein consumption while levels of **beneficial indoles** (i.e. indolelactate, indoleacetate, indolepropionate and 2-oxindole-3-acetate) decreased (Ephraim *et al.*, 2020). The higher level of around 46 % protein (compared to a FEDIAF recommendation of 18 % protein in diet) increased significantly urinary metabolites associated to inflammation and chronic kidney disease. In addition, *Faecalibacterium prausnitzii*, a beneficial butyrate-producer bacteria increased with the low-protein diet (19 % in this study). High-fiber diet (supplemented with 7.5 % beet-pulp) also reshapes gut microbiota by increasing faecal relative abundance of *Lactobacillus spp.*, *Faecalibacterium* and *Clostridium* in adult dogs (Middelbos *et al.*, 2010; Swanson *et al.*, 2011; Maria *et al.*, 2017).

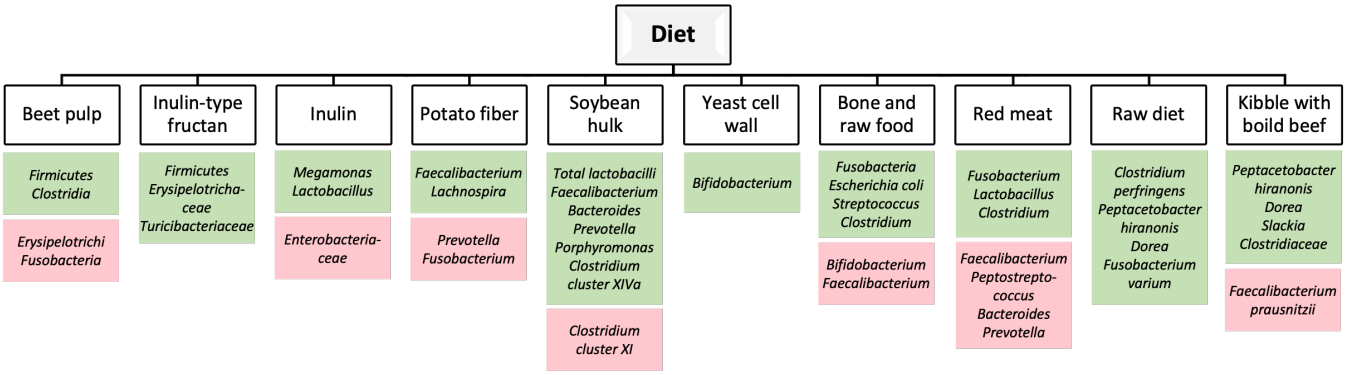

Figure 3.4: Impact of different types of diet on canine faecal gut microbiota. Green boxes: upward, increased relative abundance or red boxes, decreased relative abundance of faecal bacterial populations. Extracted and modified from Tuniyazi *et al.*, (2022).

Human-pet interplay. Human-pet pairs with a close relationship are more likely to share bacteria in their faecal profiles, especially *Streptococcus intermedius*, *E. coli*, *E. faecalis*, and *Acinetobacter lwoffii*, than pairs with a more distant relationship (Wipler *et al.*, 2017). In addition, a recent study revealed that human and dogs have coevolved in the same environment which may lead to the modulation of similar set of genes between the two groups (Huang *et al.*, 2020). Of high interest, the canine gene catalog (extracted from faecal microbiota) mapped at 63 % (versus 33 % for pigs and 22 % for mice) with the human faecal gene catalog (Coelho *et al.*, 2018). Inversely, only 28 % of the human reads mapped on the canine catalog, suggesting that canine genes may have been transmitted by human, or acquired by the same environmental conditions. To go further, this could indicate that some horizontal transmission events may have occurred between human and dogs during domestication and after, forever modifying dog's microbiota (**Figure 3.5**).

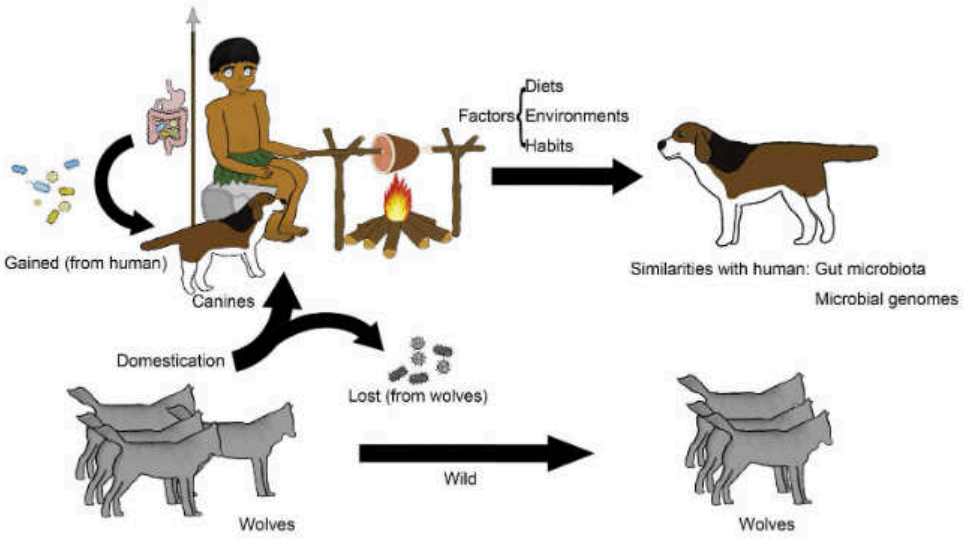

Figure 3.5: Role of domestication in evolution of the canine gut microbiota. Canine domestication led to the loss of some gut bacteria compared with those of non-domesticated wolves, while interaction with humans resulted in new gastrointestinal bacteria in dogs. *Extracted and modified from Huang et al., (2020).*

Lifestyle. Geographic localization matters on the intestinal microbial development of the dog, by mainly affecting the diversity of bacterial populations (Vilson *et al.*, 2018). In particular, the living environment of dogs impact bacterial diversity and higher diversity was observed in puppies living in big cities during their first 1.5 year of life compared to dogs living in smaller cities or in the countryside (Vilson *et al.*, 2018).

3.2. Factors driving microbiota under diseased situations

As for humans, the gut microbiota can shift from an equilibrated state called eubiosis to a perturbated one named dysbiosis. Gut dysbiosis is associated with alterations in gut microbiota composition that result in functional changes in the microbial transcriptome, proteome, or metabolome (Pilla & Suchodolski, 2020). An increase in the relative abundance of *Enterobacteriaceae* family is a common marker of human gut dysbiosis (Rivera-Chávez, Lopez & Bäumler, 2017), also observed in dogs (Vázquez-Baeza *et al.*, 2016). A canine dysbiosis index was recently developed to quantify and monitor gut dysbiosis (AlShawaqfeh *et al.*, 2017). This mathematical model was based on qPCR quantification of total bacteria and seven bacterial groups (i.e. *Faecalibacterium spp*., *Turicibacter spp*., *Escherichia coli*, *Streptococcus spp*., *Blautia spp*., *Fusobacterium spp*. and *Peptacetobacter* (ex-*Clostridium) hiranonis*) that are known to be modified in dysbiotic conditions (especially associated to chronic enteropathies). In dogs, gut microbial dysbiosis has been associated to digestive pathologies like antibiotic-induced dysbiosis, chronic enteropathies (Cassmann *et al.*, 2016; Minamoto *et al.*, 2019) including IBD (Minamoto *et al.*, 2014; AlShawaqfeh *et al.*, 2017), chronic diarrhea (Jia *et al.*, 2010), chronic inflammation (Honneffer *et al.*, 2014), but also extra-digestive pathologies such as obesity (Kieler *et al.*, 2017), cancer (Zitvogel *et al.*, 2017), neurological disfunctions (Wu *et al.*, 2016), chronic stress, arthritis (Cintio *et al.*, 2020) or metabolic disorders (Montoya-Alonso *et al.*, 2017). In addition, significant alterations of the gut microbiota by enteric parasites were evidenced, especially with *Giardia intestinalis* infection which was associated to diarrhea and a decrease of faecal bacterial richness (Šlapeta *et al.*, 2015). Similar observations

were also revealed with parvovirus infection, responsible for weaning diarrhea associated to severe gut microbiota perturbations and characterized by an increase in *Enterobacteriaceae* and a decrease in *Bacteroidetes* and *Fusobacteria* abundance (Park *et al.*, 2019). Here, a special emphasis was made on dysbiosis associated to antibiotherapy in accordance with the main aims of this PhD, but also linked to obesity and IBD in relation to future development of the *in vitro* CANIM-ARCOL model (see part 4 discussion).

3.2.1. Antibiotic treatment

Antibiotics are commonly used in veterinary medicine to treat infectious diseases caused by bacteria and other microorganisms (such as parasites like *Giardia intestinalis* or *Leishmania infantis*). As for human, inappropriate use of antibiotics is recognized as a key driver of antimicrobial resistance, this is why their mode of action and impact on gut microbiota are e increasingly studied in dogs. In particular, antibiotics are used for the treatment of acute and chronic gastrointestinal diseases, which can lead to intestinal microbiota disturbance. Studies evaluating the impact of those orally administered antibiotics on canine gut microbiota are presented in **Table 3.1**. Most of the studies that have evaluated the impact of antibiotic treatments on canine gut microbiota were performed *in vivo* using stools, involving a total amount of 134 dogs in only 10 studies. For each study, a **resilience** of the microbiota (defined by Dogra, Doré & Damak, (2020) as the property of an ecosystem to maintain its state and recover from perturbations) can be observed after the treatment, but restoration time varied depending on taxa and studies. To the best of our knowledge, up to now, no study related to the impact of antibiotics on canine microbiota has been performed *in vitro*. Antibiotics commonly used by veterinarians or known to induce microbiota damages and diarrhea were further detailed below.

Metronidazole is an antibiotic and antiparasitic drug from the nitroimidazole family. This compound is commonly and widely prescribed for acute diarrhea in dogs associated to a suspicion of *Giardia* or *Clostridium perfringens* infection. This antibiotic is able to inhibit nucleic acid synthesis and target selectively anaerobic bacteria. A treatment of 15 mg/kg of body weight/12h during 14 days result in a global decrease of bacterial richness and evenness, and a decrease in the relative abundance of *Bacteroidetes* and *Fusobacteria* phyla in dogs (Pilla *et al.*, 2020). In addition, a significant increase in *Actinobacteria* and *Proteobacteria* (associated to dysbiosis) can be observed (Igarashi *et al.*, 2014). The relative abundance of *Firmicutes* was not impacted but the composition changed with a decrease of *Clostridiales* and an increase of *Lactobacillales*, previously associated to chronic enteropathies and pancreatic insufficiency in dogs (Blake *et al.*, 2019). These modifications are mainly (but not totally) recovered 14 days after the end of the treatment. Especially, the proportion of *Peptacetobacter hiranonis* (known to be protective against *Clostridium difficile* in dogs) decreased significantly and wasn't recovered after 4 weeks for 7 over 16 dogs of the study. This alteration is also associated to a reduction in faecal secondary bile acids concentration in these dogs, consistent with the capacity of *P. hiranonis* to dehydroxylate primary bile acids into secondary bile acids (Blake *et al.*, 2020). Similar observations were also made in another study with a smaller dose of 12.5 mg/kg of body weight/12h during 14 days (Igarashi *et al.*, 2014). Combining similar amounts of metronidazole with **enrofloxacin** (a fluoroquinolone antibiotic,

targeting gram-negative bacteria) for 21 days, bile acids metabolism was also altered, coupled with an increase in the faecal dysbiosis index associated to vomiting and diarrhea.

Enrofloxacin's impact on gut microbiota was more recently evaluated *in vivo* but only in combination with metronidazole (Whittemore, Moyers & Price, 2019; Whittemore *et al.*, 2021). Enrofloxacin is a fluoroquinolone with broad spectrum. According to ANSES, enrofloxacin is efficient on gram negative bacteria including *E. coli*, *Pasteurella spp*., and *Klebsiella spp* and also gram-positive *Staphylococcus spp*. In dogs, around 40 % of the oral dose of enrofloxacin is de-ethylated into ciprofloxacin which is the main active metabolite (Cester & Toutain, 1997). Enrofloxacin is covalently ligated to DNA replication and transcription enzymes, inhibiting their action.

Tylosin is a macrolide antibiotic commonly prescribed as symptomatic treatment for acute or chronic diarrhea in dogs (German, Halladay & Noble, 2010b; Volkmann *et al.*, 2017). Its mode of action remains poorly described but one hypothesis is the decrease in total bacterial load in the small intestine and suppression of anormal mucosal immune response since tylosin may exert anti-inflammatory effects (Manchester *et al.*, 2019). Four studies have evaluated tylosin effects and all evidenced microbiota disturbance (Suchodolski *et al.*, 2009; Kilpinen *et al.*, 2015; Manchester *et al.*, 2019; Bottero *et al.*, 2022). In particular, an increase in the relative abundance of *Enterococcaceae* family was observed whereas *Fusobacteriaceae* (associated to a good health status in dogs), *Veillonellaceae* and *Bacteroidaceae* decreased whatever the treatment duration. After tylosin withdrawal, microbiota composition returned to baseline through an individual-dependent manner (Manchester *et al.*, 2019). Suchodolski *et al.*, (2009a) also reported a long-lasting microbiota modification over several weeks after treatment.

Amoxicillin is a ß-lactam antibiotic derivate from penicillin, able to inhibit peptidoglycan synthesis in the cell wall of bacteria to achieve its bactericidal activity. Amoxicillin is active against most of gram-positive bacteria, many gram-negative and most of anaerobic bacteria (except *Staphylococcus* and *Bacteroides fragilis* which produced ß-lactamases). Amoxicillin is generally used to treat bacterial infections but also frequently prescribed in dogs with acute diarrhea, despite limited efficacy evidence (Werner *et al.*, 2020). In a first study, an increase in *Enterobacteriaceae*, generally acknowledged as a sign of dysbiosis establishment, was observed with amoxicillin treatment during 7 days (Grønvold *et al.*, 2010) whereas more recently, (Werner *et al.*, (2020) didn't observed any microbiota perturbation (amoxicillin and **clavulanic acid** combined; using culturation and qPCR only). However, amoxicillin treatment significantly increased the amount of *E. coli* together with resistant *E. coli* isolated in feces in both studies. Relative abundances of some gut bacteria were also reduced such as *Roseburia*, *Oscillospira*, *Dialister* and *Lachnospiraceae*.

Table 3.1: Effect of orally administered antibiotics commonly used in veterinary clinics to treat gastrointestinal diseases in canine gut microbiota. Only statistically different results are presented. *ARE: antibiotic responsible enteropathy; BA: bile acids; DGGE: denaturing gradient gel electrophoresis; NA: not applicable; qPCR: quantitative polymerase chain reaction; RNA: ribonucleic acid.*

Reference	Dogs	Antibiotic used	Dose	Treatment period	Method	Microbiota alteration	Decrease	Increase	Recovery period
Pilla *et al.*, (2020)	Healthy (n=24)	**Metronidazole**	15 mg/kg/12h	14 days	16S rRNA (V4 region) qPCR	Yes	Richness et evenness *Fusobacteria* *Bacteroidetes* *Clostridium hiranonis*	Dysbiosis index Faecal lactate Oxidative stress markers Cholesterol (plasma)	4 weeks
Igarashi *et al.*, (2014)	Healthy (n=10)	**Metronidazole**	12,5 mg/kg/12h	14 days	16S rRNA (V4 region)	Yes	*Bacteroides* *Turicibacter* *Clostridiales (*whose *Clostridium, Faecalibacterium, Ruminococcus, Lachnospiraceae)*	*Bifidobacterium* *Lactobacillales (including Enterococcus, Lactobacillus, Streptococcus)* *Enterobacteriales (Escherichia)*	4 weeks
		Prednisolone	1.0 mg/kg/24h	14 days	16S rRNA (V4 region)	**No**	NA	NA	4 weeks
Pignataro *et al.*, (2021)	Acute diarrhea (n=15)	**Metronidazole + Spiramycin**	12.5 mg/kg 7500 UI/kg	6 days	qPCR	**No**	NA	NA	NA
Whittemore *et al.*, (2021)	Healthy (n=11)	**Enrofloxacin + Metronidazole**	10 mg/kg/24h + 12.5 mg/kg/12h	21 days	qPCR 16S rRNA (V4 region)	Yes	Shannon index *Bacteroidetes* *Fusobacteria* *Proteobacteria Clostridium hiranonis* *Faecalibacterium* *Turicibacter* Faecal indoles	BA dysmetabolism Dysbiosis index *Firmicutes* *Actinobacteria*	12 weeks
Manchester *et al.*, (2019)	Healthy (n=16)	**Tylosin**	20 mg/kg/12h	14 days	16S rRNA (V4 region) qPCR	Yes	*Bacteroidaceae* *Veillonellaceae* *Fusobacteriaceae*	*Enterococcaceae*	8 weeks
Suchodolski *et al.*, (2009a)	Healthy (n=5)	**Tylosin**	20-22 mg/kg/24h	14 days	16S rRNA (V4-V5 regions)	Yes	*Diversity, richness* *Fusobacteria* *Bacteroidales* *Moraxella*	*Enterococci* *Pasteurella spp.* *Dietzia spp.*	NA
Kilpinen *et al.*, (2015)	ARE (n=14)	**Tylosin**	25 mg/kg/24h	7 days	Cultivation	Yes	NA	*Enterococcus spp.* Lactic acid bacteria Faecal consistency	8 weeks
Bottero *et al.*, (2022)	ARE (n=15)	**Tylosin**	10 mg/kg/12h	30 days	16S rRNA (V3-V4 regions)	Yes	Alpha-diversity	Faecal score	4 weeks
Grønvold *et al.*, (2010)	Healthy (n=8)	**Amoxicillin**	20 mg/kg/12h	7 days	DGGE-16S rRNA (V3 regions), qPCR	Yes	NA	*Enterobacteriales*	3 weeks
Werner *et al.*, (2020)	Acute diarrhea (n=16)	**Amoxicillin + clavulanic acid**	25 + 50 mg/kg/24h	7 days	Cultivation qPCR	**No**	NA	NA	3 weeks

3.2.2. Obesity

In Western countries, obesity is considered as the most common nutritional disorder in pets, due to imbalance between energy intake and expenditure (Osto & Lutz, 2015). Dogs are considered as clinically obese when their body weight is at least 20-30 % above ideal weight and a universal body condition score (ranging from 1 to 9) defines overweighed dogs at 7 and obese dogs at 8/9 (Apper *et al.*, 2020). Both sexes have a similar incidence and all dogs are concerned whatever their size, even if certain breeds seem to be more predisposed, such as Labrador Retriever, Bernese mountain dog, cavalier King Charles or Beagles (Osto & Lutz, 2015). Canine obesity is generally associated to insulin resistance, altered lipid profiles, hypertension, orthopedic and cardiorespiratory diseases and the development of low-grade systemic inflammation (Tvarijonaviciute *et al.*, 2012). While gene mutations are associated with increased body weight in Beagles and Labrador, diet is clearly a determinant of obesity through excess energy intake (Zeng, Zhang & Du, 2014; Raffan *et al.*, 2016).

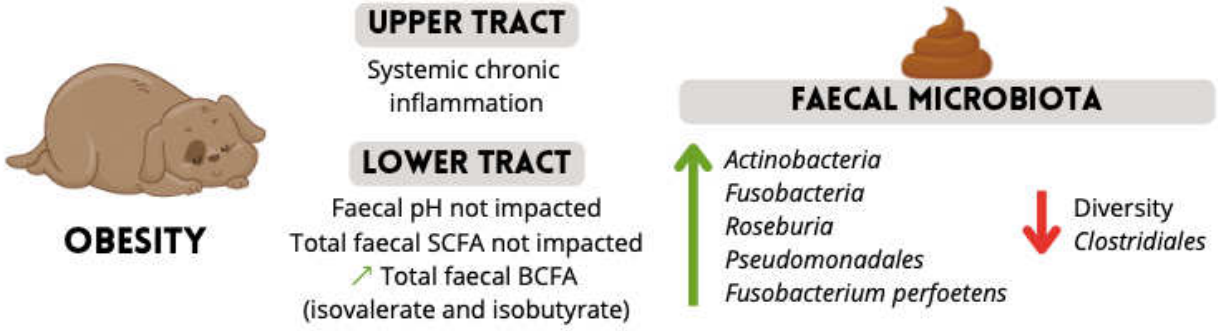

Figure 3.6: Impact of obesity on dog digestive physiology. Main variations in upper and lower digestive physiology and changes in faecal microbiota composition associated to canine obesity. Increased parameters are indicated by a rising green arrow, while decreased ones are symbolized by a falling red arrow. *BCFA: branched-chain fatty-acids; SCFA: short-chain fatty-acids.*

Several mechanisms may implicate gut microbiome in the onset and evolution of dog obesity. Based on human and mice data, this includes higher energy utilization from non-digestible carbohydrates, manipulation of host gene functions and exacerbation of inflammation (Hamper, 2016). Impacts of obesity on the canine digestion and microbiota is summarized in **Figure 3.6**. Using 16S rRNA gene pyrosequencing in companion and laboratory dogs, dominance of *Firmicutes* (> 90 %) was observed in feces of both obese and lean groups, but mean abundance of *Actinobacteria* and *Roseburia* was greater in obese dogs (Handl *et al.*, 2013). Using the same method, Salas-Mani *et al.*, (2018) showed that *Proteobacteria* predominated in obese dogs (76 %) whereas faecal microbiota of lean dogs was mainly composed by *Firmicutes* (85 %). In addition, *Clostridiales* appeared to be less abundant in obese compared to lean dogs, while opposite result was found for *Pseudomonadales*. However, in a recent study involving 17 healthy and 22 obese companion dogs, no significant difference in any taxa was highlighted between the two groups using Illumina 16S rRNA gene sequencing (Forster *et al.*, 2018). With the same method, Bermudez Sanchez and colleagues (2020) described a relative abundance of 92 % of *Firmicutes*, 2 % *Fusobacteria*, 1 % *Bacteroidetes* and a median *Firmicutes*/*Bacteroidetes* ratio of 0.123 in 20 obese dogs (Bermudez Sanchez *et al.* , 2020). Lastly, in a very recent study, a positive association between

Fusobacteria level, especially *Fusobacterium perfoetens*, and body score condition in 24 overweight laboratory Beagles was established using metagenomic analysis (Chun *et al.*, 2020). In dog like in human, microbial diversity seems to decrease in obese compared to lean dogs, with Shannon index of 1.3 and 2.3, respectively (Park *et al.*, 2015). However, more investigations are required to characterize canine obese microbiota, in feces but also in other digestive compartments, to determinate if some species should be used as obesity markers. As an example, *Proteobacteria* were recently correlated to increased weight in overweighed dogs, as it has been suggested in human (Apper *et al.*, 2020). These authors also found that the presence of lipopolysaccharides (LPS) in plasma was associated with insulin resistant status, suggesting the presence of a sub-acute pro-inflammatory status in dogs like in humans (Apper *et al.*, 2020).

In addition to microbiota changes, other physiological modifications have been demonstrated in obese humans compared to healthy individuals, including an increase in bile acids production by liver (coupled with high amounts of primary bile acids in stool), and a higher SCFA production leading to a decrease in colonic pH (Rahat-Rozenbloom *et al.*, 2014). Due to similarities between dog and human GIT and lifestyle, it would be interesting to establish if similar phenomena yet poorly investigated occur in obese dogs. Mean faecal pH of obese companion Beagles (6.6) was not significantly different from that of lean dogs (6.8) whatever the diet, i.e., high-fat or low-fat diet (Xu *et al.*, 2017). In the same study, total faecal SCFA concentration was also equivalent between the two groups, whereas faecal BCFA such as isovalerate and isobutyrate were significantly more concentrated in obese compared to lean dogs. According to our knowledge, there is until now no study that has investigated bile acids production in obese *versus* lean dogs. However, recent studies recommend to monitor faecal bile acids concentrations along with microbiota in lean and obese dogs, as they appear to be interesting markers of glucose homeostasis failure in obese dogs (Forster *et al.*, 2018; Apper *et al.*, 2020).

3.2.3. Inflammatory bowel disease

In dogs, IBD is classified in chronic enteropathies, but defining its prevalence remains difficult because diagnosis of the disease is not easy. IBD is characterized by an alternation of clinically active (with pain and diarrhea) and insignificant phases that occur irregularly. Outside active phases, there are recurring gastric symptoms with histopathological changes in mucosa of small and large intestines (Malewska *et al.*, 2011). The most predominant causes of canine IBD include bacterial and environmental factors, genetic predisposition of selected breeds, food allergies and some drugs (Malewska *et al.*, 2011). Pathogenesis of IBD includes loss of tolerance for endogenous microbiota, chronic inflammation of the GIT associated with an increase in intestinal permeability, and immune cells infiltration in the *lamina propria* (Junginger *et al.*, 2014). Clinical scenarios include decline in activity level and appetite, vomiting, increase in stool frequency, loss of stool consistency (increase in faecal water content), and weight loss.

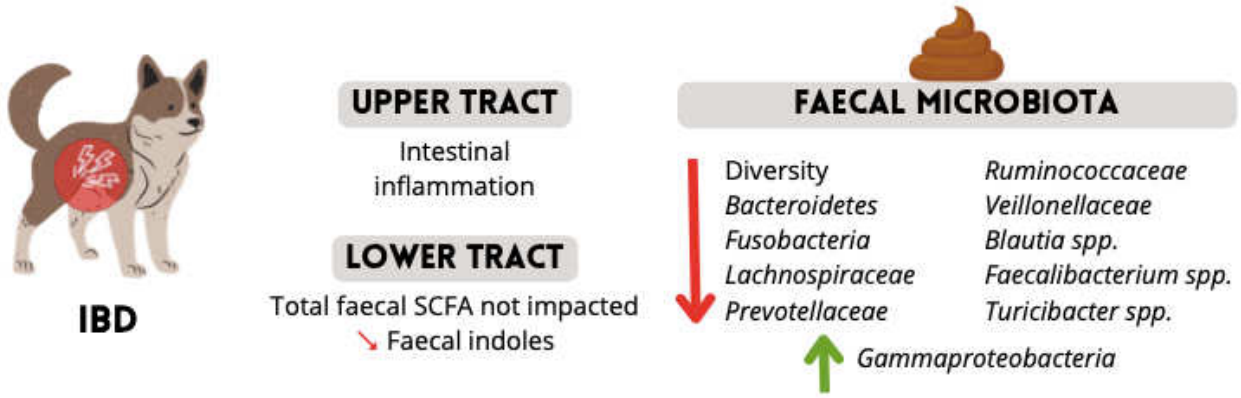

Figure 3.7: Impact of inflammatory bowel disease on dog digestive physiology. Main variations in upper and lower digestive physiology and changes in faecal microbiota composition associated to canine IBD are represented. Increased parameters are indicated by a rising green arrow, while decreased ones are symbolized by a falling red arrow. *IBD: inflammatory bowel disease; SCFA: short-chain fatty-acids.*

Recent reviews on IBD in dogs report modifications in gut microbiota structure (compared to healthy animals) similar to that found in human, with a decrease in faecal relative abundance of *Firmicutes* and *Bacteroides* together with an increase in the relative abundance of *Proteobacteria* (Hooda *et al.*, 2012) (**Figure 3.7**). This was confirmed in a recent study by Pilla & Suchodolski, (2020) who observed a decrease in *Firmicutes* (i.e. *Ruminococcaceae*, *Veillonellaceae* and *Lachnospiraceae*), *Bacteroidetes* (i.e. *Bacteroidaceae* and *Prevotellaceae*) and *Fusobacteria* relative abundancy. Nevertheless, there is no absolute consensus since Xu *et al.*, (2016) didn't observe any significant difference in *Firmicutes*, *Bacteroidetes* and *Enterobacteriaceae* abundance between healthy and IBD groups (quantified by qPCR). In their study, Minamoto and collaborators used real-time PCR to quantify some underrepresented populations, such as *Blautia spp.*, *Faecalibacterium spp.*, *Turicibacter spp.* and *Escherichia coli* (Minamoto *et al.*, 2015). The authors observed that these three first populations were less abundant in IBD group, whereas *E. coli* was non-significantly increased. They also employed 454-pyrosequencing analysis and showed a significant decrease in faecal diversity in IBD compared to healthy dogs, as also described in humans (Minamoto *et al.*, 2015). Other studies investigated gut microbial changes directly using mucosal biopsies. Molecular-phylogenetic studies have revealed a bacterial and/or fungal dysbiosis in the **duodenum** of dogs with idiopathic IBD (Suchodolski *et al.*, 2008, 2010, 2012b, 2012a; Xenoulis *et al.*, 2008; Díaz-Regañón *et al.*, 2023). Most of the time, *Clostridiales* and *Fusobacteria* proportions were decreased in IBD compared to healthy dogs, whereas *Proteobacteria* increased. Fungal DNA was more frequently detected in dogs with chronic enteropathies (76.1 %) than in healthy animals (60.9 %), but also more prevalent in mucosal (82.8 %) than in luminal samples (42.9 %). In addition, Cassmann *et al.*, (2016) showed from ileal and colonic biopsies a significantly increase in relative abundance of *Enterobacteriaceae* and *E. coli* bacteria attached onto surface epithelia or invading intestinal mucosa in IBD compared to healthy dogs, as observed in human. FISH analysis of colonic biopsies from Boxer with granulomatous colitis revealed mucosa colonization by an unknown adherent and invasive *E. coli* strain (Simpson *et al.*, 2006). Taken all together, these data indicate that global microbial structure and diversity more than a single taxa should be followed to discriminate healthy and IBD dog microbiota (Scarsella *et al.*, 2020). In accordance to these observations, a

dysbiosis score based on the difference abundances of 8 faecal microbial groups (i.e. Universal bacteria, *Faecalibacterium*, *Turicibacter*, *Streptococcus*, *E. coli*, *Blautia*, *Fusobacterium* and *C. hiranonis*) was developed to characterize dysbiosis severity (AlShawaqfeh *et al.*, 2017). Results showed that these 8 populations act as markers of IBD dysbiosis and allowed by themselves to distinguish healthy from IBD microbiota in dogs. In addition, a very recent paper showed, for the first time, an impact of dog size on both duodenal and faecal microbiota of healthy and IBD dogs (Díaz-Regañón *et al.*, 2023).

Concerning functional activity, there is no significant difference in faecal SCFA concentrations between IBD and healthy dogs but a lower indole concentration was measured in diseased dogs (Xu *et al.*, 2016; Pilla & Suchodolski, 2020). This is an important point because some indoles harbors well-known anti-inflammatory effects, strengthen epithelial barrier and decrease *E. coli* attachment to epithelium wall in dogs (Chèvreton, 2018). Alterations in microbial functions associated with IBD were estimated using a prediction tool (PICRUSt) from 16S rRNA gene data, highlighting a significant increase in secretion system pathways and transcription factor (Minamoto *et al.*, 2015). Other parameters modified in humans during IBD (Duboc *et al.*, 2013; Rana *et al.*, 2013; Fitzpatrick & Jenabzadeh, 2020), such as transit time and bile acids dysmetabolism (increase in faecal primary bile acids) have not been investigated yet in dogs.

3.2.4. Restoration strategies of the canine microbiota

Recently, better definition and understanding of gut microbiota communities in companions' animals have been achieved, especially thanks to the improvement of large-scale genomic sequencing techniques. Evidence of divergence between microbiota of healthy and diseased dogs has encouraged the willingness to develop new modulation strategies. This section will give an overview on main restoration strategies in dogs, including prebiotics, probiotics, postbiotics (including paraprobiotics) and faecal microbiota transplantation (FMT), with a special focus on paraprobiotic strategy developed during this PhD work.

3.2.4.1. Prebiotics

Prebiotics are defined as "substrates that are selectively utilized by host microorganisms conferring a health benefit" (Gibson *et al.*, 2017). According to the last consensus statement (Gibson *et al.*, 2017), prebiotics encompass oligosaccharides and milk oligosaccharides, but also potentially poly-unsaturated fatty-acids, conjugated linoleic acid and phenolic compounds, although the authors precised that for the latter, more scientific evidence were required. The number of molecules fitting with this definition is increasing and there are still debates to know if a new compound has to be included or not in this definition. Following the introduction of the Nutrition and Health Claims Regulation in 2006, the European Commission has classified the term "prebiotic" as health claims in humans. This implies that prebiotics require authorization in order to be commercialized that could theoretically be granted by providing strong scientific evidence (Laser Reuterswärd, 2007). In the petfood industry, a "Code of good labelling practice for pet food" has been proposed by the FEDIAF and evaluated by ANSES in 2018 in order to properly claim effect of diet compounds, including prebiotics.

Usually, in dogs, prebiotics include **disaccharides** (lactulose), **oligosaccharides** (fructooligosaccharides -**FOS**, mannan oligosaccharides -**MOS**-, xylooligosaccharides -**XOS**-, polydextrose, galacto-oligosaccharides -**GOS**) or **polysaccharides** like **inulin**, pectin or resistant starch (Schmitz & Suchodolski, 2016). Fibers used as canine prebiotics can be extracted from different sources but mainly from cereals. Different MOS, FOS and inulin prebiotics are actually commercialized by diverse companies and integrated in dried kibbles of veterinary diets from brands like Royal Canin, Hill's or Virbac. Beneficial effects of fibers are generally related to increase in digesta viscosity, decrease in gastric emptying (which improves satiety), reduce rate of glucose uptake, reduce blood cholesterol concentrations and promotion of beneficial bacteria growth, such as *Clostridium*, *Lactobacilli*, *Faecalibacterium* or *Bifidobacteria* (de Godoy, Kerr & Fahey, 2013). Fermented fibers provide substrates for SCFA production by microbiota in the large intestine, while non-fermentable fiber sources improve intestine health by promoting laxation, reducing transit time and increasing stool weight (Sunvold *et al.*, 1995a, 1995b, 1995c). Prebiotics impact on canine faecal microbiota and health remains poorly investigated but an increasing number of studies was published the last years reaching around one hundred articles in PubMed. As an example, inulin-type fructan increased the relative abundance of *Erysipelotrichaceae* and *Turicibacteraceae* from the *Firmicutes* phylum while *Proteobacteria* (e.g. *Enterobacteriaceae*) decreased (Alexander *et al.*, 2018). The prebiotic treatment was also associated to an increase in total faecal bile acids. In addition, some dietary fibers like beet pulp, potato fibers or soybean husk could be interesting prebiotics candidates, but detailed fiber characterization and microbial selectivity have to be established (Panasevich *et al.*, 2015a; Myint *et al.*, 2017; Donadelli & Aldrich, 2019).

3.2.4.2. Probiotics

Probiotics are defined as) "live microorganisms that, when administered in adequate amounts, confer a health benefit on the host" (Hill *et al.*, 2014). They include exogenous and commensal (i.e. next generation probiotics isolated from canine stool) bacterial species. To date, different bacterial strains or their commercial forms have been examined by the European Food Safety Authority (EFSA) for their safety and efficacy as **probiotics or feed additives** in dogs, including for example one *Bacillus velezensis* strain, two *Enterococcus faecium*, *Lactobacillus acidophilus,* a cocktail of *L. fermentum, L. plantarum* and *L. rhamnosus* and *Saccharomyces cerevisiae* (**Table 3.2**). In addition, many bacterial strains have been tested in scientific studies as potential probiotics in both healthy and diseased dogs (**Table 3.3**). In a first study, *E. faecium* orally administered during one year to young healthy dogs showed good immune modulation capabilities through increase in serum immunoglobulin A (IgA) (Benyacoub *et al.*, 2003). Healthy dogs treated during one week with *E. faecium* showed a persistence of the probiotic in faeces until 3 months after the end of the treatment (Marcináková *et al.*, 2006). In addition, authors observed a decrease of total serum lipid and protein and suggested a potential anti-obesity effect. Some *Lactobacillus* and *Bifidobacterium* strains have also been tested in healthy dogs. Especially, *L. fermentum* revealed a good probiotic potential with notable adhesion properties to canine mucus and no unacceptable antimicrobial resistance (Strompfová *et al.*, 2006; Strompfová, Lauková & Gancarčíková, 2012). Two studies have also investigated the probiotic potential of *L. acidophilus*, the first observed some modifications on hematological (e.g. increased red blood cells, hemoglobin) and immunological

(e.g. increased IgG) parameters but without demonstrating their interest in dog health (Baillon, Marshall-Jones & Butterwick, 2004). In addition, some beneficial aspects have been described with *L. acidophilus* associated to FOS, but main effects have been attributed to FOS rather than *L. acidophilus* only (Swanson *et al.*, 2002). Finally, in healthy American Staffordshire Terrier dogs, a treatment with the yeast ***S. boulardii*** showed an improvement of global well-being and stress state of dogs with a decrease in faecal calprotectin immunoglobulin A and cortisol levels but those changes were not associated with significant impact on faecal microbiota (Meineri *et al.*, 2022). Another trial using various breed of medium and large sizes showed that giving *S. boulardii* CNCM I-1079 to pregnant and lactating bitches resulted in decreasing number of low birthweight puppies, while increasing energy content in colostrum and stabilizing faecal microbiota during the whole period (Garrigues *et al.*, 2022c, 2022b). In addition, *S. boulardii* was also shown to significantly improve clinical activity score and serum albumin levels compared to the placebo group in IBD dogs (D'Angelo *et al.*, 2018). In diseased dogs, the main therapeutic applications of probiotics are chronic diarrhea and IBD treatment. A combination of different lactic acid producing bacteria (LAB) induced a decrease in duodenal IL-10 and interferon gamma associated to a decrease in *Enterobacteriaceae* and an increase in *Lactobacillus spp* (Sauter *et al.*, 2005). A different bacterial cocktails including four *Lactobacilli* (especially *Lactobacillus helveticus* -ex-*acidophilus*), three *Bifidobacteria* and *Streptococcus thermophilus* led to clinical and immunological improvement in IBD dogs (Rossi *et al.*, 2014).

Probiotics are also able to enhance mucosal health in dogs through several mechanisms such as displacement of intestinal pathogens, antimicrobial substances production, immune system improvement and/or up-regulation of various metabolites, depending on the context (healthy or disease status of the dog) or tested strains (some mechanisms appears to be strain-specific) (Schmitz & Suchodolski, 2016) (**Figure 3.8**). Compared to the human situation where the probiotic mechanisms of action have been largely investigated (e.g. production of antimicrobials, modulation of immune intestinal response, effect on barrier integrity…), many studies are still necessary in dogs. Mechanistic observations and benefits evidenced in human cannot be directly translated to dogs, even if there are many similarities between human and canine GIT. Host specificity should be considered when selecting probiotic candidates because of differences in digestive physiology, immune system and microbiota composition (Lee *et al.*, 2022). As an example, *Lactobacillus rhamnosus* GG isolated from healthy human and yet commercialized didn't persist in the canine GIT (Weese & Anderson, 2002). To go further, *in vitro* gut models are useful tools to provide further insight into probiotic mechanisms of action, as described in part 4.3.3 and **Table 4.2**.

Table 3.2: Main results obtained for probiotics candidates receiving a positive opinion by EFSA for canine use. *Faecal score: 1 = very soft feces; 5 = shaped, hard dry feces. [a]: top dressed on the kibbles; [b]: in a small portion of wet feed, [c]: mixed in a small amount of food. CFU: colony forming units.*

Product/company Probiotic strains	Dose	Main outcomes	Significant results	EFSA conclusions
Prosol SpA/Biosprint *Saccharomyces cerevisiae* MUCL 39885	7×10^{10} CFU/kg feed	**16 adult** English Setter, 14.5 kg	↗ Faecal dry matter content: 37.4 *vs* 38.4 %	➔ Improvement in the faecal consistency, but biological relevance? ⇨ Authorized as "**gut flora stabilizer**" since 2021
		16 adult Basenji and Lagotto Romagnolo, 10.5 kg	↗ Faecal dry matter content: 35.5 *vs* 38.8 %	
		16 adult German Shorthaired Pointer and Bracco Italiano, 27 kg	↗ Faecal dry matter content: 40.9 *vs* 43.4 %	
CSL *Lactobacillus acidophilus* CECT 4529	5×10^9 CFU/kg feed [a]	**15 dogs**: 6 control, 9 treated, English cocker Spaniel, 12-13 kg	↘ Moisture: 0.66 *vs* 0.63 % overall ↘ Faecal score: day 28, 3.8 *vs* 2.6	➔ Variable results on faecal moisture with respect to time but overall analysis: consistent effect on faecal moisture but biological relevance? ⇨ Authorized as "**gut flora stabilizer**" since 2018
		40 dogs: 16 control, 24 treated, Boxer, 23-24 kg	↘ Moisture: 0.69 *vs* 0.67 % overall ↘ Faecal score: 3.9 *vs* 3.3 (day 35)	
		15 dogs: 6 control and 9 treated, Labrador, 30-31 kg	↘ Moisture:0.68 *vs* 0.64 % overall ↘ Faecal score: d14, 3.7 *vs* 2.7	
Provet AG/Calsporin *Bacillus velezensis* DSM 15544	1×10^9 CFU/kg feed [a]	**12 young** Beagle dogs (7-8 months)	↗ DM: 39.1 *vs* 36.5 % ↗ Faecal score: 3.4 *vs* 3, both optimal ↘ NH_3: 0.45 *vs* 0.56 %	➔ Small but significant differences on faecal consistency but biological relevance? ⇨ Authorized as "**gut flora stabilizer**" since 2017
	1×10^9 CFU/kg feed [b]	**14 puppies** (8 weeks) from 3 litters	↘ C-reactive protein d15: 0.06 *vs* 0.11 mg/d ↗ Faecal IgA: 6.76 *vs* 3.48 mg/g wet matter	
	1×10^9 CFU/kg feed [a]	**16 adult** Beagles (4-8 year)	↘ Faecal score: 2.85 *vs* 3.3 at day 28 ↗ DM	
	1×10^9 CFU/kg feed [a]	**16 adult** Beagles (4-8 year)	↗ DM: 33.9 *vs* 30.3 % ↗ Faecal score of 4 (55.9 % *vs* 32 % frequency)	
Probiotic AG/Oralin *Enterococcus faecium* DSM 10663/NCIMB 10415	1×10^9 CFU/day	Very few information and details in the opinion 7 trials performed	Small but significant change in faecal score in 3/4 studies In 4 trials: ↗ of Gram + bacteria or ↘ Salmonella, Clostridium cluster I or XIVa counts	➔ The limited improvement in faecal scores is questionable in terms of biological relevance ⇨ Authorized as "**gut flora stabilizer**" since 2015
Cerbios Pharma SA/ Cylactin *Enterococcus faecium* NCIMB 10415	2×10^9 CFU/kg feed [a]	**16 puppies,** 4 different breeds, (8 to 52 weeks), n=4/group. 44 weeks duration	↗ 50 % in total faecal IgA after 44 weeks ↗ Serum IgA (30 %) and IgG (60 %) ↗ Mature B lymphocytes at 31 and 44 weeks ↘ Faecal score (1.36 *vs* 1.51)	➔ Beneficial effect in dogs supplemented with 2.5×10^9 CFU/kg feed, by increasing IgA intestinal or serum concentrations ⇨ Authorized as "**other zootechnical additives**" since 2013
	2×10^8 CFU/kg feed or 4×10^8 CFU/kg feed – by capsules daily	**30 dogs, 3 breeds,** 1 control and 2 treated	↗ Serum IgA with higher dose (2615 ng/mL) *vs* baseline (1804 ng/mL) and *vs* control (1340 ng/mL)	
	2.5×10^9 CFU/kg feed [c]	**16** elderly Beagle **dogs**	↗ Faecal IgA *vs* baseline and *vs* control	

Table 3.3: List of bacterial strains used as probiotic properties in canines. *Modified from Lee et al., (2022). SCFAs, short-chain fatty acids; ALT, alanine aminotransferase; ALP, alkaline phosphatase; BW, body weight; HDL, high-density lipoprotein; LDL, low-density lipoprotein. IgG, Immunoglobulin G; IFN, Interferon; TNF, tumor necrosis factor.*

Probiotic strains	Amount	Source	Animal characteristics	Tested parameters	Results	Reference
Bifidobacterium animalis AHC7	2×10^{10} CFU/day	Canine	Young adult with acute diarrhea	Effect of the postbiotic on the resolution rate of acute idiopathic diarrhea in dogs	↘ Diarrhea	Kelley *et al.*, (2009)
Bifidobacterium animalis B/12	1 mL of 1.04×10^9 CFU/mL for 14 days	Canine	Healthy dogs	Effects of *B. animalis* on faecal microbiota, faecal characteristics, faecal organic acid concentrations, blood biochemistry, hematological and immunological parameters	↘ Triglycerides and albumin concentration in blood serum ↗ ALT and ALP ↗ Faecal acetic, acetoacetic and valeric acids	Strompfová *et al.*, (2014)
Enterococcus faecium DSM 32820	10^9 CFU/day for 14 days	Canine	Healthy dogs	Evaluate effect of bacteriocin non-producing *E. faecium* DSM 32820	↘ Serum glucose concentration	Strompfová *et al.*, (2019)
Lactobacillus fermentum AD1	3 mL of 10^9 CFU/mL for 14 days	Canine	Healthy dogs	Assessment of blood sample and composition of faecal microbiome	↗ Total lipid and protein in blood ↘ Glucose in bloodstream ↗ *Lactobacilli* and *Enterococci* in feces	Strompfová *et al.*, (2006)
Lactobacillus fermentum CCM 7421	10^7–10^9 CFU/day for 4-14 days	Canine	Dogs suffering from gastrointestinal disorder	Effects of *L. fermentum* on dogs suffering from gastrointestinal disorders regarding faecal microbiota and serum biochemical parameters	↗ Total protein, cholesterol and ALT (blood) ↗ Lactic acid bacteria population ↘ *Clostridia* population and gram-negative bacterial genera ↗ Faecal consistency	Strompfová, Kubašová & Lauková, (2017)
Lactobacillus johnsonii CPN23	2.3×10^8 CFU/day for 9 weeks	Canine	Adult female Labrador	Evaluation of the potential probiotic *L. johnsonii* for its possible use in dogs fed a homemade vegetarian diet regarding nutrient digestibility and faecal fermentative metabolites	↗ Crude fiber digestibility ↗ Faecal SCFAs ↘ Faecal ammonia	Kumar *et al.*, (2017)
Lactobacillus johnsonii CPN23	10^8 CFU/ mL (0.1 mL/kg BW) for 9 weeks	Canine	Adult female dogs	Effects of the dietary supplementation of a probiotic of canine-origin on blood biochemical profile and antioxidant indices in Labrador dogs	↘ Plasma glucose and cholesterol levels ↗ HDL/LDL ratio	Kumar *et al.*, (2016)
Lactobacillus murinus LbP2	5×10^9 CFU/day for 5 days	Canine	Dogs with distemper virus + diarrhea	Effect of the probiotic *L. murinus* native strain on general clinical parameters of dogs with distemper-associated diarrhea	↗ Faecal consistency, mental status and appetite	Delucchi, Fraga & Zunino, (2017)
Lactobacillus rhamnosus MP01	10^9 CFU/day for 8 weeks	Canine	1 month old puppies	Evaluate the probiotic potential of two strains isolated from canine milk regarding survival, production of antimicrobial compounds, adherence	↗ Faecal *Lactobacillus* and *Faecalibacterium* ↗ Faecal SCFAs	Fernández *et al.*, (2019)

Probiotic strains	Amount	Source	Animal characteristics	Tested parameters	Results	Reference
Lactobacillus plantarum MP02				to intestinal mucin, degradation of mucin, and antibiotic sensitivity.	↘ Gastrointestinal infection	
Enterococcus faecium SF68	5 × 10^8 CFU/day for 7 days	Feces of a healthy breast-fed baby	Dogs with diarrhea	Impact of metronidazole combined to *E. faecium* to treat diarrhea	↘ Diarrhea more than administering metronidazole alone ↘ Giardia cysts	Fenimore, Martin & Lappin, (2017)
Enterococcus faecium SF68	5 × 10^8 CFU/day for 14 days	Feces of a healthy breast-fed baby	Healthy dogs	Effect of *E. faecium* administration on serum alanine transferase and alkaline phosphatase activity and total cholesterol and triglyceride concentrations	↘ Mean cholesterol concentration ↗ Mean triglyceride concentration	Lucena *et al.*, (2019)
Lactobacillus acidophilus D2/CSL	5.0 × 10^9 CFU/kg food for 35 days	Gastrointestinal tract of a healthy chicken	Healthy dogs	Effects of *L. acidophilus* probiotic strain on nutritional status and faecal and microbiological parameters in purebred boxer dogs	↗ Body condition score ↗ Faecal consistency	Marelli *et al.*, (2020)
Lactobacillus casei *Lactobacillus plantarum* P-8 *Bifidobacterium animalis subsp. Lact*is V9	2 × 10^9 CFU/g (2 g for young, 4 g for training, 10 g for elderly dogs) for 60 days	Fermented dairy products Feces of a healthy child	Young, training and elderly dogs	Evaluation of a multi-strain probiotic compound on canine health regarding respiration rate, breathing rate, body temperature, feed intake, and weight gain, immune function and microbiota composition	↗ Daily feed intake of elderly dogs ↗ Daily weight gain ↗ Level of serum IgG, IFN-α, and faecal secretory IgA ↘ TNF-α ↗ Beneficial bacteria ↘ Potentially harmful bacteria	Xu *et al.*, (2019)
Saccharomyces boulardii	1 x 10^9 CFU/kg of BW per 12 h for 10 days	ND	Healthy dogs and dogs with chronic enteropathies	Impact of *S. boulardii* in healthy dogs and dogs with chronic enteropathies regarding clinical activity index, stool frequency, stool consistency and body condition score	↗ Global well-being ↘ Stress state of dogs ↘ Faecal calprotectin immunoglobulin A ↘ Cortisol levels No significant impact on gut microbiota	D'Angelo *et al.*, (2018)
Saccharomyces boulardii	1 x 109 CFU/kg of food for 35 days	ND	Healthy dogs	Effects of *S. boulardii* in breeding dogs regarding nutritional parameters and inflammatory, immunological, and stress indicators, and impact on microbiota and mycobiota	↘ Faecal calprotectin Immunoglobulin A ↘ Faecal cortisol ↗ Global well-being No impact on gut microbiota and mycobiota	Meineri *et al.*, (2022)

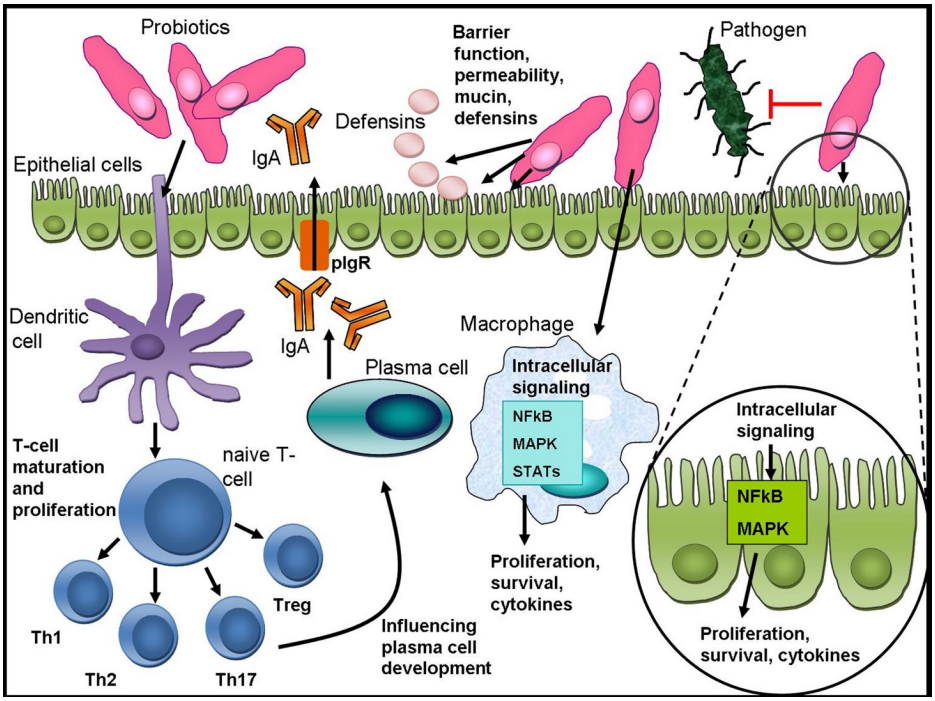

Figure 3.8: Proposed mechanisms of action of probiotics. *Extracted from Schmitz & Suchodolski, (2016) modified from Thomas & Versalovic, (2010).*

3.2.4.3. Postbiotics and paraprobiotics

Postbiotics are defined as "non-viable bacterial products or metabolic products from microorganisms that have biological activity in the host" (e.g. secreted by live bacteria or released after bacterial lysis such as organic acids, peptides, proteins, peptidoglycan-derived peptides, polysaccharides, cell surface proteins, organic acids and enzymes) and **paraprobiotics** (also called ghost or inactivated probiotics) as "non-viable microbial cells, i.e. either intact or broken, or crude cell extracts which when administered in adequate amounts, confer a benefit on the human or animal consumer", produced for example by tyndallisation (Martín & Langella, 2019). A recent International Scientific Association of Probiotics and Prebiotics (ISAPP) consensus statement finally gives the following definition of postbiotics: "preparation of inanimate microorganisms and/or their components that confers a health benefit on the host", which implies that **paraprobiotics** are part of postbiotics (Salminen *et al.*, 2021). As there is still a lot of debates related to those new concepts, we will here, for a sake of clarity, present the main results obtained for postbiotics and for paraprobiotics, which can be understood as a sub-class of postbiotics.

Postbiotics can be naturally found in fermented foods like yogurt or produced by various bacterial and fungal species such as *Lactobacillus*, *Bifidobacterium*, *Streptococcus*, *Faecalibacterium* and *Saccharomyces*. Industrial postbiotics production involves cell disruption techniques like heating, enzymatic or chemical treatments and sonication (Cuevas-González, Liceaga & Aguilar-Toalá, 2020). To the best of our knowledge, there is no regulatory authority framing the development of canine food or dietary supplements with postbiotics, whereas some regulatory standards have been established for postbiotic formulation for medical or pharmaceutical purposes (e.g. related to bacterial lysates-containing medicinal products for respiratory

conditions) (European Medicine Agency, 2019). However, the use of postbiotics in pet's diet and health is still in infancy and modes of actions remain hypothetical. In particular, very few information is available on their impact on canine microbiota (as previously described in part 2.2.3 to 2.2.5 and summarized in **Figure 2.6**). As we know, no study has evaluated the impact of oral supplementation of postbiotics in dogs. Most studies focused on postbiotic production in response to a diet, a fiber supplementation or a disease. The only information available concern potential postbiotics that may affect pets' health was provided by Wernimont *et al.*, (2020) but was totally based on human studies (**Table 3.4**).

Paraprobiotics are even more an emerging topic in dogs. To date, three studies have investigated the impact of parabiotics on canine faecal microbiota (Spears, Ameho & Reynolds, 2016; Guidi *et al.*, 2021; Panasevich *et al.*, 2021). Atopic dermatitis dogs supplemented for two months with blackcurrant seed oil, heat-killed *Lactobacillus reuteri*, zinc oxide and nucleotides in association to an hypoallergenic diet leads to an improvement of dysbiosis scores (Guidi *et al.*, 2021). In another study, heat-treated *Lactobacillus* blend (no more details) improved faecal scores in puppies and protective effect against viral diarrhea in adult dogs (Spears *et al.*, 2016). After 10 months supplementation, an increase in faecal *Firmicutes* and faecal diversity were also observed. In the most recent study, the effects of oral administration of inactivated *Lactobacillus acidophilus* (ex-*helveticus*) alone and combined with mixed prebiotics was investigated for 21 days on healthy dogs (Panasevich *et al.*, 2021). A minimal impact on gut health outcomes was observed with *L. helveticus* alone but the combination with prebiotics allowed to decrease faecal bacterial protein fermentation markers (especially isovalerate, isobutyrate, phenol and indoles that are significantly reduced). For both, no microbiota modification was observed, except a slight increase in *Prevotella* percentage (1.7 % for combined treatments *versus* 0.8 % in control dogs). Paraprobiotic modes of action have been very poorly evaluated in dogs, but those compounds have already shown anti-inflammatory and positive immune responses in both animals (mice and pigs especially) and humans (Cuevas-González *et al.*, 2020). It would be of high interest to further investigate them in dogs since they present many advantages compared to probiotics. First, as paraprobiotics are non-viable cells, they may exhibit enhanced safety with reduced risks of antibiotic resistance or sepsis. In addition, compared to probiotics, no cold chain is required for microorganism's viability and stability; while their use during petfood production is facilitated compared to live bacteria which are killed during extrusion process. Second, paraprobiotics are very stable in the gut environment (as long as they are consumed) and their presence in the large intestine is not impacted by acidity of the stomach or bile for example, nor by antibiotics or antifungal treatments. Third, inactivation processes (e.g. tyndallisation, ionization, radiations or high-pressure treatments, **Figure 3.9**) allow to modify bacterial membrane structure, increasing permeability and antimicrobial peptides release (Siciliano *et al.*, 2021). Lastly, another hypothesis is that surface proteins should be more exposed on inactivated bacteria than in viable probiotics.

Table 3.4: Example of postbiotics that may impact pet health based on human data. *Extracted from Wernimont et al., (2020). SCFA: short-chain fatty acids; bSCFA: branched short-chain fatty acids.*

Predominant Type	Postbiotic	Nutrient substrate (macronutrient class; substrate)	Target organ system	Mechanism of action	References
Saccharolytic; fermentative	SCFA; acetate	Carbohydrate; indigestible polysaccharides	Neuroendocrine; systemic energy availability	Increase satiety; substrate for hepatic lipogenesis	Macfarlane and Macfarlane, 2012; Canfora et al., 2015; Kasubuchi et al., 2015; Koh et al., 2016
Saccharolytic; fermentative	SCFA; propionate	Carbohydrate; indigestible polysaccharides	Neuroendocrine; systemic energy availability	Increase satiety; substrate for hepatic gluconeogenesis	Macfarlane and Macfarlane, 2012; De Vadder et al., 2014; Canfora et al., 2015; Kasubuchi et al., 2015; Koh et al., 2016
Saccharolytic; fermentative	SCFA; butyrate	Carbohydrate; indigestible polysaccharides	Colon	Energy substrate for colonocytes; epigenetic modulation; colon electrolyte balance, motility, blood flow	Wächtershäuser and Stein, 2000; Leonel and Alvarez-Leite, 2012; Macfarlane and Macfarlane, 2012; Canfora et al., 2015; Bultman, 2017
Proteolytic; putrefactive	Indole, indole-3-propionate	Protein; tryptophan	Colon, neuroendocrine	Bind to the arylhydrocarbon receptor; increase epithelial-cell tight-junction resistance and gut barrier integrity; decrease markers of inflammation; improve host-microbiome immune homeostasis; modulate GLP-1 secretion	Macfarlane and Macfarlane, 2012; Agus et al., 2018; Gilbert et al., 2018; Kim, 2018; Zhao et al., 2018
Proteolytic; putrefactive	Polyamines (spermidine, spermine, putrescine, and cadaverine)	Protein; arginine, lysine	Colon	Delay intestinal epithelial senescence; maintenance of intestinal barrier function through promotion of occludin and cadherin expression	Timmons et al., 2012; Kibe et al., 2014; Michael, 2016
Proteolytic; putrefactive	bSCFA; isobutyrate (2-methylpropionate)	Protein; valine	Colon	Source of energy for colonocytes; refeed starved colonocytes with greater efficiency and rapidity than butyrate	Jaskiewicz et al., 1996; Smith and Macfarlane, 1997; Koh et al., 2016
Proteolytic; putrefactive	Hydrogen sulfide	Protein; cyst(e)ine, methionine, taurine	Colon	Inhibition of mitochondrial metalloproteins; reduction in SCFA butyrate oxidation; associated with ulcerative colitis	Pun et al., 2010; De Preter et al., 2012; Macfarlane and Macfarlane, 2012; Stein and Baley, 2013; Singh and Lin, 2015; Ridlon et al., 2016
Proteolytic; putrefactive	Uremic toxins (Indoxyl sulfate, p-cresyl sulfate, 4-ethylphenyl sulfate, phenylacetylglutamine)	Protein; tryptophan, phenylalanine, tyrosine	Kidney	Proinflammation, exacerbate decline in kidney function	Lau et al., 2018
Lipolytic	10-hydroxy-*cis*-12-octadecenoic acid	Fat; linoleic acid	Oral, Dermis	Increased gingival epithelial barrier integrity; decreased dermal atopy	Kaikiri et al., 2017; Yamada et al., 2018

3.2.4.4. Faecal microbial transplantation

Faecal microbiota transplantation (FMT) is defined as transferring a suspension of faecal microorganisms from a healthy donor into the GIT of a recipient subject to favor the restoration of microbial balance of a dysbiotic gut. Compared to humans, canine FMT is more intended for research purposes than practical applications in most cases, due to safety concerns. Studies on FMT applications in canine clinical medicine are still limited, as recently reviewed by Tuniyazi *et al.* (2020) (**Table 3.5**). However, this approach was recently successfully adapted in dogs suffering from gastrointestinal disorders like acute diarrhea (Chaitman *et al.*, 2020), IBD (Niina *et al.*, 2019), or canine *Clostridium difficile* infection (Sugita *et al.*, 2019). Mechanisms of FMT modes of action remain uncertain but there are different hypotheses: niche exclusion, increase competition for nutrients, production of antimicrobials and increased production of secondary bile acids. Despite the current lack of knowledge, FMT should be a promising tool to cure canine non-treatment-responding diseases, as previously demonstrated by many clinical applications for human.

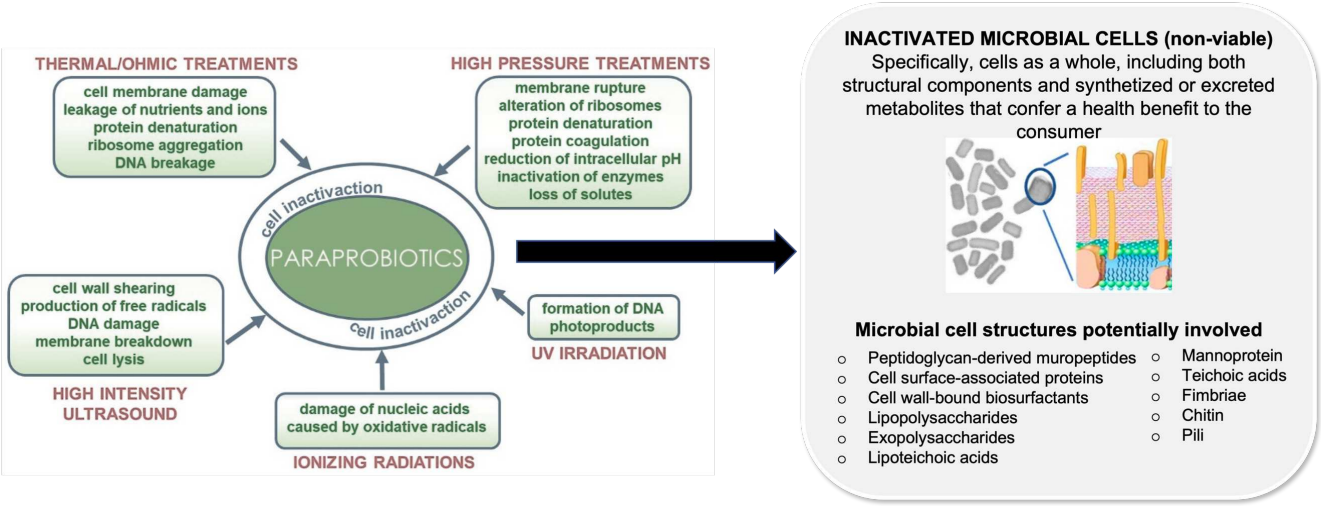

Figure 3.9: Technological processes for paraprobiotics production, associated impacts on bacterial cells, and potentially involved cell structures in beneficial health effects in the host. *Modified from Siciliano et al., (2021)*

Bullet points - ***Factors reshaping gut microbiota***

- Many internal factors can modify canine gut microbiota composition and activity such as breed, size, age or diet
- Health status is important to consider, since many gastrointestinal or extra-digestive disorders have been associated to a gut perturbated situation named dysbiosis, especially antibiotic treatments, obesity or inflammatory bowel disease
- Different restauration strategies (i.e. prebiotics, probiotics, postbiotics, paraprobiotics or FMT) have been evaluated in dogs but the associated mechanisms of action, especially in relation to gut microbiota composition, remain poorly described

Table 3.5: Overview of studies evaluating the impact of FMT on canine health and microbiota. *Modified from Tuniyazi et al., (2022). CCECAI: canine chronic enteropathy clinical activity index; CIBDAI: canine inflammatory bowel disease activity index; FMT: faecal microbiota transplantation; IBD: inflammatory bowel disease; NA: not applicable; ND: not determined; SCFAs, short-chain fatty acids.*

Dog recipient feature	Frequency of FMT	Clinical effects	Effects on faecal microbiota	Reference
Weaning puppies, postweaning diarrhea N=11 FMT, 12 control dogs	5 days, once per day	No difference in faecal consistency	Wide variability of microbiome in puppies, no clustering with donor microbiome observed	Burton *et al.*, (2016)
IBD refractory to conventional treatment N=16 adult dogs	Oral treatment group received FMT each 48-72h	↘ Mean CCECAI in dogs following FMT Heterogeneous clinical presentation and concurrent treatments complicate evaluation	NA	(Bottero, Benvenuti & Ruggiero, 2017)
Parvovirus infection N=33 received standard treatment, 33 received FMT in addition	FMT administered within 5-12h of admission and 48h thereafter	No difference in mortality rate, ↗ Resolution speed of diarrhea ↘ Hospitalization time	NA	(Pereira *et al.*, 2018)
IBD refractory to antibiotic and immunosuppressive treatment over time 10-year-old toy poodle	9 treatments within 6 months	↗ CIBDAI index	↗ Fusobacteria, *Firmicutes* and *Bacteroidetes* ↘ *Proteobacteria* Clustered phylogenetically with donor	(Niina *et al.*, 2019)
Intermittent large bowel diarrhea, 4 months of duration, feces positive for chronic diarrhea	ND	↗ Faecal consistency and defecation frequency within 2–3 days, without recurrence of diarrhea over 190 days	NA	(Sugita *et al.*, 2019)
Uncomplicated acute diarrhea of < 14 days duration N=18 dogs (11 FMT, 7 metronidazole)	11 dogs received a single FMT, 7 dogs received metronidazole 15 mg/kg/12 h for 7 days	↗ Faecal score at days 7 and 28 for both treatments, FMT faecal score lower than metronidazole at day 28	↗ Faecal dysbiosis indexes better with FMT than metronidazole at days 7 and 28 FMT dogs tended to cluster healthy dogs at day 28, unlike metronidazole dogs	(Chaitman *et al.*, 2020)
Chronic-recurring pasty large bowel diarrhea 4-year-old female golden retriever	One FMT via colonoscopy	↘ Faecal *Clostridium difficile*	NA	(Diniz *et al.*, 2021)
Canine acute hemorrhagic diarrhea syndrome N=8 dogs aged 3-12 years old	One FMT via colonoscopy	There were no significant differences in median AHDS clinical scores between FMT-recipients and sham-treated controls	↗ Diversity ↘ SCFA producers including *Eubacterium biforme*, *Faecalibacterium prausnitzii*, and *Prevotella copri*	(Gal *et al.*, 2021)

Part 4 - *In vitro* canine models as an alternative to *in vivo* assays in dogs

Since *in vivo* studies in dogs are increasingly restricted by ethical, regulatory, societal, and cost pressures, an alternative option to study dog digestion is the use of *in vitro* models simulating the different compartments of the canine GIT. The incoming part provides an in-depth description of currently available models of the canine digestive tract, discusses technical and scientific challenges that need to be addressed, and introduces potential applications of *in vitro* gut models in the food and veterinary fields. Noteworthy, some parts of this state of the art on canine *in vitro* gut models have been published in a second review article published in the journal *Alternative to Animal Experimentations* (ALTEX), and redrafted/updated for the present section.

REVIEW ARTICLE **DESCHAMPS, C.**, DENIS, S., HUMBERT, D., ZENTEK, J., PRIYMENKO, N., APPER, E. & BLANQUET-DIOT, S. (2022) *In vitro* models of the canine digestive tract as an alternative to *in vivo* assays: Advances and current challenges. *ALTEX* **39**, 235–257. doi: 10.14573/altex.2109011 **(IF 6.25)**

4.1. Generalities on *in vitro* gut models: static versus dynamic and comparison with *in vivo*

A wide range of *in vitro* gut models has been already developed, from the simplest static mono-compartmental models to the most complex dynamic and multi-compartmental models (Payne *et al.*, 2012; Guerra *et al.*, 2012). These *in vitro* models have been primarily developed to mimic human digestion, but are more and more frequently adapted to simulate animal digestion, mainly that of **pig or piglet** (Meunier *et al.*, 2008; Tanner *et al.*, 2014; Fleury *et al.*, 2017; Dufourny *et al.*, 2019), **cat** (Sunvold *et al.*, 1995c; Van den Abbeele *et al.*, 2020b) or **dog** (Sunvold *et al.*, 1995c; Smeets-Peeters *et al.*, 1999; Tzortzis *et al.*, 2004; Hervera *et al.*, 2007; Bosch *et al.*, 2008; Cutrignelli *et al.*, 2009; Panasevich *et al.*, 2013; Lee *et al.*, 2017; Vierbaum *et al.*, 2019; Van den Abbeele *et al.*, 2020b; Oba *et al.*, 2020; Verstrepen *et al.*, 2021; de Castro Santos Melo *et al.*, 2021). Such models will be described in the next 4.2 part.

Simple static models of the **upper gut** (Minekus *et al.*, 2014) reproduce in a single vessel maintained at body temperature the successive oral, gastric and/or small intestinal phases of human digestion, by changing pH conditions and adding appropriate digestive secretions (e.g. α-amylase in the oral phase, pepsin and/or lipase in the stomach and bile and/or pancreatic juice in the intestinal phase). Simplest models of the colon compartment are thermostatic batch culture systems. These models are inoculated with faeces to simulate colonic fermentation and maintained under anaerobic conditions by flushing with nitrogen or carbon dioxide, but without any renewal of nutritive growth medium until the end of experience. Such approaches are therefore limited in time by substrate availability (24 to 72 h) and parameters like pH or redox potential are not regulated. Compared to static systems, dynamic models reproduce changes in at least one parameter, such as pH kinetics, variation in digestive secretions or chyme transit. They can be mono-compartmental or composed of sequential vessels simulating the successive digestive compartments. **Dynamic mono-compartmental models** of the

upper gut are only gastric digester (Kong & Singh, 2010; Thuenemann *et al.*, 2015), while multi-compartmental models include gastric and small intestinal compartments, most frequently simulating the duodenal section (Tompkins, Mainville & Arcand, 2011; Ménard, Picque & Dupont, 2015). All these models only reproduce physicochemical parameters of the upper digestive tract, such as temperature, gastric and intestinal pH, gastric and ileal deliveries, transit time, digestive secretions and passive absorption of nutrients and water. **Dynamic large intestine models** are based on the principle of continuous or semi-continuous fermentation and just like batch systems are inoculated with faecal samples. Such models are maintained under anaerobiosis and reproduce colonic temperature, pH and transit time, and redox potential can be monitored. Moreover, a nutritive medium aiming to mimic ileal effluents and composed of various complex sources of carbon and nitrogen, electrolytes, bile acids, and vitamins is continually added to the bioreactor, while fermentation medium is regularly removed. This allows maintaining functional microbiota up to several weeks (or even several months with specific adaptations) without microbial washout (Fehlbaum *et al.*, 2015). Several configurations of these colon models include the use of three-stage bioreactors in series to mimic the different sections of the human colon (Gibson, Cummings & Macfarlane, 1988; Cinquin *et al.*, 2006; Van de Wiele *et al.*, 2015a) or the addition of mucin beads to distinguish luminal from mucosal colonic environments and their associated microbiota (Van den Abbeele *et al.*, 2009; Deschamps *et al.*, 2020). Up to now, if the TNO gastroIntestinal Model (TIM-1) is probably the most complete *in vitro* system with its four compartments reproducing the stomach and small intestine of monogastrics (Minekus *et al.*, 1995; Meunier *et al.*, 2008; Denis *et al.*, 2016), only two models simulate the whole digestive tract from the stomach to colon: the Simulator of Human Intestinal Microbial Ecosystem (SHIME) (Molly, Vande Woestyne & Verstraete, 1993; Roussel *et al.*, 2020), and the SIMulator of the Gastro-Intestinal tract (SIMGI) (Barroso *et al.*, 2015).

Despite the obvious limitations of *in vitro* approaches, i.e. no input from nervous, endocrine or immune systems, artificial gut models have many advantages in terms of low cost, technical flexibility and reproducibility. Especially, the spatial compartmentalization of bi- and multi-compartmental models allows sample collection over time and in the desired segment of the GIT, while *in vivo* studies mainly provide end-point measurements (e.g. in faecal samples), since access to the different segments of the digestive tract (from the stomach to proximal colon) remains very restrictive. Besides, in canine *in vivo* assays (like in human), there is frequently a huge discrepancy between studies due to different diets (e.g. homemade, canned or dry foods), lifestyle (companion or laboratory animals), and sizes, breeds or genetic background. Therefore, biological interpretation of *in vivo* data is complexified by this myriad of factors, among which inter-individual variability is one of the main challenges. On the contrary, *in vitro* approaches enable a high level of experimental control and reproducibility, excluding confounding environmental or dietary factors, and therefore allow to carry out in-depth mechanistic studies on pharma and food compounds; making this tool complementary to the *in vivo* approach.

4.2. Currently available canine *in* vitro gut models

Since 1995, twelve *in vitro* models of the canine gut have been developed (**Table 4.1**). There is no available model of the oral phase and only three are mimicking the upper GIT (Smeets-Peeters *et al.*, 1999; Hervera *et al.*, 2007; Lee *et al.*, 2017) (**Figure 4.1**).

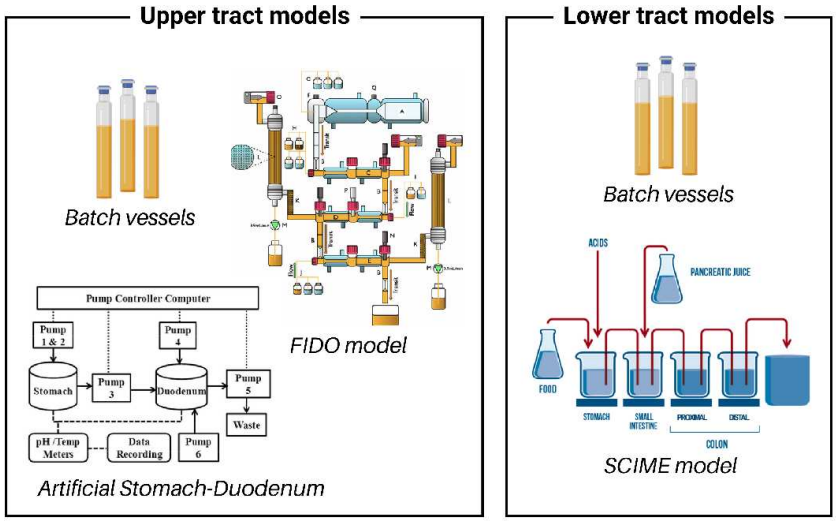

Figure 4.1: Schematic representation of currently available canine *in vitro* models. *In vitro* models of the upper tract (i.e. stomach and small intestine) are presented on the left and that of the lower tract (i.e. large intestine) are presented on the right.

4.2.1. In vitro models of the upper gut

The first canine batch model developed was that of Hervera and colleagues (2007), which simulates stomach and small intestine digestion in batch vessels by adding crushed dog food to pepsin and pancreatin secretions only. More recently, another batch model of the upper GIT was developed but no significant improvement was made except the addition of bile salts in intestinal juice (de Castro Santos Melo *et al.*, 2021). Besides, a very complete model of the canine upper gut was developed in 1999 based on the TIM-1 technology, first set-up to reproduce human digestive conditions (Smeets-Peeters *et al.*, 1999). The FIDO model (for Functional gastroIntestinal Dog Model) integrates all the upper digestive compartments (stomach, duodenum, jejunum and ileum) and simulates body temperature, kinetics of gastric and small intestine pH, half-time delivery of gastric and ileal compartment, transit time and chyme mixing, sequential delivery of digestive secretions (gastric juice containing *Rhizopus* lipase and porcine pepsin, porcine pancreatic juice, bovine trypsin, electrolytes and porcine bile), and intestinal passive absorption through dialysis hollow fibres (Smeets-Peeters, 2000). FIDO was set-up to mimic canine digestive parameters of medium dogs according to a large review of the literature (Smeets-Peeters *et al.*, 1998). All the parameters were therefore adapted to *in vivo* data, except for temperature that was kept at 37°C like in human and parameters of passive absorption, probably due to a lack of data. The model was validated only for nutritional applications, following protein digestibility and calcium bioaccessibility, both in the FIDO model and *in vivo* in ileal cannulated dogs (5 dogs). Even if TIM-1 model is still the most complete simulator of the upper gut, it only reproduces physicochemical and not microbial

digestive parameters. Another main limitation of this model is that tested food should be finely mixed before digestion, which can widely influence nutrient digestibility. More recently, the Artificial Stomach-Duodenum (ASD) dissolution model was adapted to dog digestion to allow mechanistic understanding through formulation solubility studies (Lee *et al.*, 2017). This bi-compartmental model, set at 37°C, simulate both the stomach and duodenum with associated pH (6.8 and 6.8-7, respectively), transit time (adapted from *in vivo* data) and pancreatic secretions. It's interesting to note that in this model the gastric pH is particularly high compared to the two others (6.8 for the ASD model *versus* pH 2 for Hervera's model and 2-6 for FIDO). Contrarily, values set for the small intestine are quite similar (i.e. 6.8-7, 6.8 and 6.2-7, respectively).

4.2.2. In vitro models of the lower gut: batch and continuous models

Eight other available devices are *in vitro* static models of the canine colon, based on batch fermentation. The simplest model is that of Cutrignelli *et al.* (2009) which aimed to reproduce the colon of adult dogs. A single vessel was inoculated with diluted faeces from adult large dogs, maintained at 39°C under anaerobiosis without any addition of nutritional medium, except for tested carbohydrates. Another batch model set-up by Sunvold *et al.* (1995a) to reproduce the colon from adult medium dogs, used a simulated growth medium supposed to be adapted to dog digestion.

This simple model was validated based on *in vivo* data from 30 medium dogs, regarding fibre digestibility and production of SCFAs. Another static model was very recently developed by Van den Abbeele and collaborators (Van den Abbeele *et al.*, 2020b). This batch system was inoculated with dog faecal samples but there is no information in the paper on the age and size of animals. They introduced a nutritive medium aiming to simulate dog ileal effluents but in fact, almost similar to that used for human experiments (Van den Abbeele *et al.*, 2018). The same limitation on the lack of adaptation of nutritive medium composition to dog situation could be raised on batch models developed by other teams (Tzortzis *et al.*, 2004; Panasevich *et al.*, 2013; Vierbaum *et al.*, 2019).

Bosch *et al.* (2008) developed a more complete batch fermentation model mimicking the ileum, proximal colon, transverse colon, or rectum compartment in different vessels inoculated with corresponding digestive fluids from 3 adult small or large dogs. In this study, the authors used a nutritive medium previously adapted for piglet fermentation, from another medium initially developed for rumen bacteria maintenance, without any modification in relation to dog digestion (Williams *et al.*, 2005). The main disadvantage of this model is the requirement of *in vivo* digestive fluids to inoculate *in vitro* vessels, and inter-individual variability associated with such approach. Finally, only one static batch model integrates mucin covered microcosms in order to represent the intestinal mucus but they don't discuss associated results (Oba *et al.*, 2020). To conclude on these batch models, apart for temperature setting, faecal inoculation and anaerobiosis, *in vitro* parameters were generally not adapted to canine digestion.

Table 4.1: Main *in vitro* models developed to simulate the gastrointestinal tract of dogs and their characteristics. *CO2: carbon dioxide; FIDO: Functional gastroIntestinal DOg model; GET: gastric emptying time; GI: gastrointestinal; LITT: large intestine transit time; N2: nitrogen; N/A: not applicable; ND: not defined; M-SCIME: Mucosal Simulator of the Canine Intestinal Microbial Ecosystem; SITT: small intestine transit time*

References			Dog's generalities		GI compartment modelized	Adaptations from bibliographic research	Validation processes	Physicochemical parameters								Microbiota			
			Age (years)	Dog's size				Temperature	Agitation	pH		Transit time	Food reproduction	Digestive secretions	Absorption	Presence of microbiota	Process type	Anaerobiosis	Mucus
										pH kinetic	Value								
UPPER TRACT																			
de Castro Santos Melo *et al.*, (2021)	**STATIC**	MONO-COMPARTMENTAL	ND	ND	Stomach and small intestine	But no reference to *in vivo* data	No validation	Stomach: 38.9°C Small intestine: 37°C	Magnetic bar	No	Stomach: 2 Small intestine: 6.5	No	No	Gastric juice: pepsin Intestinal juice: trypsin, bile salts	No	No	Stomach: batch 3 h Small intestine: batch 4 h	No	No
Hervera *et al.*, (2007)			ND	ND	Stomach and small intestine	But no reference to *in vivo* data	*In vivo* digestibility trial (n=54)	39°C	Magnetic bar	No	Stomach: 2 Small intestine: 6.8	No	Crushed dry extruded canine food	Gastric digestion: pepsin Intestinal digestion: pancreatin	No	No	N/A	No	No
Lee *et al.*, (2017) **Artificial Stomach-Duodenum**	**DYNAMIC**	MULTI-COMPARTMENTAL	ND	Medium	Stomach and duodenum	Adapted from Smeets-Peeters *et al.*, 1998; Carino, Sperry, & Hawley, 2006; Bhattachar *et al.*, 2011	*In vivo* pharma trial (n=6)	37°C	Paddle	No	Stomach: 6.8 Duodenum: 6.8-7	Yes	No	Pancreatin solution	No	No	N/A	No	No
Smeets-Peeters *et al.*, (1999) **FIDO**			"adult"	Medium	Stomach, duodenum, jejunum and ileum	Adapted from Smeets-Peeters *et al.*, 1998	*In vivo* digestibility trial (5 ileal cannulated dogs)	37°C	Water pressure on flexible wall	Yes	Stomach: 2-6 Duodenum: 6.2 ± 0.2 Jejunum: 6.5 ± 0.2 Ileum: 7.0 ± 0.2	GET: $T_{1/2}$: 1.5 h SITT: $T_{1/2}$: 5 h	Crushed dry or canned dog food	Gastric juice, pancreatic juice, intestinal electrolyte solution, bile solution	Passive	No	N/A	No	No
LOWER TRACT																			
Vierbaum *et al.*, (2019)	**STATIC**	MONO-COMPARTMENTAL	4.3 ± 0.9	Medium	Large intestine		No validation	37°C	Continuous shaking at 370 rpm	No	N/A	No	No dog food. Pre-reduced anaerobe sterilized medium	No	No	Yes, from faeces	Batch 24 h	Yes	No
Cutrignelli *et al.*, (2009)			3	Large	Large intestine		Based on a literature review	39°C	No	No	N/A	No	No	No	No	Yes, from faeces	Batch 48 h	Yes	No
Panasevich *et al.*, (2013)			ND	ND	Large intestine		*In vivo* digestibility trial (n=10)	39°C	Periodic mixing	No	N/A	No	No dog food Anaerobe medium	No	No	Yes, from faeces	Batch 12 h	Yes CO_2-gas	No

References			Dog's generalities		GI compartment modelized	Adaptations from bibliographic research	Validation processes	Physicochemical parameters								Microbiota			
			Age (years)	Dog's size				Temperature	Agitation	pH		Transit time	Food reproduction	Digestive secretions	Absorption	Presence of microbiota	Process type	Anaerobiosis	Mucus
										pH kinetic	Value								
						But no reference to *in vivo* data													
Sunvold *et al.*, (1995a)			5-6	Medium	Large intestine	⊗	*In vivo* fermentation study (n=30)	39°C	No	No	N/A	No	No dog food. Nutritive medium based on several solutions of vitamins, oligo-elements, supplemented with fibrous substrates	No	No	Yes, from faeces	Batch 24 h	Yes CO_2-gas	No
Van den Abbeele *et al.*, (2020b)			ND	ND	Large intestine	⊗	Based on a literature review	39°C	Magnetic bar	No	N/A	No	No dog food. Colonic background medium	No	No	Yes, from faeces	Batch 48 h	Yes N_2-gas flow	No
Tzortzis *et al.*, (2004)			ND	ND	Large intestine	⊗	No validation	37°C	Magnetic bar	No	6.8	No	No dog food. Colonic background medium	No	No	Yes, from faeces	Batch 24 h	Yes N_2-gas flow	No
Oba *et al.*, (2020)			4.6	Large	Large intestine	⊗	No validation	39°C	Continuous shaking at 90 rpm	No	N/A	No	Colonic background medium	No	No	Yes, from faeces	Batch 48 h	Yes N_2-gas flow	Mucin-covered microcosms
Bosch *et al.*, (2008)			Adult and mature	Small and large	Ileum, proximal colon, transverse colon or rectum	⊗	No validation	39°C	No	No	N/A	No	No dog food. Filtered digestive fluids added to a nutritive medium previously adapted for rumen bacteria growth	No	No	Yes, from digesta	Batch 72 h	Yes CO_2-gas	No
Duysburgh *et al.*, (2020) **SCIME** Verstrepen *et al.*, (2021) **M-SCIME**	**DYNAMIC**	MULTI-COMPARTMENTAL	ND	Medium	Stomach, small intestine, proximal colon and distal colon	⊗ But no reference to *in vivo* data	**SCIME** *In vivo* fermentation study (n=10) and literature **M-SCIME** Comparison with SCIME results -Comparison of *in vitro* results with faecal inoculum (microbiota)	39°C	Magnetic bar	No	Stomach: 2 Small intestine: 6.8 Proximal colon: 5.6-5.9 Distal colon: 6.65-6.9	Residence times GET: 1 h SITT: 4 h LITT: 6 h (transverse) 10 h (distal)	Dog food added at 9 g/L in stomach juice. Small and large intestine effluents simulated by addition of digested suspension from the previous compartment	Pancreatic juice and bile	Passive (feed)	Yes, from faeces, in the large intestinal compartments only	Continuous	Yes N_2-gas flow	Mucin-covered microcosms

Even if there are nice *in vitro* to *in vivo* correlations that have been established for some of these models, *in vitro* digestion conditions remained far from *in vivo* complexity, and do not consider nutrient composition of dog digestive fluids, digestive secretions, nor pH variations between small and large intestinal compartments and residence time in each gut section.

The only dynamic *in vitro* model of the lower gut in dog was adapted from the SHIME system, first set-up to reproduce human conditions. The SCIME model (for simulation of canine intestinal microbial ecosystem), is currently the only one reproducing the entire canine GIT from the stomach to the large intestine (Duysburgh *et al.*, 2020). SCIME is composed of four bioreactors simulating the stomach, small intestine, proximal and distal colon. Only colonic compartments were inoculated with faecal samples from medium dogs. *In vivo* parameters that are reproduced include body temperature, regionalized gastric and intestinal pH, gastrointestinal transit time, digestive secretions (pancreatic juice and bile) and anaerobiosis. The authors mentioned that most of these parameters have been adapted to medium dog digestion even if associated *in vivo* data are not clearly mentioned in the publication. SCIME was validated through comparison with *in vivo* data in ten Beagles when digesting fructooligosaccharides, regarding microbial composition and SCFA/BCFA production. Of note, *in vitro* results in proximal and distal colon (even if clearly distinct profiles were obtained) were only compared to *in vivo* data in faecal samples. Recently, SCIME was optimized with the addition of mucin-covering plastic beads, based on Mucosal-SHIME (M-SHIME) technology (Van den Abbeele *et al.*, 2009), to reproduce luminal and mucosal microenvironment of the canine colon, resulting in the M-SCIME (Van den Abbeele *et al.*, 2020a; Verstrepen *et al.*, 2021). Due to the lack of *in vivo* data, this recent optimization was not validated compared to bacterial mucosal profiles in dog, but only compared to previous results obtained in the M-SHIME. Once again, *in vitro* colonic pH varies widely between current available models, which could be explained by the fact that authors generally base their model settings on a unique *in vivo* study, whereas large inter-individual variations are observed in dogs, depending on age, size, and breed.

4.3. *In vitro* gut models as powerful tools to study canine digestion

4.3.1. Scientific and technical challenges to be addressed

As described before, parameters of *in vitro* models have been not fully adapted to *in vivo* data, probably due to the rarity of information in dogs. Therefore, many scientific and technical challenges still need to be addressed to get closer to canine digestion and consider the complexity of this environment (**Figure 4.2**).

First, technical improvements should be considered to simulate more realistically canine digestive conditions at each level of the GIT. Currently, as mentioned earlier, there is no canine chewing simulator, but such development is certainly not a priority since most of dogs do not chew but swallow large pieces. Regarding the upper gut, the FIDO model already shows a high level of complexity.

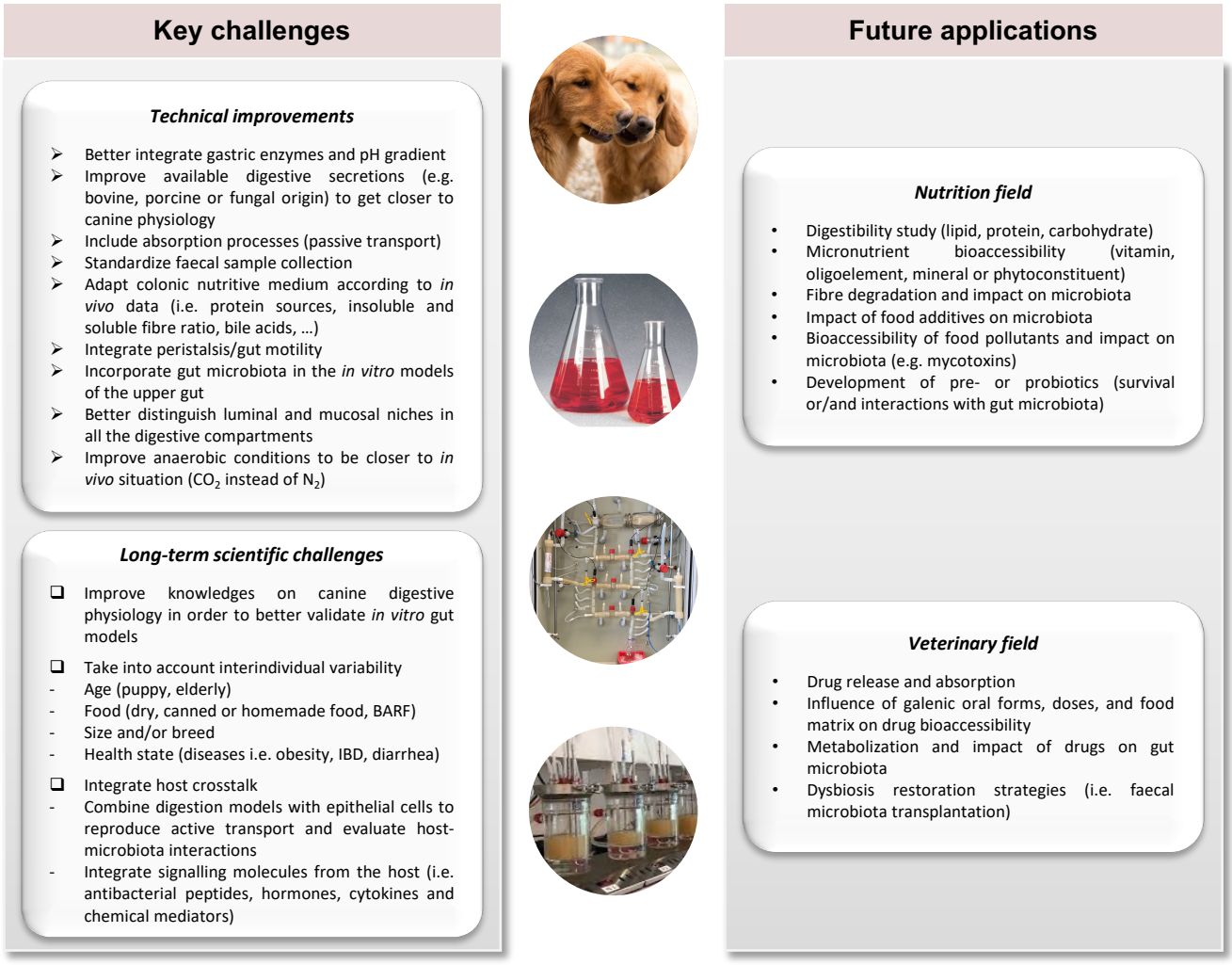

Figure 4.2: Main challenges in the development of *in vitro* gut models of the canine digestive tract and their applications in nutritional and veterinary fields. Overview of the main technical and scientific challenges and applications of canine *in vitro* gut models as reliable tools to test or develop new products in the food and pharma fields.

The M-SCIME also possesses a gastric compartment that would merit improvements such as a progressive acidification of the chyme (already made in the M-SHIME).This change in gastric pH during canine digestion is certainly a key parameter in food disruption and digestion as it influences gastric pepsin and lipase activities (Carrière *et al.*, 1993; Sams *et al.*, 2016). FIDO and M-SCIME also both homogenize food before *in vitro* digestion. In dogs, higher food particle sizes seem to reach the stomach. Even if there is very few available data on this subject in dogs (unlike in human), some canine studies showed no correlation between food size and density of particles on gastric emptying time, but also on the entire upper gut digestion process (Gruber *et al.*, 1987; Meyer *et al.*, 1988; Chen *et al.*, 2008; De Cuyper *et al.*, 2018), while others observed an increase gastric half emptying time with a higher meal viscosity and high-fat content (Ehrlein & Pröve, 1982; Palerme *et al.*, 2020). Recently, a new gastric and small intestinal model, the Engineered Stomach and Small Intestine (ESIN) has been developed to fill this gap and better handle both ingested liquids and real-size food particles in human simulated digestion studies (Guerra *et al.*, 2016). Even if this model has been primarily set-up for human

applications, we can easily imagine future developments to reproduce dog digestion. Another main issue in upper gut models is the use of porcine, bovine, or fungal secretions/enzymes instead of canine ones. Of course, due to obvious ethical constraints, digestive secretions collected from dogs cannot be used (and are not commercially available). Therefore, further investigations are needed to ensure that digestive secretions from other sources are close enough to canine ones (in terms of composition and enzymatic activities) to ensure relevant *in vitro* simulation. For example, bile composition and conjugation profiles widely differ between species (Thakare *et al.*, 2018). Thus, further analysis are needed to check if porcine bile (largely used in *in vitro* models) matches or not with the canine one (Alvaro *et al.*, 1986). Another main limitation of current upper gut models is their inability to accurately mimic gastric and intestinal peristalsis. In M-SCIME, peristaltic mixing is reproduced by using magnetic stirrers, far from *in vivo* situation. FIDO more closely reproduces peristaltic movements through gentle mixing with pressurized water jackets, but peristaltic forces and frequency have not been adapted between human and dog models, whereas *in vivo* data indicate clear differences between the two species (Boscan *et al.*, 2013; Warrit *et al.*, 2017a; Farmer *et al.*, 2018). Efforts should be therefore pursued to more accurately simulate mechanical deformations resulting from peristalsis in dogs, based on what has been already made in humans, mainly in gastric models (Kong & Singh, 2010; Li, Fortner & Kong, 2019). Regarding nutrient absorption in the small intestine, FIDO incorporates dialysis fibre modules in the jejunal and ileal compartments. In a very recent publication on the M-SCIME (Verstrepen *et al.*, 2021), a dialysis step of the grinded dog feed was integrated to simulate small intestinal absorption by removing high-molecular weight proteins. Adding such dialysis devices to other upper gut model would be beneficial to get closer to the *in vivo* situation, even if dialysis modules only reproduce passive absorption of small molecules (e.g. fatty acids, oligo and monosaccharides, small peptides, and amino acids, but also drugs and chemicals) and water. Reproducing passive absorption also ensures bile reabsorption in the distal intestine, as occurred *in vivo*, and therefore adequate decrease bile concentrations from the duodenal to the ileal compartments, which is a key point in dog like in human gut physiology. To further reproduce absorption phenomenon and integrate active transport, canine dog models of the upper gut should be coupled with immortalized canine intestinal epithelial cells (cIEC) (Farquhar *et al.*, 2018), as previously done in human with TIM-1 and Caco-2 cells (Déat *et al.*, 2009; Bahrami *et al.*, 2011) or with organoids generated from canine duodenal, jejunal and colonic biopsies (Kramer *et al.*, 2020). A last key point to be raised is the lack of intestinal microbiota in all the upper gut models, whereas bacterial concentrations up to 10^7 CFU/g can be found in the distal small intestine of dogs (Benno *et al.*, 1992; Mentula *et al.*, 2005). Even if the role of intestinal microbiota is poorly defined in dogs (Hooda *et al.*, 2012; Deng & Swanson, 2015; Enright *et al.*, 2016; Mondo *et al.*, 2019; Pilla & Suchodolski, 2020), we can assume that intestinal microbiota is involved at least in carbohydrate digestion and may exert a barrier effect against enteric pathogens as observed in humans (Andoh, 2016). This is even more important since unlike in human, an appreciable fraction of dietary fibre seems to be degraded in the canine small intestine (Bednar *et al.*, 2000). This microbial component of the canine digestive tract was nonetheless integrated in *in vitro* colon models through inoculation with faecal samples. A major issue of all available *in vitro* models is that the nutritive medium used to maintain bacterial growth and activity was not adapted to adequately mimic the composition

of ileal effluents entering the colon *in vivo*. Using digestive fluids as previously done by Bosch *et al.* (2008) is not a simple and sustainable solution as it makes *in vitro* model strongly dependent of unstandardized and poorly available *in vivo* samples. Therefore, efforts are still needed to better define growth medium composition based on available data on dog diet, but also protein, lipid and carbohydrate ileal digestibility (Bednar *et al.*, 2000; Flickinger *et al.*, 2003; Propst *et al.*, 2003). It is also very important to consider relevant bile acids concentrations and profiles reaching the colon, as it may shape gut microbiota (Ridlon *et al.*, 2014). Besides, all available *in vitro* colonic models are flushed with nitrogen or carbon dioxide to maintain anaerobic conditions inside vessels or bioreactors, which is obviously far from *in vivo* situation. In the human ARCOL model (**Figure 4.3**), anaerobiosis is maintained by the sole activity of resident microbiota to get closer to *in vivo* gut physiology (Friedman *et al.*, 2018; Deschamps *et al.*, 2020; Verdier *et al.*, 2021). Such adaptation would deserve attention to increase the relevance of current *in vitro* canine colon models.

Figure 4.3: Picture of the ARCOL model with its mucin-alginate beads module, resulting in the M-ARCOL configuration. The ARCOL model is a single-stage model. Faecal microbiota was used to inoculate the bioreactor. Nutritive medium, temperature, pH and transit time are controlled. Recently, the model has been

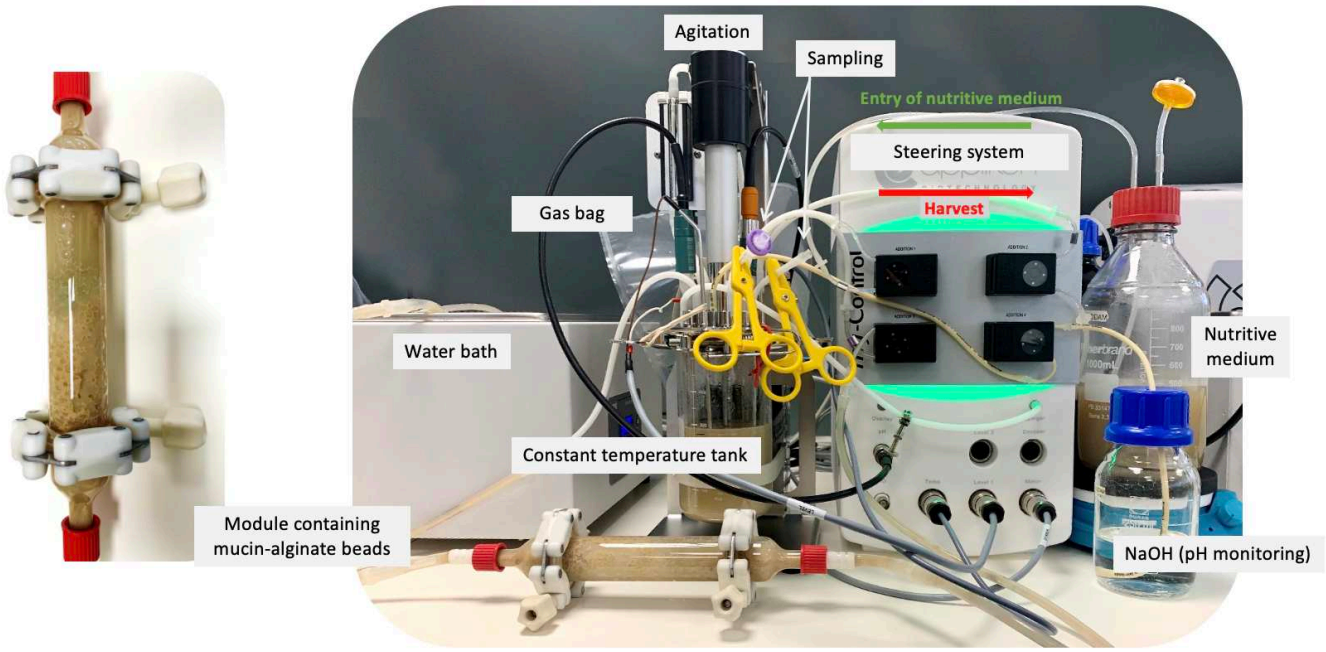

adapted in the M-ARCOL configuration with a glass vessel filled with mucin-alginate beads and connected to the main bioreactor allowing the continuous flow of luminal medium on mucin beads.

Moreover, currently, only bacteria have been followed as the main component of gut microbiota. Given the increase importance of other constituents, such as fungi, methanogen Archaea or even phages or viruses in gut physiology (Barko *et al.*, 2018), it would be of great interest to extend microbial sequencing to these populations. Lastly, as previously mentioned for upper gut models, to further investigate host-microbiome crosstalk in a close future, canine *in vitro* models should be coupled to cell culture assays, as previously described in human ones (Bahrami *et al.*, 2011; Chassaing *et al.*, 2017; Geirnaert *et al.*, 2017; Defois *et al.*, 2018). Of interest, more complex units, such as the Host Microbiota Interaction Module already coupled to

SHIME system (Marzorati *et al.*, 2014) integrates another important parameters of the colon ecosystem, such as microaerobiosis in close proximity of the epithelium that shapes mucus-associated gut microbiota.

4.3.2. Future developments and quality requirements

Up to now, most of available *in vitro* models, and especially the most complex FIDO and M-SCIME systems, have been designed to reproduce medium dog's digestive conditions when ingesting dry food. As previously described in parts 1 and 2 of this work (and reviewed in Deschamps *et al.* 2022), canine digestion and associated gut microbiota are impacted by dog's body weight or breeds (Kendall, Blaza & Smith, 1983; Bourreau *et al.*, 2004; Hernot *et al.*, 2005; Weber, 2006; Weber *et al.*, 2017; Deschamps *et al.*, 2022b). Considering in future developments the influence of body weight and/or breeds on canine digestive physicochemical and microbial parameters is undoubtedly a promising line of research to develop more relevant *in vitro* models. Further adaptations regarding dog diet (e.g. dry, canned or homemade food, BARF) and age (puppies, adults and elderly dogs) would also bring substantial added value to *in vitro* canine gut simulation. This has been already performed with success in *in vitro* human models (Blanquet *et al.*, 2004; Fehlbaum *et al.*, 2015; Denis *et al.*, 2016; Roussel *et al.*, 2016; Bondue *et al.*, 2020; Roussel *et al.*, 2020). To move forward, we can even foresee the development of *in vitro* gut models simulating not only physiological but also diseased situations, such as those associated with obesity or IBD, as previously done in human (Bussolo de Souza *et al.*, 2014). In this case, the main objective would be to maintain gut microbiota dysbiosis (considered as a typical feature of these pathologies) inside the *in vitro* models. For this purpose, small intestinal and/or colonic models will be inoculated with faeces collected from dogs suffering from obesity or IBD, but also all the associated gut parameters, such as composition of digestive effluents (including bile profiles), pH and retention time should be modified to fulfil specific diseased conditions.

Of course, all these technical and scientific improvements would be possible if corresponding canine *in vivo* data are available in the literature (or provided by clinical trials), for setting-up of *in vitro* models but also for the validation of their robustness through strong *in vivo-in vitro* correlations. Such validation is necessary to convince future users of the relevance of *in vitro* gut models but is unfortunately rarely performed due to cost, time, or technical limitations. Up to date, main gaps in *in vivo* data concern digestive secretions in the upper gut, but also microbial profiles all along the digestive tract and characterization of mucus-associated bacteria. Recent developments of non-invasive methods to follow digestive parameters, such as pH, motility or transit time in dogs (wireless motility capsules e.g. SmartPill) (Warrit *et al.*, 2017a) and in humans (Schwizer *et al.*, 2002; Wang *et al.*, 2005; Zhang *et al.*, 2014) open new avenues and may help to fill these scientific and technological gaps. Regarding such *in vivo* reference studies, it would be of high importance to standardize the experimental conditions in terms of age, breed, weight, but also diet and dog's lifestyle, which all impact digestive parameters (Mahar *et al.*, 2012; Panasevich *et al.*, 2015b; Pilla & Suchodolski, 2020; Apper *et al.*, 2020; You & Kim, 2021). It should be also relevant to exclude from these *in vivo* assays those performed with breeds showing well-known specific digestive particularities (like German Shepherd) or specific energy needs (like Husky, Great Danes or Terriers) (Zentek & Meyer, 1995). Obviously, standardization of procedures also

concerns *in vitro* studies and some interesting clues are already available in the guidance document on good *in vitro* method practice (namely GIVIMP) recently published (OECD, 2018), especially for cell culture practices.

In addition to robustness, canine *in vitro* model development also involves reproducibility and transferability. Reproducibility is considered as a key advantage of *in vitro* studies over *in vivo* experiments and should be systematically tested. Contrarily to the human situation, transferability of canine *in vitro* gut models is hampered by their stage of development, still in infancy. Simplest *in vitro* systems (such as batch models) can be more easily shared between laboratories than complex ones, like TIM or M-SHIME which require specific technical expertise. Transferability of canine gut models would be speed-up by exchanges between international experts in artificial digestion, as previously done in the frame of the INFOGEST network leading to the harmonization of static and semi-dynamic *in vitro* protocols in humans (Minekus *et al.*, 2014; Brodkorb *et al.*, 2019).

4.3.3. Potential applications of canine gut models in food and pharma

In vitro models represent a powerful platform to study the fate in the canine digestive environment of food and veterinary products, help to elucidate their mechanism of action and promote innovation in these fields. As their parameters can be adjusted in terms of food matrix, age and dog breed or body size, but also by mimicking physiological or pathological situations, we can consider unlimited applications of these systems once developed and validated (**Figure 4.2**). They can thus provide valuable information to promote the evolution of products already on the market (generic, range extension…) and/or develop new products such as specialized food or innovative drugs. All types of *in vitro* gut models from the simplest to the more complex ones can be useful. Static mono-compartmental models are ideal tools to perform pre-screening of a large number of compounds, due to low cost and easy manipulation. On the opposite, dynamic multi-compartmental systems, which are more expensive and require expertise to be handle but reproduce more physiological digestive conditions, can be applied only on a reduced number of tested compounds. The wide number of applications already performed under human conditions (Souliman *et al.*, 2006; Cordonnier *et al.*, 2015; Lyng *et al.*, 2016; Bianchi *et al.*, 2019; Kubbinga *et al.*, 2019; Blancquaert, Vervaet & Derave, 2019) in food and pharma fields can inspire potential of canine *in vitro* gut models, especially for screening or characterization of gut microbiota restauration strategies, as described in 3.2.4.

Nowadays, *in vitro* models simulating dog's digestive environment have been only used for nutritional applications, mainly to assess fibre digestibility (Sunvold *et al.*, 1995c; Bosch *et al.*, 2008; Cutrignelli *et al.*, 2009; Musco *et al.*, 2018; Van den Abbeele *et al.*, 2020b, 2020a) (**Table 4.2**). Other applications include evaluation of protein (Kim *et al.*, 2021) or lipid digestibility and bioaccessibility of micronutrients such as vitamins, minerals (van Zelst *et al.*, 2015; Lee *et al.*, 2017) or phytoconstituents like polyphenols. In addition to digestibility, *in vitro* models can provide valuable information on fibre effects on gut microbiota composition and activity, through SCFA/BCFA, ammonia or gas measurements (Bosch *et al.*, 2008b; Cutrignelli *et al.*, 2009; Van den Abbeele *et al.*, 2020b). This will help to assess the **prebiotic** status of soluble fibres and perform mechanistic studies on gut microbiota modulation independently of the host. In addition to prebiotics, **probiotic**

strains can be tested in the *in vitro* models to evaluate their interactions with gut microbiota (Ogué-Bon *et al.*, 2011), but also their survival (and the effect of mode of administration) and the production of antimicrobial compounds such as bacteriocins.

Regarding veterinary applications, kinetics of drug release and absorption can be monitored all along the GIT, as well as the influence of oral formulations (Lee *et al.*, 2017), different doses, fed or fasted state and food matrix (food-drug interactions). At this time, drug posology is only established based on dog body weight or metabolic weight, but many associated variations in digestive parameters that influence drug bioaccessibility must be considered (Oswald *et al.*, 2015). In addition, *in vitro* gut models can enhance knowledge on drug metabolization by gut microbiota and/or effects of drugs on gut microbiota composition and function (Sjögren *et al.*, 2014). Hence, gut microbial dysbiosis induced by oral antibiotherapy, as described in 3.2.1, can be simulated in the colonic models (as performed by El Hage *et al.*, (2019) in the M-SHIME with human microbiota) and further applied to evaluate the efficiency of prebiotics, probiotics, postbiotics and/or parabiotics in restoring microbiota eubiosis. Lastly, *in vitro* models can be employed to assess the efficiency of new microbial restoration therapy strategies in a safe way before using animals, such as FMT (see part 3.2.4.2). As described earlier, this therapy has been recently experimented in dogs for the treatment of post-weaning diarrhea, acute diarrhea, IBD, chronic enteropathies or parvovirus infections and seems to be promising (Burton *et al.*, 2016; Pereira *et al.*, 2018; Niina *et al.*, 2019; Chaitman *et al.*, 2020; Chaitman & Gaschen, 2020).

Bullet points – ***In vitro canine models as an alternative to in vivo assays in dogs***

- Up to now, only a restricted number of *in vitro* models has been developed to simulate the canine upper or lower digestive tract
- These devices show various levels of complexity, i.e., from static mono-compartmental to dynamic multi-compartmental models
- *In vitro* parameters have not yet been fully adapted to *in vivo* canine digestion, and some of the models are not yet totally validated, mainly due to a paucity of *in vivo* data. Of importance, none of them is simulating specific digestive conditions associated with different dog sizes, breeds, or ages, under healthy or diseased conditions
- *In vitro* canine gut models are a relevant alternative to *in vivo* assays for testing new food or pharma products, especially gut microbiota restoration strategies such as pre, pro, post and paraprobiotics

Table 4.2: Application studies of the currently available canine *in vitro* gut models in food and pharma fields. *BCFA: branched-chain fatty acids; BCS: body condition score; FOS: fructooligosaccharides; GIT: gastro-intestinal tract; GOS: galactooligosaccharides; SCFA: short-chain fatty acids; XOS: xylooligosaccharides.*

References	Applications							Aim of the study
	Macro-nutrients	Micro-nutrients	Fibers/ Prebiotics	Probiotics/ Postbiotics	Parabiotics	Drugs	Antibiotics	
	Upper GIT models							
Smeets-Peeters *et al.*, (1999)	✓	✓						Effects of small intestinal transit time on protein digestibility and calcium availability from canned dog food
Hervera *et al.*, (2007)	✓							*In vitro* percentage of organic matter disappearance used as a predictor of apparent organic matter and energy digestibility of extruded dog food
Silva *et al.*, (2013)				✓				*In vitro* assessment of functional properties of lactic acid bacteria isolated from faecal microbiota of healthy dogs for potential use as probiotics. Strains were tested for resistance to gastric acidity and bile salts, cell surface hydrophobicity, antagonism against pathogenic bacteria, production of hydrogen peroxide, and antibiotic susceptibility
van Zelst *et al.*, (2015)		✓						Identification of dietary factors that affect selenium accessibility in commercial petfood
Lee *et al.*, (2017)						✓		Evaluation of *in vitro* dissolution performance of five formulations of an acidic BCS Class II compound
Coman *et al.*, (2019)				✓				Screening potential probiotic *Lactobacillus* strains for dietary supplement in dogs' feedings based on survival to gastric and pancreatic juices and bile salts, resistance to antibiotics and antipathogenicity
Penazzi *et al.*, (2021)	✓							Effect of supplementation with Black Soldier fly (*Hermetia illucens*) larvae meal in extruded dog food on *in vivo* and *in vitro* digestibility
Kim *et al.*, (2021)	✓							Effect of thermal processing on ileal digestibility of dry matter and crude protein from raw chicken meat
de Castro Santos Melo *et al.*, (2021)				✓				Probiotic potential of *Enterococcus hirae* from goat milk and its survival in canine gastrointestinal conditions simulated *in* , acidification ability, exopolysaccharide formation, virulence and antibiotic resistance
	Lower GIT models							
Sunvold *et al.*, (1995c)			✓					Effects of cellulose, beet pulp, citrus pulp and citrus pectin on microbiota fermentation (organic matter disappearance, SCFA and lactate)
Sunvold *et al.*, (1995a)			✓					*In vitro* fermentation of selected fibrous substrates: influence of diet composition on substrate organic matter disappearance and SCFA production
Sunvold *et al.*, (1995b)			✓					*In vitro* fermentation of selected fiber sources and metabolism of fiber-supplemented diets
Swanson *et al.*, (2001)			✓					Fermentation of vegetable and fruit fiber sources compared to fiber standards following SCFA production, organic matter disappearance, and gas production

References	Applications							Aim of the study
	Macro-nutrients	Micro-nutrients	Fibers/ Prebiotics	Probiotics/ Postbiotics	Parabiotics	Drugs	Antibiotics	
Tzortzis *et al.*, (2004)			✓					Fermentation properties of galactooligosaccharides synthesized by α-galactosidase from *Lactobacillus reuteri* (SCFA)
Biagi, Cipollini & Zaghini, (2008)			✓					Effects of fiber sources on microbiota composition and activity (SCFA, ammonia and gas)
Bosch *et al.*, (2008)			✓					Fermentation kinetics of fibers from canine foods (gas and SCFA)
Cutrignelli *et al.*, 2009)			✓					Impact of different carbohydrate sources on microbiota fermentation (gas, SCFA, BCFA, ammonia)
Ogué-Bon *et al.*, (2010) with adaptation to 39°C			✓	✓				Evaluation of a symbiotic combination on probiotic growth and microbiota activity (SCFA)
Ogué-Bon *et al.*, (2011) with adaptation to 39°C			✓	✓				Effects of rice bran combined with *Lactobacillus acidophilus* and *Bifidobacterium longum* on microbiota activity (SCFA)
Panasevich *et al.*, (2013)			✓					Characterization of potato fiber fermentability by canine microbiota (SCFA and BCFA)
Panasevich *et al.*, (2015)			✓					Effect of soluble corn fibers on nitrogen-corrected true metabolizable energy and fermentability by microbiota (SCFA)
Vierbaum *et al.*, (2019)			✓					Effects of *Yucca schidigera* powder and inulin on protein fermentation metabolites (SCFA, BCFA, phenols and indoles, biogenic amines, ammonia)
Donadelli, Titgemeyer & Aldrich, (2019)			✓					Effects of different fiber sources used in petfood on organic matter disappearance and SCFA/BCFA production
Oba *et al.*, (2020)			✓					Potential fermentation and prebiotic effects of GNU100, an animal milk oligosaccharide biosimilar on microbial communities and metabolites production (gas, SCFA, BCFA, lactate)
Van den Abbeele *et al.*, (2020b)			✓					Effects of yeast-derived formulation on microbial composition and activity (gas, SCFA, ammonium)
Traughber *et al.*, (2020)			✓					Fermentability of legumes by microbiota and metabolites production (SCFA, BCFA and gas)
Duysburgh *et al.*, (2020)			✓					Effect of fructooligosaccharide supplementation on microbial community composition and activity (SCFA, BCFA and ammonium)
Van den Abbeele *et al.*, (2020a)			✓					Effect of a *S. cerevisiae*-based product on the modulation microbiota composition and production of fermentation metabolites (SCFA, BCFA and lactate)
Pinna *et al.*, (2020)		✓	✓					Effects of tylosin alone or associated with three prebiotics (FOS, GOS, and XOS) on canine faecal microbial populations and metabolites

SECTION II

EXPERIMENTAL WORK

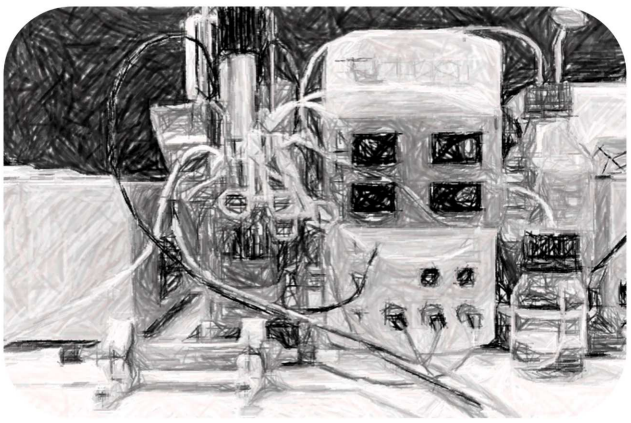

Chapter 1 – Comparative methods for faecal sample storage to preserve gut microbial structure and function in an *in vitro* model of the human colon

In vitro gut models are relevant alternatives to *in vivo* assays, providing efficient platforms to perform mechanistic studies on the role of human and animal microbiota in health and disease. Most of the time, those models are inoculated with fecal samples to introduce the microbial component of the gut ecosystem. Processing fresh stool samples within 6 h after collection appears as the ideal strategy, but it is not always possible and storage methods such as freezing or lyophilization are often used. Up to now, few studies have evaluated the impact of preservation methods on fecal microbiota, mostly from human origin. However, the impact of such methods on microbiota establishment in *in vitro* gut models has not been investigated yet, particularly under canine conditions. Consequently, this study aimed to assess the effect of short-term storage and cryopreservation on the kinetics of luminal and mucus-associated microbiota colonization and associated metabolic activities in the M-ARCOL model. Experimentations related to this study were performed during my master 2 internship at MEDIS laboratory in 2019 on human fecal samples in a collaborative work with Dr Marion Leclerc from INRAE MICALIS unit (Jouy-en-Josas, France). The corresponding paper was written at the beginning of my thesis and results used to select the most suitable option for the following experiments of this PhD work on canine fecal samples. Fecal samples from two healthy volunteers were subjected to different preservation protocols: freezing 48 h at -80°C (raw frozen stool, RFS), freezing 48 h at -80°C with glycerol as a preservative agent (glycerol frozen stool, GFS) or lyophilization with maltodextrin/trehalose following the protocol developed by MICALIS team (lyophilized stool, LS), and results obtained were compared to fresh fecal samples. This work has been published in *Applied Microbiology and Biotechnology* in 2020.

ORIGINAL ARTICLE

Comparative methods for fecal sample storage to preserve gut microbial structure and function in an *in vitro* model of the human colon

DESCHAMPS, C., FOURNIER, E., URIOT, O., LAJOIE, F., VERDIER, C., COMTET-MARRE, S., THOMAS, M., KAPEL, N., CHERBUY, C., ALRIC, M., ALMEIDA, M., ETIENNE-MESMIN, L. & BLANQUET-DIOT, S. (**2020**)

Applied Microbiology and Biotechnology **104**, 10233–10247. doi: 10.1007/s00253-020-10959-4 (**IF 5.56**)

Abstract

In vitro gut models, such as the Mucosal Artificial Colon (M-ARCOL), provide timely and cost-efficient alternative to *in vivo* assays allowing mechanistic studies to better understand the role of human microbiome in health and disease. Using such models inoculated with human fecal samples may require a critical step of stool storage. The effects of preservation methods on microbial structure and function in *in vitro* gut models have been poorly investigated. This study aimed to assess the impact of three commonly used preserving methods, compared to fresh fecal samples used as a control, on the kinetics of lumen and mucus-associated microbiota colonization in the M-ARCOL model. Feces from two healthy donors were frozen 48 h at -80°C with or without cryoprotectant (10 % glycerol) or lyophilized with maltodextrin and trehalose prior to inoculation of four parallel bioreactors (e.g. fresh stool, raw stool stored at -80 °C, stool stored at -80 °C with glycerol and lyophilized stool). Microbiota composition and diversity (qPCR and 16S metabarcoding) as well as metabolic activity (gases and short chain fatty acids) were monitored throughout the fermentation process (9 days). All the preservative treatments allowed the maintaining inside the M-ARCOL of a complex and functional microbiota but considering stabilization time of microbial profiles and activities (and not technical constraints associated with the supply of frozen material), our results highlighted 48 h freezing at -80 °C without cryoprotectant as the most efficient method. These results will help scientists to determine the most accurate method for fecal storage prior to inoculation of *in vitro* gut microbiome models.

Keywords: human gut microbiota, fecal sample, preservation method, *in vitro* M-ARCOL model

Key points:

- *In vitro* ARCOL model reproduces luminal and mucosal human microbiome
- Short-term storage of fecal sample influences microbial stabilization and activity
- 48 h freezing at -80 °C: most efficient method to preserve microbial ecosystem
- Scientific and technical requirements influencers of preservation method

1.1. Introduction

The human gastrointestinal tract (GIT) harbors a complex community including 100 trillion microorganisms including bacteria, fungi, archaea and virus-like particles, collectively referred as gut microbiota. Bacteria mainly represent this tremendous number of microbes with the highest proportion found in the colon (Sender, Fuchs & Milo, 2016). It is now well established that each individual has a unique gut microbiota composition with bacteria belonging to the predominant phyla *Bacteroidetes*, *Firmicutes*, *Actinobacteria* and to a lesser extend to *Proteobacteria* and *Verrucomicrobia* (Cheng *et al.*, 2013; Ndeh & Gilbert, 2018). This diverse microbial ecosystem provides benefits to the host through its role in digestion and assimilation of dietary nutrients, immunity and protection against invasion by pathogenic microorganisms (Andoh, 2016; Rooks & Garrett, 2016). Short chain fatty acids (SCFAs) and gas are the main fermentation products derived from microbiota-accessible carbohydrates and dietary proteins, which exert crucial physiological effects as energy supply and trophic factors (Lavelle & Sokol, 2020). Perturbations in gut microbiota structure or function (termed dysbiosis) have been associated with many gastrointestinal and extra-digestive disorders (Cheng *et al.*, 2020).

Many insights into the complex interactions between the host and the members of the gut microbiota have been performed in well-validated *in vivo* rodent models or using *in vitro* cell-based approaches (Pearce *et al.*, 2018). However, these approaches are hampered by differences between animal and human digestive physiology (including resident microbiota) and the ignorance of other niches encountered during gastrointestinal passage prior to host cell interactions, respectively. Alternative solution is to use *in vitro* models enabling the maintenance of the human gut ecosystem while reproducing the main physicochemical parameters of the human gut, i.e. pH, temperature, retention time, nutrient availability and anaerobiosis. The TNO gastrointestinal model TIM-2 (Minekus *et al.*, 1999), the PolyFermS (Zihler Berner *et al.*, 2013), the Simulator of Human Intestinal Microbial Ecosystem SHIME (Molly *et al.*, 1993) and the Artificial Colon ARCOL (Cordonnier *et al.*, 2015) are among the most relevant and well validated *in vitro* models reproducing the human colonic environment. ARCOL has been recently upgraded to distinguish the luminal and mucosal microenvironments of the colon, leading to the M-ARCOL configuration. These models are suitable platforms allowing mechanistic studies on the role of gut microbiota in health and disease (Fleury *et al.*, 2017). One of their main advantage is the possibility to set them up for an extended period of time, under controlled laboratory settings, without any ethical constraints and independently from the host.

To reproduce the microbial ecosystem of the human colon, these *in vitro* models are inoculated with a liquid suspension of feces collected from human volunteers (Aguirre *et al.*, 2014). Overall, fresh stools are preferably used for bioreactor inoculation to be as close as possible from *in vivo* situation, but scientific or technical constraints may lead to require fecal samples storage (due to geographic restriction or long-term experiments with the same fecal inoculum). Several studies have already investigated the impact of various storage protocols for downstream gut microbiota nucleic acid analysis. These studies have focused on the impact of preserving methods, mainly freezing at different temperatures (4 °C, -20 °C or -80 °C) with the addition of

cryoprotectants (ethanol, RNA later, DNA shield) on the microbial composition of the stool (Gorzelak *et al.*, 2015; Choo, Leong & Rogers, 2015; Flores *et al.*, 2015; Song *et al.*, 2016; Bassis *et al.*, 2017; Al *et al.*, 2018). To date, only one study has evaluated the impact of freezing preservative techniques on the onset of luminal (but not mucus-associated) gut microbiota in *in vitro* gut models (Aguirre *et al.*, 2015).

Therefore, in the present study, we investigated the impact of short-term storage and cryopreservation on the establishment of luminal and mucus-associated gut microbiota in M-ARCOL. To this endeavor, before inoculation in the *in vitro* gut model, fecal samples from two healthy volunteers were subjected to different preservation protocols: freezing 48 h at -80 °C (raw freezing stool, RFS), freezing 48 h at -80 °C with glycerol as a preservative agent (glycerol frozen stool, GFS) or lyophilization with maltodextrin/trehalose (lyophilized stool, LS). Impact of preservation methods was assessed by monitoring microbiota composition and microbial metabolic activity (gas and SCFAs production) throughout the fermentation process after inoculation with RFS, GFS or LS, and compared at each time point to fresh stool (FS) condition.

1.2. Materials and methods

1.2.1. Fecal sample collection and treatments

Fecal samples used to inoculate the M-ARCOL model were collected from two healthy volunteers, a female aged 22 years old (donor A) and a male aged 52 years old (donor B). Both donors have no history of antibiotic treatment or probiotic consumption for 3 months prior to sample collection. Immediately after defecation, fecal samples were transferred into a sterile recipient, placed in an airtight anaerobic box (GENbag anaer gas pack systems, Biomerieux, France), transported and processed at the laboratory within 6 hours. In an anaerobic chamber (COY laboratories, Grass Lake, USA), stool samples were manually homogenized in a hermetic freezer bag and then divided into 4 pieces of 16 g each: (i) one fresh aliquot was used to generate the fresh stool (FS) condition; (ii) the second aliquot of raw stool was directly frozen at -80°C for 48 h without any preservative (raw frozen stool, RFS condition); (iii) the third aliquot of stool was resuspended in 45 mL sterile 10 % glycerol and frozen at -80°C for 48 h (glycerol frozen stool, GFS condition); (iv) the last aliquot of stool was resuspended in 45 mL of a maltodextrin/trehalose solution, then frozen at -80°C for 12 h before lyophilization at -15°C during 36 h, as described in patent n°WO 2017/103225 (Reygner *et al.*, 2020) (lyophilized stool, LS condition). Prior to inoculation into M-ARCOL, fresh and stored fecal samples were resuspended with 30 mM sterile sodium phosphate buffer and filtered (500 µm inox sieve).

1.2.2. Description and set-up of M-ARCOL model

ARtificial COLon is a one-stage fermentation system (MiniBio, Applikon, Delft, The Netherlands), used under semi-continuous conditions, which simulates both the microbial and physicochemical conditions encountered in the human colon (Blanquet-Diot *et al.*, 2012; Thévenot *et al.*, 2015). The model has been recently adapted to distinguish the specific microenvironments found in the digestive lumen and in the mucosa (Van den Abbeele *et al.*, 2009), resulting in the Mucosal Artificial Colon configuration (M-ARCOL). It consists of a pH

and temperature-controlled main bioreactor reproducing the luminal colonic medium connected to a glass vessel containing mucin beads and reproducing the mucus-associated microbiota. A sterile nutritive medium (Thévenot *et al.*, 2015) containing various sources of carbohydrates, proteins, lipids, minerals and vitamins was sequentially introduced into the main bioreactor to simulate sequential input of ileal effluents. To ensure anaerobic condition at the beginning of fermentation, the bioreactor was operated with an initial sparging with O_2-free N_2 gas. Afterwards, during the fermentation course, the anaerobic condition inside the bioreactor was maintained by the sole activity of resident microbiota and by ensuring the airtightness of the system. Redox potential was constantly measured using a redox sensor (Mettler Toledo, Columbus, USA) and corrected into an Eh value by adding 200 mV to the recorded values, according to the manufacturer's instructions. In the present study, M-ARCOL was set-up to reproduce the mean conditions found in a healthy human adult colon with a fixed temperature of 37°C, a constant pH of 6.3 maintained by the addition of 2M NaOH, a stirring speed at 400 rpm and a mean retention time of 24 h.

1.2.3. Mucin beads and mucin compartment

Mucin from porcine stomach type II (Sigma-Aldrich, Saint-Louis, USA) and sodium alginate (Sigma-Aldrich, Saint-Louis, USA) were diluted in sterile distilled water, at a concentration of 5 % and 2 %, respectively. To produce mucin beads, the mucin/alginate solution was dropped using a peristaltic pump into a 0.2M solution of sterile $CaCl_2$ under agitation. Mucin beads were introduced into the airtight glass compartment (total area of beads 556 cm^2) connected to the bioreactor and allowing a continuous flow of the luminal medium on mucin beads. Mucin bead compartment was kept at 37°C during the experiment using a hot water bath. Every 2 days, mucin/alginate beads were renewed by fresh sterile ones under a constant flow of CO_2 to avoid oxygen entrance.

1.2.4. Experimental design and sampling

Experimental design and sampling in the M-ARCOL are presented in **Figure I.1** and **Figure I.2**, respectively. For each experiment, four bioreactors inoculated with the fecal sample from the same donor (fresh or stored) were run in parallel, corresponding to the four tested conditions (FS, RFS, GFS and LS). Two series of experiments were performed with the fecal samples from two different donors (corresponding to two biological replicates). All the fermentations were run under batch condition for 24 h and then under semi-continuous condition for additional 8 days. Samples from the main bioreactor, referred to as luminal microbiota, were collected daily for microbiota characterization and SCFA analysis. Additional samples from the mucin beads compartment, referred to as mucus-associated microbiota, were collected every 2 days for microbiota characterization. Mucin/alginate beads were washed thrice in sterile Phosphate Buffer Saline (PBS) and stored at -80°C for downstream analyzes. Samples were also harvested daily from the atmospheric phase of the bioreactor to ascertain anaerobic conditions and evaluate gas composition. The daily total volume of gas produced was also measured.

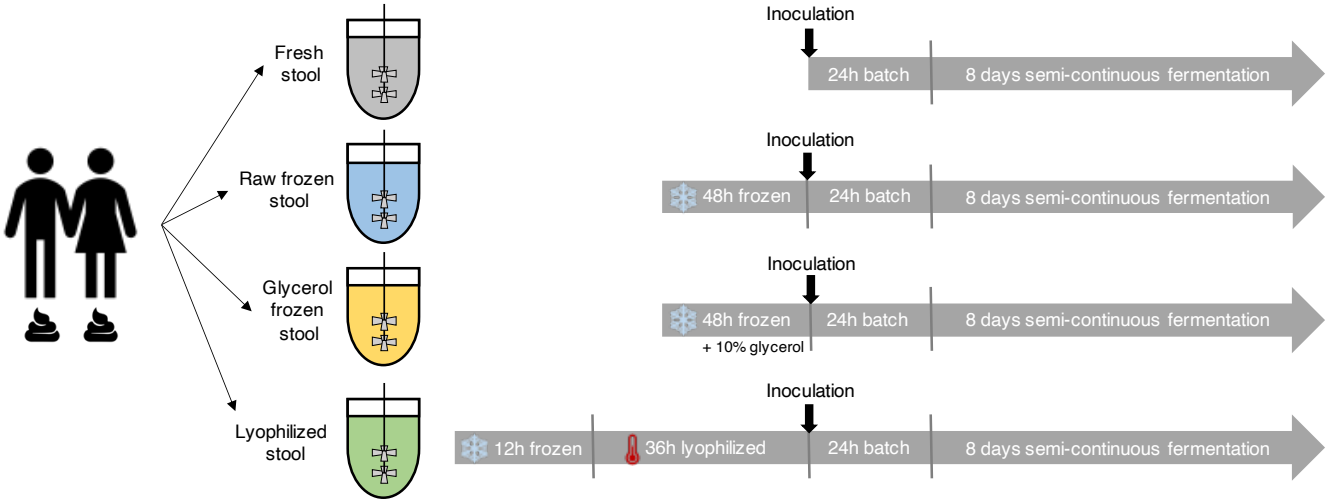

Figure I.1: Experimental design of the *in vitro* fermentation experiments in the M-ARCOL. Stools from two donors (one male, one female) were used to inoculate two independent experiments (two biological replicates) of four bioreactors, allowing testing four conditions in parallel: fresh stool (control), raw frozen stool (48 h, -80°C), glycerol-frozen stool (48 h, -80°C) and lyophilized stool (36 h, -15°C). Each fermentation was carried for a total period of 9 days including 24 h of batch and 8 days of semi-continuous fermentation.

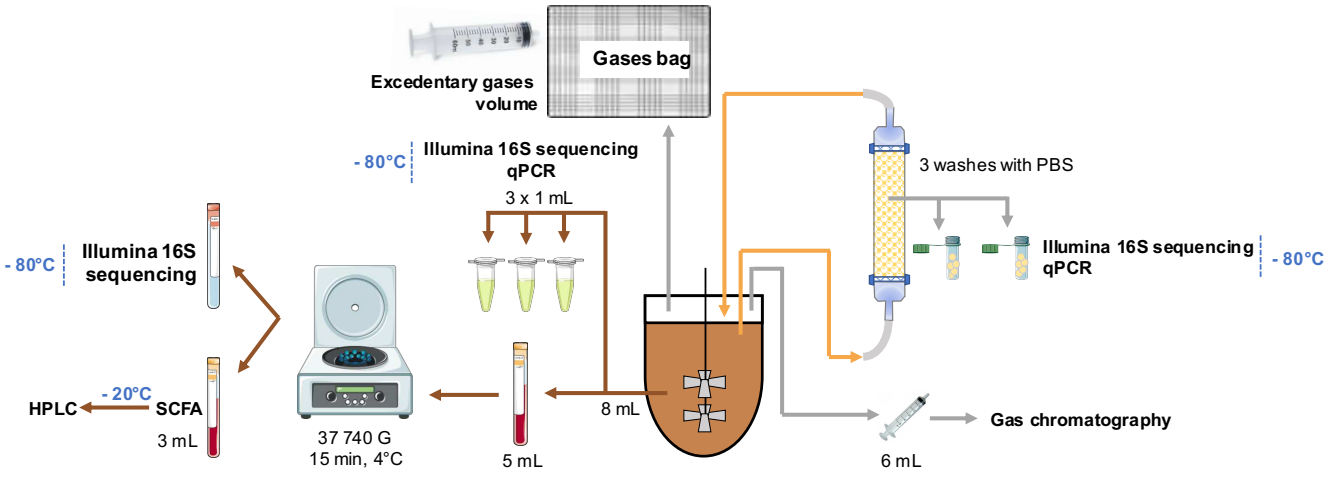

Figure I.2: Experimental set-up and sampling procedure during M-ARCOL experiments. Every day, samples were collected from the fermentation medium and frozen at -80°C for downstream analysis. After centrifugation, the supernatant was used for short chain fatty acid measurement while DNA was extracted from the pellet for further 16S metabarcoding and qPCR analyses. Daily overflow gas was measured, and gas composition was determined by gas chromatography. Every two days, mucin beads were collected to determine the composition of mucin-associated microbiota by qPCR and 16S metabarcoding. *HPLC: High Performance Liquid Chromatography; PBS: Phosphate Buffer Saline; SCFA: short chain fatty acids.*

1.2.5. DNA extraction

Genomic DNA was extracted from bioreactor samples and mucin/alginate beads using the QIAamp Fast DNA Stool Mini Kit (Qiagen, Hilden, Germany) following manufacturer's instructions with the following modifications. Prior to DNA extraction, bioreactor samples were centrifuged (2000 g, 10 min) and the pellet

was subjected to mechanical disruption using a bead beater (3 min, 20 beat/sec) with 300 mg sterile glass beads (diameter ranging in size from 0.1 to 0.6 mm), incubated (70°C, 5 min) and centrifuged again (12000 g, 1 min). Mucin/alginate beads were subjected to the following modifications prior to DNA extraction: 10 min of incubation with citrate buffer (37°C), as previously described by Capone and colleagues (Capone *et al.*, 2013), before vortexing (maximal speed, 3 min) and centrifugation (8000 g, 1 min). DNA integrity was checked by agarose gel electrophoresis. DNA quantity was evaluated using the Qubit dsDNA Broad Range Assay Kit (Invitrogen, Carlsbad, USA) with a Qubit 2.0 Fluorometer (Invitrogen, Carlsbad, USA). Samples were stored at -20°C prior to microbiota analysis (qPCR and 16S Metabarcoding).

1.2.6. Quantitative PCR

Total bacteria, Bacteroidetes and Firmicutes were quantified by qPCR. Primers and qPCR conditions are listed in **Table I.1**. Real-time PCR assays were performed in a Mx3005P apparatus (Stratagene, San Diego, USA) based on SYBR Green technology using Takyon™ Low Rox SYBR® kit (Eurogentec, Seraing, Belgium). Each reaction was run in duplicate in a final volume of 10 µL with 5 µL of Master Mix, 0,45 µL of each primer (10 µM), 1 µL of DNA sample (10 ng/µL) and, 3.1 µL of ultra-pure water. Amplifications were carried out using the following ramping profile: 1 cycle at 95°C for 5 min, followed by 40 cycles of 95°C for 30 s, 60°C for 1 min. A melting step was added to ensure primer specificity. Standard curves were generated from 10-fold dilutions of bacterial DNA (isolated from reference strain) and allowed the calculation of DNA concentrations from extracted samples.

1.2.7. 16S metabarcoding and data analysis

The bacterial V3-V4 region of 16S ribosomal DNA (rDNA) and the Archaeal 16S rDNA were amplified with primers described in **Table I.1**. Amplicons were generated using a Fluidigm Access Array followed by high-throughput sequencing on an Illumina MiSeq system (Illumina, USA) performed at the Carver Biotechnology Center of the University of Illinois (Urbana, USA). Raw data are available at NCBI under the Sequence Read Archive database with accession no. PRJNA638256. Bioinformatic analysis was performed with QIIME 2 (version 2020.2) (Bolyen *et al.*, 2019). Raw sequence data were demultiplexed and quality filtered using the q2-demux plugin followed by denoising with DADA2. Diversity analysis was estimated using q2-diversity after samples were rarefied. All amplicon sequence variants (ASVs) were aligned with mafft and used to construct a phylogeny with fasttree2. Taxonomy was assigned for Bacteria and Archaea to ASVs using the q2-feature-classifier coupled to SILVA release 132 database (Quast *et al.*, 2012).

Table I.1: Primers used for qPCR and 16S metabarcoding

Primer name	Sequence 5'-3'	Target	Annealing temperature (°C)	References
Primers qPCR				
BAC338R	ACTCCTACGGGAGGCAG	Total Bacteria	58	Yu *et al.* 2005

BAC516F	GTATTACCGCGGCTGCTG			
789cfbF	CRAACAGGATTAGATACCCT	*Bacteroidetes*	61	Bachetti De Gregoris *et al.* 2011
cfb976R	GGTAAGGTTCCTCGCGTAT			
928F-Firm	TGAAACTYAAAGGAATTGACG	*Firmicutes*	61	Bachetti De Gregoris *et al.* 2011
1040FirmR	ACCATGCACCACCTGTC			
Primers 16S				
V3_F357_N	CCTACGGGNGGCWGCAG	Bacteria	-	Klindworth *et al.* 2013
V4_R805	GACTACHVGGGTATCTAATCC		-	
Arch349F	GYGCASCAGKCGMGAAW	Archaea	-	Takai et Horikoshi, 2000
Arch806R	5GGACTACVSGGGTATCTAAT		-	

1.2.8. Gas and SCFA analysis

Analysis of O_2, N_2, CO_2, CH_4 and H_2 produced during the fermentation process was performed using HP 6890 gas chromatograph (Agilent Technologies, Santa Clara, USA) coupled with a micro-TCD detector (Agilent Technologies, Santa Clara, USA). Two series columns, Molecular Sieve 5A and Porapack Q (Aligent Technologies, Santa Clara, USA) were used. Gas composition was determined using calibration curves made from ambient air (78.09 % N_2, 20.95 % O_2, 0.04 % CO_2) and 3 gas mixtures A (5 % CO_2, 5 % H_2, 90 % N_2), B (19.98 % CO_2, 80.02 % H_2) and C (19.89 % CO_2, 19.88 % CH_4, 20 % H_2, 40.23 % N_2).

For SCFA analysis, two mL of luminal samples were centrifuged (5000 g, 15 min, 4°C) and 900 µL of supernatant were diluted at 1/10 in the H_2SO_4 0.04 M mobile phase, vortexed and filtered (0.22 µm). The three major SCFAs (acetate, propionate and butyrate) were quantified by high-performance liquid chromatography (HPLC) (Elite LaChrom, Merck HITACHI, USA) coupled with a DAD diode. The HPLC column (150x7.8 mm) contains a stationary phase of polystyrene divinylbenzene grafted with sulfonic groups, negatively charged and carries an eluent containing acidified water. Data were obtained and analyzed by the EZChrom Elite software at 205 nm. SCFAs concentrations were calculated from calibration curves established from known concentration solutions of acetate, propionate and butyrate (0, 10, 25 and 40 mM).

1.3. Results

1.3.1. Microbiota composition of initial fecal samples

Microbiota from starting stools (without any treatment) appeared highly different between the two donors (289 OTUs for donor A, 201 OTUs for donor B). As revealed by 16S metagenomics data, stool microbiota from donor A was mainly composed of *Firmicutes* (34 %), *Bacteroidetes* (33 %) and *Verrucomicrobia* (28 %) while donor B was almost exclusively constituted by *Firmicutes* (42 %) and *Bacteroidetes* (57 %) (**Suppl. Figure I.1**). Predominant family taxa (Stool samples, **Figure I.3)** emphasize divergences in the structure of fecal microbiota. The most abundant families in donor A were *Akkermansiaceae*

(29 %), *Ruminococcaceae* (16 %), *Bacteroidaceae* (15 %), *Rikenellaceae* (10 %), and *Lachnospiraceae* (9 %). Lower number of different families was identified for donor B with mainly *Bacteroidaceae* (50 %), *Ruminococcaceae* (19 %), *Lachnospiraceae* (14 %) and *Veillonellaceae* (8 %). In the same way, when considering species diversity on initial fecal samples, Shannon's indexes indicate that donor A exhibited a higher microbial diversity than donor B (5.5 *versus* 4.2) (Stool samples, **Figure I.4**). This important discrepancy was also confirmed by data from whole metagenome shotgun analysis performed on initial stools in the frame of another study (data not shown) with microbial richness higher in stool from donor A (326 species) compared to donor B (239 species). Methanogenic *Archaea* were detected only in the donor A's stool and identified as *Euryarchaeota*, *Methanobacteriaceae* and *Methanobrevibacter* at the phylum, family and genus levels, respectively (data not shown).

1.3.2. Effect of stool short-time storage on microbial composition and stabilization in M-ARCOL

In the present study, we assessed the effect of different preservative methods on luminal and mucus-associated gut microbiota composition and compared at each time point during fermentation to fresh stool used as a positive control. Two parameters were followed to determine the most efficient method: i) the time of stabilization of microbial profiles in M-ARCOL and ii) the microbiota profiles obtained after stabilization compared to the fresh stool.

Luminal medium – For the FS condition, total bacteria level reached and stabilized at 10^{10} copies of 16S rDNA/mL in the luminal phase at day 2 (qPCR data, **Figure I.5a**). Similar results were obtained for RFS and GFS conditions, while for LS condition, this stabilization level at 10^{10} copies of 16S rDNA/mL was only reached at day 4. Population levels of *Firmicutes* and *Bacteroidetes* stabilized at 10^{9} and 10^{10} copies of 16S rDNA /mL respectively, with a two-day delay for LS condition compared to the FS control and the two other experimental conditions (**Figure I.5b** and **Figure I.5c**). Regarding bacterial composition at the family level, stabilization time of major luminal populations is reached after 6-8 days (depending on the donor A or B) for all the preservative methods, as observed for control FS condition (**Figure I.3**).

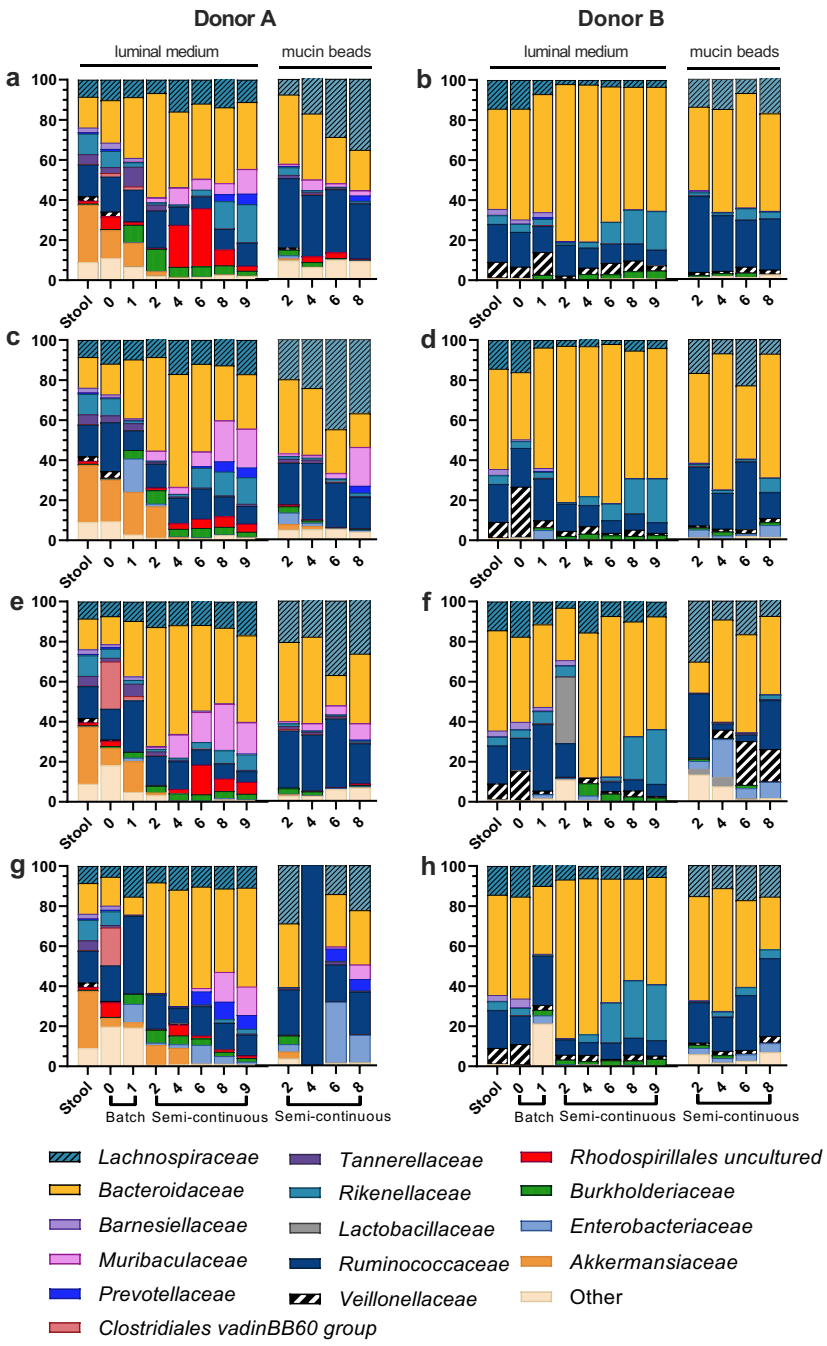

Figure I.3: Relative abundance of bacterial families retrieved in the initial stools and in the luminal medium and mucin beads from M-ARCOL. Fecal samples from two donors (donor A: left panel; donor B: right panel) were submitted to different preservative protocols: control non-treated fresh stool (FS, a and b), raw frozen stool (RFS, c and d), glycerol-frozen stool (GFS, e and f) and lyophilized stool (LS, g and h). The composition of luminal medium and mucin bead samples from M-ARCOL inoculated with fresh or treated stools was determined at the family level by analysis of 16S amplicon sequencing data.

At day 9 (end of the experiment), bacterial microbiota kept consistent differences between the two donors with families of *Bacteroidaceae* (33 % in donor A *versus* 62 % in donor B), *Rikenellaceae* (19% *versus*

19 %), *Muribaculaceae* (12 % *versus* 0 %), *Ruminococcaceae* (12 % *versus* 8 %), *Prevotellaceae* (5 % *versus* 0 %) and *Lachnospiraceae* (11 % *versus* 3 %). Microbial profiles of control and preservative treatments were comparable at the phylum level at day 9 (**Suppl. Figure I.1**), but differences may be highlighted for donor A at the family level. Specifically, *Prevotellaceae* decreased from 5 to 0.5 % in GFS, while *Rikenellaceae* decreased from 19 to 2 % in LS. Also, microbial profiles obtained for RFS were very similar to those from FS for both donors. Interestingly, *Akkermansiaceae* (from the *Verrucomicrobia* phylum), only present in donor A, disappeared after 2 days of semi-continuous fermentation from luminal medium in all conditions except for LS where these microbes persist until day 4 (**Figure I.3**). Species diversity of all luminal-associated microbiota defined by the Shannon's index was not affected during fermentation with values close to 5 in donor A and 3 in donor B (**Figure I.4**). β-diversity analysis revealed no impact of preservative treatment on microbial structure while samples highly clustered according to the donor (data not shown). Regarding methanogenic Archaea, whatever the treatment *Methanobrevibacter* population is present in the luminal phase of M-ARCOL and remains stable from day 2. In addition, *Archaea* were not impacted by any of the preservative techniques (data not shown).

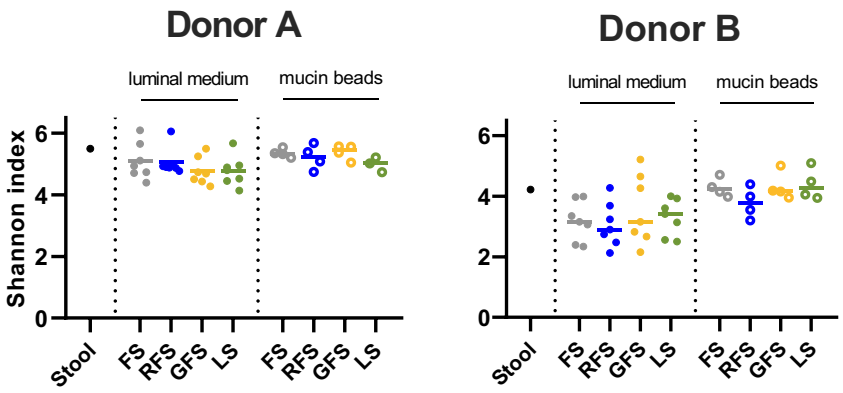

Figure I.4: Effect of different stool storage conditions on the Shannon diversity index values. Fecal samples from two donors (donor A: left graph; donor B: right graph) were submitted to different preservative protocols: control non-treated fresh stool (FS, in grey), raw frozen stool (RFS, in blue), glycerol-frozen stool (GFS, in yellow) and lyophilized stool (LS, in green). Shannon diversity indexes were determined in the initial stool and in the luminal medium and mucin beads samples collected from M-ARCOL inoculated with fresh or treated stools.

Mucin beads – For mucin beads, qPCR analysis revealed that total bacteria, *Bacteroidetes* and *Firmicutes* stabilized around 10^8 copies of 16S rDNA/mL for both FS and RFS conditions (**Figure I.5**). These populations stabilized at a slightly lower level for GFS, especially for *Bacteroidetes* (10^7 copies of 16S rDNA/mL), and the level of *Bacteroidetes* regularly decreased through the experiment for LS. At the phylum level, stabilization of the mucus-associated microbiota was reached between day 4 to 6 depending on the donor, for both FS and treated stool (**Suppl. Figure I.1**). At day 8, for donor A, no difference was observed between FS, RFS and GFS, whereas an increase in *Proteobacteria* was noticed in LS condition (14 % *versus* 2 % in FS) (**Suppl. Figure I.1**). For donor B, none of the profiles obtained at day 8 were similar from those of FS. In particular, GFS and LS conditions were characterized by an increase in *Actinobacteria* compared to control fresh stool (at day 8, 4 % and 1 % respectively *versus* 0.2 % for FS). At the family level, at the end of the experiments, all microbial profiles from processed tools originated from both donors differed from that of FS control (**Figure I.3**). For

donor A, RFS condition seemed to benefit *Muribaculaceae* (19 % *versus* 2.5 % in FS) while LS condition was associated with an increase in *Enterobacteriaceae* (14 % *versus* 0.1 % in FS). For donor B, *Enterobacteriaceae* also increased in all treatment conditions compared to FS (6 % for RFS, 8 % for GFS and 5 % for LS, *versus* 0.07 % for FS). In addition, *Veillonellaceae* proportion raised in GFS compared to FS (16 % *versus* 2 %), as well as *Ruminococcaceae* in LS compared to FS (39 % *versus* 25 %), at the expense of *Bacteroidaceae* (26 % *versus* 49 %). Interestingly, *Akkermansiaceae* was able to maintain in mucin beads up to day 4, with higher levels at day 2 in LS (3.4 %) and RFS (2.8 %) conditions compared to FS (1 %) and GFS (0.6 %). As for luminal medium, no difference in Shannon's index values was observed between treated and fresh stools for the mucin beads, with values close to 6 in donor A and 4 in donor B (**Figure I.4**). Similarly, β-diversity analysis revealed no impact of preservative treatment on mucus-associated microbiota (data not shown). *Archaea* were also detected in the mucin beads and *Methanobrevibacter* population was not impacted by any treatment (data not shown).

1.3.1. Effect of stool short-time storage on microbial activity in M-ARCOL

As an efficient fermentation yields to production of gut microbiota-derived metabolites among which SCFA and gas are important functional end-products, both were monitored in M-ARCOL. As previously described for microbiota composition, the efficiency of preservative methods was determined by analyzing stabilization time and comparing final levels with the one obtained for control FS.

Gas – Gas composition (CH_4, CO_2, N_2 and H_2) was determined in the atmospheric phase of M-ARCOL throughout fermentations and expressed as mean relative percentages (**Figure I.6**). O_2 levels remained during all the fermentations below 1 %, indicating that the anaerobiosis was efficiently maintained by the sole microbiota activity. In addition, CH_4 was detected only during experiments inoculated with fecal samples from donor A, in accordance with 16S metabarcoding data on methanogenic *Archaea*. For FS control condition, gas composition reached stable values at day 4 and day 3 in donor A and B, respectively.

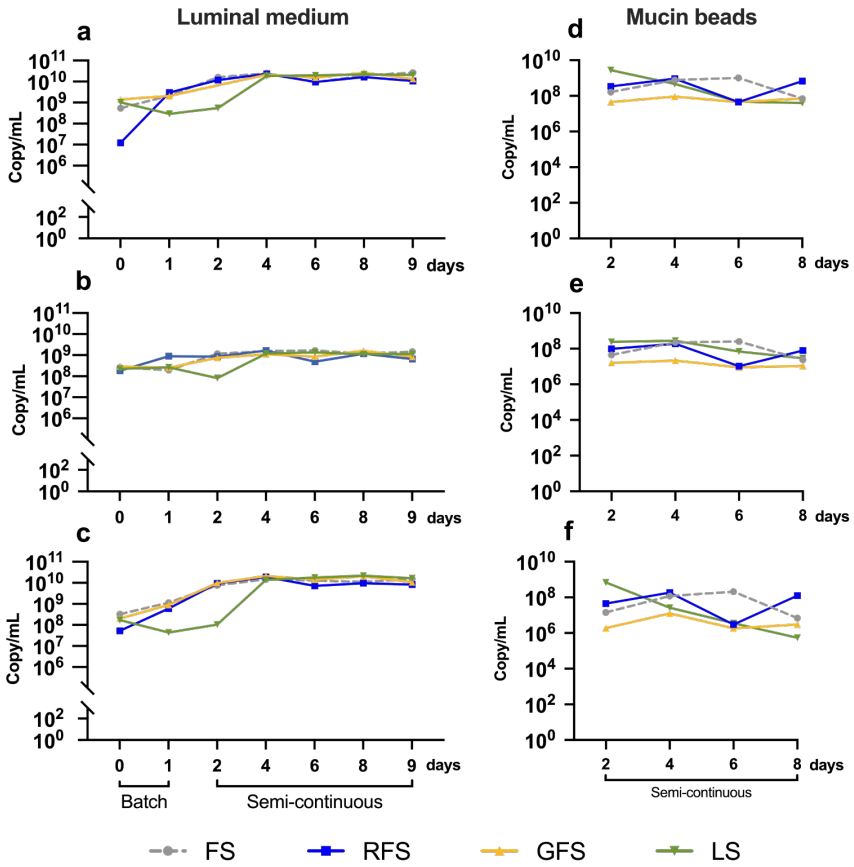

Figure I.5: Effect of different stool storage conditions on qPCR enumeration of main bacterial groups. Fecal samples from two donors were submitted to different preservative protocols: control non-treated fresh stool (FS, grey circles), raw frozen stool (RFS, blue squares), glycerol-frozen stool (GFS, yellow triangles) and lyophilized stool (LS, green triangles). Total bacteria (a and d), *Firmicute*s (b and e) and *Bacteroidetes* (c and f) were evaluated by qPCR in luminal medium (top panel) and mucin beads samples (bottom panel) collected from M-ARCOL inoculated with fresh or treated stools. Results are expressed as mean copy of 16S rDNA per mL (n=2).

Stabilization was reached at a similar period for all other tested conditions except for GFS in donor B where stable state was reached only after day 7. Stable gas pattern of donor A was composed of around 20 % N_2, 65 % CO_2 and 15 % CH_4, while that of donor B (non-methane producer) was characterized by about 20 % N_2 and 80 % CO_2. For donor A, gas profiles observed after stabilization were all similar to that of FS, even if H_2 production was observed until day 4 in GFS and LS conditions only. Conversely for donor B, all gas profiles after fecal storage differed from FS with a higher percentage of N_2 (40 *versus* 20 %) and consequently a lower percentage of CO_2 (60 *versus* 80 %). Uncommonly, an increase in H_2 production was noticed from day 3 to day 7 with GFS for donor B. On average, a higher total gas volume (1600 mL *versus* 1100 mL) was measured in LS condition when compared to FS (**Figure I.6i)**, mainly due to a sharp increase in gas production (multiply by 6 compared to FS) at day 1 (i.e. during batch experiment) (**Figure I.6j**). Lastly, during semi-continuous

fermentations, average daily gas production seemed to be lower for all the conservative methods compared to FS, and particularly for GFS condition.

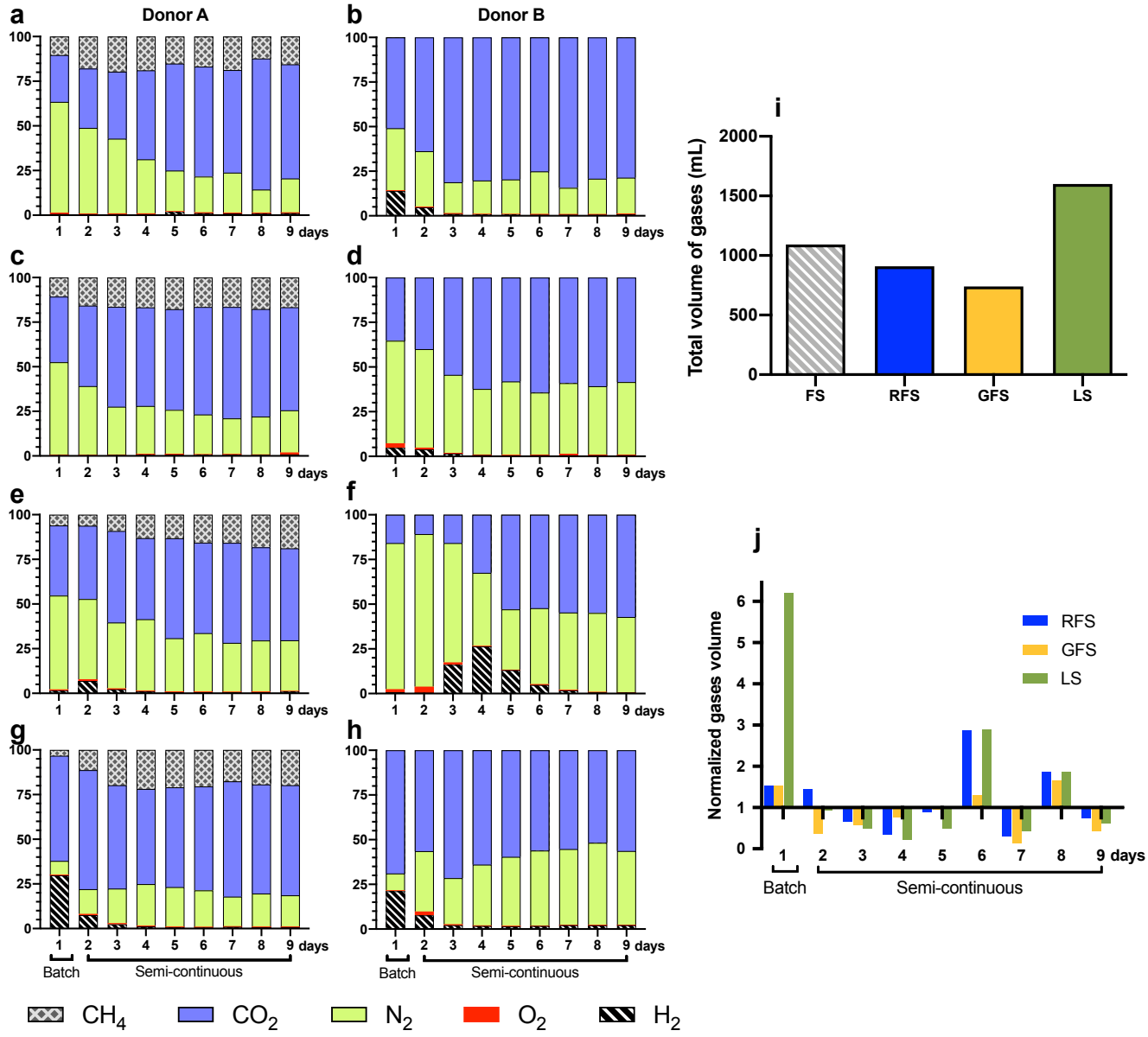

Figure I.6: Gas composition and production in M-ARCOL according to stool storage conditions. Fecal samples from two donors (donor A: left panel; donor B: right panel) were submitted to different preservative protocols: control non-treated fresh stool (FS, a and b), raw frozen stool (RFS, c and d), glycerol-frozen stool (GFS, e and f) and lyophilized stool (LS, g and h). Gas composition was analyzed by gas chromatography and results were expressed as relative percentages (graphs a to h) or as total mean volumes (in mL) produced during the fermentations (graph i). Daily gas volume productions were also averaged (n=2) and normalized to FS condition (graph j). *CH_4: methane, CO_2: carbon dioxide, N_2: nitrogen, O_2: dioxygen, H_2: dihydrogen.*

SCFA – The three main SCFAs, acetate, butyrate and propionate were quantified in the luminal medium of M-ARCOL and expressed as mean relative percentages (**Figure I.7a to 7h**). During the experiments with FS, SCFA profiles were stabilized at day 3 for the two donors. Similar stabilization time was observed for RFS

while an additional 1 or 2 days was necessary to reach stable profiles under GFS and LS conditions. At day 9 for the FS control, SCFA composition was stabilized with 48 % acetate, 30 % propionate and 22 % butyrate for donor A, compared to 58 % acetate, 22 % propionate and 20 % butyrate for donor B. Profiles obtained after stabilization for both donors are stackable with those obtained with FS regardless tested conditions (RFS, GFS or LS). As previously observed for microbial structure, stabilization profiles exhibited a more pronounced donor-dependent effect than a storage-dependent effect. However, for donor B, a distinct increase in acetate percentages was noticed from day 1 to day 4 with GFS **(Figure I.7f)**. When the total SCFA concentration was calculated throughout the total duration of the fermentation process **(Figure I.7i)**, similar levels were obtained for FS and RFS, while a slight increase was observed for LS (1420 mM *versus* 1220 mM) together with a greater decline for GFS (890 mM *versus* 1220 mM). These data are confirmed by the daily normalization of total SCFA concentrations with FS values (**Figure I.7i**). A sharp increase in SCFA production was evidenced at day 1 for LS (multiply by 2 *versus* FS) while reduced levels were maintained from day 2 to day 9 with GFS.

Redox potential – Redox potential was recorded during the overall fermentation process in M-ARCOL as an indicator of microbial fermentative activity (**Suppl. Figure I.2**). For FS control, stable levels were obtained from day 3 and low values confirmed an important reduced colonic environment (-225 mV). Similar or lower time was required to reach stabilization time for LS (3 days) and RFS (1 day) whereas increased time period was needed to obtain a stable redox potential for GFS (4 days). In addition, for donor B, abnormal elevated values were noticed until day 3 with GFS (up to +200 mV). However, once stabilized, all conditions showed similar levels compared to FS.

1.4. Discussion

Inoculation of *in vitro* gut models with fecal samples from patients or healthy donors aims to reproduce the complexity and diversity of the microbial ecosystem encountered within human colon, with obvious differences in microbial structure and activity compared to initial stools due to faecal-colon and *in vivo-in vitro* transitions. Use of fresh stools is not always feasible, defining an appropriate preservation method of fecal samples is crucial to prevent loss of important microbial populations and maintain efficient fermentation activities in the bioreactor. To date, a unique study had investigated the effects of preservation methods on the gut microbial structure and functions using the TIM-2 *in vitro* human colon model (Aguirre *et al.*, 2015). For the first time, in the current study, we assessed the effect of three preservation methods on the luminal and mucus-associated microbiota using M-ARCOL *in vitro* gut model and, in a unique way, we investigated both the bacterial and archaeal populations. As fecal microbiota exhibits important inter-individual variability, this study was conducted on fecal samples collected from two healthy donors, chosen to represent “extreme” conditions, i.e. donor A is a methane producer female while donor B is a non-methanogen male (Chaudhary, Conway & Schlundt, 2018; Kim *et al.*, 2020). Likewise, donor A harbors a much higher microbial diversity

than donor B, very likely associated due to differences in dietary habits (De Filippis *et al.*, 2016; De Angelis *et al.*, 2019).

Figure I.7: SCFA composition and production in M-ARCOL according to stool storage conditions. Fecal samples from two donors (donor A: left panel; donor B: right panel) were submitted to different preservative

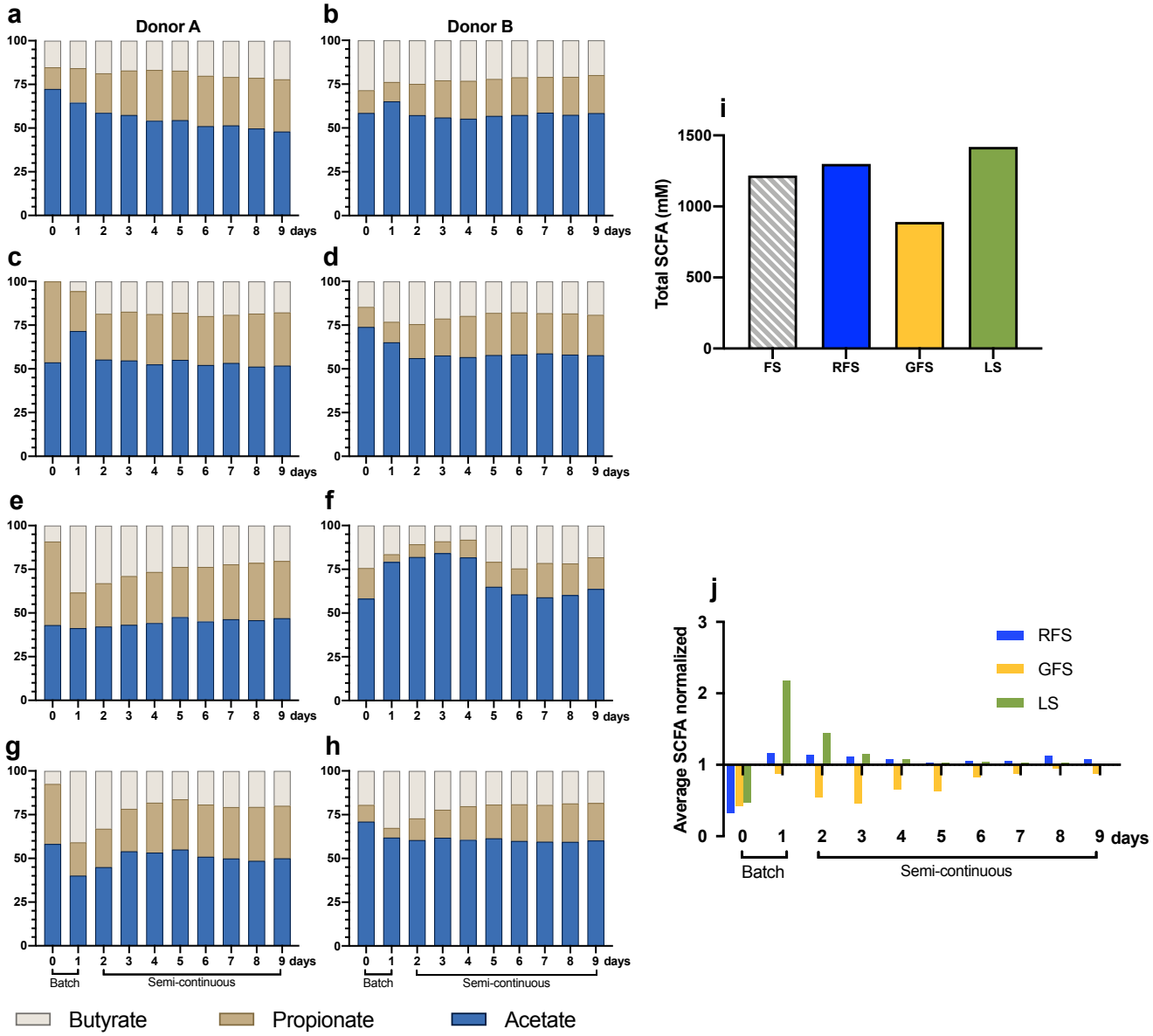

protocols: control non-treated fresh stool (FS, **a** and **b**), raw frozen stool (RFS, **c** and **d**), glycerol-frozen stool (GFS, **e** and **f**) and lyophilized stool (LS, **g** and **h**). Main SCFA (acetate, propionate and butyrate) were analyzed by liquid chromatography and results were expressed as relative percentages (graphs **a-h**) or as total mean concentrations (in mM) produced during the fermentations (graph **i**). Daily SCFA concentrations were also averaged (n=2) and normalized to FS condition (graph **j**). *SCFA: short chain fatty acids.*

Conservative treatments used previously by others for stool conservation were tested before inoculation of M-ARCOL and compared to the fresh stool condition. The simplest alternative to fresh feces is stool freezing at -80°C without any preservative treatment nor fecal samples mixing ("raw" samples), leading to the RFS condition in our study. To improve the stability of fecal microbiota during freezing and subsequent storage,

different cryoprotectants have been previously described in the literature, such as dimethyl sulfoxide, polyethylene glycol, RNA later, ethanol or glycerol (Gorzelak *et al.*, 2015; Flores *et al.*, 2015; Khanna *et al.*, 2016; Gaci *et al.*, 2017). This later (GFS condition) has been chosen as it is undoubtedly the most frequently applied for bacterial storage and currently recommended and used in clinical practice for fecal microbiota transplantation (Cammarota *et al.*, 2017, 2018, 2019). Lastly, lyophilization has been tested as a new alternative to freezing for fecal sample storage (LS condition) since various protocols of this process have been recently developed for fecal microbiota transplantation (Burz *et al.*, 2019; Reygner *et al.*, 2020). Lyophilization with trehalose/maltodextrin solutions appears as a suitable mean for preserving highly sensitive oxygen populations and sub-dominant species (Burz *et al.*, 2019; Reygner *et al.*, 2020). This preservation method also allows the maintenance of major functional activities of gut microbiota and a better revivification after reheating. Maltodextrin and trehalose sugars increase media viscosity, thus limiting crystallization and osmotic disturbance to prevent cell lysis (Al *et al.*, 2018; Burz *et al.*, 2019). Interestingly, Reygner and colleagues demonstrated that freeze-drying in maltodextrin/trehalose or freezing in glycerol better preserved SCFA for 12 months storage compared to samples frozen without any cryoprotectant (Reygner *et al.*, 2020). In the present study, the time of storage was restricted to 48 hours for all the tested conditions as our primary aim was to study the impact of preservative methods and not that of storage which is recognized to further influence microbial structure and activity (Song *et al.* 2016, Gaci *et al.* 2017).

To offer a complete picture of the effects of such preservative methods on gut microbiota in *in vitro* gut models, we investigated in M-ARCOL both luminal and mucus-associated gut microbiota and fermentation activity through gas and SCFA measurements. Mucin beads were recently integrated in M-ARCOL based on a technology similar to that implemented in M-SHIME (Van den Abbeele *et al.*, 2009), with some adaptations allowing the physiological maintenance of anaerobiosis through microbiota activity. *In vitro* colonic models involving a mucosal phase represent a valuable alternative to consider the fine-scale spatial organization present *in vivo* in the human gut microbial ecosystem. In particular, mucin beads allow a better capture of initial fecal microbial diversity and favor the development of specific mucus colonizers (e.g. *Ruminococcaceae* and *Lachnospiraceae*) and thus the restoration of a high *Firmicutes*/*Bacteroidetes* ratio, as observed *in vivo* (Liu *et al.*, 2018). Our results showed that all the preservative treatments allowed the maintaining inside M-ARCOL of a complex and functional microbiota for the two donors A and B. Interestingly, methanogenic Archaea are not impacted by the treatments neither in luminal nor in mucosal phase. Maintaining anaerobiosis without flushing with N_2 or CO_2 is certainly a key parameter enabling the persistence of *Archaea in vitro* (Gaci *et al.*, 2017). Nevertheless, applying preservative methods seemed to limit the expansion of some dominant populations normally present in the mucosal phase, leaving the opportunity for *Proteobacteria* (e.g. *Enterobacteriaceae*) and *Actinobacteria* (mainly with GFS) to colonize this ecological niche. In particular, *Enterobacteriaceae* (opportunistic pathobionts and enteric pathogens) are well-known efficient colonizers of unoccupied ecological niches after transient changes in microbiota composition (Kamada *et al.*, 2013; Chassaing *et al.*, 2014).

To represent all the facets of the human colonic ecosystem, stabilization time was evaluated on both microbial activity (gas and SCFA measurement) and composition (qPCR and 16S rRNA sequencing). In control

condition (FS), a stabilization period of 2-3 days was necessary for metabolic activities compared to 6-8 days for microbiome structure, in accordance to previous studies in *in vitro* gut models (Zihler Berner *et al.*, 2013; Fehlbaum *et al.*, 2015). Therefore, when considering all these parameters, a stabilization time of 8 days (corresponding to 8 residence times) was observed in the M-ARCOL, in accordance to Tottey *et al.*, (2015). Differences in stabilization time and/or in final stabilized levels for each parameter analyzed compared to FS control were observed, indicating that freezing stool without any preservative (RFS condition) was the most efficient method, followed by lyophilization and then freezing with glycerol. These results are in accordance with the studies from Tang and colleagues demonstrating that frozen fecal microbiota is as effective as fresh fecal sample for fecal microbiota transplantation (Tang, Yin & Liu, 2017) and from Choo's study showing the efficiency of freezing at -80°C without cryoprotectant (Choo *et al.*, 2015). Similarities between fresh and raw frozen stools can be explained by the absence of stool mixing and destructuration that may help microbiota to withstand temperature decrease. Compared with raw fecal freezing, freezing with 10% glycerol or lyophilization increased *in vitro* stabilization time in the bioreactor with notable changes in SCFA and gases production. This could be explained by the important microbial metabolism of cryoprotectants at the beginning of fermentations that may negatively affect repeatability between experiments. An increased level of acetate was thus observed until day 4 for glycerol-treated stool experiment of donor B, reflecting glycerol metabolization by gut microbiota-acetate producers (De Weirdt *et al.*, 2010). These results contrast with those from Aguirre and colleagues that did not observe any modifications of SCFA production in the TIM-2 after one week freezing at -80°C with 1.5 g glycerol (Aguirre *et al.*, 2015). This difference may be explained by different settings between the two studies, since in TIM-2 study, storage time was longer while the total duration of the fermentation experiment was shortened, and mucin beads were absent. A sharp increase in gas and SCFA production was also evidenced in both donors with lyophilized samples, which may reflect the consumption by gut microbiota of maltodextrin, an intermediate product of starch hydrolysis, and trehalose, a diholoside (Collins *et al.*, 2018). In general, adding glycerol as a preservative agent led to a reduced metabolic activity compared to all the other conditions, suggesting cellular damage during the preservative step. Interestingly, 16S metabarcoding demonstrated that lyophilization seemed to preserve beneficial microbes such as *Akkermansiaceae* (only identified in donor A) for a longer period than for the other treatments, as previously described (Burz *et al.*, 2019; Reygner *et al.*, 2020).

Our results showed that raw freezing of stools is the most efficient short-term preservative technique. Other parameters, such as technical constraints, need to be considered to determine the most appropriated method to inoculate *in vitro* gut bioreactors (**Table I.2**). Shipping frozen stools is challenging since the samples require specific preserving containers (usually shipping proceed with dry ice). Samples can face temperature fluctuations during storage (freezing failure due to power outage) and transport (exposure to high temperatures that increase the risk of thawing-freezing cycles) that may influence further microbial colonization and activity in *in vitro* gut models. Lyophilized stool samples encompass the above concerns and represent a good alternative since they are easier to deliver (no requirement of specific freezing containers), they can be stored at room

temperature and require less storage capacity. However, this technique requires time and expensive specific equipment (freeze dryer price is about 8 to 55 k$).

To conclude, the present study gives useful insight into the effects of short-term stool preservative methods, namely freezing and lyophilization, on further gut microbiota structure and fermentation activity in an *in vitro* model of the human colon. All the preservative treatments allowed the maintaining inside M-ARCOL of a complex and functional microbiota. Considering both stabilization time of microbial profiles and metabolic activities, we showed in the current study that 48 h freezing at -80°C without cryoprotectant was the most efficient method. This result has to be balanced by technical constraints associated with the use of frozen fecal materials.

Table I.2: Scientific and technical comparative data on preservative methods applied to fecal samples. From low € to high €€€€ costs; from low ★ to high ★★★★ score. F/B ratio: *Firmicutes*/*Bacteroidetes* ratio; ↗ increase or ↘ decrease; NA: not applicable.

				Fresh stool	Raw frozen stool	Glycerol frozen stool	Lyophilized stool
Scientific aspects (compared to FS)	Composition	Stabilization time		Day 6-8	Day 6-8	Day 6-8	Day 6-8
		Final microbial profiles		NA	No loss of microbial diversity as measured by Shannon index Increase of *Proteobacteria* and *Actinobacteria* in the mucin beads		
	Activity	Stabilization time	Gas	(A) day 4 (B) day 3	(A) day 3 (B) day 4	(A) day 5 (B) day 7	(A) day 4 (B) day 5
			SCFA	(A) day 3 (B) day 3	(A) day 2 (B) day 3	(A) day 5 (B) day 7	(A) day 4 (B) day 4
		Final metabolic profiles		NA	↗ N_2 (donor B)	↗ N_2(donor B) ↘ Total gas and total SCFA production	↗ N_2 (donor B) ↗ Total gas production
	Score (/5)			5/5	4/5	2/5	3/5
Technical requirements	Preparation steps			No	One step (i) Freezing	Two steps (i) Preparation including sterilization of the glycerol solution (ii) Freezing	Three steps (i) Preparation including sterilization of the maltodextrin/trehalose solution (ii) Freezing (iii) Lyophilization
	Time to implement the method			Immediate	Immediate	Up to 2 hours	Up to 2 hours
	Duration of storage			Few hours	Months (Dorsaz *et al.* 2020)	Months (Costello *et al.* 2015)	Years (Reygner *et al.*, 2020)
	Costs			€	€€	€€€	€€€€
	Storage facility			No storage	★	★	★★★
	Ease of sending			★★	★★	★★★	★★★★
	Score (/5)			4/5	3/5	3/5	4/5
TOTAL RANKING				**1**	**2**	**3**	**2**

Author's contributions EML and BDS conceived and designed research. FE, LF, DC and UO performed the experiments, analyzed and interpreted data. VC provided technical assistance during fermentations and SCFA analysis. CC, KN and TM helped to design lyophilization protocol. CMS and AM provided help for bioinformatics analysis. EML, BDS, FE and DC wrote the manuscript with input from co-authors. All authors critically revised and approved the manuscript.

Acknowledgments The authors thank Dr Ghislain Garrait and Dr Sylvain Denis for technical assistance with lyophilization and *in vitro* fermentation.

Declarations

Fundings This work was supported by fellowships from Ministère de la Recherche (France) to F. E. and MITACS (Canada) to L. F., OBFIBRE SCUSI grant from Auvergne Rhone Alpes Region to D.C. and PSPC-Bpi France RESTORBIOME funding for consumables.

Conflicts of interest/Competing interests (include appropriate disclosures). The authors declare that they have no conflict of interest.

Ethics approval (include appropriate approvals or waivers) No ethical approval was obtained because this study did not involve a prospective evaluation, did not involve laboratory animals and only involved non-invasive procedures (fecal sample collection).

Availability of data and material (data transparency).

1.5. Supplementary figures

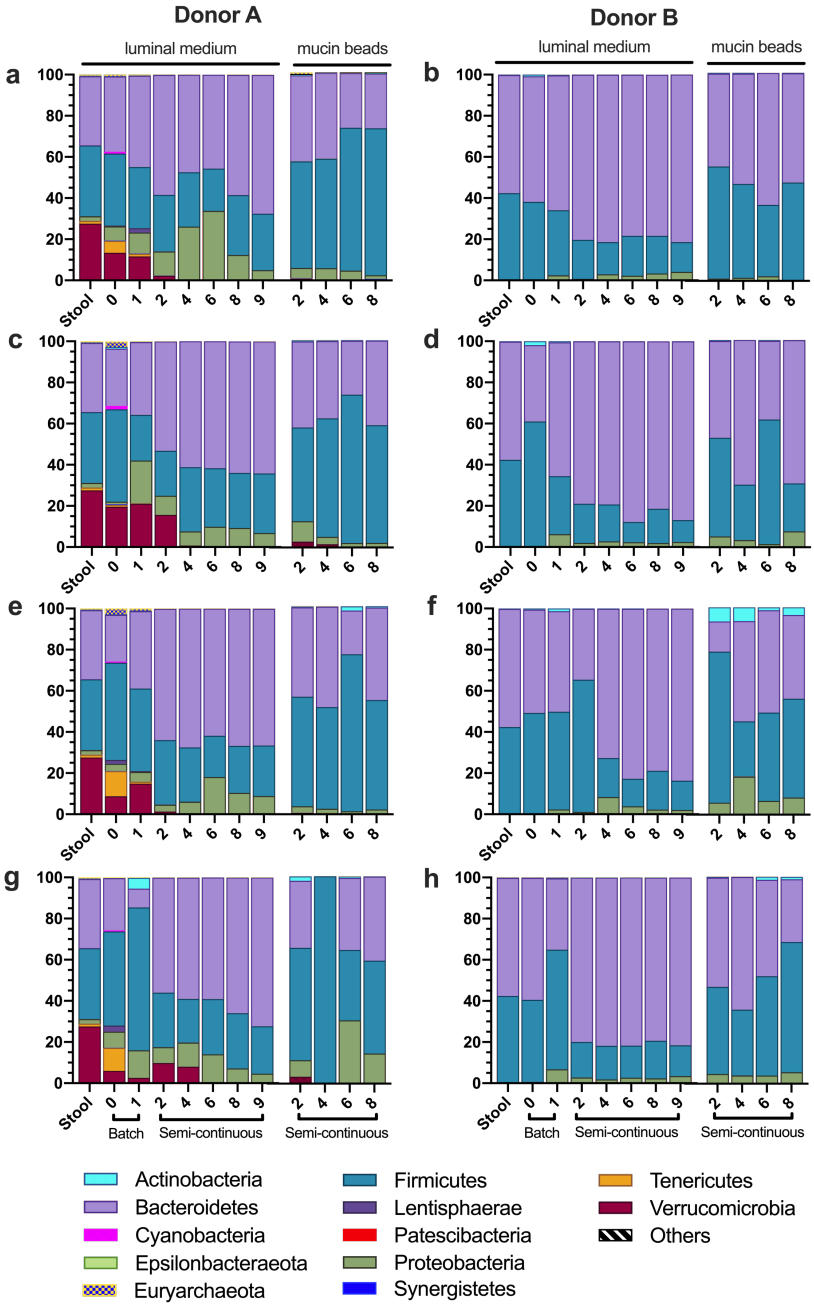

Supplementary figure I.1: Effect of different stool storage conditions on community structure at the phylum level. Fecal samples from two donors (donor A: left panel; donor B: right panel) were submitted to different preservative protocols: control non-treated fresh stool (FS, **a** and **b**), raw frozen stool (RFS, **c** and **d**), glycerol-frozen stool (GFS, **e** and **f**) and lyophilized stool (LS, **g** and **h**). The composition of luminal medium and mucin bead samples from M-ARCOL inoculated with fresh or treated stools was determined at the phylum level by analysis of 16S rDNA gene abundance. *FS: fresh stool, RFS: raw frozen stool, GFS: glycerol-frozen stool, LS: lyophilized stool.*

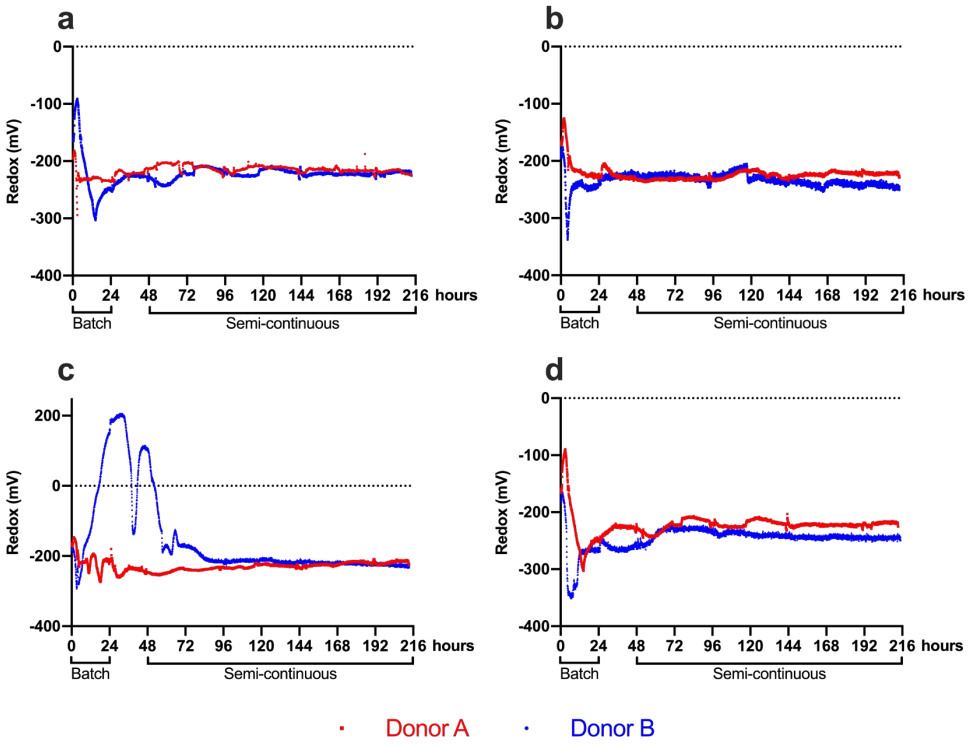

Supplementary figure I.2: Redox potential values measured in the M-ARCOL. Fecal samples from two donors (donor A in red; donor B in blue) were submitted to different preservative protocols: control non-treated fresh stool (FS, graph **a**), raw frozen stool (RFS, graph **b**), glycerol-frozen stool (GFS, graph **c**) and lyophilized stool (LS, graph **d**). Redox potential values were daily measured in the M-ARCOL inoculated with fresh or treated stools. *FS: fresh stool, RFS: raw frozen stool, GFS: glycerol-frozen stool, LS: lyophilized stool.*

1.6. Conclusion on canine faecal sample preparation and storage

In this study, we have demonstrated that freezing human faeces at -80°C without cryoprotectant until 48 h didn't impact the time needed for stabilization of microbial profiles and metabolic activities in the M-ARCOL and the profiles obtained. Regarding stools from canine origin, there is currently no guideline for collection, storage, and preparation of faecal samples. Recently, authors have investigated the effect of faecal sampling method applied to dog stools on the abundance of microbial populations and bacterial metabolites (Pinna *et al.*, 2021). Subsamples were collected from the surface to the inner part of the stools and from three equally sized areas all along the faecal materials, and therefore homogenized. Compared to the stool surface, inner subsamples resulted in greater concentrations of SCFA and ammonia and lower pH values. Because there are volatile compounds, the hypothesis was made that some evaporation during contact to ambient air may have impacted surface SCFA concentrations. However, qPCR targeting Firmicutes, Bacteroidetes, *Clostridium* cluster I, *Lactobacillus spp*., *Bifidobacterium spp*. and *Enterococcus spp*. didn't show any significant difference between subsamples. Authors concluded on the necessity for homogenization of the whole stool before sampling. A recent study has also evaluated the impact of temperature collection and stabilization strategies during storage on canine faecal microbiota (Lin *et al.*, 2020). The authors compared freshly extracted samples to unstabilized faecal samples stored at room temperature and stabilized samples placed in a PERFORMAbiome•GUT collection device stored at different temperatures or undergoing repeated freeze-thaw cycles. Sample stabilization allowed protection against alteration at 37°C and 50°C for up to 3 days, at room temperature for up to 14 days and permitted undergoing until 6 freeze-thaw cycles. No impact of temperature on both alpha and beta diversities was evidenced on stabilized samples, while alpha-diversity increased in unstabilized samples stored at room temperature for 14 days, showing growth of microorganisms. Sequencing also revealed an alteration of relative abundances of dominant phyla (i.e. Firmicutes, Fusobacteriota, Bacteroidota and Actinobacteriota) and 24 genera in unstabilized samples stored at room temperature, whereas no significant change was observed for stabilized samples under similar storage condition. In addition, authors showed a significant intra-sampling variation with a modification in the relative abundances of 9 genera depending on collection sites within a canine faecal sample. Of note, this was previously demonstrated in human faeces by Gorzelak *et al.*, (2015) and confirmed the importance of stool homogenization before sampling. A single study has evaluated the impact of storage period on *in vitro* microbial activities. Effect of chilling or freezing canine faeces for 24 h on gas production and fermentation end-products was evaluated in 72h-batch fermentation model (Bosch *et al.*, 2013). Freezing decreased maximum rate of gas production and increased overall indole or phenol concentrations depending on fermentation substrates. However, chilling for 24h in crushed ice have maintained fermentation characteristics of initial fresh stools. Considering those results, it was decided for all the experiments of this thesis to make a particular attention on **homogenization of the entire stool** before sampling. In addition, as far as possible, **fresh canine feces** was used. If necessary, freezing **raw feces at -80°C for 12h** without cryoprotectant and under anaerobic condition was applied.

Chapter 2 – Canine Mucosal Artificial Colon: *in vitro* simulation of physicochemical and microbial colonic ecosystem adapted to different dog sizes

After an in-depth review of the available literature to characterize both microbial, nutritional and physicochemical parameters of dog digestion, we observed that important modifications exist between small, medium and large dogs, especially related to the large intestine. In particular, colonic transit time, colonic pH, but also bile acids profiles and also industrial feed composition were different (e.g. type of fibers or ratio of soluble/insoluble fiber) between the three sizes. Then, we referenced all available *in vitro* canine gut models and emphasized that most of them reproduce canine lower (and not upper) gastrointestinal tract but using simple batch vessels. Only one *in vitro* dynamic model (M-SCIME) reproduces efficiently the canine colon of medium size dogs. In this context, the next step is this PhD work was to develop a new relevant and dynamic *in vitro* colonic model reproducing the specific digestive conditions associated to different dog sizes. This new model is based on M-ARCOL technology, first developed to simulate human then porcine large intestine. Of interest this system allows to distinguish the luminal and mucus-associated microbiota thanks to a mucin-beads compartment. In the frame of this work, we collaborated for stool collection with Dr Nathalie Priymenko from Toxalim team and the 'École Nationale Vétérinaire de Toulouse' (ENVT) to find canine donors meeting our criteria for feeding, age and body weight. Main BCFA measurement and bile acid identification and quantification were performed in collaboration with Pr Tom Van de Wiele (CMET, Ghent University, Belgium), Dr Ignacio Ipharraguerre (Institute of Human Nutrition and Food Science of Kiel, Germany) and Mrs. Inma Alvarez-Acero (Institute of Food Science of Madrid, Spain). This work was submitted for publication in *ALTEX*.

ORIGINAL ARTICLE

Canine Mucosal Artificial Colon: *in vitro* simulation of physicochemical and microbial colonic ecosystem adapted to different dog sizes

DESCHAMPS, C., DENIS, S., HUMBERT, D., PRIYMENKO, N., CHALANCON, S., DE BODT, J., VAN DE WIELE, T., IPHARRAGUERRE, I., ALVAREZ-ACERO, I., ACHARD, C., APPER, E., & BLANQUET-DIOT, S. (**2023**)

Submitted in ALTEX (**IF 6.25**)

For the entire manuscript this article will be cited as **Deschamps *et al.* (2023a)**.

Abstract

Differences dog breeds sizes of are an important determinant of variations in digestive physiology, mainly related to the large intestine. *In vitro* gut models are increasingly used as an alternative to animal experiments for technical, cost, societal and regulatory reasons. Up to now, only one *in vitro* model of the canine colon incorporates the dynamics of different canine gut regions, yet no adaptations exist to reproduce size-related digestive parameters. To address this limitation, we developed a new model of the canine colon, the CANIne Mucosal ARtificial COLon (CANIM-ARCOL), simulating main physiochemical (pH, transit time, anaerobiosis), nutritional (ileal effluent composition) and microbial (lumen and mucus-associated microbiota) parameters of this ecosystem, and adapted to three dog sizes (i.e. small under 10 kg, medium 10-30 kg and large over 30 kg). To validate the new model regarding microbiota composition and activities, *in vitro* fermentations were performed in bioreactors inoculated with stools from 13 dogs (4 small, 5 medium and 4 large). After a stabilization period, microbiota profiles clearly clustered depending on dog size. *Bacteroidota* and *Firmicutes* abundances were positively correlated with dog size both *in vitro* and *in vivo*, while opposite trends were observed for *Actinobacteria* and *Proteobacteria*. As observed *in vivo*, microbial activity also increased with dog size *in vitro*, as evidenced from gas production, short-chain fatty acids, ammonia and bile acid dehydroxylation. In line with the 3R regulation, CANIM-ARCOL could be a relevant platform to assess bilateral interactions between food and pharma compounds and gut microbiota, capturing inter-individual or breed variabilities.

Keywords: dog, large intestine, microbiota, *in vitro* gut model, body weight

2.1. Introduction

Digestion is a complex and regionalized process involving physicochemical, mechanical and microbial mechanisms and, as for other mammals, is acknowledged as a crucial element in canine health, with an increased awareness of the central role of gut microbiota (Redfern *et al.*, 2017; Mondo *et al.*, 2019). Since dogs are facultative carnivores, their digestion is processed by a short and simple gastrointestinal tract adapted to high-protein and high-fat diets (Kararli, 1995). More than 400 canine breeds have been genetically selected by humans, leading to huge variations in size, weight, and appearance, but also to changes in digestive anatomy and genetic profile adaptation, such as the apparition of amylase-encoding gene (Axelsson *et al.*, 2013; Botigué *et al.*, 2017). How canine digestion is influenced by dog size was recently reviewed (Deschamps *et al.*, 2022b), highlighting that most of identified variations were related to the large intestinal compartment. Large intestine length, area and volume were shown to increase with dog weight, in association with a higher colonic transit time. In close relation with this longer transit time, fermentative capacity and especially fiber degradation seems to be amplified with body weight (Weber *et al.*, 2002b; Detweiler *et al.*, 2019; Nogueira *et al.*, 2019), resulting in an important production of short-chain fatty acids (SCFA) in large dogs and a lower colonic pH (Weber *et al.*, 2004). Fecal concentrations of phenol, indole, ammonium and branched-chain fatty acids (BCFA) were also positively correlated with body weight, again probably in relation to the longer colonic transit time favoring protein fermentation (Goudez *et al.*, 2011; Beloshapka, Wolff & Swanson, 2012; Beloshapka *et al.*, 2014;

Alexander *et al.*, 2019). This is in accordance with an increased abundance of fecal *Fusobacteria* with body weight (Gazzola *et al.*, 2017; Kim *et al.*, 2017; Algya *et al.*, 2018). Fecal bile acid profiles are also impacted by dog sizes, with an apparent decrease of total bile acids, as well as primary to secondary bile acid ratios, when body weight increases (Guard *et al.*, 2019). Lastly, the intestinal mucosa of large dogs is also characterized by a higher permeability which could induce a backflow of electrolyte absorbed and explain their poorer faecal consistency (Bjarnason *et al.*, 1995; Zentek & Meyer, 1995; Weber *et al.*, 2002a, 2017). In-depth characterization of the variations with dog sizes of colonic physicochemical parameters and microbiota composition and functions is of high interest, especially because those factors can reshape not only essential processes such as nutrient digestibility but also drug bio-accessibility (notably for colon-targeted formulations) or probiotic/enteric pathogen survival and activity.

Even if *in vivo* experiments still remain the ultimate goal in nutrition or pharma studies, the use of animals in research is more and more limited by ethical, regulatory and cost reasons. The number of dogs used in research and testing has decrease of 26 % between 2018 and 2019 but 13,076 dogs were still involved in European countries in 2019 (European Commission, 2022). Among them, more than 2000 were used for legislation on medicinal products for veterinary use and over 8100 for human use (European Commission, 2022). The European 3Rs rules widely encourage the use of alternative strategies such as *in vitro* models reproducing digestion or fermentation processes occurring within the gut. Up to now, most of the *in vitro* systems developed to reproduce the canine large intestine are simple static batch models (Sunvold *et al.*, 1995c; Tzortzis *et al.*, 2004; Bosch *et al.*, 2008; Cutrignelli *et al.*, 2009; Panasevich *et al.*, 2013; Vierbaum *et al.*, 2019; Van den Abbeele *et al.*, 2020b; Oba *et al.*, 2020). These models are inoculated with dog stools, but most of them have not been adapted to the canine specific digestive environment. In addition, they cannot simulate colonic transit time and are limited to 24-72 h experiments due to a shift in major parameters such as pH, preventing the evaluation of repeated administration of drugs or food compounds. Only one dynamic model called M-SCIME (Mucosal Simulator of the Canine Intestinal Microbial Ecosystem) was very recently developed to reproduce the canine GI tract from the stomach to the large intestine, with a distinction between the luminal and mucus-associated microbiota in the colon (Duysburgh *et al.*, 2020; Verstrepen *et al.*, 2021). This model is based on semi-continuous fermentation processes in the three colonic parts, allowing to reproduce *in vivo* parameters such as pH evolution, transit time, supply of non-digested nutrients and anaerobiosis by continuous N_2 flushing. However, up to date, none of the available models, including the M-SCIME, was set up to differentiate colonic conditions depending on dog's size.

In this context, the aim of this study was to develop and *in vivo* validate a new *in vitro* model of the canine colon adapted to dog body weight, as a relevant alternative to animal assays. Based on the continuous fermentation Mucosal Artificial Colon Model (M-ARCOL) (Deschamps *et al.*, 2020), the newly developed system aims to accurately reproduce both the physicochemical, nutritive and microbial parameters specific to the colonic ecosystem of three different dog's sizes, namely "small" (under 10 kg), "medium" (from 10 to 30 kg) and "large" (over 30 kg).

2.2. Materials and methods

2.2.1. Fecal sample collection and treatment

Feces from 13 clinically healthy dogs of several breeds, ages and weights (see **Table II.1** and **Figure II.1** for details) were collected. All dogs were adult owner-pets and fed with commercial dry food. They had a body score condition of 3 under a 5-points scale, meaning all of them had a normal body weight. Immediately after defecation, fecal samples were transferred into a sterile recipient, placed in an airtight anaerobic box (GENbag anaer gas pack systems, Biomerieux, France), transported and frozen at -80°C within 6 h until processing in the next 24 h. In an anaerobic chamber (COY laboratories, USA), stool samples were manually homogenized, and 3.3 g of feces was resuspended with 30 mM sterile sodium phosphate buffer (pH 6.0) to reach a total volume of 100 mL. Because of the small amount of feces provided by small size dogs, only 1.8 g can be resuspended into 100 mL for donor S1 and 2.1 g for donor S2, S3 and S4. Feces were then mixed and filtered using a 500 µm inox sieve.

Table II.1: Characteristics of healthy adult dogs included in the study and ranked by small, medium and large dog sizes. *M: male, F: female, BCS: body condition score (ranging from 1 -very thin- to 5 -obese-, 3 corresponding to ideal weight)*

Size	*Dog_id*	*Breed*	*Sex*	*Sterilization*	*Age (years)*	*BCS*	*Weight (kg)*	*Garden access*	*Feed*
Small	S1	Shih Tzu	M	No	6	3	5	No	Dry
	S2	Chihuahua	F	No	7	3	1,9	Yes	Dry
	S3	Cavalier King Charles	F	No	5.5	3	8	No	Dry
	S4	Spitz	F	Yes	2	3	4	No	Dry
Medium	M1	Border collie x Beauceron	M	Yes	2.5	3	30	Yes	Dry
	M2	French bulldogged	F	Yes	6	3	13	Yes	Dry
	M3	Border collie	M	Yes	6	3	18	Yes	Dry
	M4	Flat coater Retriever	F	No	2.5	3	28	Yes	Dry
	M5	Golden Retriever	F	No	6.5	3	29	Yes	Dry
Large	L1	Saint-Bernard	M	No	6	3	80	Yes	Dry
	L2	Beauceron	F	Yes	3	3	40	Yes	Dry
	L3	Leonberg	F	No	3	3	52	Yes	Dry
	L4	German Shepherd	M	No	5	3	42	Yes	Dry

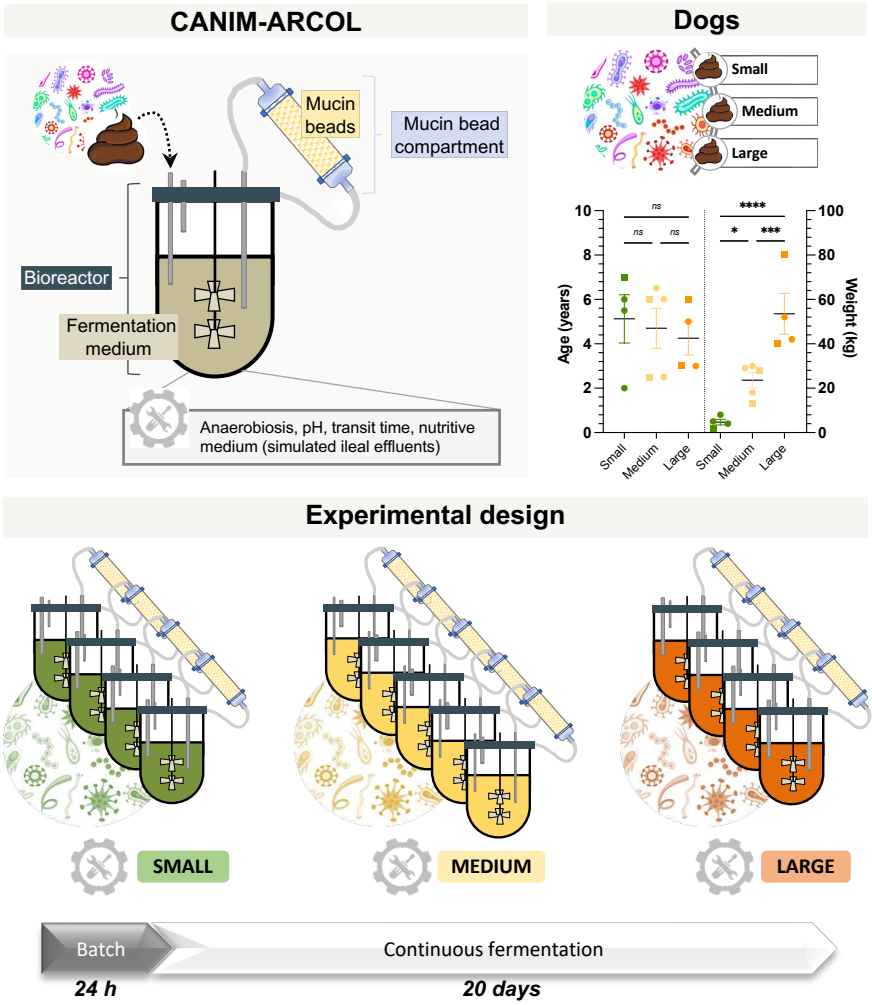

Figure II.1: Overview of experimental design in the CANIM-ARCOL model.

Once adapted to three dog sizes conditions, the CANIM-ARCOL was inoculated with fecal samples from 13 healthy dogs (n=4 small in green, n=5 medium in yellow and n=6 large in orange) and fermentations were run for 21 days. Age and weight of all dogs involved in the study (males and females are represented by square and circle, respectively) were plotted and significant differences were analyzed by one-way ANOVA (mean ± SD, *: $p<0.05$; ***: $p<0.001$; ****: $p<0.0001$). Samples were regularly collected in the atmospheric phase, in the luminal compartment and from mucin beads to monitor microbiota composition and metabolic activities.

2.2.2. Description and parameters of CANIM-ARCOL model

The newly developed Canine Mucosal Artificial Colon (CANIM-ARCOL) was adapted from the one stage continuous fermentation system previously set-up under human condition and called M-ARCOL (Deschamps *et al.*, 2020). The *in vitro* model allows to reproduce both luminal and mucosal phases of the large intestine by the use of respectively a bioreactor (MiniBio, Applikon, The Netherlands) and an airtight glass vessel connected to the bioreactor and containing mucin beads (**Figure II.1**). At the beginning of the experiment, 100 mL of faecal suspension were added per bioreactor to 200 mL of canine-adapted nutritive medium simulating the composition of ileal effluents (**Table II.2**) and containing various sources of carbohydrates, proteins, lipids, minerals, and vitamins. After an initial sparging of O_2-free N_2-gas, anaerobiosis was maintained during the total course of the fermentation by the sole activity of the resident microbiota and through ensuring the system airtightness. Bioreactor was kept at body temperature. Colonic pH and redox potential were constantly recorded (Applikon, The Netherlands) and pH was adjusted with 2 M NaOH. The nutritive medium was continuously introduced into the bioreactor, while the fermentation medium was automatically withdrawn, ensuring the appropriate mean retention time and maintaining the colonic volume constant. The mucosal compartment was dived in a water bath maintained at body temperature. It was filled with mucin-alginate beads offering an overall surface of 556 cm2 in average. The mucin/alginate solution was dropped using a peristaltic pump into a sterile solution of 0.2 M $CaCl_2$ dihydrate under agitation. Every 2 days, mucin/alginate beads remaining into the mucosal compartment were renewed by fresh sterile ones under a constant flow of CO_2 to avoid oxygen entrance.

In the present study, the *in vitro* colon model was adapted to reproduce the mean conditions found in the large intestine of healthy adult dogs and adapted to three canine sizes as summarized in **Table II.2** and detailed in the result part. Briefly, temperature was set at 39°C, residence time and pH were revised according to *in vivo* data and set-up at 5 h and pH 6.5 for small, 9 h and pH 6.5 for medium and 15 h and pH 6.2 for large dog conditions, respectively. The composition of the nutritive medium was also adapted to three dog size diet and digestive physiology.

2.2.1. Experimental design and sampling

Experimental design in the CANIM-ARCOL is presented in **Figure II.1**. In all the experiments, each bioreactor was inoculated with a fecal sample from a unique donor (from either small, medium or large dogs). Bioreactors corresponding to one dog size were run in parallel (n=4 for small and large conditions and n=5 for medium ones) and set-up with specific parameters. Fermentations were run under batch conditions for 24 h and then under continuous conditions for 20 additional days. Samples were collected daily in the fermentative medium (corresponding to the luminal phase) for analysis of microbiota composition (qPCR and 16S Metabarcoding) and metabolic activities through short chain fatty acids (SCFA), branched chain fatty acids (BCFA), total bile acids and ammonia dosage. The atmospheric phase was also sampled to follow anaerobiosis and evaluate gas composition and production thanks to a sampling bag connected to the condenser (**Figure II.1**).

Table II.2: Adaptation of physicochemical and nutritional parameters of CANIM-ARCOL to three dog sizes. *rpm: rotation per minute.*

Size	*Small*	*Medium*	*Large*
Weight (kg)	**< 10**	**10-30**	**> 30**
Bioreactor's parameters			
Temperature	39 °C	39 °C	39 °C
Residence time	5 h	9 h	15 h
pH	6.6	6.5	6.2
Stirring	400 rpm	400 rpm	400 rpm
Nutritive medium composition (in %)			
Proteins	17.2	27.0	35.6
Carbohydrates	0.9	1.3	1.8
Lipids	1.6	2.4	3.2
Fibers	3.3	5.2	6.8
Bile acids composition in the nutritive medium (mg/L)			
Cholic acid (CA)	108 mg 35 %	55 mg 10 %	32 mg 5 %
Chenodeoxycholic acid (CDCA)	31 mg 10 %	27 mg 5 %	32 mg 5 %
Deoxycholic acid (DCA)	124 mg 40 %	327 mg 60 %	418 mg 65 %
Lithocholic acid (LCA)	46 mg 15 %	136 mg 25 %	161 mg 25 %

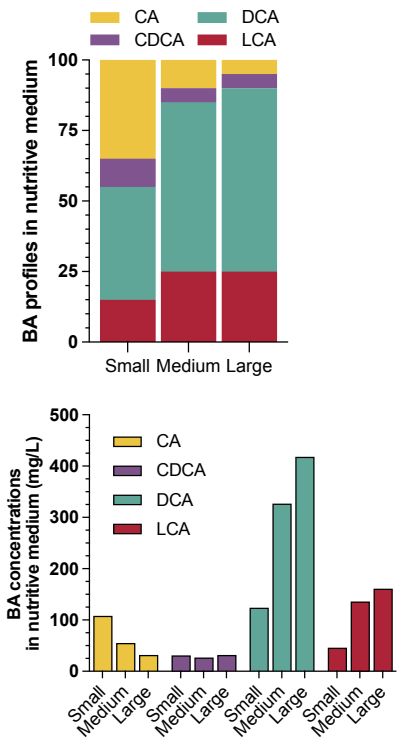

Every two days, mucin beads were collected for mucus-associated microbiota analysis (qPCR and 16S metabarcoding). Mucin beads were washed twice in sterile sodium phosphate buffer and stored at -80°C before downstream analysis.

2.2.2. DNA extraction

Genomic DNA was extracted from fermentative medium samples and mucin/alginate beads using the QIAamp Fast DNA Stool Mini Kit (Qiagen, Germany) following manufacturer's instructions with the following modifications. Prior to DNA extraction, luminal samples were centrifuged (18 000 rcf, 15 min, 4°C) and the pellets were collected. Pellets and mucin/alginate beads samples were then incubated 10 min with sterile citrate buffer (sodium citrate 55 mM and NaCl 154 mM) at 37°C (Capone *et al.*, 2013), before vortexing (maximal speed, 15 sec) and centrifuge again (8000 rcf, 1 min). Then, a step of mechanical disruption using a bead beater (5 min, 20 beat/s) was made with 300 mg sterile glass beads (diameter ranging from 100 to 600 µm). DNA quantity was evaluated using the Qubit dsDNA Broad Range Assay Kit (Invitrogen, USA) with a Qubit 3.0 Fluorometer (Invitrogen, USA). Samples were stored at -20°C prior to microbiota analysis (qPCR and rRNA 16S Metabarcoding).

2.2.3. Quantitative PCR

Total bacteria were quantified by qPCR using primers described in **Table II.3**. Real-time PCR assays were performed in a Biorad CFX96TM Real-Time System (Bio-Rad Laboratories, USA) using Takyon Low ROX SYBR 2X MasterMix blue dTTP kit (Eurogentec, Belgium). Each reaction was run in duplicate in a final

volume of 10 µL with 5 µL of MasterMix, 0.45 µL of each primer (10 µM), 1 µL of DNA sample, and 3.1 µL of ultra-pure water. Amplifications were carried out using the following ramping profile: 1 cycle at 95 °C for 5 min, followed by 40 cycles of 95 °C for 30 s, 58 °C for 30 sec. A melting step was added to ensure primer specificity. Standard curve was generated from 10-fold dilutions of bacterial DNA (isolated from a pure culture of bacteria), allowing the calculation of DNA concentrations from extracted samples.

Table II.3: Primers used for qPCR and 16S Metabarcoding analysis

Primer names	*Sequence 5'-3'*	*Target*	*Annealing temperature (°C)*	*References*
qPCR primers				
BAC338R	ACTCCTACGGGAGGCAG	Total bacteria	58	Yu *et al.* (2005)
BAC516F	GTATTACCGCGGCTGCTG			
Metabarcoding primers				
V3_F357_N	CCTACGGGNGGCWGCAG	Bacteria	-	Klindworth *et al.* (2013)
V4_R805	GACTACHVGGGTATCTAATCC			
Arch349F	GYGCASCAGKCGMGAAW	*Archaea*	-	Takai and Horikoshi (2000)
Arch806R	5GGACTACVSGGGTATCTAAT			

2.2.4. 16S Metabarcoding and data analysis

Bacterial V3-V4 regions of 16S ribosomal DNA (rRNA) and the archaeal 16S rRNA were amplified using primers described in **Table II.3**. Amplicons were generated using a Fluidigm Access Array followed by high throughput sequencing on an Illumina MiSeq system (Illumina, USA) performed at the Carver Biotechnology Center of the University of Illinois (Urbana, USA). Raw data are available at NCBI under the Sequence Read Archive database with accession number PRJNA955438. Bioinformatic analysis were performed using R studio software and helped by rANOMALY package (Theil & Rifa, 2021). Prior to analysis, raw data were demultiplexed and quality filtered using DADA2 R-package (Callahan *et al.*, 2016). Reads with quality score under 2 were truncated. Reads under 100 pb length were removed as well as sequences similar to PhiX DNA used as a spike-in control for MiSeq runs. Filtered sequences were dereplicated and cleaned for chimeras (DADA2). Taxonomic classification of the sequences was then performed with DECIPHER package (Murali *et al.,* 2018). Assignations from both SILVA 138 release (Quast *et al.*, 2013) and GTDB_bac120_arc122 (Parks *et al.*, 2022) databases were merged using the assign_taxo_fun function from rANOMALY R-package based on IDTAXA, with a 60% confidence cut-off (Theil & Rifa, 2021). A phylogenetic tree was then reconstructed using DECIPHER.

2.2.5. Gas analysis

Analysis of O_2, N_2, CO_2, CH_4, and H_2 gas produced during the fermentation process was performed using 490 micro-gas chromatography (Agilent Technologies, USA) coupled with a micro-TCD detector (Agilent Technologies, USA). Molecular Sieve 5A and Porapack Q (Aligent Technologies, USA) series columns were used. Gas composition was determined using calibration curves made from ambient air (78.09 % N_2, 20.95 % O_2, 0.04 % CO_2) and three gas mixtures A (5 % CO_2, 5 % H_2, 90 % N_2), B (20 % CO_2, 80 % H_2), and C (20 %

CO_2, 20 % CH_4, 20 % H_2, 40 % N_2). Technical replicates were performed for each sample and results were expressed as relative percentages.

2.2.6. Fatty acid analysis

For SCFA analysis, 1.5 mL of luminal samples were centrifuged (18 000 rcf, 15 min, 4°C) and 900 µL of supernatant was diluted at 1/10 into H_2SO_4 0.04 M mobile phase, vortexed, and filtered (0.22 µm). The three major SCFAs (acetate, propionate, and butyrate) were quantified by high-performance liquid chromatography (HPLC) (Elite LaChrom, Merck HITACHI, USA) coupled with a DAD diode. The HPLC column (Concise Separations, ICE-99-9865) and its guard column were maintained at 50°C. Sulfuric acid 0.04 M was used as mobile phase and SCFA were separated at a flow rate of 0.6 mL/min. Data were obtained and analyzed by the EZChrom Elite software at 205 nm. SCFA concentrations were calculated from calibration curves established from known concentration solutions of acetate, propionate, and butyrate (0, 10, 25, and 40 mM) and data expressed as mM or relative percentages. BCFA (isobutyrate, isovalerate, valerate, isocaproate, caproate, heptanoate) were measured by gas chromatography (GC-2014, Shimadzu®, The Netherlands) with a DB-FFAP 123-3232 column (30 m x 0.32 mm x 0.25 µm; Agilent, Belgium) and a flame ionization detector (FID). Liquid samples were conditioned with sulfuric acid and sodium chloride and 2-methyl hexanoic acid as internal standard for quantification and further extracted with diethyl ether. Prepared sample (1 µL) was injected at 280ºC with a split ratio of 60 and a purge flow of 3 mL min^{-1}. The oven temperature increased by 6ºC min-1 from 110ºC to 158ºC and by 8°C min-1 from 158°C to 175°C where it was kept for 1 min. FID had a temperature of 220ºC. The carrier gas was nitrogen at a flow rate of 2.49 mL/min. BCFA concentrations were calculated from calibration curves established from known concentration of pure solutions of each fatty acid and data expressed as mM or relative percentages.

2.2.7. Bile acids quantification and ammonia dosage

For bile acids extraction water:acetonitrile (1:1) and CDCA-d4 as the internal standard were used. Bile acids were quantified by HPLC-QQQ-MS, employing as external standards cholic acid (CA), deoxycholic acid (DCA), lithocholic acid (LCA), chenodeoxycholic acid (CDCA), glycodesoxycholic acid (GDCA), glycolic acid (GCA), taurodeoxycholic acid (TDCA), taurocholic acid (TCA), hyodeoxycholic acid (HDCA), ursodeoxycholic acid (UDCA), and hyocholic acid (HCA) in a range of concentrations between 5 and 0.001 µg/mL. The separation was done using a Phenomenex Kinetex XB-C18 100A column, ammonium acetate 2 mM in water and acetonitrile: methanol (1:1) as mobile phases and a constant flow rate of 1 mL/min at a temperature of 50ºC. The HPLC used was an Agilent 1200 coupled to a Triple Quadrupole (QQQ) Agilent (G6410B). Data processing was performed with Masshunter Qualitative Analysis (B.07.00), and quantification performed in the multiple reaction monitoring mode by integration of ion areas based on standard curves using authentic standards and chenodeoxycholic acid-d4 as internal standard (IS).

Total ammonia was measured using the Ammonia assay kit (LIBIOS, France) following manufacturer's instructions. Results were expressed in mM.

2.2.8. Statistical analysis

Statistical analyses on microbiota activity (gas, SCFA, BCFA, ammonia, total bile salts) and α-diversity indexes (number of observed ASVs and Shannon index) from metabarcoding data were processed using GraphPad Prism software version 9.4.1 (GraphPad Software, USA). Data normal distribution was verified by combining Anderson-Darling, D'Agostino & Pearson, Shapiro-Wilk and Kolmogorov-Smirnov tests and homoscedasticity was checked using the Fisher test. Then, appropriate statistical analysis was applied (either one-way ANOVA, *t*-test, Mann-Whitney or Welch's tests). First, principal coordinate analysis (PCoA, data not shown) were performed followed by Non-Metric Multidimensional Scaling (NMDS), highlighting important size and microenvironment (i.e. luminal medium and mucin beads) effects. Constraint Redundancy analysis (RDA) were then performed with age, weight, sex, size, microenvironment, donor and time as variables of the model, first will all parameters and then with removal of either size or microenvironment variables. Bray Curtis distances were used for each analysis and significance between groups was assessed with a one or two-way Anova. Discriminant analyses (sPLS-DA) were finally performed using MixOmics package (Lê Cao, González & Déjean, 2009).

2.3. Results

2.3.1. Characterization of canine donors and faecal microbiota

Stool samples from 13 adult dogs (including 5 females and 8 males), gathered into three size groups as previously defined (i.e. small, medium and large), were collected to inoculate CANIM-ARCOL bioreactors. Mean body weights of the dogs were respectively 4.7 ± 1.3, 23.6 ± 3.4 and 53.5 ± 9.2 kg for small, medium and large dogs with, as expected, significant differences between those three groups (**Figure II.1**). Mean ages were respectively 5.1 ± 1.0, 4.7 ± 0.9 and 4.3 ± 0.8 years, with no significant differences between groups (**Figure II.1**).

Microbiota composition and key microbial metabolites were characterized in the initial stools as a global description of the biological material used for bioreactor inoculation (**Suppl. Figure II.1**). Metabarcoding analysis showed at phylum level a higher abundance of *Firmicutes* and a lower amount of *Fusobacteriota* in the large dogs compared to other sizes (**Suppl. Figure II.1D**). A high variability in microbial profiles at the family level was also noticed between different dog sizes and between individuals (**Suppl. Figure II.1D**), body weight being the predominant explanatory variable (P=0.001) for dissimilarities in fecal microbiota composition (**Suppl. Figure II.1B**). Interestingly, total SCFA increased with dog size ($p>0.05$, **Suppl. Figure II.1E**) while BCFA showed opposite trends ($p<0.0001$, **Suppl Figure II.1G**) and no clear tendency was observed for ammonia (**Suppl**. **Figure II.1I**) and total bile acids (data not shown). Profiles obtained for SCFAs (**Suppl**. **Figure II.1F**), BCFAs (**Suppl**. **Figure II.1H**) and bile salts (**Suppl. Figure II.1J**) also showed size-dependent effects. Note that heptanoic acid was found only in the fecal samples from small dogs, and in high relative abundance (**Suppl**. **Figure II.1H**).

2.3.2. Set-up of the *in vitro* model with specific canine size-related colonic parameters

2.3.2.1. Colonic physicochemical parameters

Temperature was set at 39°C for all size groups according to veterinary recommendations. Regarding pH, there is no study evaluating colonic pH of small and large dogs and only two in medium dogs. Koziolek *et al.,* (2019) described a pH from 5 to 8 and Smith, (1965) reported a pH of 6.5 but none specified dog diet even if it is well known to influence gastrointestinal pH (Scarsella *et al.*, 2020). From our previous literature review (Deschamps *et al.*, 2022b), we determined faecal pH mean values of 6.6, 6.5 and 6.2 respectively for small, medium and large dogs. Since these data are in accordance with the negative correlation between fecal pH and canine body weight described in the literature (reviewed in Deschamps *et al.*, (2022b)), and the value for medium dogs was in line with that of Smith (1965), those three values were chosen for the model set-up (**Table II.2**). Lastly, a previous study showed that large intestinal transit time can be estimated as a percentage of total transit time, with a positive correlation between large intestinal transit time and body weight (Hernot *et al.*, 2006). Authors established that the large intestinal transit time represents 40, 55 and 70 % of total transit time for small, medium and large dogs, respectively. Applicated to the mean total transit times established from our literature review for each dog size (in total 23 studies, (Deschamps *et al.*, 2022b), we calculated average large intestinal transit time of 10, 18 and 30 h for small, medium and large dog, respectively. Those estimations were fully in line with *in vivo* data from studies which estimated this digestive parameter in various dog sizes (Bruce *et al.*, 1999; Hernot *et al.*, 2006; Boillat *et al.*, 2010; Lidbury *et al.*, 2012; Gazzola *et al.*, 2017; Koziolek *et al.*, 2019). When applied to the *in vitro* model, this led to residence time (time for renewal of half of fermentation medium) of 5, 9 and 15h, respectively (**Table II.2**).

2.3.2.2. Nutrient supply in simulated ileal effluents

The canine nutritive medium simulating ileal effluent composition was adapted from that initially developed for human by Macfarlane *et al.* (1998) and typically used in the M-ARCOL model (Deschamps *et al.*, 2020), as summarized in **Table II.2**. Composition was adapted to consider canine dry diet composition and energetical requirements for the three dog sizes, as well ileal digestibility indices for each type of nutrients. Calculations were based on a mean energy requirement of respectively 730, 1160 and 1523 kcal/day for small, medium and large dogs (Case *et al.*, 2011). Quantities of nutrients supplied to the *in vitro* model (simulated ileal effluents) were calculated assuming that they are corresponding to the fraction that has been not digested and absorbed in the upper gut. Thus, the percentage of nutrients delivered into the colon was estimated as the difference between food intake and ileal digestibility. Since no study had evaluated the ileal digestibility of macronutrients in small and large dogs, we used the data available from medium dogs for all size conditions (Bednar *et al.*, 2000; Flickinger *et al.*, 2003; Propst *et al.*, 2003; Hendriks *et al.*, 2013), i.e. 77, 95 and 99 % of initial intake for protein, lipid and carbohydrate, respectively. Protein sources were adapted with 80 and 20 % from animal and vegetal origin, respectively, to cover the entire set of amino acids (FEDIAF, 2019). Lipids were given by addition of linoleic acid (poly-unsaturated omega-6 fatty-acid) and palmitic acid (essential

saturated fatty acid for dogs) (FEDIAF, 2019). Regarding carbohydrate sources, purified starch from corn, rice and wheat (1/3 each) were added in the *in vitro* nutritive medium based on in-field proportion (commercial dry food). The same quantity of fiber per day and per kg body weight was provided for each size group but the ratio between soluble to insoluble fibers was changed according to dog size (Weber *et al.*, 2017). Therefore, a 70/30, 50/50 and 30/70 soluble to insoluble ratio was applied for small, medium and large conditions, respectively. Based on 2 g fibers/100 g of dry food, soluble fibers were provided in the *in vitro* nutritive medium by 22 % pectin, 53 % inulin and 25 % oligosaccharides (2/3 fructo-oligosaccharides and 1/3 mano-oligosaccharides), while insoluble fibers were given by a 50/50 ratio of arabinogalactan and cellulose.

2.3.2.3. Bile acid content

Faecal total bile acids were quantified in all dog sizes in only one study (Guard *et al.*, 2019) and measured 5.1, 4.7 and 3.4 µg bile acids/mg lyophilized feces for small, medium and large dogs, respectively. The amount of total bile acids per gram of fresh stools was then estimated as 1657.5, 1428.8 and 958.8 µg for small, medium and large dogs, respectively, based on a faecal moisture tendency curve established by Weber's team (Weber *et al.*, 2004). To further estimate bile acids amount transiting in the large intestine within 24 h, we considered in the calculations the colonic transit time associated to each size group and the amount of feces produced per day, i.e. 5.6 g feces/kg body weight/24 h (Algya *et al.*, 2018). This led to a total amount of bile acids in the nutritive medium per 24 h of 445, 432 and 257.5 for small, medium and large dogs, respectively (**Table II.2**). Primary to secondary bile acids ratio of 40/60, 15/85 and 10/90 for small, medium and large conditions, respectively, were determined according to Guard *et al.*, (2019). Composition in major bile acids (i.e. cholic acid, chenodeoxycholic acid, lithocholic acid and deoxycholic acid) was also estimated using Guard quantifications.

2.3.2.4. In vitro stabilization of colonic microbiota

CANIM-ARCOL was used to run colonic fermentations using small, medium or large parameters (as described above) and inoculated respectively with small, medium and large canine stools. Gut microbiota activity and composition were followed daily to determine the time period necessary for microbiota stabilization. The stabilization state was generally reached after 7 to 10 days based on individual gas (**Suppl**. **Figure II.2**) and SCFA (**Suppl**. **Figure II.3**) profiles, even if gas profiles for most of small dogs still fluctuated at the end of fermentation (especially methane production). As expected, after stabilization, anaerobiosis was efficiently maintained by the sole activity of resident microbiota with percentages of oxygen remaining below 4 %. At the phylum level (**Suppl. Figure II.4**), microbiota composition was also generally stabilized after 10 days both in the luminal and mucosal compartments, even if in some donors and/or under large dog conditions, stabilization was difficult to reach. Taken together, those data indicated that at least 10 days were necessary to stabilize the canine microbiota composition and activity. Redundancy analysis (RDA) confirmed that this time period is sufficient to reach stabilization in the *in vitro* colon model since no significant time effect could be observed from day 10 to day 21 in both luminal and mucosal compartments, whatever the dog size (time effect was significant including days 1 to 21, data not shown) (**Figure II.2C**). Stabilization in the CANIM-ARCOL was also associated to a decrease in microbial richness and evenness compared to the initial stool (**Figure II.2A**

and **2B** and **Suppl. Figure II.1A**), as previously reported in other *in vitro* models (Van den Abbeele *et al.*, 2010b; Deschamps *et al.*, 2020). The stabilization was also associated with a shift from faecal (**Suppl**. **Figure II.1D**) to colonic profiles (**Suppl**. **Figure II.4**), mainly characterized by an increase in relative abundance of *Bacteroidota* in accordance with *in vivo* data (Suchodolski *et al.*, 2008; Honneffer *et al.*, 2017).

2.3.3. Region-specific colonic microbiota composition and inter-individual variability

We also observed for the first time in a canine *in vitro* colon model, whatever the size conditions, a significant difference using constraint RDA approach ($p<0.001$) between lumen and mucus associated microbiota after stabilization, as shown by RDA analysis of microbiota composition (**Figure II.2D**). At the phylum level (**Suppl**. **Figure II.4**), for all dog sizes, higher abundances in Firmicutes together with lower amounts of Fusobacteriota were noticed in the mucosal microenvironment compared to the luminal one. Discriminant analysis showed that ASVs identified as *Ruminococcus* sp. and *Sporanaerobacter acetigenes* were enriched in the mucosal compartment (**Figure II.3A**). On the contrary, the luminal phase was enriched in *Fusobacterium mortiferum* and different ASVs identified as *Sutterella stercoricanis*. Of note, the mucus compartment was associated to a higher number of observed ASVs compared to the luminal phase, whatever the dog size (**Figure II.2A** and **2B**). The CANIM-ARCOL model also allows to capture inter-individual variabilities in microbial profiles. As an example, *Rikenellaceae* and *Dethiosulfovibrionaceae* were only found in the bioreactor inoculated with the fecal sample from donor S3, while *Negativicocacceae* were only observed for M1 and *Anaerovoraceae* for L2 (**Figure II.4**). Regarding metabolic profiles, important methane levels (up 25 % at the end of fermentation) were observed in the small dogs (especially in bioreactors inoculated with stools from S2 and S3 dogs), while CH_4 production did not exceed 0.1 % in the medium and large size conditions. This was linked with the identification of methanogenic *Archaea* sequences (**Suppl**. **Figure II.5**) in both the lumen and mucus-associated microbiota of small dog bioreactors only. Whatever the colonic microenvironment, Archaea were identified as *Methanobrevibacter smithii* (data not shown).

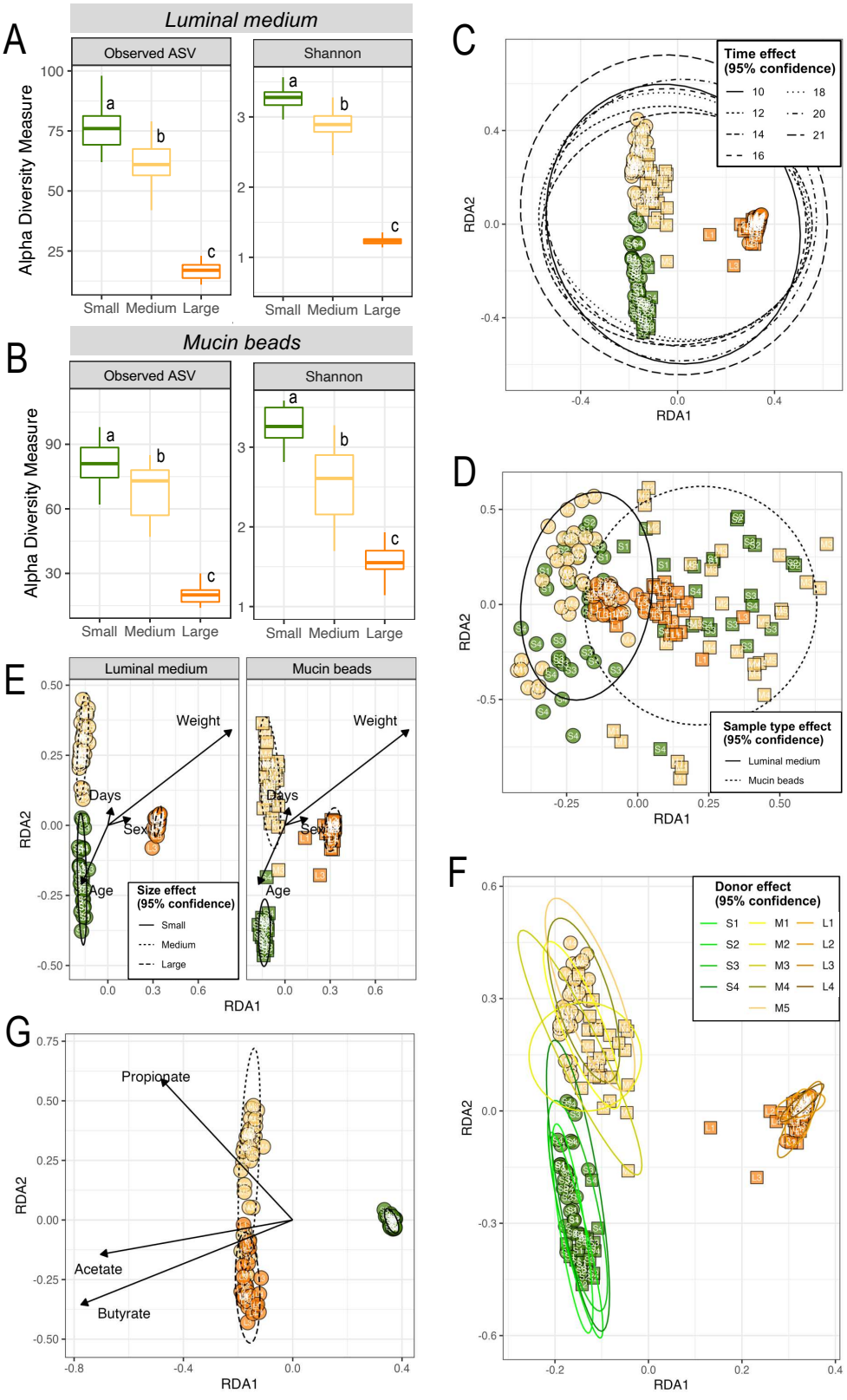

Figure II.2: Impact of dog sizes on α and β-diversity of microbial populations in the CANIM-ARCOL model. Fermentations were performed in the CANIM-ARCOL under three dog size conditions. Lumen and mucus-associated microbiota composition were analyzed by 16S Metabarcoding and diversity indexes were calculated based on ASV table. Only stabilized points (from days 10 to 21) are represented. α-diversity (observed ASVs and Shannon index) is represented as box plots in the luminal medium (**A**) and mucin-beads (**B**), with significant differences indicated by different letters ($p<0.05$). Redundancy analysis (RDA) two-dimension plot visualizations reported bacterial community β-diversity, showing the effects of fermentation time (**C**), dog size (**E**) or donor effect (**F**). Size effect was removed (partial-RDA) to visualize the impact of colonic microenvironment, i.e. luminal medium or mucin beads (**D**). For luminal samples only, corresponding SCFA concentrations were added as environmental variables and RDA was recalculated accordingly (G). Samples from luminal medium are represented in circles while mucin beads are in squares. Numbers correspond to dog ID.

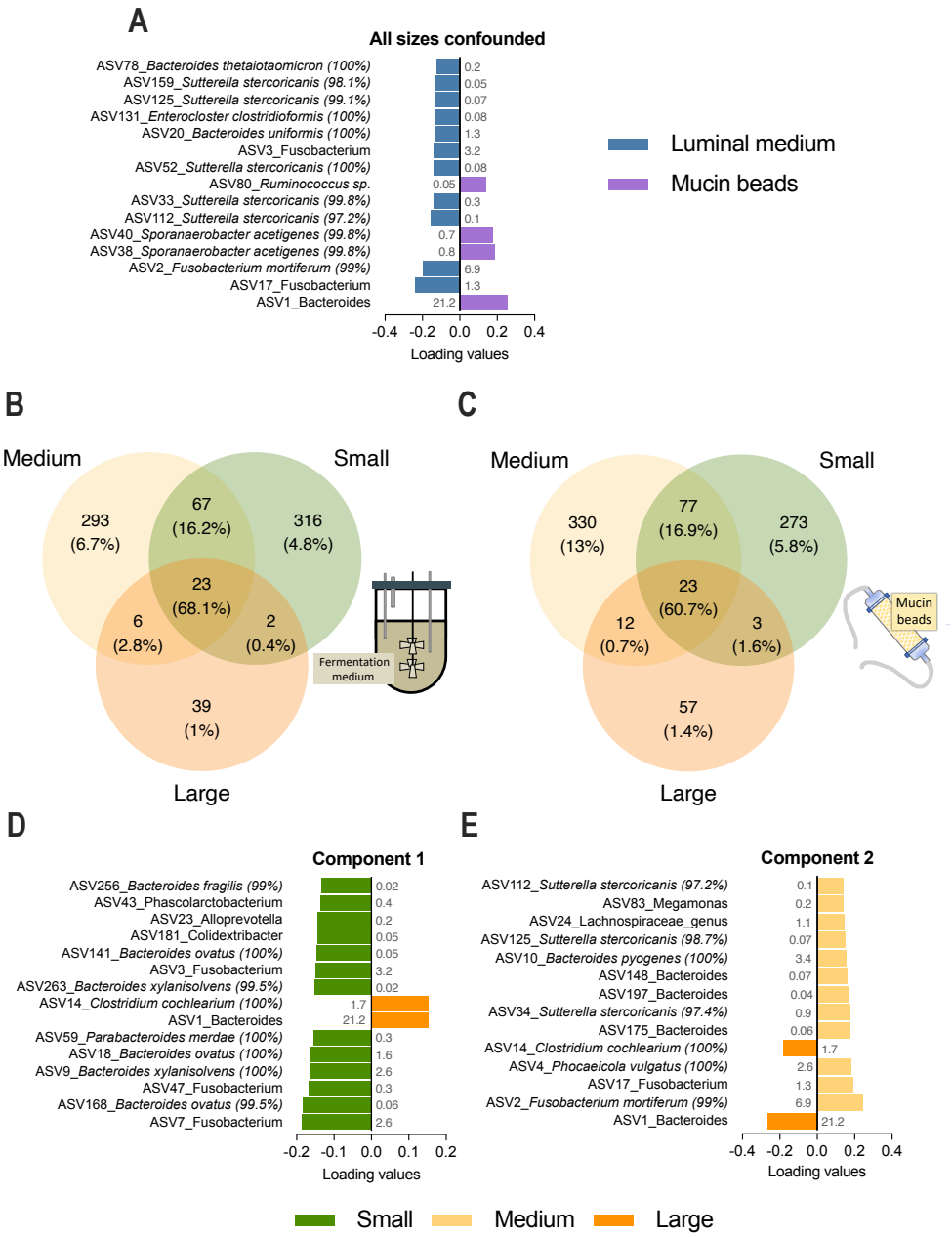

Figure II.3: Impact of colonic microenvironment and dog size on microbiota composition in the CANIM-ARCOL. Fermentations were performed in the CANIM-ARCOL under three dog size conditions. Lumen and mucus-associated microbiota compositions were analyzed by 16S Metabarcoding and differential analysis were further performed at the ASV level. Only stabilized points (from days 10 to 21) were included in the analysis. sPLS-DA analysis was performed to generate loading plots of the 15 most contributing ASVs between the luminal medium and mucin beads -all size confounded- (**A**) and between sizes -whatever the microenvironment- on component 1 (**D**) and 2 (**E**). Bars are colored according to the group in which the median abundance is maximal, which for each ASV, the relative abundancy indicated in grey. Species annotations are provided when a sequence identity percentage higher than 97 % was identified using BLAST (given into bracket). Venn diagrams based on ASV repartition were also generated on both luminal medium (**B**) and mucin beads (**C**). ASV numbers and corresponding percentages (sequence number of ASV over total sequence number) are indicated.

2.3.1. Size-specific colonic microbiota composition

As mentioned before, three dog size conditions were reproduced in the CANIM-ARCOL, leading to clear different microbial profiles between sizes after stabilization (**Figure II.4**). At the phylum level (**Figure II.5A**), stabilized microbiota in the luminal fraction displayed from small to large size conditions an increase in *Firmicutes* (12, 17 and 33 % for small, medium and large, respectively, p<0.0001) and *Bacteroidota* (39, 38 and 63 %, respectively, p<0.0001 between small/medium *versus* large), whereas *Fusobacteriota* decreased with size (40, 36 and 0.1 %, respectively, p<0.0001 between small/medium *versus* large). At the family level (**Figure II.5B**), there were slight differences between small and medium sizes. However, *Lachnospiraceae*, *Prevotellaceae,* and *Sutterellaceae* decreased with size while *Clostridiaceae* and *Bacteroidaceae* increased from small to large group, with differences reaching significance between small/medium and large (**Figure II.5B)**. In the mucosal compartment, at the phylum level (**Fig II.5A**), stabilized mucus-associated microbiota was characterized by decreases with size in *Fusobacteriota* (13, 12 and 0 % for small, medium and large groups, respectively, p<0.0001 between small/medium *versus* large), *Proteobacteria* (7, 5 and 1 %, respectively, p<0.0001 between small *versus* large) and *Actinobacteriota* (0.2, 0.4 and 0 %, respectively, p<0.0001 between medium *versus* large). At the family level (**Figure II.5B**), *Bacteroidaceae* increased with size (26, 29 and 45 % for small, medium and large size conditions, respectively, p<0.0001 between small/medium *versus* large), while *Fusobacteriaceae* (13, 12 and 0 %, respectively, p<0.0001 between small/medium *versus* large) and *Lachnospiraceae* decreased (9, 8 and 0 %, respectively, p<0.0001 between small/medium *versus* large). sPLS-DA analysis of 16S Metabarcoding data showed that a core microbiota was shared between the three groups, composed by only 23 ASVs from 10 different families, representing 68.1 and 60.7 % of total sequences in the luminal and mucosal compartments, respectively (**Figure II.3B** and **C**). The highest number of shared ASVs was found between small and medium group, whatever the compartment studied. Those results also displayed that a high number of low abundance-ASVs is constituting the size-specific microbiota, e.g. 316 ASVs (4.8 % abundance), 293 (6.7 %), 39 (1 %) in the luminal phase of small, medium and large size conditions, respectively. Discriminant analysis performed at the ASV level between the three size groups (whatever the colonic microenvironment, i.e. luminal or mucosal) revealed no significant difference between the small and medium groups and that the highest dissimilarities were observed between the small and large conditions (**Figure II.3D**). *Clostridium cochlearum* was enriched in the large group compared to the small one, while opposite trends were observed for *Fusobacterium sp*., *Bacteroides ovatus* and *Bacteroides xylanisolvens*. Less discriminant differences were revealed by PLS-DA (second component analysis, **Figure II.3E**) between medium and large groups with an enrichment in *Phocaeicola vulgatus*, *Fusobacterium mortiferum* and *Sutterella stercoricanis* in the medium one. Mean alpha-diversity indices (number of observed ASVs and Shannon index) were inversely correlated to canine size, in both lumen and mucus-associated microbiota (**Figure II.2A** and **2B**). Redundancy analysis based on ASVs composition after stabilization demonstrated an obvious clustering by size (p=0.001), stronger than that observed for donors (**Figure II.2G**). Moreover, weight (P=0.001) was clearly identified as the main environmental parameters driving microbiota composition (**Figure II.2D**).

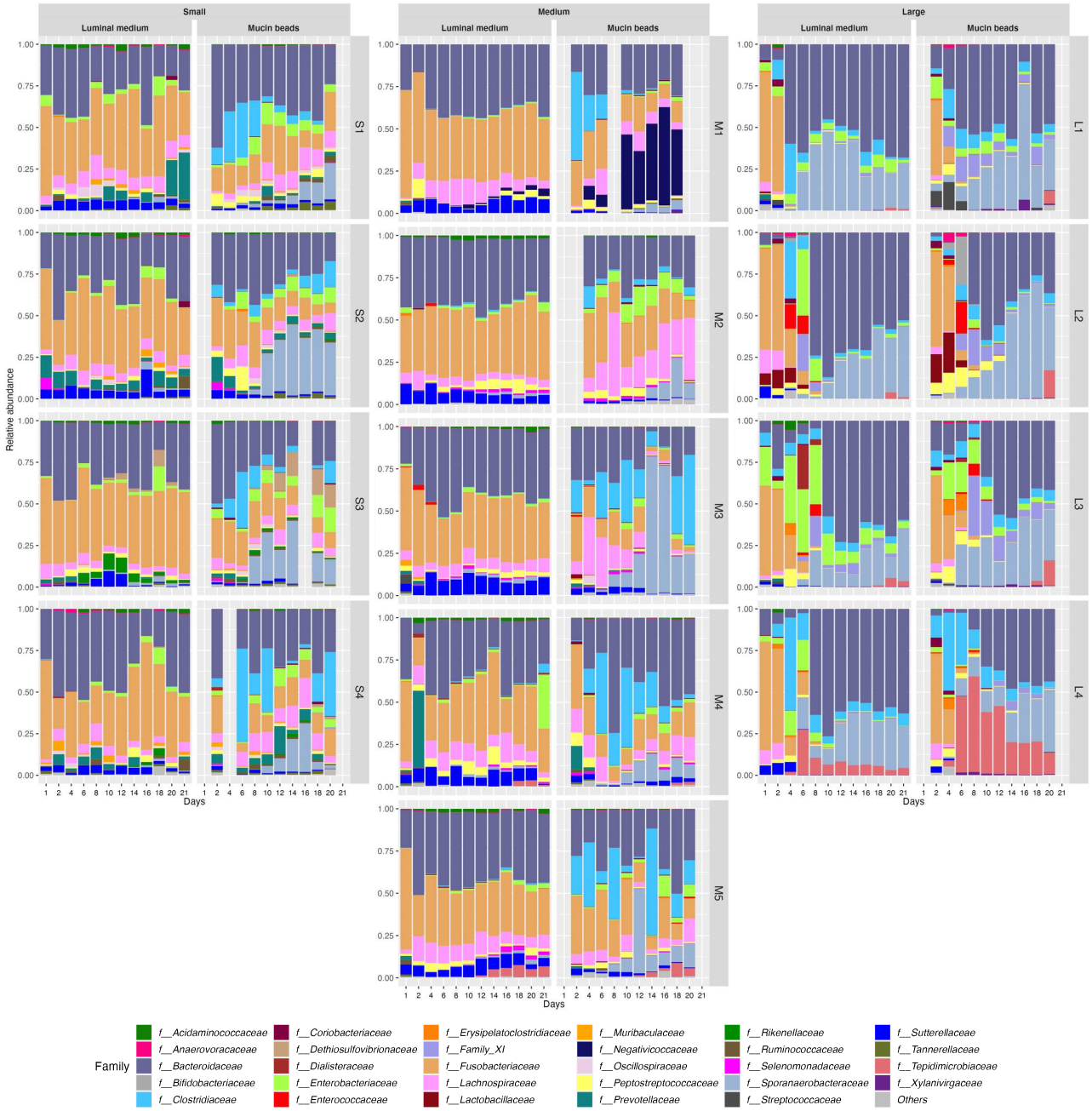

Figure II.4: Microbiota composition of luminal medium and mucin beads at the family level. Fermentations were performed in the CANIM-ARCOL under three dog size conditions. Lumen and mucus-associated microbiota composition were analyzed by 16S Metabarcoding at the family level. The most 30 abundant families are represented.

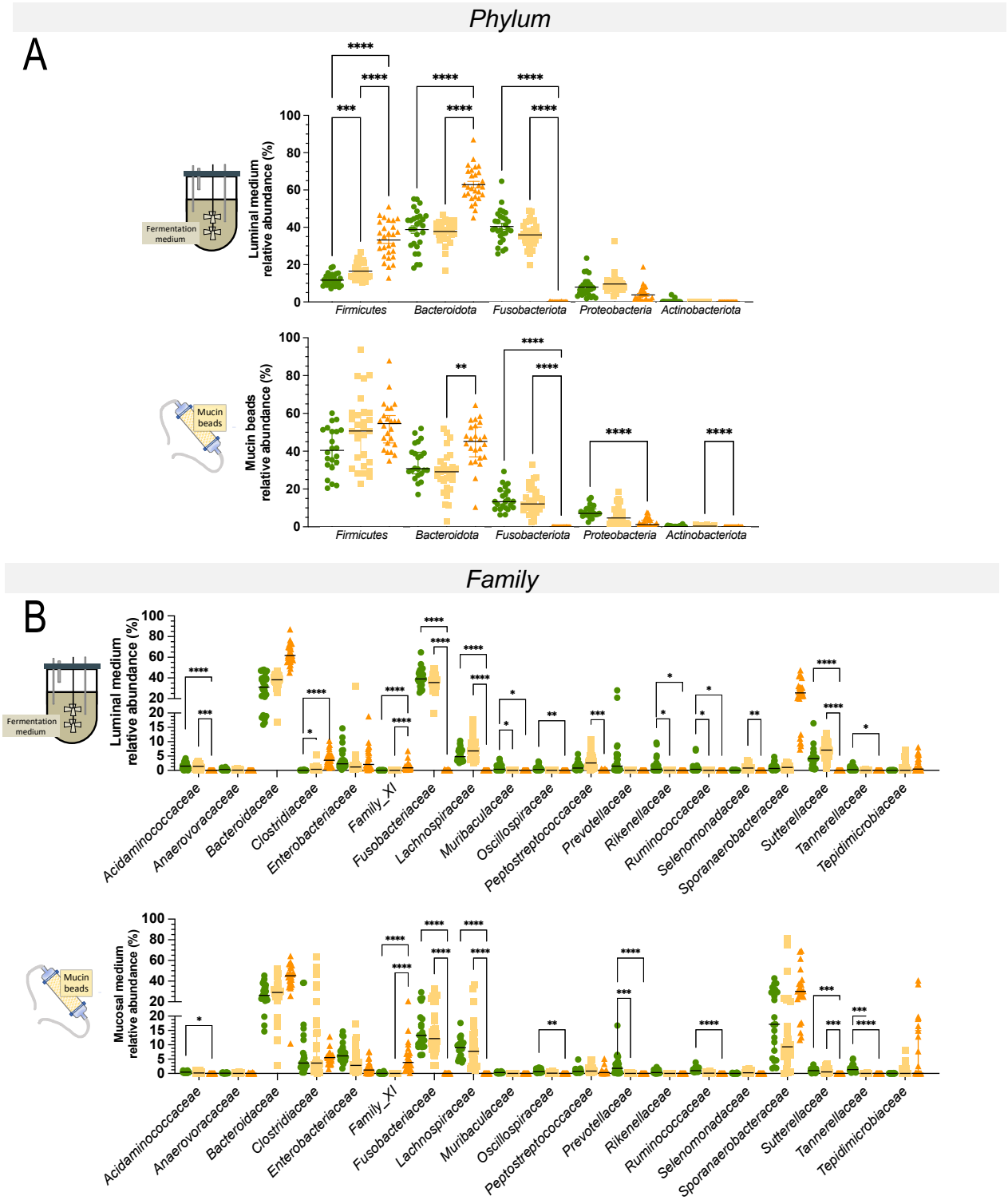

Figure II.5: Impact of three dog sizes on microbiota composition at the phylum and family levels. Fermentations were performed in the CANIM-ARCOL under three dog size conditions. Lumen and mucus-associated microbiota composition were analyzed by 16S Metabarcoding. Significant impacts of dog sizes on most abundant bacterial population are indicated at the phylum (**A**) and family (**B**) levels (one-way ANOVA, **: $p<0.01$; ***: $p<0.001$; ****: $p<0.0001$).

2.3.2. Size-specific colonic microbiota activity

Total gas production significantly increased ($p<0.01$) with size (**Figure II.6A**), with a mean total production over the stabilized phase (10-21 days) of 475, 3,775 and 17,920 mL for the small, medium and large groups, respectively). This was associated to clear different gas profiles between the three size groups (**Figure II.6B** and **6C)**. CO_2 percentages significantly increased ($p<0.0001$) with sizes, ranging from 30 to 94 % from the small to large conditions. Methane and oxygen tended to be more abundant in the small size group, with average oxygen percentages of 1.3, 0.6 and 0.4 % and methane percentages of 1.9, 0.01 and 0.03 %, for the small, medium and large groups, respectively.

A clear size effect on SCFA and BCFA production was also shown (**Figure II.6D** and **6G**). Daily SCFA concentration in the stabilized phase (**Figure II.6D**) increased with size from 83 mM for small to 179 mM for large, with differences reaching significance for small *versus* medium and small *versus* large conditions ($p<0.0001$). Similarly, daily BCFA production (**Figure II.6G**) was positively correlated to canine size with 14, 16 and 40 mM for small, medium and large dogs, respectively ($p<0.0001$ for small *versus* large and $p<0.001$ for medium *versus* large). Mean SCFA profiles also differed between groups with a significant increase in the ratio and concentration of butyrate ($p<0.001$) from small to large dogs (**Figure II.6E** and **6F**). The percentages of acetate and propionate (but not their concentrations) also decreased with size. BCFA profiles were also widely impacted by size effect. Caproate and heptanoate were found only under small size condition while isocaproate was medium size-specific (**Figure II.6H**). Isobutyrate and isovalerate ratios and concentrations significantly ($p<0.01$) increased with canine size whereas valerate decreased (**Figure II.6H** and **I**). RDA analysis of sequencing data implemented with SCFA concentrations indicated that luminal composition of medium dog size is mostly correlated to propionate level whereas luminal composition of large dog size is mostly correlated to butyrate concentration (**Figure II.2G**).

Daily bile acid concentrations significantly increased with size ($p<0.05$), with around 200 µg/mL in the fermentation medium from small bioreactors *versus* 400 and 500 µg/mL under medium and large conditions, respectively (**Figure II.6J**). Associated profiles also significantly differed with dog size, with a significant decrease of LCA percentage together with a rise in DCA in large *versus* small and medium conditions (**Figure II.6K**). In addition, in large bioreactors, percentages of CDCA tended to be higher and those of I-LCA lower compared to the two other conditions. Lastly, both DCA and LCA concentrations increased significantly ($p<0.0001$) with dog size (**Figure II.6L**). Daily ammonia concentration (**Figure II.6M**) in the luminal compartment increased with size ($p<0.0001$ for small *versus* large and medium *versus* large), with a mean total value over the stabilized phase (10-21 days) of 5.2, 5.7 and 8.7 mM for small, medium and large dogs, respectively.

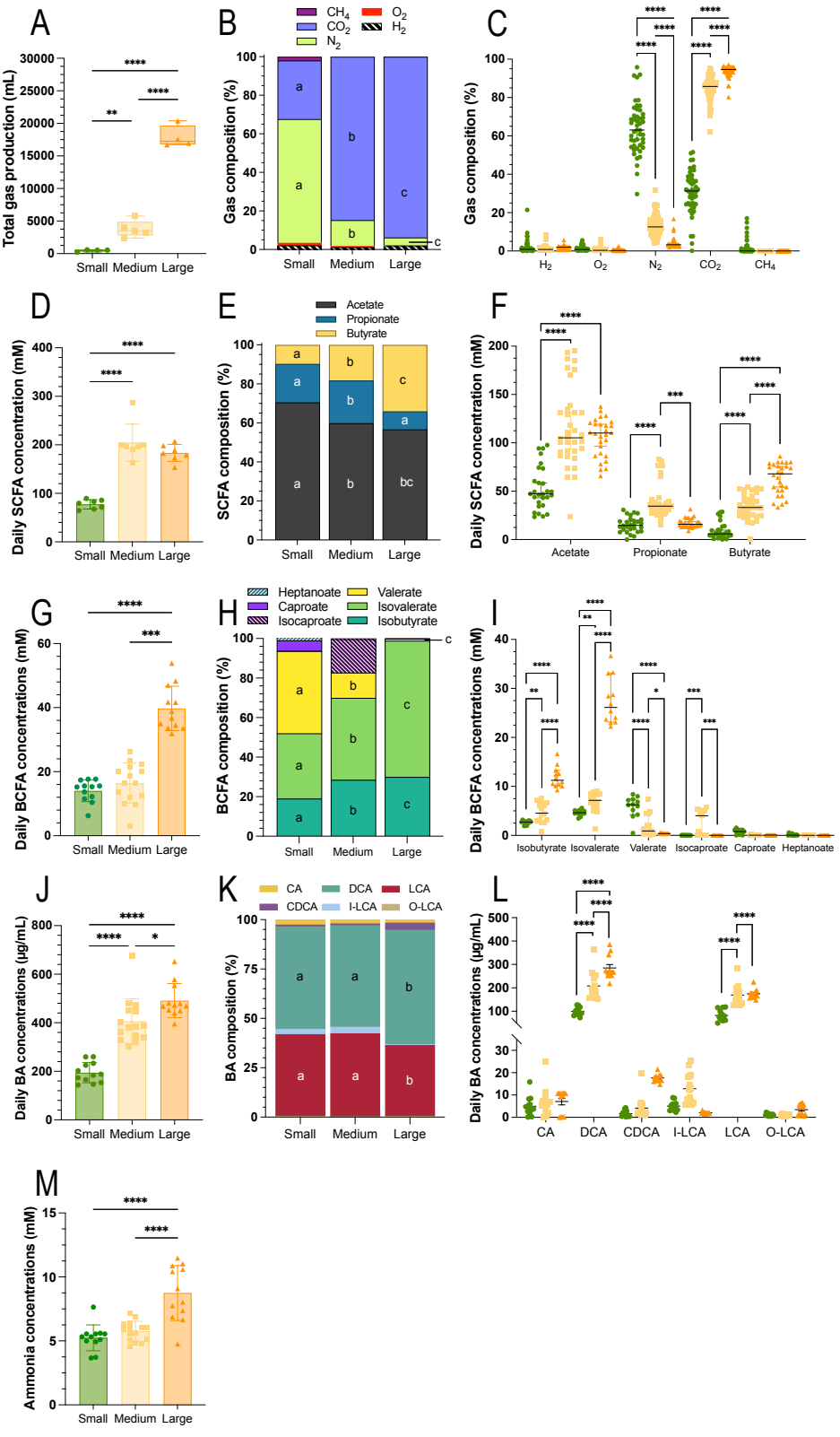

Figure II.6: Impact of dog sizes on microbiota activity in the CANIM-ARCOL. Fermentations were performed in the CANIM-ARCOL under three dog size conditions. Samples were regularly collected from atmospheric phase to determine total gas production in mL (A) and gas composition in relative percentages depending on dog size conditions (B) or type of gas (C). The three main short chain fatty acids (D, E, F), the six major branched chain fatty acids (G, H, I), ammonia (J) and main primary and secondary bile acids (K, L, M) were quantified in the luminal medium. Results are expressed as mean daily concentrations in mM ± SD (D, F, G, I, K, M) or relative percentages (E, H, L). All stabilized points (from 10 to 21 days) are represented for gas and SCFA, while only end points (from 18 to 21 days) are kept for BCFA, ammonia and BA. Statistical differences are indicated by letters or *: $p<0.05$, **: $p<0.01$; ***: $p<0.001$; ****: $p<0.0001$ (ANOVA one-way). *BA I: primary bile acids, BA II: secondary bile acids, BCFA: branched-chain fatty acids, CA: cholic acid, CDCA: chenodeoxycholic acid, CH_4: methane, CO_2: carbon dioxide, DCA: deoxycholic acid, H_2: dihydrogen, I-LCA: Isoallo-3-ketocholate, LCA: lithocholic acid, N_2: nitrogen, O-LCA: 3-oxolithocholic/ dehydrolithocholic acid, O_2: dioxygen, SCFA: short-chain fatty acids.*

2.4. Discussion

In accordance with the "3Rs" rules (adapted from Russel and Burch, 1959) which prone the reduction of animal use and the development of *in vitro* alternative strategies, the main objective of this study was to develop and validate through *in vitro-in vivo* comparisons the first model reproducing the canine colonic ecosystem adapted to three dog sizes, the CANIM-ARCOL. This was achieved thanks to a wide literature review (150 publications) we previously performed on canine colonic physicochemical (pH and transit time), nutritional (composition of simulated ileal effluents including nutrients and bile acids) and microbial (gut microbes' composition and functionalities) parameters (Deschamps, Humbert, *et al.*, 2022a). Up to now, most of the systems (8 out of 10) developed to reproduce the canine colonic environment are static batch models (Sunvold *et al.*, 1995c; Tzortzis *et al.*, 2004; Bosch *et al.*, 2008; Cutrignelli *et al.*, 2009; Panasevich *et al.*, 2013; Vierbaum *et al.*, 2019; Duysburgh *et al.*, 2020; Van den Abbeele *et al.*, 2020b; Oba *et al.*, 2020). Compared to CANIM-ARCOL, such systems are much more simplified related to physiological conditions, excluding digestive regionalization and dynamism (**Table II.4**). Moreover, experiments are limited in time (up to 72h), allowing only short-term analysis and preventing *in vitro* simulation of chronic ingestion of any compound of interest. The only dynamic model currently available with a similar level of complexity is the M-SCIME (Verstrepen *et al.*, 2021). Compared to this system, besides reproducing size-related conditions, CANIM-ARCOL exhibits the unique feature to maintain anaerobiosis by the sole activity of resident microbiota, allowing an interesting follow up of atmospheric gases. However, it does not simulate like the M-SCIME the three colonic parts nor passive absorption of fermentation products which is a key feature in gut homeostasis (Weber *et al.*, 2004). For the first time, even if it was limited by the scarcity of information, we were able to compare our *in vitro* data with *in vivo*. In all other available models, if performed, validation was only based on data from canine fecal samples. Together with the batch model of Oba *et al.* (2020) and M-SCIME (Verstrepen *et al.*, 2021), our model is one of the rare systems to distinguish the luminal from the mucus-associated microbiota, aiming to recreate more physiologically the different colonic microenvironments. Here, the mucin-compartment was filled with beads made with mucin from porcine stomach, the only source yet commercialized. Even if using canine colonic mucins will be more relevant, this option is hampered by obvious technical, societal and regulatory limitations. Anyhow, MUC-5AC and MUC-5B found in pig mucins are also the most represented glycoproteins in canine large intestine mucus (Dubbelboer *et al.*, 2022). As previously observed in human and pig *in vitro* studies, adding a mucosal compartment allowed to capture a higher bacterial diversity from the fecal microbiome (Van den Abbeele *et al.*, 2009; Deschamps *et al.*, 2020; Van Herreweghen *et al.*, 2021; Gresse *et al.*, 2021a; Verstrepen *et al.*, 2021). For each size condition and donor, this compartment exhibited a higher number of observed ASVs compared to the luminal one and is particularly efficient to preserve bacteria from the *Firmicutes* phylum, such as *Ruminococcaceae* and *Clostridiaceae* (Maru *et al.*, 2018). It was particularly helpful in maintaining rare taxa from *Tannerellaceae* or *Ruminococcaceae* families, in line with their mucin-degrading bacteria status (Bell *et al.*, 2008), certainly by providing specific nutritional niches.

Table II.4: Comparison of the CANIM-ARCOL model and other currently available models of the dog large intestine. This comparison was made based on the present study and our previous literature review (Deschamps *et al.*, 2022b). The score is based on the number of parameters reproduced in the *in vitro* model compared to the *in vivo* situation and the level of validation of the model, from the lowest (●) to the highest relevance (●●●●●). illustrates the best model regarding the considered parameter.

References		Process type	Different parts of the colon	Anaerobiosis	Adaptations based on literature	Validation with colonic *in vivo* data	Colonic physicochemical parameters						Microbiota		Score
							Adapted to dog size	Body temperature	pH control	Transit time	Adaptation to dog food	Absorption	Microbiota from colonic source	Mucus	
Vierbaum *et al.*, (2019)	STATIC	Batch 24 h	No	Yes N_2-gas	No	No validation	No	No	No	No	No	No	No, from feces	No	●
Cutrignelli *et al.*, (2009)		Batch 48 h	No	Yes	No	No (faecal data from literature)	No	Yes	No	No	No	No	No, from feces	No	●
Sunvold *et al.*, (1995)		Batch 24 h	No	Yes CO_2-gas	No	No (faecal data from *in vivo* study)	No	Yes	No	No	No	No	No, from feces	No	●
Van den Abbeele *et al.*, (2020b)		Batch 48 h	No	Yes N_2-gas flow	No	No (faecal data from literature)	No	Yes	No	No	No	No	No, from feces	No	●
Tzortzis *et al.*, (2004)		Batch 24 h	No	Yes N_2-gas flow	No	No validation	No	No	No	No	No	No	No, from feces	No	●
Panasevich *et al.*, (2013)		Batch 12 h	No	Yes CO_2-gas	Yes but corresponding references are not given in the paper	No (faecal data from *in vivo* study)	No	Yes	No	No	No	No	No, from feces	No	●●
Oba *et al.*, (2020)		Batch 24 h	No	Yes N_2-gas flow	No	No validation	No	Yes	No	No	No	No	No, from feces	Yes	●●
Bosch *et al.*, (2008)		Batch 72 h	No	Yes CO_2-gas	No	No validation	No	Yes	No	No	No	No	Yes, from digesta	No	●●●
Duysburgh *et al.*, (2020) **SCIME** Verstrepen *et al.*, (2021) **M-SCIME**	DYNAMIC	Continuous	Yes	Yes N_2-gas flow	Yes but corresponding references are not given in the paper	No (faecal data from *in vivo* study or literature)	No	Yes	Yes	Yes	Yes	Passive (feed)	No, from feces	Yes	●●●●
CANIM-ARCOL		Continuous	No	No Maintained by the sole activity of resident microbiota	Yes Based on a published literature review	Yes (only from medium dog, based on literature review)	Yes Small, medium and large	Yes	Yes Small: 6.5 Medium: 6.4 Large: 6.2	Yes Small: 5h Medium: 9h Large: 15h	Yes	No	No, from feces	Yes	●●●●●

Lastly, as previously described for the M-SCIME, making use of different fecal samples enabled our new *in vitro* model to capture the interindividual variability in colonic microbiome. Keeping variability associated to an individual or its breed is of high importance, since it is acknowledged as an important feature in canine gut microbiota and health (Oswald *et al.*, 2015).

As previously mentioned, a major advance associated with this *in vitro* gut model development is the possibility to reproduce and discriminate digestive conditions associated to different dog sizes (i.e. "small" under 10 kg, "medium" from 10 to 30 kg and "large" over 30 kg). To ensure the relevance of the newly developed size-related colonic model, our *in vitro* results were compared to *in vivo* data. Due to the paucity of information on canine colonic microbiota (only two studies performed in medium dogs, none with medium and large dogs), *in vitro-in vivo* comparisons on colonic data were only made on medium dog size (**Table II.5**). In addition, since there is no information on colonic microbiota activity *in vivo*, such analysis was only based on microbiota composition. In both luminal and mucosal compartments, the CANIM-ARCOL model allowed to maintain the dominant bacterial phyla inhabiting the canine colon (**Table II.5**), i.e. *Firmicutes*, *Bacteroidota*, *Fusobacteriota* and *Proteobacteria*, based on data collected from intraluminal colonic content (Suchodolski *et al.*, 2008) and colonic biopsies (Honneffer *et al.*, 2017). Interestingly, our *in vitro* system preserved 27 of the 31 families detected *in vivo*, apart from *Prevotellaceae*, *Streptococcaceae*, *Turicibacteraceae* and *Veillonellaceae*. Of note, these four populations were only found in colonic biopsies, but not in the study on intraluminal colonic content, suggesting interindividual or breed specificities (Suchodolski *et al.*, 2008; Honneffer *et al.*, 2017). The second level of *in vitro-in vivo* comparisons was made on the three dog sizes conditions between our *in vitro* colonic results and data from dog fecal samples collected in our previous literature review (Deschamps *et al.*, 2022b, **Table 6**). The impact of dog sizes on *in vitro* results was in line with *in vivo* data for 4 out of the 5 main bacterial phyla (*Actinobacteria*, *Bacteroidota*, *Firmicutes* and *Proteobacteria*), but not *Fusobacteriota,* described as a typical phylum in canine healthy microbiota (Pilla and Suchodolski, 2020). In the present study, this population almost disappeared from large bioreactors while an abundance around 6 % was assumed in fecal samples from large dogs by two *in vivo* studies (Sandri *et al.*, 2016; Hullar *et al.*, 2018). This inhibition might be related to the high levels of BCFA found under large conditions *in vitro*, and not observed *in vivo*, as explained later. In our study, microbial alpha-diversity was inversely correlated with dog size. This is not fully in accordance with *in vivo* funding which indicates the highest diversity for medium dog. However, both *in vitro* and *in vivo* results associated the lowest microbial diversity with large dog size condition (Sandri *et al.* 2016). This might be related to the lower amount of soluble fibers (compared to insoluble ones) introduced in the nutritive medium under large dog conditions *in vitro*, in accordance with in-field recommendations in this population with particular digestive sensitivity (Weber *et al.*, 2017). Increasing the amount of soluble fibers has already been associated with a higher fecal diversity in dogs (Biagi, Cipollini & Zaghini, 2008; Chen *et al.*, 2019). In any event, alpha-diversity indexes measured *in vitro* in large bioreactors looked low compared to the physiological situation (Sandri *et al.*, 2016).

Table II.5: Comparison of main bacterial populations found in the CANIM-ARCOL model under medium size conditions and *in vivo* in the large intestine of medium size dogs. *ND: not determined.*

Similarity or discordance between *in vitro* and *in vivo* data are indicated by a green and red color code, respectively.

	Dog large intestine *in vivo*		**CANIM-ARCOL *in vitro***		Adequation between *in vivo* and *in vitro* data
	Suchodolski *et al.* 2008	Honneffer *et al.* 2017			
	Intraluminal colonic content	*Colonic biopsies*	*Luminal medium*	*Mucin beads*	
TAXA	Hound dogs n=6	Hound dogs n=6	Medium condition n=5		
Phylum *Actinobacteriota*	ND	Detected	Detected	Detected	Yes
Family Bifidobacteriaceae	ND	Detected	Not detected	Detected	Yes
Family Coriobacteriaceae	ND	Detected	Detected	Detected	Yes
Phylum *Bacteroidota*	Detected	Detected	Detected	Detected	Yes
Family Bacteroidaceae	Detected	Detected	Detected	Detected	Yes
Family Muribaculaceae	ND	Detected	Not detected	Detected	Yes
Family Prevotellaceae	ND	Detected	Not detected	Not detected	No
Family Rikenellaceae	ND	Not detected	Detected	Detected	Yes
Family Tannerellaceae	ND	Detected	Detected	Detected	Yes
Phylum *Firmicutes*	Detected	Detected	Detected	Detected	Yes
Family Acidaminococcaceae	ND	Detected	Detected	Detected	Yes
Family Anaerovoraceae	ND	Not detected	Detected	Detected	Yes
Family Dialisteraceae	ND	Not detected	Detected	Detected	Yes
Family Enterococcaceae	Detected	Not detected	Detected	Detected	Yes
Family Erysipelotrichaceae	ND	Detected	Detected	Detected	Yes
Family Lactobacillaceae	Detected	Detected	Not detected	Detected	Yes
Family Negativicoccaceae	ND	Not detected	Detected	Detected	Yes
Family Oscillospiraceae	ND	Detected	Detected	Detected	Yes
Family Streptococcaceae	ND	Detected	Not detected	Not detected	No
Family Clostridiaceae	Detected	Detected	Detected	Detected	Yes
Family Lachnospiraceae	ND	Detected	Detected	Detected	Yes
Family Peptostreptococcaceae	ND	Detected	Detected	Detected	Yes
Family Ruminococcaceae	ND	Not detected	Detected	Detected	Yes
Family Selenomonadaceae	ND	Detected	Detected	Detected	Yes
Family Sporanaerobacteraceae	ND	Not detected	Detected	Detected	Yes
Family Tepidimicrobiaceae	ND	Detected	Detected	Detected	Yes
Family Turicibacteraceae	ND	Detected	Not detected	Not detected	No
Family Erysipelatotrichaceae	ND	Detected	Detected	Detected	Yes
Family Veillonellaceae	ND	Detected	Not detected	Not detected	No
Phylum *Fusobacteriota*	Detected	Detected	Detected	Detected	Yes
Family Fusobacteriaceae	Detected	Detected	Detected	Detected	Yes
Phylum *Proteobacteria*	Detected	Detected	Detected	Detected	Yes
Family Enterobacteriaceae	ND	Detected	Detected	Detected	Yes
Family Succinivibrionaceae	ND	Detected	Detected	Detected	Yes
Family Sutterellaceae	ND	Detected	Detected	Detected	Yes
Family Campylobacteraceae	ND	Not detected	Detected	Not detected	Partial

Lastly, of particular interest, methanogens *Archaea*, represented by *Methanobrevibacter smithii*. were found in our *in vitro* model, but under small size conditions only. This constitutes the first description of methanogens *Archaea* maintenance under *in vitro* canine digestive conditions. *In vivo*, this population is also very poorly described since only one study reported their presence in medium dog stools (Deng & Swanson, 2015), and evidently no data is available on the effect of dog size. Such *Archaea* distribution in bioreactors cannot be related to initial load in fecal sample, this population being detected in two medium dog fecal samples only. *Archaea* occurrence under small dog size condition *in vitro* is in contradiction with previous funding in human showing a positive correlation between their abundance and prolonged gastrointestinal transit time (Gaci *et al.*, 2014). One hypothesis would be related to lower isobutyrate concentrations found in small size conditions, which was negatively correlated to total methanogens in a study performed with isovalerate supplementation in steers rumen (Liu *et al.*, 2014).

In an original way, this *in vitro* model development also provided for the first time plenty of data on colonic microbiota activities related to dog size conditions (**Table 6**), with measurement of main end-fermentation products such as atmospheric gases (allowed by the lack of flushing in bioreactors with N_2 or CO_2), SCFA, BCFA, ammonia and bile acid dehydroxylation activities through primary and secondary bile acids dosage. In the canine large intestine, complex polysaccharides are degraded into monosaccharides leading to gas and SCFA production. In the present study, total gas production increased with dog size, in line with a higher microbial fermentation activity in large dogs compared to smaller sizes (Weber *et al.*, 2004). This study provides the first set of data on gas profiles under canine colonic conditions since there is no information in dogs. Higher O_2 and lower CO_2 levels in the atmospheric phase of small bioreactors is directly related to a lower microbial fermentation activity. More remnant H_2 in large bioreactors also correlates with a higher abundance of H_2-producers bacteria such as *Bacteroides* and *Clostridium* (Wolf *et al.*, 2016). In addition, high proportion of CH_4 under small size condition is perfectly correlated with the presence of *Methanobrevibacter smithii,* as previously mentioned. Regarding SCFA, total concentrations *in vitro* was positively associated with dog size, in accordance with *in vivo* data in fecal samples and the higher transit time in large dogs favoring microbial fermentation (Weber *et al.*, 2004). Effect of dog size on acetate relative percentage was in line with *in vivo* data (Cutrignelli *et al.*, 2009; Beloshapka *et al.*, 2014; Sandri *et al.*, 2016; Paßlack *et al.*, 2021; Meineri *et al.*, 2022), but not that of butyrate and propionate. The highest concentrations in butyrate were observed in large bioreactors, certainly linked to the presence of *Clostridiaceae* in the luminal medium, known to be involved in carnivorous butyrate production pathway (Vital *et al.*, 2015). The lack of correlation between *in vitro* and *in vivo* data regarding butyrate might be related to the absence of colonocytes in CANIM-ARCOL, which use butyrate as a preferential energy source. BCFA and ammonia result from metabolization by microbiota of undigested dietary proteins (Davila *et al.*, 2013). Total BCFA concentrations increased with dog size *in vitro*, while no clear conclusion was provided by *in vivo* studies (Deschamps, Humbert, *et al.*, 2022a). Besides, opposite trends were observed between our *in vitro* colonic results and *in vivo* data in dog stools regarding isovalerate, isobutyrate and valerate concentrations (Cutrignelli *et al.*, 2009; Beloshapka *et al.*, 2014; Sandri *et al.*, 2016). Again, this might be linked to the lack of intestinal cells which are involved in BCFA absorption (Ran-Ressler *et al.*, 2013). Regarding ammonia, also resulting from protein fermentation, *in vitro* concentrations increased with dog sizes, accordingly with data in dog stools (Deschamps *et al.*, 2022b). Such a rise might be associated to the bloom of *Clostridiaceae* and *Sporanaerobacteraceae* observed in large bioreactors (Hardy *et al.*, 2021). Lastly, we followed bile acid dehydroxylation of primary (CA and CDCA) into secondary bile acids (LCA and DCA) by colonic microbiota *in vitro*. Such process was identified as a key health marker disturbed in canine diseases such as antibiotic-induced dysbiosis (Whittemore *et al.*, 2021), chronic enteropathies (Guard *et al.*, 2019) or obesity (Apper *et al.*, 2020). Total bile acids concentrations increased *in vitro* with dog size while opposite trends seemed to be observed in dog stools, in the only available study (Guard *et al.*, 2019). Our study described for the first time that deconjugation of primary bile acids (supplied by the nutritive medium, **Table II.2**) into secondary bile acids efficiently occurs in an *in vitro* canine model.

Table II.6: *In vitro-in vivo* comparisons of dog size impact on gut microbial composition and activity based on fecal data. This table makes a comparison between *in vitro* data in CANIM-ARCOL and *in vivo* data in dog fecal samples, gathered from our previous literature review (Deschamps *et al.*, 2022b) or issued from the analysis of stool samples used in this study to inoculate the bioreactors (Figure S1). Inclusive parameters for *in vivo* data are the following: healthy adult dogs, fed with dry food, and classified according to their size in small (body weight under 10 kg), medium (from 10 to 30 kg) or large dogs (over 30 kg). Green box: *in vitro* data obtained in CANIM-ARCOL are in line with canine *in vivo* data; yellow: no clear conclusion can be found due to lack of *in vivo* data; red: *in vivo* and *in vitro* data are contradictory; ↘: less abundant from small to large conditions; ↗: more abundant from small to large conditions; ↭: no clear change with size conditions, *: significant variation ($p<0.05$). *BA: bile acids, BCFA: branched chain fatty acids, CA: cholic acid, CDCA: chenodeoxycholic acid, DCA: deoxycholic acid, LCA: lithocholic acid, SCFA: short chain fatty acids*. Lack of data is symbolized by a diagonal black line.

		In vivo		*In vitro*	
		Review faeces	**Faecal inoculum**	**Luminal medium**	**Mucin beads**
					
Phylum	*Actinobacteria*	↘	↭	↘	↘*
	Bacteroidota	↗	↗	↗*	↗*
	Firmicutes	↭	↗*	↗*	↗
	Fusobacteriota	↭	↭	↘*	↘*
	Proteobacteria	↘	↗	↘*	↘*
Alpha-diversity		↭	↗	↘*	↘*
Total SCFA		↗	↗	↗*	
Acetate	Relative (%)	↘	↘	↘*	
Propionate	Relative (%)	↗	↗	↘*	
Butyrate	Relative (%)	↘	↘	↗*	
Total BCFA		↭	↘*	↗*	
Isovalerate	Absolute (mM)	↘	↭	↗	
Isobutyrate	Absolute (mM)	↘	↭	↗	
Valerate	Absolute (mM)	↗	↗	↘	
Total bile acids		↘	↭	↗	
Primary BA	Relative (%)	↘	↭	↗	
Secondary BA	Relative (%)	↗	↭	↗	
Total ammonia		↗	↭	↗*	
Total gas production				↗*	
CO_2	Relative (%)			↗*	
H_2	Relative (%)			↭	
O_2	Relative (%)			↘	
N_2	Relative (%)			↘*	
CH_4	Relative (%)			↘	

This certainly results from the activity of bile acid metabolizing bacteria such as *Bacteroides*, *Clostridium* and *Lactobacillus* (Rowland *et al.*, 2018). In addition, relative percentages of secondary bile acids raised with dog size, consistent with *in vivo* data in fecal samples (Guard *et al.*, 2019).

To conclude, for the first time, we set up a new size-related *in vitro* model of the dog large intestine, the CANIM-ARCOL. This model was well validated through *in vitro-in vivo* comparisons for the medium size condition and a discriminant size-effect was reproduced. The model development also provided useful data regarding mucus-associated microbiome and microbiota metabolic activities under canine colonic simulated conditions. However, the validation of small and large size bioreactors suffered from the lack of colonic *in vivo* data and the paucity of fecal ones. Recent developments of non-invasive methods like wireless motility capsules (Warrit *et al.*, 2017a) or medical device aiming to collect microbiota during gastrointestinal transit open new avenues to fill these scientific and technological gaps. This *in vitro* model represents a powerful platform to study the fate of food and veterinary products in the canine digestive environment, help to elucidate their mechanisms of action in relation with colonic microbiota and promote innovation in these fields. Of particular interest, CANIM-ARCOL allows to study the bilateral interactions between gut microbiota and any positive (e.g. nutrients, fiber, pre-, pro or postbiotics, drugs) or deleterious compounds (e.g. pathogens, pollutants, mycotoxins) crossing the large intestine in dogs, without confounding host effect. Therefore, valuable information regarding the impact of those compounds on microbiota composition and activities, but also reversely their metabolization by microbiota, can be obtained. This model will also help to move toward personalized nutrition or medication, by capturing interindividual or breed variabilities in gut microbiome and considering dog body weight (Oswald *et al.*, 2015; You & Kim, 2021). Further developments would include the coupling of CANIM-ARCOL model with intestinal or immune cells to integrate host interactions and the adaptation of the model to diseased situations, such as antibiotic-induced dysbiosis (Igarashi *et al.*, 2014), chronic enteropathies (AlShawaqfeh *et al.*, 2017) or obesity (Apper *et al.*, 2020).

Supplementary figure II.1: Stool characterization for each canine donor. Stool samples were collected from 13 healthy dogs (n=4 small in green, n=5 medium in yellow and n=6 large in orange). Microbiota composition was analyzed by 16S Metabarcoding. Diversity indexes were calculated based on ASV table. α-diversity (observed ASVs and Shannon Index) is represented as box plots for each dog size (**A**). Redundancy analysis (RDA) two-dimension plot visualizations reported bacterial community β-diversity, showing the effects of dog size (**B**), numbers refer to dog_id mentioned in **Table II.1**. Total bacteria were also determined by quantitative-PCR and plotted as boxplots (**C**). Bacterial abundances are shown at the phylum and family levels (**D**). The three main short-chain fatty acids (**E, F**), the six major branched-chain fatty acids (**G, H**), ammonia (**I**) and main primary and secondary bile acids (**J**) were quantified in the stool samples. Results are expressed as mean daily concentrations in mM/g of fresh stool ± SD (**E, G, I**) or relative percentages (**F, H, J**). Statistical differences are indicated by ****: $p<0.0001$ (ANOVA one-way). *BCFA: branched-chain fatty acids, CA: cholic acid, CDCA: chenodeoxycholic acid, DCA: deoxycholic acid, I-LCA: Isoallo-3-ketocholate, LCA: lithocholic acid, O-LCA: 3-oxolithocholic/dehydrolithocholic acid, SCFA: short-chain fatty acids, TCA: taurocholic acid.*

2.5. Supplementary figures

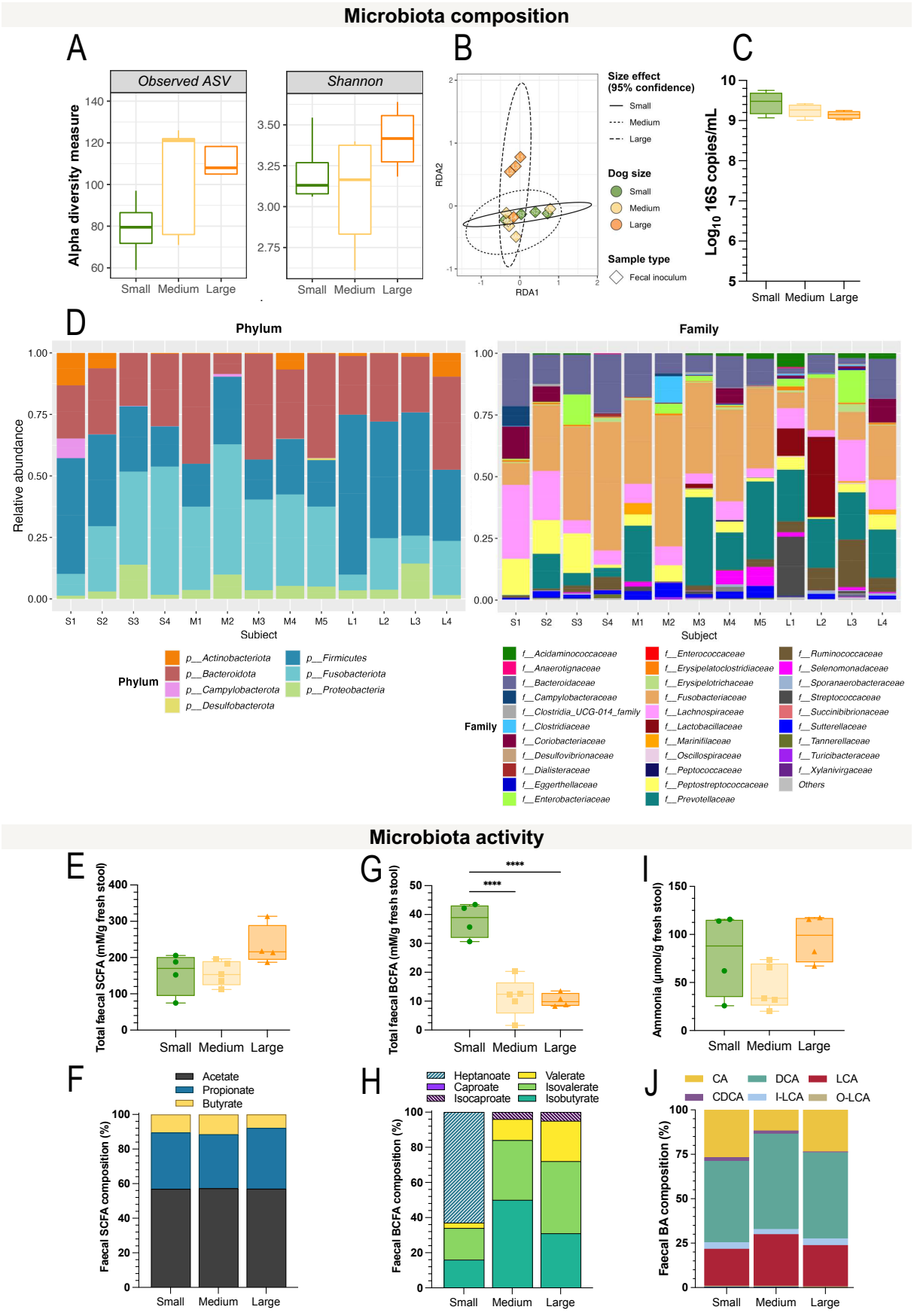

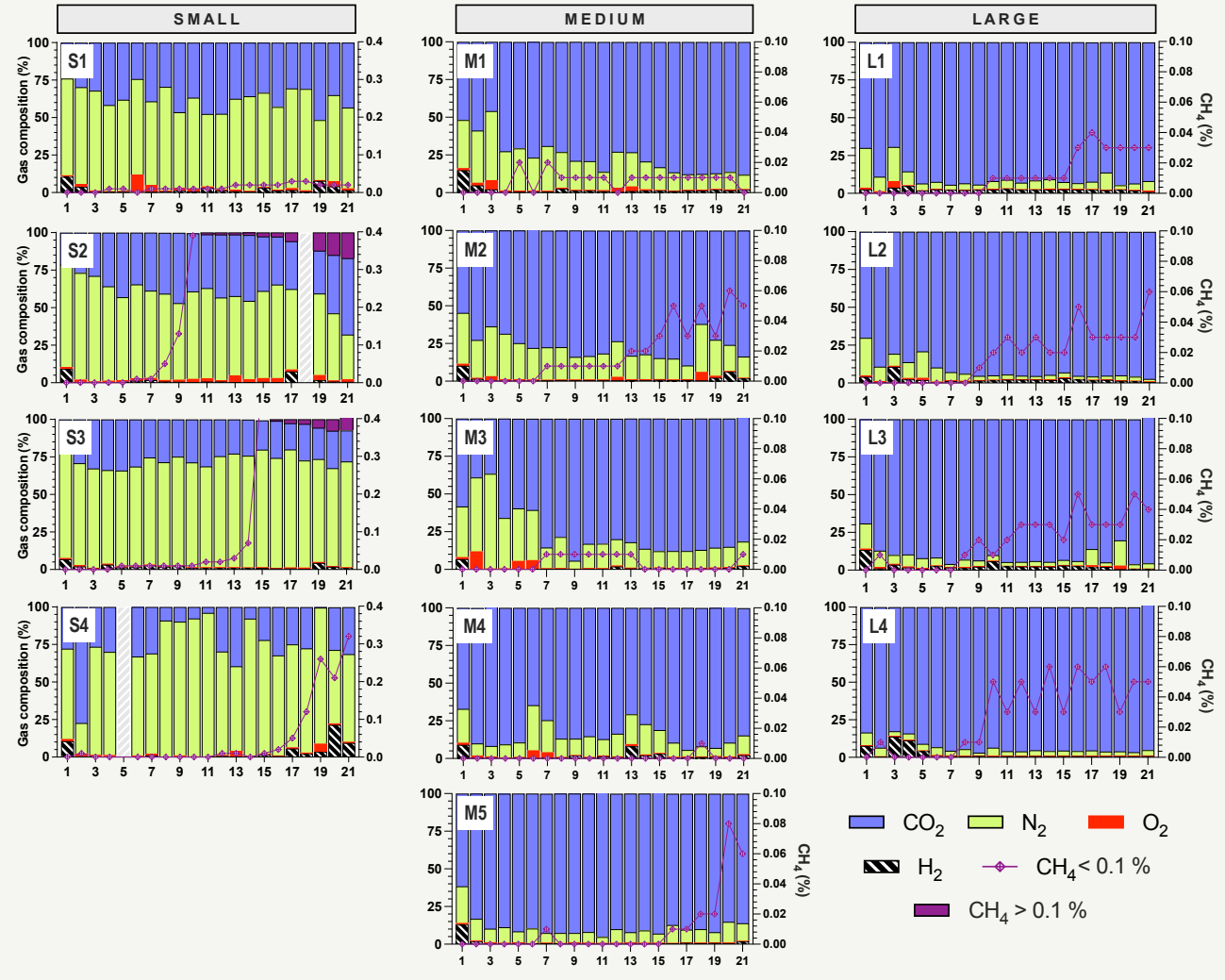

Supplementary figure II.2: Impact of three dog sizes on gas composition in the CANIM-ARCOL at the individual level. Fermentations were performed in the CANIM-ARCOL under three dog size conditions, when bioreactors were inoculated with fecal samples from 13 healthy dogs (n=4 small "S", n=5 medium "M" and n=6 large "L"). Atmospheric phase of bioreactors was sampled daily to monitor gas composition throughout fermentations. Results are expressed as relative percentages of main gases. *CH_4: methane, CO_2: carbon dioxide, H_2: dihydrogen, N_2: nitrogen, O_2: dioxygen.*

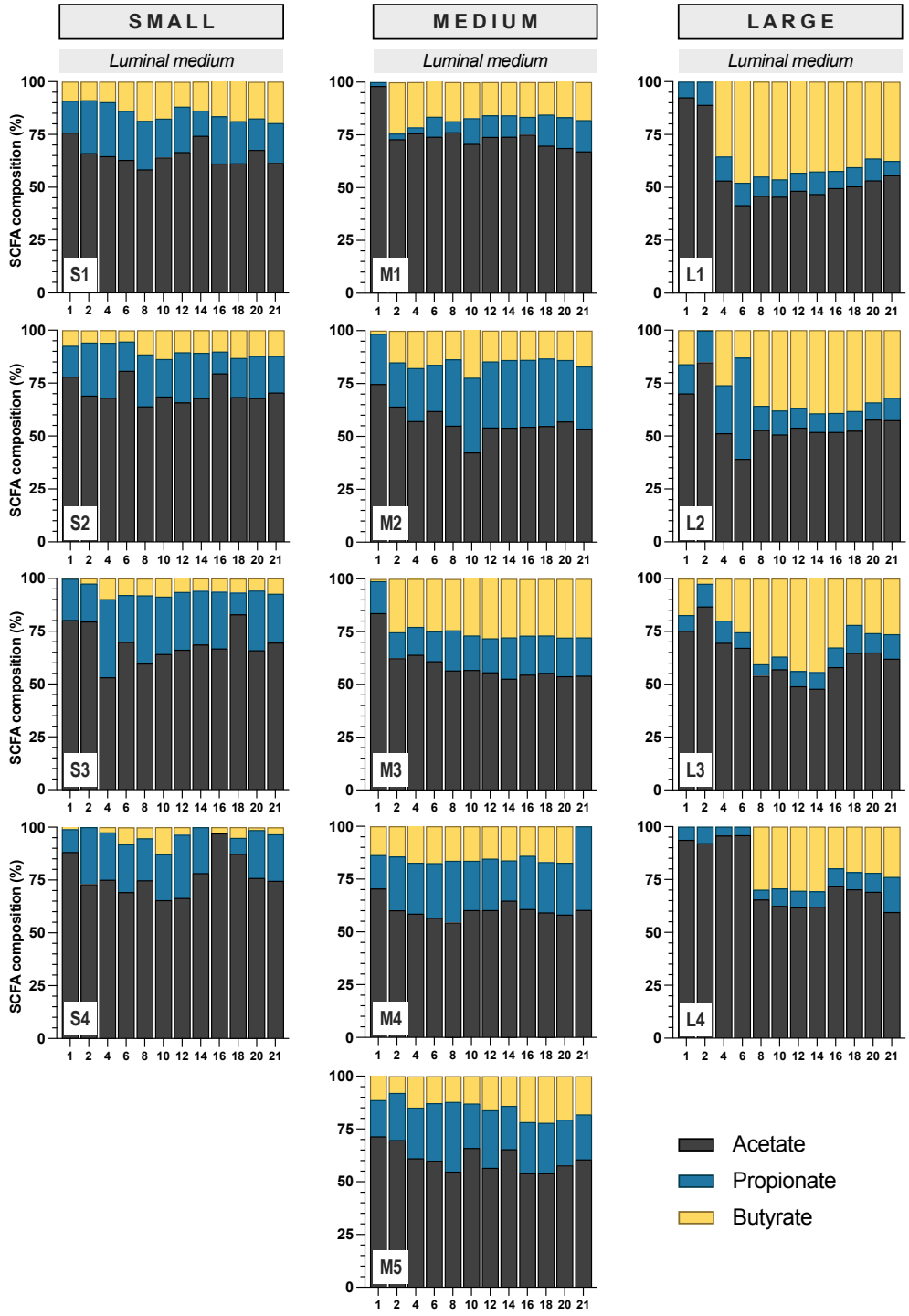

Supplementary figure II.3: Impact of three dog sizes on SCFA composition in the CANIM-ARCOL at the individual level. Fermentations were performed in the CANIM-ARCOL under three dog size conditions, when bioreactors were inoculated with fecal samples from 13 healthy dogs (n=4 small "S", n=5 medium "M" and n=6 large "L"). Luminal medium of bioreactors was sampled daily to monitor short chain fatty acid composition throughout fermentations. Results are expressed as relative percentages of main SCFA (i.e. acetate, propionate and butyrate).

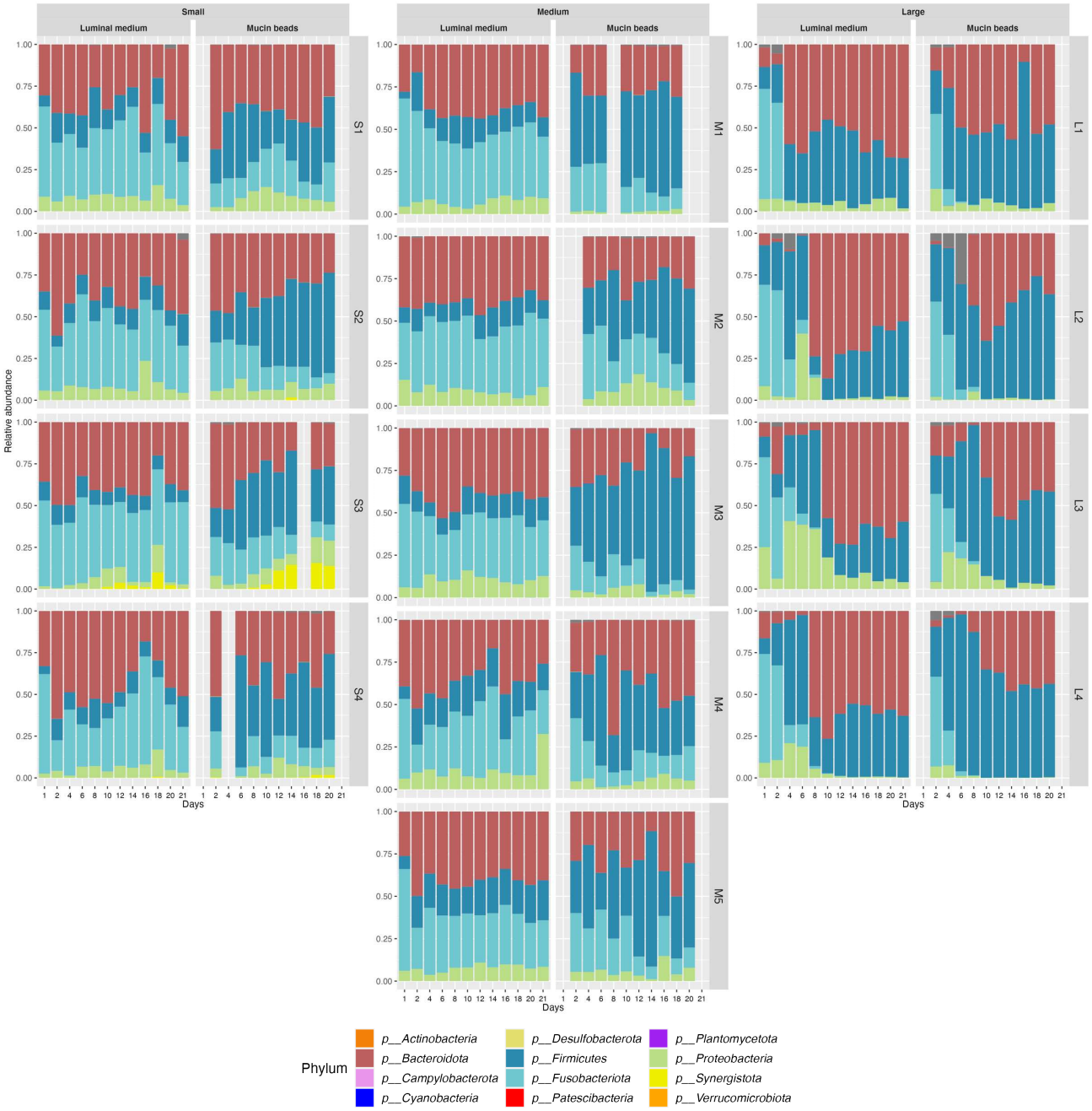

Supplementary figure II.4: Impact of three dog sizes on microbiota composition in the CANIM-ARCOL at the individual level. Fermentations were performed in the CANIM-ARCOL under three dog size conditions, when bioreactors were inoculated with fecal samples from 13 healthy dogs (n=4 small "S", n=5 medium "M" and n=6 large "L"). Luminal medium of bioreactors and mucin beads were sampled daily to monitor microbiota composition at the phylum level. Results are expressed as relative abundances of main phyla.

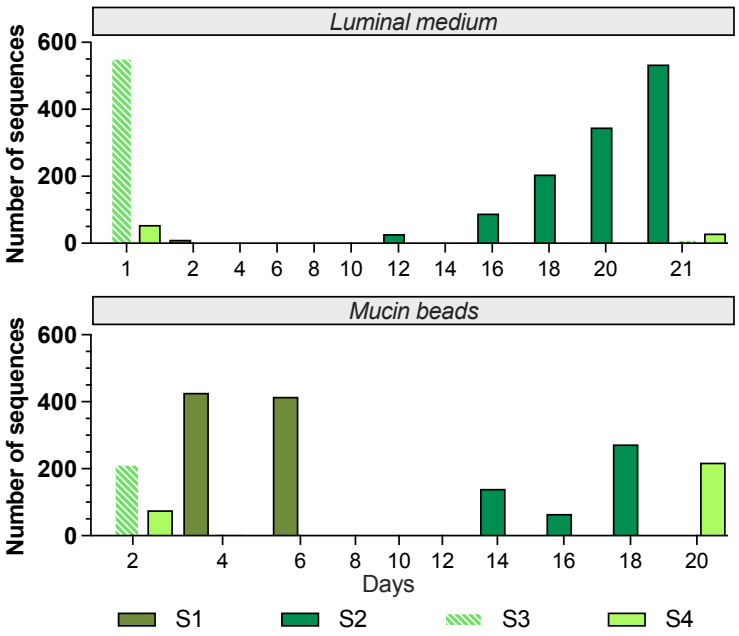

Supplementary figure II.5: Detection of archaea methanogens in the CANIM-ARCOL. Fermentations were performed in the CANIM-ARCOL under three dog size conditions, when bioreactors were inoculated with fecal samples from 13 healthy dogs (n=4 small "S", n=5 medium "M" and n=6 large "L"). Luminal medium of bioreactors and mucin beads were sampled daily to monitor *Archaea methanogens*. Results are expressed as archaeal sequence number (*Methanobrevibacter smithii* only) for small condition only, since no *Archaeal* sequence was amplified from the medium and large samples.

2.6. Additional results

Material and methods

Monitoring redox potential and pH in the CANIM-ARCOL

Redox potential was constantly measured using a redox sensor (Mettler Toledo, Columbus, USA). pH was also followed and controlled by the addition of 2M NaOH.

Functional pathways predictions using Tax4Fun2

Computational predictions of the functional bacterial capabilities using data from 16S rDNA sequencing were performed using Tax4fun2 R-tool (Wemheuer *et al.*, 2020), based on the KEGG (Kyoto Encyclopedia of Genes and Genomes) database (Kanehisa & Goto, 2000). Briefly, Tax4Fun2 transforms ASVs picked up against the Ref99NR database into taxonomic profiles of KEGG organisms and normalize these predictions by the 16S rDNA copy number.

Results and discussion

Impact of dog size on redox potential and pH in the CANIM-ARCOL

Redox potential and pH values were monitored daily in the bioreactors and presented in **Figure II.7**. Similar redox potential values were observed between size conditions (around -450 mV). However, regarding pH values, some specificities could be observed depending on dog size conditions. An almost perfect fit of values compared to setpoints for small and medium condition was noticed. In small bioreactors, short picks of around 0.1 value were observed each two days. Such picks were also observed under medium conditions but with lower increase (around 0.05). This seems to be associated to mucin-beads or nutritive medium bottle renewal. Regarding large size bioreactors, we observed that pH curve is always higher than setpoint (closer to

6.5 more than 6.2), and values took time to stabilize. Such observations are contrary to expectations, since high amounts of SCFA produced under large size conditions should have reduced pH values. However, this is consistent to the higher ammonia concentrations (basic compounds) also quantified in large bioreactors This could be related to the higher protein content contained in the nutritive medium under large size condition, since high-protein diet was previously associated to a shift to proteolytic gut bacteria and higher faecal pH observed (Ephraim *et al.*, 2020).

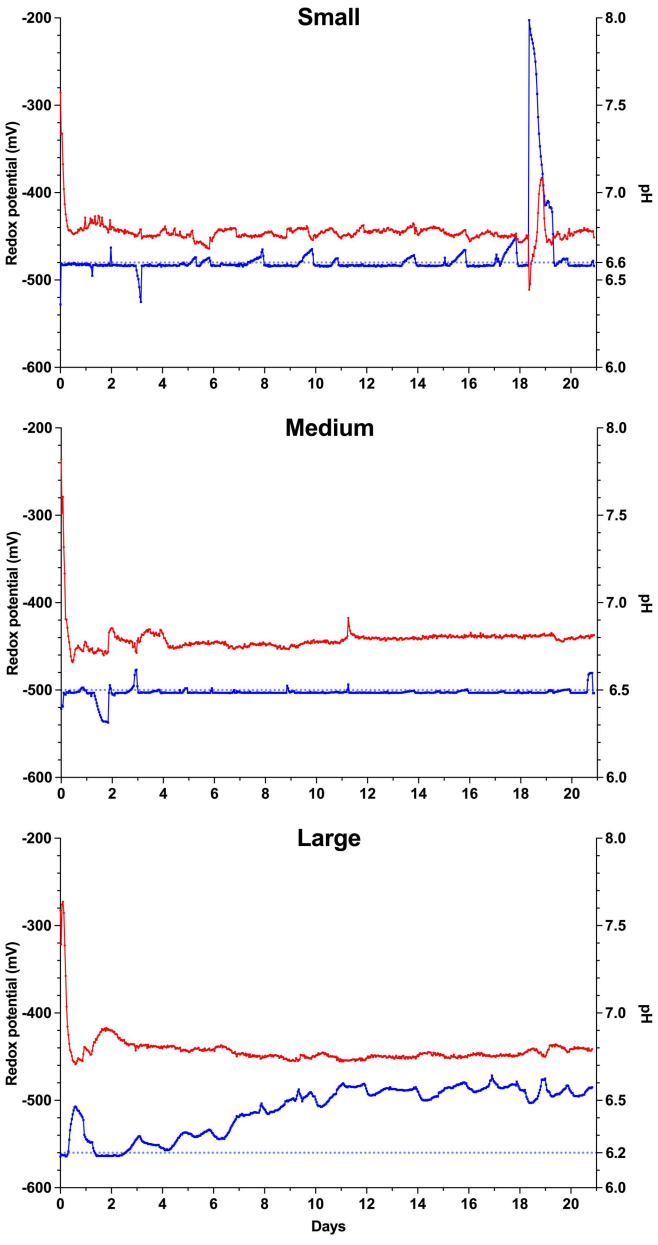

Figure II.7: Impact of dog size on redox potential and pH in the CANIM-ARCOL. Fermentations were performed in the CANIM-ARCOL under three dog sizes conditions. For each one, redox potential was averaged for the different donors and plotted in red (left y-axis). Similarly, pH values are plotted in blue (right y-axis) with setpoint materialized by a blue dotted line.

II-2

Impact of dog sizes on faecal bile acid profiles

Bile acids profiles were assessed in faecal samples from the 13 dogs involved in the study (**Figure II.8).** Such analyses revealed an important variability between dogs within a same size. For instance, inside the small size group, profile of S4 was very different compared to the three other ones (S1 to S3) with around 50 % CA and higher percentages of CDCA and TCA. This high fraction of primary bile acids (around 65 %) questions the digestive health of this dog, since decrease in secondary bile acids was previously associated to intestinal inflammation, chronic enteropathies and microbiota dysbiosis in dogs (Guard *et al.*, 2019; Jergens *et al.*, 2019; Blake *et al.*, 2019; Whittemore *et al.*, 2021). Nevertheless, fecal microbiota composition of dog S4 was similar to other small dogs (at family and genus levels, **Suppl. Figure II.1**) except maybe that it contains the higher fraction of *Fusobacteriaceae*. In addition, values of bile acids recorded for each size were not in line with that of Guard *et al.*, (2019). Guard' study showed a negative correlation of CA with dog size while DCA and LCA increased. In this work, no impact of dog size was observed for CA, LCA and DCA. In both studies, dogs were

owner-client. However, feed composition was not provided in Guard' study, and dogs involved were 1-15 years old, which is probably important to notice since age is known to impact bile acids levels and profiles in human (Frommherz *et al.*, 2016). In addition, different quantification methods were used which can impact of course the results (GC-MS in Guard study *versus* HPLC-QQQ-MS for the PhD work).

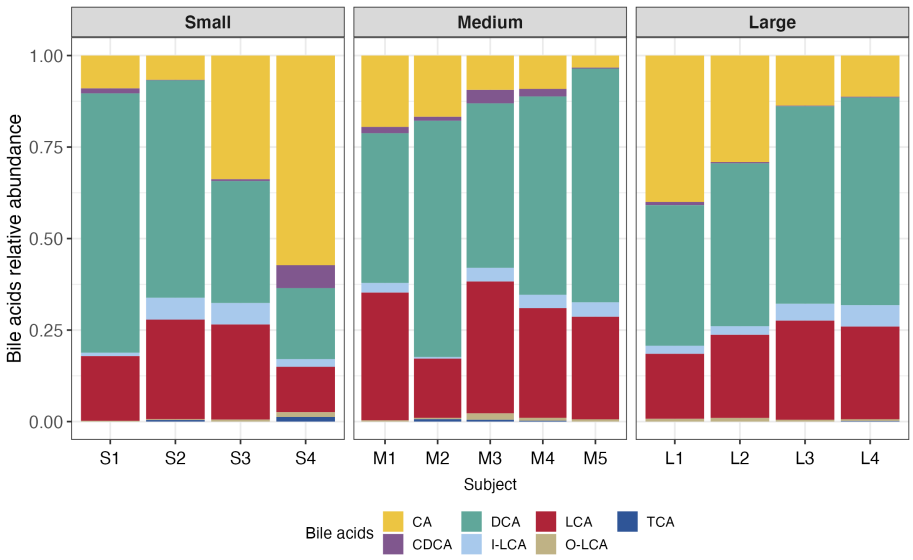

Figure II.8: Impact of dog size on faecal bile acids profiles. Bile acids profiles were analyzed by HPLC-QQQ-MS in faecal samples and presented for each canine donor. *CA: cholic acid, CDCA: chenodeoxycholic acid, DCA: deoxycholic acid, I-LCA: Isoallo-3-ketocholate, LCA: lithocholic acid, O-LCA: 3-oxolithocholic/ dehydrolithocholic acid, TCA: taurocholic acid.*

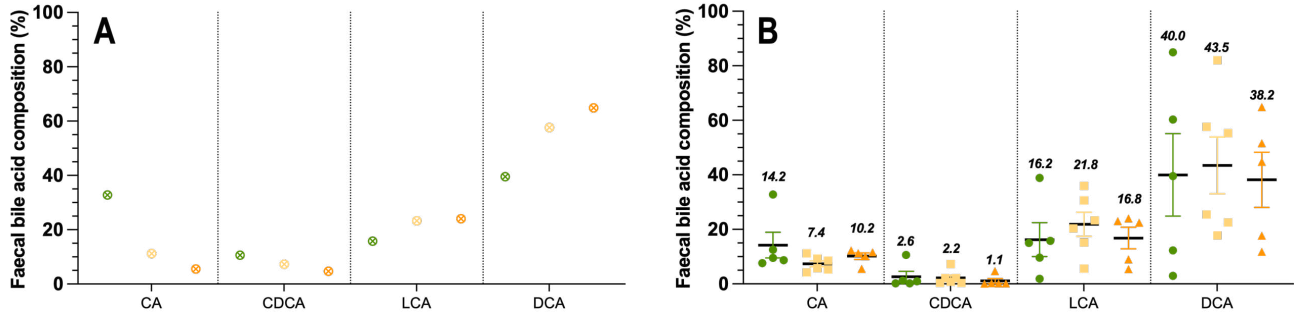

Figure II.9: Impact of dog size on faecal bile acids. Data extracted from Guard *et al.* (2019) are plotted in (**A**), and same results completed by faecal bile acids profiles of the 13 dogs involved in our study are presented in (**B**). *CA: cholic acid, CDCA: chenodeoxycholic acid, LCA: lithocholic acid and DCA: deoxycholic acid.*

Of interest also, at the beginning of the PhD work, bile acid profiles in the nutritive medium were adapted to each dog sizes, based on faecal data from Guard *et al.*, (2019)**.** A clear impact of dog size was described with a decrease in CA and CDCA while LCA and DCA increased with dog size (Figure II.9). After implementation of faecal data obtained in the current study, size effect can be observed only on CDCA percentages, while an important interindividual variability was evidenced, especially regarding secondary bile acids composition. The important differences within a same dog size may be explained by interindividual differences like breed or age (Guard *et al.*, 2019)**.**

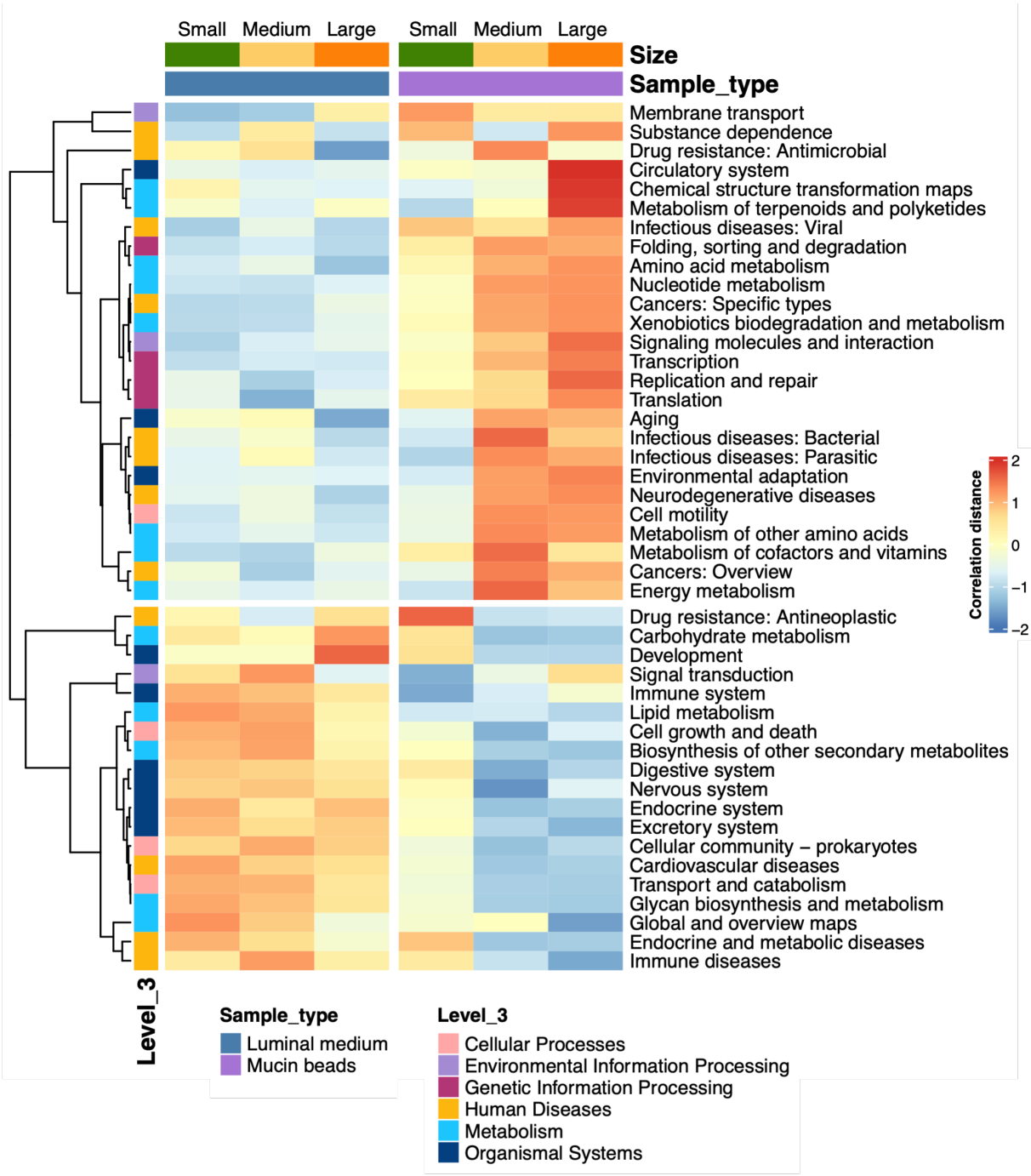

Figure II.10: Impact on colonic microenvironment and dog size on microbiota metabolic pathways predictions. Fermentations were performed in the CANIM-ARCOL under three dog size conditions. Lumen and mucus-associated microbiota compositions were analyzed by 16S metabarcoding. Functional pathways were predicted using Tax4Fun2 R-package, based on ASV table. Stabilized points (from days 10 to 21) were averaged to calculate correlation distances (Bray-Curtis) and results represented as an heatmap.

Impact of colonic microenvironment and dog size on microbiota metabolic pathways predictions

KEGG database was used to generate functional pathways predictions (**Figure II.10**). Two clusters were observed, inversely correlated between luminal and mucosal environments showing that in addition to microbiota composition, some functional specificities also differentiate the two microenvironments. Of interest, in the luminal medium, dog size was positively correlated with different pathways such as 'membrane transport', while others were negatively correlated like 'drug resistance: antimicrobial' or 'endocrine and metabolic diseases'. In mucin beads, size effect was also observed for 'metabolism of terpenoids and polyketides' and 'amino acid metabolism' (positive association). Such predictive analyses highlight for the first-time potential differences in microbiota functionality between different dog sizes, contrarily to previous *in vivo* observations in dogs. Also based on PICRUSt tool, Guard and Suchodolski (2016) observed constant functional predictions on faecal microbiota of 8 healthy dogs from 2.7 to 31.8 kg. In addition, we also evidenced here for the first time different functional pathways and size effect between colonic luminal and mucus-associated canine microbiota. However, these preliminary results are based on prediction based on microbial populations and not on gene expression. Further analyses have to be performed to confirm these predictions such as RNA-seq, to obtain a global gene expression profiling between samples from different dog sizes. Metabolomic analysis can also be considered as a complementary approach, providing a glimpse of bacterial metabolism and function associated to dog sizes.

2.7. Conclusion

In this work, a new canine *in vitro* colonic model called CANIM-ARCOL was developed and validated through *in vivo-in vitro* correlations. This model is one of only two in the world which reproduce both nutritional, physicochemical, and microbial parameters of the canine colon, in a dynamic approach. In an original way, this model is the first one to be adapted to reproduce specific colonic environment of small, medium and large size dogs. Two levels of validation were performed with comparisons of our *in vitro* results to colonic (medium size only) and faecal (all three sizes) *in vivo* data. However, robustness of such validations would be improved if we had additional *in vivo* data on three dog sizes, especially regarding colonic and mucus-associated microbiota and associated microbiota activity. To complete our current analyses, biogenic amines, indoles, and phenols dosages might be performed on both faecal and bioreactor samples, especially to increase our knowledge on proteins fermentation by canine microbiota *in vitro*. Metabolomic analysis might be also performed to investigate the complexity of the canine microbiota metabolism and improve comprehension of the entire large intestine ecosystem in dogs (Guard *et al.*, 2015; Honneffer *et al.*, 2017; Ephraim *et al.*, 2020; Whittemore *et al.*, 2021).

Chapter 3 – Mechanistic study: towards a better understanding of the relative importance of gut microbes and environmental parameters to reshape canine microbiota *in vitro* in relation to dog sizes

Once the CANIM-ARCOL was developed and validated for each dog size (i.e. small, medium and large conditions), we chose in a next step to go deeper into mechanistic approaches. In our literature review and then of course in the CANIM-ARCOL, we evidenced both nutritional, physicochemical and microbial differences between the three dog sizes, such as colonic pH and transit time, bile acid profiles and macronutrients contents in the ileal effluents. In this third chapter, taking benefit of the flexibility of our *in vitro* approach, we aimed to investigate the relative importance of microbes (fecal inoculum) and colonic environmental conditions (nutritional and physicochemical parameters) on canine colonic microbiota structure and functions. With this objective in mind, we performed additional fermentations when the CANIM-ARCOL was set-up to reproduce, as previously defined, the colonic conditions of small, medium or large dogs, but when the bioreactors were only inoculated with fecal samples from medium size dogs (2 donors, one male and one female). This study aims also to verify if the nutritional and physicochemical parameters alone, deprived of host conditions (i.e. crosstalk with host cells, hormones, intestinal permeability or immune system) and size-related fecal inoculum, are sufficient or not to shift microbiota from a medium size profile to small and large profiles. This work will be submitted for publication in *Applied Microbiology and Biotechnology*.

ORIGINAL ARTICLE

Large intestinal nutritional and physicochemical parameters from different dog sizes reshape canine microbiota structure and functions *in vitro*

DESCHAMPS, C., DENIS, S., HUMBERT, D., CHALANCON, S., ACHARD, C., APPER, E., & BLANQUET-DIOT, S. (**2023**)

To be submitted in Applied Microbiology and Biotechnology (**IF 5.6**)

For the entire manuscript this article will be cited as **Deschamps *et al.* (2023b)**.

Abstract

Different dog sizes are associated with variations in large intestinal physiology including gut microbiota, which plays a key role in animal health. This study aims to evaluate, using the CANIM-ARCOL (Canine Mucosal Artificial Colon), the relative importance of gut microbes *versus* physicochemical and nutritional parameters of the canine colonic environment in shaping microbiota structure and functions. CANIM-ARCOL was set-up to reproduce nutrient availability, bile acid profiles, colonic pH and transit time from small, medium or large dogs according to *in vivo* data, while bioreactors were all inoculated with a fecal sample collected from medium size dogs (n=2). Applying different dog size parameters resulted in a positive association between size and gas or SCFA production, as well as distinct microbiota profiles as revealed by 16S metabarcoding. Comparisons with *in vivo* data from canine stools and previous *in vitro* results obtained when CANIM-ARCOL was inoculated with fecal samples from three dog sizes revealed that environmental colonic parameters were sufficient to drive microbiota functions. However, size-related fecal microbes were necessary to accurately reproduce *in vitro* the colonic ecosystem of small, medium and large dogs. For the first time, this study provides mechanistic insights on which parameters from colonic ecosystem mainly drive canine microbiota in relation to dog size. The CANIM-ARCOL can be used as a relevant *in vitro* platform to unravel interactions between food or pharma compounds and canine colonic microbiota, under different dog size conditions. The potential of the model will be extended soon to diseased situations (e.g. chronic enteropathies or obesity).

3.1. Introduction

It is now acknowledged that gut microbiota plays a crucial role in the health of mammalian hosts, including dogs. Each compartment of the canine gastrointestinal tract is colonized by a resident microbiota mainly composed by bacteria, viruses, fungi, and protozoa, with the higher diversity and abundance found in the large intestine (Hooda *et al.*, 2012; Honneffer *et al.*, 2017). Even if evidences remain scarce in dogs (Simpson *et al.*, 2006; Cassmann *et al.*, 2016; Dubbelboer *et al.*, 2022), it can be assumed, based on the human situation, that canine microbiota varies from the digestive lumen to the intestinal epithelium surface, where a mucus layer provides nutrients and habitat for specific microbes. The intestinal microbiome protects against pathogens, educates the host immune system, and has important metabolic functions, such as food digestion leading to major end-fermentation products like short-chain fatty acid (SCFA), ammonia and gases, and bile acids metabolism (Blake & Suchodolski, 2016; Kakimoto *et al.*, 2017).

Up to now, there are few data in dogs investigating how canine body weight can impact digestive physiology and gut microbiota (Deschamps *et al.*, 2022b). Most of recognized changes in gastrointestinal physiology are related to the large intestine, with a decrease in colonic pH together with increase in transit time and permeability associated to dog size (Bjarnason *et al.*, 1995; Zentek & Meyer, 1995; Weber *et al.*, 2002b, 2002a, 2004, 2017). Regarding the effect of canine body weight on gut microbiota composition and activities, the only available data are provided from stool analysis. Those studies seem to indicate a positive correlation between body weight and carbohydrate/protein fermentation capacity (Goudez *et al.*, 2011; Beloshapka *et al.*,

2012, 2014; Alexander *et al.*, 2019; Detweiler *et al.*, 2019; Nogueira *et al.*, 2019), resulting in higher SCFA and ammonia concentrations in fecal samples from large dogs (Weber *et al.*, 2004). Fecal bile acid profiles are also impacted by dog size, with an apparent decrease of total bile acids, as well as primary to secondary bile acid ratios, when body weight increases (Guard *et al.*, 2019). Lastly, data from dog stools suggest that relative abundances of *Proteobacteria* and *Actinobacteria* decreased with body weight (Deschamps *et al.*, 2022b).

Given the paucity of data related to dog size effect on large intestinal microbiota structure and functions in dogs, an alternative option is to use *in vitro* models of the canine colon to answer such question. This alternative strategy is fully in line with European "3R" rules and provides cost, technical, ethical and regulatory benefits compared to *in vivo* assays (Russel & Burch, 1959; Deschamps *et al.*, 2022a). Two dynamic models of the canine colon have been recently developed, namely the Mucosal Simulator of the Canine Intestinal Microbial Environment (M-SCIME, Van den Abbeele *et al.* 2020a) and the Canine Mucosal Artificial Colon (CANIM-ARCOL, Deschamps *et al.* 2023a). Only the second one has been adapted to simulate the specific conditions (i.e. pH, transit time, nutrients, bile acid profiles) found in the colon of three dog sizes (i.e. small under 10 kg, medium from 10 to 30 kg and large size over 30 kg), with great *in vivo-in vitro* correlations. In those studies, *in vitro* colon models have been inoculated with fecal samples from size-related colonic conditions (e.g. medium size bioreactors were inoculated with stool from medium size dogs). It would be now of great interest to investigate if colonic nutritional and physicochemical parameters from different dog sizes are sufficient to reshape microbiota profiles *in vitro*.

In this context, we performed *in vitro* fermentations in the CANIM-ARCOL inoculated with medium dog size stools, but set-up to reproduce small, medium or large colonic conditions. Samples were regularly collected in bioreactors to analyze the composition of both lumen and mucus-associated microbiota and monitor gut microbes' activities through SCFA, gas and ammonia measurement.

Table III.1 Characteristics of healthy adult dogs from medium size used as fecal donors for *in vitro* experiments. *M: male, F: female, BCS: body condition score (ranging from 1 -very thin- to 5 -obese-, 3 corresponding to ideal weight)*

Size	*Dog_id*	*Breed*	*Sex*	*Sterilization*	*Age (years)*	*BCS*	*Weight (kg)*	*Garden access*	*Feed*
Medium	A	Labrador	F	Yes	9	4	25	Yes	Dry
	B	Samoyed	M	Yes	2.5	3	22.5	Yes	Dry

3.2. Materials and methods

3.2.1. Fecal samples collection and treatment

Two healthy dogs from medium size were used as stool donors for *in vitro* experiments (**Table III.1**): a female Labrador (dog A, 25 kg) and a male Samoyed (dog B, 22.5 kg). Both dogs were owner-pets, fed with

commercial dry food, with access to outdoor. Immediately after defecation, fecal samples were transferred into a sterile recipient, placed in an airtight anaerobic box (GENbag anaer gas pack systems, Biomerieux, France), transported and processed at the laboratory within 3 h. In an anaerobic chamber (COY laboratories, Grass Lake, USA), stool samples were manually homogenized, and 3.75 g of feces were resuspended in 100 mL of 30 mM sterile sodium phosphate buffer (pH 6.0), mixed and filtered (500 µm inox sieve).

3.2.2. Description and set-up of the CANIM-ARCOL model

CANIM-ARCOL is a one-stage fermentation system (MiniBio, Applikon, Delft, The Netherlands), inoculated with stool samples and used under continuous conditions to simulate the nutritional, physicochemical and microbial conditions found in the large intestine of dogs (Deschamps *et al.* 2023a). Briefly, the *in vitro* model is composed of a main bioreactor simulating the colonic luminal medium and an airtight glass vessel connected to this bioreactor and containing mucin beads to reproduce the mucosal compartment (**Figure III.1a**). At the beginning of experiments, 100 mL of faecal suspension from each dog were added per bioreactor to 200 mL of sterile canine-adapted nutritive medium simulating the composition of ileal effluents (**Table III.2**). To ensure anaerobic condition at the beginning of fermentation, the bioreactor was operated with an initial sparging with O_2-free N_2 gas. Afterwards, during the fermentation course, anaerobic condition was maintained by the sole activity of resident microbiota. The *in vitro* model was kept at canine body temperature (i.e. 39°C). pH and redox potential were constantly recorded (Applikon, The Netherlands) and pH was adjusted to the setpoint values with 2 M NaOH. The nutritive medium was continuously introduced into the main bioreactor, while the fermentation medium was automatically withdrawn, ensuring the appropriate colonic retention time. Every two days, mucin beads from the mucosal compartment were renewed by fresh sterile ones under a constant flow of CO_2 to avoid oxygen entrance, as previously described (Deschamps *et al.*, 2020). In the present study, the CANIM-ARCOL was set-up with nutritional and physicochemical parameters adapted to three dog sizes as previously validated and detailed in **Table III.2** (Deschamps *et al.* 2023a).

3.2.3. Experimental design and sampling

For each experiment, three bioreactors were inoculated with a same faecal sample from a medium size dog and run in parallel (**Figure III.1a**). Each bioreactor was set-up with parameters corresponding to one of the three sizes conditions (i.e. small, medium or large dog sizes), based on *in vivo* data as previously reviewed (Deschamps *et al.*, 2022b). Fermentations were run under batch conditions for 24h and then under continuous conditions for 8 additional days. Samples were collected daily (**Figure III.1b**) in the fermentation medium (luminal medium) for further analysis of microbiota composition (qPCR and 16S Metabarcoding) and gut microbial activities through SCFA and ammonia measurement. Every two days, mucin beads were collected for analysis of mucus-associated microbiota (qPCR and 16S Metabarcoding). Mucin beads were washed twice in sterile sodium phosphate buffer and stored at -80°C before downstream analysis. The atmospheric phase was also sampled every day to follow anaerobiosis and determine gas composition and production (total volume of gas) thanks to a sampling bag connected to the condenser (**Figure III.1b**).

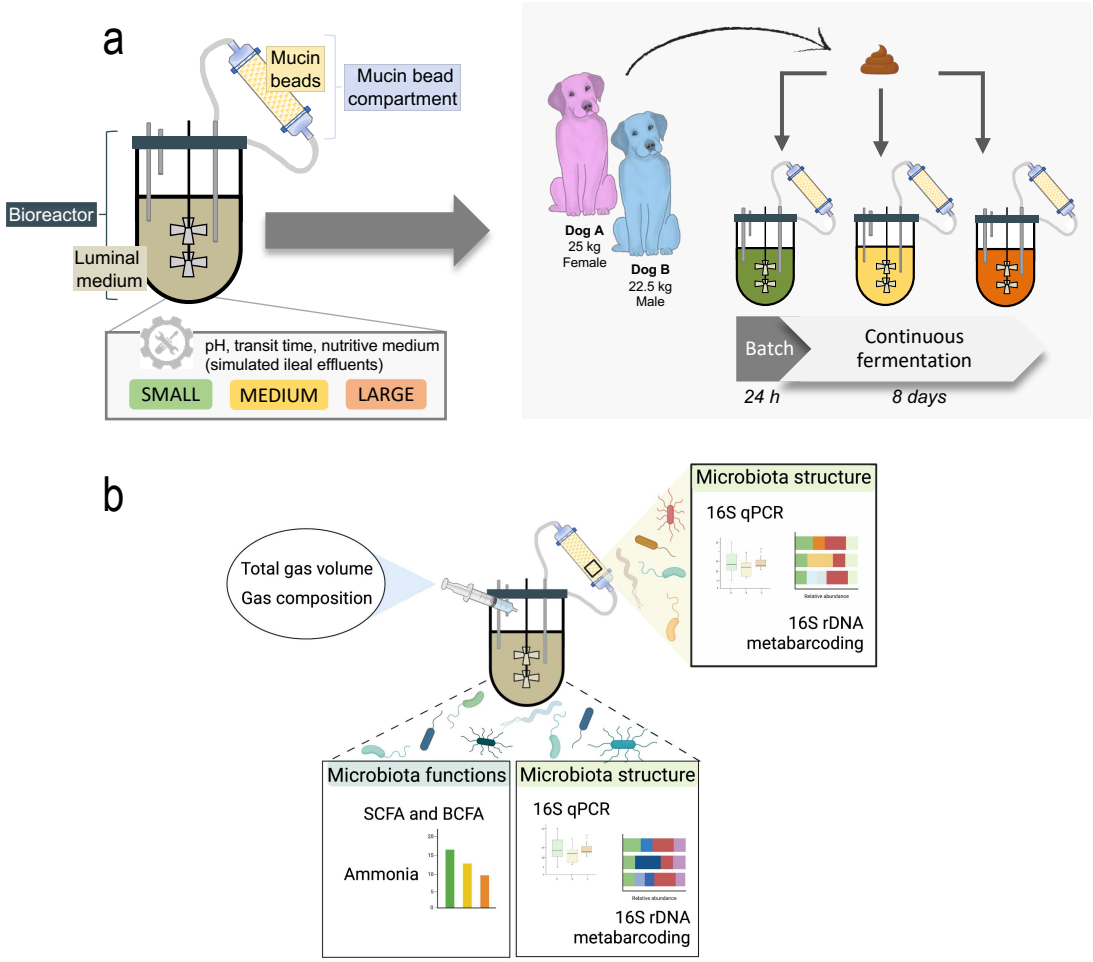

Figure III.1 Experimental design in the CANIM-ARCOL. (**a**) The CANIM-ARCOL was inoculated with faecal samples from two medium dogs (one female and one male, i.e. two biological replicates). Three bioreactors corresponding to three sizes conditions (i.e. small under 10 kg, medium from 10 to 30 kg and large over 30 kg) were run in parallel for 9 days. (**b**) Samples were regularly collected in the atmospheric phase, in the luminal medium and from mucin beads to monitor microbiota composition and fermentation metabolites.

Table III.2 Nutritional and physicochemical parameters used to set-up the CANIM-ARCOL under three dog sizes conditions. rpm: rotation per minute

Size	***Small***	***Medium***	***Large***
Weight (kg)	**< 10**	**10-30**	**> 30**
Bioreactor's parameters			
Temperature	39 °C	39 °C	39 °C
Residence time	5 h	9 h	15 h
pH	6.6	6.5	6.2
Stirring	400 rpm	400 rpm	400 rpm
Nutritive medium composition (in %)			
Proteins	17.2	27.0	35.6
Carbohydrates	0.9	1.3	1.8
Lipids	1.6	2.4	3.2
Fibers	3.3	5.2	6.8

Bile acids composition in the nutritive medium (mg/L)

Cholic acid	108 mg 35 %	55 mg 10 %	32 mg 5 %
Chenodeoxycholic acid	31 mg 10 %	27 mg 5 %	32 mg 5 %
Deoxycholic acid	124 mg 40 %	327 mg 60 %	418 mg 65 %
Lithocholic acid	46 mg 15 %	136 mg 25 %	161 mg 25 %

3.2.4. DNA extraction

Genomic DNA was extracted from luminal medium samples and mucin beads using the QIAamp Fast DNA Stool Mini Kit (Qiagen, Germany) following manufacturer's instructions with the following modifications. Prior to DNA extraction, luminal samples were centrifuged (18 000 rcf, 15 min, 4°C) and the pellets were collected. Pellets and mucin beads samples were then incubated 10 min with sterile citrate buffer (sodium citrate 55 mM and NaCl 154 mM) at 37°C, before vortexing (maximal speed, 15 sec) and centrifuging again (8000 rcf, 1 min). Then, a step of mechanical disruption using a bead beater (5 min, 20 beat/s) was made with 300 mg sterile glass beads (diameter ranging from 100 to 600 µm). DNA quantity was evaluated using the Qubit dsDNA Broad Range Assay Kit (Invitrogen, USA) with a Qubit 3.0 Fluorometer (Invitrogen, USA). Samples were stored at -20°C prior to microbiota analysis.

3.2.5. Quantitative PCR

Total bacteria were quantified by qPCR using primers described in **Table III.3**. Real-time PCR assays were performed in a Biorad CFX96TM Real-Time System (Bio-Rad Laboratories, USA) using Takyon Low ROX SYBR 2X MasterMix blue dTTP kit (Eurogentec, Belgium). Each reaction was run in duplicate in a final volume of 10 µL with 5 µL of MasterMix, 0.45 µL of each primer (10 µM), 1 µL of DNA sample and 3.1 µL of ultra-pure water. Amplifications were carried out using the following ramping profile: 1 cycle at 95°C for 5 min, followed by 40 cycles of 95°C for 30 s, 58°C for 30 sec. A melting step was added to ensure primer specificity. Standard curve was generated from 10-fold dilutions of bacterial DNA (isolated from a pure culture of bacteria), allowing the calculation of DNA concentrations from extracted samples.

Table III.3 Primers used for qPCR and 16S Metabarcoding analysis.

Primer name	*Sequence 5'-3'*	*Target*	*Annealing temperature (°C)*	*References*
qPCR primers				
BAC338R	ACTCCTACGGGAGGCAG	Total bacteria	58	Yu *et al.* (2005)
BAC516F	GTATTACCGCGGCTGCTG			
Metabarcoding primers				
V3-341F	CCTACGGGAGGCAGCAG	Bacteria	-	
V4-806R	GGACTACNVGGGTWTCTAAT			

3.2.6. 16S Metabarcoding and data analysis

Bacterial V3-V4 regions of 16S ribosomal DNA (rRNA) were amplified using primers described in **Table III.3**. High-throughput sequencing was performed on an Illumina MiSeq sequencer by the GeT-PlaGe

core facility (INRAe Transfer, Toulouse, France). MiSeq Reagent Kit v3 was used according to the manufacturer's instruction (Illumina Inc., San Diego, CA). Bioinformatic analysis were performed using R studio software and using rANOMALY package (Theil & Rifa, 2021). Prior to analysis, raw data were demultiplexed and quality filtered using DADA2 R-package (Callahan *et al.*, 2016). Reads with quality score under 2 were truncated. Reads under 100 pb length were removed as well as sequences similar to PhiX DNA used as a spike-in control for MiSeq runs. Filtered sequences were dereplicated and cleaned for chimeras (DADA2). Taxonomic classification of the sequences was then performed with DECIPHER package (Murali *et al.*, 2018). Assignations from both SILVA 138 release (Quast *et al.*, 2013) and GTDB_bac120_arc122 (Parks *et al.*, 2022) databases were merged using the assign_taxo_fun function from rANOMALY R-package based on IDTAXA, with a 60% confidence cut-off (Theil & Rifa, 2021). A phylogenetic tree was then reconstructed using DECIPHER.

3.2.7. Gas analysis

Analysis of O_2, N_2, CO_2, CH_4, and H_2 gas produced during the fermentation process was performed using 490 micro-gas chromatography (Agilent Technologies, USA) coupled with a micro-TCD detector (Agilent Technologies, USA). Molecular Sieve 5A and Porapack Q (Aligent Technologies, USA) series columns were used. Gas composition was determined using calibration curves made from ambient air (78.09 % N_2, 20.95 % O_2, 0.04 % CO_2) and three gas mixtures A (5 % CO_2, 5 % H_2, 90 % N_2), B (20 % CO_2, 80 % H_2), and C (20 % CO_2, 20 % CH_4, 20 % H_2, 40 % N_2). Technical replicates were performed for each sample and results were expressed as relative percentages.

3.2.8. Short chain fatty acid analysis

For SCFA analysis, 1.5 mL of luminal medium samples were centrifuged (18 000 rcf, 15 min, 4°C) and 900 µL of supernatant was diluted at 1/10 into H_2SO_4 0.04 M mobile phase, vortexed, and filtered (0.22 µm). The three major SCFAs (acetate, propionate, and butyrate) were quantified by high-performance liquid chromatography -HPLC- (Elite LaChrom, Merck HITACHI, USA) coupled with a DAD diode. The HPLC column (Concise Separations, ICE-99-9865) and its guard column were maintained at 50°C. Sulfuric acid 0.04 M was used as mobile phase and SCFA were separated at a flow rate of 0.6 mL/min. Data were obtained and analyzed by the EZChrom Elite software at 205 nm. SCFA concentrations were calculated from calibration curves established from known concentration solutions of acetate, propionate, and butyrate (0, 10, 25, and 40 mM) and data expressed as mM or relative percentages.

3.2.9. Ammonia quantification

Total ammonia was measured using the Ammonia assay kit (LIBIOS, France) following manufacturer's instructions. Results were expressed in mmol/L.

3.2.10. Statistical analysis

Statistical analyses on microbiota activity (gas, SCFA, ammonia) and α-diversity indexes (number of observed ASVs and Shannon index) from metabarcoding data were processed using GraphPad Prism software

version 9.4.1 (GraphPad Software, USA). Data normal distribution was verified by combining Anderson-Darling, D'Agostino & Pearson, Shapiro-Wilk and Kolmogorov-Smirnov tests and homoscedasticity was checked using the Fisher test. Then, appropriate statistical analysis was applied (either one-way ANOVA, *t*-test, Mann-Whitney or Welch's tests). First, principal coordinate analysis (PCoA, data not shown) were performed followed by Non-Metric Multidimensional Scaling (NMDS), highlighting important size and microenvironment (i.e. luminal medium and mucin beads) effects. Constraint Redundancy analysis (RDA) were then performed with age, weight, sex, size, microenvironment, donor and time as variables of the model, first will all parameters and then with removal of either size or microenvironment variables. Bray Curtis distances were used for each analysis and significance between groups was assessed with a one or two-way Anova. Discriminant analyses (sPLS-DA) were finally performed using MixOmics package (Lê Cao *et al.*, 2009). Pearson correlations between physicochemical or nutritional variables and bacterial families were established using the 'microeco' R-package (Liu *et al.*, 2021a).

3.1. Results

3.1.1. Faecal inoculum characterization

Stools used for bioreactor inoculation were characterized (**Figure III.2**). Alpha-diversity was similar between the two faecal samples with a Shannon index of 2.99 for dog A and 2.98 for dog B.Faecal bacterial profiles at the phylum level (**Figure III.2a**) were similar between the two donors with a majority of *Bacteroidota* (67% in dog A and 42% in dog B), followed by *Fusobacteriota* (15% in dog A, 36% in dog B), *Firmicutes* (13%), and *Proteobacteria* (3% in dog A, 9% in dog B). At the family level (**Figure III.2b**), dog B showed higher abundance in *Bacteroidaceae, Burkholderiaceae, Clostridiaceae*, and *Fusobacteriaceae* families compared to dog A, whereas *Prevotellaceae* was less abundant. Even if total fecal SCFA concentration **(Figure III.2c)** was similar between the two dogs, different SCFA profiles (**Figure III.2d** and **2e**) were observed with a majority of acetate in both donors, but no butyrate in dog A. Similarly, ammonia concentrations differed between the two dogs with a 10-fold higher concentration in dog B (**Figure III.2f**).

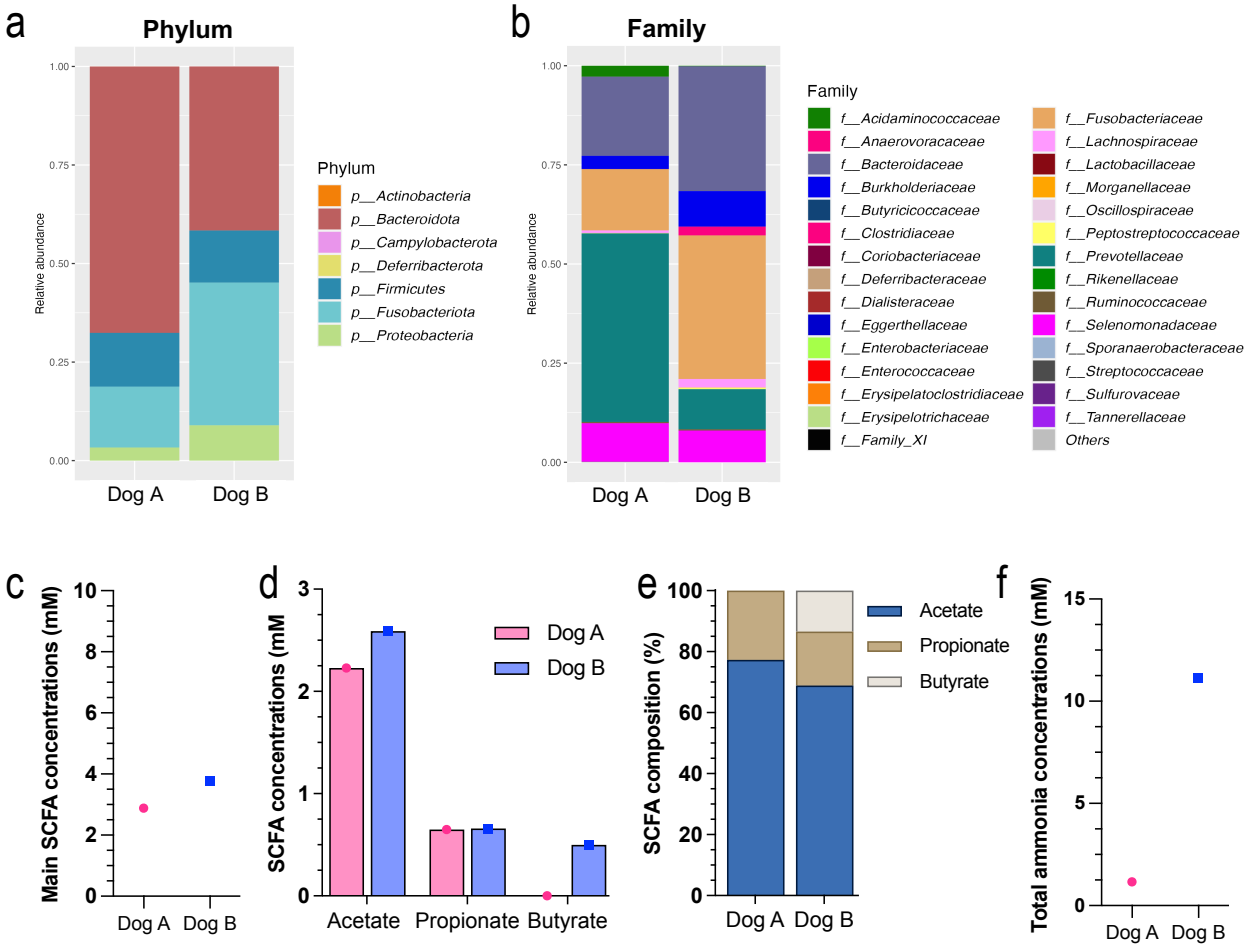

Figure III.2 Stool characterization for each canine donor. Stool samples were collected from two healthy medium dogs. Microbiota composition was analyzed by 16S Metabarcoding. Bacterial abundances are represented at the phylum (**a**), family (**b**) and genus (**c**) levels. The three main SCFA (i.e. acetate, propionate and butyrate) were measured and expressed as total concentration (**d** and **e**) and relative percentages (**f**). Ammonia concentrations are given in (**g**)

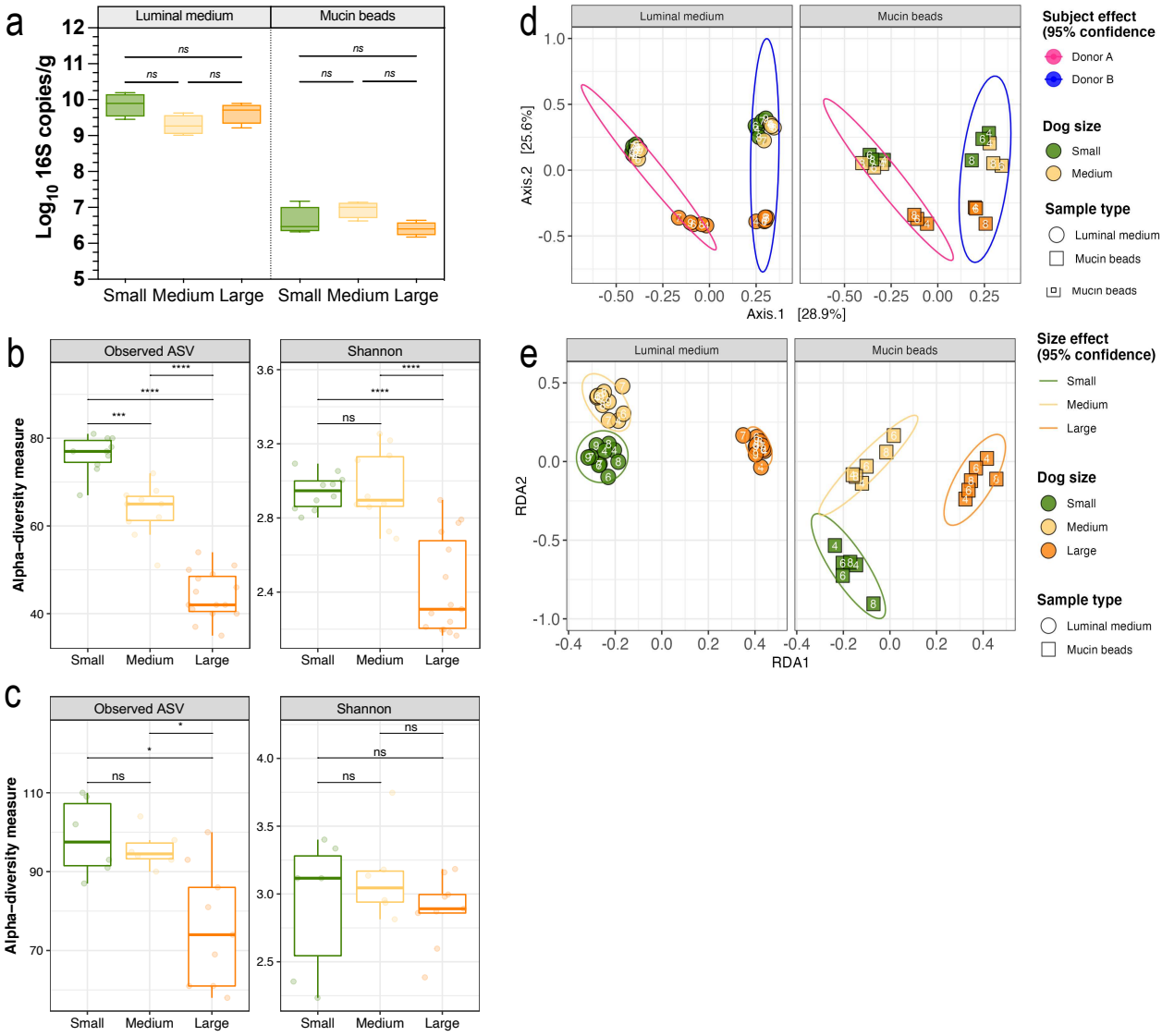

Figure III.3 Impact of dog size on bacterial load and microbial diversity in the CANIM-ARCOL. Fermentations were performed in the CANIM-ARCOL under three dog size conditions (i.e. small, medium, large), after inoculation with stools from medium size dogs (n=2). Total bacteria were quantified and expressed as Log_{10} 16S copies/g (**a**). Lumen and mucus-associated microbiota composition was analyzed by 16S Metabarcoding and diversity indexes were calculated based on ASV table. α-diversity indexes (observed ASVs and Shannon) calculated from days 4 to 9 are represented as box plots in the luminal medium (**b**) and mucin beads (**c**). Beta-diversity of samples from days 4 to 9 was analyzed by PCoA showing clear donor (**d**) effect. Redundancy analysis (RDA) without donor effect based on Bray-Curtis distances indicated strong size effect (**e**). Significant differences based on Kruskal and Wallis test are presented as * $p<0.05$, *** $p<0.001$, **** $p<0.0001$. *ns: non-significant difference ($p>0.05$)*

3.1.2. Impact of size conditions on canine colonic microbiota structure

CANIM-ARCOL was used to run colonic fermentations using small, medium or large size parameters while inoculated only with a medium stool. Total bacteria levels (**Figure III.3a**) were similar whatever the size

condition, but with higher amounts in the luminal medium (10 Log_{10} 16S copies/g) than in mucin beads (6 Log_{10} 16S copies/g). In the luminal medium (**Figure III.3b)**, number of observed ASV was negatively correlated with breed format ($p<0.001$), while only Shannon index from large size condition was significantly lower than the one obtained for small and medium ($p<0.0001$). In the mucin beads (**Figure III.3c)**, number of observed ASV was significantly lower for large condition ($p<0.05$) whereas Shannon index was not different. Whatever the size condition, alpha diversity was higher in mucin beads compared to luminal medium. Principal component analysis (PCoA) based on ASV composition and Bray-Curtis distance showed strong effects of stool donor, in both colonic microenvironments (**Figure III.3d**). Redundancy analysis (RDA) removing donor effect demonstrated a clear ($p<0.0001$) clustering by size, again in both the luminal medium and mucin beads (**Figure III.3e**). In addition, samples associated to large condition clustered apart from small and medium groups.

Whatever taxonomic levels and colonic microenvironments, profiles obtained with small and medium size conditions were more closely related than large one (**Figure III.4**). At the phylum level (**Figure III.4a**), in the luminal medium, for both donors, we can observe from small to large condition an increase in relative abundances of *Fusobacteriota* (from 22 % in small to 33 % in large condition), *Firmicutes* (from 14 % to 35 %) and *Proteobacteria* (from 5 % to 28 %) whereas *Bacteroidota* decreased (from 59 % to 3 %). At family level (**Figure III.4b**), *Lactobacillaceae, Coriobacteriaceae*, and *Dialisteraceae* and *Streptococcaceae* (the last one for dog A only) were only present in the large size condition in luminal and mucosal fractions. Moreover, the large size condition presented an important luminal proportion of *Peptostreptococcaceae* (around 5-15 %) for dog A and *Enterobacteriaceae* (until 30 %) for dog B, balanced by a reduced *Bacteroidaceae* and *Prevotellaceae* proportions (< 5%) compared to small and medium groups. Interestingly, some differences observed between donor A and B were kept in the artificial colon, such as higher abundances in *Clostridiaceae*, *Enterobacteriaceae* and *Lachnospiraceae* in bioreactors inoculated with stool from dog B. At the genus level (**Figure III.4c**), main results obtained at a higher taxonomic level were confirmed with higher relative abundances under large size condition of *Fusobacterium*, *Prevotella*, *Proteus, Peptacetobacter*, *Lactobacillus* and *Clostridium* (only for dog B), together with lower amounts of *Bacteroides* and *Alloprevotella*.

Discriminant analysis (**Figure III.5**) between the three size groups confirmed that small and medium size conditions were more similar (at the family level) between them than with large size condition (*i.e.* small *vs* large and medium *vs* large). In the luminal compartment (**Figure III.5a**), *Lactobacillaceae*, *Enterococcaceae*, *Sporanaerobacteraceae*, *Clostridiaceae Peptostreptococcaceae, Coriobacteriaceae, Dialisteraceae, Bifidobacteriaceae* and *Fusobacteriaceae* were significantly enriched in the large size conditions compared to both medium and small ($p<0.05$).

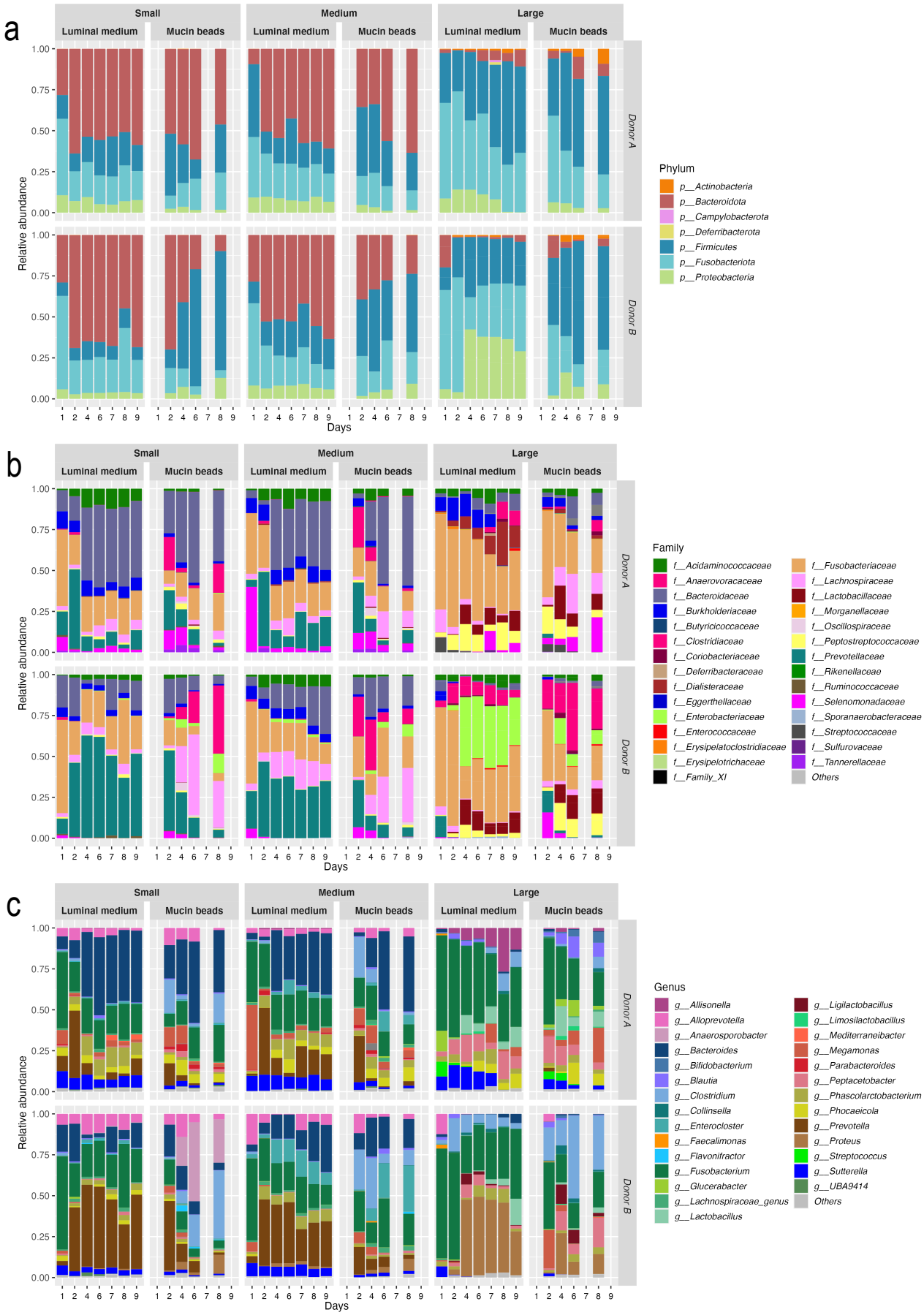
a
Small
Medium
Large
Luminal medium
Mucin beads
Donor A
Donor B
Relative abundance
Days
Phylum
p__Actinobacteria
p__Bacteroidota
p__Campylobacterota
p__Deferribacterota
p__Firmicutes
p__Fusobacteriota
p__Proteobacteria
b
Family
f__Acidaminococcaceae
f__Anaerovoracaceae
f__Bacteroidaceae
f__Burkholderiaceae
f__Butyricicoccaceae
f__Clostridiaceae
f__Coriobacteriaceae
f__Deferribacteraceae
f__Dialisteraceae
f__Eggerthellaceae
f__Enterobacteriaceae
f__Enterococcaceae
f__Erysipelatoclostridiaceae
f__Erysipelotrichaceae
f__Family_XI
f__Fusobacteriaceae
f__Lachnospiraceae
f__Lactobacillaceae
f__Morganellaceae
f__Oscillospiraceae
f__Peptostreptococcaceae
f__Prevotellaceae
f__Rikenellaceae
f__Ruminococcaceae
f__Selenomonadaceae
f__Sporanaerobacteraceae
f__Streptococcaceae
f__Sulfurovaceae
f__Tannerellaceae
Others
c
Genus
g__Allisonella
g__Alloprevotella
g__Anaerosporobacter
g__Bacteroides
g__Bifidobacterium
g__Blautia
g__Clostridium
g__Collinsella
g__Enterocloster
g__Faecalimonas
g__Flavonifractor
g__Fusobacterium
g__Glucerabacter
g__Lachnospiraceae_genus
g__Lactobacillus
g__Ligilactobacillus
g__Limosilactobacillus
g__Mediterraneibacter
g__Megamonas
g__Parabacteroides
g__Peptacetobacter
g__Phascolarctobacterium
g__Phocaeicola
g__Prevotella
g__Proteus
g__Streptococcus
g__Sutterella
g__UBA9414
Others

Figure III.4 Impact of dog size on microbial composition in the CANIM-ARCOL. Fermentations were performed in the CANIM-ARCOL under three dog size conditions (i.e. small, medium, large), after inoculation with stools from medium size dogs (n=2). Lumen and mucus-associated microbiota composition was analyzed by qPCR and 16S Metabarcoding. Relative abundance of the main bacterial populations in both colonic microenvironments are represented at the phylum (**a**), family (**b**) and genus (**c**) levels

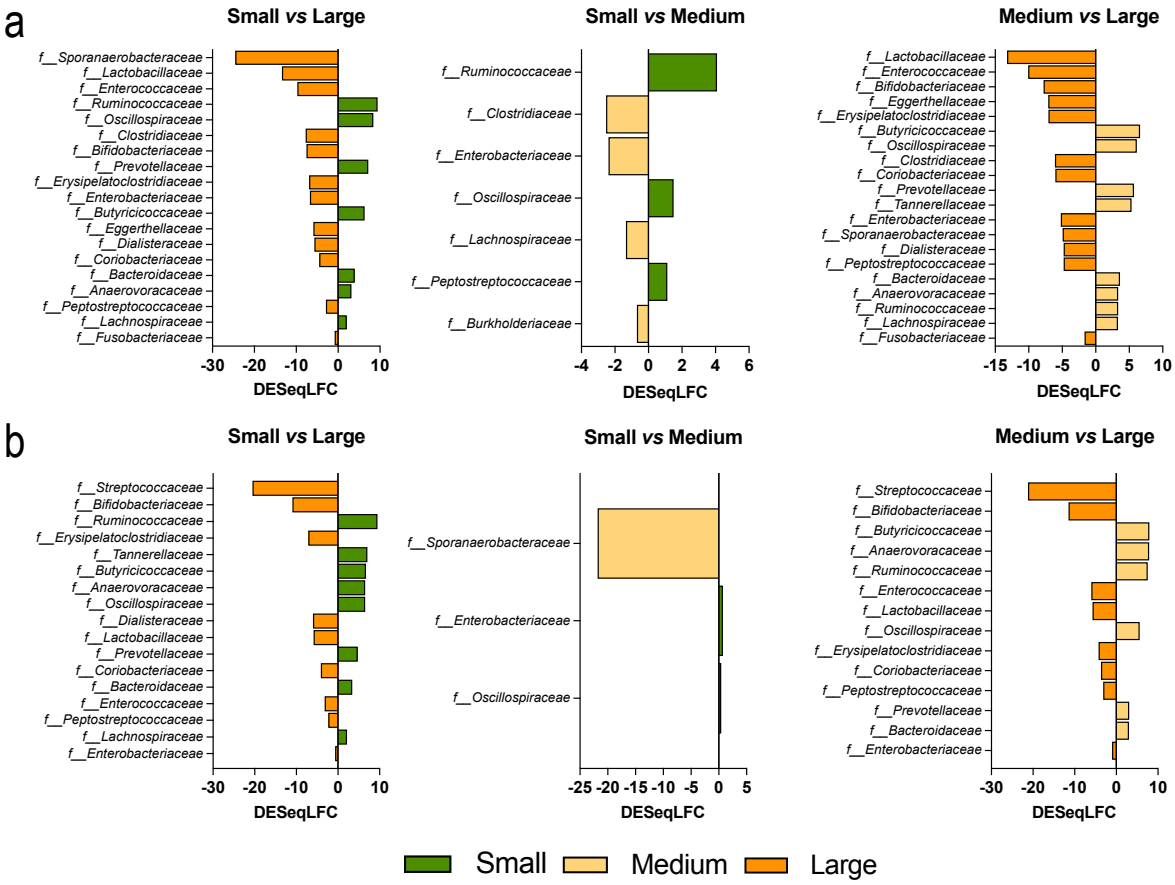

Figure III.5 Differential analysis on dog size impact on microbiota composition at the genus level. Fermentations were performed in the CANIM-ARCOL under three dog size conditions (i.e. small, medium, large), after inoculation with stools from medium size dogs (n=2). Lumen and mucus-associated microbiota composition was analyzed by 16S Metabarcoding and differential analysis were further performed on days 2 to 9. Differential analyses based on DESeq2 method were performed to generate loading plots of the 10 most contributing genera between sizes in luminal medium (**a**) and mucin beads (**b**). Bars are colored according to the group in which the median abundance is maximal, small in green, medium in yellow and large condition in orange

The most striking differences between small and medium size conditions were the enrichment of *Ruminococcaceae* and *Oscillospiraceae* in small condition, together with an increase in relative abundance of *Clostridiaceae*, *Enterobacteriaceae* and *Lachnospiraceae* under medium one. In the mucin beads (**Figure III.5b**), some discriminant families of the luminal medium (large *versus* medium and small) are conserved, such as higher relative abundance of *Enterococcaceae*, *Bifidobacteriaceae, Oscillospiraceae* and *Lactobacillaceae*. Other families, like *Streptococcaceae*, are highly selective of the large size condition, but only in the mucus-associated microbiota.

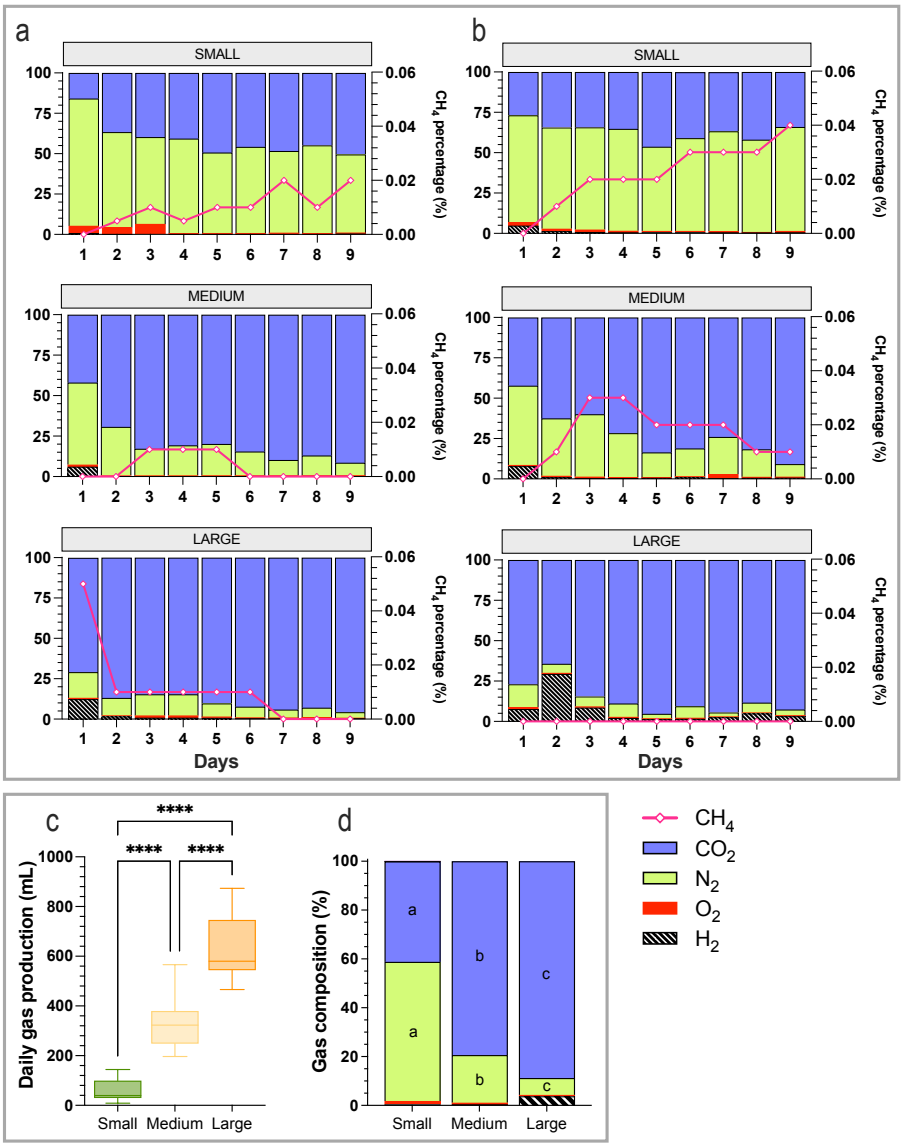

Figure III.6 Impact of dog size on gas production in the CANIM-ARCOL. Fermentations were performed in the CANIM-ARCOL under three dog size conditions (i.e. small, medium, large), after inoculation with stools from medium size dogs (n=2). Samples were regularly collected from atmospheric phase of bioreactors to determine gas composition. Results are expressed in relative percentages for dog A **(a)** and dog B **(b)**. Daily total gas production is given in mL (**c**). Average gas composition from day 4 to day 9 was calculated per size condition and represented in (**d**). Statistical differences are indicated by different letters ($p<0.05$) or ****: $p<0.0001$ (ANOVA one-way)

3.1.3. Impact of size conditions on canine colonic microbiota activity

Total gas production was evaluated every day and a significant ($p<0.0001$) increase with size was observed, with medians of 40, 320 and 580 mL per day for small, medium and large size, respectively (**Figure III.6c**). Gas composition was clearly different depending on size, but for each category quite similar between the two donors (**Figure III.6a** and **6b**). Relative percentages of CO_2 (**Figure III.6d**) significantly increased with size format (41, 79 and 89 % for small, medium and large size conditions, respectively) as well as H_2 (0.4, 0.4 and 3.7 %). Opposite trends were observed for O_2, decreasing with dog size from 1.4 for small condition to 0.6 % for large one. Both donors were CH_4-producers with clear impact of size on CH_4 levels, even if associated percentages remained very low (< 1%). The highest percentages were found under small size conditions, with up to 0.04 % at the end of fermentations for dog B. In large dog condition, CH_4 percentages dropped under detection levels for both dogs.

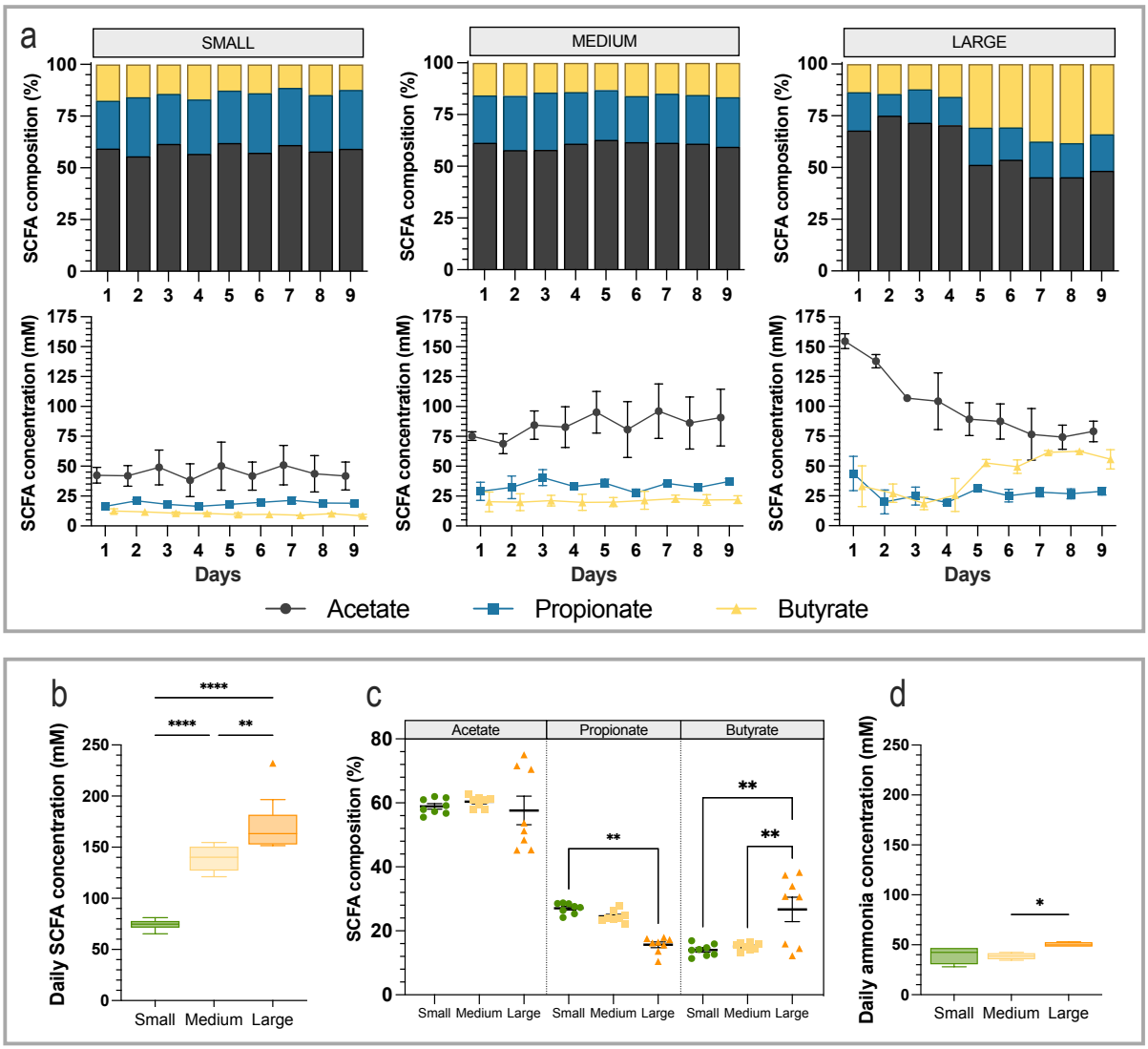

Figure III.7 Impact of dog size on short-chain fatty acids and ammonia production. Fermentations were performed in the CANIM-ARCOL under three dog size conditions (i.e. small, medium, large), after inoculation with stools from medium size dogs (n=2). Samples were regularly collected from luminal medium of the bioreactors to determine short-chain fatty acids (SCFA) and ammonia concentrations. The three main SCFA (i.e. acetate, propionate and butyrate) were measured daily throughout fermentations and results expressed in mean relative percentages (**a**, top) and concentrations (**a**, bottom). Average SCFA concentrations (**b**), SCFA composition (**c**) and ammonia concentrations (**d**) were calculated per size condition from day 2 to day 9. Statistical differences are indicated by *: p<0.05, **: p<0.01; ****: p<0.0001 (ANOVA one-way)

The three main SCFA (i.e. acetate, propionate and butyrate) were quantified in the fermentation medium of the bioreactors (**Figure III.7**). Similar profiles of acetate, propionate and butyrate were observed between small and medium groups with around 60 % acetate, 30 % propionate and 10 % butyrate (**Figure III.7a**). Bioreactors mimicking large size condition were characterized by around 45-50 % acetate, 20 % propionate and an increased proportion of 30-35 % butyrate at the end of the experiment. Daily acetate concentrations (average from days 2 to 9, data calculated from **Figure III.7a**) significantly increased from 41.7 mM (small condition) to 94.4 mM (large condition), with differences observed between small and medium (p<0.0001) and small and large conditions (p<0.0001). Daily propionate concentrations did not differ with dog size condition, whereas butyrate

increased from 10.5 for small to 44 mM for large with significant differences observed between small and large ($p<0.0001$) and medium and large ($p<0.001$) conditions. Daily SCFA production also significantly increased with size, from 75 to 165 mM per day ($p<0.001$) (**Figure III.7b**). Total SCFA production differences were associated to higher butyrate relative abundance in the large condition bioreactors (**Figure III.7c**).

Lastly, ammonia levels quantified in the luminal medium varied between 40 and 50 mM and were significantly higher in the large size condition than in the medium one (**Figure III.7d**).

3.1.4. Interactions between explainable variables and family abundances

Based on Pearson correlations, we further analyzed our data to try to evidence correlations between day of fermentation, physicochemical (i.e. pH, transit time, bile acid profiles) or nutritional (i.e. lipid, protein, carbohydrate and fiber content) parameters of bioreactors, as well as gut microbial metabolites (i.e. gas and SCFA) and bacterial family relative abundances (**Figure III.8**). This was performed by combining results from luminal medium and mucin beads, since similar data were obtained with separate analysis (data not shown). Pearson correlations based on the variable 'size condition' confirmed previous discriminant bacterial populations between dog sizes (notably *Ruminococcaceae*, *Prevotellaceae*, *Bacteroidaceae*, *Lactobacillaceae*, *Peptostreptococcaceae* and *Fusobacteriaceae*). We also confirmed the lack of effect of 'day of fermentation' variable on bacterial relative abundances, attesting the stability of those populations in the artificial colon. Similar significant correlations were obtained between 'size condition', 'transit time', and all nutritional parameters ('lipid, protein, carbohydrate, fiber'), suggesting that all those parameters widely patterned bacterial profiles in the bioreactors. Exactly opposite trends were observed with 'pH', indicating that this variable also broadly impacts bacterial population *in vitro*, but this time with a negative correlation with dog size. Regarding bile acids, cholic acid content showed a markedly different correlations with main discriminant populations compared to the three other ones, i.e. chenodeoxycholic, deoxycholic and lithocholic acids. Besides, even if total SCFA concentration significantly increased with dog size (**Figure III.7b**), Pearson correlations showed no impact of this variable ($p>0.05$). With regards to each main SCFA, acetate was negatively correlated to relative abundance of *Burkholderiaceae* and *Acidaminococcaceae*, but positively correlated with the one of *Clostridiaceae*. In addition, propionate concentration was significantly linked to an increase in *Lachnospiraceae* relative abundance, whereas butyrate was negatively associated to relative abundance of *Burkholderiaceae.* Lastly, Pearson correlations obtained for total gas production was quite similar to that of acetate concentrations, except for *Bacteroidaceae*.

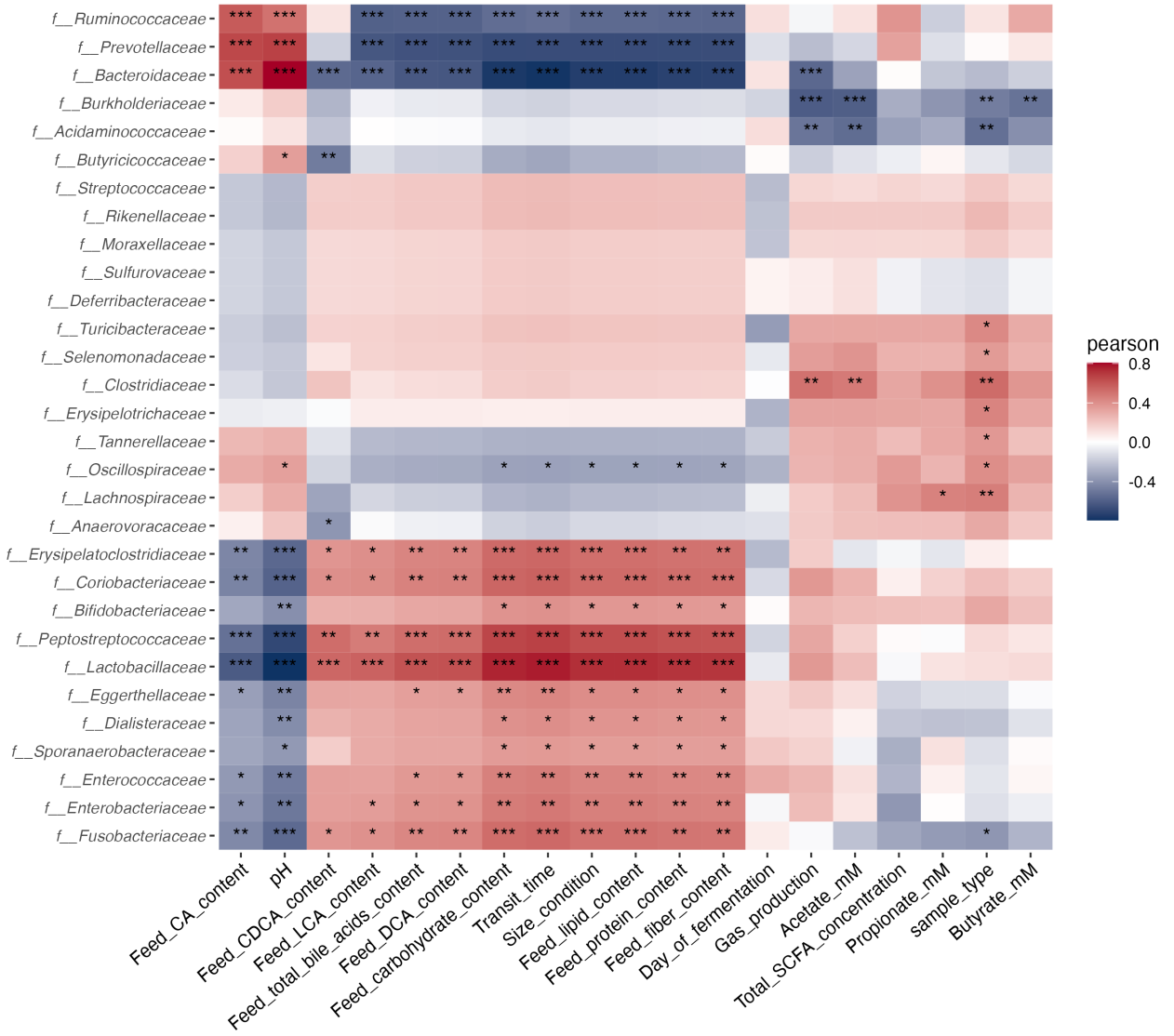

Figure III.8 Correlations between explainable variables and microbial family abundances. Fermentations were performed in the CANIM-ARCOL under three dog size conditions (i.e. small, medium, large), after inoculation with stools from medium size dogs (n=2). Lumen and mucus-associated microbiota composition was analyzed by 16S Metabarcoding. Explainable variables included day of fermentation, sample type (i.e. luminal medium or mucin beads), physicochemical (i.e. pH, transit time, bile acid profiles) or nutritional (i.e. lipid, protein, carbohydrate and fiber content) parameters of bioreactors, as well as gut microbial metabolites (i.e. gas and SCFA) and bacterial family relative abundances. Luminal medium and mucin beads were combined, and Pearson correlations were calculated on days 2 to 9. Statistical differences are indicated by *: $p<0.05$, **: $p<0.01$; ***: $p<0.001$

3.2. Discussion

In a previous study, we developed a new *in vitro* gut model, the CANIM-ARCOL, reproducing the main parameters of the canine colonic ecosystem and adapted to three dog sizes, i.e. small, medium and large sizes (Deschamps *et al.* 2023a). The model was set-up to reproduce the main physicochemical, nutritional and microbial parameters specific to each dog size and inoculated with fecal samples from size-related conditions (e.g. small size bioreactors were inoculated with stool from small size dogs). In particular, we simulated *in vitro*

the increase in colonic transit time, feed nutrients (proteins, carbohydrates, lipids and fibers), and secondary bile acids concentrations (DCA and LCA) associated to dog size, while pH and primary bile acid (CA) decreased (**Table III.2**), in line with *in vivo* data (Flickinger *et al.*, 2003; Case *et al.*, 2011; Hendriks *et al.*, 2013; Gazzola *et al.*, 2017; Weber *et al.*, 2017; Algya *et al.*, 2018; Koziolek *et al.*, 2019; Guard *et al.*, 2019). After validating this model through *in vivo-in vitro* correlations, we aimed in the present work to provide a mechanistic understanding of how colonic parameters are able to shape microbiota depending on dog size conditions. Of interest, such an *in vitro* approach allows to dissociate the microbial component from nutritional and physicochemical parameters of the colonic ecosystem, which is obviously impossible *in vivo*. Therefore, we inoculated the CANIM-ARCOL with stools from medium-size dogs while bioreactors were set-up to reproduce small, medium or large colonic conditions. The main objective was then to provide a comprehensive understanding on the relative importance of microbes (based on fecal inoculum) and colonic parameters in modelling microbiota at structural and functional levels, between the three dog sizes.

With this objective in mind, we first performed comparisons on the effect of dog size between the present results and those previously obtained in the CANIM-ARCOL inoculated with fecal samples from small, medium and large dogs (Deschamps *et al.* 2023a), as described in **Table III.4**. We should keep in mind that, even if there are of interest, such comparisons should be hampered by differences between the two studies in time of fermentation (9 days here *versus* 21 days in the previous study) and number of fecal samples (2 dogs *versus* 13 dogs). Impact of dog size on microbial alpha-diversity was in line to previous *in vitro* results, i.e. decreasing with size. However, at the phylum level, we observed opposite tendency or no clear conclusion for the main phyla (*Actinobacteria*, *Bacteroidota*, *Fusobacteriota* and *Proteobacteria*) in both microenvironments, except for *Firmicutes* in the luminal medium. At the family level, changes in 7 and 5 families out of 12, in the luminal medium and mucin beads respectively, were in accordance with previous *in vitro* results. However, major families from canine gut microbiota such as *Bacteroidaceae* and *Fusobacteriaceae* demonstrated opposite or unclear size effects between the two studies. Regarding microbiota activity, we evidenced great correlations between the present study and the previous results (Deschamps *et al.* 2023a), with 10 out of 11 tested parameters showing similar trends, including total and main SCFAs and gases, as well as ammonia. This suggests functional overlaps between different bacterial taxa resulting in quite consistent microbiota activity.

The second level of comparisons to assess the relative importance of microbial and environmental colonic parameters was to compare the present results to *in vivo* data in dogs (**Table III.5**). Due to the paucity of information on canine colonic microbiota *in vivo*, with only two studies in medium dogs (Suchodolski *et al.*, 2008; Honneffer *et al.*, 2017) and none with small and large dogs, *in vitro-in vivo* comparisons were based on fecal data extracted from our literature review (23 studies, Deschamps *et al.* 2022b).

Table III.4 ***In vitro - in vitro*** **correlations related to dog size effect on colonic microbial populations and metabolic activities between previous results in the CANIM-ARCOL and those obtained in the present study**. Previous results were extracted from Deschamps *et al.* (2023a) and found when the model was inoculated with fecal samples from three dog sizes. Size effect was indicated by symbols: ↭ no size effect, ↘ decrease with size or ↗ increase with size. Color code indicates similar tendency between the two studies (in green), clear opposite trends (in red) or no clear conclusion (in yellow). *: significant variations between sizes ($p<0.05$). ND: not detected.

		Size effect			
		CANIM-ARCOL (Deschamps *et al.* 2023a)		Present study	
		Luminal medium	Mucin beads	Luminal medium	Mucin beads
Alpha diversity		↘*	↘*	↘	↘
Phylum	*Actinobacteria*	↘	↘*	↭	↗
	Bacteroidota	↗*	↗*	↘	↘
	Firmicutes	↗*	↗	↗	↭
	Fusobacteriota	↘*	↘*	↭	↗
	Proteobacteria	↘*	↘*	↗	↭
Families	*Acidaminococcaceae*	↘*	↘	↭	↭
	Bacteroidaceae	↗	↗	↘	↭
	Clostridiaceae	↗	↗	↗	↭
	Enterobacteriaceae	↭	↘	↗	↭
	Erysipelotrichaceae	↭	↭	↭	↗
	Fusobacteriaceae	↘	↘	↭	↗
	Lachnospiraceae	↭	↘	↭	↘
	Peptostreptococcaceae	↭	↭	↭	↭
	Prevotellaceae	↘	↘	↘	↘
	Ruminococcaceae	↘	↘	↘	↘
	Sutterellaceae	↭	↘	↭	ND
	Veillonellaceae	ND	ND	↭	ND
Total SCFA		↗*		↗	
Acetate	Relative (%)	↗*		↘	
Propionate	Relative (%)	↘*		↘	
Butyrate	Relative (%)	↗*		↗	
Ammonia		↗*		↗	
Total gas production		↗*		↗	
CO_2	Relative (%)	↗*		↗	
H_2	Relative (%)	↭		↗	
O_2	Relative (%)	↘		↘	
N_2	Relative (%)	↘*		↘	
CH_4	Relative (%)	↘		↘	

Main families observed in faecal samples of different dog sizes were successfully found *in vitro* (**Table III.5a**), except for *Acidaminococcaceae* (not detected in small and medium dog stools but present under three dog size conditions in the CANIM-ARCOL) and *Veillonellaceae* (previously described in large dog feces but not found *in vitro*). Regarding size effect, we observed similar trends for 6 out of 12 families, no clear conclusion for 4 and opposite trends for *Prevotellaceae* and *Veillonellaceae*. This indicates that physicochemical and nutritional parameters applied *in vitro* were able to shift microbiota according to *in vivo* data for half of the followed families, regardless of the microbial inoculum. Similarly, size effect on microbiota activity was in line with fecal *in vivo* data for 3 over 5 studied parameters, including total SCFA and ammonia (**Table III.5b**). One explanation can be that environmental colonic parameters can drive microbiota *in vitro*, especially at the functional level, but are not sufficient to shape bacterial populations with adequate

profiles compared to *in vivo* data. This means that inoculating CANIM-ARCOL with fecal samples from three dog sizes remains necessary to obtain relevant *in vitro-in vivo* comparisons.

Of interest, this *in vitro* study allowed to better understand how different parameters from the canine colonic ecosystem can drive major bacterial family's relative abundances (**Figure III.8**). Our results indicated that nutritional and physicochemical parameters related to different dog sizes, but not the main microbial fermentation end-products (i.e. SCFA and gas) are microbiota drivers. In this study, *Coriobacteriaceae* and *Fusobacteriaceae* relative abundances were positively correlated with dog size and protein content (in the simulated ileal effluents), in accordance with *in vivo* studies in medium dogs, where high-protein diet increased the fecal levels of those two bacterial populations (Hang *et al.*, 2012, 2013). Such observations are in line with previous works reporting the involvement of *Fusobacterium* in protein fermentation to produce butyrate (Pilla & Suchodolski, 2020). A discriminant enrichment in *Clostridiaceae* and *Lactobacillaceae* was also observed *in vitro* from small to large dog size conditions, associated with higher fiber contents. This is also in adequacy with *in vivo* results showing similar trends in adult medium dog stools when they were fed with a high-fiber diet containing 7.5 % beet-pulp (Middelbos *et al.*, 2010; Swanson *et al.*, 2011; Maria *et al.*, 2017). Those two families are known to produce SCFA from carbohydrate fermentation in the gut (Oliphant & Allen-Vercoe, 2019), in line with the positive correlation we evidenced in the CANIM-ARCOL between total SCFA concentrations and dog size. In addition to feeding, bile acids are also acknowledged as key factors shaping the intestinal microbiota composition (Larabi, Masson & Bäumler, 2023). In the CANIM-ARCOL model, primary bile salts content in the ileal effluents decreased with dog size, while secondary bile salts increased, extrapolated from *in vivo* data in dog feces (Guard *et al.*, 2019). Changes in bile salts concentrations depending on dog sizes were primarily correlated with modifications in *Bacteroidaceae*, *Lactobacillaceae*, *Clostridiaceae* and *Ruminococcaceae* abundances, in accordance with the main families involved in bile salts metabolism, through dihydroxylation, oxidation or epimerization (Suchodolski, 2011a; Guard *et al.*, 2019; Larabi *et al.*, 2023).

Besides nutrients and bile salts, we also showed that physicochemical parameters of the canine colonic ecosystem are key factors shaping microbiota *in vitro*. In particular, negative correlations between transit time and *Bacteroidaceae* relative abundances were evidenced in the CANIM-ARCOL. Once again, this result should be linked to *in vivo* data since *Bacteroidaceae* raised in stools from dogs with chronic diarrhea, showing a reduced transit time (Jia *et al.*, 2010). Faster transit time can impact nutrient supply in the gut (leading to excess of resources) and select species from *Bacteroidaceae* able to grow rapidly during reduced competition (Kashyap *et al.*, 2013). In addition, we observed in the present work a negative correlation between bacterial alpha-diversity and dog size, meaning that diversity decreased with transit time.

Table III.5 *In vivo* - *in vitro* correlations related to dog size effect on gut microbial populations (a) and metabolic activities (b) between our *in vitro* results in the CANIM-ARCOL and data from fecal samples *in vivo*. Data from dog fecal samples are extracted from Deschamps *et al.* (2022a). Presence of bacterial populations was indicated by 'Yes' if present or 'No' if absent (not found in the main bacterial populations). Size effect was indicated by symbols: ↭ no size effect, ↘ decrease with size or ↗ increase with size. Color

code indicates similar tendency between *in vitro* and *in vivo* data (in green), clear opposite trends (in red) or no clear conclusion due to lack of data or inconsistencies (in yellow). *ND: not determined.*

a

Families	Fecal samples (literature)				CANIM-ARCOL (present study)				*Similar tendency in vivo and in vitro*
	Small[a]	Medium[b]	Large[c]	Size effect	Small	Medium	Large	Size effect	
Acidaminococcaceae	ND	ND	Yes	↭	Yes	Yes	Yes	↭	=
Bacteroidaceae	Yes	Yes	Yes	↘	Yes	Yes	Yes	↘	=
Clostridiaceae	Yes	Yes	Yes	↭	Yes	Yes	Yes	↗	±
Enterobacteriaceae	Yes	Yes	Yes	↭	Yes	Yes	Yes	↗	±
Erysipelotrichaceae	ND	Yes	Yes	↭	Yes	Yes	No	↭	=
Fusobacteriaceae	Yes	Yes	Yes	↭	Yes	Yes	Yes	↭	=
Lachnospiraceae	Yes	Yes	Yes	↘	Yes	Yes	Yes	↭	±
Peptostreptococcaceae	Yes	Yes	Yes	↭	Yes	Yes	Yes	↭	=
Prevotellaceae	Yes	Yes	Yes	↗	Yes	Yes	Yes	↘	≠
Ruminococcaceae	Yes	Yes	Yes	↭	Yes	Yes	No	↘	±
Sutterellaceae	ND	ND	Yes	ND	No	No	No	ND	ND
Veillonellaceae	ND	Yes	Yes	↭	No	No	No	ND	ND

[a] Kim *et al.* (2017), Omatsu *et al.* (2018), You and Kim (2021)
[b] Nogueira *et al.* (2019), Garcia-Mazcorro *et al.* (2020), Kubinyi *et al.* (2020), Paßlack *et al.* (2021)
[c] Sandri *et al.* (2016), Hullar *et al.* (2018)

b

Activity	Faecal samples (literature)	CANIM-ARCOL (present study)	*Similar tendency in vivo and in vitro*
	Size effect		
Total SCFA	↗	↗	=
Acetate %	↘	↘	=
Propionate %	↗	↘	≠
Butyrate %	↘	↗	≠
Ammonia	↗	↗	=

Our results are in line with a previous study in an *in vitro* model of the human large intestine showing that a longer transit time (associated with aging in human) led to a drop in microbial diversity and an increase in *Clostridiaceae*, *Enterobacteriaceae* and *Coriobacteriaceae* abundances and total SCFAs (Tottey *et al.*, 2017). Moreover, increasing transit time in the CANIM-ARCOL induced enrichment in *Lactobacillaceae*, *Enterococcaceae* and *Bifidobacteriaceae*, in full accordance with a previous work in an *in vitro* human gut

model showing that an increased transit time (from 5 to 10 h *versus* 5 to 15 h in the present study) was associated with a rise in *Lactobacillus*, *Enterococcus* and *Bifidobacterium* (Pham *et al.*, 2019). These families are involved in carbohydrates fermentation and lactate production, which can be promoted by increased transit time allowing a longer contact between bacteria and macronutrients (Pham *et al.*, 2019). Lastly, transit time was negatively correlated with CH_4 percentages. CH_4 is primarily produced by methanogenic *Archaea*, poorly described up to now in dog stools *Archaea* (Swanson *et al.*, 2011), but previously recovered in the CANIM-ARCOL (and identified as *Methanobrevibacter smithii*), especially under small size conditions (Deschamps *et al.* 2023a). A slow transit time was previously described as facilitating factor for *Archaea* development, and associated to an increased methane production in human (Asnicar *et al.*, 2021), which is contradictory with our results and suggests that in addition to transit time, other parameters such as availability of nutrients can favor CH_4 production. The other physicochemical parameters driving microbiota in our study is colonic pH. In the CANIM-ARCOL, values decreased from 6.5 to 6.2 from small to large size conditions, associated to a decrease in propionate but an increase in butyrate concentrations. pH was positively correlated with *Bacteroidaceae*, while *Actinobacteria* and *Firmicutes* decreased. All those results are in perfect line with those found by Haindl *et al.* (2021) *in vitro* in human feces. However, these authors also observed an increase in total SCFA concentrations when pH increased (from 6 to 7), while opposite results were obtained here, certainly due to differences in nutrient availability.

To conclude, this study provides for the first time relevant mechanistic insights about the relative importance of gut microbes and colonic physicochemical and nutritional parameters in modeling canine microbiota by using the CANIM-ARCOL. We showed that environmental colonic parameters (such as nutrient availability, transit time or pH) were sufficient to drive microbiota at the functional level, but that size-related fecal microbes were necessary to accurately reproduce the colonic environment of small, medium and large dogs. This *in vitro* study also allowed to evidence main bacterial populations shaped by nutritional or physicochemical parameters in the canine colonic ecosystem. Further investigations would be necessary to confirm the relative importance of each of those parameters in shaping gut microbes. In a next future, the CANIM-ARCOL model can be used as a relevant *in vitro* tool to decipher the relative importance of microbiota *versus* environmental colonic parameters in food and pharma studies, e.g. when studying nutrient/drug bio-accessibility or probiotic/enteric pathogen survival and activity. This study was focused on the effect of dog sizes, but the potential of our model can be extended to the simulation of different ages or healthy *versus* diseased situations (e.g. chronic enteropathies or obesity).

3.3. Additional results

Material and methods

Metabolomic analysis

Luminal samples were analyzed by GC-QToF at the PFEM platform (INRAE, Theix, France) to obtain metabolomic profiles. Samples were prepared as follows: 200 µL of fermentation samples were centrifuged at 4°C at 15,000 rpm for 10 min twice per sample. 400 µL of ice-cold methanol (stored at -20°C) were added to

the supernatants and mixed. Samples were then kept at -20°C for 30 min and centrifugated at 4°C at 15,000 rpm for 10 min. A 500 µL supernatant and 20 µL of [$^{13}C_1$]-L-valine (200 µg/mL) were added to each vial. At the same time, a control derivatization sample (fecal water sample was substituted by deionized water) was prepared in order to remove the background noise produced during sample preprocessing, derivatization, and GC-QToF analysis. GC-QToF analysis was performed following the method published by Gao, Pujos-Guillot & Sébédio, (2010).

Results and discussion

Metabolomic analyses were performed on the sterile nutritive media and fermentation samples collected in the CANIM-ARCOL set under the three dog sizes (**Figure III.9**). Despite some promising results obtained with preliminary testing and on nutritive medium samples, the method failed to obtain accurate technical replicates (data not shown), with too many particles from biological sample. In samples from the small size condition only, some metabolites annotations were performed, allowed by a lower number of suspended particles. Few putative annotations can be completed (**Table III.6**) among which valeric acid, lactic acid and oxalic acid were certainly identified and seemed to be produced over time in small size bioreactors (**Figure III.9B**). However, the metabolomic platform concluded on the impossibility to exploit our results. This failure could be explained by a different centrifugation speed used compared to Gao, Pujos-Guillot & Sébédio, (2010) (15,000 rpm for 10 min here *versus* ultracentrifugation at 50,000 rpm for 2 h) which may have impacted the repeatability of the samples. Of note, in MEDIS lab we usually used supernatants from fermentation samples after two centrifugations of 18,000 rpm for 15 min. For future analysis, the centrifugation parameter and number of technical replicates will be key parameters to improve. In addition, differences between the two biological replicates (i.e. dog A and dog B) were observed, indicating an important interindividual variability to be considered for future metabolomic analysis.

Table III.6: Putative annotations of metabolites identified by metabolomic analysis on small dog size samples.

Metabolites	Retention time (min)	Exploitable intensity[1]	Class	Formula
Valeric acid	5.66	Yes	Fatty acyls	$C_5H_{10}O_2$
Lactic acid	7.06	Yes	Hydroxy acids and derivatives	$C_3H_6O_3$
2-hydroxybutyric acid	8.13	No	Hydroxy acids and derivatives	$C_4H_8O_3$
Oxalic acid	8.33	Yes	Carboxylic acids and derivatives	$C_2H_2O_4$
3-hydroxybutyric acid	8.63	No	Hydroxy acids and derivatives	$C_4H_8O_3$
4-hydroxybutyric acid	9.72	No	Fatty acyls	$C_4H_8O_3$
L-leucine	10.3	No	Carboxylic acids and derivatives	$C_6H_{13}NO_2$
Glycerol	10.37	No	Organooxygen compounds	$C_3H_8O_3$
Niacin	10.53	No	Pyridines and derivatives	$C_6H_6N_2O$
Glycine	10.82	No	Carboxylic acids and derivatives	$C_2H_5NO_2$
L-proline	15.91	No	Carboxylic acids and derivatives	$C_5H_9NO_2$
Phloretic acid	19.8	Yes	Phenylpropanoic acids	$C_9H_{10}O_3$
Glucose o-methyloxyme	23.7	Yes	Organooxygen compounds	$C_6H_{12}O_6$
Myo-inositol	27.91	No	Organooxygen compounds	$C_6H_{12}O_6$
Maltose	39.48	Yes	Organooxygen compounds	$C_{12}H_{22}O_{11}$

[1] for some identified molecules, chromatograph intensity was not sufficient to exploit results.

3.4. Conclusion

In this third chapter, the impact of nutritional and physicochemical colonic parameters and the importance of size-related faecal inoculum on canine gut microbiota structure and activity were evaluated in the CANIM-ARCOL, set-up to reproduce the three dog size conditions but inoculated only with fecal samples from medium size dogs. We have demonstrated here that environmental parameters alone were sufficient to drive microbiota metabolic activities according to dog sizes but that fecal size-related inoculum were necessary to accurately reproduce bacteria composition. Such *in vitro* study provides interesting mechanistic insights on parameters from the large intestine shaping microbiota in dogs, independently from interactions with host cells. However, since combinations of various physicochemical and nutritional parameters were associated to the different size conditions, it was still difficult to evidence the relative role of each parameter alone (e.g. pH, transit time, each nutrient concentration, bile acid concentrations and profiles). To go further into such a mechanistic approach, it would be also of importance to characterize metabolites composition more deeply under each dog size condition, by using metabolomic approaches, that unfortunately failed during this PhD work. As done in this chapter for other analyses, metabolomic data obtained on samples from the present experiments might be compared to those found on samples from the previous study in the CANIM-ARCOL using size-related fecal samples (Chapter 2).

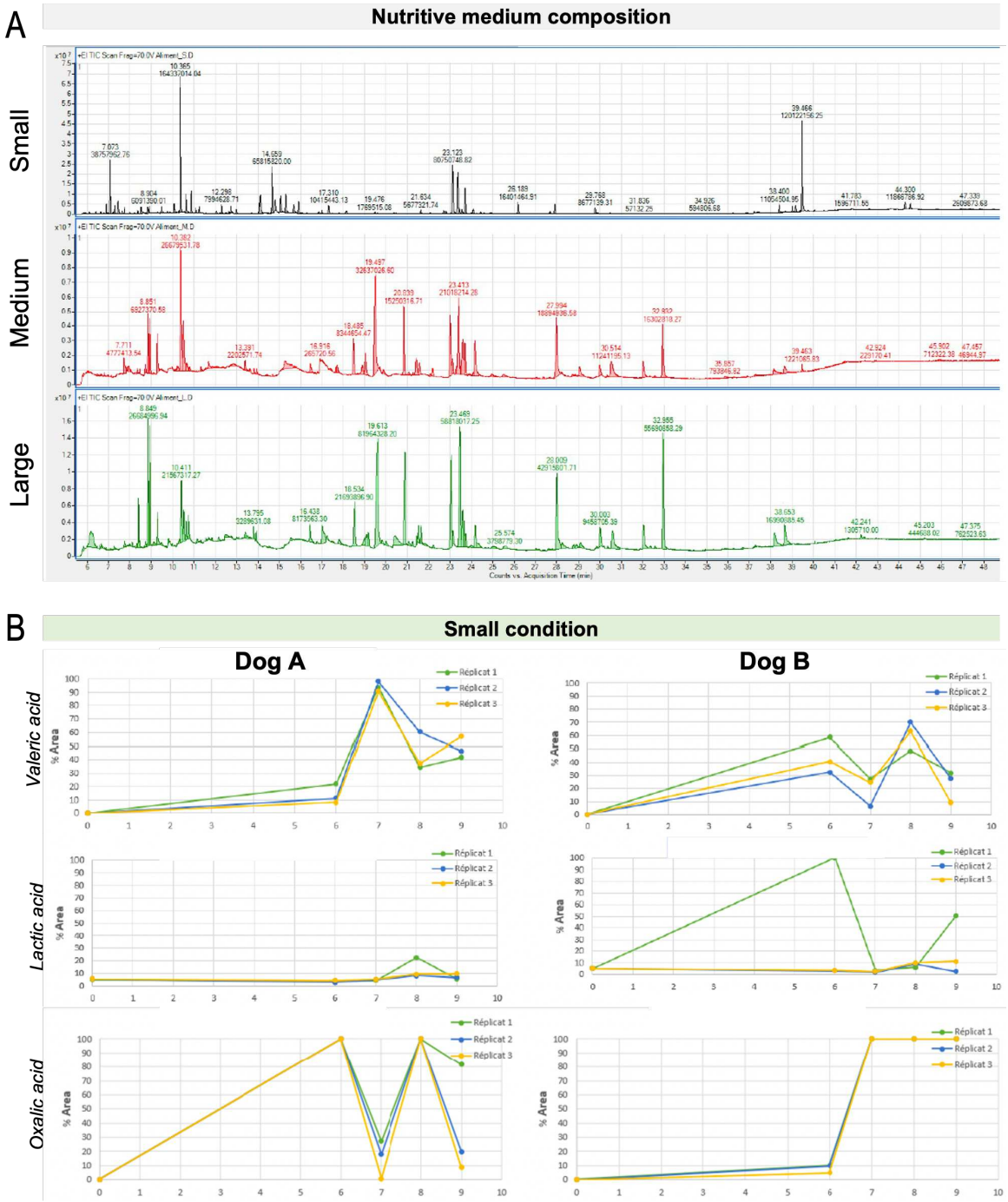

Figure III.9: Preliminary results of metabolomic analyses. Chromatogram profiles of the three sterile nutritive media (**A**). Kinetics of valeric acid, lactic acid and oxalic acid production in the small bioreactors over time for the two donors and the three technical replicates (**B**).

Chapter 4 – Development of a new dysbiotic model of the canine large intestine microbiome associated to antibiotherapy

After evaluating the impact of body size and the relative importance of faecal inoculum *versus* environmental parameters on canine microbiota in the CANIM-ARCOL under healthy condition, we then moved towards the *in vitro* simulation of a disturbed situation. We were first interested in reproducing the dysbiotic state of canine microbiota associated to diseases such as obesity or IBD, as previously done in the lab for human. Reproducing obesity was at first the preferred option since it gave very interesting results in human (I took part to this study during a 6-month master's degree internship, resulting in another first author publication submitted to *Microbiome*, see Appendix 5). However, the current lack of relevant *in vivo* data in dogs (especially related to colonic physicochemical parameters) discouraged us to adapt the CANIM-ARCOL to those diseases for now. We therefore switched toward another common canine disorder, chronic enteropathy. Such disease is frequently treated by antibiotherapy by veterinarian without looking for other alternative strategies. Nevertheless, recent studies pointed out the increase in antibiotic resistance in dogs, in response to unappropriated use of antibiotherapy. This is a subject of global concern, due to the increasing bond between pets and their owners (called "pet parenting"). Indeed, gut microbes' horizontal transfers between the two species could occur and result in transmission of antibiotic resistance. However, up to now, the impact of antibiotherapy on microbiota was poorly described in dogs with only 10 *in vivo* studies mainly focused on stools, and no study in *in vitro* gut models. In 8 over those 10 studies, authors observed microbiota perturbations, including decrease in bacterial diversity and alteration of phyla relative abundances. Then, we decided to use antibiotics as a dysbiosis inducer to develop the first *in vitro* gut model giving a picture of antibiotherapy impact on lumen and mucus-associated microbiota structure and function in dogs, focusing on medium size dog condition. This work will be submitted for publication in *Microbiology Spectrum*.

ORIGINAL ARTICLE

Development of a new dysbiotic model of the canine large intestine microbiome associated to antibiotherapy

DESCHAMPS, C., APPER, E., BRUN, M., DURIF, C., DENIS, S., HUMBERT, D., & BLANQUET-DIOT, S. (**2023**)

To be submitted in Microbiology Spectrum (**IF 9.04)**

For the entire manuscript this article will be cited as **Deschamps *et al.* (2023c)**.

Figure IV.0: Graphical abstract

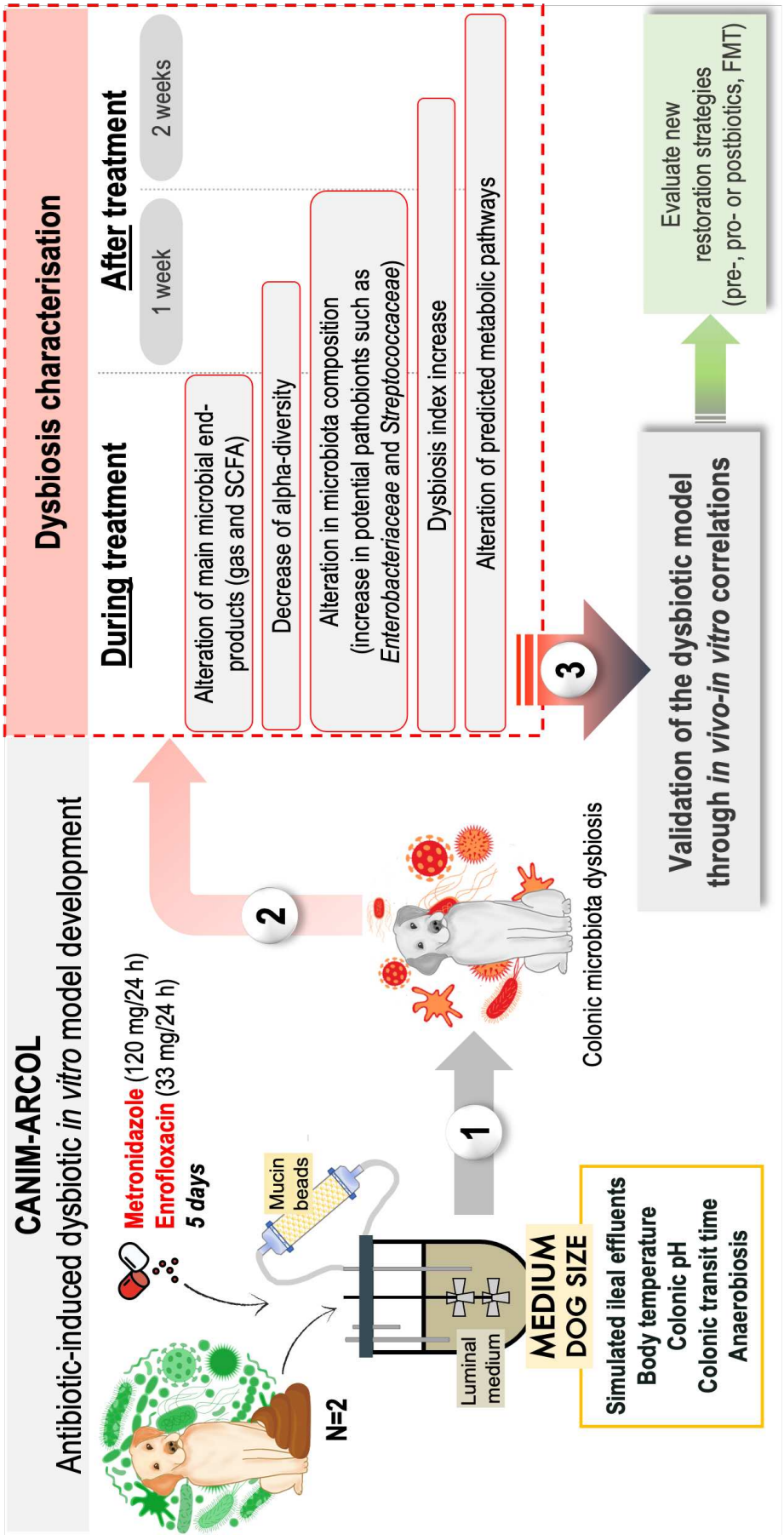

II-4

Abstract

Like in human, antibiotics are widely used in dogs to treat gastrointestinal infections, contributing to their global burden on both human and animal health. Close relationship between pet and their owners led to gut microbes' horizontal transfers between the two species, that may be associated with transmission of antibiotic resistance. Nevertheless, up to now, the impact of antibiotics on canine gut microbiota has been poorly described. The aim of this study was to adapt the Canine Mucosal Artificial Colon (CANIM-ARCOL), reproducing the main nutritional, physicochemical and microbial parameters found in the dog large intestine, to simulate an antibiotic-induced perturbation. A pre-screening was performed on five antibiotic cocktails at in-field doses, leading to the selection of 5 days metronidazole/enrofloxacin (ME) treatment for further model development. Two CANIM-ARCOL bioreactors were inoculated with a faecal sample (n=2 donors) and run in parallel for 26 days under control or antibiotic conditions. ME treatment reduced microbial diversity and induced major shifts in bacterial populations leading to a dysbiosis state characterized by an increased in *Streptococcaceae*, *Lactobacillaceae* and *Enterobacteriaceae* relative abundances while *Bacteroidaceae*, *Fusobacteriota* and *Clostridiaceae* decreased. Overall, mucus-associated microbiota was less impacted by antibiotics than luminal microbes. Microbial alterations were associated with drastic decreases in gas production and SCFA concentrations. Lastly, the model was fully validated through *in vitro-in vivo* comparison with one study in dogs. CANIM-ARCOL provides a relevant platform as an alternative to *in vivo* assays for an in-depth understanding of antibiotic-microbiota interactions and further testing of restoration strategies at the individual level.

Importance

Gut microbiota plays a key role in human and animal health. Antibiotics, which are widely used in dogs like in their owners, can disturb this key player in gut homeostasis. This study led for the first time to the development of a new *in vitro* model of antibiotic-induced dysbiosis in the canine large intestine, fully validated through *in vitro-in vivo* comparisons. In line with European 3R rules aiming to reduce animal experimentations, this *in vitro* model can be used as an alternative to *in vivo* assays for in-depth mechanistic studies on gut microbes-antibiotic interactions, considering both microbiota structure and functionalities. The ultimate goal would be to use this model for testing new restorations strategies such as prebiotics, probiotics, postbiotics or fecal microbiota transplantation. By using fecal samples from different healthy or diseased donors, this *in vitro* approach captures interindividual variabilities in gut microbes, allowing to move toward personalized medication.

Keywords: dog, large intestine, microbiota, *in vitro* gut model, CANIM-ARCOL, antibiotics, dysbiosis.

4.1. Introduction

Antibiotics are commonly used in dogs to treat infectious gastrointestinal diseases caused by bacteria or parasites. Especially, antibiotherapy is the most commonly used treatment for acute diarrhea regardless of the underlying cause, with around 50-71 % dogs treated with antimicrobials before being tested for any infectious agent (German, Halladay & Noble, 2010a; Singleton *et al.*, 2019). However, antibiotics can have damaging side effects depending on the molecule used, such as diarrhea (Pilla *et al.*, 2020), vomiting (Whittemore *et al.*, 2019), weight loss, increase of oxidative stress markers (Pilla *et al.*, 2020), and in the worse cases bile acids dysmetabolism (Whittemore *et al.*, 2021). Furthermore, inappropriate use of antibiotics is known as a key driver of antimicrobial resistance in dogs (Allerton *et al.*, 2021). Transmission of such resistance to human is exacerbated by the increasing human-pet interplays, leading to gut microbes horizontal transfers between the two species (Wipler *et al.*, 2017; Huang *et al.*, 2020). At therapeutic doses, antibiotics can induce in fecal microbes a bloom of potential pathogens, such as *Enterobacteriaceae* (9–13), generally associated to a decrease in species diversity and richness in dogs (Suchodolski *et al.*, 2009; Whittemore *et al.*, 2019, 2021; Pilla *et al.*, 2020; Bottero *et al.*, 2022), which are common markers of gut microbial perturbation called dysbiosis. Nevertheless, up to now, the impact of antibiotics on canine gut microbes' activities remains poorly described and there is no available data on the effect of antibiotherapy on colonic microbiota.

Colonic microbiota has been poorly described in dogs, but is dominated by bacteria from Firmicutes, Bacteroidetes, Fusobacteria, Proteobacteria and Actinobacteria phyla (Suchodolski *et al.*, 2008; Honneffer *et al.*, 2017). As previously reviewed by Deschamps *et al.* (2022b), gut microbiota composition seems to be clearly variable depending on gastrointestinal regions in dogs and probably differs between the lumen and the vicinity of intestinal epithelium, where mucus layer constitutes for microbes both an ecological niche and nutrient supply. The gut microbiota is known to play several key roles in dog health by maintaining host homeostasis, since it is involved in different nutritional (e.g. vitamin synthesis, fiber degradation and lipid digestion through the metabolism of primary into secondary bile acids), immunological and physiological processes, such as epithelium integrity and "barrier" effect against pathogens (Durand, 2010; Andoh, 2016). Metabolic activities of the gut microbiota led to the production of main end fermentation products, such as short-chain fatty acids (SCFA) and gases. SCFA are also important for dog health since they can be used as preferential energy source for colonocytes, liver and brain.

To evaluate the effect of antibiotics on canine colonic microbiota, and particularly the impact of parameters (Rochegüe *et al.*, 2021) such as type of molecules, dose, administration routes, duration of treatment and health status of animals, *in vivo* studies remain the golden standard. Nevertheless, such studies in dogs are increasingly restricted by ethical, regulatory, societal and cost pressures. An alternative option is the use of *in vitro* models simulating the canine gastrointestinal tract. Up to now, only two dynamic canine *in vitro* colonic models have been developed, namely the Mucosal Simulator of the Canine Intestinal Microbial Ecosystem (M-SCIME) (Verstrepen *et al.*, 2021) and the Canine Mucosal Artificial Colon (CANIM-ARCOL, Deschamps *et al.* 2023a). Both of them are inoculated with fecal samples, reproduce the main nutritional and physicochemical

parameters of the canine colon under healthy status and distinguish the lumen from mucus-associated microbes. However, only the second one has been adapted, based on a literature survey, to simulate the specific conditions (i.e. pH, transit time, nutrient availability and bile acid profiles) found in the colon of dogs from different sizes (i.e. small, medium and large dogs) and validated through *in vivo-in vitro* correlations. To the best of our knowledge, up to now, no study has investigated the impact of antibiotics on canine microbiota structure and function in *in vitro* gut models.

In this context, the objective of the present study was to set-up for the first time an *in vitro* gut model of antibiotic-induced dysbiosis using the CANIM-ARCOL model. With this objective in mind, we first performed a pre-screening experiment to select among five antibiotic treatments (i.e. metronidazole, metronidazole/enrofloxacin, metronidazole/enrofloxacin/ciprofloxacin, tylosin and amoxicillin) the most relevant for further model development. Then, in a second set of experiments, the selected antibiotic cocktail (i.e. metronidazole/enrofloxacin) was administered at field dose for 5 days in the CANIM-ARCOL model, set-up to reproduce the large intestinal conditions of medium dog size. Impact of antibiotic treatment on microbiota composition (16S Metabarcoding) and metabolic activities (gas, SCFA and bile acid profiles) was evaluated before, during and after antibiotic treatment, to describe antibiotic-induced gut microbial dysbiosis in the lumen and mucus and assess subsequent resilience of microbiota.

4.2. Results

4.2.1. Metronidazole/enrofloxacin cocktail was selected among five antibiotic cocktails for further development of the in vitro dysbiotic model in the CANIM-ARCOL

CANIM-ARCOL, set-up under medium size dog colonic conditions and inoculated with a single fecal sample, was treated with different antibiotic cocktails, i.e. metronidazole (M), metronidazole/enrofloxacin (ME), metronidazole/enrofloxacin/ciprofloxacin (MEC), tylosin (TY) and amoxicillin (AM), to select the most relevant one for further dysbiotic model development (**Figure IV.1**). This selection was based on changes observed in both microbiota composition and metabolic activities during antibiotic treatment compared to the stabilized phase in bioreactors, i.e. day 6 to 8.

Regarding gas composition, only slight modifications were observed for M and AM conditions (**Figure IV.2A**), with mainly a small increase in H_2 relative abundance in M bioreactor. Contrarily, ME, MEC and TY treatments clearly impacted gas composition, with a raise in H_2 percentage (reaching 35 % for TY), together with an increase in O_2 (up to 10 % in MEC) and a decrease in CO_2 (reaching around 25 %, 15 % and 5 % in TY, ME and MEC, respectively). Interestingly, gas profiles, especially for MEC and TY, changed over treatment time. Daily gas production (**Figure IV.2B**) was also widely reduced by antibiotics from the first day of administration, with the highest impact for ME and MEC (no gas overproduced from day 10 until the end of the treatment).

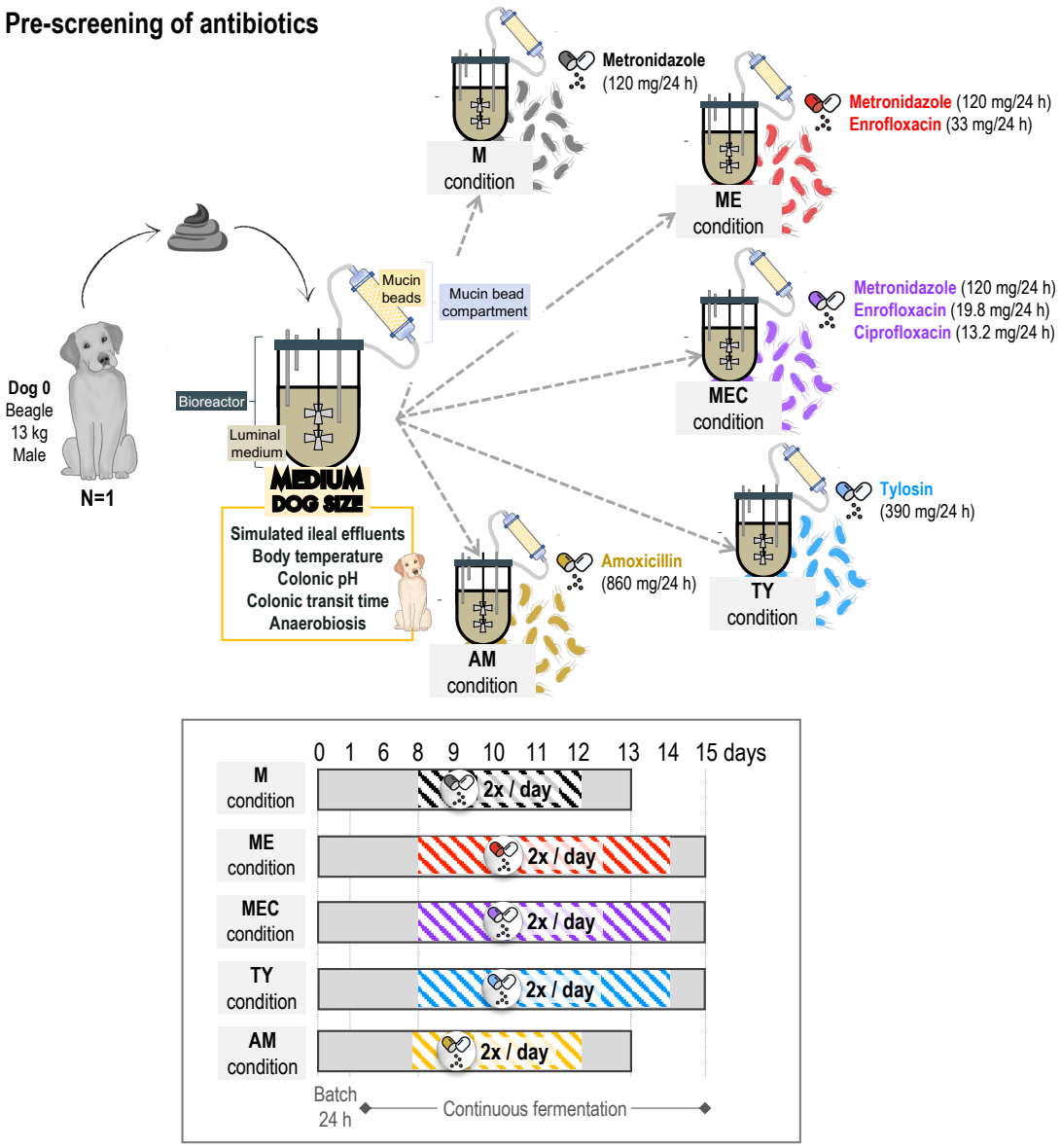

Figure IV.1: Experimental design of antibiotics pre-screening experiment in the CANIM-ARCOL. The CANIM-ARCOL model was inoculated with a fecal sample from one medium dog (one Beagle male, 13 kg) and set-up to reproduce medium dog size colonic condition. Five bioreactors were run in parallel to evaluate the effect of five different antibiotic treatments (i.e. metronidazole, metronidazole/enrofloxacin, metronidazole/enrofloxacin/ciprofloxacin, tylosin and amoxicillin) on canine colonic microbiota. After a stabilization phase of 8 days, antibiotics were twice daily introduced into the bioreactors for 5 days (metronidazole and amoxicillin) or 7 days (for the three other treatments) at in-field doses. Samples were regularly collected in the atmospheric phase, in the luminal medium and from mucin beads to monitor microbiota composition and fermentation metabolites.

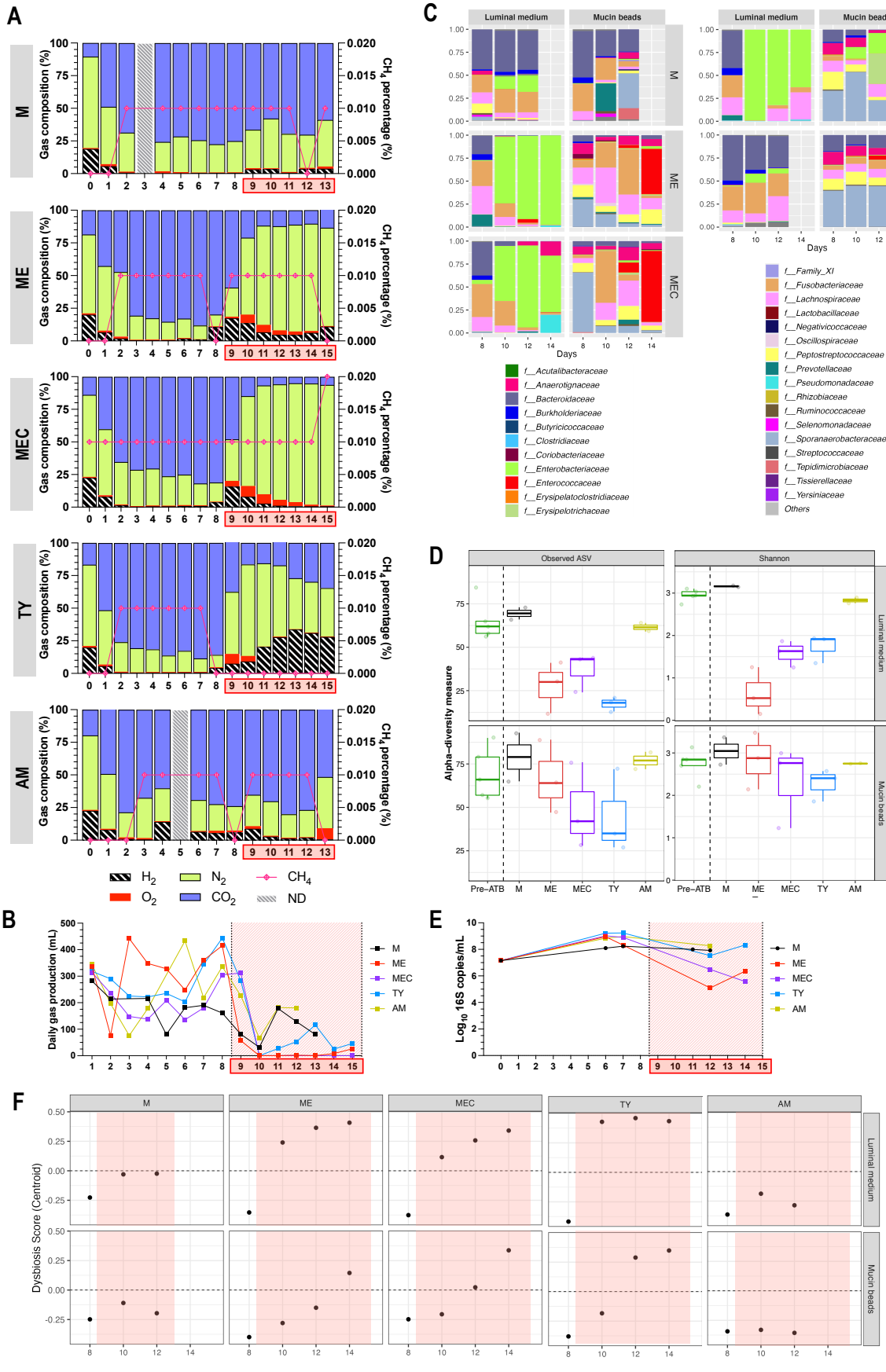
A
M
ME
MEC
TY
AM
Gas composition (%)
CH4 percentage (%)
H2
O2
N2
CO2
CH4
ND
B
Daily gas production (mL)
M
ME
MEC
TY
AM
C
Luminal medium
Mucin beads
Days
f__Family_XI
f__Fusobacteriaceae
f__Lachnospiraceae
f__Lactobacillaceae
f__Negativicoccaceae
f__Oscillospiraceae
f__Peptostreptococcaceae
f__Prevotellaceae
f__Pseudomonadaceae
f__Rhizobiaceae
f__Ruminococcaceae
f__Selenomonadaceae
f__Sporanaerobacteraceae
f__Streptococcaceae
f__Tepidimicrobiaceae
f__Tissierellaceae
f__Yersiniaceae
Others
f__Acutalibacteraceae
f__Anaerotignaceae
f__Bacteroidaceae
f__Burkholderiaceae
f__Butyricicoccaceae
f__Clostridiaceae
f__Coriobacteriaceae
f__Enterobacteriaceae
f__Enterococcaceae
f__Erysipelatoclostridiaceae
f__Erysipelotrichaceae
D
Observed ASV
Shannon
Alpha-diversity measure
Pre-ATB
E
Log10 16S copies/mL
F
Dysbiosis Score (Centroid)

Figure IV.2: Effect of five different antibiotic treatments on canine microbiota activity and composition. Fermentations were performed in the CANIM-ARCOL under medium dog size colonic conditions, after inoculation with stool from a single medium size dog. Samples were regularly collected from atmospheric phase of bioreactors to determine gas composition over time. Results are expressed in relative percentages of main gases (**A**) or total daily gas production in mL (**B**). Lumen and mucus-associated microbiota composition was analyzed by 16S Metabarcoding and 16S qPCR. Relative abundance of the main bacterial populations in both colonic microenvironments from day 8 are represented at the family level (**C**). Alpha-diversity indexes (observed ASVs and Shannon) (**D**) were calculated based on ASV table at day 8 ('Pre-ATB' box plot) and average on treated days (from day 9 to 13 for M and AM and from days 9 to 15 for ME, MEC and TY conditions, respectively) in the luminal medium (top) and mucin beads (bottom). Total bacteria were quantified throughout fermentation and expressed as Log_{10} 16S copies/mL (**E**). Lastly, a dysbiosis score based on 16S Metabarcoding results for seven bacterial populations (i.e. *Blautia, Escherichia*, *Faecalibacterium*, *Fusobacterium*, *Peptacetobacter*, *Streptococcus* and *Turicibacter*) was calculated from day 8 using AlShawaqfeh and colleagues' method (**F**) (AlShawaqfeh *et al.*, 2017). Antibiotic treatment period was symbolized by a red square or zone. *AM: amoxicillin, ND: not determined, M: metronidazole, ME: metronidazole/enrofloxacin, MEC: metronidazole/enrofloxacin/ciprofloxacin, TY: tylosin*.

Metabarcoding analysis at the family level (**Figure IV.2C**) corroborated metabolic activities results, with the lowest impact of M and even more AM on bacterial profiles in the luminal medium. On the contrary, a huge effect of ME, MEC and TY antibiotics was noted on lumen-associated bacteria, characterized by a bloom of *Enterobacteriaceae*, with relative abundance reaching up to 95% in ME bioreactor. Of note, mucus-associated microbiota was both less and differentially impacted by antibiotic treatment compared to the luminal fraction. ME and MEC treatments were associated with a sharp increase in *Enterococcaceae*, while *Erysipelotrichaceae* were the most abundant bacteria in TY bioreactor at the end of antibiotherapy. Alpha-diversity indexes (**Figure IV.2D**) once again confirmed that M and AM treatments had the lowest impact on colonic microbiota, with no significant difference between control (pre-ATB, day 8) and treated period ($p>0.05$) for both observed ASVs and Shannon, whatever the microenvironment (i.e. luminal medium or mucin beads). Contrarily, in the luminal medium, ME, MEC and TY antibiotics led to a wide decrease in the number of observed ASV (from 62 before treatment to 30, 42, and 20, respectively) and Shannon index (from 3 before treatment to 0.5, 1.6, and 1.9, respectively). Alpha-diversity of mucus-associated microbes was less impacted by antibiotic treatment than the luminal fraction, with the highest impact on both observed ASVs and Shannon observed under TY condition. Total bacteria were also quantified by 16S qPCR in the luminal medium (**Figure IV.2E**). Those analyses revealed no impact of M, TY and AM antibiotics on total bacteria load, but a decrease of around 3 Log10 16S copies/mL for both ME and MEC. Lastly, dysbiosis scores were calculated based on centroid distances (AlShawaqfeh *et al.*, 2017) for each antibiotic treatment and colonic microenvironment and compared to control conditions (day 8), as shown in **Figure IV.2F**. In accordance with all the other tested parameters, dysbiosis scores stayed under the zero value (corresponding to a non-disturbed 'eubiosis' state) during the entire antibiotic treatment for M and AM conditions, in both luminal medium and mucin beads. For ME and MEC treatments, dysbiosis scores increased over the zero value (corresponding to a perturbated 'dysbiotic' state) from day 10 in the luminal compartment and only at day 14 in mucin beads, showing again a lower perturbation for mucus-associated microbiota. The highest scores were found with TY, with a maximum level reached from day 10 in

the luminal medium and a perturbated state already observed from day 12 in mucin beads. Based on those results, ME was selected for the further steps of dysbiotic model development. In addition, since main antibiotic-associated perturbations were already observed at day 5, we decided to shorten the duration of antibiotic treatment from 7 to 5 days for the upcoming experiments.

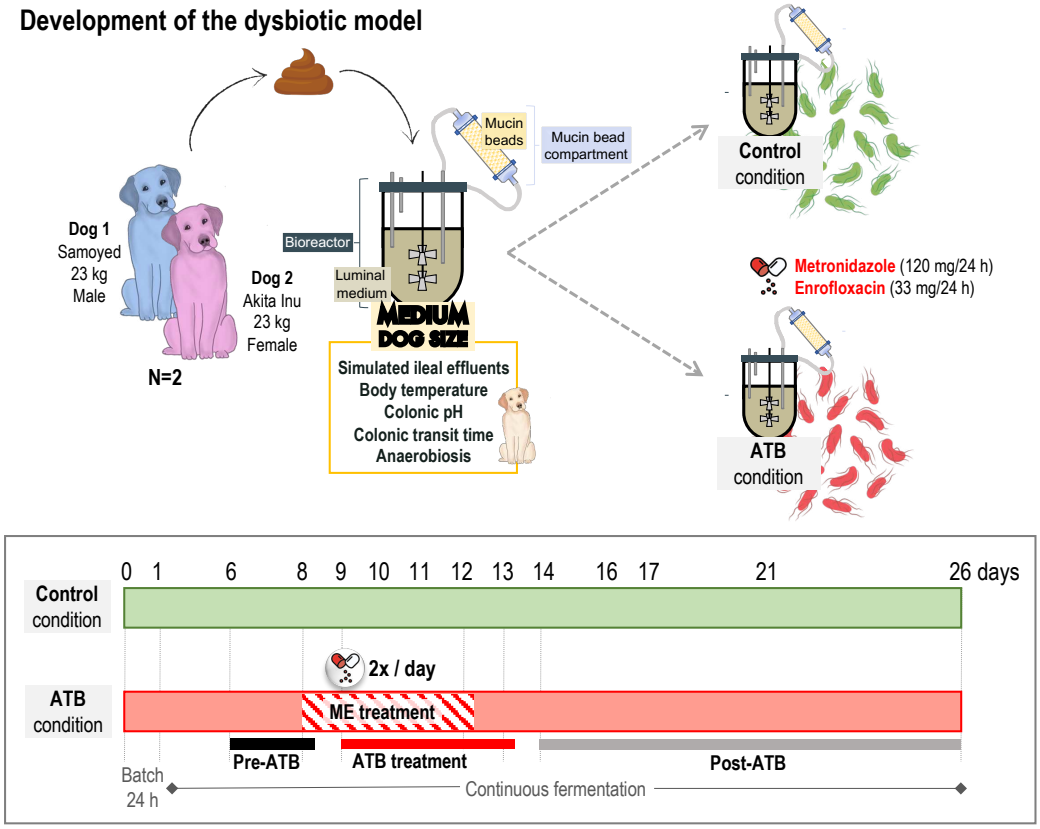

Figure IV.3: Experimental design used for the set-up of the antibiotic-induced dysbiosis model in the CANIM-ARCOL. The CANIM-ARCOL model was inoculated with fecal sample from two medium dogs (one male and one female, corresponding to two biological replicates) and set-up to reproduce medium dog size colonic conditions. For each replicate, two bioreactors were run in parallel (i.e. 'control' condition *versus* antibiotic 'ATB' condition) to evaluate the effect of the metronidazole/enrofloxacin cocktail on canine colonic microbiota. After a stabilization phase of 8 days, antibiotics were twice daily administered in the ATB bioreactor at in-field doses (i.e. 120 mg/24 h of metronidazole and 33 mg/24 h of enrofloxacin) for 5 days, while no treatment was applied to the 'control' bioreactor. Fermentations were further run until day 26 to assess microbiota resilience after antibiotherapy. Samples were regularly collected throughout fermentation in the atmospheric phase, the luminal medium and from mucin beads to monitor microbiota composition and main end-fermentation metabolites.

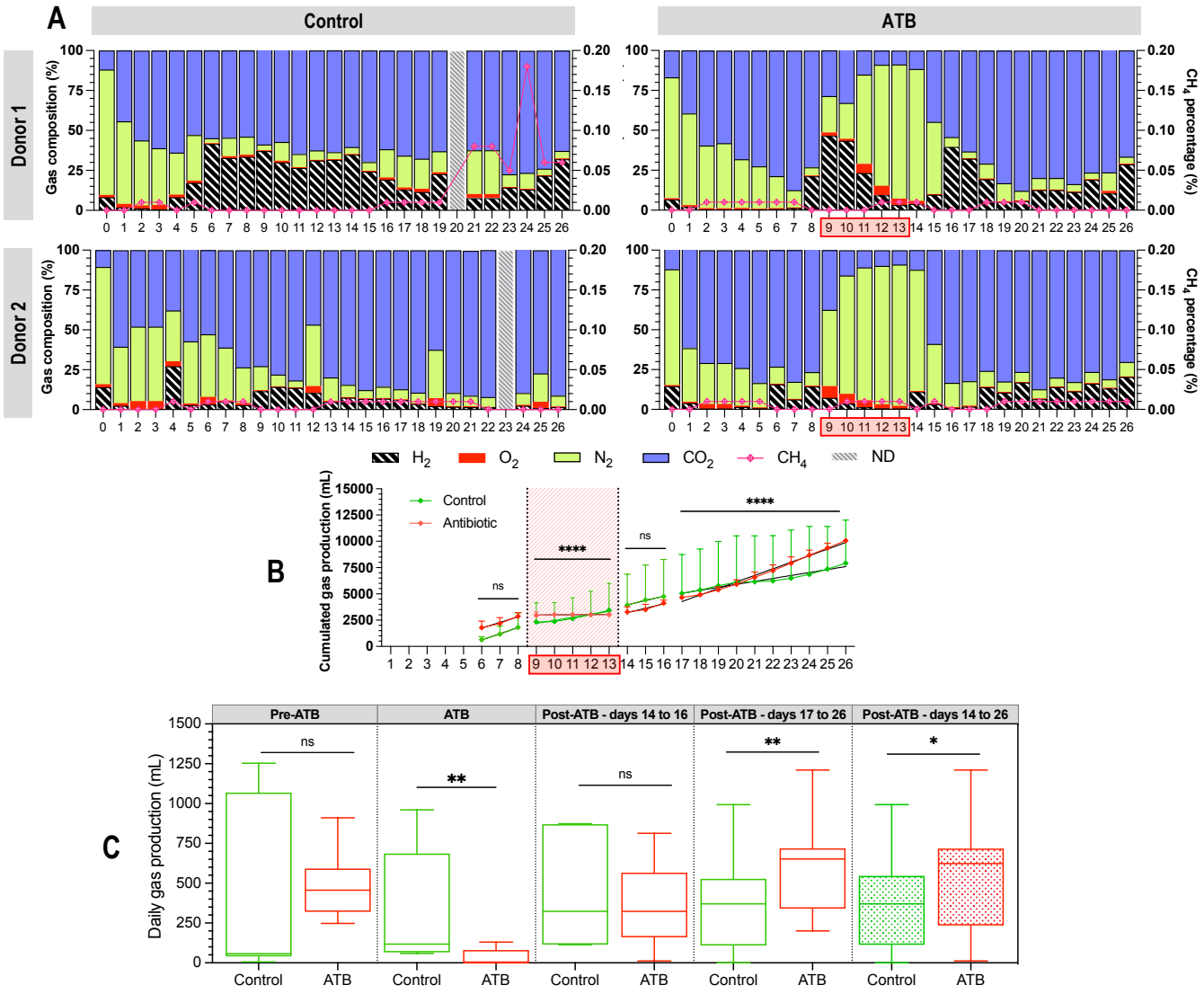

Figure IV.4: Impact of metronidazole/enrofloxacin treatment on gas production and bile acid profiles. Fermentations were performed in the CANIM-ARCOL under medium dog size colonic conditions, after inoculation with stools from medium size dogs (n=2). Samples were regularly collected from atmospheric phase of bioreactors to determine gas composition. Results are expressed in relative percentages throughout fermentation for dog 1 (top) and dog 2 (bottom) (**A**). Daily cumulated gas production is given in mL (**B**) and linear regression was calculated for each time period (i.e. pre-ATB, ATB, and post-ATB on the overall period or from days 14 to 16 and days 17 to 26). Average gas production for each time period was calculated under control and ATB condition and represented as box plots (**C**). Antibiotic treatment was symbolized by a red square or a red zone. Statistical differences are indicated by *: p<0.05, **: p<0.01 and ****: p<0.0001 (Mann-Whitney test). *ns: non-significant difference (p>0.05). ATB: antibiotic condition. ND: not determined.*

4.2.1. Production of main microbial end-fermentation products was altered during but not after antibiotherapy in the CANIM-ARCOL

In a second set of experiments, we performed additional fermentations in the CANIM-ARCOL (two biological replicates, dog 1 and dog 2, **Figure IV.3**), either under control (no treatment) or antibiotic condition

(administration of ME from day 8 to day 13) to further set-up the dysbiotic *in vitro* model. Microbiota activity was daily followed before ('pre-ATB' period), during ('ATB') and after ('post-ATB') antibiotic treatment.

Gas analysis under control conditions (**Figure IV.4A**) revealed different profiles between the two donors, with a higher percentage of H_2 in donor 1 (around 30 %) compared to donor 2 (10 %), together with lower amount of CO_2 (50% in donor 1 *versus* 75% for donor 2). ME treatment led to similar changes in gas profiles between the two donors, i.e. a decrease in H_2 and CO_2 relative abundances but a rise in O_2. From day 15 (i.e. two days after ATB treatment), a recovery of the microbiota was yet observed with an increase in CO_2 and H_2 percentages. A new stable state in gas profiles was observed from day 21 for donor 1 and a little earlier, from day 18, in donor 2. Mean (n=2) cumulated gas production was plotted (**Figure IV.4B**) and linear regressions during the different time periods (i.e. pre-ATB, ATB and post-ATB) confirmed the highly significant impact of ME ($p<0.001$) during the antibiotic treatment. A quick recovery was observed at the end of ME treatment with non-significant difference between control and ATB conditions from day 14 to 16. Curiously, gas production from days 17 to 26 under ATB condition overpassed that of the negative control ($p<0.001$). Comparison of daily gas production between control and treated conditions confirmed those results (**Figure IV.4C**).

Analysis of the three main SCFAs confirmed interindividual variations between donor 1 and 2. Under control condition, donor 1 showed higher percentages of butyrate than donor 2, but lower amounts of propionate (**Figure IV.5A**). SCFA profiles were also less stable in donor 2 compared to donor 1. However, in both donors, ME treatment resulted in a sharp decrease in propionate and butyrate relative abundances, together with an increase in acetate. Propionate and butyrate concentrations (**Figure IV. 5A**) decreased from around 25-30 mM under control condition to 0-5 mM during ATB treatment, while acetate concentrations stayed more stable. Total SCFA concentrations (**Figure IV.5B** and **5C**) significantly dropped during ATB treatment from around 140 mM to 80 mM ($p<0.01$). SCFA production and profiles were rapidly restored (from day 15-16) after cessation of antibiotic treatment (**Figure IV.5A** and **5B**), with non-significant difference between control and ATB conditions from day 14 to day 16 (**Figure IV.5C**). As previously observed for gas, SCFA production was significantly higher under ATB condition compared to control one from day 17 to day 26 ($p<0.05$).

Figure IV.5: Impact of metronidazole/enrofloxacin treatment on short-chain fatty acids production. Fermentations were performed in the CANIM-ARCOL under medium dog size colonic conditions, after inoculation with stools from medium size dogs (n=2). Samples were regularly collected from luminal medium of the bioreactors to determine short-chain fatty acids (SCFA) concentrations. The three main SCFA (i.e. acetate, propionate and butyrate) were measured daily throughout fermentations and results expressed in mean relative percentages for both donors (A, top) and concentrations in mM (A, bottom). Total SCFA concentrations (mM) over time of fermentation (B) and averaged on each time period (C) were calculated under control and ATB conditions and expressed as box plots. Antibiotic treatment was symbolized by a red square and a red zone. Statistical differences are indicated by *: $p<0.05$, **: $p<0.01$ and ****: $p<0.0001$ (Mann-Whitney test). *ns: non-significant difference ($p>0.05$). ATB: antibiotic condition.*

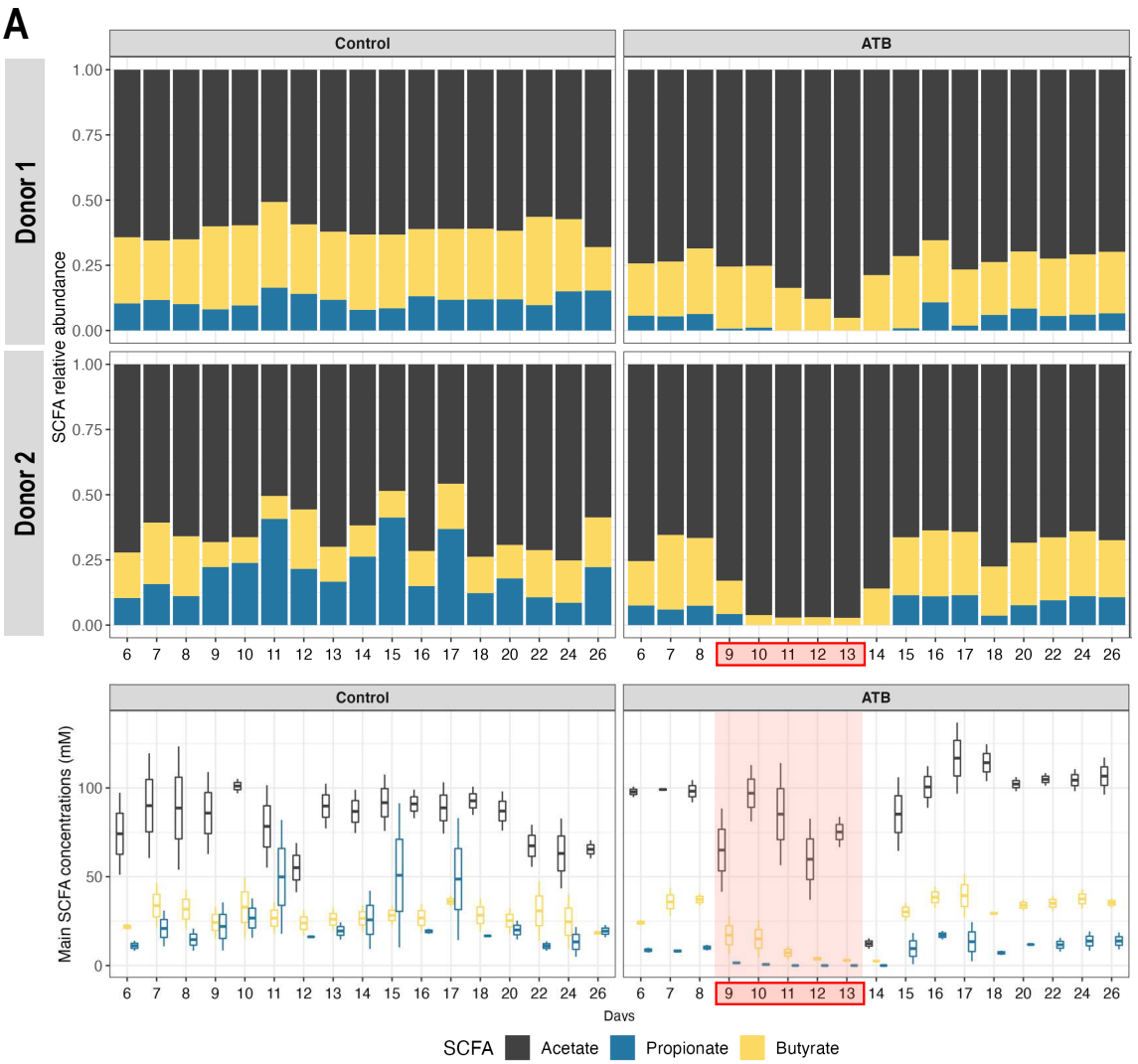
A
Control
ATB
Donor 1
Donor 2
SCFA relative abundance
1.00
0.75
0.50
0.25
0.00
6 7 8 9 10 11 12 13 14 15 16 17 18 20 22 24 26
Main SCFA concentrations (mM)
100
50
0
Days
SCFA
Acetate
Propionate
Butyrate

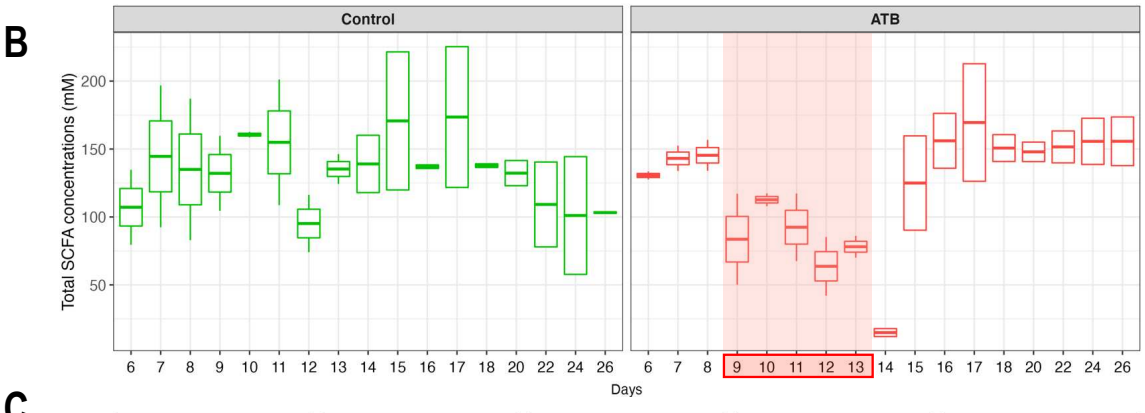
B
Control
ATB
Total SCFA concentrations (mM)
200
150
100
50
6 7 8 9 10 11 12 13 14 15 16 17 18 20 22 24 26
Days

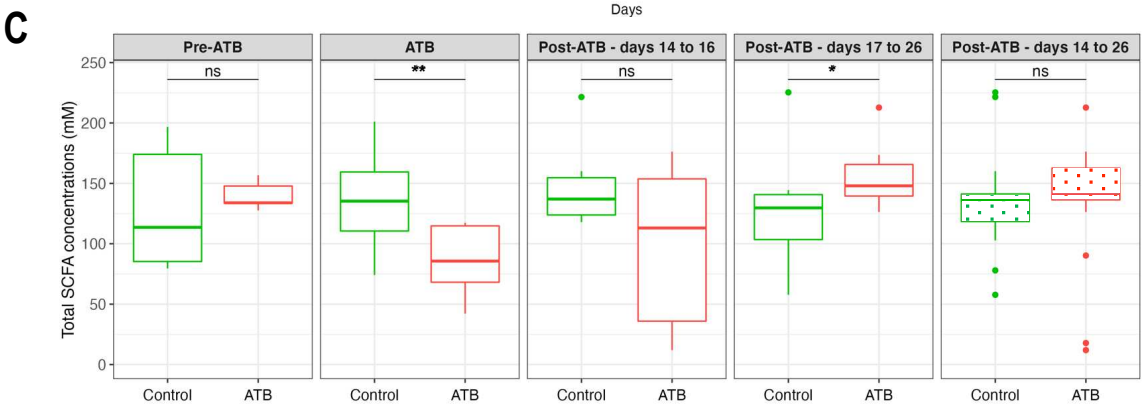
C
Pre-ATB
ATB
Post-ATB - days 14 to 16
Post-ATB - days 17 to 26
Post-ATB - days 14 to 26
ns
**
*
Total SCFA concentrations (mM)
250
200
150
100
50
0
Control
ATB

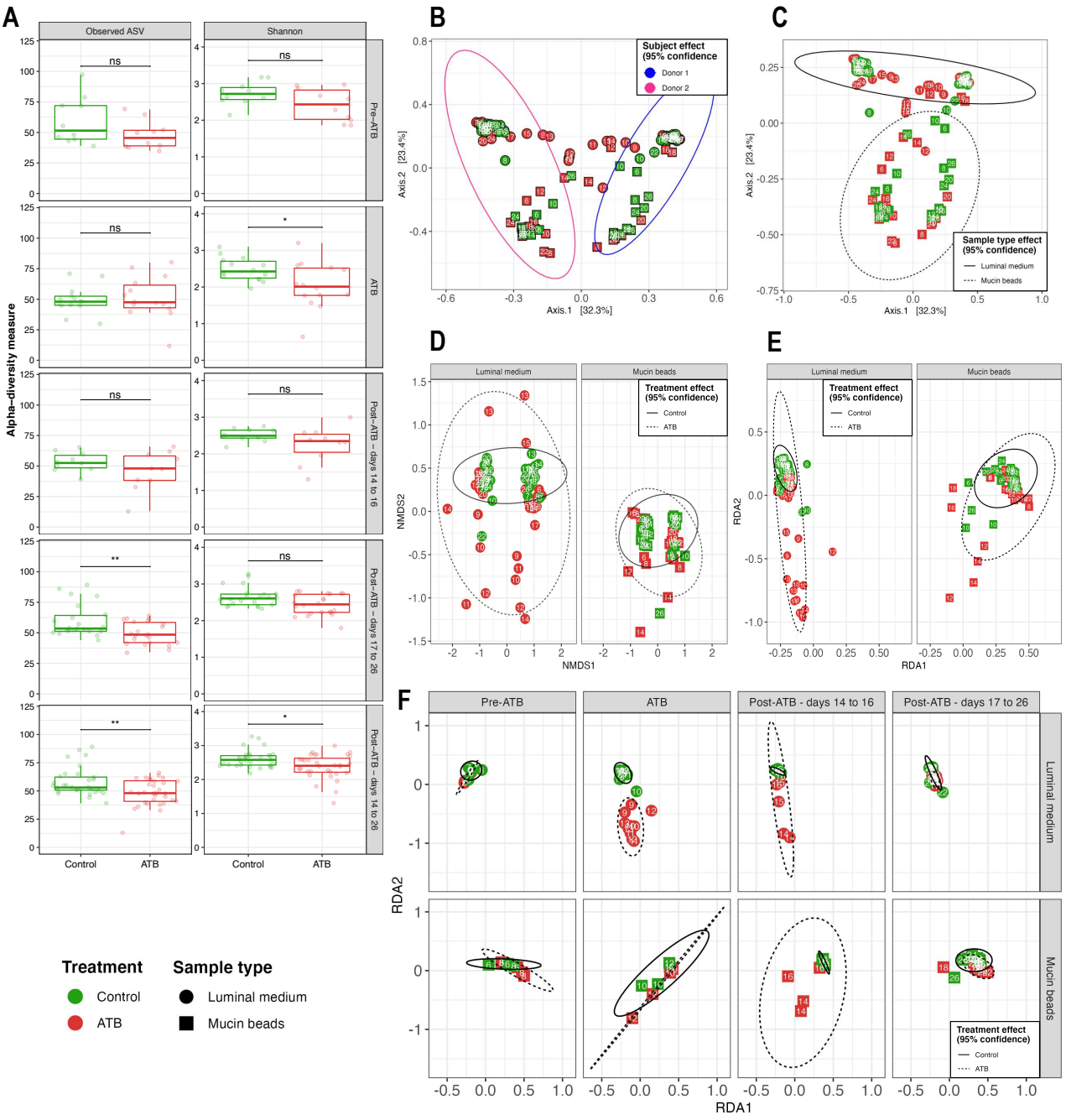

Figure IV.6: Impact of metronidazole/enrofloxacin treatment on canine microbial diversity. Fermentations were performed in the CANIM-ARCOL under medium dog size colonic conditions, after inoculation with stools from medium size dogs (n=2). Lumen and mucus-associated microbiota composition was analyzed by 16S Metabarcoding and diversity indexes were calculated based on ASV table. Alpha-diversity indexes (observed ASVs and Shannon) were calculated for each time period, averaged on both luminal medium and mucin beads and represented as box plots (**A**). Beta-diversity of samples from days 6 to 26 was analyzed by PCoA showing a clear clustering by donor (**B**) and microenvironment, i.e. luminal medium versus mucin beads (**C**). Both NMDS (**D**) and RDA analysis based on Bray-Curtis distances without donor effect (**E, F**) reveal effect of ATB treatment, when results were split by microenvironment or time period. Significant differences based on Kruskal-Wallis test are given at * $p<0.05$ and ** $p<0.01$. *ns: non-significant difference ($p>0.05$). ATB: antibiotic condition.*

4.2.1. Lumen but not mucus-associated colonic microbiota was widely modified during antibiotherapy

Bacterial alpha-diversity (**Figure IV.6A**) was significantly decreased by ME treatment ($p<0.01$ for Shannon index). Alpha-diversity indexes calculated on the overall post-ATB period (from day 14 to 26) showed that the antibiotic effects are still visible after end of administration, with a significant lower number of observed ASVs ($p<0.01$) and Shannon index ($p<0.05$) in ATB compared to control condition. Principal component analysis (PCoA) based on ASV composition and Bray-Curtis distance showed strong effects of stool donor on microbiota composition (**Figure IV.6B**), and a clear clustering of samples by colonic microenvironments, i.e. luminal or mucosal (**Figure IV.6C**). Both NMDS (**Figure IV.6D**) and redundancy analysis (RDA) removing donor effect (**Figure IV.6E**) highlighted a clear impact of antibiotic treatment on colonic microbiota, both in the luminal medium and mucin beads. Interestingly, samples collected under ATB condition showed a clear higher dispersion than control ones, especially in the luminal medium. When considering the different time periods (**Figure IV.6F**), we could clearly evidence an impact of ME on microbiota during antibiotic administration, more pronounced in the luminal medium. Samples were still clustering depending on the treatment from day 14 to 16, but no more from day 17 to 26, showing microbiota recovery.

Total bacteria were quantified in both luminal medium and mucin beads by qPCR to assess the effect of ME treatment on bacterial loads (**Figure IV.7A** and **7B**). A decrease of around 2.5 and 1.5 Log10 16S copies/mL was observed for lumen and mucus-associated microbes respectively during ATB administration. Return to baseline levels was reached within 5 and 3 days respectively for luminal and mucin beads samples. Metabarcoding analysis of lumen and mucus-associated microbiota showed, under control condition, interindividual variabilities between donor 1 and 2 in microbiota composition (**Suppl**. **Figure IV.1** and **Figure IV.7**). However, in both donors, ME treatment induced in luminal medium an increase in *Enterobacteriaceae* and *Enterococcaceae* relative abundances, while *Bacteroidaceae*, *Fusobacteriaceae* and *Burkholderiaceae* proportions decreased (**Figure IV.7C**). For the second donor, an increase in *Streptococcaceae* relative abundance was observed during ATB treatment. At the genus level (**Figure IV.7D**), percentage of *Proteus* increased while percentages of *Fusobacterium* and *Sutterella* decreased during ATB treatment for both donors. Other changes in genera were donor dependent. In the luminal medium of donor 1, relative abundance of *Ruminococcus* increased during ATB treatment while the one of *Clostridium*, *Enterocloster* and *Prevotellamassilia* decreased. In donor 2, relative abundances of *Streptococcus* together with *Escherichia* and *Enterococcus* increased, whereas proportion of *Phocaeicola* decreased. Of note, mucus-associated microbiota was less impacted by ME treatment than the luminal ones, for both donors. Most of changes occurred from day 12 (i.e. after 3 days of treatment), with an important drop of *Sporanaerobacteraceae* relative abundance, replaced by either *Enterobacteriaceae* (donor 1) or *Enterococcaceae* (donor 2).

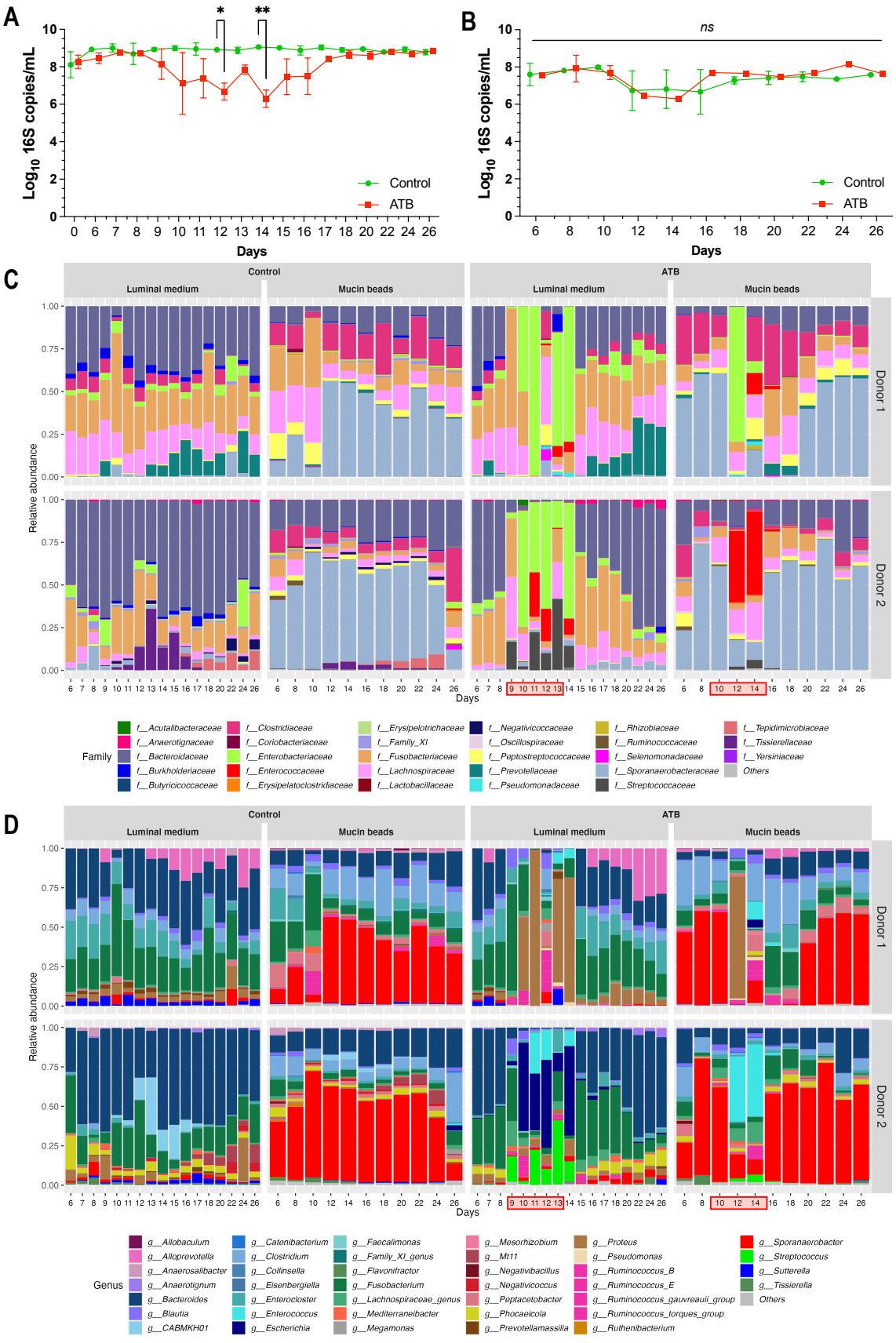

Figure IV.7: Impact of metronidazole/enrofloxacin treatment on canine bacterial populations. Fermentations were performed in the CANIM-ARCOL under medium dog size colonic conditions, after

inoculation with stools from medium size dogs (n=2). Lumen and mucus-associated microbiota composition was analyzed by 16S qPCR and 16S Metabarcoding. Total bacteria load was quantified in luminal medium (**A**) and mucin beads (**B**) and expressed as Log_{10} 16S copies/g. Relative abundance of the main bacterial populations in both colonic microenvironments are represented at the family (**C**) and genus (**D**) levels. Antibiotic treatment was symbolized by a red square and red zone. *ATB: antibiotic condition*.

In addition, for donor 2 only, the small fraction of *Negativicoccaceae* observed in the control bioreactor disappeared after antibiotic treatment. Overall, changes observed in the luminal medium occurred in the mucin beads with a 3-days delay, like *Proteus* blooming on mucin beads of donor 1 or *Enterococcus* and *Streptococcus* for donor 2. Interestingly, recovery of the microbiota globally occurs within one week for both donors except for *Burkholderiaceae* and *Tissierellaceae* (donor 2) that never recovered in the luminal medium and

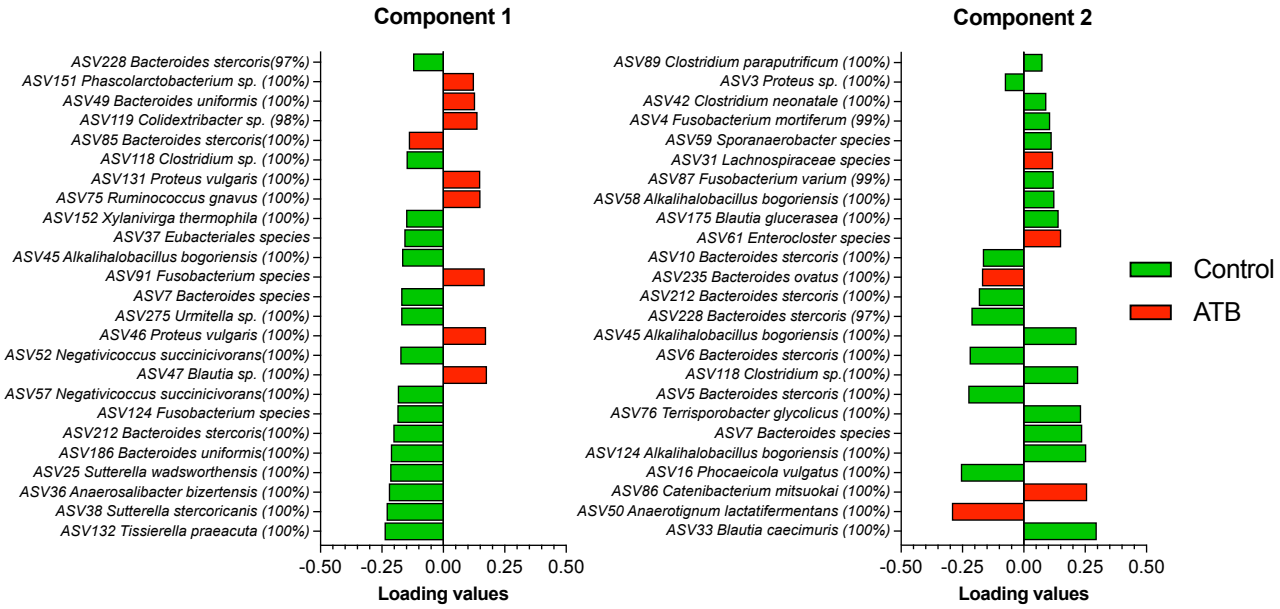

Negativicoccaceae (donor 2) in the mucin beads. Lastly, discriminant analysis based on metabarcoding data showed a significant enrichment in various ASVs associated to antibiotherapy, mainly *Blautia*, *Proteus vulgaris* and *Ruminococcus gnavus* (**Figure IV.8**).

Figure IV.8: Discriminant analysis of antibiotic effect on canine bacterial population at the ASV level. sPLS-DA analysis was performed on ATB and post-ATB periods to generate loading plots of the 25 most contributing ASVs between control and ATB conditions -all microenvironment confounded- and expressed for component 1 (explaining 7 % of data variability) and component 2 (6 %). Bars are colored according to the group in which the median abundance is maximal. Species annotations are provided when a sequence identity percentage higher than 97 % was identified using BLAST (given into bracket).

4.2.2. Metronidazole/enrofloxacin treatment was associated with a remnant dysbiosis state of colonic microbiota

Calculated dysbiosis scores remained below zero level under control condition, which confirmed that no dysbiosis was observed in both the luminal medium and mucin beads when antibiotics were not administered

(**Figure IV.9A** and **B**). As expected, ME treatment induced an increase in dysbiosis score, but much more marked in the luminal medium than in the mucin beads (**Figure IV.9A** and **9B**). When samples from both environments were gathered (**Figure IV.9C**), ME treatment induced a highly significant increase in dysbiosis score ($p<0.001$). At the end of antibiotic administration, dysbiosis scores progressively returned to the baseline in the luminal medium (**Figure IV.9A**). Values below zero were recovered earlier in the mucin beads (from day 16) compared to the luminal medium (from day 22), as shown in **Figure IV.9B**. When this recovery was analyzed by time period (**Figure IV.9C**), we observed that antibiotic-induced perturbations were maintained during the overall post-ATB period (from days 14 to 26, $p<0.001$).

4.2.1. Microbiota predicted metabolic pathways were significantly altered during but also after antibiotic treatment

Prediction of metabolic pathways was performed by PICRUSt2 based on metabarcoding analysis, with luminal medium and mucin beads samples confounded. The results obtained during and after ME treatment are shown in **Figure IV.10A** and **10B**, respectively. Thirty-one metabolic pathways were differentially expressed (LEFSe analysis) between control and ATB condition, during antibiotic administration (days 9 to 13, **Figure IV.10A**). Among them, 20 pathways were still disturbed after the end of antibiotic treatment (days 14 to 26, **Figure IV.10B**), even if their relative abundances were decreased. Most of the pathways were increased by antibiotherapy, both during (26 over 31 pathways) and after treatment (29 over 33 pathways). In particular, 'super pathway of L-tryptophan biosynthesis' and 'enterobactin biosynthesis' were activated ($p<0.05$) by ME treatment both during and after administration of the antibiotic, while 'pyruvate fermentation to propanoate I' and 'mannan degradation' were decreased ($p<0.05$). In addition, 11 pathways were only modified during ATB administration (from day 9 to day 13), such as 'super pathway of L-alanine biosynthesis', 'sucrose degradation IV (sucrose phosphorylase)' or 'hexitol fermentation to lactate, formate, ethanol and acetate' which increased, and 'acetyl-coA fermentation to butanoate II', 'superpathway of L-aspartate and L-asparagine biosynthesis', and '6-hydroxymethyl-dihydropterin diphosphate biosynthesis I' which decreased. Besides, 13 pathways were only significantly altered after the end of antibiotic administration. Among them, 'superpathway of hexuronide and hexuronate degradation' and peptidoglycan biosynthesis IV (*Enterococcus faecium*)' increased under ATB condition, while 'NAD salvage pathway I' and 'aromatic biogenic amine degradation (bacteria)' decreased ($p<0.05$).

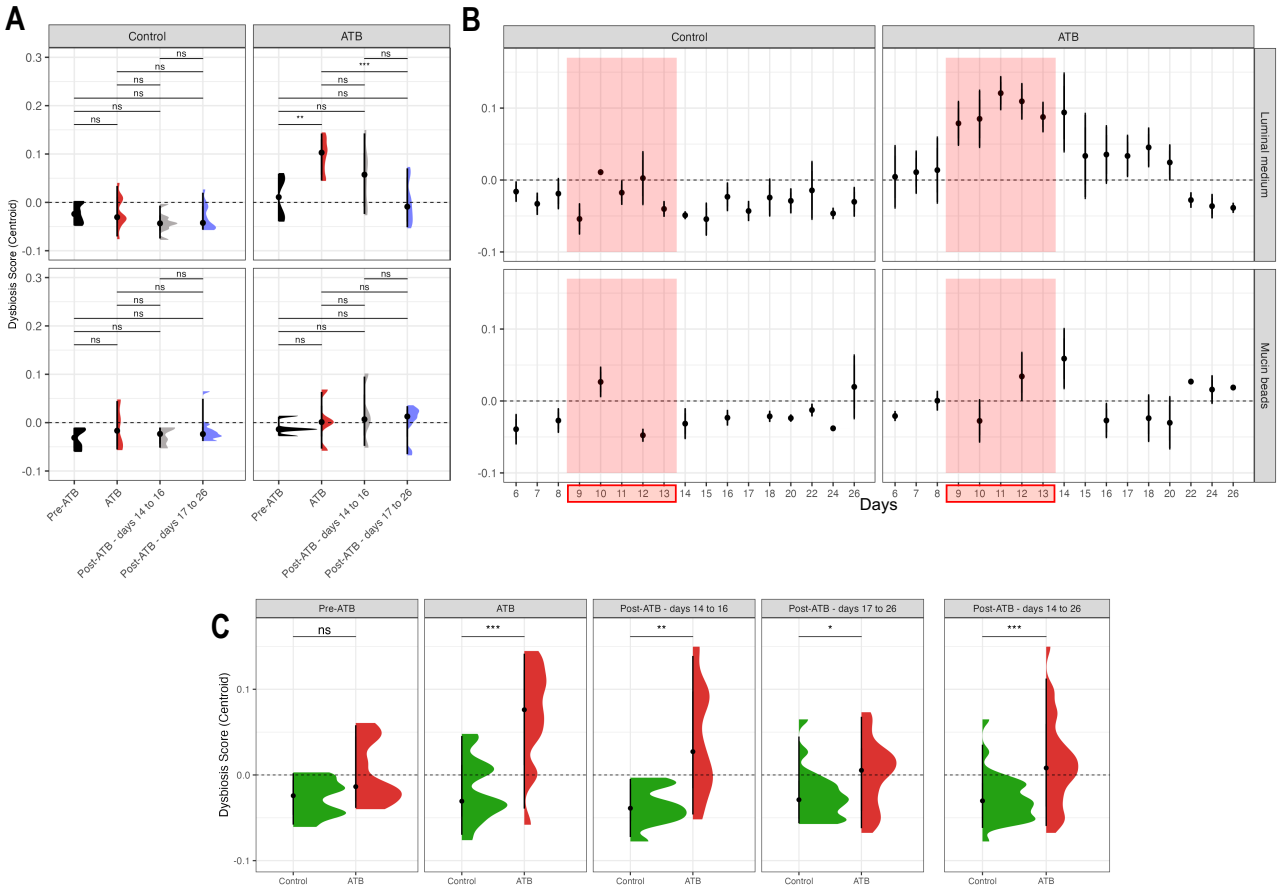

Figure IV.9: Impact of antibiotherapy on dysbiosis index in the CANIM-ARCOL. A dysbiosis score was calculated based on 16S Metabarcoding results for seven bacterial populations (i.e. *Blautia, Escherichia*, *Faecalibacterium*, *Fusobacterium*, *Peptacetobacter*, *Streptococcus* and *Turicibacter*) in both the luminal compartment and mucin beads, based on AlShawaqfeh and colleagues' method. Dysbiosis indexes were presented over period (**A**) or each day of fermentation (**B**) in the luminal medium (top) and mucin beads (bottom). The effect of antibiotherapy on dysbiosis score was also calculated on each time-period when samples from the two microenvironments were gathered (**C**). Antibiotic treatment period was symbolized by a red square and a red zone. Statistical differences are indicated by *: $p<0.05$, **: $p<0.01$ and ***: $p<0.001$ (Mann-Whitney test). *ns: non-significant difference ($p>0.05$). ATB: antibiotic condition.*

II-4

4.3. Discussion

Antibiotics are frequently used in dogs, contributing to their global burden on animal and human health. In accordance with the need to reduce *in vivo* experiments in dogs, we developed for the first time an *in vitro* model simulating an antibiotic-induced dysbiosis of the canine colonic microbiota in medium dogs and we validated it through *in vivo-in vitro* correlations. In a preliminary set of experiments, we performed a screening of five antibiotic cocktails to select the most relevant for further dysbiotic model development. Those antibiotics were selected among the most frequently used in veterinary practices and based on the availability of *in vivo* data regarding their impact on fecal microbiota (Suchodolski *et al.*, 2009; Grønvold *et al.*, 2010; Igarashi *et al.*, 2014; Kilpinen *et al.*, 2015; Manchester *et al.*, 2019; Werner *et al.*, 2020; Pilla *et al.*, 2020; Whittemore *et al.*, 2021; Pignataro *et al.*, 2021; Bottero *et al.*, 2022). Treatment doses in the CANIM-ARCOL were based on in-field recommendations for oral administration to a 20 kg dog (300 mg/12h for metronidazole, 100 mg/12h for

enrofloxacin, 200 mg/12h for tylosin and 1200 mg/12h for amoxicillin) and data on drug pharmacokinetics, i.e. absorption and potential metabolization of the active compounds in the upper digestive tract. Therefore, we established that around 20 % of the oral dose of metronidazole reached the large intestine *in vivo* (Neff-Davis, Davis & Gillette, 1981), 16 % of enrofloxacin (40 % being metabolized into ciprofloxacin) (Cester & Toutain, 1997), 98 % of tylosin (ANSES) and 35.8 % of amoxicillin (Küng & Wanner, 1994), allowing us to determine to daily dose to be added in the *in vitro* colon model. Based on the impacts of the five antibiotic cocktails on both microbiota composition and metabolic activities (gas and SCFA production), our results indicate that M and AM treatments had a too low impact on colonic microbiota composition and activity to be considered as leading to a dysbiosis state. Contrarily, TY led to extremely altered situation regarding most of tested parameters, making it a non-relevant model. Since ME and MEC had quite similar effect, we finally opted for ME for the following reasons: 1- gas profile was more stable over antibiotic treatment, 2- bacterial alpha-diversity was more altered, and 3- ME is the only form of antibiotics that is orally given to dogs, ciprofloxacin resulting from enrofloxacin metabolization (Cester & Toutain, 1997).

Since gut microbiota dysbiosis is characterized by an alteration of both its structure and function (Pilla & Suchodolski, 2020), those two facets were considered in the present study when developing the ME antibiotic-induced dysbiotic model. With this objective in mind, during *in vitro* fermentations, microbiota composition was followed using qPCR and metabarcoding and microbial metabolic activities were assessed through main fermentation end-products measurement (gas and SCFA) and prediction of functional pathways. Regarding microbiota composition, antibiotic treatment with ME induced a significant decrease in bacterial alpha-diversity mostly in the luminal medium. This is a well acknowledged effect of antibiotherapy in mammals *in vivo*, obviously also observed in dog fecal samples (Suchodolski *et al.*, 2009; Pilla *et al.*, 2020; Whittemore *et al.*, 2021; Bottero *et al.*, 2022). Accordingly, we showed that antibiotherapy led to major alterations in bacterial profiles in the luminal medium and/or mucin beads, with a decrease in *Bacteroidaceae*, *Clostridiaceae* and *Fusobacteriota* relative abundances, in accordance with metronidazole spectrum (Freeman, Klutman & Lamp, 1997). On the contrary, *Lactobacillaceae*, *Streptococcaceae* and *Lachnospiraceae* fractions increased, in line with the effects described in healthy dog stools when metronidazole was administered alone (Igarashi *et al.*, 2014). Of interest, our *in vitro* study also evidenced a bloom of *Proteobacteria*, especially from the *Enterobacteriaceae* family. Such a rise in fecal *Proteobacteria* was already associated in dogs to metronidazole (Igarashi *et al.*, 2014), tylosin ((Kilpinen *et al.*, 2015) and amoxicillin (Grønvold *et al.*, 2010) oral antibiotherapy, but also linked to microbiota dysbiosis in acute diarrhea (Park *et al.*, 2019) or inflammatory bowel disease (Cassmann *et al.*, 2016; Vázquez-Baeza *et al.*, 2016). Among *Enterobacteriaceae* strains, some are well-known opportunistic pathogens which benefit from microbiota alteration to overgrowth (Marks *et al.*, 2011).

A- During ATB treatment

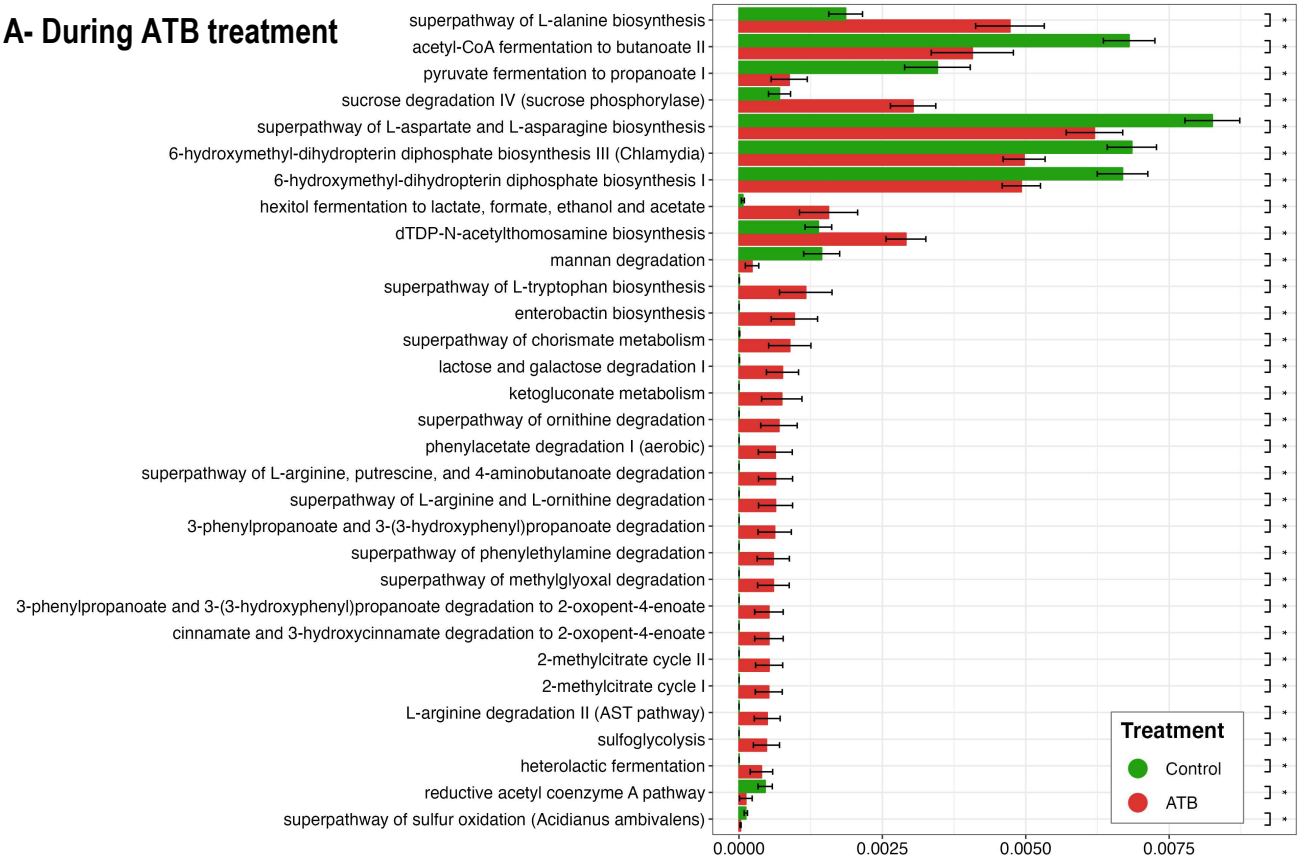

B- Post-ATB treatment

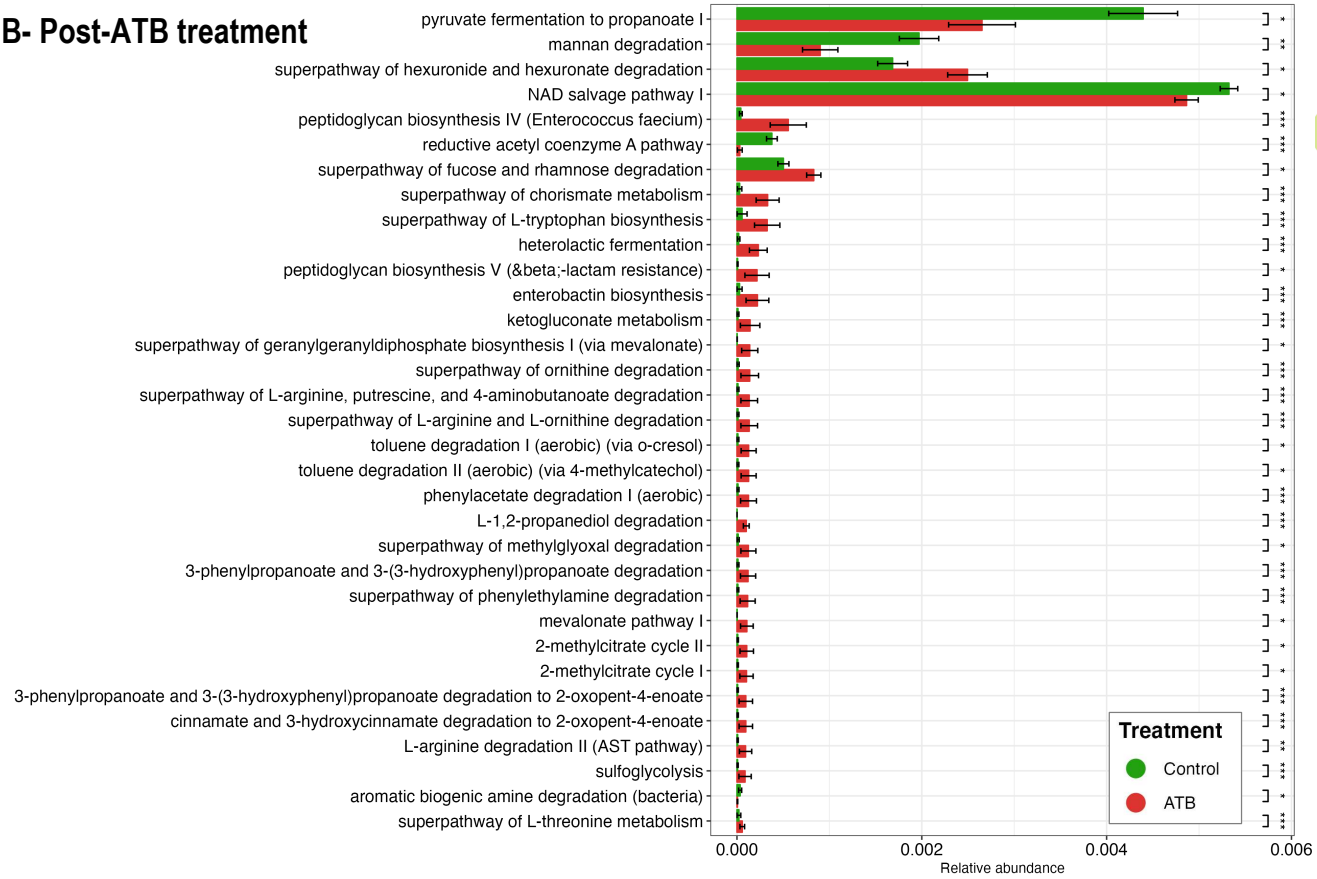

II-4

Figure IV.10: Impact of antibiotherapy on metabolic pathway predictions in the CANIM-ARCOL. PICRUSt2 software was used to predict bacterial metabolic pathways from 16S Metabarcoding data. LEFSE analysis was then performed to evidence significant differentially expressed pathways. Relative abundance of those pathways is plotted for control (green) and ATB (red) conditions during antibiotherapy from day 9 to 13 (**A**) and after ATB treatment from day 14 to 26 (**B**). Statistical differences are indicated by *: $p<0.05$, **: $p<0.01$ and ***: $p<0.001$ (Kruskal-Wallis test). *ATB: antibiotic condition.*

Differential analysis highlighted *Proteus vulgaris*, *Blautia sp*. and *Ruminococcus gnavus* as main discriminant ASVs associated with antibiotherapy. There is no specific literature on those strains in dogs but Rock and Donnenberg described *Proteus vulgaris* as an opportunistic pathogen in human, mainly responsible for urinary infection (Rock & Donnenberg, 2014) and are described as having acquired antibiotic resistance genes (Girlich *et al.*, 2020). Then, in order to assess a global effect of ME antibiotic treatment on canine colonic microbiota, we calculated a dysbiosis score, as previously defined by AlShawaqfeh and collaborators (AlShawaqfeh *et al.*, 2017). This score is based on the quantification of eight bacterial populations (total bacteria, *Fusobacteriota*, *Faecalibacterium*, *Blautia*, *Turicibacter*, *Streptococcus*, *Escherichia coli* and *Peptacetobacter hiranonis*) identified as key markers of dysbiosis in dogs with chronic enteropathies (AlShawaqfeh *et al.*, 2017), and successfully applied to other diseased situations such as diarrhea associated to *Clostridium perfringens* infection (Minamoto *et al.*, 2014) or atopic dermatitis (Guidi *et al.*, 2021). As expected, dysbiosis scores increased with ME treatment, reaching significance in the luminal medium but not in the mucin beads. Accordingly, most of our *in vitro* data suggest that antibiotherapy had less deleterious effect of mucus-associated microbiota compared to the luminal one. This was illustrated by a lower impact of ME on total bacterial load, drop in bacterial diversity and bloom of *Enterobacteriaceae*. These observations are consistent with those of Roussel and colleagues showing a lower disturbance effect of polyunsaturated fatty acids in the mucosal compartment of the M-SHIME (Mucosal Simulator of the Human Intestinal Microbial Ecosystem) compared to the luminal one (Roussel *et al.*, 2022). These authors described mucin beads as a robust microenvironment allowing a physical attachment of bacteria which confer them a competitive advantage. We can also speculate that this mucosal microenvironment may act as a bacterial reservoir to re-inoculate the luminal medium after disturbance such as antibiotherapy.

In parallel to changes in microbial composition, ME treatment also had a great impact on microbial fermentation process *in vitro*. Interestingly, the present study provides a first description of antibiotic impact on gas production (total production and profiles) by canine microbiota, since to our knowledge this has been never investigated before in dogs. Antibiotherapy led almost immediately to a stop in gas production, together with a drop in H_2 and CO_2 relative percentages. Those changes are associated with a significant decrease in total SCFA concentrations, mainly due to a reduction in propionate and butyrate amounts. All together, these results reflect the deleterious effect of ME on carbohydrate-degrading bacteria, such as *Bacteroidaceae* (Oliphant & Allen-Vercoe, 2019). Especially, decrease in propionate and butyrate levels may be correlated to the diminution of *Clostridiaceae* and *Prevotellaceae* relative abundances (Oliphant & Allen-Vercoe, 2019). Regarding SCFA, the effect of antibiotic treatment has been previously evaluated in only one study in healthy dogs, showing,

according to our results a decrease in total SCFA in fecal samples (5). Of note, after cessation of antibiotic administration, initial levels in gas and SCFA production were rapidly recovered, i.e. within 24 to 48 h, while recovery of bacterial profiles required a longer time period (up to one week). PICRUSt2 analysis revealed several metabolic pathways altered during antibiotherapy and related to microbial fermentation, such as in 'hexitol fermentation to lactate, formate, ethanol and acetate', and in 'superpathway of L-tryptophan biosynthesis' which increased, while 'acetyl-CoA fermentation to butanoate II' and 'pyruvate fermentation to propanoate I' decreased. Since tryptophan can be biosynthesized from indole, such an increase in 'superpathway of L-tryptophan biosynthesis' with ME supplementation *in vitro* is in line with the drop of faecal indole concentrations observed by Whittemore and colleagues when the same antibiotic cocktail was given to dogs (Whittemore *et al.*, 2021). Similarly, as propanoate is a precursor of propionate, the decrease in 'pyruvate fermentation to propanoate I' pathway is in adequacy with lower propionate concentrations found in CANIM-ARCOL during antibiotherapy.

Once the antibiotic-induced dysbiosis model set-up, the next step was to validate it through *in vivo-in vitro* comparisons to show its relevance compared to the physiological situation. This validation was performed thanks to the only available study in dogs which evaluated the effect of the same antibiotic cocktail on fecal microbiota composition and metabolic activities (Whittemore *et al.*, 2021). In this study, an oral dose of 250 mg/12h metronidazole (*versus* an equivalent of 300 mg in CANIM-ARCOL) and 200 mg/24h enrofloxacin (same dose than in the *in vitro* model) was administered for 21 days (compared to 5 here) to eleven medium size healthy dogs. Such *in vitro-in vivo* comparisons (**Table IV.1**) indicated that most of the parameters followed, regarding both microbiota composition (12 out of 21) and metabolic functions (3 out of 4) were similarly impacted by ME in the CANIM-ARCOL and dogs, showing the relevance of the model. However, *Actinobacteria*, *Ruminococcaceae*, *Erysipelotrichaceae* and *Proteobacteria* showed opposite trends in our *in vitro* study compared to *in vivo* data. This might be due to differences in antibiotherapy duration (5 *versus* 21 days), lack of interactions with host cells in CANIM-ARCOL (e.g. inflammation, Manchester *et al.*, (2019)) or possible re-inoculation by bacteria from food or environment *in vivo* which is not simulated *in vitro*. Surprisingly, *Proteobacteria* decreased and *Enterobacteriaceae* were almost not detected after antibiotherapy in the study from Whittemore and colleagues (Whittemore *et al.*, 2021), in total contradiction with outcomes from another publication on metronidazole in dogs (Igarashi *et al.*, 2014). Besides, *in vitro* like *in vivo*, ME induced changes in bacterial taxa that persisted after cessation of treatment, up to the end of experimentations in the CANIM-ARCOL and until 12 weeks in dogs. Lastly, our *in vitro* results which showed within 5 days many similar results with 21-days antibiotic treatment in healthy dogs, questioned the relevance of such a long period of administration in dogs.

Table IV.1: *In vivo-in vitro* comparisons regarding the effects of metronidazole/enrofloxacin treatment on gut microbial populations and metabolic activities. Effects of the metronidazole/enrofloxacin cocktail on the colonic microbiota and main end-fermentation products in the CANIM-ARCOL were compared to *in vivo* results obtained in fecal samples of healthy dogs (weight range 7.3-21.0 kg). Effects of antibiotherapy on each population or compound was indicated by '↗' if it was increased by the antibiotic treatment, '↘' if it was decreased or 'ND' if not detected. Color code indicates similar tendency between *in vitro* and *in vivo* data (in green), clear opposite trends (in red) or no full concordance (in yellow). Impossibility to conclude due to lack of *in vivo* data or no detection of the population is indicated by a grey color.

Impact of antibiotherapy on microbiota		***In vivo* study Whittemore *et al.*, (2021) N=11 dogs**	***In vitro* study CANIM-ARCOL N=2 dogs**		***In vivo-in vitro* correlations**
Treatment dose		[a] Oral dose: Metronidazole: 250 mg/12 h Enrofloxacin: 200 mg/24 h	[b] Colonic dose: Metronidazole: 60 mg/12h Enrofloxacin: 33 mg/12h		
Duration of treatment		21 days	5 days		
Type of samples		Feces	Luminal medium	Mucin beads	
Diversity	Shannon index	↘	↘	=	
Composition	**Actinobacteria**	↗	=	=	
	Coriobacteriaceae	↘	↗	↗	
	Bacteroidota	↘	↘	↘	
	Bacteroidaceae	↘	↘	↘	
	Prevotellaceae	↘	=	↘	
	Firmicutes	↗	↗	=	
	Lactobacillaceae	↗	↗	↗	
	Streptococcaceae	↗	↗	↗	
	Streptococcus	↗	↗	↗	
	Clostridiaceae	↘	↘	↘	
	Lachnospiraceae	↗	↗	↗	
	Ruminococcus	↗	↗	↗	
	Ruminococcaceae	↘	=	↗	
	Erysipelotrichaceae	↘	↗	↗	
	Fusobacteriota	↘	↘	=	
	Fusobacteriaceae	↘	↘	↗	
	Fusobacterium	↘	↘	↗	
	Proteobacteria	↘	↗	=	
	Enterobacteriaceae	ND	↗	↗	
Dysbiosis score		↗	↗	↗	
SCFA production [c]	Total SCFA	↘	↘		
	Acetate	↘	=		
	Propionate	↘	↘		
	Butyrate	↘	↘		

[a]: Oral dose calculated for a 20 kg medium size dog.
[b]: Calculated dose arriving to the large intestine of a 20 kg medium size dog, corresponding to an oral dose of 300 mg/ 12 h metronidazole and 100 mg/ 12 h enrofloxacin.
[c]: SCFA production was quantified by gas chromatography time-of-flight mass spectrometry and expressed as median pick height in Whittemore *et al.* 2021 while in the present study HPLC was used and results expressed in mM.

To conclude, we set-up for the first time an antibiotic-induced dysbiosis model of the canine large intestine, fully validated through *in vitro-in vivo* comparisons. This *in vitro* model also provided useful data, not available in dogs, on the impact of metronidazole/enrofloxacin cocktail on mucus-associated microbiome and colonic microbiota metabolic activities. CANIM-ARCOL represents a powerful platform to investigate the impact of various orally administered antibiotics on canine microbiota composition and activities, the effect of posology (e.g. duration of treatment and doses), but also the possible drug metabolization by gut microbes or antibiotic resistance gene transfer (Rochegüe *et al.*, 2021). In a next step, this *in vitro* model could be applied as an alternative to *in vivo* assays to assess the relevance of microbial restoration strategies such as prebiotics (Pinna & Biagi, 2014; Apper *et al.*, 2020), probiotics (Bell *et al.*, 2020; Bastos *et al.*, 2023), postbiotics (Spears *et al.*, 2016) or fecal microbiota transplantation (Bottero *et al.*, 2017; Gal *et al.*, 2021). Of particular interest, such an *in vitro* approach will allow to move toward personalized medicine by inoculating bioreactors with fecal samples from different healthy (e.g. different ages, breeds, feeding…) or diseased donors, suffering from instance of chronic enteropathies (AlShawaqfeh *et al.*, 2017) or obesity (Apper *et al.*, 2020). Further developments would include the coupling of CANIM-ARCOL model with intestinal or immune cells to integrate host interactions, which obviously play a role during antibiotherapy.

4.4. Material and methods

4.4.1. Preparation of antibiotic solutions

Five cocktails of antibiotic were tested during *in vitro* experiments: metronidazole (M), metronidazole/enrofloxacin (ME), metronidazole/enrofloxacin/ciprofloxacin (MEC), tylosin (TY) and amoxicillin (AM). Commercially available antibiotics were directly resuspended in distilled sterile water. ME was prepared with metronidazole (Sigma Aldrich) 1% and enrofloxacin (Sigma Aldrich) at 2.75 g/L and MEC with metronidazole 1%, enrofloxacin at 1.65 g/L and ciprofloxacin (Sigma Aldrich) at 1.1 g/L. TY preparation was made with tylosin at 48.75 g/L and AM suspension with amoxicillin at 430 g/L. Antibiotics were conserved at room temperature and protected from light until administration to CANIM-ARCOL.

4.4.2. Fecal samples collection and treatment

Three healthy dogs from medium size were used as stool donors for *in vitro* experiments (**Table IV.2**): two males, one Beagle (dog 0, 13 kg) and one Samoyed (dog 1, 23 kg) and a female Akita Inu (dog 2, 23 kg). Each dog was owner-pets, fed with commercial dry food, with access to outdoor. Immediately after defecation, fecal samples were transferred into a sterile recipient, placed in an airtight anaerobic box (GENbag anaer gas pack systems, Biomerieux, France), transported and processed at the laboratory within 3h. In an anaerobic chamber (COY laboratories, Grass Lake, USA), stool samples were manually homogenized, and 3.75 g of feces were resuspended in 100 mL of 30 mM sterile sodium phosphate buffer (pH 6.0), mixed and filtered (500 µm inox sieve).

Table IV.2: Characteristics of healthy adult dogs from medium size used as fecal donors for *in vitro* experiments. *M: male, F: female, BCS: body condition score (ranging from 1 -very thin- to 5 -obese-, 3 corresponding to ideal weight)*

Size	*Dog_id*	*Breed*	*Sex*	*Sterilization*	*Age (years)*	*BCS*	*Weight (kg)*	*Garden access*	*Feed*
Medium	Dog 0	Beagle	M	No	3	3	13	Yes	Dry
	Dog 1	Samoyed	M	No	4	3	23	Yes	Dry
	Dog 2	Akita Inu	F	No	4	3	23	Yes	Dry

4.4.3. Description and set-up of the CANIM-ARCOL model

CANIM-ARCOL is a one-stage fermentation system (MiniBio, Applikon, Delft, The Netherlands), inoculated with stool samples and used under continuous conditions to simulate the nutritional, physicochemical and microbial conditions found in the large intestine of dogs (Deschamps *et al.* 2023a). Here, in all *in vitro* experiments, the model was set-up to reproduce the colonic conditions of healthy medium size dogs, as previously described (Deschamps *et al.* 2023a). Briefly, the *in vitro* model is composed of a main bioreactor simulating the colonic luminal medium and an airtight glass vessel connected to this bioreactor and containing mucin beads to reproduce the mucosal compartment (**Figure IV.1** and **IV.3**). At the beginning of experiments, 100 mL of faecal suspension from each dog were added per bioreactor to 200 mL of sterile canine-adapted nutritive medium simulating the composition of ileal effluents of medium size dog (**Table IV.3**). To ensure anaerobic condition at the beginning of fermentation, the bioreactor was operated with an initial sparging with O_2-free N_2 gas. Afterwards, anaerobic condition was maintained by the sole activity of resident microbiota. The *in vitro* model was kept at canine body temperature. pH and redox potential were constantly recorded (Applikon, The Netherlands) and pH was adjusted to the setpoint value with 2 M NaOH. The nutritive medium was continuously introduced into the main bioreactor, while the fermentation medium was automatically withdrawn, ensuring the appropriate colonic retention time. Every two days, mucin beads from the mucosal compartment were renewed by fresh sterile ones under a constant flow of CO_2 to avoid oxygen entrance, as previously described (Deschamps *et al.*, 2020).

4.4.4. Pre-screening of antibiotics in the CANIM-ARCOL

In a first set of experiments (**Figure IV.1**), different antibiotic cocktails were administered to the CANIM-ARCOL model to investigate their effects on canine colonic microbiota composition and activity and select the most relevant for further dysbiotic model development (see part 5.). Five bioreactors were inoculated with a same fecal sample from dog 0 and run in parallel. Fermentations were run under batch conditions for 24h and then under continuous conditions for 11 to 13 additional days, depending on the antibiotics. The last day of stabilization phase (day 8) constitutes control conditions for each bioreactor. Antibiotics were twice daily introduced from day 9 for 5 days for M and AM and for 7 days for ME, MEC and TY, according to veterinary common prescriptions. Daily antibiotic doses introduced in the bioreactors were as follow: metronidazole (120 mg/24h, M condition), metronidazole (120 mg/24h) and enrofloxacin (33 mg/24h) for ME, metronidazole (120

mg/24h), enrofloxacin (19.8 mg/24h) and ciprofloxacin (13.2 mg/24h) for MEC, tylosin (390 mg/24h, TY) and amoxicillin (860 mg/24h, AM).

Table IV.3: Nutritional and physicochemical parameters used to set-up the CANIM-ARCOL under medium size canine colonic conditions. *rpm: rotation per minute, residence corresponds to half-emptying time of bioreactors.*

Size	***Medium***
Weight (kg)	**10-30**
Bioreactor's parameters	
Temperature	39 °C
Residence time	9 h
pH	6.5
Stirring	400 rpm
Nutritive medium composition (in %)	
Proteins	27.0
Carbohydrates	1.3
Lipids	2.4
Fibers	5.2
Bile acids composition in the nutritive medium (mg/L)	
Cholic acid	55 mg 10 %
Chenodeoxycholic acid	27 mg 5 %
Deoxycholic acid	327 mg 60 %
Lithocholic acid	136 mg 25 %

4.4.5. Antibiotic-induced dysbiosis in vitro model

The metronidazole/enrofloxacin cocktail was selected as the most appropriated to further reproduce an antibiotic-induced dysbiosis in the CANIM-ARCOL model. In this second set of experiments, two bioreactors were inoculated with a same faecal sample and run in parallel under either control or antibiotic conditions (**Figure IV.3**). The experiment was performed twice with fecal samples from two medium size dogs (one male and one female, dog 1 and dog 2), as biological replicates. Fermentations were run under batch conditions for 24h and then under continuous conditions for 25 additional days. Suspension of ME antibiotics was administered twice daily in the "ATB" bioreactor to reach an in-field dose of 120 mg metronidazole and 33 mg enrofloxacin per day, while the "control" bioreactor received no treatment.

4.4.6. Sampling from the CANIM-ARCOL model

In both series of experiments, samples were collected daily in the fermentation medium (luminal medium) for further analysis of microbiota composition (qPCR and 16S Metabarcoding) and metabolic activities through SCFA measurement. Every two days, mucin beads were collected to analyze the mucus-associated microbiota (qPCR and 16S Metabarcoding). Mucin beads were washed twice in sterile sodium phosphate buffer and stored at -80°C before downstream analysis. The atmospheric phase of bioreactors was also sampled every day to follow anaerobiosis and determine gas composition and production (total volume of gas) thanks to a sampling bag connected to the condenser.

4.4.7. DNA extraction

Genomic DNA was extracted from luminal medium samples using the QIAamp Fast DNA Stool Mini Kit (Qiagen, Germany) following manufacturer's instructions with the following modifications. Prior to DNA extraction, luminal samples were centrifuged (18 000 rcf, 15 min, 4°C) and the pellets were collected. Pellets

were then incubated 10 min with sterile citrate buffer (sodium citrate 55 mM and NaCl 154 mM) at 37°C, before vortexing (maximal speed, 15 sec) and centrifuge again (8000 rcf, 1 min). Then, a step of mechanical disruption using a bead beater (5 min, 20 beat/s) was made with 300 mg sterile glass beads (diameter ranging from 100 to 600 µm). Genomic DNA was extracted from around 150-200 mg of mucin beads samples using the Quick-DNA Fecal/Soil Microbe Miniprep kit (Zymo Research, Germany) following manufacturer's instructions. For both types of samples, DNA quantity was evaluated using the Qubit dsDNA Broad Range Assay Kit (Invitrogen, USA) with a Qubit 3.0 Fluorometer (Invitrogen, USA). Samples were stored at -20°C prior to microbiota analysis.

4.4.8. Quantitative PCR

Total bacteria were quantified by qPCR using primers described in **Table IV.4**. Real-time PCR assays were performed in a Biorad CFX96TM Real-Time System (Bio-Rad Laboratories, USA) using Takyon Low ROX SYBR 2X MasterMix blue dTTP kit (Eurogentec, Belgium). Each reaction was run in duplicate in a final volume of 10 µL with 5 µL of MasterMix, 0.45 µL of each primer (10 µM), 1 µL of DNA sample and 3.1 µL of ultra-pure water. Amplifications were carried out using the following ramping profile: 1 cycle at 95°C for 5 min, followed by 40 cycles of 95°C for 30 s, 58°C for 30 s, then 72°C for 30 sec. A melting step was added to ensure primer specificity. Standard curve was generated from 10-fold dilutions of bacterial DNA (isolated from a pure culture of bacteria), allowing the calculation of DNA concentrations from extracted samples.

Table IV.4: Primers used for qPCR and 16S Metabarcoding analyses

Primer name	*Sequence 5'-3'*	*Target*	*Annealing temperature (°C)*	*References*
qPCR primers				
BAC338R	ACTCCTACGGGAGGCAG	Total bacteria	58	(Yu *et al.*, 2005)
BAC516F	GTATTACCGCGGCTGCTG			
Metabarcoding primers				
V3_F357_N	CCTACGGGNGGCWGCAG	Bacteria	-	(Klindworth *et al.*, 2013)
V4_R805	GACTACHVGGGTATCTAATCC			

4.4.9. 16S Metabarcoding and data analysis

Bacterial V3-V4 regions of 16S ribosomal DNA (rRNA) were amplified using primers described in **Table IV.4**. Amplicons were generated using a Fluidigm Access Array followed by high throughput sequencing on an Illumina MiSeq system (Illumina, USA) performed at the Carver Biotechnology Center of the University of Illinois (Urbana, USA). Prior to analysis, raw data were demultiplexed and quality filtered using 'DADA2' R-package (Callahan *et al.*, 2016). Reads with quality score under 2 were truncated. Reads under 100 pb length were removed as well as sequences similar to PhiX DNA used as a spike-in control for MiSeq runs. Filtered sequences were dereplicated and cleaned for chimeras (DADA2). Taxonomic classification of the sequences was then performed with 'DECIPHER' package (Murali *et al.*, 2018). Assignations from both SILVA 138 release (Quast *et al.*, 2013) and GTDB_bac120_arc122 (Parks *et al.*, 2022) databases were merged using the

assign_taxo_fun function from rANOMALY R-package based on IDTAXA, with a 60% confidence cut-off (Theil & Rifa, 2021). A phylogenetic tree was then reconstructed using DECIPHER. Incorrect taxonomic affiliation of *Prevotella* genus in *Bacteroidaceae* family (instead of *Prevotellaceae*) was manually corrected.

4.4.10. Predicted community functional potential

The software PICRUSt2 (Phylogenetic Investigation of Communities through Reconstruction of Unobserved States) (Douglas *et al.*, 2020) was used to generate a new ASV table comprised of predicted KEGG Orthologs (KOs; Kyoto Encyclopedia of Genes and Genomes). The resultant tables were analyzed using the 'microeco' R-package by processing LEFSe analysis to identify predicted pathways that were significantly altered between control and ATB conditions. Then, Mann-Whitney test were performed on pathways relative abundancies.

4.4.11. Calculation of dysbiosis index

The 'dysbiosisR' R-package (Shetty & de Steenhuijsen Piters, 2022) was used to calculate dysbiosis scores based on 16S Metabarcoding results, as previously described by AlShawaqfeh and colleagues (AlShawaqfeh *et al.*, 2017). Dysbiosis index was defined as the difference between Euclidean distance between the test sample and the healthy class centroid and the Euclidean distance between the test sample and the diseased class centroid. The 'control' condition was related to the healthy class while the 'ATB' condition was the diseased one. A value of zero means that the test sample lies at equal distance from the center of both classes. Deviation of sample from eubiosis increases with dysbiosis index.

4.4.12. Gas analysis

Analysis of O_2, N_2, CO_2, CH_4, and H_2 gas produced during the fermentation process was performed using 490 micro-gas chromatography (Agilent Technologies, USA) coupled with a micro-TCD detector (Agilent Technologies, USA). Molecular Sieve 5A and Porapack Q (Agilent Technologies, USA) series columns were used. Gas composition was determined using calibration curves made from ambient air (78.09 % N_2, 20.95 % O_2, 0.04 % CO_2) and three gas mixtures A (5 % CO_2, 5 % H_2, 90 % N_2), B (20 % CO_2, 80 % H_2), and C (20 % CO_2, 20 % CH_4, 20 % H_2, 40 % N_2). Technical replicates were performed for each sample and results were expressed as percentages.

4.4.13. Short-chain fatty acids analysis

For SCFA analysis, 1.5 mL of luminal medium samples were centrifuged (18 000 rcf, 15 min, 4°C) and 900 µL of supernatant was diluted at 1/10 into H_2SO_4 0.04 M mobile phase, vortexed, and filtered (0.22 µm). The three major SCFAs (acetate, propionate, and butyrate) were quantified by high-performance liquid chromatography -HPLC- (Elite LaChrom, Merck HITACHI, USA) coupled with a DAD diode. The HPLC column (Concise Separations, ICE-99-9865) and its guard column were maintained at 50°C. Sulfuric acid 0.04 M was used as mobile phase and SCFA were separated at a flow rate of 0.6 mL/min. Data were obtained and analyzed by the EZChrom Elite software at 205 nm. SCFA concentrations were calculated from calibration

curves established from known concentration solutions of acetate, propionate, and butyrate (0, 10, 25, and 40 mM) and data expressed as mM or relative percentages.

4.4.14. Statistical analysis

Statistical analyses on microbiota activity (gas and SCFA) and α-diversity indexes (number of observed ASVs and Shannon index) from metabarcoding data were processed using GraphPad Prism software version 9.4.1 (GraphPad Software, USA) and/or R software (version 4.1.2). Data normal distribution was verified by combining Anderson-Darling, D'Agostino & Pearson, Shapiro-Wilk and Kolmogorov-Smirnov tests and homoscedasticity was checked using the Fisher test. Then, appropriate statistical analysis was applied (either one-way ANOVA, *t*-test or Mann-Whitney tests). Differential analysis on metabarcoding data (sPLS-DA) based on ATB and post-ATB periods only were performed using MixOmics package (Lê Cao *et al.*, 2009). Discriminant analysis on metabarcoding data (sPLS-DA) for ATB and post-ATB periods were performed using MixOmics package (Lê Cao *et al.*, 2009) while using microeco R-package (Liu *et al.*, 2021a) based of LEFSE method for PICRUSt pathways predictions First, principal coordinate analysis (PCoA) were performed followed by Non-Metric Multidimensional Scaling (NMDS), highlighting important size and microenvironment (i.e. luminal medium and mucin beads) effects. Constraint Redundancy analysis (RDA) were then performed with age, weight, sex, size, microenvironment, donor and time as variables of the model, first will all parameters and then with removal of either size or microenvironment variables. Bray Curtis distances were used for each analysis and significance between groups was assessed with a one or two-way Anova. Discriminant analyses (sPLS-DA) were finally performed using MixOmics package (Lê Cao *et al.*, 2009).

4.5. Additional figures

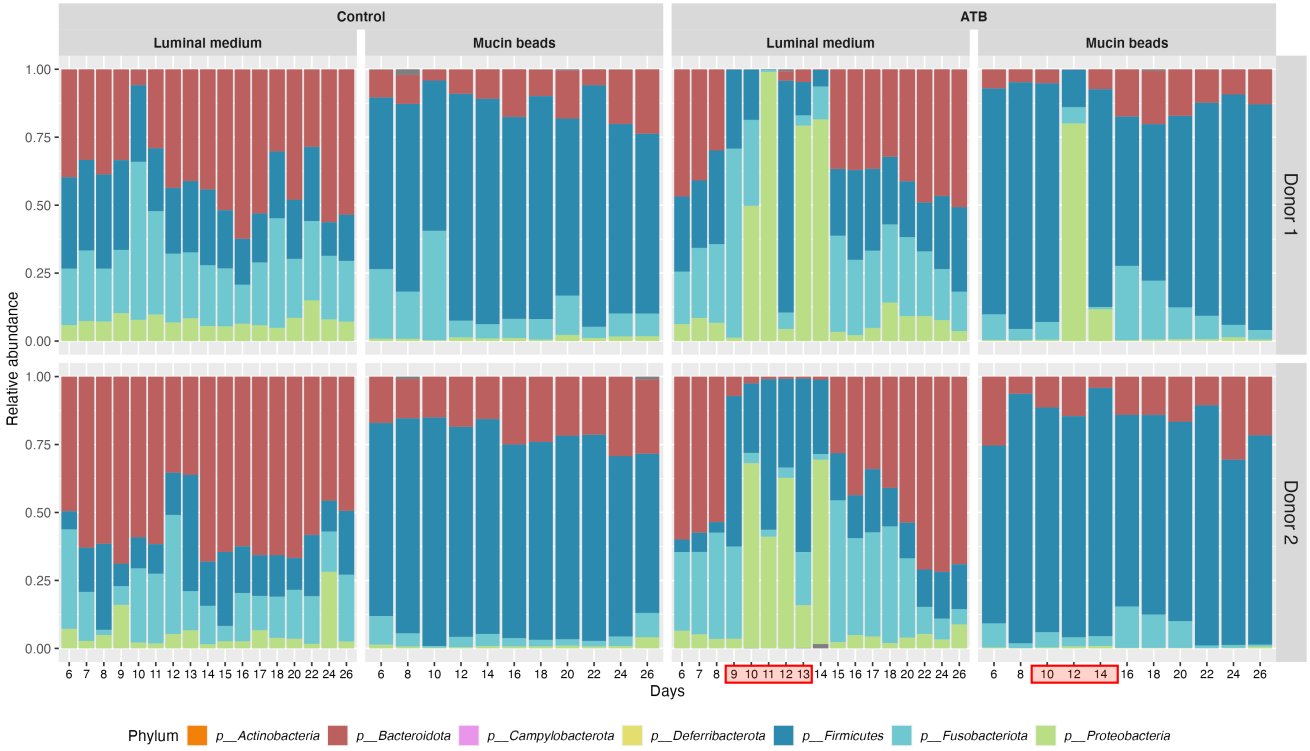

Supplementary figure IV.1: Impact of metronidazole/enrofloxacin treatment on bacterial populations at the phylum level. Fermentations were performed in the CANIM-ARCOL under medium dog size colonic conditions, after inoculation with stools from medium size dogs (n=2). Lumen and mucus-associated microbiota composition was analyzed by 16S Metabarcoding. Relative abundance of the main bacterial populations in both colonic microenvironments are represented at the phylum level. Antibiotic treatment was symbolized by a red square. *ATB: antibiotic condition.*

II-4

4.6. Additional discussion

As a marker of microbiota alteration induced by antibiotherapy, dysbiosis indexes were calculated based on the method developed by AlShawaqfeh *et al.*, (2017). Initially, the method was based on qPCR quantifications of seven bacterial populations (i.e. *Blautia, Escherichia*, *Faecalibacterium*, *Fusobacterium*, *Peptacetobacter*, *Streptococcus* and *Turicibacter*). Very recently, the 'dysbiosisR' R-package (Shetty & de Steenhuijsen Piters, 2022) allowed to calculate the same score with 16S Metabarcoding results instead of qPCR quantifications. Here, the analysis was first performed with the complete ASV table, showing a good capacity to evidence microbiota alteration induced by antibiotherapy (**Figure IV.11**).

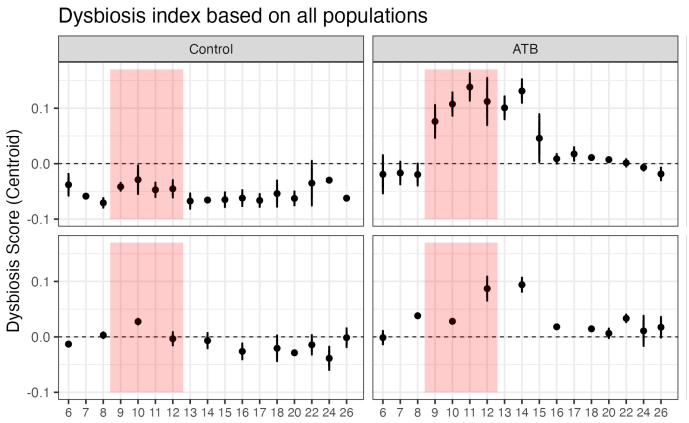

Figure IV.11: Impact of antibiotherapy on dysbiosis index in the CANIM-ARCOL, calculated for all bacteria populations. Dysbiosis score was calculated based on 16S Metabarcoding results for all bacterial populations detected. Results are presented for each day of fermentation in the luminal medium (top) and mucin beads (bottom). Antibiotic treatment period was symbolized by a red zone. *ATB: antibiotic condition.*

Nevertheless, the dysbiosis score was previously designed to evidence dysbiosis associated to canine chronic enteropathies, so we were interested to appreciate if the selected 7 populations were also able to discriminate antibiotic-induced dysbiosis based on 16 Metabarcoding data (**Figure IV.9**). Of great interest, such populations showed relevant potential to discriminate healthy and dysbiosis states, since they seemed to drive major changes associated to antibiotic-induced dysbiosis. These results are also in accordance with previous description of antibiotic induced dysbiosis, showing alterations of *Fusobacteria, Turicibacter, Streptococcus, Enterococcaceae,* and *Faecalibacterium* (see Section 1, Table 3.1). However, such index described a divergence in microbiota composition compared to a reference sample (healthy control) and results have to be considered with caution. Of note, dysbiosis is characterized by microbial alterations at the levels of both structure and functions and calculation of the dysbiosis index should be used as a complementary approach.

Analysis performed throughout this study would benefit from additional investigations, especially related to the antibiotic treatment. Of note, antibiotic concentration in the bioreactor was not dosed in this study and could be measured in future experiments using HPLC. In addition, it could be of interest to follow potential antibiotic-derived metabolites that could be produced during antibiotic degradation or metabolization by the microbiota using metabolomic approaches by RMN for example. In human, the gut microbiota reduced metronidazole, leading to N-(2-hydroxyethyl)-oxamic acid and acetamide production (Zemanová *et al.*, 2021), while enrofloxacin in mainly metabolized in the liver (Cester & Toutain, 1997). However, to date, there is no information on metronidazole or enrofloxacin metabolization by the canine microbiota. Finally, further analysis including bile acids and indoles measurement would be of great concern, since bile acid dysmetabolism and reduced indoles levels were previously described *in vivo* in dogs treated with metronidazole and enrofloxacin (Whittemore *et al.*, 2021).

4.7. Conclusion

Face to the lack of *in vitro* gut models simulating diseased situations in dogs, we adapted the newly developed CANIM-ARCOL to reproduce antibiotic-induced microbial dysbiosis inn medium dogs, for which some *in vivo* data were available in the literature. The new dysbiotic CANIM-ARCOL model is the first canine *in vitro* model to accurately simulate microbial perturbations induced by a metronidazole/enrofloxacin cocktail, as validated by great *in vivo-in vitro* correlations. Of interest, this study provides for the first time a comprehensive *in vitro* picture of antibiotic impact on both lumen and mucus-associated microbiota composition and associated gut metabolic activities. However, validation robustness may be further improved if additional *in vivo* data were available, mainly on mucosal microbes and gut metabolites.

Chapter 5 – Dysbiosis-protective or microbiota restoration strategies: *Lactobacillus helveticus*-derived parabiotic and *Saccharomyces boulardii* are efficient to restore gut microbiota after antibiotic disturbance in an *in vitro* canine gut model

The CANIM-ARCOL was successfully adapted and validated to reproduce an antibiotic-induced dysbiosis with great *in vivo-in vitro* correlations. Then, the last step of this PhD thesis was dedicated to the *in vitro* testing of microbial restoration strategies. The bibliographic research had highlighted a clear gap regarding restoration strategies associated to antibiotherapy in dogs (Section I part 3.2.4). Different strategies can be useful in this context including prebiotics, probiotics and postbiotics. A single *in vivo* study has evaluated the effect of *Enterococcus faecium* administered with metronidazole to diarrheic dogs, showing a positive impact of *E. faecium* in clinical responses and diarrhea occurrence (Fenimore *et al.*, 2017). Of interest also, the well-known probiotic *S. boulardii* could be an interesting probiotic candidate for dogs, in relation to the great effects observed in human on the reduction of antibiotic-associated diarrhea (Szajewska & Kołodziej, 2015). Yeast *S. boulardii* was up to now only tested in healthy dogs, lactating female or animals suffering from IBD, but was never tested in the context of canine antibiotherapy. In addition, postbiotics (including paraprobiotics), defined as 'a preparation of inanimate microorganisms and/or their components conferring a health benefit on the host' constitute a promising alternative strategy, still poorly documented in dogs (only 3 studies). In this context, we decided, as a final step of this PhD work, to evaluate the impact of one live probiotic yeast (*S. boulardii* CNCM I-1079) and one paraprobiotic bacteria (heat-inactivated *L. helveticus* HA-122) on canine microbiota composition and activity in a context of antibiotherapy in the CANIM-ARCOL. The impact of those products was assessed during and after antibiotherapy to test their relevance as dysbiosis-protective treatment or microbiota restoration strategies. Both *S. boulardii* and tyndallized *L. helveticus* are produced by Lallemand company. This work will be submitted for publication in *Food research international.*

ORIGINAL ARTICLE

***Lactobacillus helveticus*-derived parabiotic is as efficient as *Saccharomyces boulardii* to restore gut microbiota after antibiotic disturbance in an *in vitro* canine gut model**

DESCHAMPS, C., HUMBERT, D., DENIS, S., BRUN, M., DURIF, C., APPER, E., & BLANQUET-DIOT, S. (**2023**)

To be submitted in Food research international (**IF 7.4**)

For the entire manuscript this article will be cited as **Deschamps *et al.* (2023d)**.

Abstract

Gut microbiota plays a central role in dog health, supporting nutritional and physiological processes. Nevertheless, antibiotic treatment can disturb microbiota equilibrium, leading to a perturbated state called dysbiosis. Among modulation strategies, probiotics and postbiotics are increasingly studied but have been yet poorly evaluated in dogs in the frame of antibiotherapy. Demonstrate the efficiency and safety of these feed additives is ideally performed *in vivo* in dogs, however *in vitro* gut models may constitute relevant alternative approaches for regulatory, technical and costs reasons. In the present study, we evaluated for the first time the effect of two restoration strategies, the probiotic live yeast *Saccharomyces boulardii* CNCM I-1079 and the postbiotic heat-inactivated *Lactobacillus helveticus* HA-122 on antibiotic-induced dysbiosis in the Canine Mucosal Artificial Colon (CANIM-ARCOL). Restoration strategies were twice daily administered at in-field doses, to assess their ability to both increase resistance during antibiotic perturbation and improve restoration of lumen and mucus-associated microbiota equilibrium afterwards. Most notable effects were observed within two days after antibiotic treatment, when *S. boulardii* and *L. helveticus* mitigated *Enterobacteriaceae* bloom and promoted a quicker microbiota resilience regarding bacterial load and diversity and short-chain fatty acid production. Both microorganisms were able to downregulate metabolic pathways selected by antibiotherapy and potentially involved in pathobionts metabolism. Given those promising results, further mechanistic insights would include the characterization of products impact on host cells and enteric pathogens, by coupling CANIM-ARCOL with canine intestinal cells and extended its potential to diseased situations.

Keywords: dogs, food additives, probiotic, postbiotic, antibiotherapy, *in vitro* gut model, microbiota, restoration strategies.

5.1. Introduction

Gastrointestinal microbiota plays a key role in the health and well-being of companion animals such as dogs, by maintaining host homeostasis, physiological and immunological processes (Durand, 2010; Andoh, 2016). The microbiota inhabiting the large intestine harbors the higher number and diversity of microorganisms in the whole canine gastrointestinal tract (Hooda *et al.*, 2012). The bacterial fraction has been mostly described with around 52 % *Firmicutes*, 21 % *Fusobacteriota*, 19 % *Bacteroidota*, 4% *Proteobacteria* and 1 % *Actinobacteriota* in healthy dogs (Suchodolski *et al.*, 2008; Honneffer *et al.*, 2017). Bacterial metabolism provides beneficial nutrients for the host, such as short-chain fatty acids (SCFA) used as preferential energy source for colonocytes, increasing intestinal barrier strength, and lowering intestinal pH, thus making the environment inhospitable to pathogens (Blake & Suchodolski, 2016). This intimate relationship between microbiota and its host can be disrupted by antibiotics, commonly administered to treat canine diseases such as chronic enteropathies or acute diarrhea. Antibiotherapy may lead to side effects in dogs, namely diarrheas (Pilla *et al.*, 2020), vomiting (Whittemore *et al.*, 2019), weight loss, increase of oxidative stress markers (Pilla *et al.*,

2020), and in the worse cases bile acids dysmetabolism (Whittemore *et al.*, 2021). In addition, inappropriate use of antibiotics is known as a key driver of antimicrobial resistance in dogs (Allerton *et al.*, 2021). The closeness of dogs and humans may lead to gut microbes horizontal transfers between the two species making it a general burden (Wipler *et al.*, 2017; Huang *et al.*, 2020). Antibiotics generally induce a decrease in species diversity and richness in the canine fecal microbiota (Suchodolski *et al.*, 2009; Whittemore *et al.*, 2019, 2021; Pilla *et al.*, 2020; Bottero *et al.*, 2022), associated to an alteration of metabolite profiles (Whittemore *et al.*, 2021), contributing to a general microbial perturbation, called dysbiosis.

In order to limit perturbations and/or restore microbial equilibrium after antibiotherapy, different strategies have been envisaged in dogs, mainly translated from the human situation, such as probiotics or postbiotics (Fenimore *et al.*, 2017; Whittemore *et al.*, 2021; Pignataro *et al.*, 2021; Belchik *et al.*, 2023). Probiotics are defined as 'live microorganisms that when administered in adequate amounts confer a health effect on the host' (Hill *et al.*, 2014). Up to now, only one study has tested if a single probiotic strain fed in dogs can exert beneficial effects on antibiotic-induced gut microbial dysbiosis. This study showed that the oral administration of the bacterial strain *Enterococcus faecium* led to a decrease of diarrhea incidence in dogs treated with metronidazole (Fenimore *et al.*, 2017). Improvement of antibiotic-induced diarrhea by the yeast strain *Saccharomyces boulardi*i is well acknowledged in human (Szajewska & Kołodziej, 2015), suggesting it can be also a good probiotic candidate in dogs. This yeast significantly decreases fecal inflammatory and stress markers without impacting microbiota composition in both healthy dogs (Meineri *et al.*, 2022) and dogs with chronic enteropathies (D'Angelo *et al.*, 2018). Such probiotic strategy requires strain viability in the gastrointestinal tract, which may be challenging because of industrial constraints and conservation issues (high sensitivity to water and heat). An alternative solution is the use of heat-inactivated strains, called 'paraprobiotics' or 'postbiotics'. Postbiotics are defined as a "preparation of inanimate microorganisms and/or their components that confers a health benefit on the host" (Salminen *et al.*, 2021), while the concept of paraprobiotics refers to inactivated microbial cells or cell fractions that confer health benefit on the host (Taverniti & Guglielmetti, 2011). To date, paraprobiotics have been poorly investigated in dogs and never to counteract antibiotic effects. In healthy puppies and adult dogs, inactivated *Lactobacillus* strains improved faecal quality, microbial diversity and immune health, but also decreased fecal stress markers (Spears *et al.*, 2016; Panasevich *et al.*, 2021).

To evaluate the effect of probiotics and postbiotics on canine colonic microbiota, *in vivo* studies remain the golden standard. Nevertheless, such studies in dogs are increasingly restricted by ethical, regulatory, societal and cost pressures. An alternative option is the use of *in vitro* models simulating the canine gastrointestinal tract. Up to now, only two dynamic *in vitro* model of the canine large intestine have been developed, namely the Mucosal Simulator of the Canine Intestinal Microbial Environment (M-SCIME, Verstrepen *et al.* 2021) and the Canine Mucosal Artificial Colon (CANIM-ARCOL, Deschamps *et al.* 2023a). Both of them are inoculated with stool samples, reproduce the main nutritional and physicochemical parameters of the canine colon (i.e. pH, transit time, nutrient availability and bile acid profiles) and distinguish the lumen from mucus-associated

microbes. However, only the second one has been adapted to simulate antibiotic-induced dysbiosis and validated through *in vivo-in vitro* correlations (Deschamps *et al.* 2023c).

The objective of the present study was to evaluate the effect of two restoration strategies, namely the probiotic yeast *Saccharomyces boulardii* CNCM I-1079 and the parapostbiotic heat-inactivated *Lactobacillus helveticus* HA-122 on antibiotic-induced dysbiosis in the CANIM-ARCOL, set-up to reproduce colonic medium dog size conditions. Antibiotic disturbance was induced by 5 days administration of metronidazole/enrofloxacin cocktail. Restoration strategies were twice daily administered during and after antibiotherapy, to assess their effects on lumen and mucus-associated microbiota composition (16S metabarcoding) and metabolic activities (gas and SCFA).

5.2. Material and methods

5.2.1. Fecal samples collection and treatment

Two healthy dogs from medium size were used as stool donors for *in vitro* experiments (**Table V.1**): a male Samoyed (dog 1, 23 kg) and a female Akita Inu (dog 2, 23 kg). Each dog was owned, fed with commercial dry food, with access to outdoor. Immediately after defecation, fecal samples were transferred into a sterile recipient, placed in an airtight anaerobic box (GENbag anaer gas pack systems, Biomerieux, France), transported and processed at the laboratory within 3h. In an anaerobic chamber (COY laboratories, Grass Lake, USA), stool samples were manually homogenized, and 3.75 g of feces were resuspended in 100 mL of 30 mM sterile sodium phosphate buffer (pH 6.0), mixed and filtered (500 µm inox sieve).

Table V.1: Characteristics of healthy adult dogs from medium size used as fecal donors for *in vitro* experiments. *M: male, F: female, BCS: body condition score (ranging from 1 -very thin- to 5 -obese-, 3 corresponding to ideal weight)*

Size	*Dog_id*	*Breed*	*Sex*	*Sterilization*	*Age (years)*	*BCS*	*Weight (kg)*	*Garden access*	*Feed*
Medium	Dog 1	Samoyed	M	No	4	3	23	Yes	Dry
	Dog 2	Akita Inu	F	No	4	3	23	Yes	Dry

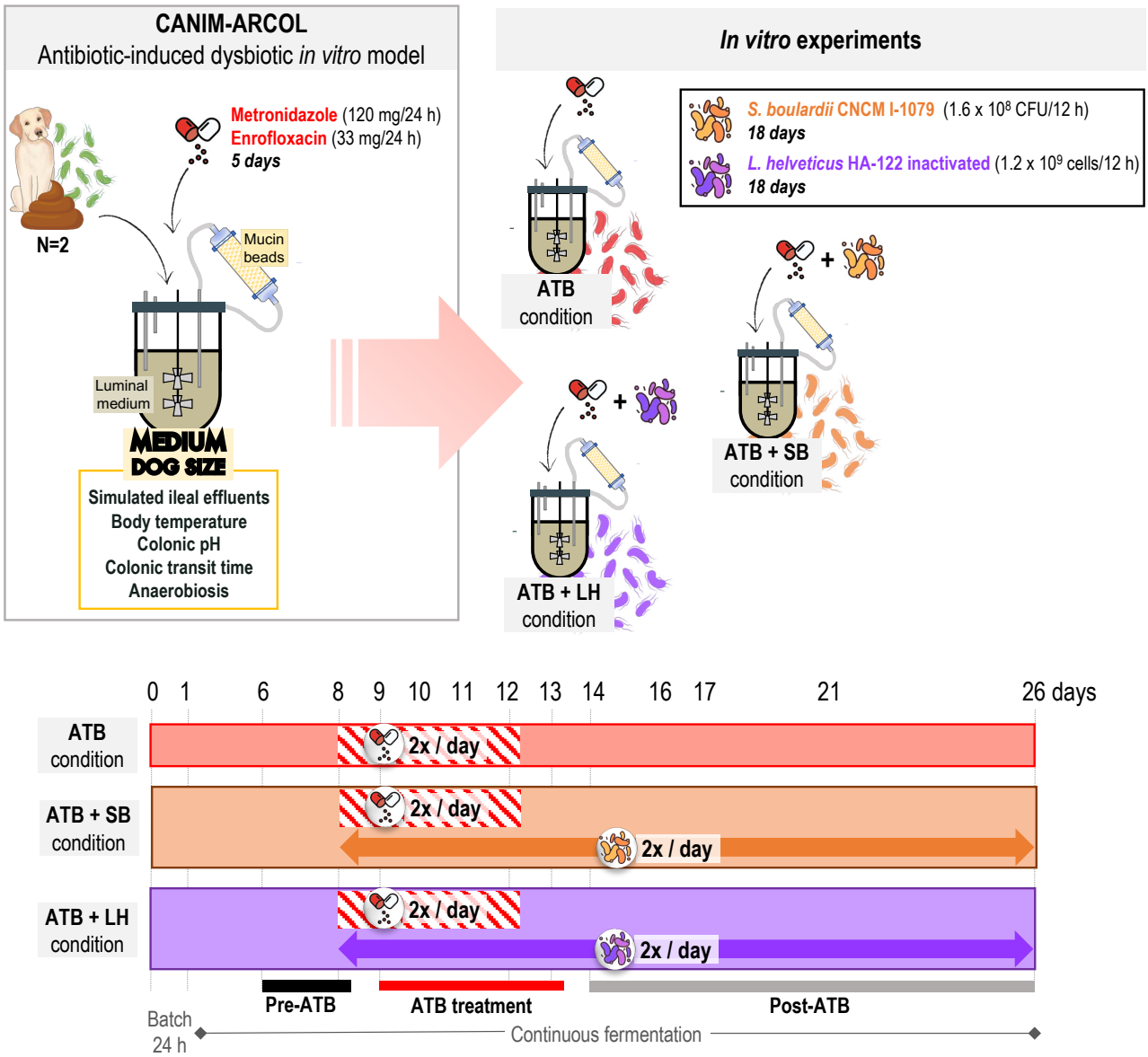

Figure V.1: Experimental design to evaluate the impact of tested restoration strategies on antibiotic-induced dysbiosis in the CANIM-ARCOL model. The CANIM-ARCOL model was inoculated with fecal sample from two medium dogs (one male and one female, corresponding to two biological replicates;) and set-up to reproduce medium dog size colonic conditions. For each replicate, three bioreactors were run in parallel to evaluate the effect of remediation strategies on antibiotic-induced canine microbiota dysbiosis: 1- antibiotic 'ATB' control condition, 2- antibiotic supplemented with alive *Saccharomyces boulardii* CNCM I-1079 'ATB + SB' and 3- antibiotic supplemented with inactivated *Lactobacillus helveticus* HA-122 'ATB + LH'. After a stabilization phase of 8 days, antibiotics were twice daily administered in all bioreactors at in-field doses for 5 days. In the 'ATB + SB' and 'ATB + LH' bioreactors, restoration strategies were twice daily administered from day 8 to 26 to assess their impact during and after antibiotherapy. Samples were regularly collected throughout fermentations in the atmospheric phase, luminal medium and mucin beads to monitor microbiota composition and main end-fermentation metabolites.

5.2.2. Description and set-up of the dysbiotic CANIM-ARCOL model

CANIM-ARCOL is a one-stage fermentation system (MiniBio, Applikon, Delft, The Netherlands), inoculated with stool samples and used under continuous conditions to simulate the nutritional, physicochemical and microbial conditions found in the large intestine of dogs (Deschamps *et al.* 2023a). Here, in all *in vitro* experiments, the model was set-up to reproduce the colonic conditions of healthy medium size dogs (Deschamps *et al.* 2023b). The model was previously adapted to reproduce an antibiotic-induced dysbiosis of colonic microbiota, with the use of metronidazole/enrofloxacin cocktail (Deschamps *et al.* 2023c). Briefly, the *in vitro* model is composed of a main bioreactor simulating the colonic luminal medium and an airtight glass vessel connected to this bioreactor and containing mucin beads to reproduce the mucosal compartment (**Figure V.1**). At the beginning of experiments, 100 mL of faecal suspension from each dog were added per bioreactor to 200 mL of sterile canine-adapted nutritive medium simulating the composition of ileal effluents of medium size dog (**Table V.2**).

Table V.2: Nutritional and physicochemical parameters used to set-up the CANIM-ARCOL under medium size canine colonic conditions. *rpm: rotation per minute, residence corresponds to half-emptying time of bioreactors.*

Size	***Medium***
Weight (kg)	**10-30**
Bioreactor's parameters	
Temperature	39 °C
Residence time	9 h
pH	6.5
Stirring	400 rpm
Nutritive medium composition (in %)	
Proteins	27.0
Carbohydrates	1.3
Lipids	2.4
Fibers	5.2
Bile acids composition in the nutritive medium (mg/L)	
Cholic acid	55 mg 10 %
Chenodeoxycholic acid	27 mg 5 %
Deoxycholic acid	327 mg 60 %
Lithocholic acid	136 mg 25 %

To ensure anaerobic condition at the beginning of fermentation, the bioreactor was operated with an initial sparging with O_2-free N_2 gas. Afterwards, anaerobic condition was maintained by the sole activity of resident microbiota. The *in vitro* model was kept at canine body temperature. pH and redox potential were constantly recorded (Applikon, The Netherlands) and pH was adjusted to the setpoint value with 2 M NaOH. The nutritive medium was continuously introduced into the main bioreactor, while the fermentation medium was automatically withdrawn, ensuring the appropriate colonic retention time. Every two days, mucin beads from the mucosal compartment were renewed by fresh sterile ones under a constant flow of CO_2 to avoid oxygen entrance, as previously described (Deschamps *et al.*, 2020).

5.2.3. Experimental design of in vitro fermentations

Three bioreactors were inoculated with a same faecal sample, run in parallel and used as follows (**Figure V.1**): the first bioreactor received only antibiotic treatment (ATB) as a negative control, the second received antibiotic and heat-inactivated *Lactobacillus helveticus* HA-122 strains (ATB + LH), and the third antibiotic and *Saccharomyces boulardii* CNCM I-1079 (ATB + SB). The experiments were performed twice with fecal

samples from two medium size dogs as biological replicates. Fermentations were run under batch conditions for 24h and then under continuous conditions for 25 additional days.

After a stabilization period of 8 days, the antibiotic suspension was administered twice daily for 5 days (from day 8 to 12) in all bioreactors to reach an in-field dose of 120 mg metronidazole (Sigma-Aldrich, Saint-Louis) and 33 mg enrofloxacin (Sigma-Aldrich, Saint-Louis) per day. Lyophilized *S. boulardii* CNCM I-1079 and heat-inactivated *L. helveticus* HA-122 were rehydrated in sterile physiological distilled water (NaCl 9 g/L) for 15 min and vortexed few seconds before administration. They were introduced twice daily from the beginning of antibiotic treatment (day 8) until the end of experiment (day 26) at the following doses: 1.2 x 10^9 cells per 12h for *L. helveticus* HA-122 (Lallemand Animal Nutrition, Blagnac) and 1.6 x 10^8 CFU per 12h for *S. boulardii* CNCM I-1079 (Lallemand Animal Nutrition, Blagnac).

5.2.4. Sampling from the CANIM-ARCOL model

Samples were collected daily in the fermentation medium (luminal medium) for further analysis of microbiota composition (qPCR and 16S Metabarcoding) and metabolic activities through SCFA measurement. Every two days, mucin beads were collected to analyze the mucus-associated microbiota (qPCR and 16S Metabarcoding). Mucin beads were washed twice in sterile sodium phosphate buffer and stored at -80°C before downstream analysis. The atmospheric phase of bioreactors was also sampled every day to follow anaerobiosis and determine gas composition and production (total volume of gas) thanks to a sampling bag connected to the condenser.

5.2.5. DNA extraction

Genomic DNA was extracted from luminal medium samples using the QIAamp Fast DNA Stool Mini Kit (Qiagen, Germany) following manufacturer's instructions with the following modifications. Prior to DNA extraction, luminal samples were centrifuged (18 000 rcf, 15 min, 4°C) and the pellets were collected. Pellets were then incubated 10 min with sterile citrate buffer (sodium citrate 55 mM and NaCl 154 mM) at 37°C, before vortexing (maximal speed, 15 sec) and centrifuged again (8000 rcf, 1 min). Then, a step of mechanical disruption using a bead beater (5 min, 20 beat/s) was made with 300 mg sterile glass beads (diameter ranging from 100 to 600 µm). Genomic DNA was extracted from around 150-200 mg of mucin beads samples using the Quick-DNA Fecal/Soil Microbe Miniprep kit (Zymo Research, Germany) following manufacturer's instructions. For both types of samples, DNA quantity was evaluated using the Qubit dsDNA Broad Range Assay Kit (Invitrogen, USA) with a Qubit 3.0 Fluorometer (Invitrogen, USA). Samples were stored at -20°C prior to microbiota analysis.

5.2.6. Quantitative PCR

Total bacteria were quantified by qPCR. Primers and hybridization temperatures are listed in **Supplementary Table V.1**. Real-time PCR assays were performed in a Biorad CFX96TM Real-Time System (Bio-Rad Laboratories, USA) using Takyon Low ROX SYBR 2X MasterMix blue dTTP kit (Eurogentec, Belgium). Each reaction was run in duplicate in a final volume of 10 µL with 5 µL of MasterMix, 0.45 µL of

each primer (10 µM), 1 µL of DNA sample and 3.1 µL of ultra-pure water. Amplifications were carried out using the following ramping profile: 1 cycle at 95°C for 5 min, followed by 40 cycles of 95°C for 30 s, at 58°C for 30 s and at 72°C for 30 s. A melting step was added to ensure primer specificity. Standard curve was generated from 10-fold dilutions of bacterial DNA (isolated from a pure culture of *Bacteroides fragilis*), allowing the calculation of DNA concentrations from samples.

5.2.7. 16S Metabarcoding and data analysis

Bacterial V3-V4 regions of 16S ribosomal DNA (rRNA) were amplified using primers described in **Supplementary Table V.1**. Amplicons were generated using a Fluidigm Access Array followed by high throughput sequencing on an Illumina MiSeq system (Illumina, USA) performed at the Carver Biotechnology Center of the University of Illinois (Urbana, USA). Prior to analysis, raw data were demultiplexed and quality filtered using 'DADA2' R-package (Callahan *et al.*, 2016). Reads with quality score under 2 were truncated. Reads under 100 pb length were removed as well as sequences similar to PhiX DNA used as a spike-in control for MiSeq runs. Filtered sequences were dereplicated and cleaned for chimeras (DADA2). Taxonomic classification of the sequences was then performed with 'DECIPHER' package (Murali *et al.*, 2018). Assignations from both SILVA 138 release (Quast *et al.*, 2013) and GTDB_bac120_arc122 (Parks *et al.*, 2022) databases were merged using the assign_taxo_fun function from rANOMALY R-package based on IDTAXA, with a 60% confidence cut-off (Theil & Rifa, 2021). A phylogenetic tree was then reconstructed using DECIPHER. Incorrect taxonomic affiliation of *Prevotella* genus in *Bacteroidaceae* family (instead of *Prevotellaceae*) was manually corrected.

5.2.8. Predicted community functional potential

The software PICRUSt2 (Phylogenetic Investigation of Communities through Reconstruction of Unobserved States) (Douglas *et al.*, 2020) was used to generate a new ASV table comprised of predicted KEGG Orthologs (KOs; Kyoto Encyclopedia of Genes and Genomes). The resultant tables were analyzed using the 'microeco' R-package by processing LEFSe analysis to identify predicted pathways that were significantly altered between control and treated (restoration strategies) conditions. Then, Mann-Whitney test were performed on pathways relative abundancies.

5.2.9. Calculation of dysbiosis index

The 'dysbiosisR' R-package (Shetty & de Steenhuijsen Piters, 2022) was used to calculate dysbiosis scores based on 16S Metabarcoding results, as previously described by AlShawaqfeh and colleagues (AlShawaqfeh *et al.*, 2017). Dysbiosis index was defined as the difference between Euclidean distance between the test sample and the healthy class centroid and the Euclidean distance between the test sample and the diseased class centroid. The 'pre-ATB' period was related to the healthy class while the 'ATB' period was the diseased one. A value of zero means that the test sample lies at equal distance from the center of both classes. Deviation of sample from eubiosis increases with dysbiosis index.

5.2.10. Gas analysis

Analysis of O_2, N_2, CO_2, CH_4, and H_2 gas produced during the fermentation process was performed using 490 micro-gas chromatography (Agilent Technologies, USA) coupled with a micro-TCD detector (Agilent Technologies, USA). Molecular Sieve 5A and Porapack Q (Agilent Technologies, USA) series columns were used. Gas composition was determined using calibration curves made from ambient air (78.09 % N_2, 20.95 % O_2, 0.04 % CO_2) and three gas mixtures A (5 % CO_2, 5 % H_2, 90 % N_2), B (20 % CO_2, 80 % H_2), and C (20 % CO_2, 20 % CH_4, 20 % H_2, 40 % N_2). Technical replicates were performed for each sample and results were expressed as percentages.

5.2.11. Short-chain fatty acids analysis

For SCFA analysis, 1.5 mL of luminal medium samples were centrifuged (18 000 rcf, 15 min, 4°C) and 900 µL of supernatant was diluted at 1/10 into H_2SO_4 0.04 M mobile phase, vortexed, and filtered (0.22 µm). The three major SCFAs (acetate, propionate, and butyrate) were quantified by high-performance liquid chromatography -HPLC- (Elite LaChrom, Merck HITACHI, USA) coupled with a DAD diode. The HPLC column (Concise Separations, ICE-99-9865) and its guard column were maintained at 50°C. Sulfuric acid 0.04 M was used as mobile phase and SCFA were separated at a flow rate of 0.6 mL/min. Data were obtained and analyzed by the EZChrom Elite software at 205 nm. SCFA concentrations were calculated from calibration curves established from known concentration solutions of acetate, propionate, and butyrate (0, 10, 25, and 40 mM) and data expressed as mM or relative percentages.

5.2.12. Statistical analysis

Statistical analyses on microbiota activity (gas and SCFA) and α-diversity indexes (number of observed ASVs and Shannon index) from metabarcoding data were processed using GraphPad Prism software version 9.4.1 (GraphPad Software, USA) and/or R software (version 4.1.2). Data normal distribution was verified by combining Anderson-Darling, D'Agostino & Pearson, Shapiro-Wilk and Kolmogorov-Smirnov tests and homoscedasticity was checked using the Fisher test. Then, appropriate statistical analysis was applied (either one-way ANOVA, t-test or Mann-Whitney test). Principal coordinate analysis (PCoA) and Redundancy analysis (RDA) based on Bray Curtis distances were calculated and significance between groups was assessed with a Permutational Multivariate Analysis of Variance (PERMANOVA) using ADONIS (999 permutations) with non-parametric tests.

5.3. Results

5.3.1. Impact of Saccharomyces boulardii CNCM I-1079 and tyndallized Lactobacillus helveticus HA-122 on antibiotic-induced dysbiosis in the CANIM-ARCOL

Impact of restoration strategies on microbiota activities and composition was first evaluated during antibiotic administration. Redox potential was followed as a global indicator of microbial fermentation activities. Antibiotics induced a regular and extensive increase (>200 mV) in redox potential during treatment period (**Suppl**. **Figure V.1a**). Compared to ATB control, SB supplementation led to a significant ($p<0.0001$) reduction in redox potential upsurge, whereas LH had no effect (**Suppl**. **Figure V.1b**). Antibiotherapy also led to an increase in H_2 and O_2, together with a decrease in CO_2 relative percentages (**Figure V.2a**). Gas profiles were not clearly impacted by SB or LH administration, and opposite trends were observed for some gases in the two donors (**Figure V.2a**). Antibiotics also induced a clear decrease in the volume of gas produced (**Figure V.2b** and **2c**). Cumulated gas production was not significantly impacted by restoration treatments (**Figure V.2b**), but SB and LH tended to decrease daily gas production, from 31.5 mL under ATB condition to 3 and 0 mL in ATB + SB and ATB + LH, respectively (**Figure V.2c**). SCFA profiles were also impacted by antibiotherapy with an increase in acetate relative percentage, while both proportions and concentrations of propionate and butyrate clearly decreased (**Figure V.3a** and **3b**). Restoration strategies had no significant impact on the three main SCFA concentrations, even if acetate levels tended to increase with LH supplementation (Figure 3b and 3d). Antibiotic treatment was associated with a clear reduction in total SCFA concentrations, from around 140 to 80 mM (**Figure V.3c**). SB impeded this drop in SCFA concentrations, but only at day 9 (**Figure V.3c**). On its side, LH allowed to maintain from day 11 a higher level in total SCFA (> 100 mM), compared to the ATB alone (around 80 mM) or treated with SB (60 mM) (**Figure V.3c**). Nevertheless, on the global period of antibiotherapy, no significant effect of restoration strategies was evidenced (**Figure V.3d**).

Regarding bacterial diversity, antibiotherapy led to a decrease in Shannon index, particularly marked at day 11, but followed before the end of treatment by a new rise (**Figure V.4a**). The two restoration strategies had no significant influence on alpha microbial diversity, as measured by both observed ASVs and Shannon index (**Figure V.4b**). Beta-diversity was also impacted by antibiotic treatment, with a clear different clustering of samples between 'pre-ATB' and 'ATB' periods, even more marked in the luminal medium (**Figure V.4c**). RDA analysis showed that both SB and LH led to a reduced dispersion of samples during antibiotherapy, both in the luminal medium and mucin beads (**Figure V.4e**). Antibiotherapy also diminished total bacterial load by around 2 Log_{10} copies/mL (**Figure V.5a** and **b**). No effect of restoration treatments was evidenced in the luminal medium while in the mucin beads, a significant drop of total bacteria was observed at day 12 for ATB + LH compared to the two other conditions (**Figure V.5a** and **b**). Interestingly, the calculated coefficient of variations during ATB treatment was lower for SB and LH compared to ATB control in both microenvironments (**Figure V.5a** and **b)**.

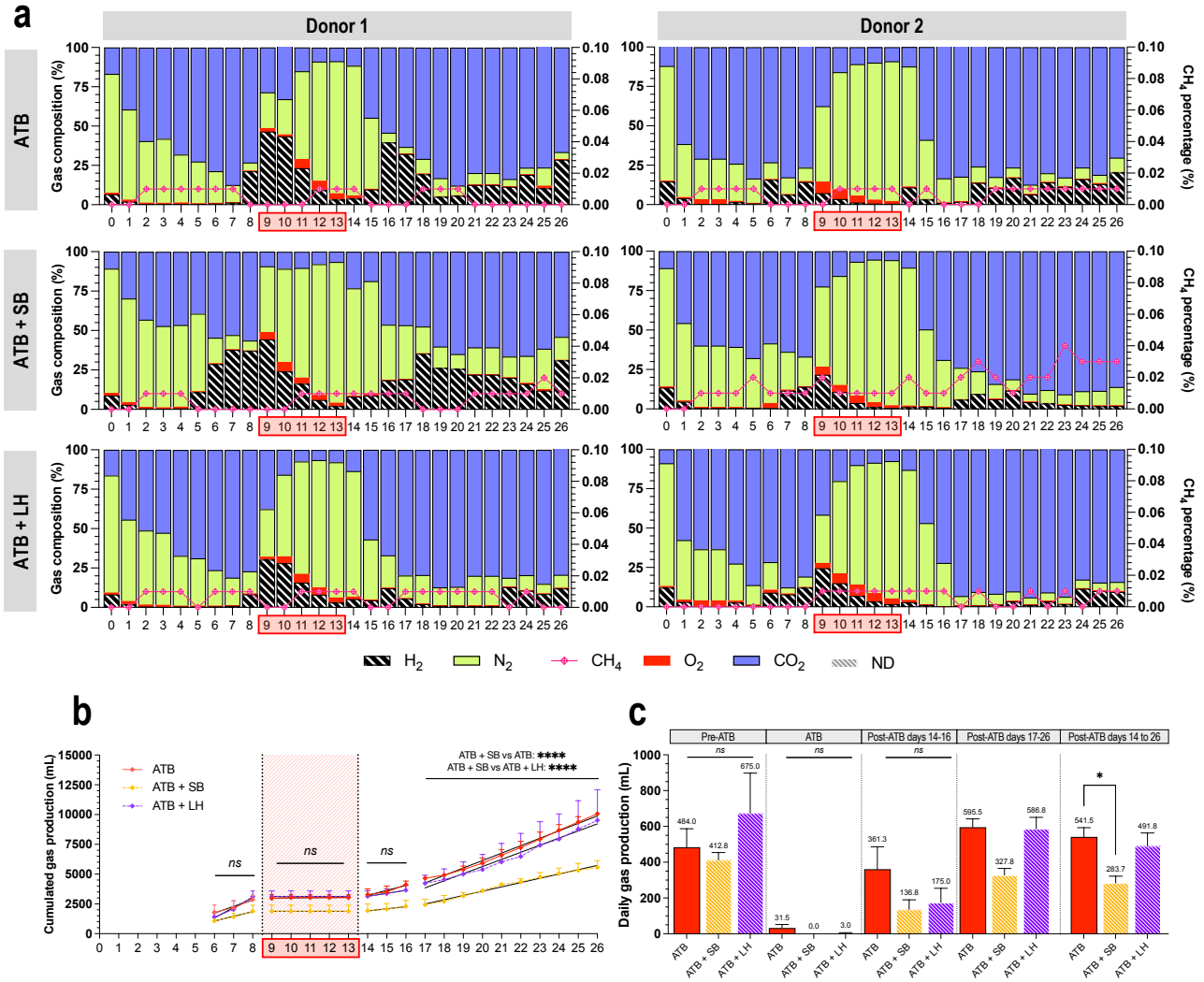

Figure V.2: Impact of *S. boulardii* and tyndallized *L. helveticus* on gas production during and after antibiotherapy. Fermentations were performed in the CANIM-ARCOL under medium dog size colonic conditions, after inoculation with stools from two dogs. Three conditions were tested: 'ATB' for the antibiotic control, 'ATB + SB' for antibiotic supplemented with CNCM I-1079 and 'ATB + LH' for antibiotic supplemented with inactivated HA-122. Samples were regularly collected to determine gas composition of the atmospheric phase and results were expressed in relative percentages for donor 1 (left) and donor 2 (right) (a). Total volume of gases produced was also measured and presented as mean cumulated production in mL (b). Linear regression was plotted for each time period (i.e. pre-ATB, ATB, post-ATB from days 14 to 16, post-ATB from days 17 to 26 and post-ATB on the overall recovery period). Average daily gas production was also represented as bar plots (c). Antibiotic treatment was symbolized by a red square or a red zone. Statistical differences are indicated by *: $p<0.05$ or ****: $p<0.0001$ (Mann-Whitney test). ns: non-significant difference ($p>0.05$). *ATB: antibiotic, LH: L. helveticus HA-122, SB: S. boulardii CNCM I-1079.*

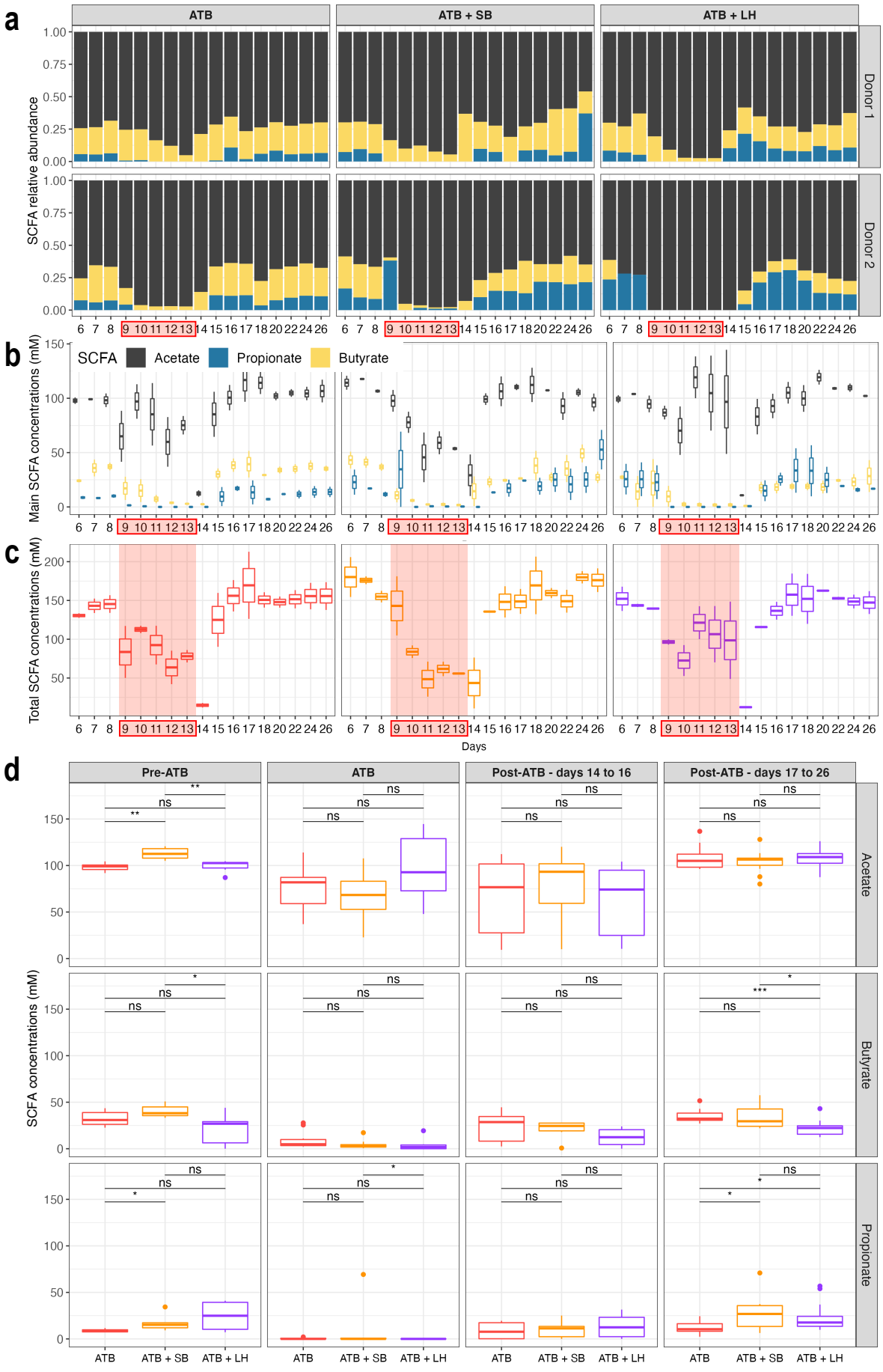
a
ATB
ATB + SB
ATB + LH
Donor 1
Donor 2
SCFA relative abundance
b
SCFA
Acetate
Propionate
Butyrate
Main SCFA concentrations (mM)
c
Total SCFA concentrations (mM)
Days
d
Pre-ATB
ATB
Post-ATB - days 14 to 16
Post-ATB - days 17 to 26
Acetate
Butyrate
Propionate
SCFA concentrations (mM)
ATB
ATB + SB
ATB + LH

II-5

Figure V.3: Impact of *S. boulardii* and tyndallized *L. helveticus* on short-chain fatty acids production during and after antibiotherapy. Samples were regularly collected from the luminal medium to determine short-chain fatty acids (SCFA) concentrations. The three main SCFA (i.e. acetate, propionate and butyrate) were measured daily throughout fermentations and results expressed in relative abundances for donor 1 (top) and donor 2 (bottom) (**a**) or given as mean concentrations in mM (**b**). Mean total SCFA concentration (mM) was daily plotted (**c**). Averaged SCFA concentrations in acetate, propionate and butyrate were given by time period and expressed as box plots (**d**). Antibiotic treatment was symbolized by a red zone or square. Statistical differences are indicated by *: $p<0.05$, **: $p<0.05$ (Mann-Whitney test), ns: non-significant difference ($p>0.05$). *ATB: antibiotic, LH: L. helveticus* HA-122*, SB: S. boulardii CNCM I-1079.*

Bacterial composition was further investigated by metabarcoding analysis (**Figure V.5c and Suppl. Figure V.2**). Antibiotics induced a bloom in *Enterobacteriaceae* in both donors in the luminal medium, mainly represented at the genus level by *Escherichia* and *Enterococcus*. *Streptococcaceae* also increased with antibiotics but only in donor 2. Perturbations in mucin beads are delayed compared to the luminal medium and characterized by a surge in *Enterobacteriaceae* in donor 1 while *Enterococcaceae* exploded in donor 2. Both SB and LH reduced *Enterobacteriaceae* relative abundance in mucin beads in donor 1 but had a less clear effect in the luminal medium, except for SB in donor 2. The two restoration strategies led to a decrease in *Enterococcaceae* and *Streptococcaceae*, but this effect was donor-dependent (only in donor 2). On the contrary, SB and LH resulted in an increase in *Lactobacillaceae* in both luminal medium and mucin beads of donor 2. SB treatment also allowed to maintain *Clostridiaceae* fraction in donor 1. Dysbiosis indexes clearly increased with antibiotherapy, with a more marked effect in the luminal medium compared to mucin beads (**Figure V.6a** and **6b**). These scores tended to be higher in the luminal medium under ATB + SB and ATB + LH conditions compared to the ATB control but associated with a strong reduction in variability (**Figure V.6a**). However, on the global period of antibiotic treatment, SB and LH had no significant effect of dysbiosis scores (**Figure V.6b**). Lastly, antibiotics had significant impacts on many metabolic pathways as predicted by PICRUSt2 (**Suppl**. **Figure V.3**) but only one related to 'norspermidine biosynthesis' was increased when LH was added (**Figure V.7a**).

5.3.1. Effects of Saccharomyces boulardii CNCM I-1079 and tyndallized Lactobacillus helveticus HA-122 on the kinetic of microbiota recovery after antibiotherapy

The effects of restoration strategies on the kinetic of microbiota recovery was evaluated on days 14 to 16 post-ATB administration where most of changes were observed. As soon as antibiotics were no more administered, redox potential sharply decreased to join baseline values at day 16 (**Suppl**. **Figure V.1a**). Such return to stabilized values was reached two days before with SB, while LH seemed to have no major effect (**Suppl**. **Figure V.1a**). However, when data are averaged on days 14-16, significant ($p<0.0001$) lower redox potential was measured with both treatments (**Suppl**. **Figure V.1b**).

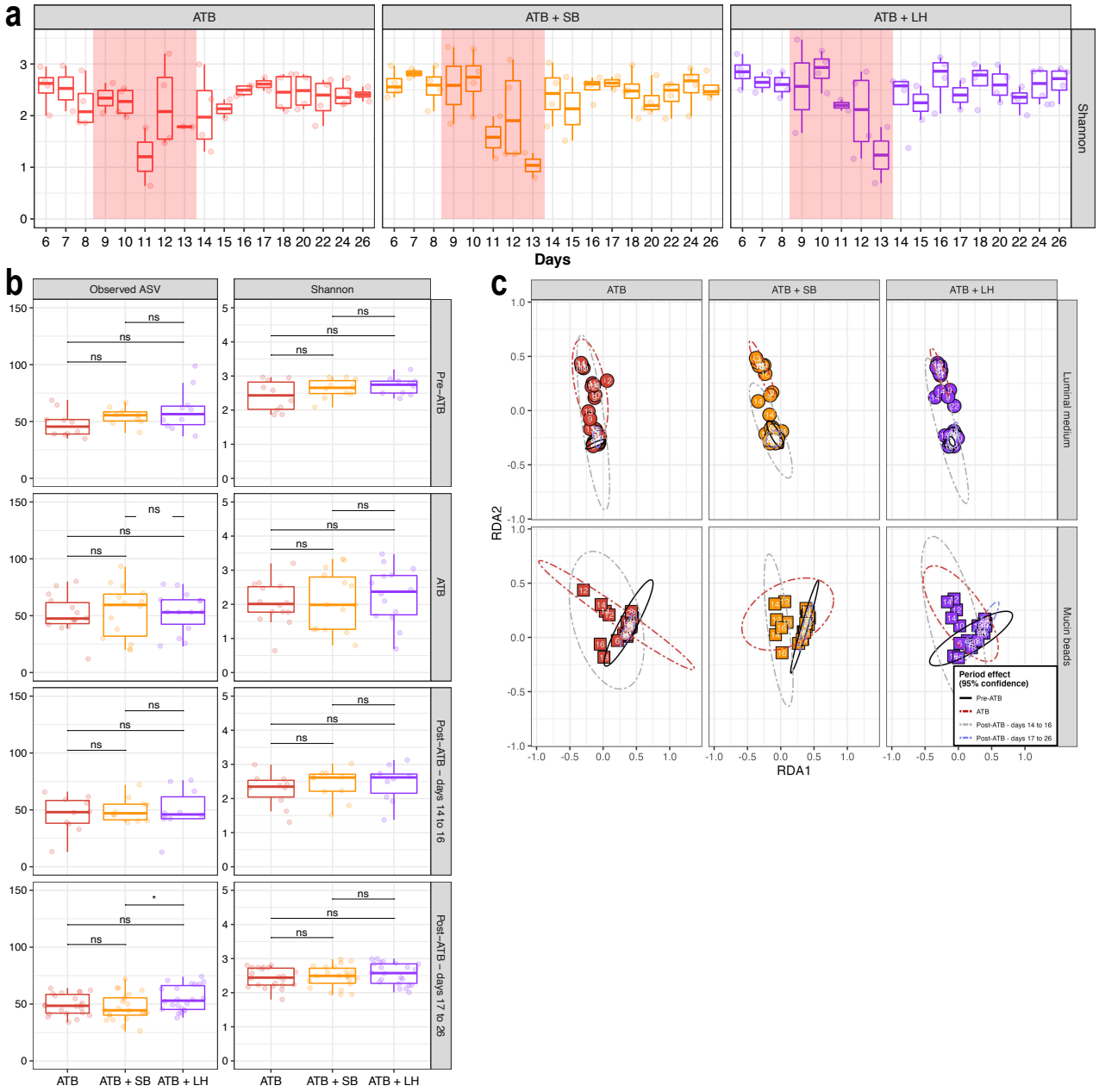

Figure V.4: Impact of S. boulardii and tyndallized L. helveticus on canine microbial diversity during and after antibiotherapy. Lumen and mucus-associated microbiota composition was analyzed by 16S Metabarcoding and diversity indexes were calculated based on ASV table. Alpha-diversity indexes (observed ASVs and/or Shannon) were calculated and represented as box plots, either daily (a) or on each time period (b), when data were averaged on luminal medium and mucin beads. Redundancy analysis (RDA) based on Bray-Curtis distances without donor effect revealed significant effects of time (c, $p<0.001$) and treatment ($p<0.001$). Antibiotic treatment was symbolized by a red zone. Significant differences based on Kruskal-Wallis test are given at *: $p<0.05$, ns: non-significant difference ($p>0.05$). ATB: antibiotic condition, LH: *L. helveticus* HA-122, SB: *S. boulardii*.

Regarding gas composition, time to return to baseline (i.e., stabilized period from days 6 to 8) varied depending on gases and donors. Percentages of H_2 remained fluctuant depending on time and donors. With regards to CO_2 which was more stable, under ATB conditions, recovery was achieved at day 18, while it seemed to be earlier with SB (day 16) and LH (days 16-17) for both donors (**Figure V.2a**). Lastly, O_2 percentages lower

than 2% were recovered whatever the conditions around day 14. In addition, no significant impact of SB or LH was observed regarding cumulated (**Figure V.2b**) and daily (**Figure V.2c**) gas production, even if lower values were found under ATB + SB (137 mL) and ATB + LH (175 mL) conditions compared to ATB control (361 mL). Besides, the two treatments led to similar kinetic of restoration of SCFA profiles and concentrations than the ATB control (**Figure V.3a** and **3b**), especially with propionate resurgence (which completely disappeared during antibiotherapy period) around day 15 whatever the conditions. Similarly, return to baseline total SCFA concentrations was not impacted by SB and LH (**Figure V.3c**). When considering the overall 14-16 days period (**Figure V.3d**), no significant difference was noticed between ATB control and treated conditions.

Regarding microbiota diversity, Shannon index turned back to baseline, i.e. around 2.5 (days 6-8), within three days under ATB control (day 16) while it was earlier (day 14) for LH and SB (**Figure V.4a**). Nevertheless, on the global 14-16 days period, no significant difference raised between the three conditions (**Figure V.4b**). As observed during antibiotherapy period, dispersion in beta-diversity was reduced with SB supplementation compared to ATB control and LH, in both luminal medium and mucin beads (**Figure V.4c**). As for diversity, return to total bacteria baseline in the luminal medium occurred two days earlier when SB and LH was added compared to non-supplemented condition (day 15 *versus* day 17) (**Figure V.5a**). However, whatever the time point, bacterial load was not significantly impacted by treatment in the luminal compartment, certainly due to the high variability observed under ATB condition. In mucin beads, recovery of total bacteria was observed at day 16 for ATB and ATB + LH but was never reached during this time period for SB (**Figure V.5b**), in accordance with a significantly ($p<0.05$) lower bacterial load (**Figure V.5b**). Interestingly, coefficients of variation (around 15 % in luminal medium and 11% in mucin beads) were still high for ATB on days 14-16, while they harshly decreased with SB, and even more LH supplementation (up to 7.6 and 4 % for SB and LH, respectively). Recovery of microbiota profiles in the luminal medium was markedly impacted by the two restoration strategies, particularly at day 14 (**Figure V.5c**). At this time point, both SB and LH counteracted the bloom of *Enterobacteriaceae* induced by antibiotherapy treatment in both donors (relative abundance of around 5 % and 35 %, respectively for SB and LH, compared to 80 % in ATB bioreactor). For donor 1, microbiota profiles were remarkably similar to the baseline from day 15 with SB and LH supplementation. In both donors, the two restoration strategies supported a better recovery of populations such as *Burkholderiaceae* and *Clostridiaceae* than the ATB control. Effect of SB and LH on microbial shift was less obvious on mucin beads. The most striking effect was probably the reduction of *Enterococcaceae* with SB and LH at day 14 for donor 2. This effect, which was not observed for LH in donor 1, seemed to be individual dependent.

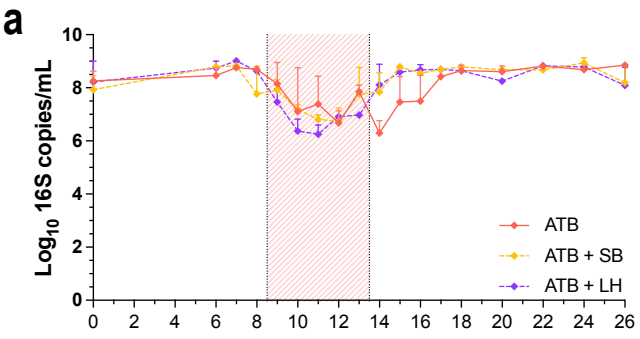

Coefficient of variation	ATB	Post-ATB days 14-16
ATB	15.6 %	15.4 %
ATB + SB	10.5 %	7.6 %
ATB + LH	8.7 %	7.0 %

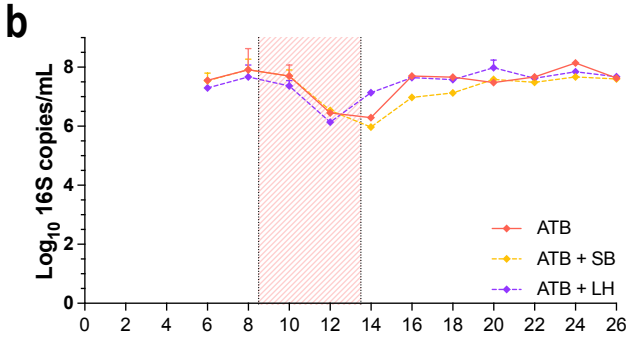

Coefficient of variation	ATB	Post-ATB days 14-16
ATB	11.0 %	11.6 %
ATB + SB	9.7 %	9.0 %
ATB + LH	10.7 %	4.0 %

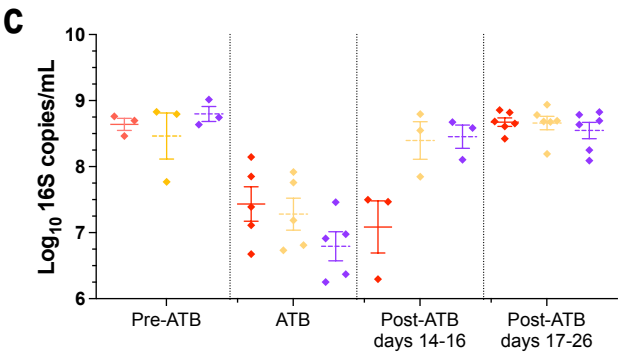

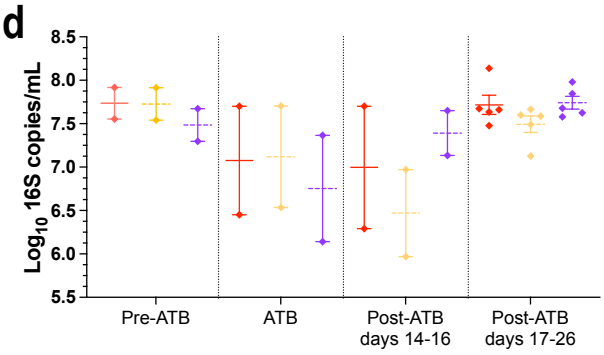

ATB ATB + SB ATB + LH

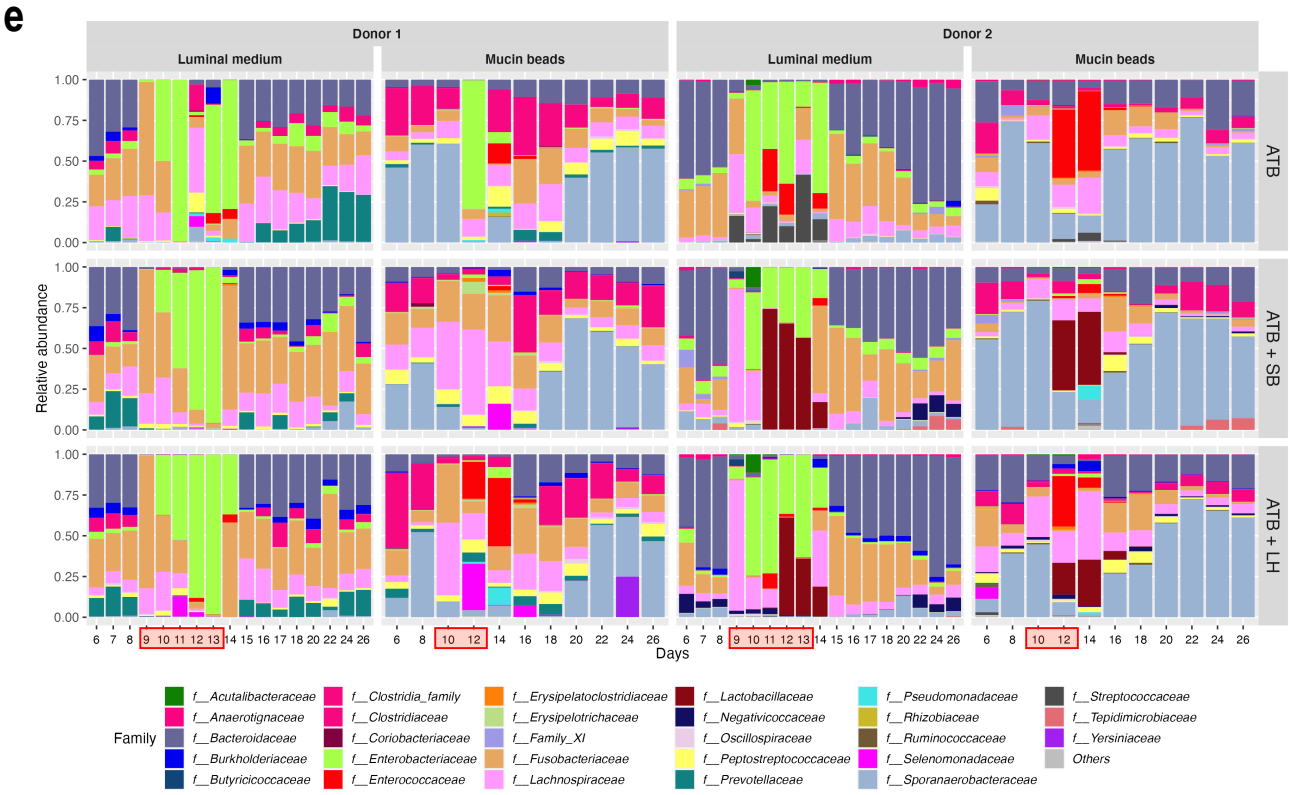

Figure V.5: Impact of *S. boulardii* and tyndallized *L. helveticus* on canine bacterial microbiota at the family level during and after antibiotherapy. Lumen and mucus-associated microbiota composition was analyzed by 16S qPCR and 16S Metabarcoding. Total bacteria load was quantified and expressed as Log_{10} 16S copies/g in the luminal medium (**a, c**) and mucin beads (**b, d**) for each day (**a, b**) or average per period (**c, d**). Coefficient of variations were calculated during antibiotic treatment and in the post-ATB phase (day 14 to 16), on both luminal medium and mucin beads (**a**, table) and results were given as percentages (**b**, table). Relative abundances of the main families in both colonic microenvironments are given for both donors (**e**). Antibiotic treatment was symbolized by a red square or a red zone. Significant differences based on 2-way Anova are given at *: $p<0.05$ and **: $p<0.01$, ns: non-significant difference ($p>0.05$). ATB: antibiotic, LH: *L. helveticus* HA-122, SB: *S. boulardii*.

This effect of treatments was further confirmed by analysis of dysbiosis scores (**Figure V.6a**). In the luminal medium only, lower values were observed with SB and LH compared to ATB control on both days 14 and 15 (e. g. at day 14, dysbiosis scores were 0.14, 0.17 and 0.25, for ATB+SB, ATB+LH and ATB, respectively). This was supported by a significant ($p<0.01$) difference between pre-ATB and post-ATB (days 14-16) under ATB condition in the luminal compartment, which was no more found with SB and LH (**Figure V.6c**). When results were analyzed on the global 14-16 days, no significant difference was observed between the three conditions (**Figure V.6b**), even if dysbiosis indexes clearly tended to be lower with treatments. Lastly, LH, and even more SB, allowed on the 14-16 days period a better recovery of predicted functional metabolic profiles compared to ATB alone in the luminal phase, but not in the mucin beads (**Figure V.7c**).

4.3.4. Impact of Saccharomyces boulardii CNCM I-1079 and tyndallized Lactobacillus helveticus HA-122 on the new microbial balance reached after restoration

The impact of restoration strategies was finally evaluated on the last time period (i.e. days 17-26), where a new balance was reached. Over the 17-26 days period, redox potential remained significantly higher ($p<0.0001$) with LH supplementation compared to ATB control and SB treatment (**Suppl**. **Figure V.1b**). On this same period, gas profiles were still not really similar to that observed before antibiotherapy, especially regarding the H_2 fraction, whatever treatment and donor (**Figure V.2a**). In addition, a significant lower cumulated gas production was observed with SB compared to the two other conditions ($p<0.0001$, **Figure V.2b**). Daily gas production with SB (328 mL/day) was also lower than that measured for ATB control (596 mL/day, $p<0.05$) and LH treatment (587 mL/day) (**Figure V.2c**). At the end of experiment, SCFA profiles returned to baseline for ATB control, but this is less obvious with SB and LH treatments which seemed to be associated to an increase in propionate fraction (**Figure V.3a**). Total SCFA concentrations at the end of fermentation were fully in line with those measured in the stabilized pre-ATB phase for all conditions (**Figure V.3c**). Over the 17-26 days, a higher concentration in butyrate and propionate was noticed under SB condition, together with a lower concentration in butyrate with LH (Figure 3d). Importantly, those differences were already observed in the pre-ATB phase.

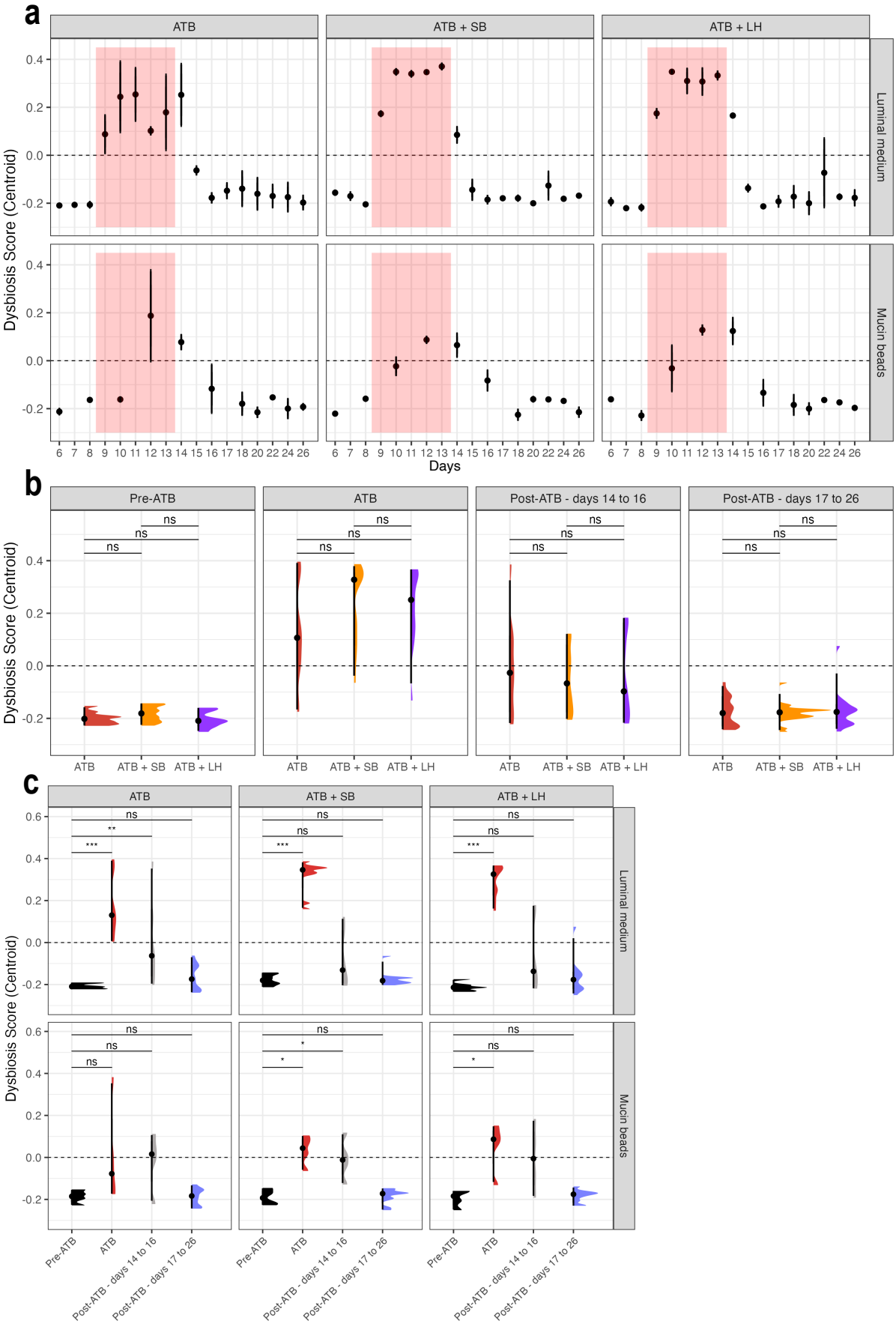
a
ATB
ATB + SB
ATB + LH
Luminal medium
Mucin beads
Dysbiosis Score (Centroid)
Days
b
Pre-ATB
ATB
Post-ATB - days 14 to 16
Post-ATB - days 17 to 26
ns
c
Pre-ATB
ATB
Post-ATB - days 14 to 16
Post-ATB - days 17 to 26

II-5

Figure V.6: Impact of antibiotherapy and *S. boulardii* or tyndallized *L. helveticus* on dysbiosis index in the CANIM-ARCOL. A dysbiosis score was calculated based on 16S Metabarcoding results in both the luminal medium and mucin beads, based on AlShawaqfeh and colleagues' method. For each condition tested ('ATB' for the antibiotic control, 'ATB + SB' for antibiotic supplemented with CNCM I-1079 and 'ATB + LH' for antibiotic supplemented with inactivated HA-122), dysbiosis indexes were daily plotted (a) in both the luminal medium (top) and mucin beads (bottom). The effect of treatments on dysbiosis scores was also calculated on each time-period when samples from the two microenvironments are gathered (b). Results were also given for each time-period (c). Antibiotic treatment period was symbolized by a red square and a red zone. Statistical differences are indicated by *: $p<0.05$, **: $p<0.01$ and ***: $p<0.001$ (Mann-Whitney test). *ns: non-significant difference ($p>0.05$). ATB: antibiotic, LH: L. helveticus HA-122, SB: S. boulardii CNCM I-1079.*

Regarding alpha-diversity, Shannon indexes were similar before antibiotherapy treatment and at the end of experiments for all conditions (**Figure V.4a**) and no significant difference was observed between treatments over the 17-26-day period (**Figure V.4b**). Notably, observed ASVs number was significantly higher under LH condition compared to SB one on this time period (**Figure V.4b**). Beta-diversity analysis also revealed very good microbial resilience for each condition, with concentrical ellipses for pre-ATB and post-ATB (days 17-26) samples, in both luminal medium and mucins beads (**Figure V.4e**). Similarly, total bacterial load returned to baseline at the end of the experiment for each condition, whatever the colonic microenvironment (**Figure V.5a** and **5b**). Regarding bacterial composition, at the end of the period of resilience, very similar profiles were observed compared to stabilized phase in mucin beads, but not in luminal samples (**Figure V.5c**). In donor 1, compared to baseline (day 8), an increase in *Prevotellaceae* relative abundance was observed in the luminal medium, while *Bacteroidaceae* decreased and *Burkholderiaceae* disappeared. In donor 2, *Anaerotignaceae* and *Sporanaerobacteraceae* percentages increased, while *Fusobacteriaceae* decreased. When SB was added, we also observed a good resilience of bacterial profiles in mucin beads and in the luminal medium of donor 1, but populations clearly differed in donor 2 between recovery and baseline (days 6-8). In addition, compared to ATB control, SB led to a reduction in *Prevotellaceae* abundance and maintained populations such as *Burkholderiaceae*. Of interest, in both donors, LH supplementation allowed to restore at days 22-26 bacterial profiles very closed to those observed before antibiotherapy period in the luminal medium and mucin beads. Over the 17-26 days, dysbiosis indexes returned to baseline, i.e. an "eubiosis" state (<0), whatever the treatment and microenvironment **(Figure V.6a** and **6c**), with no significant difference between the three conditions (**Figure V.6b**).

Finally, Picrust2 analysis was performed on days 14-26 to assess the effect of restoration strategies on predicted metabolic pathways (**Figure V.7**). PCoA analysis revealed that antibiotherapy treatment still modified predicted pathways on days 17-26, particularly in mucin beads (Figure 7c). A slight better resilience can be observed with SB and LH in the luminal medium. Over 14-26 days, 23 metabolic pathways were still differentially expressed between the three conditions (**Figure V.7b**). Most of pathways activated under ATB control condition were decreased by both restoration strategies (13 over 23).

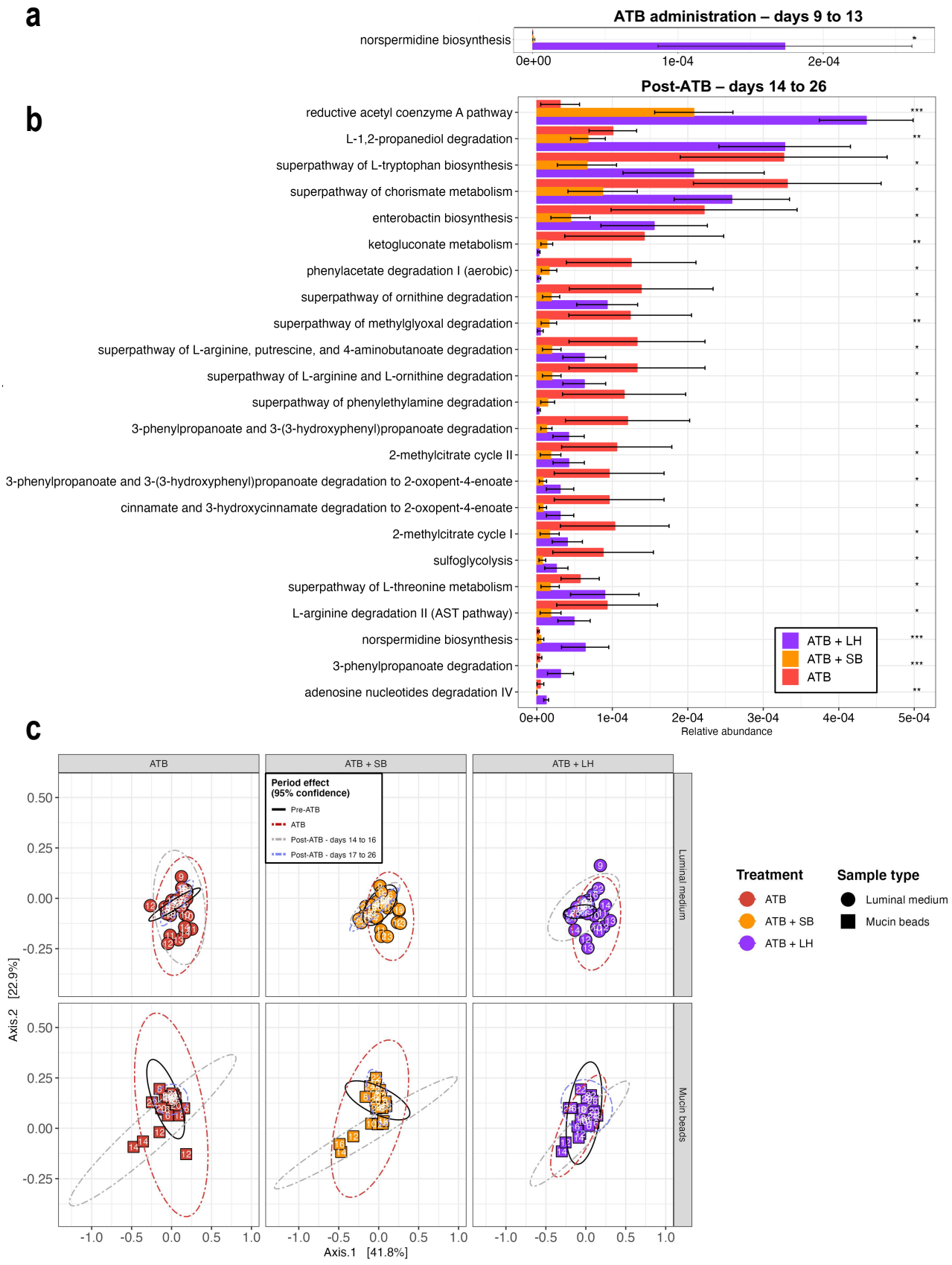
a
ATB administration – days 9 to 13
norspermidine biosynthesis
0e+00
1e-04
2e-04
b
Post-ATB – days 14 to 26
reductive acetyl coenzyme A pathway
L-1,2-propanediol degradation
superpathway of L-tryptophan biosynthesis
superpathway of chorismate metabolism
enterobactin biosynthesis
ketogluconate metabolism
phenylacetate degradation I (aerobic)
superpathway of ornithine degradation
superpathway of methylglyoxal degradation
superpathway of L-arginine, putrescine, and 4-aminobutanoate degradation
superpathway of L-arginine and L-ornithine degradation
superpathway of phenylethylamine degradation
3-phenylpropanoate and 3-(3-hydroxyphenyl)propanoate degradation
2-methylcitrate cycle II
3-phenylpropanoate and 3-(3-hydroxyphenyl)propanoate degradation to 2-oxopent-4-enoate
cinnamate and 3-hydroxycinnamate degradation to 2-oxopent-4-enoate
2-methylcitrate cycle I
sulfoglycolysis
superpathway of L-threonine metabolism
L-arginine degradation II (AST pathway)
norspermidine biosynthesis
3-phenylpropanoate degradation
adenosine nucleotides degradation IV
ATB + LH
ATB + SB
ATB
0e+00
1e-04
2e-04
3e-04
4e-04
5e-04
Relative abundance
c
ATB
ATB + SB
ATB + LH
Period effect
(95% confidence)
Pre-ATB
ATB
Post-ATB - days 14 to 16
Post-ATB - days 17 to 26
Luminal medium
Mucin beads
Axis.2 [22.9%]
Axis.1 [41.8%]
Treatment
ATB
ATB + SB
ATB + LH
Sample type
Luminal medium
Mucin beads

II-5

Figure V.7: Impact of antibiotics and pro- or postbiotic supplementation on functional pathway predictions during and after antibiotherapy. PICRUSt2 software was used to predict bacterial metabolic pathways from 16S Metabarcoding data. LEFSe analysis was then performed to evidence significant differentially expressed pathways. Relative abundances of those pathways are plotted for ATB (red), ATB + SB (orange) and ATB + LH (purple) during antibiotic administration from day 9 to 13 (**a**) and after antibiotic treatment from day 14 to 26 (**b**). PCoA based on Bray-Curtis distances calculated on samples from days 6 to 26 showed effect of time period (c) on predicted metabolic profiles. Statistical differences are indicated by *: $p<0.05$, **: $p<0.01$ and ***: $p<0.001$ (Kruskal-Wallis test). *ATB: antibiotic, LH: L. helveticus HA-122, SB: S. boulardii CNCM I-1079.*

This effect was particularly marked for SB on 8 pathways, such as 'chorismate pathway', 'enterobactin biosynthesis', 'superpathway of L-tryptophan biosynthesis' and 'superpathway of ornithine degradation'. On its side, LH particularly diminished 'superpathway of phenylethylamine degradation', 'ketogluconate metabolism' and "phenylacetate degradation'. Contrarily, some pathways were increased by LH and SB compared to ATB control, like 'reductive acetyl coenzyme A pathway', 'norspermidine biosynthesis' and 'L-1,2 propanediol degradation'. Finally, two pathways were activated by LH but decreased by SB, namely 'superpathway of L-threonine metabolism' and 'adenosine nucleotides degradation IV'.

5.4. Discussion

In the present study, we showed for the first time the restoration capacities of the probiotic live yeast *Saccharomyces boulardii* CNCM I-1079 and the heat-inactivated bacteria *Lactobacillus helveticus* HA-122 after antibiotic disturbance in an *in vitro* model of the canine large intestine (Deschamps *et al.* 2023c). Widely and extensive use of antibiotics in pets is a major concern for both humans and pets' health. Indeed, the use of antibiotics may lead to microbial dysbiosis by depleting the gut microbiota of numerous bacterial species and result in adverse gastrointestinal effects. Also, long-term exposure to antibiotics can increase the risk of metabolic diseases and lipid-metabolism disorders in adults while predisposing young animals to obesity (Wang *et al.*, 2018). Consistency in dogs, sub-therapeutic antibiotic dosages may cause the increase of relative abundance of taxa involved in sugar metabolism, suggesting a link with weight gain (Rochegüe *et al.*, 2021). Microbiota obviously exert a critical role in all those negative effects. Therefore, it is of outmost importance to characterize its resilience, defined as the property of an ecosystem to resist changes under stress or to recover from the perturbations quickly and fully (Ingrisch & Bahn, 2018). More precisely, the capacity of the system to persist during the impact is the resistance while the capacity to return to baseline after the disturbance is the recovery, both notions determining overall resilience (Dogra *et al.*, 2020).

The microbiota resilience after an antibiotic challenge could be improved by relevant nutritional strategies. Among those strategies, the supplementation with pro- or post-biotics during and after the antibiotherapy period deserves attention (Whittemore *et al.*, 2019; Pignataro *et al.*, 2021). We first checked that before antibiotic treatment (end of stabilization phase), most of the parameters monitored (except the microbiota composition due to donor effect), were similar between the different conditions, i.e. gas production, redox potential, microbial alpha- and beta-diversity, dysbiosis scores and total bacterial load. We were therefore able to monitor the true impact of our nutritional strategies on the canine microbiota resilience after antibiotic

challenge. As anticipated, antibiotherapy with metronidazole/enrofloxacin resulted in a decrease of bacterial load and fermentation activities characterized by a sharp drop of gas production and total SCFA concentrations, associated with a rise in redox potential. In addition, we achieved to create a dysbiosis status mostly in the luminal medium as confirmed by the dysbiosis score (AlShawaqfeh *et al.*, 2017) and the bloom of facultative anaerobes like *Enterobacteriaceae*, *Enterococcaceae* and *Streptococcaceae*. Since hosts' cells are not present in our *in vitro* model, those results suggest that gut microbiota alone can drive redox potential evolution in the colonic ecosystem, in agreement with the results previously obtained in fecal samples from mice and humans (Reese *et al.*, 2018). The pre-cited bacteria are able to use a broad range of electron acceptors for respiration and efficiently consume residual substrates associated to bacterial depletion, conferring them a strong competitive advantage in case of antibiotherapy. Besides, antibiotic supplementation led to the activation of metabolic pathways ($p=0.104$) related to antibiotic resistance (beta-lactam resistance) and mevalonate metabolism. The first pathway is directly related to the bloom of Gram-negative *Enterobacteriaceae*, while the second is linked to Gram-positive cocci bacteria, notably *Streptococcus* and *Enterococcus*. The end-products of mevalonate pathway include the lipid carrier undecaprenol involved in cell wall biosynthesis, as well as menaquinones and ubiquinones implicated in electron transport (Wilding *et al.*, 2000). These molecules may confer a competitive advantage to bacteria in the context of antibiotic treatment, in line with the drop in their relative abundances.

During antibiotic treatment, we observed beneficial effects of the postbiotic *L. helveticus* HA-122 on microbiota's resistance, notably a greater microbiota stabilization as shown by a reduced coefficient of variation for bacterial load. This might allow a quicker recovery after disturbance. In addition, even if the dysbiosis score was not improved by LH, in donor 2, the heat-inactivated bacteria reduced the bloom of *Enterobacteriaceae* and *Enterococcaceae* to the benefit of *Lactobacillaceae* or *Lachnospiraceae*. In donor 1, the transient increase in *Enterobacteriaceae* observed in mucin beads with the antibiotic alone was suppressed by LH supplementation. LH treatment also tended to preserve acetate production and induced the norspermidine pathway. Acetate production may result from the activity of heterofermentative bacteria from *Lactobacillaceae*, which relative abundance increased with LH. Acetate is known to exhibit anti-microbial effect, and a recent study showed that a diet-inducing acetate production in the mice gut may protect against enteric infection (Yap *et al.*, 2021). Norspermidine induced the suppression and disassembly of biofilms made by clinical or commensal strains like *E. coli* (Sun *et al.*, 2019). When SB was added to the fermenters, similar effects as those obtained with LH were observed on bacterial composition. In terms of function, the yeast led to a significant decrease in redox potential during antibiotic supplementation. Similar effect of the live yeast was already observed in the M-ARCOL model set-up under piglet colonic conditions during perturbation associated to feed deprivation in the weaning phase (Gresse *et al.*, 2021d).

The most notable effects of the two restoration strategies were obtained within two days after antibiotic treatment, highlighting their potential to support microbiota recovery. Of note, SB and LH supplementation led in the luminal medium to lower redox potential and dysbiosis scores compared to antibiotic alone, together with a higher bacterial load of around 1.5 Log_{10} copies/mL. At day 14, with LH and SB, the bloom of

Enterobacteriaceae associated to antibiotics almost disappeared, while the abundance of *Fusobacteriaceae*, a family considered as reflecting a healthy gut microbiota in dogs, increased (Pilla & Suchodolski, 2020). SB and LH also allowed a clearer recovery of bacterial profiles after day 16 compared to the antibiotic control. Besides, putative functions based on PICRUSt analysis differed between the three groups during the post-antibiotic period, with an activation of the reductive acetyl coenzyme A pathway (with SB and LH) involved in the production of acetate and butyrate (Shen *et al.*, 2021), of propanediol degradation (LH -typical of *Lactobacillaceae* heterofermentative activity) and adenosine nucleotide degradation (SB). Interestingly, addition of SB and LH also downregulated the chorismate metabolism pathway, which was recently pinpointed as a promising target for new antimicrobial solutions (Sadaka *et al.*, 2018) since it is a biochemical node to produce enterobacterin, aromatic amino acids, folate, vitamins E and K, and coenzyme Q. This result is consistent with the putative downregulation of the enterobactin and tryptophan biosynthesis pathways. Another interesting metabolic pathway downregulated by the supplementation with SB and LH was the cinnamate (or 3-phenypropanoate) pathway, typical from certain Gram-negative bacteria including *Enterobacteriaceae* and related to protein putrefaction. SB and LH also repressed the arginine/ornithine/putrescine pathway, involved in bacterial acid resistance system in *E. coli* and *Enterococcus* (Tofalo, Cocchi & Suzzi, 2019). Knowing the limitations of PICRUSt analysis, our very encouraging results should be confirmed using metabolomics analysis targeting some valuable metabolites from these key pathways.

Efficacy of live *S. boulardii* in mitigating antibiotic-induced microbiota changes and reducing antibiotic-associated diarrhea has already been shown in humans (Moré & Swidsinski, 2015; Kabbani *et al.*, 2017). Its use in dogs is much more recent but few studies yet suggested the great potential of this live probiotic in animals suffering from chronic enteropathies (D'Angelo *et al.*, 2018) and in healthy dogs receiving lincomycin antibiotic (Aktas, Borku & Ozkanlar, 2007). More recently, it was shown that *S. boulardii* CNCM I-1079 induced a better microbiota resilience in gestating and lactating bitches at whelping and a modulation of puppies' microbiota. This effect seemed to be mediated by an increase of *Lactobacillaceae* involved in milk degradation, while potential pathobionts from *Enterobacteriaceae* decreased (Garrigues *et al.*, 2022b). Properties of *S. boulardii* can be related to different direct or indirect modes of action, such as antimicrobial properties, pathogen exclusion, immune modulation and trophic effects (Pais *et al.*, 2020). In our study, *S. boulardii* seemed to act by creating a favorable growth environment (e.g. restoration of redox potential) for beneficial intestinal microbiota subjected to antibiotic challenge, improving its resilience. The use of postbiotic inactivated bacteria is much more recent and less documented, especially in canine species, with only two studies on *Lactobacilli* (Spears *et al.*, 2016; Panasevich *et al.*, 2021). The main mechanisms of action claimed for inactivated bacteria implies a crosstalk between cell wall components and host epithelial cells (Teame *et al.*, 2020). In a zebrafish model, inactivated *L. helveticus* HA-122 strengthened gut barrier by promoting goblet cells, stimulating innate humoral defenses and increasing the number of innate immune cells in the intestinal submucosa (Rawling *et al.*, 2022). Of interest, in the present study, we demonstrated for the first time a direct effect of inactivated *L. helveticus* HA-122 on gut microbiota since the CANIM-ARCOL model is devoid of epithelial cells. Co-aggregation with pathobionts could be one of the mechanisms involved, although not the only one (Holz *et al.*,

2015; Aiba *et al.*, 2017). In another study, lipoteichoic acid from inactivated *Lactobacillus plantarum* inhibited *Streptococcus mutans* biofilm formation through suppression of exopolysaccharides production (Ahn *et al.*, 2018). In accordance to the strong upregulation of norspermidine biosynthesis pathway observed in our *in vitro* study, norspermidine was able to alter *quorum* sensing gene expression in *S. mutans*, inhibiting biofilm formation (Ou & Ling, 2017). To further understand LH mechanisms of action, next steps will include cell wall characterization.

Interestingly, although we observed specific microbial composition associated to each donor prior the antibiotic challenge, both nutritional strategies resulted in similar recovery effects after antibiotherapy, with notably the quicker restoration of the microbiota. This was fully in lines with an increasing number of studies highlighted interindividual variability in extent and direction of microbiota response to perturbations, which has been attributed to the unique characteristics of each microbiome. Altogether, such information also emphasizes the necessity to follow the evolution microbiota profile of each individual to optimize the use of nutritional solutions applicable by the pet industry, and answer to specific needs associated to each animal. In an original way, our results demonstrated for the first time that the live yeast *S. boulardii* CNCM I-1079 and the postbiotic heat-inactivated *L. helveticus* HA-122 act as canine gut microbiota stabilizers after antibiotherapy *in vitro*. From a translational perspective, their ability to improve resistance during antibiotic perturbation and allow quicker restoration of microbial equilibrium would offer significant benefits to the host. For further mechanistic insights and integration of host-microbiota interactions, the CANIM-ARCOL could be coupled to canine intestinal cells, as previously done under piglet conditions (Gresse *et al.*, 2021b, 2021c). In a near future, the potential of our *in vitro* approach could be extended to the simulation of diseased situations (e.g. infection with enteric pathogens) or mimicking individual sub-groups differing by their sizes, ages or breeds.

5.5. Supplementary figures and tables

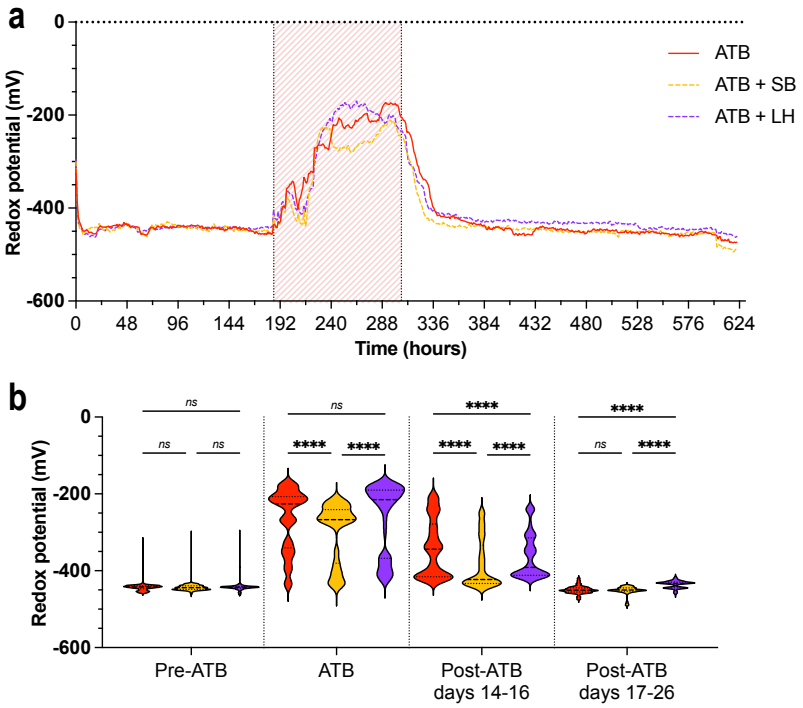

Supplementary figure V.1: Impact of antibiotics and restoration strategies on redox potential in the CANIM-ARCOL model. Fermentations were performed in the CANIM-ARCOL under medium dog size colonic conditions, after inoculation with stools from two dogs. Three conditions were tested: 'ATB' for the antibiotic control, 'ATB + SB' for antibiotic supplemented with CNCM I-1079 and 'ATB + LH' for antibiotic supplemented with inactivated HA-122. Redox potential (in mV) was averaged for both donors and plotted every six minutes (a). Results were also given for each time period to compare the effect of treatments (b). Antibiotic treatment was symbolized by a red zone. Statistical differences are indicated by ****: $p<0.0001$ (1-way Anova). *ATB: antibiotic, LH: L. helveticus HA-122, SB: S. boulardii CNCM I-1079.*

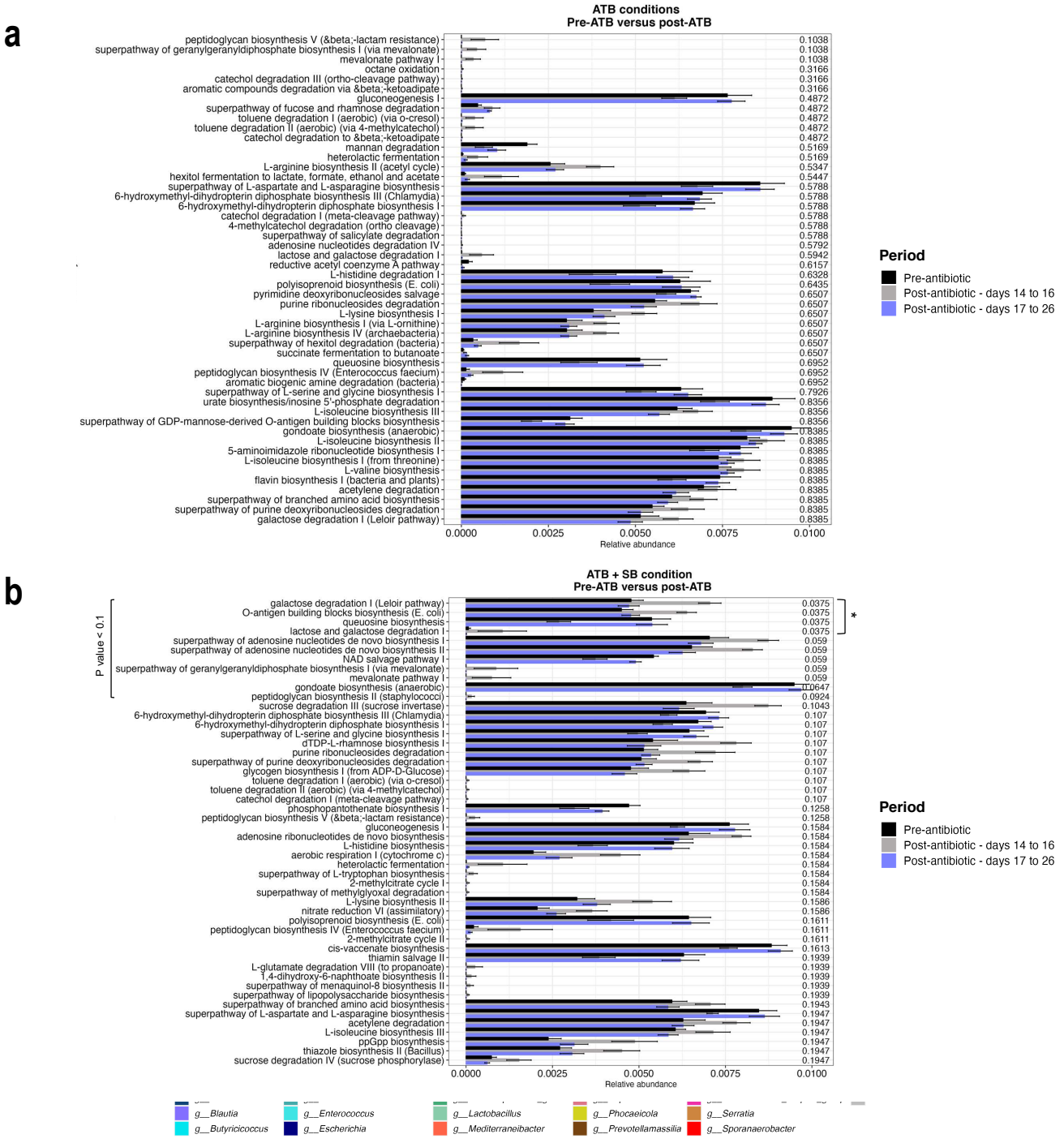

Supplementary figure V.2: Impact of *S. boulardii* and tyndallized *L. helveticus* on canine bacterial microbiota at the phylum and genus levels during and after antibiotherapy. Fermentations were performed in the CANIM-ARCOL under medium dog size colonic conditions, after inoculation with stools from two dogs. Three conditions were tested: 'ATB' for the antibiotic control, 'ATB + SB' for antibiotic supplemented with CNCM I-1079 and 'ATB + LH' for antibiotic supplemented with inactivated HA-122. Lumen and mucus-associated microbiota composition was analyzed by 16S Metabarcoding. Relative abundances of the main phyla and genus in both colonic microenvironments are given in (a) and (b), respectively. Antibiotic treatment was symbolized by a red square and red zone. *ATB: antibiotic, LH: L. helveticus HA-122, SB: S. boulardii CNCM I-1079.*

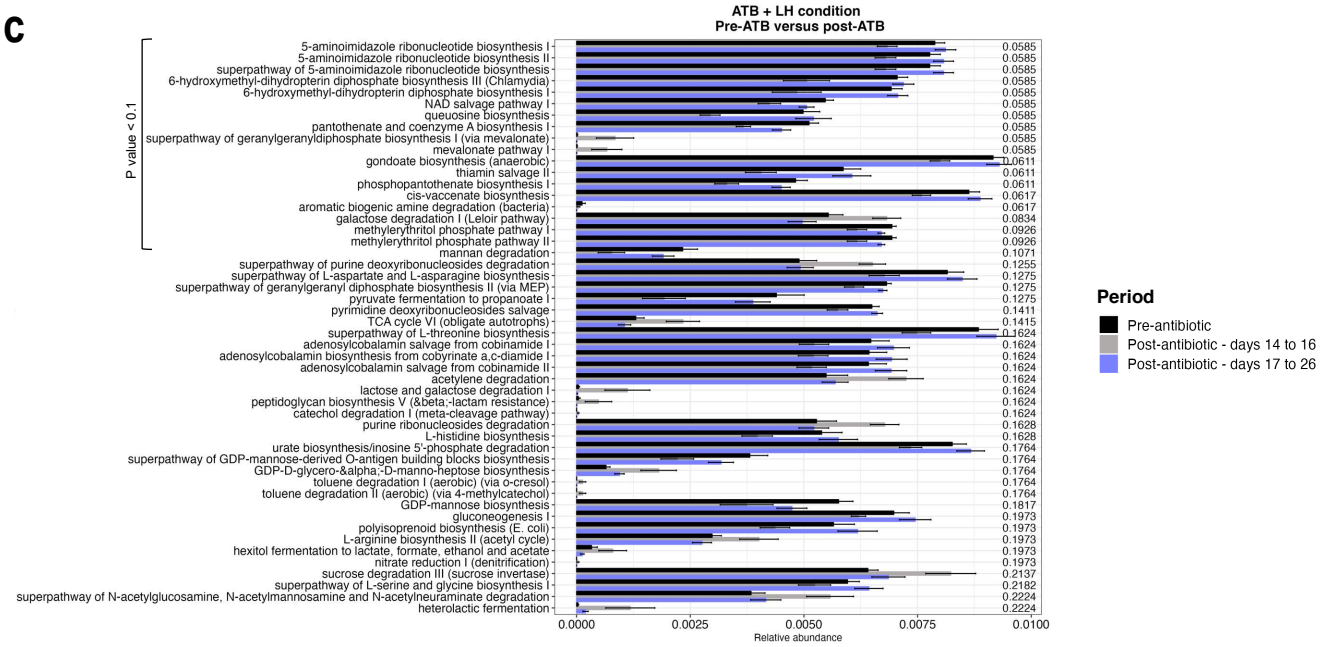

Supplementary figure V.3: Functional pathway predictions before and after antibiotherapy for each condition. PICRUSt2 software was used to predict bacterial metabolic pathways from 16S Metabarcoding data. LEFSe analysis was then performed to evidence significant differentially expressed pathways within conditions. Relative abundances of those pathways are plotted for ATB (a), ATB + SB (b) and ATB + LH (c) before (black), and after antibiotic administration from day 14 to 16 (grey) and day 17 to 26 (purple). P-values are indicated in front of each bar. Statistical differences are indicated by *: p<0.05 (Kruskal-Wallis test). *ATB: antibiotic, LH: L. helveticus HA-122, SB: S. boulardii CNCM I-1079.*

Supplementary table V.1: Primers used for qPCR and 16S Metabarcoding analyses.

Primer name	*Sequence 5'-3'*	*Target*	*Annealing temperature (°C)*	*References*
qPCR primers				
BAC338R	ACTCCTACGGGAGGCAG	Total bacteria	58	(Yu *et al.*, 2005)
BAC516F	GTATTACCGCGGCTGCTG			
Metabarcoding primers				
V3_F357_N	CCTACGGGNGGCWGCAG	Bacteria	-	(Klindworth *et al.*, 2013)
V4_R805	GACTACHVGGGTATCTAATCC			

5.6. Additional results

Material and methods

Yeasts and L. helveticus counts

S. boulardii CNCM I-1079 viability in the bioreactors was evaluated twice daily by plate count on Sabouraud agar (65 g/L Sabouraud Dextrose agar, Fisher Scientific) supplemented with chloramphenicol (50 mg/L, Sigma Aldrich) and gentamycin (10 mg/L, Sigma Aldrich). 100 µL of luminal medium samples from CANIM-ARCOL were diluted (1/10) in sterile physiological water (9 g/L NaCl). Around 200 mg mucin beads were crushed in 3 mL sterile physiological water. 100 µL of the diluted sample were inoculated on Sabouraud

agar plates in duplicates and counts performed after 48 h incubation at 30°C in aerobiosis. *L. helveticus* was quantified by qPCR using primers used by Myles *et al.*, (2020) with the same protocol used for total bacteria quantification.

Discriminant analysis

Sparse Partial Least-Squares Discriminant Analysis (sPLS-DA) were performed using MixOmics package (Lê Cao *et al.*, 2009) on days 9 to 26 with luminal and mucosal samples confounded. BLAST was used to precise species annotations.

Results and discussion

Quantification of the *S. boulardii* CNCM I-1079 yeast and total *L. helveticus* (including tyndallized strains *L. helveticus* HA-122) was achieved over fermentation time in the bioreactors (**Figure V.8**). The yeast was detected in the luminal medium samples only (not in faecal inoculum nor in mucin beads) and tended to better survive during antibiotherapy (values closer to baseline) than in the post-ATB period (**Figure V.8a**). This is in line with a previous study demonstrating that *S. boulardii* can colonize the gut when competition with intestinal microbiota was limited (Edwards-Ingram *et al.*, 2007) as it is the case here with antibiotherapy (Shannon index 2 during antibiotherapy *versus* 2.8 before and 7.2 Log_{10} total bacteria *versus* 8.5 before). Thus, the lower levels of *S. boulardii* found after antibiotherapy may be the reflect of increased competition with the recovered colonic microbiota. In this study, *S. boulardii* CNCM I-1079 was not detected in mucin beads, contrarily to previous observations showing a its capacity to adhere to mucin *in vivo* in human and pigs (Pais *et al.*, 2020). It was also demonstrated *in vitro* that *S. cerevisiae* CNCM I-3856 was able to colonize the mucosal fraction of the human simulated ascending colon in the M-SHIME (Roussel *et al.*, 2021).

Regarding *L. helveticus* quantification, we observed initial levels in the faecal inoculum (so before supplementation) similar to those measured during fermentations, in both luminal medium and mucin beads (**Figures V.8c** and **V.8d**). This is in accordance with the fact that *L. helveticus* is part of the commensal gut microbiota previously detected in dog feces. However, a slightly higher fraction of heat-inactivated *L. helveticus* was found in mucin beads compared to luminal medium. This may be due to *L. helveticus* adhesion to mucins or its potential entrapment in the bacterial biofilm formed at mucin beads surface which was observed by scanning electron microscopy in a previous study of our lab (Gresse *et al.*, 2021a).

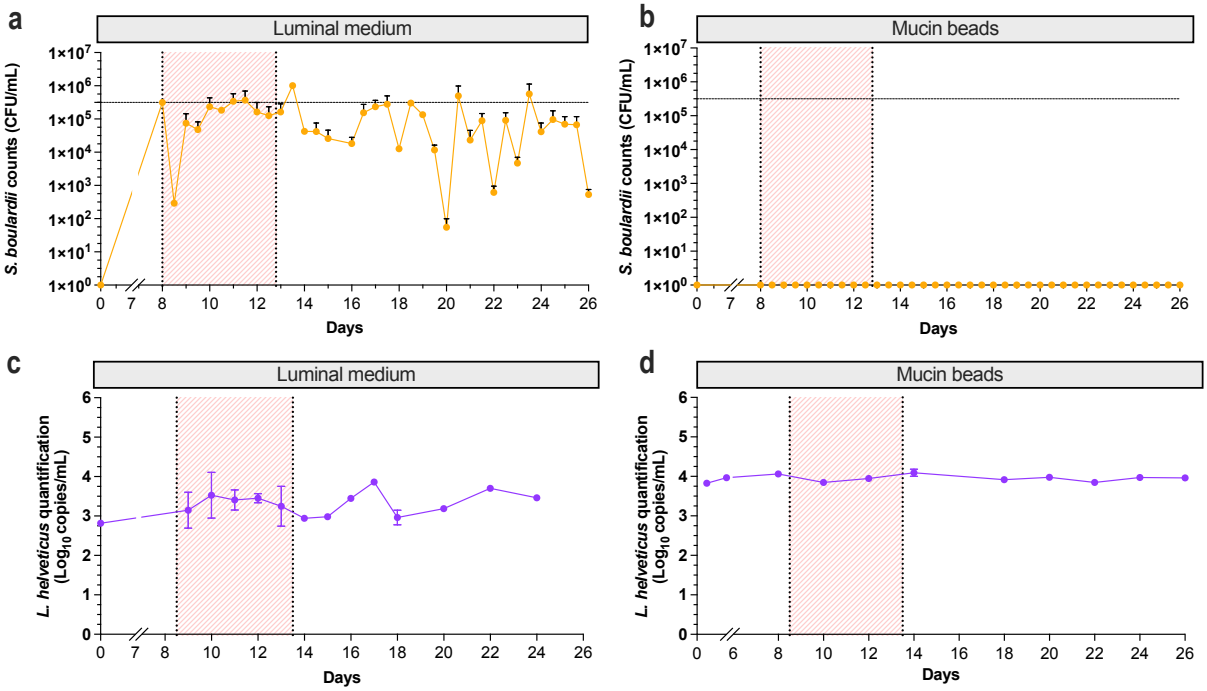

Figure V.8: Monitoring of *S. boulardii* and *L. helveticus* in the CANIM-ARCOL model. Fermentations were performed in the CANIM-ARCOL under medium dog size colonic conditions, after inoculation with stools from two dogs. *S. boulardii* CNCM I-1079 survival was followed by plate count in luminal medium (**a**) and mucin beads (**b**). *L. helveticus* bacterial load was estimated by qPCR in the luminal medium (**c**) and mucin beads (**d**). Antibiotic treatment was symbolized by a red zone. Horizontal line represents the baseline level of yeast injected each 12 h.

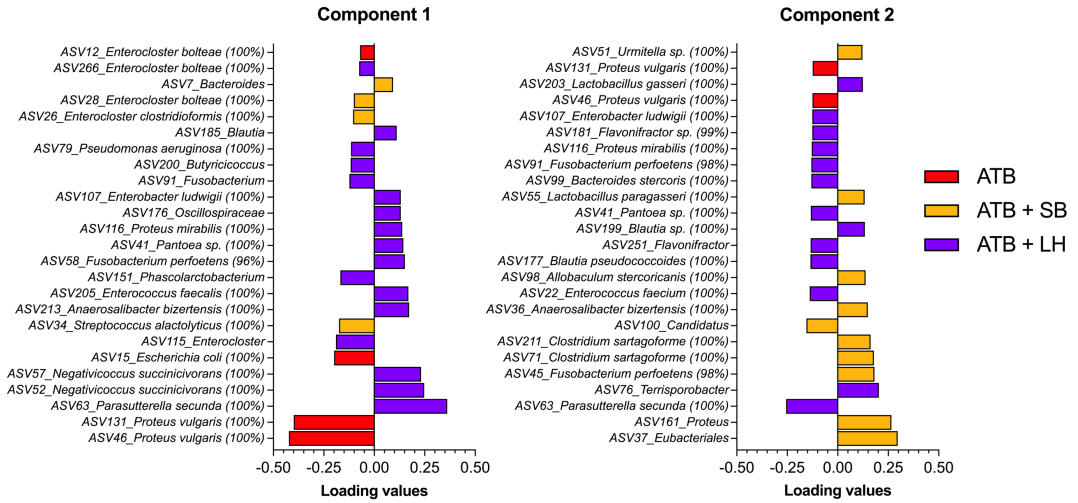

Figure V.9: Impact of restoration strategies on microbiota composition at the ASV level. sPLS-DA analysis was performed on days 9 to 26 on luminal and mucosal samples confounded to generate loading plots of the 25 most contributing ASVs between ATB, ATB + SB and ATB + LH conditions, and represented for component 1 (left) and 2 (right). Bars are colored according to the group in which the median abundance is maximal. Species annotations are provided when a sequence identity percentage higher than 97 % was identified using BLAST (given into brackets). ATB: antibiotic, LH: *L. helveticus* HA-122, SB: *S. boulardii* CNCM I-1079.

Additional discriminant analyses were also performed to identify ASVs markers of SB and LH supplementation. sPLS-DA analysis performed on global treated period (days 9 to 26) revealed significant

enrichments of ASVs from *Proteus vulgaris*, *Escherichia coli* and *Streptococcus alactolyticus* in ATB condition (**Figure V.9**). ATB + SB condition was characterized by an enrichment in species from *Bacteroides, Eubacteriales* and *Proteus*, whereas ATB + LH was more characterized by species from *Fusobacterium*, *Negativicoccus succinicivorans*, *Phascolarctobacterium* and *Parasutterella secunda*. Of interest, these analyses also confirmed that both SB and LH had an important impact on microbiota composition and may support the recovery of gut microbial metabolic activity, since they are mostly associated to enrichment in bacteria involved in SCFA production such as *Bacteroides*, *Phascolarctobacterium* (acetate and propionate), but also *Parasutterella secunda* which produced succinate, a precursor of propionate (**Figure V.9**).

5.7. Conclusion

As a final step of this PhD work, the newly adapted dysbiotic CANIM-ARCOL was used to evaluate for the first time the potential of one live probiotic yeast (*S. boulardii* CNCM I-1079) and one paraprobiotic bacteria (heat-inactivated *L. helveticus* HA-122) for their protective or restorative effects on canine microbiota composition and activity during and after antibiotherapy. During antibiotherapy, no significant effect of *S. boulardii* and *L. helveticus* was evidenced on microbiota activity. However, interestingly, both strains induced a reduction of *Enterobacteriaceae* relative abundance during antibiotic supplementation and were able to decrease variability of results especially regarding beta-diversity, total bacterial load, dysbiosis index and metabolic pathways predictions. In addition, after antibiotherapy, both strains demonstrated interesting restorative capacities such as a faster recovery in microbiota activity and composition. To move toward strains commercialization for canine application, it will be necessary to ensure the safety of those two products in dogs. This implies a better comprehension of the impact of the pro- and paraprobiotic on microbiota activity. Quantification of fermentation products including BCFA, phenol, indoles, lactate and ammonia could be performed in a next future, and profiles of bile acids be established. Of interest, metronidazole/enrofloxacin treatment was previously associated to bile acids dysmetabolism and the effect of both restoration strategies on bile acids metabolization by the colonic microbiota could be interesting to assess *in vitro* (as discussed in Chapter 4). Finally, characterization of cell walls of the heat-inactivated *L. helveticus* HA-122 will be an added value to well understand its potential interactions with the gut microbiota.

SECTION III

GENERAL DISCUSSION

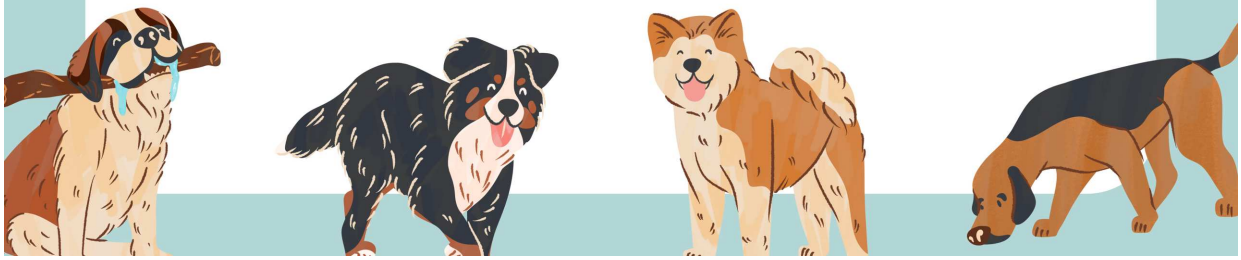

A. Repositioning the global context of the research

Thirty thousand years after domestication of the grey wolf, around 400 canine breeds have been selected, leading to **various dogs' sizes** and weight ranging from 1 kg for a Chihuahua to 100 kg for a Saint-Bernard. The emotional bond existing between dogs and their owner is stronger than ever before, leading to humanization of pets so called '**pet parenting'**. Dogs now occupy a full place in the family and their health and well-being are of paramount importance for their owners, leading to major implications for the pet food and pet care industry. In particular, **digestion and associated gut microbiota** are key parameters of dog health and an increasingly important concern for owners, veterinarians, researchers and industrialists. Besides, it should be highlighted that most studies on digestion focused on medium size dogs (mainly Beagles), and extremely sparse data are available on small and large dog sizes, as presented in Section I Part 1. Regardless of dog size population, microbiota studies are usually performed on feces and still very few data are available on **colonic** microbiota, which differs from that of stools, and on **luminal and mucus-associated microbiota** (Section I Part 2). Nevertheless, the colonic microbiota and particularly the mucosal one which is in close relationship with host cells *in vivo* most certainly play a central role in dog health, supporting nutritional, immunological and physiological processes. As well described in human, diseases such as obesity, diarrhea or chronic enteropathy, but also **antibiotherapy**, can disturb the canine gut microbiota and induce a perturbated state called **dysbiosis**. As an answer, new restoration strategies of the gut microbiota can be envisaged such as pre-, pro- or postbiotics, but up to now a very limited number of studies has been performed in dogs, especially in the frame of antibiotherapy. To study interactions with canine gut microbiota, clinical studies are limited by obvious ethical, regulatory and cost constraints, while *in vitro* gut models are more accessible. Especially, ***in vitro* dynamic colonic models** are valuable tools allowing to maintain a complex and metabolically active gut microbiota for several weeks under physiologically relevant conditions. Such *in vitro* approach allows to investigate the composition and activity of the microbiota, and the impact on them of any beneficial or deleterious compounds. However, up to now, few canine *in vitro* gut models have been developed, except for simple ones that yet remain far from the physiological conditions, but none of them integrate the specificities associated to different dog sizes. In addition, improvements of these *in vitro* gut models are continuously needed to better fit with new *in vivo* data available, if any.

In this context, the main goal of this PhD project, performed at MEDIS in the context of an industrial partnership with Lallemand Animal Nutrition and Dômes Pharma, was to set-up a new *in vitro* model of the canine colon adapted to three dog sizes (i.e. small dogs under 10 kg, medium dogs from 10 to 30 kg and large dogs over 30 kg). Once this model developed and validated compared to *in vivo* data under healthy situation regarding both microbiota composition and activities, the second step of the project was to reproduce in the *in vitro* model a perturbated situation of gut microbiota, namely called dysbiosis. Antibiotherapy was chosen since antibiotics are, like in humans, frequently administered to dogs with potential side effects. Once again, this dysbiotic colon model was validated compared to the *in vivo* situation in dogs. Finally, as potential restoration strategies, we evaluated the ability of a live probiotic yeast (i.e. *S. boulardii* CNCM I-1079) and a postbiotic

lactic acid bacteria (i.e. heat-inactivated *L. helveticus* HA-122) to preserve canine colonic microbiota during antibiotherapy and speed-up return to microbiota equilibrium afterwards.

B. *Interest and originality of the PhD work*

a. *Impact of conservative methods on faecal inoculum used in the M-ARCOL model*

For all our experiments, the CANIM-ARCOL was inoculated with faecal suspensions collected from healthy dogs. Preparation of the inoculum is a critical step to consider but there is no consensus yet regarding the collection, storage and preparation of canine faecal samples. Recently, the impact of faecal sampling method was investigated, showing no impact of sampling site on targeted microbial populations, but variations of SCFA and ammonia concentrations, as well as pH values (Pinna *et al.*, 2021). The authors concluded on the necessity for homogenization of the whole stool before sampling. Regarding storage of canine faecal samples, no impact of temperature (room-temperature, 37°C or 50°C and freeze-thaw cycles) on both alpha and beta-diversities was evidenced on samples stabilized into PERFORMAbiome•GUT collection devices, while alpha-diversity increased in unstabilized samples stored at room temperature for 14 days, showing growth of microorganisms and alteration of 24 genera (Lin *et al.*, 2020). In addition, this study revealed a significant intra-sampling variation with a modification in the relative abundances of 9 genera depending on collection sites within a canine faecal sample, as previously observed with human feces (Gorzelak *et al.*, 2015). Effect of chilling or freezing canine faeces for 24 h was also evaluated through its impact on gas production and fermentation end-products in 72h-batch fermentation model (Bosch *et al.*, 2013), showing that freezing decreased gas production while increased indole or phenol concentrations. However, no study has already evaluated the effect of storage conditions of stool samples before using them to inoculate an *in vitro* colon model.

To fill this gap of knowledge, the aim of our first experiment was to assess the effect of different preservative methods (freezing 48 h at -80°C, freezing 48 h at -80°C with glycerol as a preservative agent or lyophilization with maltodextrin/trehalose) on the colonization kinetics of both luminal and mucus-associated microbiota in the M-ARCOL model inoculated with fecal samples from two adult donors (Deschamps *et al.*, 2020, *Applied Microbiology and Biotechnology*, Section II Chapter 1). All the preservative treatments tested allowed to maintain inside the M-ARCOL of a complex and functional microbiota but considering stabilization time of microbial profiles and activities (and not technical constraints associated to the supply of frozen material), our results highlighted 48 h freezing at -80 °C without cryoprotectant as the most efficient method.

With this in mind and as far as possible, fresh canine feces were used, or raw feces were freezing at -80°C for 12h without cryoprotectant and under anaerobic condition. In addition, colleagues working on canine colonic *in vitro* models (static and dynamic ones) also usually worked with fresh faecal samples collected immediately after defecation (Sunvold *et al.*, 1995; Tzortzis *et al.*, 2004; Bosch *et al.*, 2008; Cutrignelli *et al.*, 2009; Vierbaum *et al.*, 2019; Van den Abbeele *et al.*, 2020; Oba *et al.*, 2020; Verstrepen *et al.*, 2021). In addition, during this whole PhD work, we decided to work with unpooled faecal samples, since previous studies showed important inter-individual variations in faecal microbiota composition between dogs (as reported in Deschamps

et al., 2022). This was also supported by a study from Van de Wiele and colleagues stated that "the artificially high microbial diversity in pooled *inoculum* creates disturbances in the cross-feeding processes between microorganisms that are adapted to one another in each of the separate microbiomes" (Van de Wiele *et al.*, 2015). Our experiments performed on small, medium and large dog size microbiota also highlighted important variations in microbiota composition between donors, thus confirming the importance to use unpooled stools for canine-related fermentation studies.

b. Impact of dog size on canine colonic physicochemical parameters and gut microbiota

The food and pharma context

For decades, recommendations for petfood and drug intake by industrialists and veterinarians are only based on canine body weight or metabolic weight. However, as evidenced during this PhD project, the available literature also highlighted plenty of **specificities associated to each dog size** in relation to digestive physiology, especially linked to the large intestine and its associated microbiota. For instance, this work emphasized differences in intestinal and colonic permeability and absorption capacities with dog sizes, which can obviously impact nutrient or drug bioaccessibility (Oswald *et al.*, 2015). In addition, transit time and pH vary with dog sizes, which needs to be considered since they are known to impact not only drug release (Oswald *et al.*, 2015), food digestibility (Lewis *et al.*, 1994), but also gut microbiota composition and metabolic activities (Tottey *et al.*, 2017; Pham *et al.*, 2019). In light of this knowledge, the development of new food supplements or veterinary products should consider all the facets associated with dog size effects, to move towards more personalized nutrition and veterinary medicine. To evaluate the fate and effect of such food and pharma compounds, we opted in this PhD work to use only *in vitro* approaches. This was fully in line with increasing concerns raised by public opinion about animal welfare and with the European directive ('3R' principle) that widely encourages to replace, reduce and refine the use of animal in research (Russel & Burch, 1959), increasing the pressure for developing *in vitro* alternative solutions. *In vitro* gut models can be a relevant alternative to *in vivo* assays in dogs, given they are fully set-up and validated based on *in vivo* data. Such efforts were made throughout the PhD work, as well as linking scientific objectives and technological developments.

Development of the CANIM-ARCOL model adapted to different dog sizes

First, our in-depth understanding of the **impact of body size** on nutritional, physicochemical and microbial parameters of the canine large intestine was associated to the development of a new size-related colonic *in vitro* model based on the M-ARCOL technology, so called the **CANIM-ARCOL** (Deschamps *et al.* 2023a, *submitted to ALTEX*, Section II Chapter 2). This model is the second dynamic *in vitro* model (with the M-SCIME) reproducing the canine large intestine and distinguishing lumen from mucus-associated microbiota. The CANIM-ARCOL is however the first one to be adapted to digestive specificities associated to small, medium and large dog sizes. Of interest, this work also provides an extensive description of faecal samples from 13 healthy dogs belonging to the three dog sizes, as rarely performed before in a single study. This includes

microbiota composition, with analysis of total bacteria load and metabarcoding profiles, but also metabolic activities through the dosage of main fermentation end-products such as gas, SCFA, BCFA, ammonia and the uncommon description of bile acids profiles. As a novelty in the field, we provided the first data set on gas profiles under canine colonic conditions, allowed by the lack of flushing with N_2 or CO_2 inside the bioreactors. Monitoring gas production is of high interest because both the volume of gases and their composition can be linked to health status. In dogs, an excessive gas production led to flatulence and intestinal discomfort (Jones *et al.*, 1998), and was mainly associated with a poorly digestible diet (Weber, Biourge & Nguyen, 2017). In humans, excessive gas production was associated to protein putrefaction (leading to H_2S production) and gastrointestinal diseases including IBD or irritable bowel syndrome (El-Salhy *et al.*, 2017). Depending on their type, concentration and volume, gases can induce abdominal symptoms and might also have physiological and therapeutic effects (Kalantar-Zadeh *et al.*, 2019). Thus, profiling gases could be powerful criteria to evaluate diet digestibility or dietary manipulations. Modulation of intestinal gases might be also an interesting prospect for disease prevention and/or therapy in dogs, as previously demonstrated for human (Kalantar-Zadeh *et al.*, 2019). This study also provides, for the first time, accurate data on the impact of dog size on bacterial and archaeal composition. Studying the archaeal fraction is of interest, because even it was estimated to represent 1.1 % of the canine faecal microbiota (Swanson *et al.*, 2011), up to now *Archaea* have been very poorly studied *in vivo* and never in *in vitro* gut models. Based on translation from other mammalian situations including the human one, we can hypothesize that *Archaea* may be involved in mutualistic interactions with bacteria in the canine gut. In mice model, it was suggested that H_2 transfer between bacterial and archaeal species was involved in increasing energy uptake (Zhang *et al.*, 2009). In human stools, an inverse relationship between *Archaea* abundance and body mass index (BMI) was evidenced (Schwiertz *et al.*, 2010; Million *et al.*, 2012, 2013; Goodrich *et al.*, 2016; de la Cuesta-Zuluaga *et al.*, 2018; Jinatham *et al.*, 2018), in accordance to our results showing a negative correlation between *Archaea* and dog body size. In addition, it would be also interesting to explore both the mycobiome and virome of the canine colonic microbiota, each representing 0.4 % of the canine fecal microbiota (Foster *et al.*, 2013; Shi *et al.*, 2021) and have been yet poorly described in dogs. Of interest, a very recent study evidenced an alteration of the virome composition and diversity associated to diarrhea in dogs (Wang *et al.*, 2023). In human, the mycobiome was recently described as an indispensable component of microbiome, disturbed in the context of gastrointestinal diseases including IBD and cancer (El-Jurdi & Ghannoum, 2017), suggesting once again the interest to follow it in dogs. However, previous experiments in the M-ARCOL under human situation evidenced difficulties in maintaining *in vitro* the eukaryotic fraction from gut microbiome. Lastly, the effect of dog size was here evaluated for the first time on both luminal and mucus-associated microbiota. Under canine condition, mucosal microbes were previously studied in only one *in vitro* model, the M-SCIME simulating medium dog size condition (Verstrepen *et al.*, 2021). Similar families were observed between the mucosal fractions of M-SCIME and CANIM-ARCOL, except that no *Verrucomicrobia* was detected in our study neither in faecal inoculum nor in bioreactors. The mucus fraction of the canine large intestine was only evaluated by targeted approaches such as FISH, mainly to follow pathogenic bacteria such as adherent invasive *E. coli* (Simpson *et al.*, 2006). Nevertheless, it would be highly interesting to better describe

mucus-associated microbes since there are increasing evidence of their importance in health. Our *in vitro* study suggests that in dogs, *Bacteroidaceae* (all sizes), *Fusobacteriaceae* and *Lachnospiraceae* (small and medium sizes) as well as *Clostridiaceae* and *Sporanaerobacteraceae* (large size) seem to be important families associated to mucus environment in accordance with observations on other species (for *Bacteroidaceae* and *Lachnospiraceae*). These results also reinforce the idea of a functional role of *Fusobacteriaceae* in healthy dogs, probably more typical of the canine species (Oswald *et al.*, 2015). In human, in mice, but also in dogs, invasion of the outer mucus layer was associated to disease such as granulomatous colitis (Simpson *et al.*, 2006). In human, changes in mucus thickness or composition have been related to diseases (Etienne-Mesmin *et al.*, 2019). Colonic mucus showing similar characteristics between dog and humans (Linden *et al.*, 2008) -but also pigs (Barmpatsalou *et al.*, 2021)- with a majority of MUC2 proteins (Dubbelboer *et al.*, 2022), this further supports a role of the mucus layer in dog health.

Validation of the CANIM-ARCOL model

Once developed, the CANIM-ARCOL model was well validated through *in vivo-in vitro* comparisons on colonic (medium size only) and faecal data extracted from a literature review previously published (Deschamps *et al.*, 2022). Surprisingly, until now only two studies have assessed colonic microbiota composition, in medium size dogs only, certainly due to the need of invasive methods for sampling. The recent development of new pH-sensitive sampling technology (i.e. smart capsules) may contribute to fill this gap, allowing to easily studied the entire GIT, especially microbiota composition but also pH, ileal digestibility or bile acids profiles in different dog sizes (Waimin *et al.*, 2020; Nejati *et al.*, 2022). Despite such *in vitro-in vivo* validation, considering the results obtained from our study, some additional improvements should be performed to better discriminate microbiota from small and medium dog sizes *in vitro*. In parallel, the large size condition of the model still needs to be questioned to find what can be responsible of the very low alpha-diversity and loss of *Fusobacteria* associated to a bloom of *Sporanaerobacteraceae* relative abundance. A first answer would be a fine metabolomic characterization of large size samples to better understand the potential cause of such shift. We also expected that thanks to this work, researchers can start considering size effect in canine microbiome studies or can even make accessible sequencing data from previous ones to reanalyze results considering size effect. This would lead to the possibility to fine-tune the set-up of new developed *in vitro* gut models and increase their robustness. Lastly, this study focuses on the canine lower gut, but the fate of food or veterinary products in the canine upper gastrointestinal tract can be also of high concern for industrials and academics from the food and pharma fields. This might be an important added value, especially to study probiotics survival or the fate and bioaccessibility of active compounds such as drugs in the canine upper gut. Up to now, only one dynamic model of the stomach and small intestine is accessible for dogs, the FIDO model based on the TIM technology available at MEDIS lab. This model simulates the conditions found in the upper gut of medium size dogs only (Smeets-Peeters *et al.*, 1999a). Unfortunately, the lack of *in vivo* data related to the canine upper digestive tract (i.e. pH kinetics, enzyme and bile concentrations, mucus width and microbiota composition in the different

compartments) prevented us to make adaptations of the FIDO model to small and large size conditions during this PhD work.

Mechanistic study: importance of gut microbes versus physicochemical and nutritional parameters

Afterwards, in an original way, the CANIM-ARCOL was used to evaluate the **relative importance of gut microbes *versus* physicochemical and nutritional parameters** of the canine colonic environment in shaping microbiota structure and functions *in vitro* (Deschamps *et al.* 2023b, *in preparation for Applied Microbiology Biotechnology*, Section II Chapter 3). For the first time, this study gave mechanistic insights on which parameters from the colonic ecosystem mainly drive canine microbiota in relation to dog size. This work benefits from an innovative mechanistic approach never used before in the literature, but already employed successfully in the study performed during my Master 2 internship, which aimed to investigate the impact of physicochemical and nutritional parameters from the human large intestine environment on gut microbiota dysbiosis associated to obesity (see Appendix 5). The results obtained here were compared to *in vivo* data from canine stools and previous *in vitro* results obtained when CANIM-ARCOL was inoculated with fecal samples from three dog sizes. This study demonstrated for the first time that environmental colonic parameters were sufficient to drive microbiota functions *in vitro*. This work also uncovers that size-related fecal microbes were necessary to accurately reproduce *in vitro* the colonic ecosystem of small, medium and large dogs. Our data suggest that gut metabolic activities are more quickly responsive to changes than microbiota composition. Such observations are in line with our previous studies in the ARCOL model set under human conditions and showing a quicker recovery of microbiota activity compared to composition after antibiotherapy and restoration by fecal microbiota transplantation (Verdier *et al.*, 2021). Similar results were also obtained under piglet conditions in the M-ARCOL after feed deprivation associated to weaning (Gresse *et al.*, 2021a). This capacity is certainly allowed by the functional redundancy of gut microbes (Tian *et al.*, 2020). Further investigations with a higher number of biological replicates (only 2 dogs involved in this study) and studies of each of the independently modified factors would be needed to confirm their relative importance in shaping gut microbes. As an example, a novel viewpoint would be provided using medium dog size condition and increasing or decreasing pH only to evaluate its relative impact on microbiota composition and activities.

c. Impact of antibiotherapy on microbiota structure and functions

Antibiotherapy in dogs

Antibiotics are the first treatment used by veterinarians to treat canine gastrointestinal diseases such as diarrhea. Of note, pathology curation involves an exclusion diagnosis, usually starting with antibiotherapy to exclude bacterial and/or parasite causes. As in humans, antibiotic use can have damaging side-effects in dogs, such as vomiting (Whittemore, Moyers & Price, 2019), diarrhea (Pilla *et al.*, 2020) or weight loss but can also lead to bile acids dysmetabolism and microbial dysbiosis (5). Nevertheless, up to now, the impact of antibiotherapy on canine colonic microbiota composition and functions has never been described, while available studies mainly focused on stools (Grønvold *et al.*, 2010; Igarashi *et al.*, 2014; Kilpinen *et al.*, 2015;

Manchester *et al.*, 2019; Werner *et al.*, 2020; Pilla *et al.*, 2020; Whittemore *et al.*, 2021, 2021; Pignataro *et al.*, 2021; Bottero *et al.*, 2022). In the second part of this PhD, after studying the effect of dog sizes under healthy situation, we aimed to focus on a perturbated state and investigated the impact of antibiotherapy on canine colonic microbiota, restricting the scope on medium size dogs. This work led to the development of the first canine **antibiotic-induced dysbiotic model** based on the CANIM-ARCOL, set up under medium size condition (Deschamps *et al.* 2023c, *in preparation for Microbiology Spectrum*, Section II Chapter 4).

Pre-screening experiments and development of the antibiotic-induced dysbiotic model

We performed a first set of experiments to compare the effects of five antibiotic cocktails used by veterinarians on canine microbiota and select the most appropriated for the dysbiotic colonic model development. Even if this step was used as preliminary antibiotic screening, it could be interesting to increase the number of biological replicates to assess if some donor-depending responses can be observed. Of interest, amoxicillin and metronidazole alone had a limited impact on colonic microbiota while tylosin led to a very disturbed situation. Results obtained with amoxicillin and metronidazole are a bit surprising since microbiota alterations were previously described in dog fecal samples (Grønvold *et al.*, 2010; Igarashi *et al.*, 2014; Pilla *et al.*, 2020). Nevertheless, these data were obtained after longer treatment periods (14 days for metronidazole and 7 days for amoxicillin -versus 7 days for metronidazole and 5 for amoxicillin in our experiments-, longer than veterinarians recommendations) and different sequencing methods (Rintala *et al.*, 2017), which can impact results. Results obtained with tylosin were generally in accordance with the literature reporting an increase in *Enterobacteriaceae* while alpha-diversity and *Fusobacteriaceae* relative abundance decreased (Kilpinen *et al.*, 2015; Manchester *et al.*, 2019, 2019; Bottero *et al.*, 2022). The metronidazole/enrofloxacin cocktail was selected for the development of the dysbiotic model. Metronidazole is extensively used in dogs suffering from chronic enteropathies or diarrhea, while enrofloxacin is mostly employed to treat gastrointestinal infections that have not responded to previous antibiotherapy. Of note, metronidazole/enrofloxacin cocktail is not extensively prescribed by veterinarians but this combination was described to greatly broaden the antibiotic spectrum of activity, increasing the risk for associated gastrointestinal signs in dogs (Whittemore *et al.*, 2019) and inducing severe alterations of faecal microbiome and metabolome (Whittemore *et al.*, 2021). As a dysbiosis state of gut microbiota is defined by an alteration of both composition and functionalities (Pilla & Suchodolski, 2020), during the model development, we performed both metabarcoding analysis of lumen and mucus-associated microbiota and measurement of gas and SCFA as main fermentation end-products. We also determined, for the first time in an *in vitro* gut model, dysbiosis index (AlShawaqfeh *et al.*, 2017) to characterize canine microbiota dysbiosis. This dysbiosis index was initially developed in the frame of chronic enteropathies, using qPCR quantifications of 7 key bacterial populations considered as dysbiosis markers. In the present study, dysbiosis scores were calculated using the same method but in an original way based on metabarcoding data instead of qPCR ones, thanks to the recent development of the 'dysbiosisR' R-package (Shetty & de Steenhuijsen Piters, 2022). The use of total bacterial populations and the selected 7 dysbiosis markers allowed to evidence microbiota dysbiosis associated to antibiotherapy, indicating that such 7 specific populations can be used not

only to predict dysbiosis associated to chronic enteropathies but also antibiotherapy. As expected, metronidazole/enrofloxacin induced *in vitro* an important alteration of the colonic microbiota, especially in the luminal compartment of the CANIM-ARCOL. The mucus-associated microbiota was less impacted, as previously observed *in vitro* in the M-SHIME set-up under human conditions and after addition of polyunsaturated fatty acids (Roussel *et al.*, 2022). The authors described mucin beads as a robust microenvironment allowing a physical attachment of bacteria conferring them a competitive advantage. An important biofilm formation was observed at the surface of mucin beads previously collected from the M-ARCOL model set-up under piglet conditions and analyzed by scanning electron microscopy (Gresse *et al.*, 2021a). Since biofilms are known to protect bacteria from antibiotic by acting as a 'protective clothing' (Yin *et al.*, 2019), we can formulate the hypothesis that this preserved microenvironment may act as a bacterial reservoir continually reinoculating the luminal medium. In the luminal medium of the CANIM-ARCOL, a reduction of total bacteria load, gas and SCFA production, associated to an increase of the dysbiosis index was observed during antibiotic treatment and maintained afterward. In addition, a bloom of *Enterobacteriaceae* was noticed during antibiotherapy, associated to an increase in opportunistic pathogens relative abundances such as *Enterococcus*, *Escherichia* and *Proteus*, while *Fusobacteria*, *Faecalibacterium* and *Clostridium* were reduced. This was expected because *Enterobacteriaceae* bloom was previously described as a dysbiosis common marker in human (Rivera-Chávez, Lopez & Bäumler, 2017) and also in dog (Grønvold *et al.*, 2010; Cassmann *et al.*, 2016; Park *et al.*, 2019). Of interest also, such modifications of both microbiota composition and activity were perfectly in line with results from the only *in vivo* study that evaluated in dog stools the effect on microbiome of the same antibiotic cocktail (Whittemore *et al.*, 2021), validating our dysbiotic model. However, it should be noted that gas production and profiles have never been monitored *in vivo* in dogs in a context of antibiotherapy, which has prevented *in vitro-in vivo* comparisons on these parameters. Surprisingly, the present study also demonstrated that a 5-days metronidazole/enrofloxacin treatment (which is 4 times shorter than the 21 days treatment applied in Whittemore *et al.*, 2021, and more in adequation with vet prescriptions) is able to induce critical changes in the canine colonic microbiota and this independently of the host component. In addition, most of the impacted bacterial populations were still altered after antibiotherapy, as previously observed *in vivo* (Whittemore *et al.*, 2021). However, in our *in vitro* study, microbiota alterations persisted for few days, while up to 4 weeks were necessary to recover microbiota composition *in vivo*. This is surprising because there are in dogs many sources of bacterial re-inoculation, such as food or environment, that do not exist *in vitro,* the bioreactors being a closed system. Such a difference might be primarily explained by a longer period of antibiotherapy *in vivo* than *in vitro*. Another explanation is that in the CANIM-ARCOL, the mucosal phase is more effective than *in vivo* to re-inoculate the luminal compartment, maybe due to a higher ratio of mucosal surface *in vitro* than *in vivo*. This was set-up previously at the lab based on human data and unfortunately there is no available data on canine colonic mucus thickness in the literature. Altogether, the present data confirmed the negative effects that antibiotherapy may have on gut microbiome in dogs. In accordance with PROTECT ME guidelines (BSAVA/SAMSoc, 2018), our results encourage veterinarians to take faecal samples for culture

and antibiotic resistance testing before antibiotherapy in dogs (except for urgency), in order to limit as much as possible their inappropriate use.

Toward other dysbiosis model development

This work focused on a dysbiotic state associated to antibiotic treatment under medium size dog condition. In a near future, we may also consider the adaptation of the antibiotic-induced dysbiotic model to other canine dog sizes (i.e. small and large sizes). However, this objective would be limited by the lack of *in vivo* data from small and large dogs for validation, since all antibiotic studies were until now performed in medium dogs. The potential of the CANIM-ARCOL could be also extended to other diseased situations where gut microbiota dysbiosis has been evidenced, such as obesity, IBD or chronic enteropathies (Malewska *et al.*, 2011; Guard *et al.*, 2015; AlShawaqfeh *et al.*, 2017; Dandrieux & Mansfield, 2019). Simulating a dysbiotic situation in *in vitro* gut models will necessitate the use of faecal samples from diseased donors, but also the adaptation of all associated physicochemical and nutritional parameters to reproduce the colonic environmental conditions specific of the disease. Such adaptations are crucial due to the important resilience capacity of gut microbiota which will rapidly shift to an eubiosis state if diseased parameters are not maintained. As an example, simulating canine obesity *in vitro* would imply to adapt food quantity (as overfeeding is the main driver of canine dysbiosis), but also the composition of simulated ileal effluents, such as nutrient content as altered lipid and bile profiles have been reported in obese dogs (Tvarijonaviciute *et al.*, 2012; Apper *et al.*, 2020). This type of adaptation has been already successfully performed with the M-ARCOL model to reproduce human obese conditions (see Appendix 5).

d. Evaluation of restoration strategies based on probiotics and postbiotics

Choice of tested products

The final step of this project was to **evaluate the protective and restoration potential of two microbial products** in a context of antibiotic-induced dysbiosis in dogs (Deschamps *et al.* 2023d, *in preparation for Food International Journal*, Section II Chapter 5). There is a growing number of gut microbiota restoration strategies commercialized for dogs (see Section 1 Part 3.2.1) and until now only the bacterium *Enterococcus faecium* was tested *in vivo* in the context of antibiotherapy (Fenimore, Martin & Lappin, 2017). Consequently, to fulfill this gap of knowledge, two potential candidates were selected among strains produced by one of this PhD thesis partners, Lallemand SAS, namely the live probiotic yeast *Saccharomyces boulardii* CNCM I-1079 (already commercialized as LevucellSB for pigs and poultry) and the paraprobiotic (heat-inactivated bacteria) *Lactobacillus helveticus* HA-122 (recently commercialized for dogs and cats and requiring scientific substantiation).

S. boulardii was selected here as a "positive control" since beneficial effects are already well recognized in humans in the context of antibiotherapy. In human, *S. boulardii* had remarkable effects on diarrhea associated to antibiotherapy by reducing diarrhea occurrence thanks to an increase in SCFA and especially butyrate production (Pais *et al.*, 2020). In addition, the probiotic yeast is known to secrete polyamines, reported as

beneficial for colonic mucosa health (Tofalo, Cocchi & Suzzi, 2019). Some pathogen exclusion have been shown by pathogen binding (e.g. *E. coli* or *Salmonella*) to the yeast cells or secretion of antimicrobial compounds (Pais *et al.*, 2020). Anti-toxinic effect were also described against *Clostridium difficile* and *Cholera* toxin (McFarland, 2010). Lastly, *S. boulardii* has been reported to have immunomodulatory and anti-inflammatory effects mainly by repressing NF-κB pathway and IL-8 production while inducing the production of anti-inflammatory IL-10 (Stier & Bischoff, 2016). Interesting probiotic effects of *S. boulardii* CNCM I-1079 have been also demonstrated in dogs, showing a better microbiota resilience in gestating and lactating bitches at whelping and a modulation of puppies' microbiota (Garrigues *et al.*, 2022b, 2022a). Significant decreases in fecal inflammatory and stress markers without impacting microbiota composition were also observed in both healthy dogs (Meineri *et al.*, 2022) and dogs with chronic enteropathies (D'Angelo *et al.*, 2018). Up to now, the effects of *S. boulardii* have been very poorly tested in a context of antibiotherapy in dogs but showed promising effects in healthy animals receiving lincomycin antibiotic (Aktas, Borku & Ozkanlar, 2007). Nevertheless, such probiotic strategy requires by definition strain viability in the gastrointestinal tract, which may be challenging because of industrial constraints (extrusion for kibbles) and conservation issues (high sensitivity to water and heat). In addition, live yeast is considered as a **feed additive** and requires a European authorization by EFSA (Regulation EU 68/2013) to be on the market. An alternative solution is the use of heat-inactivated strains, called 'paraprobiotics' or 'postbiotics'. These products are less sensitive to industrial and storage conditions and are considered as **raw materials** in European regulation (Regulation EU 767/2009), making them easy to be used in petfood industry. Such approaches were recently developed and to date very few *in vivo* studies were performed. Nevertheless, these products already demonstrated potential beneficial effects on canine microbiota and health. Of interest, heat-inactivated *Lactobacillus* were able to improve faecal scores in healthy puppies and showed protective effect against viral diarrhea in adult dogs, by increasing *Firmicutes* and faecal diversity after a long-term supplementation -10 months- (Spears, Ameho & Reynolds, 2016). However, the potential of microbiota modulation of heat-inactivated *L. helveticus* during antibiotherapy has never been studied in dogs.

Effect of restoration strategies on antibiotic disturbed canine microbiome

In this last study, we demonstrated promising effects of both probiotic and postbiotic strains during antibiotherapy and within the two days after treatment (Deschamps *et al.* 2023d, *in preparation for Food International Journal*, Section II Chapter 5). Especially, *S. boulardii* CNCM I-1079 and heat-inactivated *L. helveticus* HA-122 mitigated *Enterobacteriaceae* bloom and promoted a quicker microbiota resilience regarding bacterial load and diversity, and SCFA production. Both microorganisms were also able to downregulate putative metabolic pathways stimulated by antibiotherapy and potentially involved in pathobionts metabolism. Here, for the first time, we showed direct effects of *S. boulardii* CNCM I-1079 and inactivated *L. helveticus* HA-122 on microbiota composition.

S. boulardii modes of action are well described and include pathogen binding or agglutination, antimicrobial peptides secretion, immune modulation and trophic effects (Pais *et al.*, 2020). In addition, some

S. boulardii strains are able to produce high concentrations of acetic acid, which was found to exert an inhibitory effect in *E. coli* (Offei *et al.*, 2019), in accordance to the decrease in *Escherichia* abundance observed in the CANIM-ARCOL. Of note, in opposite to our results, previous canine studies reporting *S. boulardii* supplementation for 10 to 35 days to healthy dogs and dogs with chronic enteropathies did not report any impact on faecal microbiota and mycobiota (D'Angelo *et al.*, 2018; Meineri *et al.*, 2022). Besides, an *in vitro* study simulating rumen condition showed that both living and autoclaved *S. boulardii* significantly stimulated SCFA (i.e. acetate and butyrate) and BCFA (i.e. isovalerate and valerate) production, with no major differences between the two conditions (Oeztuerk *et al.*, 2005). Authors concluded to a potential prebiotic effect of the yeast, but microbial populations were not followed. This prebiotic effect was supposed to be associated with the use of yeast cell wall material (such as glucans, mannoproteins and chitin) as substrates for microbial fermentation by various SCFA-producing bacteria. We can thus speculate that the effects observed in the CANIM-ARCOL when *S. boulardii* was added was linked to pathogen binding or agglutination, antimicrobial effect or prebiotic effect, independently of any involvement of the yeast in immune response or cells interactions. This is also supported by the fact that *S. boulardii* treatment increased the relative abundance of beneficial family *Lactobacillaceae* while *Enterobacteriaceae* ones decreased in our *in vitro* study. Further investigations could be performed to verify this hypothesis such as repeating the same study with tyndallized *S. boulardii* and/or with glucans, mannoproteins and chitin purified or in cocktail to evaluate relative importance of each cell walls components in the observed effects.

The principal mode of action envisaged for heat-inactivated bacteria is related to interactions with host epithelial cells or immune system (Piqué, Berlanga & Miñana-Galbis, 2019; Pais *et al.*, 2020; Rawling *et al.*, 2022) and those of inactivated *L. helveticus* HA-122 was supposed to be mainly based on cell wall properties. The heat-inactivation process was developed by Lallemand to keep intact bacterial cells, and cell walls characterization is ongoing (not published). Based on literature data, we can yet make some hypothesis. In particular, study showed that lipoteichoic acids purified from *Lactobacillus* inhibited biofilm formation by *S. mutans*, *S. aureus* or *Enterococcus faecalis in vitro* (Ahn *et al.*, 2018). Another possibility would involve the lectin domain at the surface of bacteria which has been shown anti-biofilm effects for *E. coli* and *Salmonella* biofilm formation (Ma, Tu & Chen, 2023). Finally, some co-aggregation mechanisms may occur between heat-inactivated *L. helveticus* and live bacteria. Further characterizations of *L. helveticus* tyndallized cells are necessary to verify if adhesion site or receptors are conserved during heat treatment and also if they are still active. Altogether, these results suggested that both probiotic *S. boulardii* and postbiotic *L. helveticus* may be promising restoration strategies for canine microbiota disturbed by antibiotherapy.

Towards of a more complex model of antibiotic-induced perturbations and other applications of restoration strategies

Administration of antibiotics to dogs is generally associated to the treatment of acute diarrhea, which are induced in most of cases by enteric pathogens such as enteroinvasive (i.e. *E. coli*, *Salmonella*, *Shigella*, *Campylobacter*) or enterotoxigenic bacteria (i.e. *Clostridium*, *S. aureus* and *Klebsiella*) (Suchodolski *et al.*,

2012). In this study, microbiota disturbance was induced by antibiotic supplementation alone and we did not reproduce enteric infection. A step forward to the dysbiotic model development will be to introduce an enteric pathogen prior to the antibiotic period to be closer to the *in vivo* situation. We could therefore investigate the potential of the live yeast *S. boulardii* CNCM I-1079 or the heat-inactivated postbiotic *L. helveticus* HA-122 to mitigate the negative effects of both enteric pathogens and antibiotics. For example, we could follow pathogen colonization in the bioreactors and mucin beads but also toxin synthesis and expression of virulence genes as previously performed in human (Roussel *et al.*, 2016; Fehlbaum *et al.*, 2016; Bondue *et al.*, 2020) or pig (Gresse *et al.*, 2021b) conditions. However, further investigations will be necessary to determine the in-field dose of pathogen, since most of the time they are not quantified prior to treatment in canine faecal sample. In addition also, it was demonstrated an absence of correlation between diarrhea occurrence and toxin or endospores quantity (Marks *et al.*, 2011).

Our *in vitro* dysbiotic model (complexified or not by the addition of an enteric pathogen) can be a useful platform to evaluate the impact of new restorations strategies. As an example, very few studies have investigated the impact of prebiotics on microbiota recovery after antibiotherapy, but promising results have been evidenced in rats receiving cephalexin and supplemented with GOS for 5 days (Omer *et al.*, 2020). Effect of next generation prebiotics such as GOS, MOS and XOS on microbiota perturbation and resilience during and after antibiotherapy can be evaluated, administered alone or combined with pro-or postbiotics. In an original way also, the efficiency of FMT, which is to date more intended for research purposes than practical applications in dogs, can be also evaluated in the CANIM-ARCOL. Thanks to this *in vitro* tool, we can provide relevant information on the kinetic of gut microbiota restoration after FMT, as previously assessed under human condition (Verdier *et al.*, 2021). In a near future, depending on industrial needs, we can consider setting up screening tests or dose and frequency administration studies on different products to improve efficacy and safety for example. Finally, the model can be also easily adapted to reproduce dysbiosis associated to other antibiotic cocktails, opening new avenues for the evaluation of emerging restorations strategies.

C. *From in vitro simulation to marketing of protective microbial products*

This PhD project was divided in four parts, based all on *in vitro* approaches using the M-ARCOL model. The first one aimed to define the best conditions for stool sample storage, the second one intended to decipher the impact of dog size on canine colonic fermentation, the third focused on the impact of antibiotherapy on canine colonic microbiota, and the last one was dedicated to the study of pro- and postbiotics restoration strategies. Regarding this last part, this PhD project opens new avenues in the development of protective microbial products, but additional steps are obviously required before any commercialization in dogs.

Potential of other in vitro gut models to collect additional data

Results obtained during this PhD work can be completed by the use of additional *in vitro* gut models. First, the development of miniature bioreactors mimicking the canine large intestine, simpler and costless

compared to the CANIM-ARCOL, would allow the screening of a higher number of new feed additives or ingredients. This type of approach would permit to efficiently select the most relevant products for further *in vitro* investigation in more complex models like CANIM-ARCOL or M-SHIME and accelerate research in this field. Miniature bioreactors would also allow to increase the number of tested donors and better consider inter-individual variabilities to move towards more personalized approaches. Another complementary *in vitro* model is the FIDO system (based on the TIM-1 technology) that could be used to evaluate the fate of any compounds of interest in the upper GIT of dogs before entering the colon (Smeets-Peeters *et al.*, 1999b, 1999a). This *in vitro* model can provide valuable information about the impact of upper digestive tract parameters, such as acid pH, digestive enzymes or bile, on probiotic survival, macronutrients digestibility or micronutrients bioaccessibility, as well as their effects on enteric pathogen survival and virulence, as previously done in humans (Roussel *et al.*, 2016, 2021; Venema *et al.*, 2020; Uriot *et al.*, 2021). Up to now, this model has been set-up only under healthy medium size dog conditions, but as for the CANIM-ARCOL, if *in vivo* data are available in the future, we can fully consider its adaptation to other sizes or even diseased situation. Finally, the last but not least complementary approach would be the adaptation of the ESIN model to simulate the canine situation. To date, ESIN is the most complex *in vitro* gut model of the upper GIT, integrating all parameters found in the TIM-1 model plus the possibility to digest real size of food particles and the simulation of differential gastric emptying allowing to separate liquids and solids (Guerra *et al.*, 2016). As an example, the canine ESIN would provide first information about the importance of food particles size on nutrient digestibility, which could be of interest since dogs swallow larger pieces of food compared to humans (Kararli, 1995). The ESIN model will be soon further improved to reproduce the ileal microbiota, for which there is yet an increasing interest in human health (Roberti *et al.*, 2022). However, canine microbiota research is not enough advanced compared to the human one, and years will be necessary to reach this step.

Incorporating host response by coupling in vitro models with cell culture

All the *in vitro* gut models are obviously deprived of the host component and are not able to reproduce gut barrier functions as well as all facets of nervous, hormonal and immune systems. To improve the relevance of the healthy and dysbiotic CANIM-ARCOL models, we can integrate a part of the host components by coupling the model with canine intestinal or immune cells. It would be for the present study of particular necessity since *S. boulardii* and *L. helveticus* are supposed to act through interactions with those cells. To date, such adaptation have been already successfully performed with *in vitro* models set under human (Marzorati *et al.*, 2014; Cai *et al.*, 2017; Defois *et al.*, 2018; Calatayud *et al.*, 2021) or pig conditions (Gresse *et al.*, 2021b, 2021c), allowing to follow expression level of genes encoding for mucins, tight junction proteins but also innate immune pathway, and pro-inflammatory response. In addition, gut-on-a-chip devices should be also coupled to fermentation models. A recent adaptation of such approach allowed to perform pharmacological and toxicological analyses by coupling digestion processes in mouth, stomach and intestine (including digestive secretions) to intestinal cells (De Haan *et al.*, 2021). However, these adaptations were never achieved with canine *in vitro* gut models. Different canine cells lines are available, such as monolayers cells of jejunum (Weng,

Beyenbach & Quaroni, 2005), or canine intestinal epithelial cells (cIEC, Farquhar *et al.*, 2018). Of note, the relevance of human epithelial colorectal adenocarcinoma cells (Caco-2) and Madin-Darby canine kidney (MDCK) cells for modelling intestinal epithelial interactions of the dog was evaluated, and the authors conclude that this approach seemed to be not appropriated (Rubas, Jezyk & Grass, 1993). Especially, Caco-2 cells were not able to efficiently reproduce the intestinal permeability of the dog and several differences are still occurring between the Caco-2 model and canine small intestine regarding drug-metabolizing enzymes (Prueksaritanont *et al.*, 1996). The differences observed between human Caco-2 and canine cIEC suggest that species-specific models need to be considered when exploring barrier function. In addition, co-culture of intestinal cells and mucin-producing cells (as previously performed with human cells Caco2 and HT29 MTX cells lines, Béduneau *et al.*, 2014) or immune cells (macrophages or dendritic cells, Susewind *et al.*, 2015) can be also very informative, providing additional information on microbiota-microbial products interactions with other types of intestinal cells. However, to the best of my knowledge, such co-culture has never been achieved in dogs. Lastly, to increase again in cell complexity, it could be also envisaged to associate *in vitro* gut models with canine 3-dimensionsional organoids (Gabriel *et al.*, 2022). To date, the more complex canine organoid approach was enteroid and colonoid derived from tissue of more than 40 healthy dogs and dogs with gastrointestinal diseases, including IBD and intestinal carcinomas (Chandra *et al.*, 2019). Interestingly, coupling intestinal cells to *in vitro* gut models would be relevant to assess the impact of food, drugs or pathogens on barrier function, permeability, cell integrity and inflammation. Organoid models can be a complementary approach, allowing to study both healthy or diseased status in dogs and could be used for toxicology studies or analysis of host-pathogen interactions, providing a better simulation of the physiological and molecular features found in the tissue environment compared to two-dimensional cell cultures.

Next steps until marketing authorization for microbial products

The final step of product development will be their commercialization as **feed additives** or **veterinary medicinal products** (the only way to use the 'probiotic' or 'postbiotic' qualification). In France, EFSA regulates the use of **additives** for animal nutrition (regulation 1831/2003). Authorization could be delivered after evaluating quality and safety of additives for animals, consumers, users, and environment as well as their efficacy. To do so, ***in vivo* studies** involving dogs need to be performed with a minimum period of 28 days of product administration. ANMV (the French Agency for Veterinary Medicinal Products) within the ANSES is the competent authority in France for risk assessment and management of **veterinary medicinal products**. ANMV gives the marketing authorization after a procedure that requires providing information on the pharmaceutical quality of the product (including qualitative and quantitative constituents, manufacturing process, analysis methods and stability studies), on safety (toxicological data, pharmacokinetics and user safety study) and efficacy demonstrated by **pre-clinical and clinical** studies

Interestingly, regarding efficacy results provided by our *in vitro* study on *S. boulardii* CNCM I-1079 and heat-inactivated *L. helveticus* HA-122, we can thus speculate on a future commercialization of *S. boulardii* CNCM I-1079 as "**gut flora stabilizer**" (within feed additives category), recommended as restoration strategies

after antibiotic disturbance. The heat inactivated *L. helveticus* HA-122 is currently commercialized as raw material and our *in vitro* results demonstrated the efficacy of the product as restoration strategies after antibiotic disturbance. However, further experiments need to be performed to increase statistical power, provide further information about *L. helveticus* HA-122 modes of action and increase knowledges regarding potential host interactions. Of note, only clinical *in vivo* studies are approved by EFSA for toxicity, tolerance and efficiency studies, obviously meaning that a clinical study needs to be performed before commercialization of *S. boulardii* CNCM I-1079 for dogs. However, this PhD work have highlighted here the potential of *in vitro* gut model to provide relevant studies regarding products efficacy, in accordance with the confidence given by EFSA itself when requesting MEDIS services to evaluate the impact of nanocelluloses (used as human food additive) on the colonic gut microbiota using the M-ARCOL model. This led to the hope that dynamic *in vitro* gut models, together with complementary approaches can, in a near future, be alternative tools to replace *in vivo* clinical studies in regulatory and marketing processes.

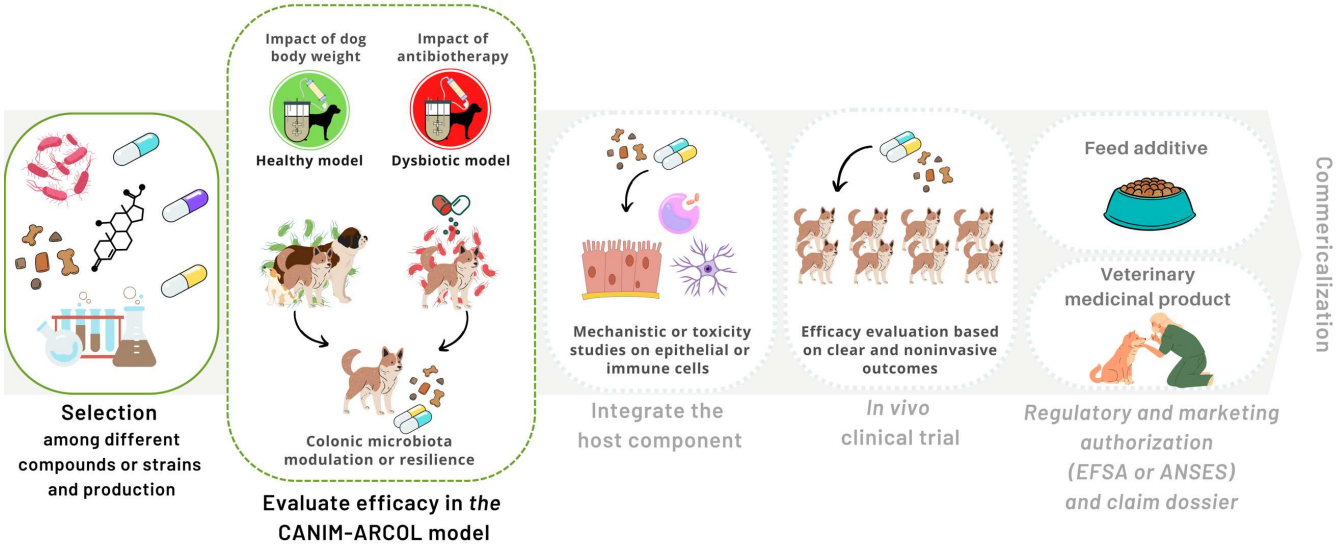

Figure III.1: Positioning of CANIM-ARCOL from compound selection to product commercialization.

CHAPTER 1

Fresh stools *are the best option if possible*

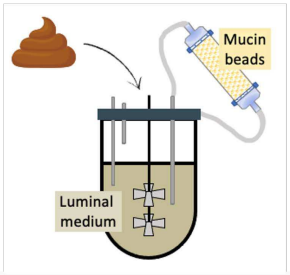

Simulation of healthy …

CHAPTER 2

Model development
In vitro simulation of physicochemical and microbial colonic ecosystem adapted to different dog sizes

ADAPTATION TO DOG SIZES
Simulated ileal effluents
Body temperature
Colonic pH
Colonic transit time
Anaerobiosis

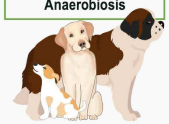

Size effect

LUMINAL MEDIUM	MUCIN BEADS
↘ Alpha-diversity ↗ *Bacteroidota* and *Firmicutes* ↘ *Actinobacteria*, *Fusobacteriota* and *Proteobacteria*	
↗ SCFA, BCFA, ammonia and gas production, total bile acids	

Validation of the model

1- with *in vivo* colonic da

- = 27/31 families maintained
- ≠ Except *Prevotellaceae*, *Streptococcaceae*, *Turicibacteraceae* and *Veillonellaceae*

Suchodolski et al., 2008 & Honneffer et al., 2017

2- with *in vivo* faecal da

- = 4/5 phyla
- = 4/12 activity parameters
- ± 5/12 activity parameters
- ≠ 3/12 activity parameters (isovalerate, isobutyrate and valerate concentrations)

Deschamps et al. 2022, IJBS

CHAPTER 3

Mechanistic study
Relative importance of gut microbes and environmental parameters to reshape size-related microbiota

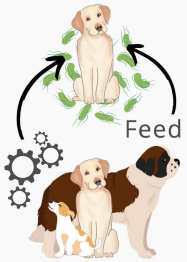

- = Environmental parameters sufficient to reproduce microbiota activities
- ≠ Faecal size-related inoculum necessary to reproduce bacteria composition

… or diseased conditions

CHAPTER 4

Model development
In vitro simulation of colonic dysbiosis associated to antibiotherapy in medium dogs

Metronidazole/ Enrofloxacin 5 days

Antibiotic effect

LUMINAL MEDIUM	MUCIN BEADS
↘ Alpha-diversity ↗ *Enterobacteriaceae*, *Streptococcaceae* and *Lactobacillaceae* ↗ Dysbiosis score ↘ SCFA production Alteration of putative metabolic pathways	Similar but lower impact

Resilience after antibiotherapy

Alpha diversity and microbiota composition (1 week after)
Alteration of dysbiosis index and putative metabolic pathways (2 weeks after)

Validation of the model with *in vivo* faecal data

- = 12/21 families
- = 3/4 activity parameters
- ≠ Except *Actinobacteria*, *Proteobacteria*, *Ruminococcaceae* & *Erysipelotrichaceae*

Whittemore et al. 2021

CHAPTER 4

Restoration strategies
Impact of probiotic and postbiotic on microbiota resilience after antibiotherapy

Metronidazole/ Enrofloxacin 5 days

SB and LH effects

During antibiotherapy ↘ *Enterobacteriaceae* ↘ Variability of results	No impact on microbiota activity
After antibiotherapy ↗ Microbiota composition and activity resilience (within 2 days) for bacterial load, diversity and SCFA production ↘ Alteration of putative metabolic pathways	

Figure III.3: Main results of the PhD thesis on the impact of body weight and antibiotic disturbance on canine gut microbiota, and testing of restoration strategies. This joint PhD between MEDIS (Clermont-Ferrand), Lallemand Animal Nutrition (Blagnac) and Dômes Pharma (Pont-du-Château) aimed to investigate the impact of body weight and antibiotic disturbance on canine gut microbiota. This PhD project was divided in four parts, all based on *in vitro* approaches using the M-ARCOL model. The first one aimed to define the best conditions for stool sample storage, the second one intended to decipher the impact of dog size on canine colonic digestive physiology and associated microbiota, the third focused on the impact of antibiotherapy on canine colonic microbiota, and the last one was dedicated to the study of pro- and postbiotics as restoration strategies. Regarding this last part, this PhD project opens new avenues in the development of protective microbial products, but additional steps are obviously required before any commercialization in dogs. *SCFA: short-chain fatty acids, BCFA: branched-chain fatty acids.*

REFERENCES

AGUIRRE, M., ECK, A., KOENEN, M.E., SAVELKOUL, P.H.M., BUDDING, A.E. & VENEMA, K. (2015) Evaluation of an optimal preparation of human standardized fecal inocula for *in vitro* fermentation studies. *Journal of Microbiological Methods* **117**, 78–84.

AGUIRRE, M., RAMIRO-GARCIA, J., KOENEN, M.E. & VENEMA, K. (2014) To pool or not to pool? Impact of the use of individual and pooled fecal samples for *in vitro* fermentation studies. *Journal of Microbiological Methods* **107**, 1–7.

AHN, K.B., BAIK, J.E., PARK, O.-J., YUN, C.-H. & HAN, S.H. (2018) Lactobacillus plantarum lipoteichoic acid inhibits biofilm formation of *Streptococcus mutans*. *PloS One* **13**, e0192694.

AIBA, Y., ISHIKAWA, H., TOKUNAGA, M. & KOMATSU, Y. (2017) Anti-*Helicobacter pylori* activity of non-living, heat-killed form of *lactobacilli* including *Lactobacillus johnsonii* No.1088. *FEMS microbiology letters* **364**.

AKIMOTO, M., NAGAHATA, N., FURUYA, A., FUKUSHIMA, K., HIGUCHI, S. & SUWA, T. (2000) Gastric pH profiles of beagle dogs and their use as an alternative to human testing. *European Journal of Pharmaceutics and Biopharmaceutics: Official Journal of Arbeitsgemeinschaft Fur Pharmazeutische Verfahrenstechnik e.V* **49**, 99–102.

AKTAS, M.S., BORKU, M.K. & OZKANLAR, Y. (2007) Efficacy of *Saccharomyces boulardii* as a probiotic in dogs with lincomycin induced diarrhoea. *Bull Vet Inst Pulawy* **51**, 365–369.

AL, K.F., BISANZ, J.E., GLOOR, G.B., REID, G. & BURTON, J.P. (2018) Evaluation of sampling and storage procedures on preserving the community structure of stool microbiota: A simple at-home toilet-paper collection method. *Journal of Microbiological Methods* **144**, 117–121.

ALBENBERG, L., ESIPOVA, T.V., JUDGE, C.P., BITTINGER, K., CHEN, J., LAUGHLIN, A., GRUNBERG, S., BALDASSANO, R.N., LEWIS, J.D., LI, H., THOM, S.R., BUSHMAN, F.D., VINOGRADOV, S.A. & WU, G.D. (2014) Correlation between intraluminal oxygen gradient and radial partitioning of intestinal microbiota. *Gastroenterology* **147**, 1055-1063.e8.

ALEXANDER, C., CROSS, T.-W.L., DEVENDRAN, S., NEUMER, F., THEIS, S., RIDLON, J.M., SUCHODOLSKI, J.S., DE GODOY, M.R.C. & SWANSON, K.S. (2018) Effects of prebiotic inulin-type fructans on blood metabolite and hormone concentrations and faecal microbiota and metabolites in overweight dogs. *The British Journal of Nutrition* **120**, 711–720.

ALEXANDER, C., GUARD, B.C., SUCHODOLSKI, J.S. & SWANSON, K.S. (2019) Cholestyramine decreases apparent total tract macronutrient digestibility and alters fecal characteristics and metabolites of healthy adult dogs. *Journal of Animal Science* **97**, 1020–1026.

ALGYA, K.M., CROSS, T.-W.L., LEUCK, K.N., KASTNER, M.E., BABA, T., LYE, L., DE GODOY, M.R.C. & SWANSON, K.S. (2018) Apparent total-tract macronutrient digestibility, serum chemistry, urinalysis, and fecal characteristics, metabolites and microbiota of adult dogs fed extruded, mildly cooked, and raw diets1. *Journal of Animal Science* **96**, 3670–3683.

ALLERTON, F., PRIOR, C., BAGCIGIL, A.F., BROENS, E., CALLENS, B., DAMBORG, P., DEWULF, J., FILIPPITZI, M.-E., CARMO, L.P., GÓMEZ-RAJA, J., HARPAZ, E., MATEUS, A., NOLFF, M., PHYTHIAN, C.J., TIMOFTE, D., *ET AL.* (2021) Overview and Evaluation of Existing Guidelines for Rational Antimicrobial Use in Small-Animal Veterinary Practice in Europe. *Antibiotics (Basel, Switzerland)* **10**, 409.

ALSHAWAQFEH, M.K., WAJID, B., MINAMOTO, Y., MARKEL, M., LIDBURY, J.A., STEINER, J.M., SERPEDIN, E. & SUCHODOLSKI, J.S. (2017) A dysbiosis index to assess microbial changes in fecal samples of dogs with chronic inflammatory enteropathy. *FEMS microbiology ecology* **93**.

ALVARO, D., CANTAFORA, A., ATTILI, A.F., GINANNI CORRADINI, S., DE LUCA, C., MINERVINI, G., DI BLASE, A. & ANGELICO, M. (1986) Relationships between bile salts hydrophilicity and phospholipid composition in bile of various animal species. *Comparative Biochemistry and Physiology Part B: Comparative Biochemistry* **83**, 551–554.

ANDOH, A. (2016) Physiological Role of Gut Microbiota for Maintaining Human Health. *Digestion* **93**, 176–181.

APPER, E., PRIVET, L., TAMINIAU, B., LE BOURGOT, C., SVILAR, L., MARTIN, J.-C. & DIEZ, M. (2020) Relationships Between Gut Microbiota, Metabolome, Body Weight, and Glucose Homeostasis of Obese Dogs Fed with Diets Differing in Prebiotic and Protein Content. *Microorganisms* **8**.

ARMOUGOM, F., HENRY, M., VIALETTES, B., RACCAH, D. & RAOULT, D. (2009) Monitoring bacterial community of human gut microbiota reveals an increase in Lactobacillus in obese patients and Methanogens in anorexic patients. *PloS One* **4**, e7125.

ASNICAR, F., LEEMING, E.R., DIMIDI, E., MAZIDI, M., FRANKS, P.W., AL KHATIB, H., VALDES, A.M., DAVIES, R., BAKKER, E., FRANCIS, L., CHAN, A., GIBSON, R., HADJIGEORGIOU, G., WOLF, J., SPECTOR, T.D., *ET AL.* (2021) Blue poo: impact of gut transit time on the gut microbiome using a novel marker. *Gut* **70**, 1665–1674.

ASPINALL, V. (2004) Anatomy and Physiology of the Dog and Cat **8. The Digestive System**. *Veterinary Nursing Journal* **19**, 94–99.

AXELSSON, E., RATNAKUMAR, A., ARENDT, M.-L., MAQBOOL, K., WEBSTER, M.T., PERLOSKI, M., LIBERG, O., ARNEMO, J.M., HEDHAMMAR, Å. & LINDBLAD-TOH, K. (2013) The genomic signature of dog domestication reveals adaptation to a starch-rich diet. *Nature* **495**, 360–364.

BACCHETTI DE GREGORIS, T., ALDRED, N., CLARE, A.S. & BURGESS, J.G. (2011) Improvement of phylum- and class-specific primers for real-time PCR quantification of bacterial taxa. *Journal of Microbiological Methods* **86**, 351–356.

BAHRAMI, B., CHILD, M.W., MACFARLANE, S. & MACFARLANE, G.T. (2011) Adherence and Cytokine Induction in Caco-2 Cells by Bacterial Populations from a Three-Stage Continuous-Culture Model of the Large Intestine. *Applied and Environmental Microbiology* **77**, 2934–2942. American Society for Microbiology.

BAILLON, M.-L.A., MARSHALL-JONES, Z.V. & BUTTERWICK, R.F. (2004) Effects of probiotic Lactobacillus acidophilus strain DSM13241 in healthy adult dogs. *American Journal of Veterinary Research* **65**, 338–343.

BALSA, I.M., CULP, W.T.N., DROBATZ, K.J., JOHNSON, E.G., MAYHEW, P.D. & MARKS, S.L. (2017) Effect of Laparoscopic-assisted Gastropexy on Gastrointestinal Transit Time in Dogs. *Journal of Veterinary Internal Medicine* **31**, 1680–1685.

BARKO, P.C., MCMICHAEL, M.A., SWANSON, K.S. & WILLIAMS, D.A. (2018) The Gastrointestinal Microbiome: A Review. *Journal of Veterinary Internal Medicine* **32**, 9–25.

BARMPATSALOU, V., DUBBELBOER, I.R., RODLER, A., JACOBSON, M., KARLSSON, E., PEDERSEN, B.L. & BERGSTRÖM, C.A.S. (2021) Physiological properties, composition and structural profiling of porcine gastrointestinal mucus. *European Journal of Pharmaceutics and Biopharmaceutics: Official Journal of Arbeitsgemeinschaft Fur Pharmazeutische Verfahrenstechnik e.V* **169**, 156–167.

BARROSO, E., CUEVA, C., PELÁEZ, C., MARTÍNEZ-CUESTA, M.C. & REQUENA, T. (2015) The Computer-Controlled Multicompartmental Dynamic Model of the Gastrointestinal System SIMGI. In *The Impact of Food Bioactives on Health: in vitro and ex vivo models* (eds K. VERHOECKX, P. COTTER, I. LÓPEZ-EXPÓSITO, C. KLEIVELAND, T. LEA, A. MACKIE, T. REQUENA, D. SWIATECKA & H. WICHERS), p. Springer, Cham (CH).

BASSIS, C.M., MOORE, N.M., LOLANS, K., SEEKATZ, A.M., WEINSTEIN, R.A., YOUNG, V.B. & HAYDEN, M.K. (2017) Comparison of stool versus rectal swab samples and storage conditions on bacterial community profiles. *BMC Microbiology* **17**.

BASTOS, T.S., SOUZA, C.M.M., LEGENDRE, H., RICHARD, N., PILLA, R., SUCHODOLSKI, J.S., DE OLIVEIRA, S.G., LESAUX, A.A. & FÉLIX, A.P. (2023) Effect of Yeast Saccharomyces cerevisiae as a Probiotic on Diet Digestibility, Fermentative Metabolites, and Composition and Functional Potential of the Fecal Microbiota of Dogs Submitted to an Abrupt Dietary Change. *Microorganisms* **11**, 506.

BAUM, B., MENESES, F., KLEINSCHMIDT, S., NOLTE, I. & HEWICKER-TRAUTWEIN, M. (2007) Age-related histomorphologic changes in the canine gastrointestinal tract: a histologic and immunohistologic study. *World Journal of Gastroenterology* **13**, 152–157.

BEDNAR, G.E., MURRAY, S.M., PATIL, A.R., FLICKINGER, E.A., MERCHEN, N.R. & FAHEY, G.C. (2000) Selected animal and plant protein sources affect nutrient digestibility and fecal characteristics of ileally cannulated dogs. *Archiv Fur Tierernahrung* **53**, 127–140.

BÉDUNEAU, A., TEMPESTA, C., FIMBEL, S., PELLEQUER, Y., JANNIN, V., DEMARNE, F. & LAMPRECHT, A. (2014) A tunable Caco-2/HT29-MTX co-culture model mimicking variable permeabilities of the human

intestine obtained by an original seeding procedure. *European Journal of Pharmaceutics and Biopharmaceutics* **87**, 290–298.

BELCHIK, S.E., OBA, P.M., WYSS, R., ASARE, P.T., VIDAL, S., MIAO, Y., ADESOKAN, Y., SUCHODOLSKI, J.S. & SWANSON, K.S. (2023) Effects of a milk oligosaccharide biosimilar on fecal characteristics, microbiota, and bile acid, calprotectin, and immunoglobulin concentrations of healthy adult dogs treated with metronidazole. *Journal of Animal Science* **101**, skad011.

BELL, J.A., KOPPER, J.J., TURNBULL, J.A., BARBU, N.I., MURPHY, A.J. & MANSFIELD, L.S. (2008) Ecological Characterization of the Colonic Microbiota of Normal and Diarrheic Dogs. *Interdisciplinary Perspectives on Infectious Diseases* **2008**, 1–17.

BELL, S.E., NASH, A.K., ZANGHI, B.M., OTTO, C.M. & PERRY, E.B. (2020) An Assessment of the Stability of the Canine Oral Microbiota After Probiotic Administration in Healthy Dogs Over Time. *Frontiers in Veterinary Science* **7**, 616.

BELOSHAPKA, A.N., ALEXANDER, L.G., BUFF, P.R. & SWANSON, K.S. (2014) The effects of feeding resistant starch on apparent total tract macronutrient digestibility, faecal characteristics and faecal fermentative end-products in healthy adult dogs. *Journal of Nutritional Science* **3**, e38.

BELOSHAPKA, A.N., DE GODOY, M.R.C., DETWEILER, K.B., NEWCOMB, M., ELLEGÅRD, K.H., FAHEY, G.C. & SWANSON, K.S. (2016) Apparent total tract macronutrient digestibility, fecal characteristics, and fecal fermentative end-product concentrations of healthy adult dogs fed bioprocessed soy protein. *Journal of Animal Science* **94**, 3826–3834.

BELOSHAPKA, A.N., WOLFF, A.K. & SWANSON, K.S. (2012) Effects of feeding polydextrose on faecal characteristics, microbiota and fermentative end products in healthy adult dogs. *The British Journal of Nutrition* **108**, 638–644.

BELZER, C., CHIA, L.W., AALVINK, S., CHAMLAGAIN, B., PIIRONEN, V., KNOL, J. & DE VOS, W.M. (2017) Microbial Metabolic Networks at the Mucus Layer Lead to Diet-Independent Butyrate and Vitamin B_{12} Production by Intestinal Symbionts. *mBio* **8**, e00770-17.

BENNO, Y., NAKAO, H., UCHIDA, K. & MITSUOKA, T. (1992) Impact of the advances in age on the gastrointestinal microflora of beagle dogs. *The Journal of Veterinary Medical Science* **54**, 703–706.

BENYACOUB, J., CZARNECKI-MAULDEN, G.L., CAVADINI, C., SAUTHIER, T., ANDERSON, R.E., SCHIFFRIN, E.J. & VON DER WEID, T. (2003) Supplementation of food with Enterococcus faecium (SF68) stimulates immune functions in young dogs. *The Journal of Nutrition* **133**, 1158–1162.

BERMUDEZ SANCHEZ, S., PILLA, R., SARAWICHITR, B., GRAMENZI, A., MARSILIO, F., STEINER, J.M., LIDBURY, J.A., WOODS, G.R.T., GERMAN, A.J. & SUCHODOLSKI, J.S. (2020) Fecal microbiota in client-owned obese dogs changes after weight loss with a high-fiber-high-protein diet. *PeerJ* **8**, e9706.

BHATTACHAR, S.N., PERKINS, E.J., TAN, J.S. & BURNS, L.J. (2011) Effect of gastric pH on the pharmacokinetics of a BCS class II compound in dogs: utilization of an artificial stomach and duodenum dissolution model and GastroPlus,™ simulations to predict absorption. *Journal of Pharmaceutical Sciences* **100**, 4756–4765.

BIAGI, G., CIPOLLINI, I. & ZAGHINI, G. (2008) *In vitro* fermentation of different sources of soluble fiber by dog faecal inoculum. *Veterinary Research Communications* **32**, 335–337.

BIANCHI, F., LOPES, N.P., ADORNO, M.A.T., SAKAMOTO, I.K., GENOVESE, M.I., SAAD, S.M.I. & SIVIERI, K. (2019) Impact of combining acerola by-product with a probiotic strain on a gut microbiome model. *International Journal of Food Sciences and Nutrition* **70**, 182–194.

BICKEL, M. & KAUFFMAN, G.L. (1981) Gastric gel mucus thickness: effect of distention, 16,16-dimethyl prostaglandin e2, and carbenoxolone. *Gastroenterology* **80**, 770–775.

BJARNASON, I., MACPHERSON, A. & HOLLANDER, D. (1995) Intestinal permeability: an overview. *Gastroenterology* **108**, 1566–1581.

BLACHIER, F., MARIOTTI, F., HUNEAU, J.F. & TOMÉ, D. (2007) Effects of amino acid-derived luminal metabolites on the colonic epithelium and physiopathological consequences. *Amino Acids* **33**, 547–562.

BLAKE, A.B., CIGARROA, A., KLEIN, H.L., KHATTAB, M.R., KEATING, T., VAN DE COEVERING, P., LIDBURY, J.A., STEINER, J.M. & SUCHODOLSKI, J.S. (2020) Developmental stages in microbiota, bile acids, and clostridial species in healthy puppies. *Journal of Veterinary Internal Medicine* **34**, 2345–2356.

BLAKE, A.B., GUARD, B.C., HONNEFFER, J.B., LIDBURY, J.A., STEINER, J.M. & SUCHODOLSKI, J.S. (2019) Altered microbiota, fecal lactate, and fecal bile acids in dogs with gastrointestinal disease. *PLOS ONE* **14**, e0224454.

BLAKE, A.B. & SUCHODOLSKI, J.S. (2016) Importance of gut microbiota for the health and disease of dogs and cats. *Animal Frontiers* **6**, 37–42.

BLANCQUAERT, L., VERVAET, C. & DERAVE, W. (2019) Predicting and Testing Bioavailability of Magnesium Supplements. *Nutrients* **11**.

BLANQUET, S., ZEIJDNER, E., BEYSSAC, E., MEUNIER, J.-P., DENIS, S., HAVENAAR, R. & ALRIC, M. (2004) A dynamic artificial gastrointestinal system for studying the behavior of orally administered drug dosage forms under various physiological conditions. *Pharmaceutical Research* **21**, 585–591.

BLANQUET-DIOT, S., DENIS, S., CHALANCON, S., CHAIRA, F., CARDOT, J.-M. & ALRIC, M. (2012) Use of Artificial Digestive Systems to Investigate the Biopharmaceutical Factors Influencing the Survival of Probiotic Yeast During Gastrointestinal Transit in Humans. *Pharmaceutical Research* **29**, 1444–1453.

BOILLAT, C.S., GASCHEN, F.P. & HOSGOOD, G.L. (2010) Assessment of the relationship between body weight and gastrointestinal transit times measured by use of a wireless motility capsule system in dogs. *American Journal of Veterinary Research* **71**, 898–902.

BOLYEN, E., RIDEOUT, J.R., DILLON, M.R., BOKULICH, N.A., ABNET, C.C., AL-GHALITH, G.A., ALEXANDER, H., ALM, E.J., ARUMUGAM, M., ASNICAR, F., BAI, Y., BISANZ, J.E., BITTINGER, K., BREJNROD, A., BRISLAWN, C.J., *ET AL.* (2019) Reproducible, interactive, scalable and extensible microbiome data science using QIIME 2. *Nature Biotechnology* **37**, 852–857.

BONDUE, P., LEBRUN, S., TAMINIAU, B., EVERAERT, N., LAPOINTE, G., CREVECOEUR, S., DAUBE, G. & DELCENSERIE, V. (2020) A toddler SHIME® model to study microbiota of young children. *FEMS microbiology letters* **367**.

BOSCAN, P., COCHRAN, S., MONNET, E., WEBB, C. & TWEDT, D. (2013) Effect of prolonged general anesthesia with sevoflurane and laparoscopic surgery on gastric and small bowel propulsive motility and pH in dogs. *Veterinary Anaesthesia and Analgesia* **41**, 73–81.

BOSCH, G., PELLIKAAN, W.F., RUTTEN, P.G.P., VAN DER POEL, A.F.B., VERSTEGEN, M.W.A. & HENDRIKS, W.H. (2008) Comparative *in vitro* fermentation activity in the canine distal gastrointestinal tract and fermentation kinetics of fiber sources. *Journal of Animal Science* **86**, 2979–2989.

BOSCH, G., WRIGGLESWORTH, D.J., CONE, J.W., PELLIKAAN, W.F. & HENDRIKS, W.H. (2013) Effects of preservation conditions of canine feces on *in vitro* gas production kinetics and fermentation end products. *Journal of Animal Science* **91**, 259–267.

BOTIGUÉ, L.R., SONG, S., SCHEU, A., GOPALAN, S., PENDLETON, A.L., OETJENS, M., TARAVELLA, A.M., SEREGÉLY, T., ZEEB-LANZ, A., ARBOGAST, R.-M., BOBO, D., DALY, K., UNTERLÄNDER, M., BURGER, J., KIDD, J.M., *ET AL.* (2017) Ancient European dog genomes reveal continuity since the Early Neolithic. *Nature Communications* **8**, 16082.

BOTTERO, E., BENVENUTI, E. & RUGGIERO, P. (2017) Faecal Microbiota Transplantation in 16 Dogs with Idiopathic Inflammatory Bowel Disease. *Veterinaria* **31**, 1–12.

BOTTERO, E., FERRIANI, R., BENVENUTI, E., RUGGIERO, P., ASTORINA, S., GIRALDI, M., BERTOLDI, L., BENVENUTO, G., SATTIN, E., GIANELLA, P. & SUCHODOLSKI, J.S. (2022) Clinical evaluation and microbiota analysis in 9 dogs with antibiotic-responsive enteropathy: A prospective comparison study. *Journal of Veterinary Internal Medicine* **36**, 1220–1228.

BOUCARD, A.-S., THOMAS, M., LEBON, W., POLACK, B., FLORENT, I., LANGELLA, P. & BERMÚDEZ-HUMARÁN, L.G. (2021) Age and Giardia intestinalis Infection Impact Canine Gut Microbiota. *Microorganisms* **9**, 1862.

BOURREAU, J., HERNOT, D., BAILHACHE, E., WEBER, M., FERCHAUD, V., BIOURGE, V., MARTIN, L., DUMON, H. & NGUYEN, P. (2004) Gastric emptying rate is inversely related to body weight in dog breeds of different sizes. *The Journal of Nutrition* **134**, 2039S-2041S.

BRESCIANI, F., MINAMOTO, Y., SUCHODOLSKI, J.S., GALIAZZO, G., VECCHIATO, C.G., PINNA, C., BIAGI, G. & PIETRA, M. (2018) Effect of an extruded animal protein-free diet on fecal microbiota of dogs with food-responsive enteropathy. *Journal of Veterinary Internal Medicine* **32**, 1903–1910.

BRODKORB, A., EGGER, L., ALMINGER, M., ALVITO, P., ASSUNÇÃO, R., BALLANCE, S., BOHN, T., BOURLIEU-LACANAL, C., BOUTROU, R., CARRIÈRE, F., CLEMENTE, A., CORREDIG, M., DUPONT, D., DUFOUR, C., EDWARDS, C., *ET AL.* (2019) INFOGEST static *in vitro* simulation of gastrointestinal food digestion. *Nature Protocols* **14**, 991–1014.

BRUCE, S.J., GUILFORD, W.G., HEDDERLEY, D.I. & MCCAULEY, M. (1999) Development of reference intervals for the large intestinal transit of radiopaque markers in dogs. *Veterinary Radiology & Ultrasound: The Official Journal of the American College of Veterinary Radiology and the International Veterinary Radiology Association* **40**, 472–476.

BSAVA/SAMSOC (2018) PROTECT ME. In *BSAVA/SAMSoc Guide to Responsible Use of Antibacterials: PROTECT ME* (ed BSAVA AND SAMSOC), p. British Small Animal Veterinary Association.

BUDDINGTON, R.K. (2003) Postnatal changes in bacterial populations in the gastrointestinal tract of dogs. *American Journal of Veterinary Research* **64**, 646–651.

BURTON, E.N., O'CONNOR, E., ERICSSON, A.C. & FRANKLIN, C.L. (2016) Evaluation of Fecal Microbiota Transfer as Treatment for Postweaning Diarrhea in Research-Colony Puppies. *Journal of the American Association for Laboratory Animal Science: JAALAS* **55**, 582–587.

BURZ, S.D., ABRAHAM, A.-L., FONSECA, F., DAVID, O., CHAPRON, A., BEGUET-CRESPEL, F., CENARD, S., LE ROUX, K., PATRASCU, O., LEVENEZ, F., SCHWINTNER, C., BLOTTIERE, H.M., BERA-MAILLET, C., LEPAGE, P., DORE, J., *ET AL.* (2019) A Guide for Ex Vivo Handling and Storage of Stool Samples Intended for Fecal Microbiota Transplantation. *Scientific Reports* **9**, 8897.

BUSSOLO DE SOUZA, C., ROESELERS, G., TROOST, F., JONKERS, D., KOENEN, M.E. & VENEMA, K. (2014) Prebiotic effects of cassava bagasse in TNO's *in vitro* model of the colon in lean versus obese microbiota. *Journal of Functional Foods* **11**, 210–220.

CAI, X., CHEN, X., YIN, N., DU, H., SUN, G., WANG, L., XU, Y., CHEN, Y. & CUI, Y. (2017) Estimation of the bioaccessibility and bioavailability of Fe, Mn, Cu, and Zn in Chinese vegetables using the *in vitro* digestion/Caco-2 cell model: the influence of gut microbiota. *Food & Function* **8**, 4592–4600.

CAI, X., LIAO, R., CHEN, G., LU, Y., ZHAO, Y. & CHEN, Y. (2022) The influence of food processing methods on serum parameters, apparent total-tract macronutrient digestibility, fecal microbiota and SCFA content in adult beagles. *PloS One* **17**, e0262284.

CALATAYUD, M., BÖRNER, R.A., GHYSELINCK, J., VERSTREPEN, L., MEDTS, J.D., ABBEELE, P.V.D., BOULANGÉ, C.L., PRIOUR, S., MARZORATI, M. & DAMAK, S. (2021) Water Kefir and Derived Pasteurized Beverages Modulate Gut Microbiota, Intestinal Permeability and Cytokine Production *In vitro*. *Nutrients* **13**, 3897.

CALLAHAN, B.J., MCMURDIE, P.J., ROSEN, M.J., HAN, A.W., JOHNSON, A.J.A. & HOLMES, S.P. (2016) DADA2: High-resolution sample inference from Illumina amplicon data. *Nature Methods* **13**, 581–583.

CAMMAROTA, G., IANIRO, G., GASBARRINI, A., & EUROPEAN FMT WORKING GROUP (2018) Faecal microbiota transplantation in clinical practice. *Gut* **67**, 196–197.

CAMMAROTA, G., IANIRO, G., KELLY, C.R., MULLISH, B.H., ALLEGRETTI, J.R., KASSAM, Z., PUTIGNANI, L., FISCHER, M., KELLER, J.J., COSTELLO, S.P., SOKOL, H., KUMP, P., SATOKARI, R., KAHN, S.A., KAO, D., *ET AL.* (2019) International consensus conference on stool banking for faecal microbiota transplantation in clinical practice. *Gut* **68**, 2111–2121.

CAMMAROTA, G., IANIRO, G., TILG, H., RAJILIĆ-STOJANOVIĆ, M., KUMP, P., SATOKARI, R., SOKOL, H., ARKKILA, P., PINTUS, C., HART, A., SEGAL, J., ALOI, M., MASUCCI, L., MOLINARO, A., SCALDAFERRI, F., *ET AL.* (2017) European consensus conference on faecal microbiota transplantation in clinical practice. *Gut* **66**, 569–580.

CAPONE, S.H., DUFRESNE, M., RECHEL, M., FLEURY, M.-J., SALSAC, A.-V., PAULLIER, P., DAUJAT-CHAVANIEU, M. & LEGALLAIS, C. (2013) Impact of alginate composition: from bead mechanical properties to encapsulated HepG2/C3A cell activities for *in vivo* implantation. *PloS One* **8**, e62032.

CARINO, S.R., SPERRY, D.C. & HAWLEY, M. (2006) Relative bioavailability estimation of carbamazepine crystal forms using an artificial stomach-duodenum model. *Journal of Pharmaceutical Sciences* **95**, 116–125.

CARRIÈRE, F., LAUGIER, R., BARROWMAN, J.A., DOUCHET, I., PRIYMENKO, N. & VERGER, R. (1993) Gastric

and pancreatic lipase levels during a test meal in dogs. *Scandinavian Journal of Gastroenterology* **28**, 443–454.

CASE, L., CAREY, D., HIRAKAWA, D. & DARISTOTLE, L. (2011) *Canine and feline nutrition: a resource for companion animal professionals*. Elsevier.

CASSMANN, E., WHITE, R., ATHERLY, T., WANG, C., SUN, Y., KHODA, S., MOSHER, C., ACKERMANN, M. & JERGENS, A. (2016) Alterations of the Ileal and Colonic Mucosal Microbiota in Canine Chronic Enteropathies. *PLOS ONE* **11**, e0147321.

DE CASTRO SANTOS MELO, C., DA SILVA FREIRE, A., GALDEANO, M.A., DA COSTA, C.F., DE OLIVEIRA GONÇALVES, A.P.D., DIAS, F.S. & MENEZES, D.R. (2021) Probiotic potential of Enterococcus hirae in goat milk and its survival in canine gastrointestinal conditions simulated *in vitro*. *Research in Veterinary Science* **138**, 188–195.

CESTER, C.C. & TOUTAIN, P.L. (1997) A comprehensive model for enrofloxacin to ciprofloxacin transformation and disposition in dog. *Journal of Pharmaceutical Sciences* **86**, 1148–1155.

CHAITMAN, J. & GASCHEN, F. (2020) Fecal Microbiota Transplantation in Dogs. *The Veterinary Clinics of North America. Small Animal Practice* **51**, 219–223.

CHAITMAN, J., ZIESE, A.-L., PILLA, R., MINAMOTO, Y., BLAKE, A.B., GUARD, B.C., ISAIAH, A., LIDBURY, J.A., STEINER, J.M., UNTERER, S. & SUCHODOLSKI, J.S. (2020) Fecal Microbial and Metabolic Profiles in Dogs with Acute Diarrhea Receiving Either Fecal Microbiota Transplantation or Oral Metronidazole. *Frontiers in Veterinary Science* **7**, 192.

CHANDRA, L., BORCHERDING, D.C., KINGSBURY, D., ATHERLY, T., AMBROSINI, Y.M., BOURGOIS-MOCHEL, A., YUAN, W., KIMBER, M., QI, Y., WANG, Q., WANNEMUEHLER, M., ELLINWOOD, N.M., SNELLA, E., MARTIN, M., SKALA, M., *ET AL.* (2019) Derivation of adult canine intestinal organoids for translational research in gastroenterology. *BMC biology* **17**, 33.

CHASSAING, B., KOREN, O., CARVALHO, F.A., LEY, R.E. & GEWIRTZ, A.T. (2014) AIEC pathobiont instigates chronic colitis in susceptible hosts by altering microbiota composition. *Gut* **63**, 1069–1080.

CHASSAING, B., VAN DE WIELE, T., DE BODT, J., MARZORATI, M. & GEWIRTZ, A.T. (2017) Dietary emulsifiers directly alter human microbiota composition and gene expression ex vivo potentiating intestinal inflammation. *Gut* **66**, 1414–1427.

CHAUDHARY, P.P., CONWAY, P.L. & SCHLUNDT, J. (2018) Methanogens in humans: potentially beneficial or harmful for health. *Applied Microbiology and Biotechnology* **102**, 3095–3104.

CHEN, E.P., MAHAR DOAN, K.M., PORTELLI, S., COATNEY, R., VADEN, V. & SHI, W. (2008) Gastric pH and gastric residence time in fasted and fed conscious cynomolgus monkeys using the Bravo pH system. *Pharmaceutical Research* **25**, 123–134.

CHEN, T., CHEN, D., TIAN, G., ZHENG, P., MAO, X., YU, J., HE, J., HUANG, Z., LUO, Y., LUO, J. & YU, B. (2019) Soluble Fiber and Insoluble Fiber Regulate Colonic Microbiota and Barrier Function in a Piglet Model. *BioMed Research International* **2019**, 7809171.

CHENG, F.P., HSIEH, M.J., CHOU, C.C., HSU, W.L. & LEE, Y.J. (2015) Detection of indoxyl sulfate levels in dogs and cats suffering from naturally occurring kidney diseases. *Veterinary Journal (London, England: 1997)* **205**, 399–403.

CHENG, J., PALVA, A.M., DE VOS, W.M. & SATOKARI, R. (2013) Contribution of the intestinal microbiota to human health: from birth to 100 years of age. *Current Topics in Microbiology and Immunology* **358**, 323–346.

CHENG, L., QI, C., ZHUANG, H., FU, T. & ZHANG, X. (2020) gutMDisorder: a comprehensive database for dysbiosis of the gut microbiota in disorders and interventions. *Nucleic Acids Research* **48**, D554–D560.

CHÈVRETON, P. (2018) The gut microbiota of domestic carnivorous: state of play. Faculté de médecine de Créteil.

CHOO, J.M., LEONG, L.E. & ROGERS, G.B. (2015) Sample storage conditions significantly influence faecal microbiome profiles. *Scientific Reports* **5**, 16350.

CHUN, J.L., JI, S.Y., LEE, S.D., LEE, Y.K., KIM, B. & KIM, K.H. (2020) Difference of gut microbiota composition based on the body condition scores in dogs. *Journal of Animal Science and Technology* **62**,

239–246.

CINQUIN, C., LE BLAY, G., FLISS, I. & LACROIX, C. (2006) New three-stage *in vitro* model for infant colonic fermentation with immobilized fecal microbiota: Model for infant colon fermentation. *FEMS Microbiology Ecology* **57**, 324–336.

CINTIO, M., SCARSELLA, E., SGORLON, S., SANDRI, M. & STEFANON, B. (2020) Gut Microbiome of Healthy and Arthritic Dogs. *Veterinary Sciences* **7**, 92.

COELHO, L.P., KULTIMA, J.R., COSTEA, P.I., FOURNIER, C., PAN, Y., CZARNECKI-MAULDEN, G., HAYWARD, M.R., FORSLUND, S.K., SCHMIDT, T.S.B., DESCOMBES, P., JACKSON, J.R., LI, Q. & BORK, P. (2018) Similarity of the dog and human gut microbiomes in gene content and response to diet. *Microbiome* **6**.

COLLINS, J., ROBINSON, C., DANHOF, H., KNETSCH, C.W., VAN LEEUWEN, H.C., LAWLEY, T.D., AUCHTUNG, J.M. & BRITTON, R.A. (2018) Dietary trehalose enhances virulence of epidemic Clostridium difficile. *Nature* **553**, 291–294.

COLLINS, S.B., PEREZ-CAMARGO, G., GETTINBY, G., BUTTERWICK, R.F., BATT, R.M. & GIFFARD, C.J. (2001) Development of a technique for the *in vivo* assessment of flatulence in dogs. *American Journal of Veterinary Research* **62**, 1014–1019.

COMAN, M.M., VERDENELLI, M.C., CECCHINI, C., BELÀ, B., GRAMENZI, A., ORPIANESI, C., CRESCI, A. & SILVI, S. (2019) Probiotic characterization of Lactobacillus isolates from canine faeces. *Journal of Applied Microbiology* **126**, 1245–1256.

CONTRERAS-AGUILAR, M.D., TECLES, F., MARTÍNEZ-SUBIELA, S., ESCRIBANO, D., BERNAL, L.J. & CERÓN, J.J. (2017) Detection and measurement of alpha-amylase in canine saliva and changes after an experimentally induced sympathetic activation. *BMC veterinary research* **13**, 266.

CORDONNIER, C., THÉVENOT, J., ETIENNE-MESMIN, L., DENIS, S., ALRIC, M., LIVRELLI, V. & BLANQUET-DIOT, S. (2015) Dynamic *In vitro* Models of the Human Gastrointestinal Tract as Relevant Tools to Assess the Survival of Probiotic Strains and Their Interactions with Gut Microbiota. *Microorganisms* **3**, 725–745.

CUEVAS-GONZÁLEZ, P.F., LICEAGA, A.M. & AGUILAR-TOALÁ, J.E. (2020) Postbiotics and paraprobiotics: From concepts to applications. *Food Research International (Ottawa, Ont.)* **136**, 109502.

CUTRIGNELLI, M.I., BOVERA, F., TUDISCO, R., D'URSO, S., MARONO, S., PICCOLO, G. & CALABRÒ, S. (2009) *In vitro* fermentation characteristics of different carbohydrate sources in two dog breeds (German shepherd and Neapolitan mastiff). *Journal of Animal Physiology and Animal Nutrition* **93**, 305–312.

DAISLEY, B.A., KOENIG, D., ENGELBRECHT, K., DONEY, L., HARDS, K., AL, K.F., REID, G. & BURTON, J.P. (2021) Emerging connections between gut microbiome bioenergetics and chronic metabolic diseases. *Cell Reports* **37**, 110087.

DANDRIEUX, J.R.S. & MANSFIELD, C.S. (2019) Chronic Enteropathy in Canines: Prevalence, Impact And Management Strategies. *Veterinary Medicine (Auckland, N.Z.)* **10**, 203–214.

D'ANGELO, S., FRACASSI, F., BRESCIANI, F., GALUPPI, R., DIANA, A., LINTA, N., BETTINI, G., MORINI, M. & PIETRA, M. (2018) Effect of *Saccharomyces boulardii* in dogs with chronic enteropathies: double-blinded, placebo-controlled study. *Veterinary Record* **182**, 258–258.

DARCY-VRILLON, B., CHERBUY, C., MOREL, M.T., DURAND, M. & DUÉE, P.H. (1996) Short chain fatty acid and glucose metabolism in isolated pig colonocytes: modulation by NH4+. *Molecular and Cellular Biochemistry* **156**, 145–151.

DAVILA, A.-M., BLACHIER, F., GOTTELAND, M., ANDRIAMIHAJA, M., BENETTI, P.-H., SANZ, Y. & TOMÉ, D. (2013) Intestinal luminal nitrogen metabolism: role of the gut microbiota and consequences for the host. *Pharmacological Research* **68**, 95–107.

DE ANGELIS, M., GARRUTI, G., MINERVINI, F., BONFRATE, L., PORTINCASA, P. & GOBBETTI, M. (2019) The Food-gut Human Axis: The Effects of Diet on Gut Microbiota and Metabolome. *Current Medicinal Chemistry* **26**, 3567–3583.

DE CUYPER, A., HESTA, M., TIBOSCH, S., WANKE, C., CLAUSS, M. & JANSSENS, G.P.J. (2018) How does dietary particle size affect carnivore gastrointestinal transit: A dog model. *Journal of Animal Physiology and Animal Nutrition* **102**, e615–e622.

DE FILIPPIS, F., PELLEGRINI, N., VANNINI, L., JEFFERY, I.B., LA STORIA, A., LAGHI, L., SERRAZANETTI, D.I., DI CAGNO, R., FERROCINO, I., LAZZI, C., TURRONI, S., COCOLIN, L., BRIGIDI, P., NEVIANI, E., GOBBETTI, M., *ET AL.* (2016) High-level adherence to a Mediterranean diet beneficially impacts the gut microbiota and associated metabolome. *Gut* **65**, 1812–1821.

DE LA CUESTA-ZULUAGA, J., CORRALES-AGUDELO, V., CARMONA, J.A., ABAD, J.M. & ESCOBAR, J.S. (2018) Body size phenotypes comprehensively assess cardiometabolic risk and refine the association between obesity and gut microbiota. *International Journal of Obesity (2005)* **42**, 424–432.

DE WEIRDT, R., POSSEMIERS, S., VERMEULEN, G., MOERDIJK-POORTVLIET, T.C.W., BOSCHKER, H.T.S., VERSTRAETE, W. & VAN DE WIELE, T. (2010) Human faecal microbiota display variable patterns of glycerol metabolism: Glycerol metabolism in the human colon. *FEMS Microbiology Ecology* **74**, 601–611.

DÉAT, E., BLANQUET-DIOT, S., JARRIGE, J.-F., DENIS, S., BEYSSAC, E. & ALRIC, M. (2009) Combining the dynamic TNO-gastrointestinal tract system with a Caco-2 cell culture model: application to the assessment of lycopene and alpha-tocopherol bioavailability from a whole food. *Journal of Agricultural and Food Chemistry* **57**, 11314–11320.

DEFOIS, C., RATEL, J., GARRAIT, G., DENIS, S., LE GOFF, O., TALVAS, J., MOSONI, P., ENGEL, E. & PEYRET, P. (2018) Food Chemicals Disrupt Human Gut Microbiota Activity and Impact Intestinal Homeostasis As Revealed By *In vitro* Systems. *Scientific Reports* **8**, 11006.

DELUCCHI, L., FRAGA, M. & ZUNINO, P. (2017) Effect of the probiotic Lactobacillus murinus LbP2 on clinical parameters of dogs with distemper-associated diarrhea. *Canadian Journal of Veterinary Research = Revue Canadienne De Recherche Veterinaire* **81**, 118–121.

DENG, P. & SWANSON, K.S. (2015) Gut microbiota of humans, dogs and cats: current knowledge and future opportunities and challenges. *British Journal of Nutrition* **113**, S6–S17.

DENIS, S., SAYD, T., GEORGES, A., CHAMBON, C., CHALANCON, S., SANTÉ-LHOUTELLIER, V. & BLANQUET-DIOT, S. (2016) Digestion of cooked meat proteins is slightly affected by age as assessed using the dynamic gastrointestinal TIM model and mass spectrometry. *Food & Function* **7**, 2682–2691.

DESCHAMPS, C., DENIS, S., HUMBERT, D., ZENTEK, J., PRIYMENKO, N., APPER, E. & BLANQUET-DIOT, S. (2022a) *In vitro* models of the canine digestive tract as an alternative to *in vivo* assays: Advances and current challenges. *ALTEX* **39**, 235–257.

DESCHAMPS, C., FOURNIER, E., URIOT, O., LAJOIE, F., VERDIER, C., COMTET-MARRE, S., THOMAS, M., KAPEL, N., CHERBUY, C., ALRIC, M., ALMEIDA, M., ETIENNE-MESMIN, L. & BLANQUET-DIOT, S. (2020) Comparative methods for fecal sample storage to preserve gut microbial structure and function in an *in vitro* model of the human colon. *Applied Microbiology and Biotechnology* **104**, 10233–10247.

DESCHAMPS, C., HUMBERT, D., ZENTEK, J., DENIS, S., PRIYMENKO, N., APPER, E. & BLANQUET-DIOT, S. (2022b) From Chihuahua to Saint-Bernard: how did digestion and microbiota evolve with dog sizes. *International Journal of Biological Sciences* **18**, 5086–5102. Ivyspring International Publisher.

DETWEILER, K.B., HE, F., MANGIAN, H.F., DAVENPORT, G.M. & DE GODOY, M.R.C. (2019) Effects of high inclusion of soybean hulls on apparent total tract macronutrient digestibility, fecal quality, and fecal fermentative end-product concentrations in extruded diets of adult dogs. *Journal of Animal Science* **97**, 1027–1035.

DEWHIRST, F.E., KLEIN, E.A., THOMPSON, E.C., BLANTON, J.M., CHEN, T., MILELLA, L., BUCKLEY, C.M.F., DAVIS, I.J., BENNETT, M.-L. & MARSHALL-JONES, Z.V. (2012) The Canine Oral Microbiome. *PLoS ONE* **7**.

DÍAZ-REGAÑÓN, D., GARCÍA-SANCHO, M., VILLAESCUSA, A., SAINZ, Á., AGULLA, B., REYES-PRIETO, M., RODRÍGUEZ-BERTOS, A. & RODRÍGUEZ-FRANCO, F. (2023) Characterization of the Fecal and Mucosa-Associated Microbiota in Dogs with Chronic Inflammatory Enteropathy. *Animals* **13**, 326.

DINIZ, A.N., SOUZA, A. DA C.F. DE, NEPOMUCENO, A.C., MARCELINO, S.A.C., PIEREZAN, F., LOBATO, F.C.F. & SILVA, R.O.S. (2021) Fecal microbiota transplantation via colonoscopy in a dog with Clostridioides (Clostridium) difficile infection. *Ciência Rural* **51**, e20200783.

DOGRA, S.K., DORÉ, J. & DAMAK, S. (2020) Gut Microbiota Resilience: Definition, Link to Health and Strategies for Intervention. *Frontiers in Microbiology* **11**, 572921.

DONADELLI, R.A. & ALDRICH, C.G. (2019) The effects on nutrient utilization and stool quality of Beagle dogs fed diets with beet pulp, cellulose, and Miscanthus grass12. *Journal of Animal Science* **97**, 4134–4139.

DONADELLI, R.A., TITGEMEYER, E.C. & ALDRICH, C.G. (2019) Organic matter disappearance and production of short- and branched-chain fatty acids from selected fiber sources used in pet foods by a canine *in vitro* fermentation model1. *Journal of Animal Science* **97**, 4532–4539.

DOUGLAS, G.M., MAFFEI, V.J., ZANEVELD, J.R., YURGEL, S.N., BROWN, J.R., TAYLOR, C.M., HUTTENHOWER, C. & LANGILLE, M.G.I. (2020) PICRUSt2 for prediction of metagenome functions. *Nature Biotechnology* **38**, 685–688.

DOULIDIS, P.G., GALLER, A.I., HAUSMANN, B., BERRY, D., RODRÍGUEZ-ROJAS, A. & BURGENER, I.A. (2023) Gut microbiome signatures of Yorkshire Terrier enteropathy during disease and remission. *Scientific Reports* **13**, 4337.

DRESSMAN, J.B. (1986) Comparison of canine and human gastrointestinal physiology. *Pharmaceutical Research* **3**, 123–131.

DUBBELBOER, I.R., BARMPATSALOU, V., RODLER, A., KARLSSON, E., FILIPE NUNES, S., HOLMBERG, J., HÄGGSTRÖM, J. & A S BERGSTRÖM, C. (2022) Gastrointestinal mucus in dog: physiological characteristics, composition, and structural properties. *European Journal of Pharmaceutics and Biopharmaceutics: Official Journal of Arbeitsgemeinschaft Fur Pharmazeutische Verfahrenstechnik e.V*, S0939-6411(22)00040-6.

DUBOC, H., RAJCA, S., RAINTEAU, D., BENAROUS, D., MAUBERT, M.-A., QUERVAIN, E., THOMAS, G., BARBU, V., HUMBERT, L., DESPRAS, G., BRIDONNEAU, C., DUMETZ, F., GRILL, J.-P., MASLIAH, J., BEAUGERIE, L., *ET AL.* (2013) Connecting dysbiosis, bile-acid dysmetabolism and gut inflammation in inflammatory bowel diseases. *Gut* **62**, 531–539.

DUFOURNY, S., EVERAERT, N., LEBRUN, S., DOUNY, C., SCIPPO, M.-L., LI, B., TAMINIAU, B., MARZORATI, M., WAVREILLE, J., FROIDMONT, E., RONDIA, P. & DELCENSERIE, V. (2019) Baby-SPIME: A dynamic *in vitro* piglet model mimicking gut microbiota during the weaning process. *Journal of Microbiological Methods* **167**, 105735.

DURAND, A. (2010) Entéropathies exsudatives chez le chien : proposition d'une stratégie thérapeutique diététique et médiacale. Université Claude Bernard.

DUYSBURGH, C., OSSIEUR, W.P., DE PAEPE, K., VAN DEN ABBEELE, P., VICHEZ-VARGAS, R., VITAL, M., PIEPER, D.H., VAN DE WIELE, T., HESTA, M., POSSEMIERS, S. & MARZORATI, M. (2020) Development and validation of the Simulator of the Canine Intestinal Microbial Ecosystem (SCIME)1. *Journal of Animal Science* **98**.

EDWARDS-INGRAM, L., GITSHAM, P., BURTON, N., WARHURST, G., CLARKE, I., HOYLE, D., OLIVER, S.G. & STATEVA, L. (2007) Genotypic and Physiological Characterization of *Saccharomyces boulardii*, the Probiotic Strain of *Saccharomyces cerevisiae*. *Applied and Environmental Microbiology* **73**, 2458–2467.

EHRLEIN, H.-J. & PRÖVE, J. (1982) Effect of viscosity of test meals on gastric emptying in dogs. *Quarterly Journal of Experimental Physiology* **67**, 419–425.

EISENHAUER, L., VAHJEN, W., DADI, T., KOHN, B. & ZENTEK, J. (2019) Effects of Brewer's spent grain and carrot pomace on digestibility, fecal microbiota, and fecal and urinary metabolites in dogs fed low- or high-protein diets1. *Journal of Animal Science* **97**, 4124–4133.

EL HAGE, R., HERNANDEZ-SANABRIA, E., CALATAYUD ARROYO, M., PROPS, R. & VAN DE WIELE, T. (2019) Propionate-Producing Consortium Restores Antibiotic-Induced Dysbiosis in a Dynamic *in vitro* Model of the Human Intestinal Microbial Ecosystem. *Frontiers in Microbiology* **10**, 1206.

EL-JURDI, N. & GHANNOUM, M.A. (2017) The Mycobiome: Impact on Health and Disease States. *Microbiology Spectrum* **5**, 5.3.11.

EL-SALHY, M., YSTAD, S.O., MAZZAWI, T. & GUNDERSEN, D. (2017) Dietary fiber in irritable bowel syndrome (Review). *International Journal of Molecular Medicine* **40**, 607–613.

ENRIGHT, E.F., GAHAN, C.G.M., JOYCE, S.A. & GRIFFIN, B.T. (2016) The Impact of the Gut Microbiota on Drug Metabolism and Clinical Outcome. *The Yale Journal of Biology and Medicine* **89**, 375–382.

EPHRAIM, E., COCHRANE, C.-Y. & JEWELL, D.E. (2020) Varying Protein Levels Influence Metabolomics and the Gut Microbiome in Healthy Adult Dogs. *Toxins* **12**.

ETIENNE-MESMIN, L., CHASSAING, B., DESVAUX, M., DE PAEPE, K., GRESSE, R., SAUVAITRE, T., FORANO, E., DE WIELE, T.V., SCHÜLLER, S., JUGE, N. & BLANQUET-DIOT, S. (2019) Experimental models to study intestinal microbes-mucus interactions in health and disease. *FEMS microbiology reviews* **43**, 457–489.

FABER, T.A., HOPKINS, A.C., MIDDELBOS, I.S., PRICE, N.P. & FAHEY, G.C. (2011) Galactoglucomannan oligosaccharide supplementation affects nutrient digestibility, fermentation end-product production, and large bowel microbiota of the dog1. *Journal of Animal Science* **89**, 103–112.

FARMER, A.D., RUFFLE, J.K. & HOBSON, A.R. (2019) Linaclotide increases cecal pH, accelerates colonic transit, and increases colonic motility in irritable bowel syndrome with constipation. *Neurogastroenterology and Motility: The Official Journal of the European Gastrointestinal Motility Society* **31**, e13492.

FARMER, A.D., WEGEBERG, A.-M.L., BROCK, B., HOBSON, A.R., MOHAMMED, S.D., SCOTT, S.M., BRUCKNER-HOLT, C.E., SEMLER, J.R., HASLER, W.L., HELLSTRÖM, P.M., DREWES, A.M. & BROCK, C. (2018) Regional gastrointestinal contractility parameters using the wireless motility capsule: inter-observer reproducibility and influence of age, gender and study country. *Alimentary Pharmacology & Therapeutics* **47**, 391–400.

FARQUHAR, M.J., MCCLUSKEY, E., STAUNTON, R., HUGHES, K.R. & COLTHERD, J.C. (2018a) Characterisation of a canine epithelial cell line for modelling the intestinal barrier. *Alternatives to laboratory animals: ATLA* **46**, 115–132.

FARQUHAR, M.J., MCCLUSKEY, E., STAUNTON, R., HUGHES, K.R. & COLTHERD, J.C. (2018b) Characterisation of a canine epithelial cell line for modelling the intestinal barrier. *Alternatives to laboratory animals: ATLA* **46**, 115–132.

FEDIAF (2019) FEDIAF Nutritional Guidelines 2019.

FEHLBAUM, S., CHASSARD, C., HAUG, M.C., FOURMESTRAUX, C., DERRIEN, M. & LACROIX, C. (2015) Design and Investigation of PolyFermS *In vitro* Continuous Fermentation Models Inoculated with Immobilized Fecal Microbiota Mimicking the Elderly Colon. *PloS One* **10**, e0142793.

FEHLBAUM, S., CHASSARD, C., POEKER, S.A., DERRIEN, M., FOURMESTRAUX, C. & LACROIX, C. (2016) Clostridium difficile colonization and antibiotics response in PolyFermS continuous model mimicking elderly intestinal fermentation. *Gut Pathogens* **8**, 63.

FELDMAN, E.J., DOWLING, R.H., MCNAUGHTON, J. & PETERS, T.J. (1976) Effects of oral versus intravenous nutrition on intestinal adaptation after small bowel resection in the dog. *Gastroenterology* **70**, 712–719.

FENIMORE, A., MARTIN, L. & LAPPIN, M.R. (2017) Evaluation of Metronidazole with and Without Enterococcus Faecium SF68 in Shelter Dogs With Diarrhea. *Topics in Companion Animal Medicine* **32**, 100–103.

FERNÁNDEZ, L., MARTÍNEZ, R., PÉREZ, M., ARROYO, R. & RODRÍGUEZ, J.M. (2019) Characterization of Lactobacillus rhamnosus MP01 and Lactobacillus plantarum MP02 and Assessment of Their Potential for the Prevention of Gastrointestinal Infections in an Experimental Canine Model. *Frontiers in Microbiology* **10**, 1117.

FITZPATRICK, L.R. & JENABZADEH, P. (2020) IBD and Bile Acid Absorption: Focus on Pre-clinical and Clinical Observations. *Frontiers in Physiology* **11**, 564.

FLEURY, M.A., LE GOFF, O., DENIS, S., CHAUCHEYRAS-DURAND, F., JOUY, E., KEMPF, I., ALRIC, M. & BLANQUET-DIOT, S. (2017) Development and validation of a new dynamic *in vitro* model of the piglet colon (PigutIVM): application to the study of probiotics. *Applied Microbiology and Biotechnology* **101**, 2533–2547.

FLICKINGER, E.A., SCHREIJEN, E.M.W.C., PATIL, A.R., HUSSEIN, H.S., GRIESHOP, C.M., MERCHEN, N.R. & FAHEY, G.C. (2003) Nutrient digestibilities, microbial populations, and protein catabolites as affected by fructan supplementation of dog diets. *Journal of Animal Science* **81**, 2008–2018.

FLORES, R., SHI, J., YU, G., MA, B., RAVEL, J., GOEDERT, J.J. & SINHA, R. (2015) Collection media and delayed freezing effects on microbial composition of human stool. *Microbiome* **3**.

FORSTER, G.M., STOCKMAN, J., NOYES, N., HEUBERGER, A.L., BROECKLING, C.D., BANTLE, C.M. & RYAN, E.P. (2018) A Comparative Study of Serum Biochemistry, Metabolome and Microbiome Parameters of Clinically Healthy, Normal Weight, Overweight, and Obese Companion Dogs. *Topics in Companion*

Animal Medicine **33**, 126–135.

FOSTER, M.L., DOWD, S.E., STEPHENSON, C., STEINER, J.M. & SUCHODOLSKI, J.S. (2013) Characterization of the fungal microbiome (mycobiome) in fecal samples from dogs. *Veterinary Medicine International* **2013**, 658373.

FREEMAN, C.D., KLUTMAN, N.E. & LAMP, K.C. (1997) Metronidazole. A therapeutic review and update. *Drugs* **54**, 679–708.

FRIEDMAN, E.S., BITTINGER, K., ESIPOVA, T.V., HOU, L., CHAU, L., JIANG, J., MESAROS, C., LUND, P.J., LIANG, X., FITZGERALD, G.A., GOULIAN, M., LEE, D., GARCIA, B.A., BLAIR, I.A., VINOGRADOV, S.A., *ET AL.* (2018) Microbes vs. chemistry in the origin of the anaerobic gut lumen. *Proceedings of the National Academy of Sciences of the United States of America* **115**, 4170–4175.

FROMMHERZ, L., BUB, A., HUMMEL, E., RIST, M.J., ROTH, A., WATZL, B. & KULLING, S.E. (2016) Age-Related Changes of Plasma Bile Acid Concentrations in Healthy Adults—Results from the Cross-Sectional KarMeN Study. *PLOS ONE* **11**, e0153959.

FU, J., YU, M., XU, W. & YU, S. (2021) Research Progress of Bile Acids in Cancer. *Frontiers in Oncology* **11**, 778258.

GABRIEL, V., ZDYRSKI, C., SAHOO, D.K., DAO, K., BOURGOIS-MOCHEL, A., ATHERLY, T., MARTINEZ, M.N., VOLPE, D.A., KOPPER, J., ALLENSPACH, K. & MOCHEL, J.P. (2022) Canine Intestinal Organoids in a Dual-Chamber Permeable Support System. *Journal of Visualized Experiments: JoVE*.

GACI, N., BORREL, G., TOTTEY, W., O'TOOLE, P.W. & BRUGÈRE, J.-F. (2014) Archaea and the human gut: new beginning of an old story. *World Journal of Gastroenterology* **20**, 16062–16078.

GACI, N., CHAUDHARY, P.P., TOTTEY, W., ALRIC, M. & BRUGÈRE, J.-F. (2017) Functional amplification and preservation of human gut microbiota. *Microbial Ecology in Health and Disease* **28**, 1308070.

GAL, A., BARKO, P.C., BIGGS, P.J., GEDYE, K.R., MIDWINTER, A.C., WILLIAMS, D.A., BURCHELL, R.K. & PAZZI, P. (2021) One dog's waste is another dog's wealth: A pilot study of fecal microbiota transplantation in dogs with acute hemorrhagic diarrhea syndrome. *PloS One* **16**, e0250344.

GAO, X., PUJOS-GUILLOT, E. & SÉBÉDIO, J.-L. (2010) Development of a Quantitative Metabolomic Approach to Study Clinical Human Fecal Water Metabolome Based on Trimethylsilylation Derivatization and GC/MS Analysis. *Analytical Chemistry* **82**, 6447–6456.

GARCIA-MAZCORRO, J.F., DOWD, S.E., POULSEN, J., STEINER, J.M. & SUCHODOLSKI, J.S. (2012a) Abundance and short-term temporal variability of fecal microbiota in healthy dogs. *MicrobiologyOpen* **1**, 340–347.

GARCIA-MAZCORRO, J.F., MINAMOTO, Y., KAWAS, J.R., SUCHODOLSKI, J.S. & DE VOS, W.M. (2020) Akkermansia and Microbial Degradation of Mucus in Cats and Dogs: Implications to the Growing Worldwide Epidemic of Pet Obesity. *Veterinary Sciences* **7**.

GARCIA-MAZCORRO, J.F., SUCHODOLSKI, J.S., JONES, K.R., CLARK-PRICE, S.C., DOWD, S.E., MINAMOTO, Y., MARKEL, M., STEINER, J.M. & DOSSIN, O. (2012b) Effect of the proton pump inhibitor omeprazole on the gastrointestinal bacterial microbiota of healthy dogs. *FEMS microbiology ecology* **80**, 624–636.

GARRIGUES, Q., APPER, E., CHASTANT, S. & MILA, H. (2022a) Gut microbiota development in the growing dog: A dynamic process influenced by maternal, environmental and host factors. *Frontiers in Veterinary Science* **9**, 964649.

GARRIGUES, Q., APPER, E., MERCIER, F., RODILES, A., ROVERE, N., MANSALIER, E., DAVID, P., CHASTANT, S. & MILA, H. (2022b) Evolution of the gut microbiome in female dogs around parturition and in early lactation and impact of live yeast Saccharomyces boulardii CNCM I-1079. Oral presentation, Amsterdam.

GARRIGUES, Q., CHASTANT, S., MILA, H. & APPER, E. (2022c) Impact of a maternal supplementation with the probiotic yeast Saccharomyces cerevisiae boulardii CNCM I-1079 on milk composition and puppies health. Oral presentation, Basel.

GAZZOLA, K.M., NELSON, L.L., FRITZ, M.C., CLANCY, M.R. & HAUPTMAN, J.G. (2017) Effects of prophylactic incisional gastropexy on markers of gastric motility in dogs as determined by use of a novel wireless motility device. *American Journal of Veterinary Research* **78**, 100–106.

GEIRNAERT, A., CALATAYUD, M., GROOTAERT, C., LAUKENS, D., DEVRIESE, S., SMAGGHE, G., DE VOS, M.,

BOON, N. & VAN DE WIELE, T. (2017) Butyrate-producing bacteria supplemented *in vitro* to Crohn's disease patient microbiota increased butyrate production and enhanced intestinal epithelial barrier integrity. *Scientific Reports* **7**, 11450.

GERMAN, A.J., HALLADAY, L.J. & NOBLE, P.-J.M. (2010) First-choice therapy for dogs presenting with diarrhoea in clinical practice. *Veterinary Record* **167**, 810–814.

GERMAN, A.J., HELPS, C.R., HALL, E.J. & DAY, M.J. (2000) Cytokine mRNA expression in mucosal biopsies from German shepherd dogs with small intestinal enteropathies. *Digestive Diseases and Sciences* **45**, 7–17.

GIBSON, G.R., CUMMINGS, J.H. & MACFARLANE, G.T. (1988) Use of a three-stage continuous culture system to study the effect of mucin on dissimilatory sulfate reduction and methanogenesis by mixed populations of human gut bacteria. *Applied and Environmental Microbiology* **54**, 2750–2755.

GIBSON, G.R., HUTKINS, R., SANDERS, M.E., PRESCOTT, S.L., REIMER, R.A., SALMINEN, S.J., SCOTT, K., STANTON, C., SWANSON, K.S., CANI, P.D., VERBEKE, K. & REID, G. (2017) Expert consensus document: The International Scientific Association for Probiotics and Prebiotics (ISAPP) consensus statement on the definition and scope of prebiotics. *Nature Reviews. Gastroenterology & Hepatology* **14**, 491–502.

GIFFARD, C.J., COLLINS, S.B., STOODLEY, N.C., BUTTERWICK, R.F. & BATT, R.M. (2001) Administration of charcoal, Yucca schidigera, and zinc acetate to reduce malodorous flatulence in dogs. *Journal of the American Veterinary Medical Association* **218**, 892–896.

GIRLICH, D., BONNIN, R.A., DORTET, L. & NAAS, T. (2020) Genetics of Acquired Antibiotic Resistance Genes in Proteus spp. *Frontiers in Microbiology* **11**, 256.

DE GODOY, M.R.C., KERR, K.R. & FAHEY, G.C. (2013) Alternative dietary fiber sources in companion animal nutrition. *Nutrients* **5**, 3099–3117.

DE GODOY, M.R.C., VERMILLION, R., BAUER, L.L., YAMKA, R., FRANTZ, N., JIA, T., FAHEY, G.C. & SWANSON, K.S. (2014) *In vitro* disappearance characteristics of selected categories of commercially available dog treats. *Journal of Nutritional Science* **3**, e47.

GOODRICH, J.K., DAVENPORT, E.R., BEAUMONT, M., JACKSON, M.A., KNIGHT, R., OBER, C., SPECTOR, T.D., BELL, J.T., CLARK, A.G. & LEY, R.E. (2016) Genetic determinants of the gut microbiome in UK Twins. *Cell host & microbe* **19**, 731–743.

GORZELAK, M.A., GILL, S.K., TASNIM, N., AHMADI-VAND, Z., JAY, M. & GIBSON, D.L. (2015) Methods for Improving Human Gut Microbiome Data by Reducing Variability through Sample Processing and Storage of Stool. *PLoS ONE* **10**.

GOUDEZ, R., WEBER, M., BIOURGE, V. & NGUYEN, P. (2011) Influence of different levels and sources of resistant starch on faecal quality of dogs of various body sizes. *The British Journal of Nutrition* **106 Suppl 1**, S211-215.

GRANDJEAN, D. & HAYMANN, F. (2010) *Encyclopédie du chien Royal Canin*.

GRESSE, R., CHAUCHEYRAS-DURAND, F., DENIS, S., BEAUMONT, M., VAN DE WIELE, T., FORANO, E. & BLANQUET-DIOT, S. (2021a) Weaning-associated feed deprivation stress causes microbiota disruptions in a novel mucin-containing *in vitro* model of the piglet colon (MPigut-IVM). *Journal of Animal Science and Biotechnology* **12**, 75.

GRESSE, R., CHAUCHEYRAS-DURAND, F., DENIS, S., BEAUMONT, M., VAN DE WIELE, T., FORANO, E. & BLANQUET-DIOT, S. (2021b) Weaning-associated feed deprivation stress causes microbiota disruptions in a novel mucin-containing *in vitro* model of the piglet colon (MPigut-IVM). *Journal of Animal Science and Biotechnology* **12**, 75.

GRESSE, R., CHAUCHEYRAS-DURAND, F., GARRIDO, J.J., DENIS, S., JIMÉNEZ-MARÍN, A., BEAUMONT, M., VAN DE WIELE, T., FORANO, E. & BLANQUET-DIOT, S. (2021c) Pathogen Challenge and Dietary Shift Alter Microbiota Composition and Activity in a Mucin-Associated *in vitro* Model of the Piglet Colon (MPigut-IVM) Simulating Weaning Transition. *Frontiers in Microbiology* **12**, 703421.

GRESSE, R., GARRIDO, J.J., JIMÉNEZ-MARÍN, A., DENIS, S., VAN DE WIELE, T., FORANO, E., BLANQUET-DIOT, S. & CHAUCHEYRAS-DURAND, F. (2021d) Saccharomyces Cerevisiae Var Boulardii CNCM I-1079 Reduces Expression of Genes Involved in Inflammatory Response in Porcine Cells Challenged by Enterotoxigenic E. Coli and Influences Bacterial Communities in an *In vitro* Model of the Weaning Piglet

Colon. *Antibiotics (Basel, Switzerland)* **10**, 1101.

GRØNVOLD, A.-M.R., L'ABÉE-LUND, T.M., SØRUM, H., SKANCKE, E., YANNARELL, A.C. & MACKIE, R.I. (2010) Changes in fecal microbiota of healthy dogs administered amoxicillin. *FEMS Microbiology Ecology* **71**, 313–326.

GRUBER, P., RUBINSTEIN, A., LI, V.H.K., BASS, P. & ROBINSON, J.R. (1987) Gastric Emptying of Nondigestible Solids in the Fasted Dog. *Journal of Pharmaceutical Sciences* **76**, 117–122.

GUARD, B.C., BARR, J.W., REDDIVARI, L., KLEMASHEVICH, C., JAYARAMAN, A., STEINER, J.M., VANAMALA, J. & SUCHODOLSKI, J.S. (2015) Characterization of Microbial Dysbiosis and Metabolomic Changes in Dogs with Acute Diarrhea. *PLOS ONE* **10**, e0127259.

GUARD, B.C., HONNEFFER, J.B., JERGENS, A.E., JONIKA, M.M., TORESSON, L., LAWRENCE, Y.A., WEBB, C.B., HILL, S., LIDBURY, J.A., STEINER, J.M. & SUCHODOLSKI, J.S. (2019) Longitudinal assessment of microbial dysbiosis, fecal unconjugated bile acid concentrations, and disease activity in dogs with steroid-responsive chronic inflammatory enteropathy. *Journal of Veterinary Internal Medicine* **33**, 1295–1305.

GUARD, B.C., MILA, H., STEINER, J.M., MARIANI, C., SUCHODOLSKI, J.S. & CHASTANT-MAILLARD, S. (2017) Characterization of the fecal microbiome during neonatal and early pediatric development in puppies. *PloS One* **12**, e0175718.

GUARD, B.C. & SUCHODOLSKI, J.S. (2016) HORSE SPECIES SYMPOSIUM: Canine intestinal microbiology and metagenomics: From phylogeny to function1. *Journal of Animal Science* **94**, 2247–2261.

GUERRA, A., DENIS, S., GOFF, O. LE, SICARDI, V., FRANÇOIS, O., YAO, A.-F., GARRAIT, G., MANZI, A.P., BEYSSAC, E., ALRIC, M. & BLANQUET-DIOT, S. (2016) Development and validation of a new dynamic computer-controlled model of the human stomach and small intestine. *Biotechnology and Bioengineering* **113**, 1325–1335.

GUIDI, E.E.A., GRAMENZI, A., PERSICO, P., DI PRINZIO, R., DI SIMONE, D. & CORNEGLIANI, L. (2021) Effects of Feeding a Hypoallergenic Diet with a Nutraceutical on Fecal Dysbiosis Index and Clinical Manifestations of Canine Atopic Dermatitis. *Animals* **11**, 2985.

HAINDL, R., SCHICK, S. & KULOZIK, U. (2021) Influence of Cultivation pH on Composition, Diversity, and Metabolic Production in an *In vitro* Human Intestinal Microbiota. *Fermentation* **7**, 156.

HAMPER, B. (2016) Current Topics in Canine and Feline Obesity. *The Veterinary Clinics of North America. Small Animal Practice* **46**, 785–795.

HANDL, S., GERMAN, A.J., HOLDEN, S.L., DOWD, S.E., STEINER, J.M., HEILMANN, R.M., GRANT, R.W., SWANSON, K.S. & SUCHODOLSKI, J.S. (2013) Faecal microbiota in lean and obese dogs. *FEMS microbiology ecology* **84**, 332–343.

HANG, I., HEILMANN, R.M., GRÜTZNER, N., SUCHODOLSKI, J.S., STEINER, J.M., ATROSHI, F., SANKARI, S., KETTUNEN, A., DE VOS, W.M., ZENTEK, J. & SPILLMANN, T. (2013) Impact of diets with a high content of greaves-meal protein or carbohydrates on faecal characteristics, volatile fatty acids and faecal calprotectin concentrations in healthy dogs. *BMC veterinary research* **9**, 201.

HANG, I., RINTTILA, T., ZENTEK, J., KETTUNEN, A., ALAJA, S., APAJALAHTI, J., HARMOINEN, J., DE VOS, W.M. & SPILLMANN, T. (2012) Effect of high contents of dietary animal-derived protein or carbohydrates on canine faecal microbiota. *BMC veterinary research* **8**, 90.

HARDY, J., BONIN, P., LAZUKA, A., GONIDEC, E., GUASCO, S., VALETTE, C., LACROIX, S. & CABROL, L. (2021) Similar Methanogenic Shift but Divergent Syntrophic Partners in Anaerobic Digesters Exposed to Direct versus Successive Ammonium Additions. *Microbiology Spectrum* **9**, e00805-21.

HART, I.R. & KIDDER, D.E. (1978) The quantitative assessment of normal canine small intestinal mucosa. *Research in Veterinary Science* **25**, 157–162.

HEIMANN, E., NYMAN, M., PÅLBRINK, A.-K., LINDKVIST-PETERSSON, K. & DEGERMAN, E. (2016) Branched short-chain fatty acids modulate glucose and lipid metabolism in primary adipocytes. *Adipocyte* **5**, 359–368.

HENDRIKS, W.H., THOMAS, D.G., BOSCH, G. & FAHEY, G.C. (2013) Comparison of ileal and total tract nutrient digestibility of dry dog foods. *Journal of Animal Science* **91**, 3807–3814.

HERNOT, D.C., BIOURGE, V.C., MARTIN, L.J., DUMON, H.J. & NGUYEN, P.G. (2005) Relationship between total

transit time and faecal quality in adult dogs differing in body size. *Journal of Animal Physiology and Animal Nutrition* **89**, 189–193.

HERNOT, D.C., DUMON, H.J., BIOURGE, V.C., MARTIN, L.J. & NGUYEN, P.G. (2006) Evaluation of association between body size and large intestinal transit time in healthy dogs. *American Journal of Veterinary Research* **67**, 342–347.

HERNOT, D.C., NERY, J., BIOURGE, V.C., MARTIN, L.J., DUMON, H.J. & NGUYEN, P.G. (2009) Colonic permeability is higher in Great Danes compared with smaller breed-dogs. *Journal of Animal Physiology and Animal Nutrition* **93**, 703–709.

HERSTAD, K.M.V., GAJARDO, K., BAKKE, A.M., MOE, L., LUDVIGSEN, J., RUDI, K., RUD, I., SEKELJA, M. & SKANCKE, E. (2017) A diet change from dry food to beef induces reversible changes on the faecal microbiota in healthy, adult client-owned dogs. *BMC veterinary research* **13**, 147.

HERSTAD, K.M.V., RØNNING, H.T., BAKKE, A.M., MOE, L. & SKANCKE, E. (2018) Changes in the faecal bile acid profile in dogs fed dry food vs high content of beef: a pilot study. *Acta Veterinaria Scandinavica* **60**, 29.

HERVERA, M., BAUCELLS, M.D., BLANCH, F. & CASTRILLO, C. (2007) Prediction of digestible energy content of extruded dog food by *in vitro* analyses. *Journal of Animal Physiology and Animal Nutrition* **91**, 205–209.

HILL, C., GUARNER, F., REID, G., GIBSON, G.R., MERENSTEIN, D.J., POT, B., MORELLI, L., CANANI, R.B., FLINT, H.J., SALMINEN, S., CALDER, P.C. & SANDERS, M.E. (2014) Expert consensus document. The International Scientific Association for Probiotics and Prebiotics consensus statement on the scope and appropriate use of the term probiotic. *Nature Reviews. Gastroenterology & Hepatology* **11**, 506–514.

HOLZ, C., BUSJAHN, A., MEHLING, H., ARYA, S., BOETTNER, M., HABIBI, H. & LANG, C. (2015) Significant Reduction in Helicobacter pylori Load in Humans with Non-viable Lactobacillus reuteri DSM17648: A Pilot Study. *Probiotics and Antimicrobial Proteins* **7**, 91–100.

HONG, H.-R., OH, Y.-I., KIM, Y.J. & SEO, K.-W. (2019) Salivary alpha-amylase as a stress biomarker in diseased dogs. *Journal of Veterinary Science* **20**, e46.

HONNEFFER, J.B., MINAMOTO, Y. & SUCHODOLSKI, J.S. (2014) Microbiota alterations in acute and chronic gastrointestinal inflammation of cats and dogs. *World Journal of Gastroenterology* **20**, 16489–16497.

HONNEFFER, J.B., STEINER, J.M., LIDBURY, J.A. & SUCHODOLSKI, J.S. (2017) Variation of the microbiota and metabolome along the canine gastrointestinal tract. *Metabolomics* **13**, 26.

HOODA, S., MINAMOTO, Y., SUCHODOLSKI, J.S. & SWANSON, K.S. (2012) Current state of knowledge: the canine gastrointestinal microbiome. *Animal Health Research Reviews* **13**, 78–88.

HUANG, Z., PAN, Z., YANG, R., BI, Y. & XIONG, X. (2020) The canine gastrointestinal microbiota: early studies and research frontiers. *Gut Microbes* **11**, 635–654.

HUGHES, R., MAGEE, E.A. & BINGHAM, S. (2000) Protein degradation in the large intestine: relevance to colorectal cancer. *Current Issues in Intestinal Microbiology* **1**, 51–58.

HULLAR, M.A.J., LAMPE, J.W., TOROK-STORB, B.J. & HARKEY, M.A. (2018) The canine gut microbiome is associated with higher risk of gastric dilatation-volvulus and high-risk genetic variants of the immune system. *PloS One* **13**, e0197686.

IACOPETTI, I., PERAZZI, A., BADON, T., BEDIN, S., CONTIERO, B. & RICCI, R. (2017) Salivary pH, calcium, phosphorus and selected enzymes in healthy dogs: a pilot study. *BMC Veterinary Research* **13**, 330.

IGARASHI, H., MAEDA, S., OHNO, K., HORIGOME, A., ODAMAKI, T. & TSUJIMOTO, H. (2014) Effect of oral administration of metronidazole or prednisolone on fecal microbiota in dogs. *PloS One* **9**, e107909.

IGARASHI, H., OHNO, K., MATSUKI, N., FUJIWARA-IGARASHI, A., KANEMOTO, H., FUKUSHIMA, K., UCHIDA, K. & TSUJIMOTO, H. (2017) Analysis of fecal short chain fatty acid concentration in miniature dachshunds with inflammatory colorectal polyps. *The Journal of Veterinary Medical Science* **79**, 1727–1734.

INGRISCH, J. & BAHN, M. (2018) Towards a Comparable Quantification of Resilience. *Trends in Ecology & Evolution* **33**, 251–259.

JERGENS, A.E., GUARD, B.C., REDFERN, A., ROSSI, G., MOCHEL, J.P., PILLA, R., CHANDRA, L., SEO, Y.-J.,

STEINER, J.M., LIDBURY, J., ALLENSPACH, K. & SUCHODOLSKI, J. (2019) Microbiota-Related Changes in Unconjugated Fecal Bile Acids Are Associated with Naturally Occurring, Insulin-Dependent Diabetes Mellitus in Dogs. *Frontiers in Veterinary Science* **6**, 199.

JIA, J., FRANTZ, N., KHOO, C., GIBSON, G.R., RASTALL, R.A. & MCCARTNEY, A.L. (2010) Investigation of the faecal microbiota associated with canine chronic diarrhoea. *FEMS microbiology ecology* **71**, 304–312.

JINATHAM, V., KULLAWONG, N., KESPECHARA, K., GENTEKAKI, E. & POPLUECHAI, S. (2018) Comparison of Gut Microbiota between Lean and Obese Adult Thai Individuals. *Microbiology and Biotechnology Letters* **46**, 277–287.

JONES, B.R., JONES, K.S., TURNER, K. & ROGATSKI, B. (1998) Flatulence in pet dogs. *New Zealand Veterinary Journal* **46**, 191–193.

JONES, M.L., MARTONI, C.J., GANOPOLSKY, J.G., LABBÉ, A. & PRAKASH, S. (2014) The human microbiome and bile acid metabolism: dysbiosis, dysmetabolism, disease and intervention. *Expert Opinion on Biological Therapy* **14**, 467–482.

JUNGINGER, J., LEMENSIECK, F., MOORE, P.F., SCHWITTLICK, U., NOLTE, I. & HEWICKER-TRAUTWEIN, M. (2014) Canine gut dendritic cells in the steady state and in inflammatory bowel disease. *Innate Immunity* **20**, 145–160.

KABBANI, T.A., PALLAV, K., DOWD, S.E., VILLAFUERTE-GALVEZ, J., VANGA, R.R., CASTILLO, N.E., HANSEN, J., DENNIS, M., LEFFLER, D.A. & KELLY, C.P. (2017) Prospective randomized controlled study on the effects of Saccharomyces boulardii CNCM I-745 and amoxicillin-clavulanate or the combination on the gut microbiota of healthy volunteers. *Gut Microbes* **8**, 17–32.

KAJDIČ, L., PLAVEC, T., ZDOVC, I., KALIN, A. & ZAKOŠEK PIPAN, M. (2021) Impact of Type of Parturition on Colostrum Microbiota Composition and Puppy Survival. *Animals: an open access journal from MDPI* **11**, 1897.

KAKIMOTO, T., KANEMOTO, H., FUKUSHIMA, K., OHNO, K. & TSUJIMOTO, H. (2017) Effect of a high-fat–high-cholesterol diet on gallbladder bile acid composition and gallbladder motility in dogs. *American Journal of Veterinary Research* **78**, 1406–1413.

KALANTAR-ZADEH, K., BEREAN, K.J., BURGELL, R.E., MUIR, J.G. & GIBSON, P.R. (2019) Intestinal gases: influence on gut disorders and the role of dietary manipulations. *Nature Reviews. Gastroenterology & Hepatology* **16**, 733–747.

KALANTZI, L., PERSSON, E., POLENTARUTTI, B., ABRAHAMSSON, B., GOUMAS, K., DRESSMAN, J.B. & REPPAS, C. (2006) Canine Intestinal Contents vs. Simulated Media for the Assessment of Solubility of Two Weak Bases in the Human Small Intestinal Contents. *Pharmaceutical Research* **23**, 1373–1381.

KAMADA, N., CHEN, G.Y., INOHARA, N. & NÚÑEZ, G. (2013) Control of pathogens and pathobionts by the gut microbiota. *Nature Immunology* **14**, 685–690.

KANEHISA, M. & GOTO, S. (2000) KEGG: kyoto encyclopedia of genes and genomes. *Nucleic Acids Research* **28**, 27–30.

KARARLI, T.T. (1995) Comparison of the gastrointestinal anatomy, physiology, and biochemistry of humans and commonly used laboratory animals. *Biopharmaceutics & Drug Disposition* **16**, 351–380.

KASHYAP, P.C., MARCOBAL, A., URSELL, L.K., LARAUCHE, M., DUBOC, H., EARLE, K.A., SONNENBURG, E.D., FERREYRA, J.A., HIGGINBOTTOM, S.K., MILLION, M., TACHE, Y., PASRICHA, P.J., KNIGHT, R., FARRUGIA, G. & SONNENBURG, J.L. (2013) Complex interactions among diet, gastrointestinal transit, and gut microbiota in humanized mice. *Gastroenterology* **144**, 967–977.

KELLEY, R.L., MINIKHIEM, D., KIELY, B., O'MAHONY, L., O'SULLIVAN, D., BOILEAU, T. & PARK, J.S. (2009) Clinical benefits of probiotic canine-derived Bifidobacterium animalis strain AHC7 in dogs with acute idiopathic diarrhea. *Veterinary Therapeutics: Research in Applied Veterinary Medicine* **10**, 121–130.

KENDALL, P.T., BLAZA, S.E. & SMITH, P.M. (1983) Influence of level of intake and dog size on apparent digestibility of dog foods. *The British Veterinary Journal* **139**, 361–362.

KHANNA, S., PARDI, D.S., KELLY, C.R., KRAFT, C.S., DHERE, T., HENN, M.R., LOMBARDO, M.-J., VULIC, M., OHSUMI, T., WINKLER, J., PINDAR, C., MCGOVERN, B.H., POMERANTZ, R.J., AUNINS, J.G., COOK, D.N., *ET AL.* (2016) A Novel Microbiome Therapeutic Increases Gut Microbial Diversity and Prevents Recurrent *Clostridium difficile* Infection. *Journal of Infectious Diseases* **214**, 173–181.

KIELER, I.N., SHAMZIR KAMAL, S., VITGER, A.D., NIELSEN, D.S., LAURIDSEN, C. & BJORNVAD, C.R. (2017) Gut microbiota composition may relate to weight loss rate in obese pet dogs. *Veterinary Medicine and Science* **3**, 252–262.

KIENZLE, E. (1988) Enzyme activity in pancreatic tissue, intestinal mucosa and chyme of dogs in relation to age and diet. *Journal of Animal Physiology and Animal Nutrition*, 276–288.

KILPINEN, S., RANTALA, M., SPILLMANN, T., BJÖRKROTH, J. & WESTERMARCK, E. (2015) Oral tylosin administration is associated with an increase of faecal enterococci and lactic acid bacteria in dogs with tylosin-responsive diarrhoea. *The Veterinary Journal* **205**, 369–374.

KIM, H., JUNG, A.H., PARK, S.H., YOON, Y. & KIM, B.G. (2021) *In vitro* Protein Disappearance of Raw Chicken as Dog Foods Decreased by Thermal Processing but Was Unaffected by Non-Thermal Processing. *Animals: an open access journal from MDPI* **11**, 1256.

KIM, H., RATHER, I.A., KIM, H., KIM, S., KIM, T., JANG, J., SEO, J., LIM, J. & PARK, Y.-H. (2015) A Double-Blind, Placebo Controlled-Trial of a Probiotic Strain Lactobacillus sakei Probio-65 for the Prevention of Canine Atopic Dermatitis. *Journal of Microbiology and Biotechnology* **25**, 1966–1969.

KIM, H., SEO, J., PARK, T., SEO, K., CHO, H., CHUN, J. & KIM, K. (2022) Obese dogs exhibit different fecal microbiome and specific microbial networks compared with normal weight dogs. preprint, In Review.

KIM, J., AN, J.-U., KIM, W., LEE, S. & CHO, S. (2017) Differences in the gut microbiota of dogs (Canis lupus familiaris) fed a natural diet or a commercial feed revealed by the Illumina MiSeq platform. *Gut Pathogens* **9**.

KIM, S. & JAZWINSKI, S.M. (2018) The Gut Microbiota and Healthy Aging: A Mini-Review. *Gerontology* **64**, 513–520.

KIM, Y.S., UNNO, T., KIM, B.Y. & PARK, M.S. (2020) Sex Differences in Gut Microbiota. *The World Journal of Men's Health* **38**, 48–60.

KLINDWORTH, A., PRUESSE, E., SCHWEER, T., PEPLIES, J., QUAST, C., HORN, M. & GLÖCKNER, F.O. (2013) Evaluation of general 16S ribosomal RNA gene PCR primers for classical and next-generation sequencing-based diversity studies. *Nucleic Acids Research* **41**, e1.

KONG, F. & SINGH, R.P. (2010) A human gastric simulator (HGS) to study food digestion in human stomach. *Journal of Food Science* **75**, E627-635.

KOZIOLEK, M., GRIMM, M., BOLLMANN, T., SCHÄFER, K.J., BLATTNER, S.M., LOTZ, R., BOECK, G. & WEITSCHIES, W. (2019) Characterization of the GI transit conditions in Beagle dogs with a telemetric motility capsule. *European Journal of Pharmaceutics and Biopharmaceutics: Official Journal of Arbeitsgemeinschaft Fur Pharmazeutische Verfahrenstechnik e.V* **136**, 221–230.

KRAMER, N., PRATSCHER, B., MENESES, A.M.C., TSCHULENK, W., WALTER, I., SWOBODA, A., KRUITWAGEN, H.S., SCHNEEBERGER, K., PENNING, L.C., SPEE, B., KIESLINGER, M., BRANDT, S. & BURGENER, I.A. (2020) Generation of Differentiating and Long-Living Intestinal Organoids Reflecting the Cellular Diversity of Canine Intestine. *Cells* **9**.

KUBBINGA, M., AUGUSTIJNS, P., GARCÍA, M.A., HEINEN, C., WORTELBOER, H.M., VERWEI, M. & LANGGUTH, P. (2019) The effect of chitosan on the bioaccessibility and intestinal permeability of acyclovir. *European Journal of Pharmaceutics and Biopharmaceutics: Official Journal of Arbeitsgemeinschaft Fur Pharmazeutische Verfahrenstechnik e.V* **136**, 147–155.

KUBINYI, E., BEL RHALI, S., SÁNDOR, S., SZABÓ, A. & FELFÖLDI, T. (2020) Gut Microbiome Composition is Associated with Age and Memory Performance in Pet Dogs. *Animals: an open access journal from MDPI* **10**, E1488.

KUMAR, S., PATTANAIK, A.K., SHARMA, S., GUPTA, R., JADHAV, S.E. & DUTTA, N. (2017) Comparative assessment of canine-origin *Lactobacillus johnsonii* CPN23 and dairy-origin *Lactobacillus acidophillus* NCDC 15 for nutrient digestibility, faecal fermentative metabolites and selected gut health indices in dogs. *Journal of Nutritional Science* **6**, e38.

KUMAR, S., PATTANAIK, A.K., SHARMA, S. & JADHAV, S.E. (2016) Species-specific probiotic Lactobacillus johnsonii CPN23 supplementation modulates blood biochemical profile and erythrocytic antioxidant indices in Labrador dogs. *Indian Journal of Animal Sciences* **86**, 918–924.

KÜNG, K. & WANNER, M. (1994) Bioavailability of different forms of amoxycillin administered orally to dogs.

The Veterinary Record **135**, 552–554.

LARABI, A.B., MASSON, H.L.P. & BÄUMLER, A.J. (2023) Bile acids as modulators of gut microbiota composition and function. *Gut Microbes* **15**, 2172671.

LARCHEVEQUE, S. (2019) Etat des connaissances sur la mucocèle biliaire chez le chien : étude bibliographique. Faculté de médecine de Créteil.

LARMAS, M. & SCHEININ, A. (1971) Studies on dog saliva. I. Some physico-chemical characteristics. *Acta Odontologica Scandinavica* **29**, 205–214.

LASER REUTERSWÄRD, A. (2007) The new EC Regulation on nutrition and health claims on foods. *Scandinavian Journal of Food and Nutrition* **51**, 100–106.

LAVELLE, A. & SOKOL, H. (2020) Gut microbiota-derived metabolites as key actors in inflammatory bowel disease. *Nature Reviews. Gastroenterology & Hepatology* **17**, 223–237.

LAVY, E., GOLDBERGER, D., FRIEDMAN, M. & STEINBERG, D. (2012) pH Values and Mineral Content of Saliva in Different Breeds of Dogs. *Israel Journal of Veterinary Medicine* **67**, 244–2448.

LÊ CAO, K.-A., GONZÁLEZ, I. & DÉJEAN, S. (2009) integrOmics: an R package to unravel relationships between two omics datasets. *Bioinformatics (Oxford, England)* **25**, 2855–2856.

LEE, C.-M., LUNER, P.E., LOCKE, K. & BRIGGS, K. (2017) Application of an Artificial Stomach-Duodenum Reduced Gastric pH Dog Model for Formulation Principal Assessment and Mechanistic Performance Understanding. *Journal of Pharmaceutical Sciences* **106**, 1987–1997.

LEE, D., GOH, T.W., KANG, M.G., CHOI, H.J., YEO, S.Y., YANG, J., HUH, C.S., KIM, Y.Y. & KIM, Y. (2022) Perspectives and advances in probiotics and the gut microbiome in companion animals. *Journal of Animal Science and Technology* **64**, 197–217.

LEWIS, L.D., MAGERKURTH, J.H., ROUDEBUSH, P., MORRIS, M.L., MITCHELL, E.E. & TEETER, S.M. (1994) Stool characteristics, gastrointestinal transit time and nutrient digestibility in dogs fed different fiber sources. *The Journal of Nutrition* **124**, 2716S-2718S.

LI, Y., FORTNER, L. & KONG, F. (2019) Development of a Gastric Simulation Model (GSM) incorporating gastric geometry and peristalsis for food digestion study. *Food Research International (Ottawa, Ont.)* **125**, 108598.

LIDBURY, J.A., SUCHODOLSKI, J.S., IVANEK, R. & STEINER, J.M. (2012) Assessment of the Variation Associated with Repeated Measurement of Gastrointestinal Transit Times and Assessment of the Effect of Oral Ranitidine on Gastrointestinal Transit Times Using a Wireless Motility Capsule System in Dogs. *Veterinary Medicine International* **2012**, 1–8.

LIN, C.-Y., CROSS, T.-W.L., DOUKHANINE, E. & SWANSON, K.S. (2020) An ambient temperature collection and stabilization strategy for canine microbiota studies. *Scientific Reports* **10**, 13383.

LINDEN, S.K., SUTTON, P., KARLSSON, N.G., KOROLIK, V. & MCGUCKIN, M.A. (2008) Mucins in the mucosal barrier to infection. *Mucosal Immunology* **1**, 183–197.

LIU, C., CUI, Y., LI, X. & YAO, M. (2021a) *microeco*: an R package for data mining in microbial community ecology. *FEMS Microbiology Ecology* **97**, fiaa255.

LIU, J.-R., MIAO, H., DENG, D.-Q., VAZIRI, N.D., LI, P. & ZHAO, Y.-Y. (2021b) Gut microbiota-derived tryptophan metabolism mediates renal fibrosis by aryl hydrocarbon receptor signaling activation. *Cellular and molecular life sciences: CMLS* **78**, 909–922.

LIU, L., FIRRMAN, J., TANES, C., BITTINGER, K., THOMAS-GAHRING, A., WU, G.D., VAN DEN ABBEELE, P. & TOMASULA, P.M. (2018) Establishing a mucosal gut microbial community *in vitro* using an artificial simulator. *PloS One* **13**, e0197692.

LIU, Q., WANG, C., PEI, C.X., LI, H.Y., WANG, Y.X., ZHANG, S.L., ZHANG, Y.L., HE, J.P., WANG, H., YANG, W.Z., BAI, Y.S., SHI, Z.G. & LIU, X.N. (2014) Effects of isovalerate supplementation on microbial status and rumen enzyme profile in steers fed on corn stover based diet. *Livestock Science* **161**, 60–68.

LÓPEZ ALBORS, O., ROJO, D., SARRIÁ, R., SORIA, F., PÉREZ CUADRADO, E. & LATORRE, R. (2011) Morphometry of the canine intestine with reference to the use of double balloon endoscopy. *Veterinary Journal (London, England: 1997)* **190**, 113–118.

LOUIS, P. & FLINT, H.J. (2017) Formation of propionate and butyrate by the human colonic microbiota.

Environmental Microbiology **19**, 29–41.

LOUIS, P., HOLD, G.L. & FLINT, H.J. (2014) The gut microbiota, bacterial metabolites and colorectal cancer. *Nature Reviews Microbiology* **12**, 661–672.

LUCENA, R., NOVALES, M., BLANCO, B., HERNÁNDEZ, E. & GINEL, P.J. (2019) Effect of probiotic *Enterococcus faecium* SF68 on liver function in healthy dogs. *Journal of Veterinary Internal Medicine* **33**, 2628–2634.

LUI, C.Y., AMIDON, G.L., BERARDI, R.R., FLEISHER, D., YOUNGBERG, C. & DRESSMAN, J.B. (1986) Comparison of gastrointestinal pH in dogs and humans: implications on the use of the beagle dog as a model for oral absorption in humans. *Journal of Pharmaceutical Sciences* **75**, 271–274.

LYNG, E., HAVENAAR, R., SHASTRI, P., HETSCO, L., VICK, A. & SAGARTZ, J. (2016) Increased bioavailability of celecoxib under fed versus fasted conditions is determined by postprandial bile secretion as demonstrated in a dynamic gastrointestinal model. *Drug Development and Industrial Pharmacy* **42**, 1334–1339.

MA, L., TU, H. & CHEN, T. (2023) Postbiotics in Human Health: A Narrative Review. *Nutrients* **15**, 291.

MACFARLANE, GT., MACFARLANE, S. & GIBSON, GR. (1998) Validation of a Three-Stage Compound Continuous Culture System for Investigating the Effect of Retention Time on the Ecology and Metabolism of Bacteria in the Human Colon. *Microbial Ecology* **35**, 180–187.

MACFARLANE, G.T., GIBSON, G.R., BEATTY, E. & CUMMINGS, J.H. (1992) Estimation of short-chain fatty acid production from protein by human intestinal bacteria based on branched-chain fatty acid measurements. *FEMS Microbiology Letters* **101**, 81–88.

MACFARLANE, G.T. & MACFARLANE, S. (2012) Bacteria, Colonic Fermentation, and Gastrointestinal Health. *Journal of AOAC International* **95**, 50–60.

MACIERZANKA, A., MACKIE, A.R. & KRUPA, L. (2019) Permeability of the small intestinal mucus for physiologically relevant studies: Impact of mucus location and ex vivo treatment. *Scientific Reports* **9**, 17516.

MADRID, J.A., SALIDO, G.M., MAÑAS, M., MARTINEZ DE VICTORIA, E. & MATAIX, F.J. (1983) Use of a bidirectional cannula to study biliary secretion in conscious dogs. *Laboratory Animals* **17**, 307–310.

MAHAR, K.M., PORTELLI, S., COATNEY, R. & CHEN, E.P. (2012) Gastric pH and Gastric Residence Time in Fasted and Fed Conscious Beagle Dogs using the Bravo® pH System. *Journal of Pharmaceutical Sciences* **101**, 2439–2448.

MALEWSKA, K., RYCHLIK, A., NIERADKA, R. & KANDER, M. (2011) Treatment of inflammatory bowel disease (IBD) in dogs and cats. *Polish Journal of Veterinary Sciences* **14**, 165–171.

MANCHESTER, A.C., WEBB, C.B., BLAKE, A.B., SARWAR, F., LIDBURY, J.A., STEINER, J.M. & SUCHODOLSKI, J.S. (2019) Long-term impact of tylosin on fecal microbiota and fecal bile acids of healthy dogs. *Journal of Veterinary Internal Medicine* **33**, 2605–2617.

MARCINÁKOVÁ, M., SIMONOVÁ, M., STROMPFOVÁ, V. & LAUKOVÁ, A. (2006) Oral application of Enterococcus faecium strain EE3 in healthy dogs. *Folia Microbiologica* **51**, 239–242.

MARELLI, S.P., FUSI, E., GIARDINI, A., MARTINO, P.A., POLLI, M., BRUNI, N. & RIZZI, R. (2020) Effects of probiotic *Lactobacillus acidophilus* D2/CSL (CECT 4529) on the nutritional and health status of boxer dogs. *Veterinary Record* **187**.

MARIA, A.P.J., AYANE, L., PUTAROV, T.C., LOUREIRO, B.A., NETO, B.P., CASAGRANDE, M.F., GOMES, M.O.S., GLÓRIA, M.B.A. & CARCIOFI, A.C. (2017) The effect of age and carbohydrate and protein sources on digestibility, fecal microbiota, fermentation products, fecal IgA, and immunological blood parameters in dogs1,2. *Journal of Animal Science* **95**, 2452–2466.

MARKS, S.L., RANKIN, S.C., BYRNE, B.A. & WEESE, J.S. (2011) Enteropathogenic Bacteria in Dogs and Cats: Diagnosis, Epidemiology, Treatment, and Control. *Journal of Veterinary Internal Medicine* **25**, 1195–1208.

MARTÍN, R. & LANGELLA, P. (2019) Emerging Health Concepts in the Probiotics Field: Streamlining the Definitions. *Frontiers in Microbiology* **10**, 1047.

MARTINEZ, M. (2002) Applying the biopharmaceutics classification system to veterinary pharmaceutical products Part II. Physiological considerations. *Advanced Drug Delivery Reviews* **54**, 825–850.

MARU, B.T., MUNASINGHE, P.C., GILARY, H., JONES, S.W. & TRACY, B.P. (2018) Fixation of CO2 and CO on a diverse range of carbohydrates using anaerobic, non-photosynthetic mixotrophy. *FEMS microbiology letters* **365**.

MARZORATI, M., VANHOECKE, B., DE RYCK, T., SADAGHIAN SADABAD, M., PINHEIRO, I., POSSEMIERS, S., VAN DEN ABBEELE, P., DERYCKE, L., BRACKE, M., PIETERS, J., HENNEBEL, T., HARMSEN, H.J., VERSTRAETE, W. & VAN DE WIELE, T. (2014) The HMI™ module: a new tool to study the Host-Microbiota Interaction in the human gastrointestinal tract *in vitro*. *BMC microbiology* **14**, 133.

MCFARLAND, L.V. (2010) Systematic review and meta-analysis of *Saccharomyces boulardii* in adult patients. *World Journal of Gastroenterology* **16**, 2202.

MEINERI, G., MARTELLO, E., ATUAHENE, D., MIRETTI, S., STEFANON, B., SANDRI, M., BIASATO, I., CORVAGLIA, M.R., FERROCINO, I. & COCOLIN, L.S. (2022) Effects of Saccharomyces boulardii Supplementation on Nutritional Status, Fecal Parameters, Microbiota, and Mycobiota in Breeding Adult Dogs. *Veterinary Sciences* **9**, 389.

MELDRUM, O.W., YAKUBOV, G.E., BONILLA, M.R., DESHMUKH, O., MCGUCKIN, M.A. & GIDLEY, M.J. (2018) Mucin gel assembly is controlled by a collective action of non-mucin proteins, disulfide bridges, Ca2+-mediated links, and hydrogen bonding. *Scientific Reports* **8**, 5802.

MÉNARD, O., FAMELART, M.-H., DEGLAIRE, A., LE GOUAR, Y., GUÉRIN, S., MALBERT, C.-H. & DUPONT, D. (2018) Gastric Emptying and Dynamic *In vitro* Digestion of Drinkable Yogurts: Effect of Viscosity and Composition. *Nutrients* **10**.

MÉNARD, O., PICQUE, D. & DUPONT, D. (2015) The DIDGI® System. In *The Impact of Food Bioactives on Health: in vitro and ex vivo models* (eds K. VERHOECKX, P. COTTER, I. LÓPEZ-EXPÓSITO, C. KLEIVELAND, T. LEA, A. MACKIE, T. REQUENA, D. SWIATECKA & H. WICHERS), p. Springer, Cham (CH).

MENTULA, S., HARMOINEN, J., HEIKKILÄ, M., WESTERMARCK, E., RAUTIO, M., HUOVINEN, P. & KÖNÖNEN, E. (2005) Comparison between cultured small-intestinal and fecal microbiotas in beagle dogs. *Applied and Environmental Microbiology* **71**, 4169–4175.

MEUNIER, J.P., MANZANILLA, E.G., ANGUITA, M., DENIS, S., PÉREZ, J.F., GASA, J., CARDOT, J.-M., GARCIA, F., MOLL, X. & ALRIC, M. (2008) Evaluation of a dynamic *in vitro* model to simulate the porcine ileal digestion of diets differing in carbohydrate composition. *Journal of Animal Science* **86**, 1156–1163.

MEYER, H., ZENTEK, J., HABERNOLL, H. & MASKELL, I. (1999) Digestibility and compatibility of mixed diets and faecal consistency in different breeds of dog. *Zentralblatt Fur Veterinarmedizin. Reihe A* **46**, 155–165.

MEYER, J.H., ELASHOFF, J., PORTER-FINK, V., DRESSMAN, J. & AMIDON, G.L. (1988) Human postprandial gastric emptying of 1-3-millimeter spheres. *Gastroenterology* **94**, 1315–1325.

MIDDELBOS, I.S., VESTER BOLER, B.M., QU, A., WHITE, B.A., SWANSON, K.S. & FAHEY, G.C. (2010) Phylogenetic characterization of fecal microbial communities of dogs fed diets with or without supplemental dietary fiber using 454 pyrosequencing. *PloS One* **5**, e9768.

MIDDLETON, R.P., LACROIX, S., SCOTT-BOYER, M.-P., DORDEVIC, N., KENNEDY, A.D., SLUSKY, A.R., CARAYOL, J., PETZINGER-GERMAIN, C., BELOSHAPKA, A. & KAPUT, J. (2017) Metabolic Differences between Dogs of Different Body Sizes. *Journal of Nutrition and Metabolism* **2017**, 4535710.

MINAMOTO, Y., DHANANI, N., MARKEL, M.E., STEINER, J.M. & SUCHODOLSKI, J.S. (2014) Prevalence of Clostridium perfringens, Clostridium perfringens enterotoxin and dysbiosis in fecal samples of dogs with diarrhea. *Veterinary Microbiology* **174**, 463–473.

MINAMOTO, Y., MINAMOTO, T., ISAIAH, A., SATTASATHUCHANA, P., BUONO, A., RANGACHARI, V.R., MCNEELY, I.H., LIDBURY, J., STEINER, J.M. & SUCHODOLSKI, J.S. (2019) Fecal short-chain fatty acid concentrations and dysbiosis in dogs with chronic enteropathy. *Journal of Veterinary Internal Medicine* **33**, 1608–1618.

MINAMOTO, Y., OTONI, C.C., STEELMAN, S.M., BÜYÜKLEBLEBICI, O., STEINER, J.M., JERGENS, A.E. & SUCHODOLSKI, J.S. (2015) Alteration of the fecal microbiota and serum metabolite profiles in dogs with idiopathic inflammatory bowel disease. *Gut Microbes* **6**, 33–47.

MINEKUS, M., ALMINGER, M., ALVITO, P., BALLANCE, S., BOHN, T., BOURLIEU, C., CARRIÈRE, F., BOUTROU,

R., CORREDIG, M., DUPONT, D., DUFOUR, C., EGGER, L., GOLDING, M., KARAKAYA, S., KIRKHUS, B., *ET AL.* (2014) A standardised static *in vitro* digestion method suitable for food - an international consensus. *Food & Function* **5**, 1113–1124.

MINEKUS, M., MARTEAU, P., HAVENAAR, R. & VELD, J.H.J.H. IN'T (1995) A Multicompartmental Dynamic Computer-controlled Model Simulating the Stomach and Small Intestine. *Alternatives to Laboratory Animals* **23**, 197–209.

MINEKUS, M., SMEETS-PEETERS, M., BERNALIER, A., MAROL-BONNIN, S., HAVENAAR, R., MARTEAU, P., ALRIC, M., FONTY, G. & HUIS IN'T VELD, J.H. (1999) A computer-controlled system to simulate conditions of the large intestine with peristaltic mixing, water absorption and absorption of fermentation products. *Applied Microbiology and Biotechnology* **53**, 108–114.

MIZUKAMI, K., UCHIYAMA, J., IGARASHI, H., MURAKAMI, H., OSUMI, T., SHIMA, A., ISHIAHRA, G., NASUKAWA, T., UNE, Y. & SAKAGUCHI, M. (2019) Age-related analysis of the gut microbiome in a purebred dog colony. *FEMS Microbiology Letters* **366**, fnz095.

MOLLY, K., VANDE WOESTYNE, M. & VERSTRAETE, W. (1993) Development of a 5-step multi-chamber reactor as a simulation of the human intestinal microbial ecosystem. *Applied Microbiology and Biotechnology* **39**, 254–258.

MONDO, E., MARLIANI, G., ACCORSI, P.A., COCCHI, M. & DI LEONE, A. (2019) Role of gut microbiota in dog and cat's health and diseases. *Open Veterinary Journal* **9**, 253–258.

MONTOYA-ALONSO, J.A., BAUTISTA-CASTAÑO, I., PEÑA, C., SUÁREZ, L., JUSTE, M.C. & TVARIJONAVICIUTE, A. (2017) Prevalence of Canine Obesity, Obesity-Related Metabolic Dysfunction, and Relationship with Owner Obesity in an Obesogenic Region of Spain. *Frontiers in Veterinary Science* **4**, 59.

MOON, C.D., YOUNG, W., MACLEAN, P.H., COOKSON, A.L. & BERMINGHAM, E.N. (2018) Metagenomic insights into the roles of *Proteobacteria* in the gastrointestinal microbiomes of healthy dogs and cats. *MicrobiologyOpen* **7**, e00677.

MORÉ, M.I. & SWIDSINSKI, A. (2015) Saccharomyces boulardii CNCM I-745 supports regeneration of the intestinal microbiota after diarrheic dysbiosis - a review. *Clinical and Experimental Gastroenterology* **8**, 237–255.

MORRIS, J.G. & ROGERS, G.R. (1989) Comparative aspects of nutrition and metabolism of dogs and cats. In *Nutrition of the dog and cat* pp. 35–66Cambridge University Press. Cambridge.

MOUILLÉ, B., DELPAL, S., MAYEUR, C. & BLACHIER, F. (2003) Inhibition of human colon carcinoma cell growth by ammonia: a non-cytotoxic process associated with polyamine synthesis reduction. *Biochimica Et Biophysica Acta* **1624**, 88–97.

MURALI, A., BHARGAVA, A. & WRIGHT, E.S. (2018) IDTAXA: a novel approach for accurate taxonomic classification of microbiome sequences. *Microbiome* **6**, 140.

MUSCO, N., CALABRÒ, S., ROBERTI, F., GRAZIOLI, R., TUDISCO, R., LOMBARDI, P. & CUTRIGNELLI, M.I. (2018) *In vitro* evaluation of Saccharomyces cerevisiae cell wall fermentability using a dog model. *Journal of Animal Physiology and Animal Nutrition* **102 Suppl 1**, 24–30.

MYINT, H., IWAHASHI, Y., KOIKE, S. & KOBAYASHI, Y. (2017) Effect of soybean husk supplementation on the fecal fermentation metabolites and microbiota of dogs. *Animal Science Journal* **88**, 1730–1736.

MYLES, E.M., O'LEARY, M.E., ROMKEY, I.D., PIANO, A., DE CARVALHO, V., TOMPKINS, T.A. & PERROT, T.S. (2020) Guidelines for best practice in placebo-controlled experimental studies on probiotics in rodent animal models. *Beneficial Microbes* **11**, 245–254.

NAGAHARA, T., OHNO, K., KANEMOTO, H., KAKIMOTO, T., FUKUSHIMA, K., GOTO-KOSHINO, Y. & TSUJIMOTO, H. (2018) Effect of prednisolone administration on gallbladder emptying rate and gallbladder bile composition in dogs. *American Journal of Veterinary Research* **79**, 1050–1056.

NAVA, G.M., CARBONERO, F., CROIX, J.A., GREENBERG, E. & GASKINS, H.R. (2012) Abundance and diversity of mucosa-associated hydrogenotrophic microbes in the healthy human colon. *The ISME journal* **6**, 57–70.

NDEH, D. & GILBERT, H.J. (2018) Biochemistry of complex glycan depolymerisation by the human gut microbiota. *FEMS microbiology reviews* **42**, 146–164.

NEFF-DAVIS, C.A., DAVIS, L.E. & GILLETTE, E.L. (1981) Metronidazole: a method for its determination in biological fluids and its disposition kinetics in the dog. *Journal of Veterinary Pharmacology and Therapeutics* **4**, 121–127.

NEJATI, S., WANG, J., SEDAGHAT, S., BALOG, N.K., LONG, A.M., RIVERA, U.H., KASI, V., PARK, K., JOHNSON, J.S., VERMA, M.S. & RAHIMI, R. (2022) Smart capsule for targeted proximal colon microbiome sampling. *Acta Biomaterialia* **154**, 83–96.

NERI, M., PHILLIPS, S.F., FICH, A. & HADDAD, A.C. (1991) Canine ileocolonic sphincter: flow, transit, and motility before and after sphincterotomy. *The American Journal of Physiology* **260**, G284-289.

NERY, J., BIOURGE, V., TOURNIER, C., LERAY, V., MARTIN, L., DUMON, H. & NGUYEN, P. (2010) Influence of dietary protein content and source on fecal quality, electrolyte concentrations, and osmolarity, and digestibility in dogs differing in body size. *Journal of Animal Science* **88**, 159–169.

NIEMIEC, B.A., GAWOR, J., TANG, S., PREM, A. & KRUMBECK, J.A. (2021) The bacteriome of the oral cavity in healthy dogs and dogs with periodontal disease. *American Journal of Veterinary Research* **83**, 50–58.

NIINA, A., KIBE, R., SUZUKI, R., YUCHI, Y., TESHIMA, T., MATSUMOTO, H., KATAOKA, Y. & KOYAMA, H. (2019) Improvement in Clinical Symptoms and Fecal Microbiome After Fecal Microbiota Transplantation in a Dog with Inflammatory Bowel Disease. *Veterinary Medicine (Auckland, N.Z.)* **10**, 197–201.

NOGUEIRA, J.P.D.S., HE, F., MANGIAN, H.F., OBA, P.M. & DE GODOY, M.R.C. (2019) Dietary supplementation of a fiber-prebiotic and saccharin-eugenol blend in extruded diets fed to dogs. *Journal of Animal Science* **97**, 4519–4531.

OBA, P.M., VIDAL, S., WYSS, R., MIAO, Y., ADESOKAN, Y. & SWANSON, K.S. (2020) Effect of a novel animal milk oligosaccharide biosimilar on the gut microbial communities and metabolites of *in vitro* incubations using feline and canine fecal inocula. *Journal of Animal Science* **98**, skaa273.

OECD (2018) *Guidance Document on Good In vitro Method Practices (GIVIMP)*. OECD.

OEZTUERK, H., SCHROEDER, B., BEYERBACH, M. & BREVES, G. (2005) Influence of Living and Autoclaved Yeasts of Saccharomyces boulardii on *In vitro* Ruminal Microbial Metabolism. *Journal of Dairy Science* **88**, 2594–2600.

OGUÉ-BON, E., KHOO, C., HOYLES, L., MCCARTNEY, A.L., GIBSON, G.R. & RASTALL, R.A. (2011) *In vitro* fermentation of rice bran combined with Lactobacillus acidophilus 14 150B or Bifidobacterium longum 05 by the canine faecal microbiota. *FEMS microbiology ecology* **75**, 365–376.

OKSANEN, J., BLANCHET, F.G., FRIENDLY, M., KINDT, R., LEGENDRE, P., MCGLINN, D., MINCHIN, P., O'HARA, R., SIMPSON, G., SOLYMOS, P., STEVENS, M., SZÖCS, E. & WAGNER, H. (2019) *vegan: Community Ecology Package. R package version 2.5-5, 2019.*

OLIPHANT, K. & ALLEN-VERCOE, E. (2019) Macronutrient metabolism by the human gut microbiome: major fermentation by-products and their impact on host health. *Microbiome* **7**, 91.

OMATSU, T., OMURA, M., KATAYAMA, Y., KIMURA, T., OKUMURA, M., OKUMURA, A., MURATA, Y. & MIZUTANI, T. (2018) Molecular diversity of the faecal microbiota of Toy Poodles in Japan. *The Journal of Veterinary Medical Science* **80**, 749–754.

OMER, R., IQBAL, S., MUSHTAQ, B.S. & HUSSAIN, M.B. (2020) Evaluating the Effect of Prebiotics in the Rehabilitation of Gut Microbiota After Antibiotic Therapy in Rats. *Gazi Medical Journal* **31**.

O'SHEA, E.F., COTTER, P.D., STANTON, C., ROSS, R.P. & HILL, C. (2012) Production of bioactive substances by intestinal bacteria as a basis for explaining probiotic mechanisms: Bacteriocins and conjugated linoleic acid. *International Journal of Food Microbiology* **152**, 189–205.

OSTO, M. & LUTZ, T.A. (2015) Translational value of animal models of obesity-Focus on dogs and cats. *European Journal of Pharmacology* **759**, 240–252.

OSWALD, H., SHARKEY, M., PADE, D. & MARTINEZ, M.N. (2015) Canine gastrointestinal physiology: Breeds variations that can influence drug absorption. *European Journal of Pharmaceutics and Biopharmaceutics* **97**, 192–203.

OU, M. & LING, J. (2017) Norspermidine changes the basic structure of S. mutans biofilm. *Molecular Medicine Reports* **15**, 210–220.

PAIS, P., ALMEIDA, V., YILMAZ, M. & TEIXEIRA, M.C. (2020) Saccharomyces boulardii: What Makes It Tick as Successful Probiotic? *Journal of Fungi (Basel, Switzerland)* **6**, 78.

PALERME, J.-S., SILVERSTONE, A., RIEDESEL, E.A., SIMONE, K.M. & POMRANTZ, J.S. (2020) A pilot study on the effect of fat loading on the gastrointestinal tract of healthy dogs. *The Journal of Small Animal Practice* **61**, 732–737.

PANASEVICH, M.R., DARISTOTLE, L., QUESNELL, R., REINHART, G.A. & FRANTZ, N.Z. (2021) Altered fecal microbiota, IgA, and fermentative end-products in adult dogs fed prebiotics and a nonviable Lactobacillus acidophilus. *Journal of Animal Science* **99**, skab347.

PANASEVICH, M.R., KERR, K.R., DILGER, R.N., FAHEY, G.C., GUÉRIN-DEREMAUX, L., LYNCH, G.L., WILS, D., SUCHODOLSKI, J.S., STEER, J.M., DOWD, S.E. & SWANSON, K.S. (2015a) Modulation of the faecal microbiome of healthy adult dogs by inclusion of potato fibre in the diet. *The British Journal of Nutrition* **113**, 125–133.

PANASEVICH, M.R., KERR, K.R., SERAO, M.C.R., DE GODOY, M.R.C., GUÉRIN-DEREMAUX, L., LYNCH, G.L., WILS, D., DOWD, S.E., FAHEY, G.C., SWANSON, K.S. & DILGER, R.N. (2015b) Evaluation of soluble corn fiber on chemical composition and nitrogen-corrected true metabolizable energy and its effects on *in vitro* fermentation and *in vivo* responses in dogs. *Journal of Animal Science* **93**, 2191–2200.

PANASEVICH, M.R., ROSSONI SERAO, M.C., DE GODOY, M.R.C., SWANSON, K.S., GUÉRIN-DEREMAUX, L., LYNCH, G.L., WILS, D., FAHEY, G.C. & DILGER, R.N. (2013) Potato fiber as a dietary fiber source in dog foods. *Journal of Animal Science* **91**, 5344–5352.

PARK, H.-J., LEE, S.-E., KIM, H.-B., ISAACSON, R.E., SEO, K.-W. & SONG, K.-H. (2015) Association of Obesity with Serum Leptin, Adiponectin, and Serotonin and Gut Microflora in Beagle Dogs. *Journal of Veterinary Internal Medicine* **29**, 43–50.

PARK, J.S., GUEVARRA, R.B., KIM, B.-R., LEE, J.H., LEE, S.H., CHO, J.H., KIM, H., CHO, J.H., SONG, M., LEE, J.-H., ISAACSON, R.E., SONG, K.H. & KIM, H.B. (2019) Intestinal Microbial Dysbiosis in Beagles Naturally Infected with Canine Parvovirus. *Journal of Microbiology and Biotechnology* **29**, 1391–1400.

PARKS, D.H., CHUVOCHINA, M., RINKE, C., MUSSIG, A.J., CHAUMEIL, P.-A. & HUGENHOLTZ, P. (2022) GTDB: an ongoing census of bacterial and archaeal diversity through a phylogenetically consistent, rank normalized and complete genome-based taxonomy. *Nucleic Acids Research* **50**, D785–D794.

PAßLACK, N., KOHN, B., VAHJEN, W. & ZENTEK, J. (2021) Effects of dietary cellobiose on the intestinal microbiota and excretion of nitrogen metabolites in healthy adult dogs. *Journal of Animal Physiology and Animal Nutrition*.

PAYNE, A.N., ZIHLER, A., CHASSARD, C. & LACROIX, C. (2012) Advances and perspectives in *in vitro* human gut fermentation modeling. *Trends in Biotechnology* **30**, 17–25.

PEARCE, S.C., COIA, H.G., KARL, J.P., PANTOJA-FELICIANO, I.G., ZACHOS, N.C. & RACICOT, K. (2018) Intestinal *in vitro* and ex vivo Models to Study Host-Microbiome Interactions and Acute Stressors. *Frontiers in Physiology* **9**, 1584.

PENAZZI, L., SCHIAVONE, A., RUSSO, N., NERY, J., VALLE, E., MADRID, J., MARTINEZ, S., HERNANDEZ, F., PAGANI, E., ALA, U. & PROLA, L. (2021) *In vivo* and *in vitro* Digestibility of an Extruded Complete Dog Food Containing Black Soldier Fly (Hermetia illucens) Larvae Meal as Protein Source. *Frontiers in Veterinary Science* **8**, 653411.

PEREIRA, A.M., PINNA, C., BIAGI, G., STEFANELLI, C., MAIA, M.R.G., MATOS, E., SEGUNDO, M.A., FONSECA, A.J.M. & CABRITA, A.R.J. (2020) Supplemental selenium source on gut health: insights on fecal microbiome and fermentation products of growing puppies. *FEMS Microbiology Ecology* **96**, fiaa212.

PEREIRA, G.Q., GOMES, L.A., SANTOS, I.S., ALFIERI, A.F., WEESE, J.S. & COSTA, M.C. (2018) Fecal microbiota transplantation in puppies with canine parvovirus infection. *Journal of Veterinary Internal Medicine* **32**, 707–711.

PHAM, V.T., CHASSARD, C., RIFA, E., BRAEGGER, C., GEIRNAERT, A., ROCHA MARTIN, V.N. & LACROIX, C. (2019) Lactate Metabolism Is Strongly Modulated by Fecal Inoculum, pH, and Retention Time in PolyFermS Continuous Colonic Fermentation Models Mimicking Young Infant Proximal Colon. *mSystems* **4**, e00264-18.

PHILLIPS-DONALDSON, D. (2019) Global pet food sales hit $91 billion in 2018. *Petfoodindustry.com*.

https://www.petfoodindustry.com/articles/7899-global-pet-food-sales-hit-91-billion-in-2018.

PIGNATARO, G., DI PRINZIO, R., CRISI, P.E., BELA, B., FUSARO, I., TREVISAN, C., DE ACETIS, L. & GRAMENZI, A. (2021) Comparison of the Therapeutic Effect of Treatment with Antibiotics or Nutraceuticals on Clinical Activity and the Fecal Microbiome of Dogs with Acute Diarrhea. *Animals* **11**, 1484.

PILLA, R., GASCHEN, F.P., BARR, J.W., OLSON, E., HONNEFFER, J., GUARD, B.C., BLAKE, A.B., VILLANUEVA, D., KHATTAB, M.R., ALSHAWAQFEH, M.K., LIDBURY, J.A., STEINER, J.M. & SUCHODOLSKI, J.S. (2020) Effects of metronidazole on the fecal microbiome and metabolome in healthy dogs. *Journal of Veterinary Internal Medicine* **34**, 1853–1866.

PILLA, R. & SUCHODOLSKI, J.S. (2020) The Role of the Canine Gut Microbiome and Metabolome in Health and Gastrointestinal Disease. *Frontiers in Veterinary Science* **6**, 498.

PINNA, C. & BIAGI, G. (2014) The Utilisation of Prebiotics and Synbiotics in Dogs. *Italian Journal of Animal Science* **13**, 3107.

PINNA, C., VECCHIATO, C.G., BOLDUAN, C., GRANDI, M., STEFANELLI, C., WINDISCH, W., ZAGHINI, G. & BIAGI, G. (2018) Influence of dietary protein and fructooligosaccharides on fecal fermentative end-products, fecal bacterial populations and apparent total tract digestibility in dogs. *BMC Veterinary Research* **14**.

PINNA, C., VECCHIATO, C.G., DELSANTE, C., GRANDI, M. & BIAGI, G. (2021) On the Variability of Microbial Populations and Bacterial Metabolites within the Canine Stool. An in-Depth Analysis. *Animals: an open access journal from MDPI* **11**.

PINNA, C., VECCHIATO, C.G., GRANDI, M., MAMMI, L.M.E., STEFANELLI, C. & BIAGI, G. (2020) *In vitro* Evaluation of the Effects of Tylosin on the Composition and Metabolism of Canine Fecal Microbiota. *Animals: an open access journal from MDPI* **10**, 98.

PIQUÉ, N., BERLANGA, M. & MIÑANA-GALBIS, D. (2019) Health Benefits of Heat-Killed (Tyndallized) Probiotics: An Overview. *International Journal of Molecular Sciences* **20**, 2534.

PROPST, E.L., FLICKINGER, E.A., BAUER, L.L., MERCHEN, N.R. & FAHEY, G.C. (2003) A dose-response experiment evaluating the effects of oligofructose and inulin on nutrient digestibility, stool quality, and fecal protein catabolites in healthy adult dogs. *Journal of Animal Science* **81**, 3057–3066.

PRUEKSARITANONT, T., GORHAM, L.M., HOCHMAN, J.H., TRAN, L.O. & VYAS, K.P. (1996) Comparative studies of drug-metabolizing enzymes in dog, monkey, and human small intestines, and in Caco-2 cells. *Drug Metabolism and Disposition: The Biological Fate of Chemicals* **24**, 634–642.

QUAST, C., PRUESSE, E., YILMAZ, P., GERKEN, J., SCHWEER, T., YARZA, P., PEPLIES, J. & GLÖCKNER, F.O. (2013) The SILVA ribosomal RNA gene database project: improved data processing and web-based tools. *Nucleic Acids Research* **41**, D590-596.

RAFFAN, E., DENNIS, R.J., O'DONOVAN, C.J., BECKER, J.M., SCOTT, R.A., SMITH, S.P., WITHERS, D.J., WOOD, C.J., CONCI, E., CLEMENTS, D.N., SUMMERS, K.M., GERMAN, A.J., MELLERSH, C.S., ARENDT, M.L., IYEMERE, V.P., *ET AL.* (2016) A Deletion in the Canine POMC Gene Is Associated with Weight and Appetite in Obesity-Prone Labrador Retriever Dogs. *Cell Metabolism* **23**, 893–900.

RAHAT-ROZENBLOOM, S., FERNANDES, J., GLOOR, G.B. & WOLEVER, T.M.S. (2014) Evidence for greater production of colonic short-chain fatty acids in overweight than lean humans. *International Journal of Obesity* **38**, 1525–1531.

RANA, S.V., SHARMA, S., MALIK, A., KAUR, J., PRASAD, K.K., SINHA, S.K. & SINGH, K. (2013) Small intestinal bacterial overgrowth and orocecal transit time in patients of inflammatory bowel disease. *Digestive Diseases and Sciences* **58**, 2594–2598.

RAN-RESSLER, R.R., GLAHN, R.P., BAE, S. & BRENNA, J.T. (2013) Branched-chain fatty acids in the neonatal gut and estimated dietary intake in infancy and adulthood. *Nestle Nutrition Institute Workshop Series* **77**, 133–143.

RAWLING, M., LECLERCQ, E., SCHIAVONE, M., MERRIFIELD, D., CASTEX, M. & APPER, E. (2022) Bacterial probiotic and postbiotics from L. helveticus HA122 and L. Plantarum HA-119 allow reinforcing gut barrier function in a zebrafish (Danio rerio) model. Amsterdam.

REDDY, K.E., KIM, H.-R., JEONG, J.Y., SO, K.-M., LEE, S., JI, S.Y., KIM, M., LEE, H.-J., LEE, S., KIM, K.-H. & KIM, M. (2019) Impact of Breed on the Fecal Microbiome of Dogs under the Same Dietary Condition.

Journal of Microbiology and Biotechnology **29**, 1947–1956.

REDFERN, A., SUCHODOLSKI, J. & JERGENS, A. (2017) Role of the gastrointestinal microbiota in small animal health and disease. *The Veterinary Record* **181**, 370.

REESE, A.T., CHO, E.H., KLITZMAN, B., NICHOLS, S.P., WISNIEWSKI, N.A., VILLA, M.M., DURAND, H.K., JIANG, S., MIDANI, F.S., NIMMAGADDA, S.N., O'CONNELL, T.M., WRIGHT, J.P., DESHUSSES, M.A. & DAVID, L.A. (2018) Antibiotic-induced changes in the microbiota disrupt redox dynamics in the gut. *eLife* **7**, e35987.

REYGNER, J., CHARRUEAU, C., DELANNOY, J., MAYEUR, C., ROBERT, V., CUINAT, C., MEYLHEUC, T., MAURAS, A., AUGUSTIN, J., NICOLIS, I., MODOUX, M., JOLY, F., WALIGORA-DUPRIET, A.-J., THOMAS, M. & KAPEL, N. (2020) Freeze-dried fecal samples are biologically active after long-lasting storage and suited to fecal microbiota transplantation in a preclinical murine model of *Clostridioides difficile* infection. *Gut Microbes* **11**, 1405–1422.

RICCI, R., PERAZZI, A., BADON, T., BEDIN, S. & IACOPETTI, I. (2018) Effect of storage on long-term stability of salivary α-amylase, lysozyme, lactate dehydrogenase, calcium and phosphorus in dogs. *Veterinary Journal (London, England: 1997)* **242**, 44–47.

RIDLON, J.M., HARRIS, S.C., BHOWMIK, S., KANG, D.-J. & HYLEMON, P.B. (2016) Consequences of bile salt biotransformations by intestinal bacteria. *Gut Microbes* **7**, 22–39.

RIDLON, J.M., KANG, D.J., HYLEMON, P.B. & BAJAJ, J.S. (2014) Bile acids and the gut microbiome: *Current Opinion in Gastroenterology* **30**, 332–338.

RINTALA, A., PIETILÄ, S., MUNUKKA, E., EEROLA, E., PURSIHEIMO, J.-P., LAIHO, A., PEKKALA, S. & HUOVINEN, P. (2017) Gut Microbiota Analysis Results Are Highly Dependent on the 16S rRNA Gene Target Region, Whereas the Impact of DNA Extraction Is Minor. *Journal of biomolecular techniques: JBT* **28**, 19–30.

RIVERA-CHÁVEZ, F., LOPEZ, C.A. & BÄUMLER, A.J. (2017) Oxygen as a driver of gut dysbiosis. *Free Radical Biology and Medicine* **105**, 93–101.

ROBERTI, M.P., RAUBER, C., KROEMER, G. & ZITVOGEL, L. (2022) Impact of the ileal microbiota on colon cancer. *Seminars in Cancer Biology* **86**, 955–966.

ROBIN, A. (2007) Les enterpathies exudatives chez le chien : actualités, diagnostiques et analyse retrospective de series de cas cliniques. Université Claude Bernard, Lyon.

ROCHEGÜE, T., HAENNI, M., MONDOT, S., ASTRUC, C., CAZEAU, G., FERRY, T., MADEC, J.-Y. & LUPO, A. (2021) Impact of Antibiotic Therapies on Resistance Genes Dynamic and Composition of the Animal Gut Microbiota. *Animals* **11**, 3280.

ROCK, C. & DONNENBERG, M.S. (2014) Human Pathogenic Enterobacteriaceae. In *Reference Module in Biomedical Sciences* p. B9780128012383000000. Elsevier.

ROLFE, V. (1999) Colonic fluid and electrolyte transport in health and disease. *The Veterinary Clinics of North America. Small Animal Practice* **29**, 577–588, viii.

ROOKS, M.G. & GARRETT, W.S. (2016) Gut microbiota, metabolites and host immunity. *Nature Reviews. Immunology* **16**, 341–352.

ROSSI, G., PENGO, G., CALDIN, M., PALUMBO PICCIONELLO, A., STEINER, J.M., COHEN, N.D., JERGENS, A.E. & SUCHODOLSKI, J.S. (2014) Comparison of Microbiological, Histological, and Immunomodulatory Parameters in Response to Treatment with Either Combination Therapy with Prednisone and Metronidazole or Probiotic VSL#3 Strains in Dogs with Idiopathic Inflammatory Bowel Disease. *PLoS ONE* **9**, e94699.

ROTA, A., DEL CARRO, A., BERTERO, A., DEL CARRO, A., STARVAGGI CUCUZZA, A., BANCHI, P. & CORRÒ, M. (2021) Does Bacteria Colonization of Canine Newborns Start in the Uterus? *Animals* **11**, 1415.

ROUSSEL, C., ANUNCIAÇÃO BRAGA GUEBARA, S., PLANTE, P.-L., DESJARDINS, Y., DI MARZO, V. & SILVESTRI, C. (2022) Short-term supplementation with ω-3 polyunsaturated fatty acids modulates primarily mucolytic species from the gut luminal mucin niche in a human fermentation system. *Gut Microbes* **14**, 2120344.

ROUSSEL, C., CORDONNIER, C., GALIA, W., LE GOFF, O., THÉVENOT, J., CHALANCON, S., ALRIC, M.,

THEVENOT-SERGENTET, D., LERICHE, F., VAN DE WIELE, T., LIVRELLI, V. & BLANQUET-DIOT, S. (2016) Increased EHEC survival and virulence gene expression indicates an enhanced pathogenicity upon simulated pediatric gastrointestinal conditions. *Pediatric Research* **80**, 734–743.

ROUSSEL, C., DE PAEPE, K., GALIA, W., DE BODT, J., CHALANCON, S., DENIS, S., LERICHE, F., VANDEKERKOVE, P., BALLET, N., BLANQUET-DIOT, S. & VAN DE WIELE, T. (2021) Multi-targeted properties of the probiotic saccharomyces cerevisiae CNCM I-3856 against enterotoxigenic escherichia coli (ETEC) H10407 pathogenesis across human gut models. *Gut Microbes* **13**, 1953246.

ROUSSEL, C., DE PAEPE, K., GALIA, W., DE BODT, J., CHALANCON, S., LERICHE, F., BALLET, N., DENIS, S., ALRIC, M., VAN DE WIELE, T. & BLANQUET-DIOT, S. (2020) Spatial and temporal modulation of enterotoxigenic E. coli H10407 pathogenesis and interplay with microbiota in human gut models. *BMC biology* **18**, 141.

ROWLAND, I., GIBSON, G., HEINKEN, A., SCOTT, K., SWANN, J., THIELE, I. & TUOHY, K. (2018) Gut microbiota functions: metabolism of nutrients and other food components. *European Journal of Nutrition* **57**, 1–24.

RUBAS, W., JEZYK, N. & GRASS, G.M. (1993) Comparison of the permeability characteristics of a human colonic epithelial (Caco-2) cell line to colon of rabbit, monkey, and dog intestine and human drug absorption. *Pharmaceutical Research* **10**, 113–118.

RUSSEL, W.M.S. & BURCH, R.L. (1959) *The Principles of Humane Experimental Technique*.

SADAKA, C., ELLSWORTH, E., HANSEN, P.R., EWIN, R., DAMBORG, P. & WATTS, J.L. (2018) Review on Abyssomicins: Inhibitors of the Chorismate Pathway and Folate Biosynthesis. *Molecules (Basel, Switzerland)* **23**, 1371.

SAITOH, Y., SUZUKI, H., TANI, K., NISHIKAWA, K., IRIE, K., OGURA, Y., TAMURA, A., TSUKITA, S. & FUJIYOSHI, Y. (2015) Structural insight into tight junction disassembly by *Clostridium perfringens* enterotoxin. *Science* **347**, 775–778.

SALAS-MANI, A., JEUSETTE, I., CASTILLO, I., MANUELIAN, C.L., LIONNET, C., IRACULIS, N., SANCHEZ, N., FERNÁNDEZ, S., VILASECA, L. & TORRE, C. (2018) Fecal microbiota composition changes after a BW loss diet in Beagle dogs. *Journal of Animal Science* **96**, 3102–3111.

SALMINEN, S., COLLADO, M.C., ENDO, A., HILL, C., LEBEER, S., QUIGLEY, E.M.M., SANDERS, M.E., SHAMIR, R., SWANN, J.R., SZAJEWSKA, H. & VINDEROLA, G. (2021) The International Scientific Association of Probiotics and Prebiotics (ISAPP) consensus statement on the definition and scope of postbiotics. *Nature Reviews Gastroenterology & Hepatology* **18**, 649–667.

SAMS, L., PAUME, J., GIALLO, J. & CARRIÈRE, F. (2016) Relevant pH and lipase for *in vitro* models of gastric digestion. *Food & Function* **7**, 30–45.

SANDRI, M., DAL MONEGO, S., CONTE, G., SGORLON, S. & STEFANON, B. (2016) Raw meat-based diet influences faecal microbiome and end products of fermentation in healthy dogs. *BMC Veterinary Research* **13**.

SANGUANSERMSRI, P., JENKINSON, H.F., THANASAK, J., CHAIRATVIT, K., ROYTRAKUL, S., KITTISENACHAI, S., PUENGSURIN, D. & SURARIT, R. (2018) Comparative proteomic study of dog and human saliva. *PloS One* **13**, e0208317.

SARRIÁ, R., LATORRE, R., HENROTEAUX, M., HENROTEAUX, N., SORIA, F., PÉREZ-CUADRADO, E. & LÓPEZ ALBORS, O. (2012) Morphometric study of the layers of the canine small intestine at five sampling sites. *Veterinary Journal (London, England: 1997)* **192**, 498–502.

SAUTER, S.N., ALLENSPACH, K., GASCHEN, F., GRÖNE, A., ONTSOUKA, E. & BLUM, J.W. (2005) Cytokine expression in an ex vivo culture system of duodenal samples from dogs with chronic enteropathies: modulation by probiotic bacteria. *Domestic Animal Endocrinology* **29**, 605–622.

SCARSELLA, E., STEFANON, B., CINTIO, M., LICASTRO, D., SGORLON, S., DAL MONEGO, S. & SANDRI, M. (2020) Learning machine approach reveals microbial signatures of diet and sex in dog. *PloS One* **15**, e0237874.

SCHMIDT, M., UNTERER, S., SUCHODOLSKI, J.S., HONNEFFER, J.B., GUARD, B.C., LIDBURY, J.A., STEINER, J.M., FRITZ, J. & KÖLLE, P. (2018) The fecal microbiome and metabolome differs between dogs fed Bones and Raw Food (BARF) diets and dogs fed commercial diets. *PLOS ONE* **13**, e0201279.

SCHMITZ, S. & SUCHODOLSKI, J. (2016) Understanding the canine intestinal microbiota and its modification by

pro-, pre- and synbiotics - what is the evidence? *Veterinary Medicine and Science* **2**, 71–94.

SCHWIERTZ, A., TARAS, D., SCHÄFER, K., BEIJER, S., BOS, N.A., DONUS, C. & HARDT, P.D. (2010) Microbiota and SCFA in lean and overweight healthy subjects. *Obesity (Silver Spring, Md.)* **18**, 190–195.

SCHWIZER, W., STEINGÖTTER, A., FOX, M., ZUR, T., THUMSHIRN, M., BÖSIGER, P. & FRIED, M. (2002) Non-invasive measurement of gastric accommodation in humans. *Gut* **51 Suppl 1**, i59-62.

SENDER, R., FUCHS, S. & MILO, R. (2016) Revised Estimates for the Number of Human and Bacteria Cells in the Body. *PLOS Biology* **14**, e1002533.

SHEN, G., WU, J., YE, B.-C. & QI, N. (2021) Gut Microbiota-Derived Metabolites in the Development of Diseases. *The Canadian Journal of Infectious Diseases & Medical Microbiology = Journal Canadien Des Maladies Infectieuses Et De La Microbiologie Medicale* **2021**, 6658674.

SHETTY, S. & DE STEENHUIJSEN PITERS, W.A. (2022) dysbiosisR: an R package for calculating microbiome dysbiosis measures.

SHI, Y., TAO, J., LI, B., SHEN, X., CHENG, J. & LIU, H. (2021) The Gut Viral Metagenome Analysis of Domestic Dogs Captures Snapshot of Viral Diversity and Potential Risk of Coronavirus. *Frontiers in Veterinary Science* **8**, 695088.

SICILIANO, R.A., REALE, A., MAZZEO, M.F., MORANDI, S., SILVETTI, T. & BRASCA, M. (2021) Paraprobiotics: A New Perspective for Functional Foods and Nutraceuticals. *Nutrients* **13**, 1225.

SILVA, B.C., JUNG, L.R.C., SANDES, S.H.C., ALVIM, L.B., BOMFIM, M.R.Q., NICOLI, J.R., NEUMANN, E. & NUNES, A.C. (2013) *In vitro* assessment of functional properties of lactic acid bacteria isolated from faecal microbiota of healthy dogs for potential use as probiotics. *Beneficial Microbes* **4**, 267–275.

SIMON, M. (2019) L'anxiété chez le chien, les répercussions sur le microbiote intestinal : intérêt de l'utilisation des probiotiques dans la prise en charge thérapeutique. Ecole Nationale Vétérinaire de Toulouse, Toulouse.

SIMPSON, K.W., DOGAN, B., RISHNIW, M., GOLDSTEIN, R.E., KLAESSIG, S., MCDONOUGH, P.L., GERMAN, A.J., YATES, R.M., RUSSELL, D.G., JOHNSON, S.E., BERG, D.E., HAREL, J., BRUANT, G., MCDONOUGH, S.P. & SCHUKKEN, Y.H. (2006) Adherent and invasive Escherichia coli is associated with granulomatous colitis in boxer dogs. *Infection and Immunity* **74**, 4778–4792.

SINGLETON, D.A., NOBLE, P.J.M., SÁNCHEZ-VIZCAÍNO, F., DAWSON, S., PINCHBECK, G.L., WILLIAMS, N.J., RADFORD, A.D. & JONES, P.H. (2019) Pharmaceutical Prescription in Canine Acute Diarrhoea: A Longitudinal Electronic Health Record Analysis of First Opinion Veterinary Practices. *Frontiers in Veterinary Science* **6**, 218.

SJÖGREN, E., ABRAHAMSSON, B., AUGUSTIJNS, P., BECKER, D., BOLGER, M.B., BREWSTER, M., BROUWERS, J., FLANAGAN, T., HARWOOD, M., HEINEN, C., HOLM, R., JURETSCHKE, H.-P., KUBBINGA, M., LINDAHL, A., LUKACOVA, V., *ET AL.* (2014) *In vivo* methods for drug absorption - comparative physiologies, model selection, correlations with *in vitro* methods (IVIVC), and applications for formulation/API/excipient characterization including food effects. *European Journal of Pharmaceutical Sciences: Official Journal of the European Federation for Pharmaceutical Sciences* **57**, 99–151.

ŠLAPETA, J., DOWD, S.E., ALANAZI, A.D., WESTMAN, M.E. & BROWN, G.K. (2015) Differences in the faecal microbiome of non-diarrhoeic clinically healthy dogs and cats associated with Giardia duodenalis infection: impact of hookworms and coccidia. *International Journal for Parasitology* **45**, 585–594.

SMEETS-PEETERS, M. (2000) Feeding FIDO: development, validation and application of a dynamic, *in vitro* model of the gastrointestinal tract of the dog. Wageningen University.

SMEETS-PEETERS, M., WATSON, T., MINEKUS, M. & HAVENAAR, R. (1998) A review of the physiology of the canine digestive tract related to the development of *in vitro* systems. *Nutrition Research Reviews* **11**, 45–69.

SMEETS-PEETERS, M.J., MINEKUS, M., HAVENAAR, R., SCHAAFSMA, G. & VERSTEGEN, M.W. (1999) Description of a dynamic *in vitro* model of the dog gastrointestinal tract and an evaluation of various transit times for protein and calcium. *Alternatives to laboratory animals: ATLA* **27**, 935–949.

SMITH, H.W. (1965) Observations on the flora of the alimentary tract of animals and factors affecting its composition. *The Journal of Pathology and Bacteriology* **89**, 95–122.

SONG, S.J., AMIR, A., METCALF, J.L., AMATO, K.R., XU, Z.Z., HUMPHREY, G. & KNIGHT, R. (2016) Preservation Methods Differ in Fecal Microbiome Stability, Affecting Suitability for Field Studies. *mSystems* **1**.

SOTO-MARTIN, E.C., WARNKE, I., FARQUHARSON, F.M., CHRISTODOULOU, M., HORGAN, G., DERRIEN, M., FAURIE, J.-M., FLINT, H.J., DUNCAN, S.H. & LOUIS, P. (2020) Vitamin Biosynthesis by Human Gut Butyrate-Producing Bacteria and Cross-Feeding in Synthetic Microbial Communities. *mBio* **11**, e00886-20.

SOULIMAN, S., BLANQUET, S., BEYSSAC, E. & CARDOT, J.-M. (2006) A level A *in vitro*/*in vivo* correlation in fasted and fed states using different methods: applied to solid immediate release oral dosage form. *European Journal of Pharmaceutical Sciences: Official Journal of the European Federation for Pharmaceutical Sciences* **27**, 72–79.

SPEARS, J., AMEHO, C. & REYNOLDS, A. (2016) Beyond Probiotics: Heat-Treated Probiotics in Companion Animal Health. *Pet Nutrition: Beyond Essential*, 79.

STIER, H. & BISCHOFF, S. (2016) Influence of Saccharomyces boulardii CNCM I-745 on the gut-associated immune system. *Clinical and Experimental Gastroenterology* **Volume 9**, 269–279.

STROMPFOVÁ, V., KUBAŠOVÁ, I. & LAUKOVÁ, A. (2017) Health benefits observed after probiotic Lactobacillus fermentum CCM 7421 application in dogs. *Applied Microbiology and Biotechnology* **101**, 6309–6319.

STROMPFOVÁ, V., KUBAŠOVÁ, I., ŠČERBOVÁ, J., MAĎARI, A., GANCARČÍKOVÁ, S., MUDROŇOVÁ, D., MILTKO, R., BELZECKI, G. & LAUKOVÁ, A. (2019) Oral administration of bacteriocin-producing and non-producing strains of Enterococcus faecium in dogs. *Applied Microbiology and Biotechnology* **103**, 4953–4965.

STROMPFOVÁ, V., LAUKOVÁ, A. & GANCARČÍKOVÁ, S. (2012) Effectivity of freeze-dried form of Lactobacillus fermentum AD1-CCM7421 in dogs. *Folia Microbiologica* **57**, 347–350.

STROMPFOVÁ, V., MARCIŇÁKOVÁ, M., SIMONOVÁ, M., BOGOVIČ-MATIJAŠIĆ, B. & LAUKOVÁ, A. (2006) Application of potential probiotic Lactobacillus fermentum AD1 strain in healthy dogs. *Anaerobe* **12**, 75–79.

STROMPFOVÁ, V., POGÁNY SIMONOVÁ, M., GANCARČÍKOVÁ, S., MUDROŇOVÁ, D., FARBÁKOVÁ, J., MAD'ARI, A. & LAUKOVÁ, A. (2014) Effect of Bifidobacterium animalis B/12 administration in healthy dogs. *Anaerobe* **28**, 37–43.

SUCHODOLSKI, J.S. (2011a) Intestinal Microbiota of Dogs and Cats: a Bigger World than We Thought. *Veterinary Clinics of North America: Small Animal Practice* **41**, 261–272.

SUCHODOLSKI, J.S. (2011b) Companion animals symposium: microbes and gastrointestinal health of dogs and cats. *Journal of Animal Science* **89**, 1520–1530.

SUCHODOLSKI, J.S., CAMACHO, J. & STEINER, J.M. (2008) Analysis of bacterial diversity in the canine duodenum, jejunum, ileum, and colon by comparative 16S rRNA gene analysis. *FEMS microbiology ecology* **66**, 567–578.

SUCHODOLSKI, J.S., DOWD, S.E., WESTERMARCK, E., STEINER, J.M., WOLCOTT, R.D., SPILLMANN, T. & HARMOINEN, J.A. (2009) The effect of the macrolide antibiotic tylosin on microbial diversity in the canine small intestine as demonstrated by massive parallel 16S rRNA gene sequencing. *BMC Microbiology* **9**, 210.

SUCHODOLSKI, J.S., DOWD, S.E., WILKE, V., STEINER, J.M. & JERGENS, A.E. (2012a) 16S rRNA gene pyrosequencing reveals bacterial dysbiosis in the duodenum of dogs with idiopathic inflammatory bowel disease. *PloS One* **7**, e39333.

SUCHODOLSKI, J.S., MARKEL, M.E., GARCIA-MAZCORRO, J.F., UNTERER, S., HEILMANN, R.M., DOWD, S.E., KACHROO, P., IVANOV, I., MINAMOTO, Y., DILLMAN, E.M., STEINER, J.M., COOK, A.K. & TORESSON, L. (2012b) The fecal microbiome in dogs with acute diarrhea and idiopathic inflammatory bowel disease. *PloS One* **7**, e51907.

SUCHODOLSKI, J.S., XENOULIS, P.G., PADDOCK, C.G., STEINER, J.M. & JERGENS, A.E. (2010) Molecular analysis of the bacterial microbiota in duodenal biopsies from dogs with idiopathic inflammatory bowel disease. *Veterinary Microbiology* **142**, 394–400.

SUGITA, K., YANUMA, N., OHNO, H., TAKAHASHI, K., KAWANO, K., MORITA, H. & OHMORI, K. (2019) Oral

faecal microbiota transplantation for the treatment of Clostridium difficile-associated diarrhoea in a dog: a case report. *BMC veterinary research* **15**, 11.

SUN, Y., PAN, Y., SUN, Y., LI, M., HUANG, S., QIU, W., TU, H. & ZHANG, K. (2019) Effects of Norspermidine on Dual-Species Biofilms Composed of Streptococcus mutans and Streptococcus sanguinis. *BioMed Research International* **2019**, 1950790.

SUNVOLD, G.D., FAHEY, G.C., MERCHEN, N.R. & REINHART, G.A. (1995a) *In vitro* fermentation of selected fibrous substrates by dog and cat fecal inoculum: influence of diet composition on substrate organic matter disappearance and short-chain fatty acid production. *Journal of Animal Science* **73**, 1110–1122.

SUNVOLD, G.D., FAHEY, G.C., MERCHEN, N.R., TITGEMEYER, E.C., BOURQUIN, L.D., BAUER, L.L. & REINHART, G.A. (1995b) Dietary fiber for dogs: IV. *In vitro* fermentation of selected fiber sources by dog fecal inoculum and *in vivo* digestion and metabolism of fiber-supplemented diets. *Journal of Animal Science* **73**, 1099–1109.

SUNVOLD, G.D., HUSSEIN, H.S., FAHEY, G.C., MERCHEN, N.R. & REINHART, G.A. (1995c) *In vitro* fermentation of cellulose, beet pulp, citrus pulp, and citrus pectin using fecal inoculum from cats, dogs, horses, humans, and pigs and ruminal fluid from cattle. *Journal of Animal Science* **73**, 3639–3648.

SUSEWIND, J., DE SOUZA CARVALHO-WODARZ, C., REPNIK, U., COLLNOT, E.-M., SCHNEIDER-DAUM, N., GRIFFITHS, G.W. & LEHR, C.-M. (2015) A 3D co-culture of three human cell lines to model the inflamed intestinal mucosa for safety testing of nanomaterials. *Nanotoxicology*, 1–10.

SWANSON, K.S., DOWD, S.E., SUCHODOLSKI, J.S., MIDDELBOS, I.S., VESTER, B.M., BARRY, K.A., NELSON, K.E., TORRALBA, M., HENRISSAT, B., COUTINHO, P.M., CANN, I.K.O., WHITE, B.A. & FAHEY, G.C. (2011) Phylogenetic and gene-centric metagenomics of the canine intestinal microbiome reveals similarities with humans and mice. *The ISME journal* **5**, 639–649.

SWANSON, K.S., GRIESHOP, C.M., CLAPPER, G.M., SHIELDS, R.G., BELAY, T., MERCHEN, N.R. & FAHEY, G.C. (2001) Fruit and vegetable fiber fermentation by gut microflora from canines. *Journal of Animal Science* **79**, 919.

SWANSON, K.S., GRIESHOP, C.M., FLICKINGER, E.A., BAUER, L.L., CHOW, J., WOLF, B.W., GARLEB, K.A. & FAHEY, G.C. (2002) Fructooligosaccharides and Lactobacillus acidophilus modify gut microbial populations, total tract nutrient digestibilities and fecal protein catabolite concentrations in healthy adult dogs. *The Journal of Nutrition* **132**, 3721–3731.

SZAJEWSKA, H. & KOŁODZIEJ, M. (2015) Systematic review with meta-analysis: Saccharomyces boulardii in the prevention of antibiotic-associated diarrhoea. *Alimentary Pharmacology & Therapeutics* **42**, 793–801.

TAKAI, K. & HORIKOSHI, K. (2000) Rapid detection and quantification of members of the archaeal community by quantitative PCR using fluorogenic probes. *Applied and Environmental Microbiology* **66**, 5066–5072.

TANG, G., YIN, W. & LIU, W. (2017) Is frozen fecal microbiota transplantation as effective as fresh fecal microbiota transplantation in patients with recurrent or refractory Clostridium difficile infection: A meta-analysis? *Diagnostic Microbiology and Infectious Disease* **88**, 322–329.

TANNER, S.A., ZIHLER BERNER, A., RIGOZZI, E., GRATTEPANCHE, F., CHASSARD, C. & LACROIX, C. (2014) *In vitro* continuous fermentation model (PolyFermS) of the swine proximal colon for simultaneous testing on the same gut microbiota. *PloS One* **9**, e94123.

TAVERNITI, V. & GUGLIELMETTI, S. (2011) The immunomodulatory properties of probiotic microorganisms beyond their viability (ghost probiotics: proposal of paraprobiotic concept). *Genes & Nutrition* **6**, 261–274.

TEAME, T., WANG, A., XIE, M., ZHANG, Z., YANG, Y., DING, Q., GAO, C., OLSEN, R.E., RAN, C. & ZHOU, Z. (2020) Paraprobiotics and Postbiotics of Probiotic Lactobacilli, Their Positive Effects on the Host and Action Mechanisms: A Review. *Frontiers in Nutrition* **7**, 570344.

TECLES, F., ESCRIBANO, D., CONTRERAS-AGUILAR, M.D., RUBIO, C.P., SZCZUBIAŁ, M., CERÓN, J.J., DĄBROWSKI, R. & TVARIJONAVICIUTE, A. (2018) Evaluation of adenosine deaminase in saliva and serum, and salivary α-amylase, in canine pyometra at diagnosis and after ovariohysterectomy. *The Veterinary Journal* **236**, 102–110.

THAKARE, R., ALAMOUDI, J.A., GAUTAM, N., RODRIGUES, A.D. & ALNOUTI, Y. (2018) Species differences in

bile acids I. Plasma and urine bile acid composition. *Journal of applied toxicology: JAT* **38**, 1323–1335.

THE BUSINESS RESEARCH COMPANY (2020) Animal medicinee global market opportunities and strategies to 2023.

THEIL, S. & RIFA, E. (2021) rANOMALY: AmplicoN wOrkflow for Microbial community AnaLYsis. *F1000Research* **10**, 7.

THÉVENOT, J., CORDONNIER, C., ROUGERON, A., LE GOFF, O., NGUYEN, H.T.T., DENIS, S., ALRIC, M., LIVRELLI, V. & BLANQUET-DIOT, S. (2015) Enterohemorrhagic Escherichia coli infection has donor-dependent effect on human gut microbiota and may be antagonized by probiotic yeast during interaction with Peyer's patches. *Applied Microbiology and Biotechnology* **99**, 9097–9110.

THOMAS, C.M. & VERSALOVIC, J. (2010) Probiotics-host communication: Modulation of signaling pathways in the intestine. *Gut Microbes* **1**, 148–163.

THUENEMANN, E.C., MANDALARI, G., RICH, G.T. & FAULKS, R.M. (2015) Dynamic Gastric Model (DGM). In *The Impact of Food Bioactives on Health: in vitro and ex vivo models* (eds K. VERHOECKX, P. COTTER, I. LÓPEZ-EXPÓSITO, C. KLEIVELAND, T. LEA, A. MACKIE, T. REQUENA, D. SWIATECKA & H. WICHERS), p. Springer, Cham (CH).

TIAN, L., WANG, X.-W., WU, A.-K., FAN, Y., FRIEDMAN, J., DAHLIN, A., WALDOR, M.K., WEINSTOCK, G.M., WEISS, S.T. & LIU, Y.-Y. (2020) Deciphering functional redundancy in the human microbiome. *Nature Communications* **11**, 6217.

TOFALO, R., COCCHI, S. & SUZZI, G. (2019) Polyamines and Gut Microbiota. *Frontiers in Nutrition* **6**, 16.

TOMPKINS, T.A., MAINVILLE, I. & ARCAND, Y. (2011) The impact of meals on a probiotic during transit through a model of the human upper gastrointestinal tract. *Beneficial Microbes* **2**, 295–303.

TOTTEY, W., FERIA-GERVASIO, D., GACI, N., LAILLET, B., PUJOS, E., MARTIN, J.-F., SEBEDIO, J.-L., SION, B., JARRIGE, J.-F., ALRIC, M. & BRUGÈRE, J.-F. (2017) Colonic Transit Time Is a Driven Force of the Gut Microbiota Composition and Metabolism: *In vitro* Evidence. *Journal of Neurogastroenterology and Motility* **23**, 124–134.

TOTTEY, W., GACI, N., BORREL, G., ALRIC, M., O'TOOLE, P.W. & BRUGÈRE, J.-F. (2015) In-vitro model for studying methanogens in human gut microbiota. *Anaerobe* **34**, 50–52.

TRAUGHBER, Z.T., HE, F., HOKE, J.M., DAVENPORT, G.M. & DE GODOY, M.R.C. (2020) Chemical composition and *in vitro* fermentation characteristics of legumes using canine fecal inoculum. *Translational Animal Science* **4**, txaa200.

TUNIYAZI, M., HU, X., FU, Y. & ZHANG, N. (2022) Canine Fecal Microbiota Transplantation: Current Application and Possible Mechanisms. *Veterinary Sciences* **9**, 396.

TVARIJONAVICIUTE, A., CERON, J.J., HOLDEN, S.L., CUTHBERTSON, D.J., BIOURGE, V., MORRIS, P.J. & GERMAN, A.J. (2012) Obesity-related metabolic dysfunction in dogs: a comparison with human metabolic syndrome. *BMC veterinary research* **8**, 147.

TZORTZIS, G., GOULAS, A.K., BAILLON, M.-L.A., GIBSON, G.R. & RASTALL, R.A. (2004) *In vitro* evaluation of the fermentation properties of galactooligosaccharides synthesised by alpha-galactosidase from Lactobacillus reuteri. *Applied Microbiology and Biotechnology* **64**, 106–111.

URIOT, O., CHALANCON, S., MAZAL, C., ETIENNE-MESMIN, L., DENIS, S. & BLANQUET-DIOT, S. (2021) Use of the Dynamic TIM-1 Model for an In-Depth Understanding of the Survival and Virulence Gene Expression of Shiga Toxin-Producing Escherichia coli in the Human Stomach and Small Intestine. *Methods in Molecular Biology (Clifton, N.J.)* **2291**, 297–315.

VAN DE WIELE, T., VAN DEN ABBEELE, P., OSSIEUR, W., POSSEMIERS, S. & MARZORATI, M. (2015a) The Simulator of the Human Intestinal Microbial Ecosystem (SHIME®). In *The Impact of Food Bioactives on Health: in vitro and ex vivo models* (eds K. VERHOECKX, P. COTTER, I. LÓPEZ-EXPÓSITO, C. KLEIVELAND, T. LEA, A. MACKIE, T. REQUENA, D. SWIATECKA & H. WICHERS), p. Springer, Cham (CH).

VAN DE WIELE, T., VAN DEN ABBEELE, P., OSSIEUR, W., POSSEMIERS, S. & MARZORATI, M. (2015b) The Simulator of the Human Intestinal Microbial Ecosystem (SHIME®). In *The Impact of Food Bioactives on Health: in vitro and ex vivo models* (eds K. VERHOECKX, P. COTTER, I. LÓPEZ-EXPÓSITO, C. KLEIVELAND, T. LEA, A. MACKIE, T. REQUENA, D. SWIATECKA & H. WICHERS), p. Springer, Cham

(CH).

VAN DEN ABBEELE, P., DUYSBURGH, C., RAKEBRANDT, M. & MARZORATI, M. (2020a) Dried yeast cell walls high in beta-glucan and mannan-oligosaccharides positively affect microbial composition and activity in the canine gastrointestinal tract *in vitro*. *Journal of Animal Science* **98**.

VAN DEN ABBEELE, P., GROOTAERT, C., MARZORATI, M., POSSEMIERS, S., VERSTRAETE, W., GÉRARD, P., RABOT, S., BRUNEAU, A., EL AIDY, S., DERRIEN, M., ZOETENDAL, E., KLEEREBEZEM, M., SMIDT, H. & VAN DE WIELE, T. (2010) Microbial community development in a dynamic gut model is reproducible, colon region specific, and selective for Bacteroidetes and Clostridium cluster IX. *Applied and Environmental Microbiology* **76**, 5237–5246.

VAN DEN ABBEELE, P., GROOTAERT, C., POSSEMIERS, S., VERSTRAETE, W., VERBEKEN, K. & VAN DE WIELE, T. (2009) *In vitro* model to study the modulation of the mucin-adhered bacterial community. *Applied Microbiology and Biotechnology* **83**, 349–359.

VAN DEN ABBEELE, P., MOENS, F., PIGNATARO, G., SCHNURR, J., RIBECCO, C., GRAMENZI, A. & MARZORATI, M. (2020b) Yeast-Derived Formulations Are Differentially Fermented by the Canine and Feline Microbiome as Assessed in a Novel *In vitro* Colonic Fermentation Model. *Journal of Agricultural and Food Chemistry*, acs.jafc.9b05085.

VAN DEN ABBEELE, P., TAMINIAU, B., PINHEIRO, I., DUYSBURGH, C., JACOBS, H., PIJLS, L. & MARZORATI, M. (2018) Arabinoxylo-Oligosaccharides and Inulin Impact Inter-Individual Variation on Microbial Metabolism and Composition, Which Immunomodulates Human Cells. *Journal of Agricultural and Food Chemistry* **66**, 1121–1130.

VAN HERREWEGHEN, F., DE PAEPE, K., MARZORATI, M. & VAN DE WIELE, T. (2021) Mucin as a Functional Niche Is a More Important Driver of *In vitro* Gut Microbiota Composition and Functionality than Akkermansia muciniphila Supplementation. *Applied and Environmental Microbiology* **87**, e02647-20.

VÁZQUEZ-BAEZA, Y., HYDE, E.R., SUCHODOLSKI, J.S. & KNIGHT, R. (2016) Dog and human inflammatory bowel disease rely on overlapping yet distinct dysbiosis networks. *Nature Microbiology* **1**, 16177.

VENEMA, K., VERHOEVEN, J., BECKMAN, C. & KELLER, D. (2020) Survival of a probiotic-containing product using capsule-within-capsule technology in an *in vitro* model of the stomach and small intestine (TIM-1). *Beneficial Microbes* **11**, 403–409.

VERDIER, C., DENIS, S., GASC, C., BOUCINHA, L., URIOT, O., DELMAS, D., DORE, J., CAMUS, C.L., SCHWINTNER, C. & BLANQUET-DIOT, S. (2021) An Oral FMT Capsule as Efficient as an Enema for Microbiota Reconstruction Following Disruption by Antibiotics, as Assessed in an *In vitro* Human Gut Model. *Microorganisms* **9**, 358.

VERSTREPEN, L., VAN DEN ABBEELE, P., PIGNATARO, G., RIBECCO, C., GRAMENZI, A., HESTA, M. & MARZORATI, M. (2021) Inclusion of small intestinal absorption and simulated mucosal surfaces further improve the Mucosal Simulator of the Canine Intestinal Microbial Ecosystem (M-SCIME™). *Research in Veterinary Science* **140**, 100–108.

VIERBAUM, L., EISENHAUER, L., VAHJEN, W. & ZENTEK, J. (2019) *In vitro* evaluation of the effects of Yucca schidigera and inulin on the fermentation potential of the faecal microbiota of dogs fed diets with low or high protein concentrations. *Archives of Animal Nutrition* **73**, 399–413.

VILSON, Å., RAMADAN, Z., LI, Q., HEDHAMMAR, Å., REYNOLDS, A., SPEARS, J., LABUDA, J., PELKER, R., BJÖRKSTÉN, B., DICKSVED, J. & HANSSON-HAMLIN, H. (2018) Disentangling factors that shape the gut microbiota in German Shepherd dogs. *PloS One* **13**, e0193507.

VINCE, A.J. & BURRIDGE, S.M. (1980) Ammonia production by intestinal bacteria: the effects of lactose, lactulose and glucose. *Journal of Medical Microbiology* **13**, 177–191.

VITAL, M., GAO, J., RIZZO, M., HARRISON, T. & TIEDJE, J.M. (2015) Diet is a major factor governing the fecal butyrate-producing community structure across Mammalia, Aves and Reptilia. *The ISME Journal* **9**, 832–843.

VOLKMANN, M., STEINER, J.M., FOSGATE, G.T., ZENTEK, J., HARTMANN, S. & KOHN, B. (2017) Chronic Diarrhea in Dogs - Retrospective Study in 136 Cases. *Journal of Veterinary Internal Medicine* **31**, 1043–1055.

WAIMIN, J.F., NEJATI, S., JIANG, H., QIU, J., WANG, J., VERMA, M.S. & RAHIMI, R. (2020) Smart capsule for

non-invasive sampling and studying of the gastrointestinal microbiome. *RSC Advances* **10**, 16313–16322.

WANG, H., LI, Z., LI, C., MA, Y., SUN, Q., ZHANG, H., NIU, G., WEI, J., YAO, H. & MA, Z. (2023) Viral Metagenomic Analysis of the Fecal Samples in Domestic Dogs (Canis lupus familiaris). *Viruses* **15**, 685.

WANG, W.-X., YAN, G.-Z., SUN, F., JIANG, P.-P., ZHANG, W.-Q. & ZHANG, G.-F. (2005) A non-invasive method for gastrointestinal parameter monitoring. *World Journal of Gastroenterology* **11**, 521–524.

WANG, X., ZHENG, Y., MA, Y., DU, L., CHU, F., GU, H., DAHLGREN, R.A., LI, Y. & WANG, H. (2018) Lipid metabolism disorder induced by up-regulation of miR-125b and miR-144 following β-diketone antibiotic exposure to F0-zebrafish (Danio rerio). *Ecotoxicology and Environmental Safety* **164**, 243–252.

WARRIT, K., BOSCAN, P., FERGUSON, L.E., BRADLEY, A.M., DOWERS, K.L., RAO, S. & TWEDT, D.C. (2017a) Minimally invasive wireless motility capsule to study canine gastrointestinal motility and pH. *The Veterinary Journal* **227**, 36–41.

WARRIT, K., BOSCAN, P., FERGUSON, L.E., BRADLEY, A.M., DOWERS, K.L. & TWEDT, D.C. (2017b) Effect of hospitalization on gastrointestinal motility and pH in dogs. *Journal of the American Veterinary Medical Association* **251**, 65–70.

WASHABAU, R.J., DAY, M.J., WILLARD, M.D., HALL, E.J., JERGENS, A.E., MANSELL, J., MINAMI, T., BILZER, T.W., & WSAVA INTERNATIONAL GASTROINTESTINAL STANDARDIZATION GROUP (2010) Endoscopic, biopsy, and histopathologic guidelines for the evaluation of gastrointestinal inflammation in companion animals. *Journal of Veterinary Internal Medicine* **24**, 10–26.

WASHIZU, T., ISHIDA, T., WASHIZU, M., TOMODA, I. & KANEKO, J.J. (1994) Changes in bile acid composition of serum and gallbladder bile in bile duct ligated dogs. *The Journal of Veterinary Medical Science* **56**, 299–303.

WEBER, M. (2006) Influence of size on the dog's digestive function. *Bulletin de l'Académie vétérinaire de France*, 327.

WEBER, M., MARTIN, L., BIOURGE, V., NGUYEN, P. & DUMON, H. (2003) Influence of age and body size on the digestibility of a dry expanded diet in dogs. *Journal of Animal Physiology and Animal Nutrition* **87**, 21–31.

WEBER, M.P., BIOURGE, V.C. & NGUYEN, P.G. (2017) Digestive sensitivity varies according to size of dogs: a review. *Journal of Animal Physiology and Animal Nutrition* **101**, 1–9.

WEBER, M.P., HERNOT, D., NGUYEN, P.G., BIOURGE, V.C. & DUMON, H.J. (2004) Effect of size on electrolyte apparent absorption rates and fermentative activity in dogs. *Journal of Animal Physiology and Animal Nutrition* **88**, 356–365.

WEBER, M.P., MARTIN, L.J., DUMON, H.J., BIOURGE, V.C. & NGUYEN, P.G. (2002a) Influence of age and body size on intestinal permeability and absorption in healthy dogs. *American Journal of Veterinary Research* **63**, 1323–1328.

WEBER, M.P., STAMBOULI, F., MARTIN, L.J., DUMON, H.J., BIOURGE, V.C. & NGUYEN, P.G. (2002b) Influence of age and body size on gastrointestinal transit time of radiopaque markers in healthy dogs. *American Journal of Veterinary Research* **63**, 677–682.

WEESE, J.S. & ANDERSON, M.E.C. (2002) Preliminary evaluation of Lactobacillus rhamnosus strain GG, a potential probiotic in dogs. *The Canadian Veterinary Journal = La Revue Veterinaire Canadienne* **43**, 771–774.

WENG, X.-H., BEYENBACH, K.W. & QUARONI, A. (2005) Cultured monolayers of the dog jejunum with the structural and functional properties resembling the normal epithelium. *American Journal of Physiology-Gastrointestinal and Liver Physiology* **288**, G705–G717.

WERNER, M., SUCHODOLSKI, J.S., STRAUBINGER, R.K., WOLF, G., STEINER, J.M., LIDBURY, J.A., NEUERER, F., HARTMANN, K. & UNTERER, S. (2020) Effect of amoxicillin-clavulanic acid on clinical scores, intestinal microbiome, and amoxicillin-resistant Escherichia coli in dogs with uncomplicated acute diarrhea. *Journal of Veterinary Internal Medicine* **34**, 1166–1176.

WERNIMONT, S.M., RADOSEVICH, J., JACKSON, M.I., EPHRAIM, E., BADRI, D.V., MACLEAY, J.M., JEWELL, D.E. & SUCHODOLSKI, J.S. (2020) The Effects of Nutrition on the Gastrointestinal Microbiome of Cats and Dogs: Impact on Health and Disease. *Frontiers in Microbiology* **11**, 1266.

WHITTEMORE, J.C., MOYERS, T.D. & PRICE, J.M. (2019) Randomized, controlled, crossover trial of prevention of antibiotic-induced gastrointestinal signs using a synbiotic mixture in healthy research dogs. *Journal of Veterinary Internal Medicine* **33**, 1619–1626.

WHITTEMORE, J.C., PRICE, J.M., MOYERS, T. & SUCHODOLSKI, J.S. (2021) Effects of Synbiotics on the Fecal Microbiome and Metabolomic Profiles of Healthy Research Dogs Administered Antibiotics: A Randomized, Controlled Trial. *Frontiers in Veterinary Science* **8**, 665713.

WILDING, E.I., BROWN, J.R., BRYANT, A.P., CHALKER, A.F., HOLMES, D.J., INGRAHAM, K.A., IORDANESCU, S., SO, C.Y., ROSENBERG, M. & GWYNN, M.N. (2000) Identification, evolution, and essentiality of the mevalonate pathway for isopentenyl diphosphate biosynthesis in gram-positive cocci. *Journal of Bacteriology* **182**, 4319–4327.

WILLIAMS, B.A., BOSCH, M.W., BOER, H., VERSTEGEN, M.W.A. & TAMMINGA, S. (2005) An *in vitro* batch culture method to assess potential fermentability of feed ingredients for monogastric diets. *Animal Feed Science and Technology* **123–124**, 445–462.

WIPLER, J., ČERMÁKOVÁ, Z., HANZÁLEK, T., HORÁKOVÁ, H. & ŽEMLIČKOVÁ, H. (2017) [Sharing bacterial microbiota between owners and their pets (dogs, cats)]. *Klinicka Mikrobiologie a Infekcni Lekarstvi* **23**, 48–57.

WOLF, P.G., BISWAS, A., MORALES, S.E., GREENING, C. & GASKINS, H.R. (2016) H_2 metabolism is widespread and diverse among human colonic microbes. *Gut Microbes* **7**, 235–245.

WU, J., ZHANG, Y., YANG, H., RAO, Y., MIAO, J. & LU, X. (2016) Intestinal Microbiota as an Alternative Therapeutic Target for Epilepsy. *Canadian Journal of Infectious Diseases and Medical Microbiology* **2016**, 1–6.

XENOULIS, P.G., PALCULICT, B., ALLENSPACH, K., STEINER, J.M., VAN HOUSE, A.M. & SUCHODOLSKI, J.S. (2008) Molecular-phylogenetic characterization of microbial communities imbalances in the small intestine of dogs with inflammatory bowel disease. *FEMS microbiology ecology* **66**, 579–589.

XU, H., HUANG, W., HOU, Q., KWOK, L.-Y., LAGA, W., WANG, Y., MA, H., SUN, Z. & ZHANG, H. (2019) Oral Administration of Compound Probiotics Improved Canine Feed Intake, Weight Gain, Immunity and Intestinal Microbiota. *Frontiers in Immunology* **10**.

XU, J., VERBRUGGHE, A., LOURENÇO, M., COOLS, A., LIU, D.J.X., VAN DE WIELE, T., MARZORATI, M., EECKHAUT, V., VAN IMMERSEEL, F., VANHAECKE, L., CAMPOS, M. & HESTA, M. (2017) The response of canine faecal microbiota to increased dietary protein is influenced by body condition. *BMC veterinary research* **13**, 374.

XU, J., VERBRUGGHE, A., LOURENÇO, M., JANSSENS, G.P.J., LIU, D.J.X., VAN DE WIELE, T., EECKHAUT, V., VAN IMMERSEEL, F., VAN DE MAELE, I., NIU, Y., BOSCH, G., JUNIUS, G., WUYTS, B. & HESTA, M. (2016) Does canine inflammatory bowel disease influence gut microbial profile and host metabolism? *BMC Veterinary Research* **12**.

YAP, Y.A., MCLEOD, K.H., MCKENZIE, C.I., GAVIN, P.G., DAVALOS-SALAS, M., RICHARDS, J.L., MOORE, R.J., LOCKETT, T.J., CLARKE, J.M., ENG, V.V., PEARSON, J.S., HAMILTON-WILLIAMS, E.E., MACKAY, C.R. & MARIÑO, E. (2021) An acetate-yielding diet imprints an immune and anti-microbial programme against enteric infection. *Clinical & Translational Immunology* **10**, e1233.

YIN, W., WANG, Y., LIU, L. & HE, J. (2019) Biofilms: The Microbial 'Protective Clothing' in Extreme Environments. *International Journal of Molecular Sciences* **20**, 3423.

YOU, I. & KIM, M.J. (2021) Comparison of Gut Microbiota of 96 Healthy Dogs by Individual Traits: Breed, Age, and Body Condition Score. *Animals* **11**, 2432.

YU, Y., LEE, C., KIM, J. & HWANG, S. (2005) Group-specific primer and probe sets to detect methanogenic communities using quantitative real-time polymerase chain reaction. *Biotechnology and Bioengineering* **89**, 670–679.

VAN ZELST, M., HESTA, M., ALEXANDER, L.G., GRAY, K., BOSCH, G., HENDRIKS, W.H., DU LAING, G., DE MEULENAER, B., GOETHALS, K. & JANSSENS, G.P.J. (2015) *In vitro* selenium accessibility in pet foods is affected by diet composition and type. *The British Journal of Nutrition* **113**, 1888–1894.

ZEMANOVÁ, N., LNĚNIČKOVÁ, K., VAVREČKOVÁ, M., ANZENBACHEROVÁ, E., ANZENBACHER, P., ZAPLETALOVÁ, I., HERMANOVÁ, P., HUDCOVIC, T., KOZÁKOVÁ, H. & JOUROVÁ, L. (2021) Gut

microbiome affects the metabolism of metronidazole in mice through regulation of hepatic cytochromes P450 expression. *PloS One* **16**, e0259643.

ZENG, R., ZHANG, Y. & DU, P. (2014) The SNPs of Melanocortin 4 Receptor (MC4R) Associated with Body Weight in Beagle Dogs. *Experimental Animals* **63**, 73–78.

ZENTEK, J., FRICKE, S., HEWICKER-TRAUTWEIN, M., EHINGER, B., AMTSBERG, G. & BAUMS, C. (2004) Dietary protein source and manufacturing processes affect macronutrient digestibility, fecal consistency, and presence of fecal Clostridium perfringens in adult dogs. *The Journal of Nutrition* **134**, 2158S-2161S.

ZENTEK, J. & MEYER, H. (1995) Normal handling of diets--are all dogs created equal? *The Journal of Small Animal Practice* **36**, 354–359.

ZHANG, Y., JEON, M., RICH, L.J., HONG, H., GENG, J., ZHANG, Y., SHI, S., BARNHART, T.E., ALEXANDRIDIS, P., HUIZINGA, J.D., SESHADRI, M., CAI, W., KIM, C. & LOVELL, J.F. (2014) Non-invasive multimodal functional imaging of the intestine with frozen micellar naphthalocyanines. *Nature Nanotechnology* **9**, 631–638.

ZIHLER BERNER, A., FUENTES, S., DOSTAL, A., PAYNE, A.N., VAZQUEZ GUTIERREZ, P., CHASSARD, C., GRATTEPANCHE, F., DE VOS, W.M. & LACROIX, C. (2013) Novel Polyfermentor intestinal model (PolyFermS) for controlled ecological studies: validation and effect of pH. *PloS One* **8**, e77772.

ZITVOGEL, L., DAILLÈRE, R., ROBERTI, M.P., ROUTY, B. & KROEMER, G. (2017) Anticancer effects of the microbiome and its products. *Nature Reviews Microbiology* **15**, 465–478.

APPENDIX

Appendix 1 - Scientific *curriculum vitae*

KEYWORDS ASSOCIATED TO RESEARCH THEME

Dog, digestive physiology, gut microbiota, size, *in vitro* gut models, faecal sample storage, dysbiosis, antibiotherapy, obesity, restoration strategies.

PROFESSIONAL CAREER AND INTERNSHIPS

2020 – 2023

PhD student - Biology and Health

PhD school Sciences de la Vie, de la Santé, Agronomie et Environnement, *Clermont-Ferrand (63)*

Supervisors: Pr Stéphanie BLANQUET-DIOT, Dr Emmanuelle APPER, Delphine HUMBERT

Host laboratory: UMR 454 Microbiology, Digestive Environment and Health (MEDIS), *Clermont-Ferrand* (63), University of Clermont Auvergne/INRAe

Subject: **Impact of body weight and antibiotic disturbance on canine gut microbiota: *in vitro* simulation and restoration strategies**

Fundings: CIFRE grant

Partner compagnies: Lallemand Animal Nutrition, Blagnac (31), France; Dômes Pharma, *Pont-du-Château* (63), France

2017 – 2019

Master's degree in Microbiology – Genome, Ecology and Microbial Physiology

University Clermont Auvergne, *Clermont-Ferrand (63)*

Average: 14/20, Mention Bien *Rank: 3/27*

- **September to November 2019 – Laboratory Technician** (2.5 months)
  Laboratory: UMR 454 Microbiology, Digestive Environment and Health (**MEDIS**), Clermont-Ferrand (63), University Clermont Auvergne in collaboration with *UMR 1319 INRAe* **MICALIS**, *Jouy-en-Josas (78)*
  Subject: "*Development of an in vitro model of the colonic environment of obese patients*" (project continuation)
- **January to July 2019 – Research internship Master 2** (*6 months*)
  Supervisors: Stéphanie BLANQUET-DIOT, Marion LECLERC
  Host laboratory: UMR 454 Microbiology, Digestive Environment and Health (**MEDIS**), Clermont-Ferrand (63), University Clermont Auvergne in collaboration with *UMR 1319 INRAe* **MICALIS**, *Jouy-en-Josas (78)*
  Subject: "*Development of an in vitro model of the colonic environment of obese patients*"
- **May to July 2018 – Research internship Master 1** (*2 months*)
  Supervisor: Marie-Cécile BADET
  Host laboratory: Microbiology Laboratory, UFR Odontology, *University of Bordeaux* (33)
  Subject: "*Improvement of a dynamic experimental model of dental biofilm*"

2014 – 2017

Bachelor of Biology – Cell Biology and Physiology University Clermont Auvergne, *Clermont-Ferrand (63)*

Average: 11.1/20 *Rank: 64/155*

2013 – 2014

First Year Common to Health Studies (PACES) Université d'Auvergne, *Clermont-Ferrand (63)*

TECHNICAL SKILLS

Microbiology: identification, culture and enumeration of microorganisms (aerobic and anaerobic bacteria)

Molecular biology: DNA analysis: DNA extraction, DNA purification, PCR amplification, qPCR, electrophoresis gel

Analytical techniques: HPLC (determination of short chain fatty acids), gas chromatography, bile acid extractions, ammonia colorimetric assays

Biotechnology: continuous *in vitro* fermentation (M-ARCOL, Mucosal Artificial Colon) in healthy condition or dysbiosis (obesity and irritable bowel syndrome), human and dog

Bioinformatics and statistics: databases (BLAST, MetaCyc), statistical software (R, Prism), Illumina RNA 16S sequencing data processing (Galaxy, Qiime2, R studio), functional predictions (Tax4Fun2, PICRUSt2), statistical analyses (parametric or non-parametric statistical tests, PCoA, NMDS, RDA, rCCA, PLS-DA)

Animal experimentation: Level 1 Animal Experimentation Training: Procedure Designer, June 2022

Software: R-Studio, Git, Zotero, office pack, Prism, Biorender, Adobe Premiere Pro (basics)

EDUCATION & MANAGEMENT

TEACHING MISSIONS - TEMPORARY TEACHING DOCTORAL STUDENT

- **2020-2023: Université Clermont Auvergne**, *Clermont-Ferrand*
  Domain: Food quality and microbiological safety
  Training: Master 1 Microbiology and Master 1 Biology-Health, 12 hours of tutorials *(distance and face-to-face) and writing of two exam subjects*

- **2023:** *IUT Biological Engineering, Clermont-Ferrand*
  Field: Microbiology
  Training: BUT 1st year - Medical Biology and Biotechnology course, 25 hours of practical work *and corrections of reports*

MANAGEMENT ACTIVITY

2022-2023 Supervision of laboratory technician (4 months)

2021-2022 Supervision of trainees

- Three high school students in 2nd technological (observation internship of 1 week, 2021)
- A License 3 student (1 week, 2021)
- A 3rd year veterinary student (8 weeks, summer 2021)
- A Master 1 Bioinformatics intern (8 weeks, summer 2022)

SCIENTIFIC PRODUCTION

PUBLICATIONS

Published articles

Etienne-Mesmin L, Meslier V, Uriot O, Fournier E, **Deschamps** C, Denis S, David A, Jegou S, Morabito C, Quinquis B, Thirion F, Plaza Oñate F, Le Chatelier E, Ehrlich S.D, Blanquet-Diot S, *et al.* (**2023**) *In vitro* modelling of oral microbial invasion in the human colon. *Microbiology Spectrum*, e04344-22. https:// doi.org/ 10.1128/spectrum.04344-22 (IF = 9.04)

Deschamps C, Humbert D, Zentek J, Denis S, Priymenko N, Apper E, Blanquet-Diot S (**2022**) From Chihuahua to Saint-Bernard: how did digestion and microbiota evolve with dog sizes. *Int J Biol Sci* 18:5086–5102. https://doi.org/10.7150/ijbs.72770 (IF = 10.75)

Deschamps C, Denis S, Humbert D, Zentek J, Priymenko N, Apper E, Blanquet-Diot S (**2022**) *In vitro* models of the canine digestive tract as an alternative to *in vivo* assays: Advances and current challenges. *ALTEX* 39:235–257. https://doi.org/10.14573/altex.2109011 (IF = 6.25)

Deschamps C, Fournier E, Uriot O, Lajoie F, Verdier C, Comtet-Marre S, Thomas M, Kapel N, Cherbuy C, Alric M, Almeida M, Etienne-Mesmin L, Blanquet-Diot S (**2020**) Comparative methods for fecal sample storage to preserve gut microbial structure and function in an *in vitro* model of the human colon. *Appl Microbiol* Biotechnol 104:10233–10247.https://doi.org/10.1007/s00253-020-10959-4 (IF = 5.56)

Articles submitted or in preparation

Uriot O*, **Deschamps** C*, Etienne-Mesmin L, Brun M, Pouget M, Chalancon S, Durif C, Chaudemanche C, Alric M, Boirie Y, Blanquet-Diot S. Colonic physicochemical parameters drive gut microbiota dysbiosis in obesity. *co-first author. **Submitted to Microbiome (IF = 16.83)**

***Deschamps C**, Denis S, Humbert D, Gresse R, Durif C, Apper E, Blanquet-Diot S. Systèmes digestifs artificiels : applications en nutrition et santé du chien et du porc.* **Submitted to Bulletin de l'Académie Vétérinaire de France (IF = 0.12)**

***Deschamps C**, Denis S, Humbert D, Priymenko N, Chalancon S, De Bodt J, Achard C, Apper E, Blanquet-Diot S. Canine Mucosal Artificial Colon: in vitro simulation of physicochemical and microbial colonic ecosystem adapted to different dog sizes.* Submitted to Altex (IF = 6.25)

***Deschamps C**,* Denis S, *Humbert D, Chalancon S, Achard C, Apper E, Blanquet-Diot S. Large intestinal nutritional and physicochemical parameters from different dog sizes reshape canine microbiota structure and functions in vitro.* In preparation for Applied Microbiology and Biotechnology (IF = 5.56)

***Deschamps C**, Apper E, Brun M, Durif C, Denis S, Humbert D, Blanquet-Diot S. Development of a new dysbiotic model of the canine large intestine microbiome associated to antibiotherapy.* In preparation for Microbial Spectrum (IF = 9.04)

***Deschamps C**,* Brun M, Denis S, *Durif C, Humbert D, Apper E, Blanquet-Diot S. Lactobacillus helveticus-derived parabiotic is as efficient as Saccharomyces boulardii to restore gut microbiota after antibiotic disturbance in an in vitro canine gut model.* In preparation for Food Research International (IF = 7.42)

ORAL COMMUNICATIONS

- Académie Vétérinaire de France, June 4th 2023, Paris, France

Deschamps C, Blanquet-Diot S. Systèmes digestifs artificiels : applications en nutrition et santé animale.

- International Probiotic Congress, 27-30 June 2022, Bratislava, Slovakia

Deschamps C, Denis S, Humbert D, Chalancon S, Apper E, Blanquet-Diot S. Development of a mucin-associated *in vitro* model adapted to size-specific canine colonic environment.

- SVSAE Doctoral School Day, 18-19 May 2022, Clermont-Ferrand, France

Deschamps C, Denis S, Humbert D, Chalancon S, Apper E, Blanquet-Diot S. Development and validation of a new *in vitro* model of the canine colon adapted to different dog sizes.

POSTER COMMUNICATIONS

- 13th International Symposium on Gut Microbiology (INRAE-ROWETT), 13-15 June 2023, Aberdeen, Scotland

Deschamps C, Apper E, Brun M, Durif C, Denis S, Humbert D, Blanquet-Diot S. *In vitro* simulation of antibiotic-induced dysbiosis in a new canine gut microbiome model.

Uriot O, Deschamps C, Brun M, Pouget M, Etienne-Mesmin L, Alric M, Chaudemanche C, Boirie Y, Blanquet Diot S. Linking diet and gut microbiota in obesity : usefulness of a new *in vitro* human mucosal colon model.

Meslier V, Etienne-Mesmin L, Uriot O, Fournier E, Deschamps C, Denis S, David A, Jegou S, Marabito C, Quinquis B, Thirion F, Plaza Oñate F, Le Chatelier E, Ehrlich D, Blanquet-Diot S, Almeida M. In vitro modelling of oral microbial invasion in the human colon.

- 4th Ghent Gut Inflammation Group Meeting, February 08-10th 2023, Ghent, Belgium

Deschamps C, Denis S, Humbert D, Chalancon S, Achard C, Apper E, Blanquet-Diot S. Colonic physicochemical parameters from different dog's sizes reshape canine microbiota activity and structure *in vitro*.

- 12th International Symposium on Gut Microbiology (INRAE-ROWETT), October 13-15th 2021, Clermont-Ferrand, France (online)

Deschamps C, Humbert D, Priymenko N, Denis S, Apper E, Blanquet-Diot S. Colonic physicochemical parameters from different dog's sizes reshape canine microbiota activity and structure in an *in vitro* gut model.

VULGARIZATION

- Movie "**Puy de Science**" (July 2022): presentation of the laboratory's *in vitro* digestion platform, dedicated to high school students
- "**Fête de la Science**" (October 2021): organization of workshops, production of posters and supervision of high school students

AWARDS

1st prize best oral communication in the category "Gut microbiota" during the 25th days of the SVSAE doctoral school, University Clermont Auvergne, May 2022, Clermont-Ferrand, France

Appendix 2 – Review in ALTEX

DESCHAMPS, C., DENIS, S., HUMBERT, D., ZENTEK, J., PRIYMENKO, N., APPER, E. & BLANQUET-DIOT, S. (**2022**) *In vitro* models of the canine digestive tract as an alternative to *in vivo* assays: Advances and current challenges. *ALTEX*. 39:235–257. https://doi.org/10.14573/altex.2109011

Review Article

In Vitro Models of the Canine Digestive Tract as an Alternative to *In Vivo* Assays: Advances and Current Challenges

Charlotte Deschamps[1,2], Sylvain Denis[1], Delphine Humbert[3], Jürgen Zentek[4], Nathalie Priymenko[5], Emmanuelle Apper[2] and Stéphanie Blanquet-Diot[1]

[1]Université Clermont Auvergne, UMR 454 MEDIS UCA-INRAE, Clermont-Ferrand, France; [2]Lallemand Animal Nutrition, Blagnac, France; [3]Dômes Pharma, Pont-du-Château, France; [4]Institute of Animal Nutrition, Freie Universität Berlin, Berlin, Germany; [5]Toxalim (Research Center in Food Toxicology), University of Toulouse, INRAE, ENVT, INP-Purpan, UPS, Toulouse, France

Abstract

Dogs occupy a full place in the family, and their well-being is of paramount importance to their owners. Digestion, a complex process involving physicochemical, mechanical, and microbial parameters, plays a central role in maintaining canine health. As *in vivo* studies in dogs are increasingly restricted by ethical, regulatory, societal, and cost pressures, an alternative option is the use of *in vitro* models simulating the different compartments of the canine gastrointestinal tract. This review introduces digestion and gut microbiota as key factors in dog nutrition and health under both healthy and diseased conditions (obesity and inflammatory bowel disease) and highlights similarities and differences between the human and canine digestive tract and processes. We provide the first in-depth description of currently available models of the canine digestive tract, discuss technical and scientific challenges that need to be addressed, and introduce potential applications of *in vitro* gut models in the food and veterinary fields. Even if the development of some *in vitro* models is still limited by a lack of *in vivo* data in dogs that is necessary for relevant configuration and validation, translation of long-term expertise on human *in vitro* gut models to dogs opens avenues for model optimization and adaptation to specific canine digestive conditions associated with various dog ages, sizes, breeds and/or diets, in both physiological and diseased states.

1 Introduction

1.1 Dogs in familial and economical contexts

Canis lupus familiaris, the domesticated dog, belongs to the *Canidae* family. The dog is thought to have been the first animal domesticated by humans around 12,000 years ago (Axelsson et al., 2013). Dogs were initially strict carnivores, but they probably acquired the ability to digest starch during the agricultural revolution to become facultative carnivores (Axelsson et al., 2013). Nowadays, canine species include approximatively 400 breeds with broad morphological and size variabilities and body weight ranging from 1 kg for a Chihuahua to 100 kg for a Saint-Bernard (Grandjean and Haymann, 2010). Dogs occupy a full place in the family, and their health and well-being are of paramount importance to their owners.

There are estimated to be more than 500 million dogs worldwide, which represents a huge market for the petfood and animal health industry. In 2018, the global petfood market size reached $91.1 billion, representing a 31% increase within 5 years (Phillips-Donaldson, 2019). A vast array of foods, snacks, and nutritional supplements have been developed to support well-being, health, improve aging, or prevent disease. According to the increased interest of owners in maintaining their dogs' health, petfood has been adapted to fit each dog's lifestyle, for example specific products for puppies or lactating bitches, sedentary or active animals, and maintenance or hypocaloric diets.

Different types of canine food are available and can be classified into three categories: dry food, canned food, and alternative food (biologically appropriate raw food (BARF), homemade food, and feedstuffs). At the interface between petfood and veterinary compounds, nutritional supplements represent an expanding market with a huge product range. As an example, micronutrients like selenium, taurine or polyphenols can be added for old dogs, calcium, phosphorus, omega-3 fatty-acids and vitamin E for lactating bitches, or L-carnitine for athletic dogs. Supplements for specific nutri-

Received September 1, 2021; Accepted January 11, 2022;
Epub January 13, 2022; © The Authors, 2022.

ALTEX 39(2), 000-000. doi:10.14573/altex.2109011

Correspondence: Stéphanie Blanquet-Diot, PhD
UMR 454 MEDIS
University Clermont Auvergne, INRAe
28 place Henri Dunant
63000 Clermont-Ferrand, France
(mailto:stephanie.blanquet@uca.fr)

tional purposes such as prebiotics or probiotics are also developed to decrease food sensitivities or for digestive or articular care.

In 2019, pet medicine, including vaccines, antiparasitic treatments or antibiotics, represented a $17.5 billion market[1]. Drugs can be administered in different forms: topically, by injection, or as oral formulations. Oral formulations can have liquid (e.g., solution or suspension), semi-solid (oily or aqueous formulations), or solid (e.g., powder, capsules, conventional or sustained-release tablets) forms. Specific treatments have been developed to avoid lipid absorption in obesity or decrease pain in inflammatory bowel disease (IBD). Of note, vulnerability to specific diseases depends on a dog's size and breed, with for instance obesity and dental trouble common in small dogs and digestive problems more common in larger animals.

1.2 Regulatory context

In Europe, the European petfood industry federation (FEDIAF) represents 16 national petfood industries and provides a framework for the production of safe, nutritious, and palatable petfood. Heads of medicine agencies or national agencies must evaluate the quality and safety of medicinal products for animals, consumers, users, and the environment as well as the effectiveness of the medicinal product before it can be marketed.

To assess the digestibility of petfood or bioaccessibility of active compounds (including drugs) in the canine gastrointestinal tract (GIT), *in vivo* studies remain the gold standard. *In vivo* experiments in dogs are also performed to model the human gut due to similarities in digestive physiology (Lui et al., 1986; Akimoto et al., 2000). More than 17,000 experiments were carried out on dogs in 2018 in the EU28 and Norway[2]. However, *in vivo* assays are increasingly restricted by regulation, ethical and societal constraints, and high associated costs.

The 3Rs proposed by Russel and Burch (1959) widely encourage a reduction in the number of animals used in research and promote the development of alternative *in vitro* approaches. Among *in vitro* alternatives, models simulating the canine digestive environment (intestinal cell culture, organoids, or *in vitro* gut models) can help to answer many scientific questions associated with food and drug behavior during canine digestion, especially on mechanistic aspects. However, this approach requires a comprehensive understanding of the canine digestive process.

1.3 Digestion and gut microbiota as key parameters in dog nutrition and health

Canine digestion involves physicochemical (e.g., pH, digestive secretions, transit time), mechanical, and microbial parameters. These digestive components affect food digestibility, nutrient absorption, and energy release, but also drug metabolism and absorption, and survival of probiotic microorganisms. Thus, the development of new petfood or veterinary products needs to consider these multi-faceted aspects of canine digestion to answer important questions such as: How do physicochemical parameters modulate food digestibility? What is the importance of gut microbiota in canine digestion and drug metabolism? Where are drugs released and absorbed? How is drug bioaccessibility impacted by food matrix, galenic form, physicochemical parameters, or microbiota? How do probiotic strains survive along the GIT? However, recommendations for petfood and drug intake are currently based only on dog body weight or metabolic weight. Development of new products should consider the variations in the digestion process associated with different canine sizes and breeds to move towards personalized nutrition and veterinary medicine.

2 Methods of literature research and aim of the review

Our literature search was performed using *PubMed*[3] and *Google Scholar*[4] using the keywords "dog" OR "canine" AND "digestion", "pH", "enzyme", "digestive secretions", "absorption", "microbiota", "bile acids", "transit time", "short chain fatty acids", "fermentation", "gas", "mucus", "*in vitro*", "model" in all available years. The online database search was last performed in August 2021 on titles, abstracts, and key words including original articles, reviews, theses, and books. Relevant studies were identified after consultation of the main text, figures and supplementary materials, and information regarding involved dogs (i.e., number of dogs, age, weight, breed, sex, reproduction state, living environment), alimentation (i.e., type of food, feeding frequency, principal components of food), health (i.e., healthy, obese or IBD dogs only), and analysis methods was extracted.

This review paper aims to give a state-of-the-art on canine digestive physiology regarding both physicochemical and microbial parameters that can be reproduced in *in vitro* gut models. Then, we explain how these parameters change under diseased conditions associated with obesity and IBD. In a third part, we provide an in-depth description of all available *in vitro* models of the canine digestive tract before discussing their limitations and challenges associated with the development of *in vitro* gut models of healthy or diseased dogs and their applications in the food and veterinary fields. This paper considers the entire canine GIT and associated microbiota and highlights similarities and differences between dog and human digestive physiology to provide new opportunities for canine *in vitro* gut simulation.

3 Canine digestion

3.1 Digestive anatomy

Because dogs are facultative carnivores, their GIT is adapted to high-protein and high-fat diets, i.e., relatively short and simple

[1] Animal medicine global market opportunities and strategies to 2023. https://www.globenewswire.com/news-release/2020/01/13/1969734/0/en/Global-Animal-Medicine-Market-Opportunities-Strategies-to-2023-Veterinary-Pharmaceuticals-Will-Gain-20-7B-of-Global-Annual-Sales-by-2023-A-6-6B-Opportunity-for-Veterinary-Parasitic.html

[2] https://webgate.ec.europa.eu/envdataportal/content/alures/section1_number-of-animals.html (accessed 3.2.2022)

[3] https://pubmed.ncbi.nlm.nih.gov

[4] https://scholar.google.fr

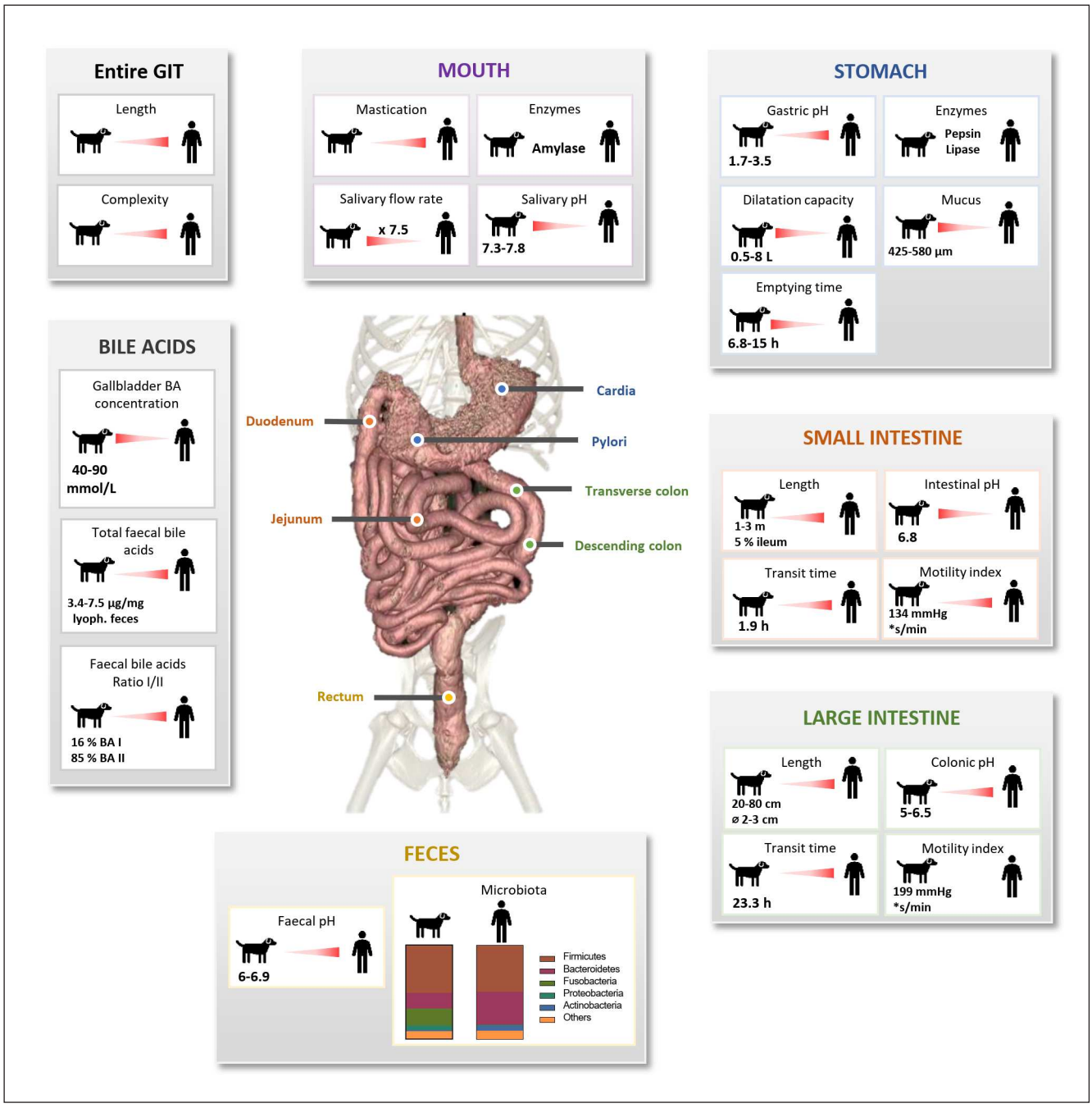

Fig. 1: Canine digestive compartments and associated mechanical, physicochemical, and microbial processes
Key parameters of the oral, gastric, intestinal, and colonic compartments of medium-sized healthy dogs are summarized and compared to *in vivo* data in healthy humans. Lack of *in vivo* data is represented by "?". BA, bile acid

compared to herbivores and even omnivores like humans or pigs, reflecting the lower retention time required for meat in comparison to grass digestion (Moon et al., 2018) (Fig. 1). A dog's digestive tract weight in relation to total body mass is inversely correlated to canine size, representing 7% and 2.8% of the total body weight in 5 and 60 kg dogs, respectively (Weber, 2006). The GIT length is correlated with shoulder height at a 6:1 ratio (Morris and Rogers, 1989).

Digestion in dogs starts in the mouth with the mechanic action of mastication, using 42 teeth and only 2000 taste buds. The canines can cut meat into pieces. The molars have a larger crown than in humans and allow grinding of bones. The mastication step

is less important than in humans as most dogs do not really chew but swallow large pieces of food. After swallowing, the food bolus crosses the esophagus, which has a length similar to that of the human esophagus, i.e., around 30 cm for a medium-sized dog (Kararli, 1995; Freiche and Hernandez, 2010). Like in humans, the canine stomach has the shape of a J-elongated bag. It is located in the abdomen, starts with the cardia and extends to the pylorus, and is composed of the antrum and the fundus (Kararli, 1995). Its dilation capacity (0.5-8 L volume) is larger than that of the human stomach, and the gastric wall measures between 3 and 5 mm in thickness (Kararli, 1995; Freiche and Hernandez, 2010).

Digestion continues along the small intestine, which is anatomically divided into the duodenum (10%), jejunum (85%) and ileum (5%), measuring from 1 to 3 m total length. In comparison, the human ileum represents 60% of the total small intestine length (Kararli, 1995; Oswald et al., 2015). This suggests that ileal function may differ between dogs and humans. Canine small intestine diameter is smaller than in humans (1 cm versus 5 cm). Duodenal thickness reaches 6 mm, whereas intestinal loops measure around 2-3 mm. The large intestine or colon is 20-80 cm in length with a diameter of 2-3 cm in medium-sized dogs, while it is 90-150 cm in humans with a diameter of 5 cm (Kararli, 1995). The large intestine is composed of the ascending, transverse, and descending colon. Finally, the rectum forms the terminal section of the large intestine ending in the anus. The three parts of the canine colon are less well defined than in humans, with the particularity of being non-sacculated and devoid of a sigmoid colon (Kararli, 1995).

As for humans, peripheral organs are involved in canine digestion. The pancreas secretes pancreatic juice into the duodenum and is involved in protein (trypsin, chymotrypsin, elastase, and carboxypeptidase), carbohydrate (α-amylase), and lipid (lipase and phospholipase) digestion. Pancreatic juice also contains antimicrobial agents that contribute to microbial balance. The liver is coupled with a gallbladder and located near the stomach. The liver plays a central role in digestion, including vitamin and glucose storage (glycogen), detoxification and excretion of toxic substances (e.g., urea), and lipid digestion by saponification of lipids by bile acids (BA). Bile is produced by the liver, stored in the gallbladder, and discharged into the duodenum.

Depending on body size and breed, dogs show a diversity in anatomical features such as intestinal length and volume, intestinal villus morphology, and intestinal or colonic permeability (Zentek and Meyer, 1995; Oswald et al., 2015). Because of the relationship between anatomy and digestive physicochemical parameters, these differences may affect dog digestion and key parameters such as pH, digestive secretions, transit time, and gut microbiota. To avoid making this discussion too complex, the following sections (3.2 and 3.3) focus on digestion processes in medium-sized dogs (from 10 to 30 kg).

3.2 Physicochemical parameters

pH

Gastrointestinal pH changes along the dog's digestive tract (Fig. 1). The mean salivary pH of medium-sized dogs is 7.3-7.8 (Smeets-Peeters et al., 1998). In the stomach, the arrival of a food bolus induces the secretion of gastrin, which in turn stimulates hydrochloric acid (HCl) production. The gastric pH of Beagles under fasted conditions is around 1.5 (range 0.9-2.5), similar to that of humans (range 1.4-2.1) (Dressman, 1986; Kararli, 1995; Mahar et al., 2012). Several studies have observed a higher gastric pH in fed dogs, ranging from 2 to 5.5 (Smith, 1965; Dressman, 1986; Kararli, 1995; Shinchi et al., 1996; Martinez, 2002; Duysburgh et al., 2020). In the small intestine, the pH increases to values close to neutrality because of the buffering capacity of pancreatic juice and bile (Kararli, 1995). The pH of the small intestine also increases from the proximal to the distal part, from 6.5 to 8 in medium-sized dogs (Koziolek et al., 2019). The few studies that have investigated the canine jejunal pH measured a mean pH of 6.8 for medium-sized dogs (Mentula et al., 2005; Kalantzi et al., 2006), which is similar to that of humans (value of 6-7) (Kararli, 1995; Martinez, 2002). Colonic pH is, like in humans, more acidic with values of 5-6.5 (Smith, 1965; Koziolek et al., 2019). The fecal pH of medium dogs has a pH range of 6-6.9 (Eisenhauer et al., 2019; Nogueira et al., 2019).

Digestive secretions

Dog digestion is accelerated by digestive secretions containing various enzymes (Fig. 1). Amylase, lactate dehydrogenase and adenosine deaminase are found in dog saliva (Lavy et al., 2012; Iacopetti et al., 2017; Ricci et al., 2018). The gastric mucosa secretes gastric juice containing proteolytic (pepsin, chymosin) and lipolytic (lipase) enzymes (Aspinall, 2004; Durand, 2010). Canine pancreatic juice contains amylase, lipase, phospholipases, cholesterases, proteases, and nucleases (Kienzle, 1988; Robin, 2007). Of note, gastric and pancreatic juices are poorly characterized in dogs, in contrast to bile, for which more data are available. Bile is discharged into the duodenum during postprandial phases. Bile is up to 10-fold more concentrated in the gallbladder than in the liver, with a total concentration around 50 (40-90) mmol/L in dogs versus 3-45 mmol/L in humans (Nakayama, 1969; Kararli, 1995; Kakimoto et al., 2017; Nagahara et al., 2018; Larcheveque, 2019). Canine bile contains up to 15 BA, but the three major BAs (taurocholic, taurodeoxycholic and taurochenodeoxycholic acid) found in healthy dogs make up 99% of the total BA pool (Washizu et al., 1994). 0.15% of BA are conjugated to glycine and 0.81% are unconjugated (Nagahara et al., 2018). Fecal samples show concentrations of 5.8-7.5 µg total BA per mg of dry feces (Schmidt et al., 2018; Blake et al., 2019; Manchester et al., 2019). Lastly, as in various mammals including humans, mucins are produced by goblet cells all along the canine GIT (Kararli, 1995). Mucus thickness has been evaluated in dogs only in the stomach, measuring 425 and 576 µm respectively in the fundus and antrum in agreement with human values (Bickel and Kauffman, 1981; Kararli, 1995; Etienne-Mesmin et al., 2019). The mucin layer protects the epithelium from the acidic pH of the stomach and withstands bone fragments (Moon et al., 2018). In the large intestine, the mucus layer is colonized by a microbial biomass, as described in Section 3.3.

Gut motility and transit time

Using wireless motility capsules, Farmer and collaborators found that gut motility indexes in dogs are higher in the large intestine (199 mmHg*sec/min) compared to the small intestine

(134 mmHg*sec/min) and stomach (55 mmHg*sec/min) (Farmer et al., 2018). Canine motility is quite different to that of humans. Maximum pressure under fed conditions is higher in humans than in dogs (241 and 119 mmHg in the human stomach and small intestine, respectively, versus 52 and 75 mmHg for dog), but with a similar maximum frequency of 3.7 contractions/min in the gastric compartment (Boscan et al., 2013; Farmer et al., 2018). Data on transit time in the different digestive compartments of dogs (Fig. 1) wary widely depending on the method used (e.g., radiopaque markers, plastic beads, ^{13}C-octanic acid breath test, sulfasalazine-sulfapyridine method, or wireless motility capsule), breed, age, feed (composition, energy density or viscosity) and environment (laboratory or owners' home, stress context or sedation). Gastric emptying time varies from 2-19.8 h in fed medium-sized dogs (Hinder and Kelly, 1977; Theodorakis, 1980; Ehrlein and Pröve, 1982; Meyer et al., 1985; Lui et al., 1986; Gupta and Robinson, 1988; Hornof et al., 1989; Arnbjerg, 1992; Carrière et al., 1993; Cullen and Kelly, 1996; Sagawa et al., 2009; Boillat et al., 2010; Mahar et al., 2012; Boscan et al., 2013; Koziolek et al., 2019). Small intestinal transit time has been reported to have a range of 1.1-3.6 h (Boillat et al., 2010; Oswald et al., 2015). Large intestine transit time in dogs ranged from 1.1-49.1 h measured in dogs from a wide range of weights and breeds (Boillat et al., 2010; Warrit et al., 2017).

3.3 Canine gut microbiota

Composition

Microorganisms colonize the entire GIT of dogs from mouth to rectum. Like in humans, there are longitudinal variations (i.e., along the GIT) in gut microbiota composition due to changes in pH, substrate concentrations (including oxygen and nutrient availability), and transit time (Hooda et al., 2012; Friedman et al., 2018; Etienne-Mesmin et al., 2019). Figure 2 gives an overview of available data on gut bacteria composition of the different gastrointestinal regions in dogs.

The stomach is the least colonized compartment with 10^4 to 10^5 colony forming units (CFU) per gram of content in medium-sized dogs, mainly composed by *Proteobacteria*, including *Helicobacter* spp. as in humans, which are potential pathogenic strains (Benno et al., 1992; Mentula et al., 2005; Hooda et al., 2012).

The small intestine contains 10^5 to 10^7 CFU/g of content (Benno et al., 1992; Mentula et al., 2005). The duodenum is colonized by *Firmicutes* (calculated median of the three available publications: 47%), *Proteobacteria* (27%), *Bacteroidetes* (9%), *Fusobacteria* (3%), and *Actinobacteria* (1%), whereas the jejunum is characterized by a higher abundance of *Proteobacteria* (37%), *Actinobacteria* (11%), and *Fusobacteria* (10%), together with lower percentages of *Firmicutes* (33%) and *Bacteroidetes* (7%) (Xenoulis et al., 2008; Suchodolski et al., 2009; Garcia-Mazcorro et al., 2012). A single study on 6 dogs investigated ileal microbiota and observed 31% *Fusobacteria*, 24% *Firmicutes*, 23% *Bacteroidetes* and 22% *Proteobacteria* (Suchodolski et al., 2008).

The colon is the most colonized part of the GIT, with up to 10^9-10^{11} CFU/g of content (Hooda et al., 2012). According to a unique publication using 16S Illumina sequencing to investigate microbiota composition, colonic digesta is dominated by 37% *Firmicutes*, 33% *Bacteroidetes*, 29% *Fusobacteria* and 1% *Proteobacteria* (Suchodolski et al., 2008a).

The majority of taxa colonizing the colon are also found in canine feces (Pilla and Suchodolski, 2020), which seems to be rather different from the human situation, where a significant number of mucus-adherent bacteria from the colon are not found in feces (Pilla and Suchodolski, 2020). In addition to bacteria (98%), canine fecal microbiota contains 1.1% archaea, 0.4% fungi and 0.4% viruses, mainly bacteriophages (Suchodolski, 2011; Swanson et al., 2011). Fecal microbiota of healthy dogs is dominated by three main bacterial phyla: *Firmicutes*, *Bacteroidetes* and *Fusobacteria* (Pilla and Suchodolski, 2020). Bacteria from *Actinobacteria* and *Proteobacteria* phyla are also found in canine feces but in a lower proportion.

Fusobacteria and *Proteobacteria* seem to be more abundant in dogs than in humans, probably related to a carnivorous versus omnivorous diet (Fig. 1) (Simon, 2019). Unlike in humans, where *Fusobacterium* is frequently associated with diseases, in dogs this genus is related to non-stressful conditions and therefore probably a healthy state, especially because its abundance increases when dogs have access to the outdoors (Oswald et al., 2015).

In addition to longitudinal variations, scarce data suggest variations in microbiota composition from the digestive lumen to the surface of the intestinal epithelium covered by a mucin layer. Only two studies have investigated the mucosa-associated bacteria on the outer mucus layer in the colon of healthy dogs (Simpson et al., 2006; Cassmann et al., 2016). Cassmann et al. (2016) demonstrated that free colonic mucus is mainly colonized by *Bacteroidetes* spp. and *Eubacteria*. Of interest, *Akkermansia muciniphila*, a well-known mucin-degrading bacterium in humans, which is inversely correlated with obesity, was not yet identified in canine feces (Garcia-Mazcorro et al., 2020).

Metabolic activities

Gut microbiota is known to play a key role in host homeostasis and health maintenance, as it is implicated in many nutritional (e.g., fiber degradation and vitamin synthesis), immunological (immune system maturation) and physiological processes (e.g., vascularization, epithelium integrity, barrier effect against pathogens, and lipid digestion via the metabolism of primary BA into secondary BA) (Durand, 2010; Andoh, 2016). Gut microbiota metabolic activity leads to short-chain fatty acid (SCFA) and gas production as mean fermentation products resulting from degradation of soluble fibers. In dogs, like in humans, the three main SCFAs are acetate, propionate and butyrate, with relative percentages in fecal samples of 60:25:15 (Mondo et al., 2019). Non-digested proteins from diet and endogenous proteins (e.g., from mucins) are also metabolized by gut microbiota, leading to the production of branched chain fatty-acids (BCFA), ammonia, indoles and phenols (Weber et al., 2017). Total fecal SCFA and BCFA were investigated, with values widely varying between studies, i.e., 91-423 and 4.7-36.1 µmol/g of lyophilized stools, respectively (Beloshapka et al., 2012; Minamoto et al., 2015; Alexander et al., 2019; Detweiler et al., 2019; Eisenhauer et al., 2019; Nogueira et al., 2019). To our knowledge there is no *in vivo* data on gas production in

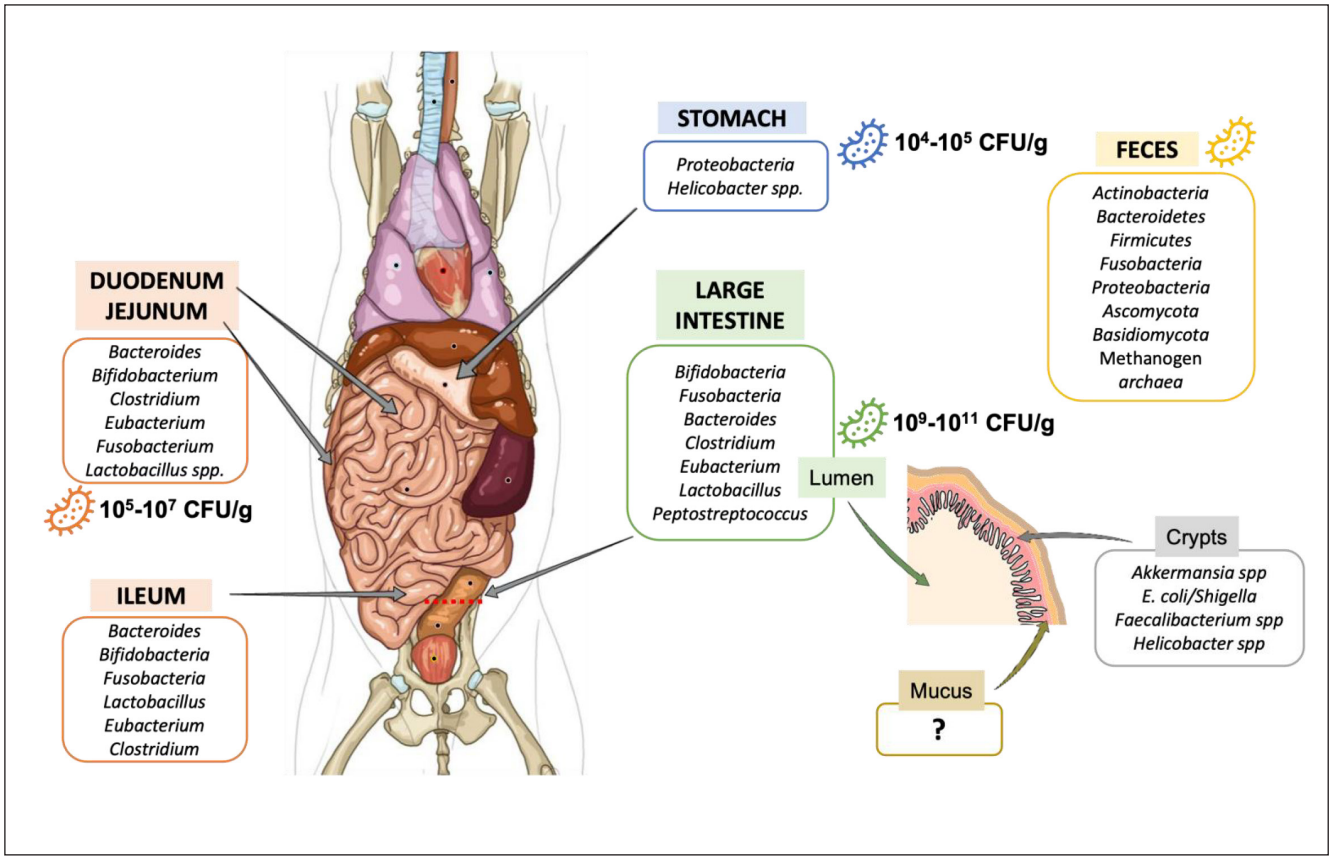

Fig. 2: Variations in gut microbiota composition along the canine digestive tract
Main bacterial populations found in the different compartments of the gastrointestinal tract of the medium-sized dog are represented. CFU, colony-forming unit

dogs, and the two available studies on gas composition focused on malodorous compounds such as hydrogen sulfide (Collins et al., 2001; Giffard et al., 2001).

4 From healthy to diseased dogs: impact on digestive physiology and gut microbiota?

As in humans, diseases such as obesity and IBD are increasingly prevalent in dogs. Because the etiology of such diseases is now better understood in humans, the emergence of similar pathologies in dogs has raised awareness of veterinary and petfood companies and motivated development of pharma and nutritional products. Most available data on obese or IBD dogs focus on the lower gut and its associated microbiota. Indeed, in many intestinal or extra-digestive diseases such as obesity and IBD, in dogs like in humans, gut microbiota appears to be in a disrupted state called "dysbiosis" where both functional and compositional states are altered (Pilla and Suchodolski, 2020).

4.1 Obesity

In Western countries, obesity is considered the most common nutritional disorder in pets due to an imbalance between energy intake and expenditure (Osto and Lutz, 2015). Dogs are considered clinically obese when their body weight is at least 20-30% above ideal weight, and a universal body condition score (ranging from 1 to 9) defines overweight dogs at 7 and obese dogs at 8/9 (Apper et al., 2020). Both sexes have a similar incidence and all dogs are affected whatever their size, even if certain breeds seem to be more predisposed, like Labrador Retriever, Bernese mountain dog, Cavalier King Charles or Beagle (Osto and Lutz, 2015). Canine obesity is generally associated with insulin resistance, altered lipid profile, hypertension, orthopedic and cardiorespiratory disease, and development of low-grade systemic inflammation (Tvarijonaviciute et al., 2012). While gene mutations are associated with increased body weight in Beagle and Labrador, diet is clearly a determinant of obesity through excess energy intake (Zeng et al., 2014; Raffan et al., 2016).

Several mechanisms may implicate gut microbiome in the onset and evolution of dog obesity. Based on human and murine data, this includes higher energy utilization from non-digestible carbohydrates, manipulation of host gene functions, and exacerbation of inflammation (Hamper, 2016). Five studies have compared fecal microbiota composition of obese and lean dogs (Fig. 3). Using 16S rRNA gene pyrosequencing in companion and laboratory dogs, dominance of *Firmicutes* (> 90%) was observed

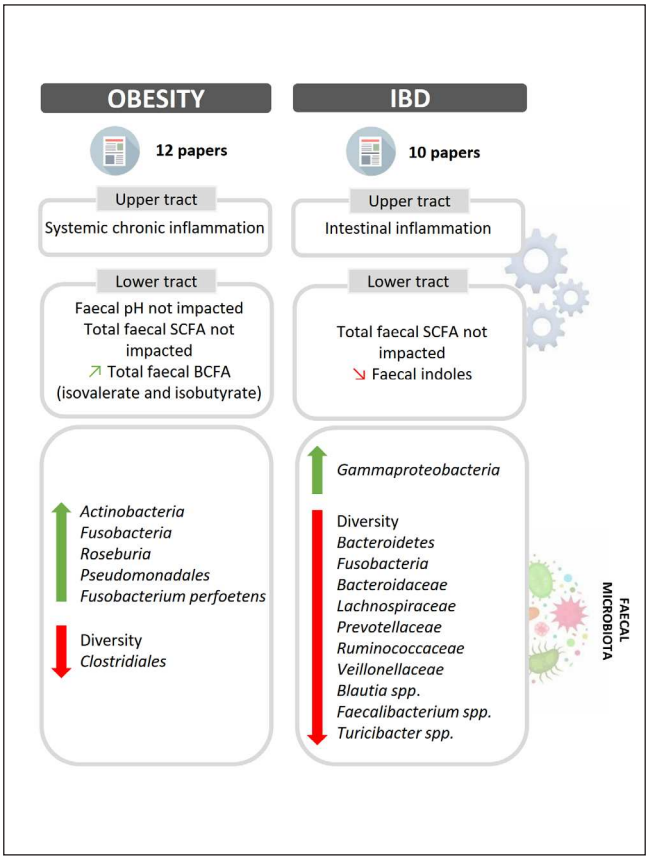

Fig. 3: Impact of obesity and inflammatory bowel disease on canine digestive physiology

Main variations in upper and lower digestive physiology and changes in fecal microbiota composition associated with canine obesity and IBD are represented. Increased parameters are indicated by green arrows, decreased parameters by red arrows. BCFA, branched-chain fatty acids; IBD, inflammatory bowel disease; SCFA, short-chain fatty acids

in both obese and lean groups, but mean abundance of *Actinobacteria* and *Roseburia* was greater in obese dogs (Handl et al., 2013). Using the same method, Salas-Mani et al. (2018) showed that *Proteobacteria* was predominant in obese dogs (76%), whereas fecal microbiota from lean dogs was mainly composed of *Firmicutes* (85%). In addition, *Clostridiales* appeared to be less abundant in obese compared to lean dogs, while the opposite result was found for *Pseudomonadales*. However, in a recent study involving 17 healthy and 22 obese companion dogs, no significant difference in any taxa was highlighted when comparing the two groups using Illumina 16S rRNA gene sequencing (Forster et al., 2018). With the same method, Bermudez Sanchez and colleagues (2020) described a relative abundance of 92% of *Firmicutes*, 2% *Fusobacteria*, 1% *Bacteroidetes* and a median *Firmicutes*/*Bacteroidetes* ratio of 0.123 in 20 obese dogs (Bermudez Sanchez et al., 2020). Lastly, in a very recent study, a positive association between *Fusobacteria* level, especially *Fusobacterium perfoetens*, and body score condition in 24 overweight laboratory Beagles was established using metagenomic analysis (Chun et al., 2020). In dogs, like in humans, microbial diversity seems to decrease in obese compared to lean dogs, with a Shannon index of 1.3 and 2.3, respectively (Park et al., 2015). However, more investigations are required to characterize canine obese microbiota, in feces but also in other digestive compartments, to determinate if some species should be used as obesity markers. As an example, *Proteobacteria* were recently correlated with increased weight in overweight dogs, as has been suggested in humans (Apper et al., 2020).

In addition to microbiota changes, other physiological modifications have been demonstrated in obese humans compared to healthy individuals, including an increase in BA production by liver (coupled with high amounts of primary BA in stool), and a higher SCFA production, leading to a decrease in colonic pH (Rahat-Rozenbloom et al., 2014). Due to similarities between dog and human GIT and lifestyle, it would be interesting to establish whether similar phenomena occur in obese dogs. Mean fecal pH of obese companion Beagles (6.6) was not significantly different from that of lean dogs (6.8) whatever the diet, i.e., high-fat or low-fat diet (Xu et al., 2017). In the same study, total fecal SCFA concentration was also equivalent in the two groups, whereas fecal BCFA such as isovalerate and isobutyrate were significantly more concentrated in obese compared to lean dogs. To our knowledge, no study has investigated BA production in obese versus lean dogs. However, recent studies recommend to monitor fecal BA concentrations along with microbiota in lean and obese dogs as they appear to be interesting markers of glucose homeostasis failure in obese dogs (Forster et al., 2018; Apper et al., 2020).

4.2 Inflammatory bowel disease

In dogs, IBD is classified as a chronic enteropathy, but defining its prevalence remains difficult because diagnosis of the disease is challenging. IBD is characterized by an irregular alternation of clinically active (with pain and diarrhea) and insignificant phases. Outside active phases, there are recurring gastric symptoms with histopathological changes in mucosa of the small and large intestines (Malewska et al., 2011). The predominant causes of canine IBD include bacterial and environmental factors, genetic predisposition of selected breeds, food allergies, and some drugs (Malewska et al., 2011). Pathogenesis of IBD includes loss of tolerance for endogenous microbiota, chronic inflammation of the GIT associated with an increase in intestinal permeability, and immune cell infiltration in the *lamina propria* (Junginger et al., 2014). Clinical scenarios include a decline in activity level and appetite, vomiting, increase in stool frequency, loss of stool consistency (increase in fecal water content), and weight loss.

Recent reviews on IBD in dogs (Fig. 3) report modifications in gut microbiota structure (compared to healthy animals) similar to those found in humans (Xenoulis et al., 2008; Hooda et al., 2012; Suchodolski et al., 2008, 2010, 2012a,b; Cassmann et al., 2016; Pilla and Suchodolski, 2020), although Xu et al. (2016) did not observe significant differences between healthy and IBD groups. Minamoto and collaborators (2015) showed an overall decrease in fecal diversity in IBD compared to healthy dogs, as also de-

scribed in humans (Minamoto et al., 2015). Furthermore, a dysbiosis index designed using qPCR targeting of eight bacterial groups to assess fecal microbial changes associated with canine chronic enteropathies allowed discrimination between healthy and diseased dogs with 95% confidence range (AlShawaqfeh et al., 2017). Fungal DNA was more frequently detected in dogs with chronic enteropathies than in healthy animals. FISH analysis of colonic biopsies from Boxers with granulomatous colitis revealed mucosa colonization by an unknown adherent and invasive *E. coli* strain (Simpson et al., 2006). The data indicate that global microbial structure and diversity, more than a single taxa, should be followed to discriminate healthy and IBD dog microbiota (Scarsella et al., 2020).

Concerning functional activity, there is no significant difference in fecal SCFA concentrations between IBD and healthy dogs, but a lower indole concentration was measured in diseased dogs (Xu et al., 2016; Pilla and Suchodolski, 2020). This is an important point because indoles have well-known anti-inflammatory effects, strengthen epithelial barrier, and decrease E.coli attachment to the epithelial wall (Chèvreton, 2018). Alterations in microbial functions associated with IBD were estimated using a prediction tool (PICRUSt) from 16S rRNA gene data, highlighting a significant increase in secretion system pathways and transcription factors (Minamoto et al., 2015). Other parameters modified in humans during IBD (Duboc et al., 2013; Rana et al., 2013; Fitzpatrick and Jenabzadeh, 2020) such as transit time and BA dysmetabolism (increase in fecal primary BA) have not been investigated in dogs yet.

5 *In vitro* canine models as an alternative to *in vivo* assays in dogs

5.1 Generalities on *in vitro* gut models: static versus dynamic and comparison with *in vivo*

A wide range of *in vitro* gut models has been developed, from simple static mono-compartmental models to more complex dynamic and multi-compartmental models (Guerra et al., 2012; Payne et al., 2012). These *in vitro* models have been primarily developed to mimic human digestion but have also been adapted to simulate animal digestion, mainly that of pig or piglet (Meunier et al., 2008; Tanner et al., 2014; Fleury et al., 2017; Dufourny et al., 2019), cat (Sunvold et al., 1995a,b; Van den Abbeele et al., 2020a) or dog (Sunvold et al., 1995a,b; Smeets-Peeters et al., 1999; Tzortzis et al., 2004; Hervera et al., 2007; Bosch et al., 2008; Cutrignelli et al., 2009; Panasevich et al., 2013; Lee et al., 2017; Vierbaum et al., 2019; Oba et al., 2020; Van den Abbeele et al., 2020a; Verstrepen et al., 2021), as described in Section 5.2.

Simple static models of the upper gut (Minekus et al., 2014) reproduce the successive oral, gastric and/or small intestinal phases of human digestion in a single vessel maintained at body temperature by changing pH conditions and adding appropriate digestive secretions (e.g., α-amylase in the oral phase, pepsin and/or lipase in the stomach, and bile and/or pancreatic juice in the intestinal phase). The simplest models of the colon compartment are thermostatic batch culture systems. These models are inoculated with feces to simulate colonic fermentation and are maintained under anaerobic conditions by flushing them with nitrogen or carbon dioxide without renewal of nutritive growth medium. Such approaches are therefore limited in the time they can be run by substrate availability (24 to 72 h), and parameters like pH or redox potential are not regulated.

Compared to static systems, dynamic models reproduce changes in at least one parameter such as pH kinetics, variation in digestive secretions, or chyme transit. They can be mono-compartmental or are composed of sequential vessels simulating the successive digestive compartments. Dynamic mono-compartmental models of the upper gut are only gastric digesters (Kong and Singh, 2010; Thuenemann et al., 2015), while multi-compartmental models include gastric and small intestinal compartments, most frequently simulating the duodenal section (Tompkins et al., 2011; Ménard et al., 2015). All these models only reproduce physicochemical parameters of the upper digestive tract, such as temperature, gastric and intestinal pH, gastric and ileal deliveries, transit time, digestive secretions and passive absorption of nutrients and water. Dynamic large intestine models are based on the principle of continuous or semi-continuous fermentation and are inoculated with fecal samples. Such models are maintained under anaerobiosis and reproduce colonic temperature, pH, and transit time, and redox potential can be monitored. Moreover, a nutritive medium aiming to mimic ileal effluents and composed of various complex sources of carbon and nitrogen, electrolytes, BA, and vitamins is continually added to the bioreactor while fermentation medium is regularly removed. This allows maintaining functional microbiota for up to several weeks (or even several months with specific adaptations) (Fehlbaum et al., 2015). Several configurations of these colon models include the use of three-stage bioreactors in series to mimic the different sections of the human colon (Gibson et al., 1988; Cinquin et al., 2006; Van de Wiele et al., 2015) or the addition of mucin beads to distinguish luminal from mucosal colonic environments and their associated microbiota (Van den Abbeele et al., 2009; Deschamps et al., 2020). Up to now, the TNO gastro-Intestinal Model (TIM-1) is probably the most complete *in vitro* system, with its four compartments reproducing the stomach and small intestine of monogastrics (Minekus et al., 1995; Meunier et al., 2008; Denis et al., 2016), while only two models simulate the whole digestive tract from the stomach to colon: the Simulator of Human Intestinal Microbial Ecosystem (SHIME) (Molly et al., 1993; Roussel et al., 2020), and the SIMulator of the Gastro-Intestinal tract (SIMGI) (Barroso et al., 2015).

Despite the obvious limitations of *in vitro* approaches, i.e., no input from nervous, endocrine or immune systems, artificial gut models have many advantages in terms of low cost, technical flexibility and reproducibility. Especially, the spatial compartmentalization of bi- and multi-compartmental models allows sample collection over time and in the desired segment of the GIT, while *in vivo* studies mainly provide endpoint measurements (e.g., in fecal samples), since access to the different segments of the digestive tract (from the stomach to proximal colon) is restricted. Besides, in canine *in vivo* assays, there is frequently a huge discrepancy between studies due to different diets, life-

style, sizes and breeds. Therefore, as in humans, inter-individual variability is one of the main challenges. In comparison, *in vitro* approaches enable a high level of experimental control and reproducibility by excluding confounding environmental or dietary factors and therefore allow in-depth mechanistic studies on pharma and food compounds.

5.2 Currently available canine *in vitro* gut models

Since 1995, twelve *in vitro* models of the canine gut have been developed (Tab. 1). There is no available model of the oral phase, and only three models mimic the upper GIT (Smeets-Peeters et al., 1999; Hervera et al., 2007; Lee et al., 2017).

In vitro *models of the upper gut*

While Hervera and colleagues (2007) simulate stomach and small intestine digestion in batch vessels by adding crushed dog food to pepsin and pancreatin secretions only, a very complete model of the canine upper gut was developed in 2000 based on the TIM-1 technology, initially set up to reproduce human digestive conditions. Though the TIM-1 model is the most complete simulator of the upper gut, it only reproduces physicochemical and not microbial digestive parameters. Another main limitation of this model is that tested food should be finely mixed before digestion, which can influence nutrient digestibility.

FIDO (for Functional gastroIntestinal Dog Model) integrates all the upper digestive compartments (stomach, duodenum, jejunum and ileum) and simulates body temperature, kinetics of gastric and small intestine pH, half-time delivery of gastric and ileal compartment, transit time and chyme mixing, sequential delivery of digestive secretions (gastric juice containing *Rhizopus* lipase and porcine pepsin, porcine pancreatic juice, bovine trypsin, electrolytes, and porcine bile), and intestinal passive absorption through hollow dialysis fibers (Smeets-Peeters, 2000). FIDO was set-up to mimic canine digestive parameters of medium dogs based on literature review (Smeets-Peeters et al., 1998). All parameters were therefore adapted to *in vivo* data, except for temperature, which was kept at 37°C like in humans, and parameters of passive absorption, probably due to a lack of data. The model was validated only for nutritional applications, by comparing protein digestibility and calcium bioaccessibility in the FIDO model and in ileal cannulated dogs (5 dogs).

More recently, the Artificial Stomach-Duodenum (ASD) dissolution model was adapted to dog digestion for formulation solubility studies (Lee et al., 2017). This bi-compartmental model, set at 37°C, simulates both the stomach and duodenum with associated pH (6.8 and 6.8-7, respectively), transit time (adapted from *in vivo* data), and pancreatic secretions. In this model the gastric pH is particularly high compared to the other two (6.8 for the ASD model versus pH 2 for Hervera's model and 2-6 for FIDO).

In vitro *models of the lower gut: batch and continuous models*

Eight other available devices are *in vitro* static models of the canine colon based on batch fermentation. The simplest model of the colon on adult dogs was developed by Cutrignelli et al. (2009). Here, a single vessel was inoculated with diluted feces from adult large dogs and maintained at 39°C under anaerobiosis without any addition of nutritional medium except for the tested carbohydrates. Another batch model set up by Sunvold et al. (1995c) to reproduce the colon of adult medium-sized dogs used a simulated growth medium adapted to dog digestion. This model was validated against *in vivo* data from 30 medium-sized dogs regarding fiber digestibility and production of SCFAs. Another static model, a batch system inoculated with dog fecal samples (no information on age and size of animals), was recently developed by Van den Abbeele et al. (2020a). A nutritive medium was introduced to simulate dog ileal effluents, but this was similar to one used previously for human experiments (Van den Abbeele et al., 2018). Batch models developed by other teams share the limitation that they lack a nutritive medium adapted to the canine situation (Tzortzis et al., 2004; Panasevich et al., 2013; Vierbaum et al., 2019). Bosch et al. (2008) developed a more complete batch fermentation model mimicking the ileum, proximal colon, transverse colon, or rectum compartment in different vessels inoculated with corresponding digestive fluids from 3 adult small or large dogs. In this study, the authors used a nutritive medium previously adapted for piglet fermentation, from another medium initially developed for rumen bacteria maintenance, without any modification in relation to dog digestion (Williams et al., 2005). The main disadvantage of this model is that it uses digestive fluids collected from dogs to inoculate the vessels, and the inter-individual variability associated with such an approach. Only one static batch model integrates mucin-covered microcosms in order to represent the intestinal mucus, but the associated results are not discussed (Oba et al., 2020). To conclude on these batch models, apart for temperature, fecal inoculation and anaerobiosis, parameters were generally not adapted to canine digestion. Even if *in vitro*/*in vivo* correlations were established for some of these models, *in vitro* digestion conditions remained far from *in vivo* complexity, and nutrient composition of dog digestive fluids, digestive secretions, or pH variations between small and large intestinal compartments and residence time in each gut section were not considered.

The only dynamic *in vitro* model of the lower dog gut, the SCIME model (for simulation of canine intestinal microbial ecosystem), was adapted from the SHIME system, first set up to reproduce human conditions. The SCIME model is currently unique in reproducing the entire canine GIT from the stomach to the large intestine (Duysburgh et al., 2020). SCIME is composed of four bioreactors simulating the stomach, small intestine, and proximal and distal colon. Only colonic compartments are inoculated with fecal samples from medium-sized dogs. *In vivo* parameters that are reproduced include body temperature, regionalized gastric and intestinal pH, gastrointestinal transit time, digestive secretions (pancreatic juice and bile), and anaerobiosis. The authors mention that most of the parameters were adapted to medium-sized dog digestion, though associated *in vivo* data are not clearly mentioned in the publication. SCIME was validated by comparison with *in vivo* data from ten Beagles digesting fructooligosaccharides regarding microbial composition and SCFA/BCFA production. Of note, *in vitro* results in proximal and distal colon (even if clearly distinct profiles were obtained) were only compared to *in vivo* data in fecal samples. Recently,

Tab. 1: Main *in vitro* models developed to simulate the gastrointestinal tract of dogs and their characteristics
CO_2, carbon dioxide; FIDO, Functional gastroIntestinal DOg model; GET, gastric emptying time; GI, gastrointestinal; LITT, large intestine transit time; N_2, nitrogen; N/A, not applicable; ND, not defined; M-SCIME, Mucosal Simulator of the Canine Intestinal Microbial Ecosystem; SITT, small intestine transit time

References			Dog's generalities		GI compartment modelized	Adaptations from bibliographic research	Validation processes	Physicochemical parameters								Microbiota			
			Age (years)	Dog's size				Temperature	Agitation	pH		Transit time	Food reproduction	Digestive secretions	Absorption	Presence of microbiota	Process type	Anaerobiosis	Mucus
										pH kinetic	Value								
UPPER TRACT																			
Hervera et al., 2007	STATIC	MONO-COMPARTMENTAL	ND	ND	Stomach and small intestine	But no reference to *in vivo* data	*In vivo* digestibility trial (n=54)	39°C	Magnetic bar	No	Stomach: 2 Small intestine: 6.8	No	Crushed dry extruded canine food	Gastric digestion: pepsin Intestinal digestion: pancreatin	No	No	N/A	No	No
Lee et al., 2017 **Artificial Stomach-Duodenum**	DYNAMIC	MULTI-COMPARTMENTAL	ND	Medium	Stomach and duodenum	Adapted from Smeets-Peeters et al., 1998; Carino et al., 2006; Bhattachar et al., 2011	*In vivo* pharma trial (n=6)	37°C	Paddle	No	Stomach: 6.8 Duodenum: 6.8-7	Yes	No	Pancreatin solution	No	No	N/A	No	No
Smeets-Peeters et al., 1999 **FIDO**			"Adult"	Medium	Stomach, duodenum, jejunum and ileum	Adapted from Smeets-Peeters et al., 1998	*In vivo* digestibility trial (5 ileal cannulated dogs)	37°C	Water pressure on flexible wall	Yes	Stomach: 2-6 Duodenum: 6.2 ± 0.2 Jejunum: 6.5 ± 0.2 Ileum: 7.0 ± 0.2	GET: $T_{1/2}$: 1.5 h SITT: $T_{1/2}$: 5 h	Crushed dry or canned dog food	Gastric juice, pancreatic juice, intestinal electrolyte solution, bile solution	Passive	No	N/A	No	No
LOWER TRACT																			
Vierbaum et al., 2019	STATIC	MONO-COMPARTMENTAL	4.3 ± 0.9	Medium	Large intestine	⊗	No validation	37°C	Continuous shaking at 370 rpm	No	N/A	No	No dog food. Pre-reduced anaerobe sterilized medium	No	No	Yes, from feces	Batch 24 h	Yes	No
Cutrignelli et al., 2009			3	Large	Large intestine	⊗	Based on a literature review	39°C	No	No	N/A	No	No	No	No	Yes, from feces	Batch 48 h	Yes	No
Panasevich et al., 2013			ND	ND	Large intestine	But no reference to *in vivo* data	*In vivo* digestibility trial (n=10)	39°C	Periodic mixing	No	N/A	No	No dog food Anaerobe medium	No	No	Yes, from feces	Batch 12 h	Yes CO_2-gas	No
Sunvold et al., 1995			5-6	Medium	Large intestine	⊗	*In vivo* fermentation study (n=30)	39°C	No	No	N/A	No	No dog food. Nutritive medium based on several solutions of vitamins, oligo-elements, supplemented with fibrous substrates	No	No	Yes, from feces	Batch 24 h	Yes CO_2-gas	No
Van den Abbeele et al., 2020a			ND	ND	Large intestine	⊗	Based on a literature review	39°C	Magnetic bar	No	N/A	No	No dog food. Colonic background medium	No	No	Yes, from feces	Batch 48 h	Yes N_2-gas flow	No

Tzortzis et al., 2004			ND	ND	Large intestine	⊗	No validation	37°C	Magnetic bar	No	6.8	No	No dog food. Colonic background medium	No	No	Yes, from feces	Batch 24 h	Yes N_2-gas flow	No
Oba et al., 2020			4.6	Large	Large intestine	⊗	No validation	39°C	Continu-ous shaking at 90 rpm	No	N/A	No	Colonic background medium	No	No	Yes, from feces	Batch 48 h	Yes N_2-gas flow	Mucin-covered microcosms
Bosch et al., 2008			Adult and mature	Small and large	Ileum, proximal colon, transverse colon or rectum	⊗	No validation	39°C	No	No	N/A	No	No dog food. Filtered digestive fluids added to a nutritive medium previously adapted for rumen bacteria growth	No	No	Yes, from digesta	Batch 72 h	Yes CO_2-gas	No
Duysburgh et al., 2020 **SCIME** Verstrepen et al., 2021 **M-SCIME**	DYNAMIC	MULTI-COMPARTMENTAL	ND	Medium	Stomach, small intestine, proximal colon and distal colon	But no reference to *in vivo* data	**SCIME** *In vivo* fermentation study (n=10) and literature **M-SCIME** Comparison with SCIME results - Comparison of *in vitro* results with fecal inoculum (microbiota)	39°C	Magnetic bar	No	Stomach: 2 Small intestine: 6.8 Proximal colon: 5.6-5.9 Distal colon: 6.65-6.9	Residence times GET: 1 h SITT: 4 h LITT: 6 h (transverse) 10 h (distal)	Dog food added at 9 g/L in stomach juice. Small and large intestine effluents simulated by addition of digested suspension from the previous compartment	Pancreatic juice and bile	Passive (feed)	Yes, from feces, in the large intestinal compartments only	Continuous	Yes N_2-gas flow	Mucin-covered microcosms

SCIME was optimized by the addition of mucin-covered plastic beads, based on Mucosal-SHIME (M-SHIME) technology (Van den Abbeele et al., 2009), to reproduce the luminal and mucosal microenvironment of the canine colon. The resulting model was called M-SCIME (Van den Abbeele et al., 2020b; Verstrepen et al., 2021). Due to a lack of *in vivo* data, this optimization was not validated compared to bacterial mucosal profiles in dogs, but only compared to previous results obtained in the M-SHIME. Once again, *in vitro* colonic pH varies widely between currently available models, which could be explained by the fact that authors generally base their model settings on a unique *in vivo* study, whereas large inter-individual variations are observed in dogs depending on age, size, and breed.

6 *In vitro* gut models as powerful tools to study canine digestion

6.1 Scientific and technical challenges to be addressed

As described above, *in vitro* models have not been fully optimized, probably due to the paucity of information on the relevant parameters in dogs. Therefore, many scientific and technical challenges still need to be addressed to improve models of canine digestion and reflect the complexity of this environment (Fig. 4).

First, technical improvements should be considered to simulate canine digestive conditions in each part of the GIT more realistically. Currently, there is no canine chewing simulator, but such a development is not a priority, since most dogs do not chew but swallow large pieces for food. Regarding the upper gut, the FIDO model already shows a high level of complexity. The M-SCIME also possesses a gastric compartment that would merit improvements such as progressive acidification of the chyme (already introduced in the M-SHIME). This change in gastric pH during canine digestion is a key parameter in food disruption and digestion as it influences gastric pepsin and lipase activities (Carrière et al., 1993; Sams et al., 2016). FIDO and M-SCIME both require homogenization of food before *in vitro* digestion. In dogs, larger food particle sizes seem to reach the stomach. Even if little data on this in dogs is available (unlike in humans), some canine studies showed no correlation between food size and density of particles on gastric emptying time or on the entire upper gut digestion process (Gruber et al., 1987; Meyer et al., 1988; Chen et al., 2008; De Cuyper et al., 2018), while others observed that gastric half emptying time increased with higher meal viscosity and fat content (Ehrlein and Pröve, 1982; Palerme et al., 2020). Recently, a new human gastric and small intestinal model, the Engineered Stomach and Small Intestine (ESIN), was developed to fill this gap and handle both ingested liquids and real-size food particles better in simulated digestion studies (Guerra et al., 2016). Even if this model was primarily set up for human applications, it could easily be adapted to reproduce dog digestion.

Another main issue in upper gut models is the use of porcine, bovine, or fungal secretions/enzymes instead of canine ones. Due to ethical constrains, digestive secretions cannot be collected from dogs for this purpose (and are not commercially avail-

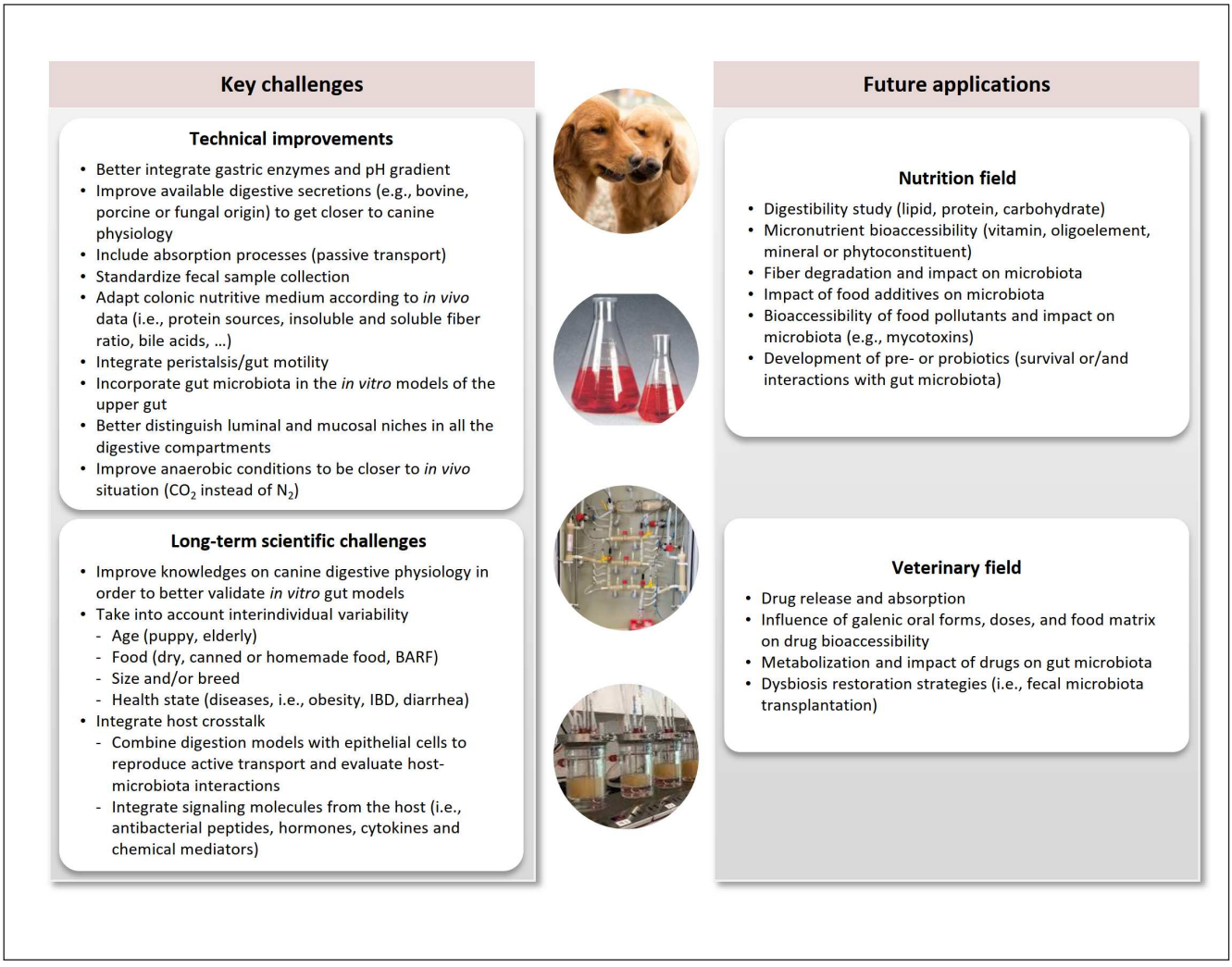

Fig. 4: Main challenges in the development of *in vitro* gut models of the canine digestive tract and their applications in nutritional and veterinary fields

Overview of the main technical and scientific challenges and applications of canine *in vitro* gut models as reliable tools to test or develop new products in the food and pharma fields.

able). Therefore, further investigations are needed to ensure that digestive secretions from other sources are suitable to represent canine ones (in terms of composition and enzymatic activities) to ensure relevant *in vitro* simulation. For example, bile composition and conjugation profiles differ widely between species (Thakare et al., 2018a,b). Thus, further analysis is needed to determine whether porcine bile (largely used in *in vitro* models) is a good model of canine bile (Alvaro et al., 1986).

Another main limitation of current upper gut models is their inability to accurately mimic gastric and intestinal peristalsis. In M-SCIME, peristaltic mixing is reproduced using magnetic stirrers, which is far from the *in vivo* situation. FIDO more closely reproduces peristaltic movements through gentle mixing with pressurized water jackets, but peristaltic force and frequency have not been adapted for dog models, whereas *in vivo* data indicate clear differences between humans and dogs (Boscan et al., 2013; Warrit et al., 2017; Farmer et al., 2018). Efforts should therefore be invested to more accurately simulate mechanical deformation resulting from peristalsis in dogs, based on what has already been done in human gastric models (Kong and Singh, 2010; Li et al., 2019).

Regarding nutrient absorption in the small intestine, FIDO incorporates dialysis fiber modules in the jejunal and ileal compartments. In a very recent publication on the M-SCIME (Verstrepen et al., 2021), a dialysis step of ground dog feed was integrated to simulate small intestinal absorption by removing high-molecular weight proteins. Adding such dialysis devices to other upper gut models would be beneficial to better represent the *in vivo* situation, even if dialysis modules only reproduce passive absorption of small molecules (e.g., fatty acids, oligo- and monosaccharides, small peptides, amino acids, but also drugs and chemicals) and water. Reproducing passive absorption also ensures bile re-

absorption in the distal intestine and, therefore, a decrease in bile concentrations from the duodenal to the ileal compartments, which is a key process in both dog and human gut physiology.

To further reproduce absorption phenomena and integrate active transport, canine dog models of the upper gut should be coupled with immortalized canine intestinal epithelial cells (cIEC) (Farquhar et al., 2018), as done in human models with TIM-1 and Caco-2 cells (Déat et al., 2009; Bahrami et al., 2011) or with organoids generated from canine duodenal, jejunal and colonic biopsies (Kramer et al., 2020).

A last key point to be raised is the lack of intestinal microbiota in all the upper gut models, whereas bacterial concentrations up to 10^7 CFU/g can be found in the distal small intestine of dogs (Benno et al., 1992; Mentula et al., 2005). Even if the role of intestinal microbiota is poorly defined in dogs (Hooda et al., 2012; Deng and Swanson, 2015; Enright et al., 2016; Mondo et al., 2019; Pilla and Suchodolski, 2020), we can assume that intestinal microbiota is involved at least in carbohydrate digestion and may exert a barrier effect against enteric pathogens as observed in humans (Andoh, 2016). This is even more important since, unlike in humans, an appreciable fraction of dietary fibers seems to be degraded in the canine small intestine (Bednar et al., 2000).

This microbial component of the canine digestive tract is integrated in *in vitro* colon models by inoculation with fecal samples. However, a major issue of all available *in vitro* colon models is that the nutritive medium used to maintain bacterial growth and activity was not adapted to adequately mimic the composition of ileal effluents entering the colon *in vivo*. Using digestive fluids as previously done by Bosch et al. (2008) is not a simple and sustainable solution as it makes *in vitro* models strongly dependent of unstandardized and poorly available *in vivo* samples. Therefore, efforts are still required to better define a growth medium composition based on available data on dog diet, but also protein, lipid and carbohydrate ileal digestibility (Bednar et al., 2000; Flickinger et al., 2003; Propst et al., 2003). It is also important to consider relevant BA concentrations and profiles reaching the colon, as they may shape gut microbiota composition (Ridlon et al., 2014).

All available *in vitro* colonic models are flushed with nitrogen or carbon dioxide to maintain anaerobic conditions inside vessels or bioreactors, which is unlike the *in vivo* situation. In the human Artificial Colon (ARCOL) model, anaerobiosis is maintained solely by the activity of resident microbiota to reflect *in vivo* gut physiology (Friedman et al., 2018; Deschamps et al., 2020; Verdier et al., 2021). Such an adaptation could further increase the relevance of *in vitro* canine colon models.

Moreover, only bacteria have been followed to date as the main component of gut microbiota. Given the importance of other constituents, such as fungi, methanogenic archaea, or even phages or viruses in gut physiology (Barko et al., 2018), it would be of great interest to extend microbial sequencing to these populations.

Lastly, as mentioned for upper gut models, to further investigate host-microbiome crosstalk, canine *in vitro* models should be coupled to cell culture assays, as previously described for human models (Bahrami et al., 2011; Chassaing et al., 2017; Geirnaert et al., 2017; Defois et al., 2018).

Of interest, the Host Microbiota Interaction Module already coupled to the SHIME system (Marzorati et al., 2014) integrates microaerobiosis in close proximity to the epithelium, shaping mucus-associated gut microbiota. This may also be of relevance for the dog colonic ecosystem.

6.2 Future developments and quality requirements

Most available *in vitro* models, and especially the more complex FIDO and M-SCIME systems, have been designed to reproduce a medium-sized dog's digestive conditions when ingesting dry food. As widely described, canine digestion is impacted by body weight or breed (Kendall et al., 1983; Bourreau et al., 2004; Hernot et al., 2005; Weber, 2006; Weber et al., 2017). Considering the influence of body weight and/or breed on canine digestive physicochemical and microbial parameters is undoubtedly a promising line of research to develop more relevant *in vitro* models.

Further, adaptations regarding dog diet (e.g., dry, canned or homemade food, BARF) and age (puppies, adults and elderly dogs) would also bring substantial added value to *in vitro* canine gut simulation. This has been already performed with success in *in vitro* human models (Blanquet et al., 2004; Fehlbaum et al., 2015; Denis et al., 2016; Roussel et al., 2016, 2020; Bondue et al., 2020).

Moving forward, we can foresee the development of *in vitro* gut models simulating not only physiological but also diseased situations, such as those associated with obesity or IBD, as previously done in humans (Bussolo de Souza et al., 2014). In this case, the main objective would be to maintain gut microbiota dysbiosis (considered a typical feature of these pathologies) inside the *in vitro* models. For this purpose, small intestinal and/or colonic models could be inoculated with feces collected from dogs suffering from obesity or IBD, but also all the associated gut parameters, such as the composition of digestive effluents (including bile profiles), pH and retention time should be modified to fulfil specific diseased conditions.

All these technical and scientific improvements would be possible if corresponding canine *in vivo* data were available in the literature (or provided by clinical trials), both for setting-up *in vitro* models and for the validation of their robustness through strong *in vivo-in vitro* correlations. Such validation is necessary to convince future users of the relevance of *in vitro* gut models but is unfortunately rarely performed due to cost, time, or technical limitations.

To date, main gaps in *in vivo* data concern digestive secretions in the upper gut as well as microbial profiles along the digestive tract and characterization of mucus-associated bacteria. Recent developments of non-invasive methods to follow digestive parameters, such as pH, motility, or transit time (wireless motility capsules, e.g., SmartPill) in dogs (Warrit et al., 2017) and in humans (Schwizer et al., 2002; Wang et al., 2005; Zhang et al., 2014) open new avenues and may help to fill these scientific and technological gaps. Regarding such *in vivo* reference studies, it would be of high importance to standardize the experimental conditions in terms of age, breed, weight, but also diet and lifestyle, which all impact digestive parameters (Mahar et al., 2012; Panasevich et al., 2015; Apper et al., 2020; Pilla and Such-

odolski, 2020; You and Kim, 2021). It is also important to exclude breeds showing well-known specific digestive particularities (like German Shepherd) or specific energy needs (like Husky, Great Danes or Terriers) (Zentek and Meyer, 1995) from such *in vivo* assays.

Standardization of procedures is also of concern for *in vitro* studies, and some important guidance is available in the guidance document on Good *In Vitro* Method Practice (GIVIMP) (OECD, 2018), especially for cell culture practices.

In addition to robustness, canine *in vitro* model development involves other quality requirements, such as reproducibility and transferability. Reproducibility is considered a key advantage of *in vitro* studies over *in vivo* experiments and should be systematically assessed. Transferability of canine *in vitro* gut models is hampered by their current early stage of development. The simple *in vitro* systems (such as batch models) can be more easily shared between laboratories than the more complex ones, which require specific technical expertise. Transferability of canine gut models could be accelerated by exchanges between international experts in artificial digestion, as previously done in the frame of the INFOGEST network, which led to the harmonization of static and semi-dynamic *in vitro* protocols in humans (Minekus et al., 2014; Brodkorb et al., 2019).

6.3 Potential applications of canine gut models in food and pharma

In vitro models represent a powerful platform to study the fate of food and veterinary products in the canine digestive environment, to help elucidate their mechanisms of action and promote innovation in these fields. As parameters can be adjusted in terms of food matrix, age, dog breed or body size, but also by mimicking physiological or pathological situations, we can imagine numerous applications of these systems once developed and validated (Fig. 4). They could provide valuable information to promote the evolution of products already on the market (generic, range extension, etc.) and/or inform the development of new products such as specialized food or innovative drugs. All types of *in vitro* gut models, from the simplest to the more complex ones, can be useful. Static mono-compartmental models are ideal tools to perform pre-screening of many compounds due to their low cost and easy manipulation. Dynamic multi-compartmental systems, which are more expensive and require expertise but reproduce more physiological digestive conditions, can be applied for a more focused study of selected candidate compounds. The applications already performed under human conditions (Souliman et al., 2006; Cordonnier et al., 2015; Lyng et al., 2016; Bianchi et al., 2019; Blancquaert et al., 2019; Kubbinga et al., 2019) in food and pharma fields can inspire similar studies in canine *in vitro* gut models.

To date, *in vitro* models simulating the canine digestive environment have only been used for nutritional applications, mainly to assess fiber digestibility (Sunvold et al., 1995c; Bosch et al., 2008; Cutrignelli et al., 2009; Musco et al., 2018; Van den Abbeele et al., 2020a,b) (Tab. 2). Other applications include evaluation of protein (Kim et al., 2021) or lipid digestibility and bioaccessibility of micronutrients such as vitamins, minerals (van Zelst et al., 2015; Lee et al., 2017) or phytoconstituents like polyphenols. In addition to digestibility, *in vitro* models can provide valuable information on the effects of fiber on gut microbial composition and activity, through SCFA/BCFA, ammonia or gas measurements (Bosch et al., 2008; Cutrignelli et al., 2009; Van den Abbeele et al., 2020a). This will help to assess the prebiotic status of soluble fibers. In addition to prebiotics, probiotic strains can be tested in the *in vitro* models to evaluate their interactions with gut microbiota (Ogué-Bon et al., 2011) but also their survival (and the effect of mode of administration) and their production of active compounds such as bacteriocins.

Regarding veterinary applications, the kinetics of drug release and absorption can be monitored all along the GIT, as well as the influence of oral formulations (Lee et al., 2017), different doses, fed or fasted state, and food matrix (food-drug interactions). Currently, drug posology is only established based on dog body weight or metabolic weight, but many associated variations in digestive parameters that influence drug bioaccessibility should be considered (Oswald et al., 2015). In addition, *in vitro* gut models can enhance knowledge of drug metabolization by gut microbiota and/or effects of drugs on gut microbiota composition and function (Sjögren et al., 2014). Hence, gut microbial dysbiosis induced by oral antibiotherapy (El Hage et al., 2019) can be simulated in colonic models and further applied to evaluate the efficiency of prebiotics and/or probiotics in restoring microbiota eubiosis.

Lastly, *in vitro* models can be employed to assess the efficiency of new microbial restoration therapy strategies such as fecal microbiota transplantation in a safe way before using animals. Fecal microbiota transplantation is based on the observation that transfer of intestinal contents from a healthy donor to a diseased one can improve gut health. This therapy has been recently tested in dogs for the treatment of post-weaning diarrhea, acute diarrhea, IBD, chronic enteropathies, or parvovirus infections and seems to be promising (Burton et al., 2016; Pereira et al., 2018; Niina et al., 2019; Chaitman and Gaschen, 2020; Chaitman et al., 2020).

7 Conclusion

Canine digestion is a complex and regionalized process involving physicochemical, mechanical, and microbial processes. It plays a central role in maintaining dog healthy and is increasingly recognized as part of the etiology of intestinal and extra-digestive diseases (such as IBD and obesity) in relation to gut microbiota dysbiosis. When testing or developing new products, food and veterinary industries need to consider these multi-faceted aspects of canine digestion and would benefit from relevant *in vitro* gut models for in-depth mechanistic studies as an alternative to *in vivo* assays.

Up to now, only a restricted number of *in vitro* models has been developed to simulate the canine upper or lower digestive tract. These devices show various levels of complexity, i.e., from static mono-compartmental to dynamic multi-compartmental models. The *in vitro* parameters have not yet been fully

Tab. 2: Application studies of the currently available canine *in vitro* gut models
BCFA, branched-chain fatty acids; GIT, gastro-intestinal tract; SCFA, short-chain fatty acids

References	Applications					Aim of the study
	Macronutrients	Micronutrients	Fibers/Prebiotics	Probiotics	Drugs	
Upper GIT models						
Smeets-Peeters et al., 1999	✓	✓				Effects of small intestinal transit time on protein digestibility and calcium availability from canned dog food
Hervera et al., 2007	✓					*In vitro* percentage of organic matter disappearance used as a predictor of apparent organic matter and energy digestibility of extruded dog food
van Zelst et al., 2015		✓				Identification of dietary factors that affect selenium accessibility in commercial petfood
Lee et al., 2017					✓	Evaluation of *in vitro* dissolution performance of five formulations of an acidic BCS Class II compound
Penazzi et al., 2021	✓					Effect of supplementation with black soldier fly (*Hermetia illucens*) larvae meal in extruded dog food on *in* vivo and *in vitro* digestibility
Kim et al., 2021	✓					Effect of thermal processing on ileal digestibility of dry matter and crude protein from raw chicken meat
Lower GIT models						
Sunvold et al., 1995b			✓			Effects of cellulose, beet pulp, citrus pulp, and citrus pectin on microbiota fermentation (organic matter disappearance, SCFA, and lactate)
Sunvold et al. 1995a			✓			*In vitro* fermentation of selected fibrous substrates: influence of diet composition on substrate organic matter disappearance and SCFA production
Sunvold et al., 1995c			✓			*In vitro* fermentation of selected fiber sources and metabolism of fiber-supplemented diets
Swanson et al., 2001			✓			Fermentation of vegetable and fruit fiber sources compared to fiber standards following SCFA production, organic matter disappearance, and gas production
Tzortzis et al., 2004			✓			Fermentation properties of galactooligosaccharides synthesized by α-galactosidase from *Lactobacillus reuteri* (SCFA)
Biagi et al., 2008			✓			Effects of fiber sources on microbiota composition and activity (SCFA, ammonia, and gas)
Bosch et al., 2008			✓			Fermentation kinetics of fibers from canine foods (gas and SCFA)
Cutrignelli et al., 2009			✓			Impact of different carbohydrate sources on microbiota fermentation (gas, SCFA, BCFA, ammonia)
Ogué-Bon et al., 2010 (39°C)			✓	✓		Evaluation of a symbiotic combination on probiotic growth and microbiota activity (SCFA)
Ogué-Bon et al., 2011 (39°C)			✓	✓		Effects of rice bran combined with *Lactobacillus acidophilus* and *Bifidobacterium longum* on microbiota activity (SCFA)
Panasevich et al., 2013			✓			Characterization of potato fiber fermentability by canine microbiota (SCFA and BCFA)
Panasevich et al., 2015			✓			Effect of soluble corn fibers on nitrogen-corrected true metabolizable energy and fermentability by microbiota (SCFA)
Vierbaum et al., 2019			✓			Effects of *Yucca schidigera* powder and inulin on protein fermentation metabolites (SCFA, BCFA, phenols and indoles, biogenic amines, ammonia)
Donadelli et al., 2019			✓			Effects of different fiber sources used in petfood on organic matter disappearance and SCFA/BCFA production
Oba et al., 2020			✓			Potential fermentation and prebiotic effects of GNU100, an animal milk oligosaccharide biosimilar, on microbial communities and metabolites production (gas, SCFA, BCFA, lactate)
Van den Abbeele et al., 2020a			✓			Effects of yeast-derived formulation on microbial composition and activity (gas, SCFA, ammonium)

References	Applications					Aim of the study
	Macronutrients	Micronutrients	Fibers/Prebiotics	Probiotics	Drugs	
Traughber et al., 2020			✓			Fermentability of legumes by microbiota and metabolites production (SCFA, BCFA and gas)
Duysburgh et al., 2020			✓			Effect of fructooligosaccharide supplementation on microbial community composition and activity (SCFA, BCFA and ammonium)
Van den Abbeele et al., 2020b			✓			Effect of a S. cerevisiae-based product on microbiota composition and production of fermentation metabolites (SCFA, BCFA and lactate)

adapted to *in vivo* canine digestion, and some of the models are not yet validated for their application, mainly due to a paucity of *in vivo* data. Therefore, many scientific and technical challenges must be overcome to optimize canine models to represent canine digestive physiology to realize their potential in food and pharma studies, e.g., by simulating specific digestive conditions associated with different dog sizes, breeds, or ages, under healthy or diseased conditions.

References

Akimoto, M., Nagahata, N., Furuya, A. et al. (2000). Gastric pH profiles of beagle dogs and their use as an alternative to human testing. *Eur J Pharm Biopharm 49*, 99-102. doi:10.1016/s0939-6411(99)00070-3

Alexander, C., Guard, B. C., Suchodolski, J. S. et al. (2019). Cholestyramine decreases apparent total tract macronutrient digestibility and alters fecal characteristics and metabolites of healthy adult dogs. *J Anim Sci 97*, 1020-1026. doi:10.1093/jas/sky437

AlShawaqfeh, M. K., Wajid, B., Minamoto, Y. et al. (2017). A dysbiosis index to assess microbial changes in fecal samples of dogs with chronic inflammatory enteropathy. *FEMS Microbiol Ecol 93*, fix136. doi:10.1093/femsec/fix136

Alvaro, D., Cantafora, A., Attili, A. F. et al. (1986). Relationships between bile salts hydrophilicity and phospholipid composition in bile of various animal species. *Comp Biochem Physiol B Comp Biochem 83*, 551-554. doi:10.1016/0305-0491(86)90295-6

Andoh, A. (2016). Physiological role of gut microbiota for maintaining human health. *Digestion 93*, 176-181. doi:10.1159/000444066

Apper, E., Privet, L., Taminiau, B. et al. (2020). Relationships between gut microbiota, metabolome, body weight, and glucose homeostasis of obese dogs fed with diets differing in prebiotic and protein content. *Microorganisms 8*, 513. doi:10.3390/microorganisms8040513

Arnbjerg, J. (1992). Gastric emptying time in the dog and cat. *Food and Agriculture Organization of the United Nations 28*, 77-81.

Aspinall, V. (2004). Anatomy and physiology of the dog and cat 8. The digestive system. *Veterinary Nursing Journal 19*, 94-99. doi:10.1080/17415349.2004.11013260

Axelsson, E., Ratnakumar, A., Arendt, M.-L. et al. (2013). The genomic signature of dog domestication reveals adaptation to a starch-rich diet. *Nature 495*, 360-364. doi:10.1038/nature11837

Bahrami, B., Child, M. W., Macfarlane, S. et al. (2011). Adherence and cytokine induction in Caco-2 cells by bacterial populations from a three-stage continuous-culture model of the large intestine. *Appl Environ Microbiol 77*, 2934-2942. doi:10.1128/AEM.02244-10

Barko, P. C., McMichael, M. A., Swanson, K. S. et al. (2018). The gastrointestinal microbiome: A review. *J Vet Intern Med 32*, 9-25. doi:10.1111/jvim.14875

Barroso, E., Cueva, C., Peláez, C. et al. (2015). The computer-controlled multicompartmental dynamic model of the gastrointestinal system SIMGI. In K. Verhoeckx, P. Cotter, I. López-Expósito et al. (eds.), *The Impact of Food Bioactives on Health: In Vitro and Ex Vivo Models*. Cham, Switzerland: Springer.

Bednar, G. E., Murray, S. M., Patil, A. R. et al. (2000). Selected animal and plant protein sources affect nutrient digestibility and fecal characteristics of ileally cannulated dogs. *Arch Tierernahr 53*, 127-140. doi:10.1080/17450390009381942

Beloshapka, A. N., Wolff, A. K. and Swanson, K. S. (2012). Effects of feeding polydextrose on faecal characteristics, microbiota and fermentative end products in healthy adult dogs. *Br J Nutr 108*, 638-644. doi:10.1017/S0007114511005927

Benno, Y., Nakao, H., Uchida, K. et al. (1992). Impact of the advances in age on the gastrointestinal microflora of beagle dogs. *J Vet Med Sci 54*, 703-706. doi:10.1292/jvms.54.703

Bermudez Sanchez, S., Pilla, R., Sarawichitr, B. et al. (2020). Fecal microbiota in client-owned obese dogs changes after weight loss with a high-fiber-high-protein diet. *PeerJ 8*, e9706. doi:10.7717/peerj.9706

Biagi, G., Cipollini, I. and Zaghini, G. (2008). In vitro fermentation of different sources of soluble fiber by dog faecal inoculum. *Vet Res Commun 32*, 335-337. doi:10.1007/s11259-008-9142-y

Bianchi, F., Lopes, N. P., Adorno, M. A. T. et al. (2019). Impact of combining acerola by-product with a probiotic strain on a gut microbiome model. *Int J Food Sci Nutr 70*, 182-194. doi:10.1080/09637486.2018.1498065

Bickel, M. and Kauffman, G. L. (1981). Gastric gel mucus thickness: Effect of distention, 16,16-dimethyl prostaglandin e2, and carbenoxolone. *Gastroenterology 80*, 770-775.

Blake, A. B., Guard, B. C., Honneffer, J. B. et al. (2019). Altered microbiota, fecal lactate, and fecal bile acids in dogs with gastrointestinal disease. *PLoS One 14*, e0224454. doi:10.1371/journal.pone.0224454

Blancquaert, L., Vervaet, C. and Derave, W. (2019). Predicting and testing bioavailability of magnesium supplements. *Nutrients 11*, 1663. doi:10.3390/nu11071663

Blanquet, S., Zeijdner, E., Beyssac, E. et al. (2004). A dynamic artificial gastrointestinal system for studying the behavior of orally administered drug dosage forms under various physiological conditions. *Pharm Res 21*, 585-591. doi:10.1023/b:pham.0000022404.70478.4b

Boillat, C. S., Gaschen, F. P. and Hosgood, G. L. (2010). Assessment of the relationship between body weight and gastrointestinal transit times measured by use of a wireless motility capsule system in dogs. *Am J Vet Res 71*, 898-902. doi:10.2460/ajvr.71.8.898

Bondue, P., Lebrun, S., Taminiau, B. et al. (2020). A toddler SHIME® model to study microbiota of young children. *FEMS Microbiol Lett 367*, fnaa135. doi:10.1093/femsle/fnaa135

Boscan, P., Cochran, S., Monnet, E. et al. (2013). Effect of prolonged general anesthesia with sevoflurane and laparoscopic surgery on gastric and small bowel propulsive motility and pH in dogs. *Vet Anaesth Analg 41*, 73-81. doi:10.1111/vaa.12093

Bosch, G., Pellikaan, W. F., Rutten, P. G. P. et al. (2008). Comparative in vitro fermentation activity in the canine distal gastrointestinal tract and fermentation kinetics of fiber sources. *J Anim Sci 86*, 2979-2989. doi:10.2527/jas.2007-0819

Bourreau, J., Hernot, D., Bailhache, E. et al. (2004). Gastric emptying rate is inversely related to body weight in dog breeds of different sizes. *J Nutr 134*, 2039S-2041S. doi:10.1093/jn/134.8.2039S

Brodkorb, A., Egger, L., Alminger, M. et al. (2019). INFOGEST static in vitro simulation of gastrointestinal food digestion. *Nat Protoc 14*, 991-1014. doi:10.1038/s41596-018-0119-1

Burton, E. N., O'Connor, E., Ericsson, A. C. et al. (2016). Evaluation of fecal microbiota transfer as treatment for postweaning diarrhea in research-colony puppies. *J Am Assoc Lab Anim Sci 55*, 582-587.

Bussolo de Souza, C., Roeselers, G., Troost, F. et al. (2014). Prebiotic effects of cassava bagasse in TNO's in vitro model of the colon in lean versus obese microbiota. *J Funct Foods 11*, 210-220. doi:10.1016/j.jff.2014.09.019

Carrière, F., Laugier, R., Barrowman, J. A. et al. (1993). Gastric and pancreatic lipase levels during a test meal in dogs. *Scand J Gastroenterol 28*, 443-454. doi:10.3109/00365529309098247

Cassmann, E., White, R., Atherly, T. et al. (2016). Alterations of the ileal and colonic mucosal microbiota in canine chronic enteropathies. *PLoS One 11*, e0147321. doi:10.1371/journal.pone.0147321

Chaitman, J. and Gaschen, F. (2020). Fecal microbiota transplantation in dogs. *Vet Clin North Am Small Anim Pract 51*, 219-223. doi:10.1016/j.cvsm.2020.09.012

Chaitman, J., Ziese, A.-L., Pilla, R. et al. (2020). Fecal microbial and metabolic profiles in dogs with acute diarrhea receiving either fecal microbiota transplantation or oral metronidazole. *Front Vet Sci 7*, 192. doi:10.3389/fvets.2020.00192

Chassaing, B., Van de Wiele, T., De Bodt, J. et al. (2017). Dietary emulsifiers directly alter human microbiota composition and gene expression ex vivo potentiating intestinal inflammation. *Gut 66*, 1414-1427. doi:10.1136/gutjnl-2016-313099

Chen, E. P., Mahar Doan, K. M., Portelli, S. et al. (2008). Gastric pH and gastric residence time in fasted and fed conscious cynomolgus monkeys using the Bravo pH system. *Pharm Res 25*, 123-134. doi:10.1007/s11095-007-9358-5

Chèvreton, P. (2018). *The Gut Microbiota of Domestic Carnivorous: State of Play*. Faculté de Médecine de Créteil.

Chun, J. L., Ji, S. Y., Lee, S. D. et al. (2020). Difference of gut microbiota composition based on the body condition scores in dogs. *J Anim Sci Technol 62*, 239-246. doi:10.5187/jast.2020.62.2.239

Cinquin, C., Le Blay, G., Fliss, I. et al. (2006). New three-stage in vitro model for infant colonic fermentation with immobilized fecal microbiota: Model for infant colon fermentation. *FEMS Microbiol Ecol 57*, 324-336. doi:10.1111/j.1574-6941.2006.00117.x

Collins, S. B., Perez-Camargo, G., Gettinby, G. et al. (2001). Development of a technique for the in vivo assessment of flatulence in dogs. *Am J Vet Res 62*, 1014-1019. doi:10.2460/ajvr.2001.62.1014

Cordonnier, C., Thévenot, J., Etienne-Mesmin, L. et al. (2015). Dynamic in vitro models of the human gastrointestinal tract as relevant tools to assess the survival of probiotic strains and their interactions with gut microbiota. *Microorganisms 3*, 725-745. doi:10.3390/microorganisms3040725

Cullen, J. J. and Kelly, K. A. (1996). Functional characteristics of canine pylorus in health, with pyloroplasty, and after pyloric reconstruction. *Dig Dis Sci 41*, 711-719. doi:10.1007/BF02213127

Cutrignelli, M. I., Bovera, F., Tudisco, R. et al. (2009). In vitro fermentation characteristics of different carbohydrate sources in two dog breeds (German shepherd and Neapolitan mastiff). *J Anim Physiol Anim Nutr 93*, 305-312. doi:10.1111/j.1439-0396.2009.00931.x

De Cuyper, A., Hesta, M., Tibosch, S. et al. (2018). How does dietary particle size affect carnivore gastrointestinal transit: A dog model. *J Anim Physiol Anim Nutr (Berl) 102*, e615-e622. doi:10.1111/jpn.12803

Déat, E., Blanquet-Diot, S., Jarrige, J.-F. et al. (2009). Combining the dynamic TNO-gastrointestinal tract system with a Caco-2 cell culture model: Application to the assessment of lycopene and alpha-tocopherol bioavailability from a whole food. *J Agric Food Chem 57*, 11314-11320. doi:10.1021/jf902392a

Defois, C., Ratel, J., Garrait, G. et al. (2018). Food chemicals disrupt human gut microbiota activity and impact intestinal homeostasis as revealed by in vitro systems. *Sci Rep 8*, 11006. doi:10.1038/s41598-018-29376-9

Deng, P. and Swanson, K. S. (2015). Gut microbiota of humans, dogs and cats: Current knowledge and future opportunities and challenges. *Br J Nutr 113*, S6-S17. doi:10.1017/S0007114514002943

Denis, S., Sayd, T., Georges, A. et al. (2016). Digestion of cooked meat proteins is slightly affected by age as assessed using the dynamic gastrointestinal TIM model and mass spectrometry. *Food Funct 7*, 2682-2691. doi:10.1039/C6FO00120C

Deschamps, C., Fournier, E., Uriot, O. et al. (2020). Comparative methods for fecal sample storage to preserve gut microbial structure and function in an in vitro model of the human colon. *Appl Microbiol Biotechnol 104*, 10233-10247. doi:10.1007/s00253-020-10959-4

Detweiler, K. B., He, F., Mangian, H. F. et al. (2019). Effects of high inclusion of soybean hulls on apparent total tract macronutrient digestibility, fecal quality, and fecal fermentative end-product concentrations in extruded diets of adult dogs. *J Anim Sci 97*, 1027-1035. doi:10.1093/jas/skz015

Donadelli, R. A., Titgemeyer, E. C. and Aldrich, C. G. (2019). Organic matter disappearance and production of short- and branched-chain fatty acids from selected fiber sources used in pet foods by a canine in vitro fermentation model. *J Anim Sci 97*, 4532-4539. doi:10.1093/jas/skz302

Dressman, J. B. (1986). Comparison of canine and human gastrointestinal physiology. *Pharm Res 3*, 123-131. doi:10.1023/A:1016353705970

Duboc, H., Rajca, S., Rainteau, D. et al. (2013). Connecting dysbiosis, bile-acid dysmetabolism and gut inflammation in inflammatory bowel diseases. *Gut 62*, 531-539. doi:10.1136/gutjnl-2012-302578

Dufourny, S., Everaert, N., Lebrun, S. et al. (2019). Baby-SPIME: A dynamic in vitro piglet model mimicking gut microbiota during the weaning process. *J Microbiol Methods 167*, 105735. doi:10.1016/j.mimet.2019.105735

Durand, A. (2010). *Entéropathies exsudatives chez le chien : Proposition d'une stratégie thérapeutique diététique et médiacale*. Université Claude Bernard.

Duysburgh, C., Ossieur, W. P., De Paepe, K. et al. (2020). Development and validation of the Simulator of the Canine Intestinal Microbial Ecosystem (SCIME). *J Anim Sci 98*, skz357. doi:10.1093/jas/skz357

Ehrlein, H.-J. and Pröve, J. (1982). Effect of viscosity of test meals on gastric emptying in dogs. *Exp Physiol 67*, 419-425. doi:10.1113/expphysiol.1982.sp002657

Eisenhauer, L., Vahjen, W., Dadi, T. et al. (2019). Effects of Brewer's spent grain and carrot pomace on digestibility, fecal microbiota, and fecal and urinary metabolites in dogs fed low- or high-protein diets. *J Anim Sci 97*, 4124-4133. doi:10.1093/jas/skz264

El Hage, R., Hernandez-Sanabria, E., Calatayud Arroyo, M. et al. (2019). Propionate-producing consortium restores antibiotic-induced dysbiosis in a dynamic in vitro model of the human intestinal microbial ecosystem. *Front Microbiol 10*, 1206. doi:10.3389/fmicb.2019.01206

Enright, E. F., Gahan, C. G. M., Joyce, S. A. et al. (2016). The impact of the gut microbiota on drug metabolism and clinical outcome. *Yale J Biol Med 89*, 375-382.

Etienne-Mesmin, L., Chassaing, B., Desvaux, M. et al. (2019). Experimental models to study intestinal microbes-mucus interactions in health and disease. *FEMS Microbiol Rev 43*, 457-489. doi:10.1093/femsre/fuz013

Farmer, A. D., Wegeberg, A.-M. L., Brock, B. et al. (2018). Regional gastrointestinal contractility parameters using the wireless motility capsule: Inter-observer reproducibility and influence of age, gender and study country. *Aliment Pharmacol Ther 47*, 391-400. doi:10.1111/apt.14438

Farquhar, M. J., McCluskey, E., Staunton, R. et al. (2018). Characterisation of a canine epithelial cell line for modelling the intestinal barrier. *Altern Lab Anim 46*, 115-132. doi:10.1177/026119291804600304

Fehlbaum, S., Chassard, C., Haug, M. C. et al. (2015). Design and investigation of PolyFermS in vitro continuous fermentation models inoculated with immobilized fecal microbiota mimicking the elderly colon. *PLoS One 10*, e0142793. doi:10.1371/journal.pone.0142793

Fitzpatrick, L. R. and Jenabzadeh, P. (2020). IBD and bile acid absorption: Focus on pre-clinical and clinical observations. *Front Physiol 11*, 564. doi:10.3389/fphys.2020.00564

Fleury, M. A., Le Goff, O., Denis, S. et al. (2017). Development and validation of a new dynamic in vitro model of the piglet colon (PigutIVM): Application to the study of probiotics. *Appl Microbiol Biotechnol 101*, 2533-2547. doi:10.1007/s00253-017-8122-y

Flickinger, E. A., Schreijen, E. M. W. C., Patil, A. R. et al. (2003). Nutrient digestibilities, microbial populations, and protein catabolites as affected by fructan supplementation of dog diets. *J Anim Sci 81*, 2008-2018. doi:10.2527/2003.8182008x

Forster, G. M., Stockman, J., Noyes, N. et al. (2018). A comparative study of serum biochemistry, metabolome and microbiome parameters of clinically healthy, normal weight, overweight, and obese companion dogs. *Top Companion Anim Med 33*, 126-135. doi:10.1053/j.tcam.2018.08.003

Freiche, V. and Hernandez, J. (2010). *Gastro-entérologie canine et féline : De la clinique à la thérapeutique*. Elsevier Masson.

Friedman, E. S., Bittinger, K., Esipova, T. V. et al. (2018). Microbes vs. chemistry in the origin of the anaerobic gut lumen. *Proc Natl Acad Sci U S A 115*, 4170-4175. doi:10.1073/pnas.1718635115

Garcia-Mazcorro, J. F., Dowd, S. E., Poulsen, J. et al. (2012). Abundance and short-term temporal variability of fecal microbiota in healthy dogs. *Microbiologyopen 1*, 340-347. doi:10.1002/mbo3.36

Garcia-Mazcorro, J. F., Minamoto, Y., Kawas, J. R. et al. (2020). Akkermansia and microbial degradation of mucus in cats and dogs: Implications to the growing worldwide epidemic of pet obesity. *Vet Sci 7*, 44. doi:10.3390/vetsci7020044

Geirnaert, A., Calatayud, M., Grootaert, C. et al. (2017). Butyrate-producing bacteria supplemented in vitro to Crohn's

disease patient microbiota increased butyrate production and enhanced intestinal epithelial barrier integrity. *Sci Rep 7*, 11450. doi:10.1038/s41598-017-11734-8

Gibson, G. R., Cummings, J. H. and Macfarlane, G. T. (1988). Use of a three-stage continuous culture system to study the effect of mucin on dissimilatory sulfate reduction and methanogenesis by mixed populations of human gut bacteria. *Applied and Environmental Microbiology 54*, 2750-2755. doi:10.1128/AEM.54.11.2750-2755.1988

Giffard, C. J., Collins, S. B., Stoodley, N. C. et al. (2001). Administration of charcoal, Yucca schidigera, and zinc acetate to reduce malodorous flatulence in dogs. *J Am Vet Med Assoc 218*, 892-896. doi:10.2460/javma.2001.218.892

Grandjean, D. and Haymann, F. (2010). *Encyclopédie du chien Royal Canin*.

Gruber, P., Rubinstein, A., Li, V. H. K. et al. (1987). Gastric emptying of nondigestible solids in the fasted dog. *J Pharm Sci 76*, 117-122. doi:10.1002/jps.2600760207

Guerra, A., Etienne-Mesmin, L., Livrelli, V. et al. (2012). Relevance and challenges in modeling human gastric and small intestinal digestion. *Trends Biotechnol 30*, 591-600. doi:10.1016/j.tibtech.2012.08.001

Guerra, A., Denis, S., Goff, O. le et al. (2016). Development and validation of a new dynamic computer-controlled model of the human stomach and small intestine. *Biotechnol Bioeng 113*, 1325-1335. doi:10.1002/bit.25890

Gupta, P. K. and Robinson, J. R. (1988). Gastric emptying of liquids in the fasted dog. *Int J Pharm 43*, 45-52. doi:10.1016/0378-5173(88)90057-9

Hamper, B. (2016). Current topics in canine and feline obesity. *Vet Clin North Am Small Anim Pract 46*, 785-795. doi:10.1016/j.cvsm.2016.04.003

Handl, S., German, A. J., Holden, S. L. et al. (2013). Faecal microbiota in lean and obese dogs. *FEMS Microbiol Ecol 84*, 332-343. doi:10.1111/1574-6941.12067

Hernot, D. C., Biourge, V. C., Martin, L. J. et al. (2005). Relationship between total transit time and faecal quality in adult dogs differing in body size. *J Anim Physiol Anim Nutr 89*, 189-193. doi:10.1111/j.1439-0396.2005.00544.x

Hervera, M., Baucells, M. D., Blanch, F. et al. (2007). Prediction of digestible energy content of extruded dog food by in vitro analyses. *J Anim Physiol Anim Nutr (Berl) 91*, 205-209. doi:10.1111/j.1439-0396.2007.00693.x

Hinder, R. A. and Kelly, K. A. (1977). Canine gastric emptying of solids and liquids. *Am J Physiol Endocrinol Metab 233*, E335. doi:10.1152/ajpendo.1977.233.4.E335

Hooda, S., Minamoto, Y., Suchodolski, J. S. et al. (2012). Current state of knowledge: The canine gastrointestinal microbiome. *Anim Health Res Rev 13*, 78-88. doi:10.1017/S1466252312000059

Hornof, W. J., Koblik, P. D., Strombeck, D. R. et al. (1989). Scintigraphic evaluation of solid-phase gastric emptying in the dog. *Veterinary Radiology 30*, 242-248. doi:10.1111/j.1740-8261.1989.tb01794.x

Iacopetti, I., Perazzi, A., Badon, T. et al. (2017). Salivary pH, calcium, phosphorus and selected enzymes in healthy dogs: A pilot study. *BMC Vet Res 13*, 330. doi:10.1186/s12917-017-1256-4

Junginger, J., Lemensieck, F., Moore, P. F. et al. (2014). Canine gut dendritic cells in the steady state and in inflammatory bowel disease. *Innate Immun 20*, 145-160. doi:10.1177/1753425913485475

Kakimoto, T., Kanemoto, H., Fukushima, K. et al. (2017). Effect of a high-fat-high-cholesterol diet on gallbladder bile acid composition and gallbladder motility in dogs. *Am J Vet Res 78*, 1406-1413. doi:10.2460/ajvr.78.12.1406

Kalantzi, L., Persson, E., Polentarutti, B. et al. (2006). Canine intestinal contents vs. simulated media for the assessment of solubility of two weak bases in the human small intestinal contents. *Pharm Res 23*, 1373-1381. doi:10.1007/s11095-006-0207-8

Kararli, T. T. (1995). Comparison of the gastrointestinal anatomy, physiology, and biochemistry of humans and commonly used laboratory animals. *Biopharm Drug Dispos 16*, 351-380. doi:10.1002/bdd.2510160502

Kendall, P. T., Blaza, S. E. and Smith, P. M. (1983). Influence of level of intake and dog size on apparent digestibility of dog foods. *Br Vet J 139*, 361-362. doi:10.1016/s0007-1935(17)30442-6

Kienzle, E. (1988). Enzymaktivität in Pancreas, Darmwand und Chymus des Hundes in Abhängigkeit von Alter und Futterart. (Enzyme activity in pancreatic tissue, intestinal mucosa and chyme of dogs in relation to age and diet). *J Anim Physiol Anim Nutr 60*, 276-288. doi:10.1111/j.1439-0396.1988.tb00203.x

Kim, H., Jung, A. H., Park, S. H. et al. (2021). In vitro protein disappearance of raw chicken as dog foods decreased by thermal processing, but was unaffected by non-thermal processing. *Animals (Basel) 11*, 1256. doi:10.3390/ani11051256

Kong, F. and Singh, R. P. (2010). A human gastric simulator (HGS) to study food digestion in human stomach. *J Food Sci 75*, E627-635. doi:10.1111/j.1750-3841.2010.01856.x

Koziolek, M., Grimm, M., Bollmann, T. et al. (2019). Characterization of the GI transit conditions in Beagle dogs with a telemetric motility capsule. *Eur J Pharm Biopharm 136*, 221-230. doi:10.1016/j.ejpb.2019.01.026

Kramer, N., Pratscher, B., Meneses, A. M. C. et al. (2020). Generation of differentiating and long-living intestinal organoids reflecting the cellular diversity of canine intestine. *Cells 9*, 822. doi:10.3390/cells9040822

Kubbinga, M., Augustijns, P., García, M. A. et al. (2019). The effect of chitosan on the bioaccessibility and intestinal permeability of acyclovir. *Eur J Pharm Biopharm 136*, 147-155. doi:10.1016/j.ejpb.2019.01.021

Larcheveque, S. (2019). *Etat des connaissances sur la mucocèle biliaire chez le chien : Étude bibliographique*. Faculté de Médecine de Créteil.

Lavy, E., Goldberger, D., Friedman, M. et al. (2012). pH values and mineral content of saliva in different breeds of dogs. *Isr J Vet Med 67*, 244-2448.

Lee, C.-M., Luner, P. E., Locke, K. et al. (2017). Application of an artificial stomach-duodenum reduced gastric pH dog

model for formulation principle assessment and mechanistic performance understanding. *J Pharm Sci 106*, 1987-1997. doi:10.1016/j.xphs.2017.02.015

Li, Y., Fortner, L. and Kong, F. (2019). Development of a gastric simulation model (GSM) incorporating gastric geometry and peristalsis for food digestion study. *Food Res Int 125*, 108598. doi:10.1016/j.foodres.2019.108598

Lui, C. Y., Amidon, G. L., Berardi, R. R. et al. (1986). Comparison of gastrointestinal pH in dogs and humans: Implications on the use of the beagle dog as a model for oral absorption in humans. *J Pharm Sci 75*, 271-274. doi:10.1002/jps.2600750313

Lyng, E., Havenaar, R., Shastri, P. et al. (2016). Increased bioavailability of celecoxib under fed versus fasted conditions is determined by postprandial bile secretion as demonstrated in a dynamic gastrointestinal model. *Drug Dev Ind Pharm 42*, 1334-1339. doi:10.3109/03639045.2015.1135935

Mahar, K. M., Portelli, S., Coatney, R. et al. (2012). Gastric pH and gastric residence time in fasted and fed conscious Beagle dogs using the Bravo® pH system. *J Pharm Sci 101*, 2439-2448. doi:10.1002/jps.23159

Malewska, K., Rychlik, A., Nieradka, R. et al. (2011). Treatment of inflammatory bowel disease (IBD) in dogs and cats. *Pol J Vet Sci 14*, 165-171. doi:10.2478/v10181-011-0026-7

Manchester, A. C., Webb, C. B., Blake, A. B. et al. (2019). Long-term impact of tylosin on fecal microbiota and fecal bile acids of healthy dogs. *J Vet Intern Med 33*, 2605-2617. doi:10.1111/jvim.15635

Martinez, M. (2002). Applying the biopharmaceutics classification system to veterinary pharmaceutical products Part II. Physiological considerations. *Adv Drug Deliv Rev 54*, 825-850. doi:10.1016/S0169-409X(02)00071-6

Marzorati, M., Vanhoecke, B., De Ryck, T. et al. (2014). The HMI™ module: A new tool to study the host-microbiota interaction in the human gastrointestinal tract in vitro. *BMC Microbiol 14*, 133. doi:10.1186/1471-2180-14-133

Ménard, O., Picque, D. and Dupont, D. (2015). The DIDGI® System. In K. Verhoeckx, P. Cotter, I. López-Expósito et al. (eds.), *The Impact of Food Bioactives on Health: In Vitro and Ex Vivo Models*. Cham, Switzerland: Springer.

Mentula, S., Harmoinen, J., Heikkilä, M. et al. (2005). Comparison between cultured small-intestinal and fecal microbiotas in beagle dogs. *Appl Environ Microbiol 71*, 4169-4175. doi:10.1128/AEM.71.8.4169-4175.2005

Meunier, J. P., Manzanilla, E. G., Anguita, M. et al. (2008). Evaluation of a dynamic in vitro model to simulate the porcine ileal digestion of diets differing in carbohydrate composition. *J Anim Sci 86*, 1156-1163. doi:10.2527/jas.2007-0145

Meyer, J. H., Dressman, J., Fink, A. et al. (1985). Effect of size and density on canine gastric emptying of nondigestible solids. *Gastroenterology 89*, 805-813. doi:10.1016/0016-5085(85)90576-1

Meyer, J. H., Elashoff, J., Porter-Fink, V. et al. (1988). Human postprandial gastric emptying of 1-3-millimeter spheres. *Gastroenterology 94*, 1315-1325. doi:10.1016/0016-5085(88)90669-5

Minamoto, Y., Otoni, C. C., Steelman, S. M. et al. (2015). Alteration of the fecal microbiota and serum metabolite profiles in dogs with idiopathic inflammatory bowel disease. *Gut Microbes 6*, 33-47. doi:10.1080/19490976.2014.997612

Minekus, M., Marteau, P., Havenaar, R. et al. (1995). A multicompartmental dynamic computer-controlled model simulating the stomach and small intestine. *Altern Lab Anim 23*, 197-209. doi:10.1177/026119299502300205

Minekus, M., Alminger, M., Alvito, P. et al. (2014). A standardised static in vitro digestion method suitable for food – An international consensus. *Food Funct 5*, 1113-1124. doi:10.1039/c3fo60702j

Molly, K., Vande Woestyne, M. and Verstraete, W. (1993). Development of a 5-step multi-chamber reactor as a simulation of the human intestinal microbial ecosystem. *Appl Microbiol Biotechnol 39*, 254-258. doi:10.1007/bf00228615

Mondo, E., Marliani, G., Accorsi, P. A. et al. (2019). Role of gut microbiota in dog and cat's health and diseases. *Open Vet J 9*, 253-258. doi:10.4314/ovj.v9i3.10

Moon, C. D., Young, W., Maclean, P. H. et al. (2018). Metagenomic insights into the roles of Proteobacteria in the gastrointestinal microbiomes of healthy dogs and cats. *MicrobiologyOpen 7*, e00677. doi:10.1002/mbo3.677

Morris, J. G. and Rogers, G. R. (1989). Comparative aspects of nutrition and metabolism of dogs and cats. In H. Burger and J. P. W. Rivers (eds.), *Nutrition of the Dog and Cat* (35-66). Cambridge, UK: Cambridge University Press.

Musco, N., Calabrò, S., Roberti, F. et al. (2018). In vitro evaluation of Saccharomyces cerevisiae cell wall fermentability using a dog model. *J Anim Physiol Anim Nutr (Berl) 102, Suppl 1*, 24-30. doi:10.1111/jpn.12864

Nagahara, T., Ohno, K., Kanemoto, H. et al. (2018). Effect of prednisolone administration on gallbladder emptying rate and gallbladder bile composition in dogs. *Am J Vet Res 79*, 1050-1056. doi:10.2460/ajvr.79.10.1050

Nakayama, F. (1969). Composition of gallstone and bile: Species difference. *J Lab Clin Med 73*, 623-630.

Niina, A., Kibe, R., Suzuki, R. et al. (2019). Improvement in clinical symptoms and fecal microbiome after fecal microbiota transplantation in a dog with inflammatory bowel disease. *Vet Med (Auckl) 10*, 197-201. doi:10.2147/VMRR.S230862

Nogueira, J. P. D. S., He, F., Mangian, H. F. et al. (2019). Dietary supplementation of a fiber-prebiotic and saccharin-eugenol blend in extruded diets fed to dogs. *J Anim Sci 97*, 4519-4531. doi:10.1093/jas/skz293

Oba, P. M., Vidal, S., Wyss, R. et al. (2020). Effect of a novel animal milk oligosaccharide biosimilar on the gut microbial communities and metabolites of in vitro incubations using feline and canine fecal inocula. *J Anim Sci 98*, skaa273. doi:10.1093/jas/skaa273

OECD (2018). Guidance Document on Good In Vitro Method Practices (GIVIMP). *OECD Series on Testing and Assessment, No. 286*. OECD Publishing, Paris. doi:10.1787/9789264304796-en

Ogué-Bon, E., Khoo, C., McCartney, A. L. et al. (2010). In vitro effects of synbiotic fermentation on the canine faecal microbiota. *FEMS Microbiol Ecol 73*, 587-600. doi:10.1111/j.1574-

6941.2010.00915.x

Ogué-Bon, E., Khoo, C., Hoyles, L. et al. (2011). In vitro fermentation of rice bran combined with Lactobacillus acidophilus 14 150B or Bifidobacterium longum 05 by the canine faecal microbiota. *FEMS Microbiol Ecol 75*, 365-376. doi:10.1111/j.1574-6941.2010.01014.x

Osto, M. and Lutz, T. A. (2015). Translational value of animal models of obesity – Focus on dogs and cats. *Eur J Pharmacol 759*, 240-252. doi:10.1016/j.ejphar.2015.03.036

Oswald, H., Sharkey, M., Pade, D. et al. (2015). Canine gastrointestinal physiology: Breeds variations that can influence drug absorption. *Eur J Pharm Biopharm 97*, 192-203. doi:10.1016/j.ejpb.2015.09.009

Palerme, J.-S., Silverstone, A., Riedesel, E. A. et al. (2020). A pilot study on the effect of fat loading on the gastrointestinal tract of healthy dogs. *J Small Anim Pract 61*, 732-737. doi:10.1111/jsap.13216

Panasevich, M. R., Rossoni Serao, M. C., de Godoy, M. R. C. et al. (2013). Potato fiber as a dietary fiber source in dog foods. *J Anim Sci 91*, 5344-5352. doi:10.2527/jas.2013-6842

Panasevich, M. R., Kerr, K. R., Serao, M. C. R. et al. (2015). Evaluation of soluble corn fiber on chemical composition and nitrogen-corrected true metabolizable energy and its effects on in vitro fermentation and in vivo responses in dogs. *J Anim Sci 93*, 2191-2200. doi:10.2527/jas.2014-8425

Park, H.-J., Lee, S.-E., Kim, H.-B. et al. (2015). Association of obesity with serum leptin, adiponectin, and serotonin and gut microflora in beagle dogs. *J Vet Intern Med 29*, 43-50. doi:10.1111/jvim.12455

Payne, A. N., Zihler, A., Chassard, C. et al. (2012). Advances and perspectives in in vitro human gut fermentation modeling. *Trends Biotechnol 30*, 17-25. doi:10.1016/j.tibtech.2011.06.011

Penazzi, L., Schiavone, A., Russo, N. et al. (2021). In vivo and in vitro digestibility of an extruded complete dog food containing black soldier fly (Hermetia illucens) larvae meal as protein source. *Front Vet Sci 8*, 653411. doi:10.3389/fvets.2021.653411

Pereira, G. Q., Gomes, L. A., Santos, I. S. et al. (2018). Fecal microbiota transplantation in puppies with canine parvovirus infection. *J Vet Intern Med 32*, 707-711. doi:10.1111/jvim.15072

Phillips-Donaldson, D. (2019). Global pet food sales hit $91 billion in 2018. *Petfoodindustry.com*. https://www.petfoodindustry.com/articles/7899-global-pet-food-sales-hit-91-billion-in-2018

Pilla, R. and Suchodolski, J. S. (2020). The role of the canine gut microbiome and metabolome in health and gastrointestinal disease. *Front Vet Sci 6*, 498. doi:10.3389/fvets.2019.00498

Propst, E. L., Flickinger, E. A., Bauer, L. L. et al. (2003). A dose-response experiment evaluating the effects of oligofructose and inulin on nutrient digestibility, stool quality, and fecal protein catabolites in healthy adult dogs. *J Anim Sci 81*, 3057-3066. doi:10.2527/2003.81123057x

Raffan, E., Dennis, R. J., O'Donovan, C. J. et al. (2016). A deletion in the canine POMC gene is associated with weight and appetite in obesity-prone labrador retriever dogs. *Cell Metab 23*, 893-900. doi:10.1016/j.cmet.2016.04.012

Rahat-Rozenbloom, S., Fernandes, J., Gloor, G. B. et al. (2014). Evidence for greater production of colonic short-chain fatty acids in overweight than lean humans. *Int J Obes 38*, 1525-1531. doi:10.1038/ijo.2014.46

Rana, S. V., Sharma, S., Malik, A. et al. (2013). Small intestinal bacterial overgrowth and orocecal transit time in patients of inflammatory bowel disease. *Dig Dis Sci 58*, 2594-2598. doi:10.1007/s10620-013-2694-x

Ricci, R., Perazzi, A., Badon, T. et al. (2018). Effect of storage on long-term stability of salivary α-amylase, lysozyme, lactate dehydrogenase, calcium and phosphorus in dogs. *Vet J 242*, 44-47. doi:10.1016/j.tvjl.2018.10.006

Ridlon, J. M., Kang, D. J., Hylemon, P. B. et al. (2014). Bile acids and the gut microbiome. *Curr Opin Gastroenterol 30*, 332-338. doi:10.1097/MOG.0000000000000057

Robin, A. (2007). *Les enterpathies exudatives chez le chien : Actualités, diagnostiques et analyse retrospective de series de cas cliniques*. Lyon, France: Université Claude Bernard.

Roussel, C., Cordonnier, C., Galia, W. et al. (2016). Increased EHEC survival and virulence gene expression indicate an enhanced pathogenicity upon simulated pediatric gastrointestinal conditions. *Pediatr Res 80*, 734-743. doi:10.1038/pr.2016.144

Roussel, C., De Paepe, K., Galia, W. et al. (2020). Spatial and temporal modulation of enterotoxigenic E. coli H10407 pathogenesis and interplay with microbiota in human gut models. *BMC Biol 18*, 141. doi:10.1186/s12915-020-00860-x

Russel, W. M. S. and Burch, R. L. (1959). *The Principles of Humane Experimental Technique*. https://caat.jhsph.edu/principles/the-principles-of-humane-experimental-technique

Sagawa, K., Li, F., Liese, R. et al. (2009). Fed and fasted gastric pH and gastric residence time in conscious beagle dogs. *J Pharm Sci 98*, 2494-2500. doi:10.1002/jps.21602

Salas-Mani, A., Jeusette, I., Castillo, I. et al. (2018). Fecal microbiota composition changes after a BW loss diet in Beagle dogs. *J Anim Sci 96*, 3102-3111. doi:10.1093/jas/sky193

Sams, L., Paume, J., Giallo, J. et al. (2016). Relevant pH and lipase for in vitro models of gastric digestion. *Food Funct 7*, 30-45. doi:10.1039/C5FO00930H

Scarsella, E., Stefanon, B., Cintio, M. et al. (2020). Learning maa chine approach reveals microbial signatures of diet and sex in dog. *PLoS One 15*, e0237874. doi:10.1371/journal.pone.0237874

Schmidt, M., Unterer, S., Suchodolski, J. S. et al. (2018). The fecal microbiome and metabolome differs between dogs fed bones and raw food (BARF) diets and dogs fed commercial diets. *PLoS One 13*, e0201279. doi:10.1371/journal.pone.0201279

Schwizer, W., Steingötter, A., Fox, M. et al. (2002). Non-invasive measurement of gastric accommodation in humans. *Gut 51, Suppl 1*, i59-62. doi:10.1136/gut.51.suppl_1.i59

Shinchi, H., Takao, S., Fukura, K. et al. (1996). Gastric acid secretion and gastroduodenal pH after pancreaticogastrostomy in dogs. *J Surg Res 61*, 152-158. doi:10.1006/jsre.1996.0097

Simon, M. (2019). *L'anxiété chez le chien, les répercussions sur le microbiote intestinal : Intérêt de l'utilisation des probiotiques dans la prise en charge thérapeutique.* Toulouse, France: Ecole Nationale Vétérinaire de Toulouse. https://oatao.univ-toulouse.fr/25833/

Simpson, K. W., Dogan, B., Rishniw, M. et al. (2006). Adherent and invasive Escherichia coli is associated with granulomatous colitis in boxer dogs. *Infect Immun 74*, 4778-4792. doi:10.1128/IAI.00067-06

Sjögren, E., Abrahamsson, B., Augustijns, P. et al. (2014). In vivo methods for drug absorption – Comparative physiologies, model selection, correlations with in vitro methods (IVIVC), and applications for formulation/API/excipient characterization including food effects. *Eur J Pharm Sci 57*, 99-151. doi:10.1016/j.ejps.2014.02.010

Smeets-Peeters, M., Watson, T., Minekus, M. et al. (1998). A review of the physiology of the canine digestive tract related to the development of in vitro systems. *Nutr Res Rev 11*, 45-69. doi:10.1079/NRR19980005

Smeets-Peeters, M. J., Minekus, M., Havenaar, R. et al. (1999). Description of a dynamic in vitro model of the dog gastrointestinal tract and an evaluation of various transit times for protein and calcium. *Altern Lab Anim 27*, 935-949. doi:10.1177/026119299902700608

Smeets-Peeters, M. (2000). *Feeding FIDO: Development, validation and application of a dynamic, in vitro model of the gastrointestinal tract of the dog*. Wageningen University. Dissertation. https://www.wur.nl/nl/Publicatie-details.htm?publicationId=publication-way-3635343534

Smith, H. W. (1965). Observations on the flora of the alimentary tract of animals and factors affecting its composition. *J Pathol 89*, 95-122. doi:10.1002/path.1700890112

Souliman, S., Blanquet, S., Beyssac, E. et al. (2006). A level A in vitro/in vivo correlation in fasted and fed states using different methods: Applied to solid immediate release oral dosage form. *Eur J Pharm Sci 27*, 72-79. doi:10.1016/j.ejps.2005.08.006

Suchodolski, J. S., Camacho, J. and Steiner, J. M. (2008). Analysis of bacterial diversity in the canine duodenum, jejunum, ileum, and colon by comparative 16S rRNA gene analysis. *FEMS Microbiol Ecol 66*, 567-578. doi:10.1111/j.1574-6941.2008.00521.x

Suchodolski, J. S., Dowd, S. E., Westermarck, E. et al. (2009). The effect of the macrolide antibiotic tylosin on microbial diversity in the canine small intestine as demonstrated by massive parallel 16S rRNA gene sequencing. *BMC Microbiol 9*, 210. doi:10.1186/1471-2180-9-210

Suchodolski, J. S., Xenoulis, P. G., Paddock, C. G. et al. (2010). Molecular analysis of the bacterial microbiota in duodenal biopsies from dogs with idiopathic inflammatory bowel disease. *Vet Microbiol 142*, 394-400. doi:10.1016/j.vetmic.2009.11.002

Suchodolski, J. S. (2011). Companion animals symposium: Microbes and gastrointestinal health of dogs and cats. *J Anim Sci 89*, 1520-1530. doi:10.2527/jas.2010-3377

Suchodolski, J. S., Dowd, S. E., Wilke, V. et al. (2012a). 16S rRNA gene pyrosequencing reveals bacterial dysbiosis in the duodenum of dogs with idiopathic inflammatory bowel disease. *PLoS One 7*, e39333. doi:10.1371/journal.pone.0039333

Suchodolski, J. S., Markel, M. E., Garcia-Mazcorro, J. F. et al. (2012b). The fecal microbiome in dogs with acute diarrhea and idiopathic inflammatory bowel disease. *PLoS One 7*, e51907. doi:10.1371/journal.pone.0051907

Sunvold, G. D., Fahey, G. C., Merchen, N. R. et al. (1995a). In vitro fermentation of selected fibrous substrates by dog and cat fecal inoculum: Influence of diet composition on substrate organic matter disappearance and short-chain fatty acid production. *J Anim Sci 73*, 1110-1122. doi:10.2527/1995.7341110x

Sunvold, G. D., Hussein, H. S., Fahey, G. C. et al. (1995b). In vitro fermentation of cellulose, beet pulp, citrus pulp, and citrus pectin using fecal inoculum from cats, dogs, horses, humans, and pigs and ruminal fluid from cattle. *J Anim Sci 73*, 3639-3648. doi:10.2527/1995.73123639x

Sunvold, G. D., Fahey, G. C., Merchen, N. R. et al. (1995c). Dietary fiber for dogs: IV. In vitro fermentation of selected fiber sources by dog fecal inoculum and in vivo digestion and metabolism of fiber-supplemented diets. *J Anim Sci 73*, 1099-1109. doi:10.2527/1995.7341099x

Swanson, K. S., Dowd, S. E., Suchodolski, J. S. et al. (2011). Phylogenetic and gene-centric metagenomics of the canine intestinal microbiome reveals similarities with humans and mice. *ISME J 5*, 639-649. doi:10.1038/ismej.2010.162

Tanner, S. A., Zihler Berner, A., Rigozzi, E. et al. (2014). In vitro continuous fermentation model (PolyFermS) of the swine proximal colon for simultaneous testing on the same gut microbiota. *PLoS One 9*, e94123. doi:10.1371/journal.pone.0094123

Thakare, R., Alamoudi, J. A., Gautam, N. et al. (2018a). Species differences in bile acids I. Plasma and urine bile acid composition. *J Appl Toxicol 38*, 1323-1335. doi:10.1002/jat.3644

Thakare, R., Alamoudi, J. A., Gautam, N. et al. (2018b). Species differences in bile acids II. Bile acid metabolism. *J Appl Toxicol 38*, 1336-1352. doi:10.1002/jat.3645

Theodorakis, M. C. (1980). External scintigraphy in measuring rate of gastric emptying in beagles. *Am J Physiol 239*, G39-43. doi:10.1152/ajpgi.1980.239.1.G39

Thuenemann, E. C., Mandalari, G., Rich, G. T. et al. (2015). Dynamic gastric model (DGM). In K. Verhoeckx, P. Cotter, I. López-Expósito et al. (eds.), *The Impact of Food Bioactives on Health: In Vitro and Ex Vivo Models*. Cham, Switzerland: Springer.

Tompkins, T. A., Mainville, I. and Arcand, Y. (2011). The impact of meals on a probiotic during transit through a model of the human upper gastrointestinal tract. *Benef Microbes 2*, 295-303. doi:10.3920/BM2011.0022

Traughber, Z. T., He, F., Hoke, J. M. et al. (2020). Chemical composition and in vitro fermentation characteristics of legumes using canine fecal inoculum. *Transl Anim Sci 4*, txaa200. doi:10.1093/tas/txaa200

Tvarijonaviciute, A., Ceron, J. J., Holden, S. L. et al. (2012). Obesity-related metabolic dysfunction in dogs: A comparison with human metabolic syndrome. *BMC Vet Res 8*, 147.

doi:10.1186/1746-6148-8-147

Tzortzis, G., Goulas, A. K., Baillon, M.-L. A. et al. (2004). In vitro evaluation of the fermentation properties of galactooligosaccharides synthesised by alpha-galactosidase from Lactobacillus reuteri. *Appl Microbiol Biotechnol 64*, 106-111. doi:10.1007/s00253-003-1427-z

Van de Wiele, T., Van den Abbeele, P., Ossieur, W. et al. (2015). The simulator of the human intestinal microbial ecosystem (SHIME®). In K. Verhoeckx, P. Cotter, I. López-Expósito et al. (eds.), *The Impact of Food Bioactives on Health: In Vitro and Ex Vivo Models*. Cham, Switzerland: Springer.

Van den Abbeele, P., Grootaert, C., Possemiers, S. et al. (2009). In vitro model to study the modulation of the mucin-adhered bacterial community. *Appl Microbiol Biotechnol 83*, 349-359. doi:10.1007/s00253-009-1947-2

Van den Abbeele, P., Taminiau, B., Pinheiro, I. et al. (2018). Arabinoxylo-oligosaccharides and inulin impact inter-individual variation on microbial metabolism and composition, which immunomodulates human cells. *J Agric Food Chem 66*, 1121-1130. doi:10.1021/acs.jafc.7b04611

Van den Abbeele, P., Moens, F., Pignataro, G. et al. (2020a). Yeast-derived formulations are differentially fermented by the canine and feline microbiome as assessed in a novel in vitro colonic fermentation model. *J Agric Food Chem 68*, 13102-13110. doi:10.1021/acs.jafc.9b05085

Van den Abbeele, P., Duysburgh, C., Rakebrandt, M. et al. (2020b). Dried yeast cell walls high in beta-glucan and mannan-oligosaccharides positively affect microbial composition and activity in the canine gastrointestinal tract in vitro. *J Anim Sci 98*, skaa173. doi:10.1093/jas/skaa173

van Zelst, M., Hesta, M., Alexander, L. G. et al. (2015). In vitro selenium accessibility in pet foods is affected by diet composition and type. *Br J Nutr 113*, 1888-1894. doi:10.1017/S0007114515001324

Verdier, C., Denis, S., Gasc, C. et al. (2021). An oral FMT capsule as efficient as an enema for microbiota reconstruction following disruption by antibiotics, as assessed in an in vitro human gut model. *Microorganisms 9*, 358. doi:10.3390/microorganisms9020358

Verstrepen, L., Van den Abbeele, P., Pignataro, G. et al. (2021). Inclusion of small intestinal absorption and simulated mucosal surfaces further improve the mucosal simulator of the canine intestinal microbial ecosystem (M-SCIME™). *Res Vet Sci 140*, 100-108. doi:10.1016/j.rvsc.2021.08.011

Vierbaum, L., Eisenhauer, L., Vahjen, W. et al. (2019). In vitro evaluation of the effects of Yucca schidigera and inulin on the fermentation potential of the faecal microbiota of dogs fed diets with low or high protein concentrations. *Arch Anim Nutr 73*, 399-413. doi:10.1080/1745039X.2019.1616498

Wang, W.-X., Yan, G.-Z., Sun, F. et al. (2005). A non-invasive method for gastrointestinal parameter monitoring. *World J Gastroenterol 11*, 521-524. doi:10.3748/wjg.v11.i4.521

Warrit, K., Boscan, P., Ferguson, L. E. et al. (2017). Minimally invasive wireless motility capsule to study canine gastrointestinal motility and pH. *Vet J 227*, 36-41. doi:10.1016/j.tvjl.2017.08.005

Washizu, T., Ishida, T., Washizu, M. et al. (1994). Changes in bile acid composition of serum and gallbladder bile in bile duct ligated dogs. *J Vet Med Sci 56*, 299-303. doi:10.1292/jvms.56.299

Weber, M. (2006). Influence of size on the dog's digestive function. *Bul de l'Ac Vét de France*, 327. doi:10.4267/2042/47851

Weber, M. P., Biourge, V. C. and Nguyen, P. G. (2017). Digestive sensitivity varies according to size of dogs: A review. *J Anim Physiol Anim Nutr (Berl) 101*, 1-9. doi:10.1111/jpn.12507

Williams, B. A., Bosch, M. W., Boer, H. et al. (2005). An in vitro batch culture method to assess potential fermentability of feed ingredients for monogastric diets. *Anim Feed Sci Technol 123-124*, 445-462. doi:10.1016/j.anifeedsci.2005.04.031

Xenoulis, P. G., Palculict, B., Allenspach, K. et al. (2008). Molecular-phylogenetic characterization of microbial communities imbalances in the small intestine of dogs with inflammatory bowel disease. *FEMS Microbiol Ecol 66*, 579-589. doi:10.1111/j.1574-6941.2008.00556.x

Xu, J., Verbrugghe, A., Lourenço, M. et al. (2016). Does canine inflammatory bowel disease influence gut microbial profile and host metabolism? *BMC Vet Res 12*, 114. doi:10.1186/s12917-016-0736-2

Xu, J., Verbrugghe, A., Lourenço, M. et al. (2017). The response of canine faecal microbiota to increased dietary protein is influenced by body condition. *BMC Vet Res 13*, 374. doi:10.1186/s12917-017-1276-0

You, I. and Kim, M. J. (2021). Comparison of gut microbiota of 96 healthy dogs by individual traits: Breed, age, and body condition score. *Animals 11*, 2432. doi:10.3390/ani11082432

Zeng, R., Zhang, Y. and Du, P. (2014). The SNPs of melanocortin 4 receptor (MC4R) associated with body weight in beagle dogs. *Exp Anim 63*, 73-78. doi:10.1538/expanim.63.73

Zentek, J. and Meyer, H. (1995). Normal handling of diets – Are all dogs created equal? *J Small Anim Pract 36*, 354-359. doi:10.1111/j.1748-5827.1995.tb02949.x

Zhang, Y., Jeon, M., Rich, L. J. et al. (2014). Non-invasive multimodal functional imaging of the intestine with frozen micellar naphthalocyanines. *Nat Nanotechnol 9*, 631-638. doi:10.1038/nnano.2014.130

Conflict of interest

The authors have no conflict of interest.

Appendix 3 – Review in International Journal of Biological Sciences

DESCHAMPS, C., HUMBERT, D., ZENTEK, J., DENIS, S., PRIYMENKO, N., APPER, E. & BLANQUET-DIOT, S. (**2022**) From Chihuahua to Saint-Bernard: how did digestion and microbiota evolve with dog sizes. *International Journal of Biological Sciences* **18**, 5086–5102. Ivyspring International Publisher. https://doi.org/10.7150/ijbs.72770

IVYSPRING INTERNATIONAL PUBLISHER

International Journal of Biological Sciences

2022; 18(13): 5086-5102. doi: 10.7150/ijbs.72770

Review

From Chihuahua to Saint-Bernard: how did digestion and microbiota evolve with dog sizes

Charlotte Deschamps[1,2], Delphine Humbert[3], Jürgen Zentek[4], Sylvain Denis[1], Nathalie Priymenko[5], Emmanuelle Apper[2], Stéphanie Blanquet-Diot[1]✉

1. Université Clermont Auvergne, UMR 454 MEDIS UCA-INRAE, Clermont-Ferrand, France
2. Lallemand Animal Nutrition, Blagnac, France
3. Dômes Pharma, Pont-du-Château, France
4. Institute of Animal Nutrition, Freie Universität Berlin, Königin-Luise-Strasse 49, Berlin, Germany
5. Toxalim (Research Center in Food Toxicology), University of Toulouse, INRAE, ENVT, INP-Purpan, UPS, Toulouse, France

✉ Corresponding author: Stéphanie Blanquet-Diot, UMR 454 MEDIS, University Clermont Auvergne, INRAe, 28 place Henri Dunant, 63000 Clermont-Ferrand, France. (+33473178390; stephanie.blanquet@uca.fr)

Received: 2022.03.10; Accepted: 2022.07.17; Published: 2022.08.01

Abstract

Health and well-being of dogs are of paramount importance to their owners. Digestion plays a key role in dog health, involving physicochemical, mechanical and microbial actors. However, decades of breeding selection led to various dog sizes associated with different digestive physiology and disease sensitivity. Developing new products requires the consideration of all the multi-faceted aspects of canine digestion, the evaluation of food digestibility, drug release and absorption in the gut. This review paper provides an exhaustive literature survey on canine digestive physiology, focusing on size effect on anatomy and digestive parameters, with graphical representation of data classified as "small", "medium" and "large" dogs. Despite the huge variability between protocols and animals, interesting size effects on gastrointestinal physiology were highlighted, mainly related to the colonic compartment. Colonic measurements, transit time permeability, fibre degradation, faecal short-chain fatty acid concentration and faecal water content increase while faecal bile acid concentration decreases with body size. A negative correlation between body weight and *Proteobacteria* relative abundance was observed suggesting an effect of dog body size on faecal microbiota. This paper gathers helpful *in* vivo data for academics and industrials and supports the development of new food and pharma products to move towards canine personalized nutrition and health.

Key words: canine, digestive physiology, gut microbiota, petfood, veterinary products

Introduction

Canis lupus familiaris, also known as the domesticated dogs, belong to the *Canidae* family like the grey wolf (*Canis lupus*) and the dingo, a domestic dog returned to the wild. Descending from the grey wolf, dogs might have been the first animal domesticated by humans around 20.000 to 40.000 years ago [1]. Dogs were initially strict carnivores, but during the agricultural revolution they probably acquired the ability to digest starch and became facultative carnivores. Genes playing key roles in starch digestion (i.e. encoding for pancreatic amylase, membrane-bound intestinal maltase-glucoamylase and gene involved in glucose uptake) were selected during dog domestication [2]. Depending on their usefulness for humans, the *Canis lupus familiaris* subspecies have differentiated slowly, with the development of new canine species designated for specific tasks, such as herd protection (Mastiff), hunting (Pointer), cold hardiness (Siberian husky) or companion (Pekinese). Nowadays, the canine species includes approximatively 400 breeds with high size variability and weight ranging from 1 kg for a Chihuahua to 100 kg for a Saint-Bernard [3]. Dogs now occupy a full place in many families. Their health and well-being are therefore of paramount importance to their owners, to the extent that 7 % of

French dogs have their own health insurance against 30 % of dogs homed in the United Kingdom and 80 % of dogs homed in Sweden (SantéVet/Ipsos, 2018). Digestion, a complex process involving many physicochemical, mechanical, and microbial mechanisms, is a key parameter in dog health. In particular, gut microbiota and its involvement in canine nutrition and health have increasingly been studied during the last decade. Developing new food or pharma products needs to consider all these multi-faceted aspects of canine digestion, to answer important questions such as food digestibility, micronutrient bioaccessibility, probiotic survival and activity, or drug release and absorption in the gut. Petfood manufacturers and veterinary companies aim to develop personalized ranges adapted to size (e.g. long-term growth of large breeds puppies, poor digestive tolerance and gastric dilatation volvulus for large dogs) or to address certain breed predispositions such as obesity in Labrador Retrievers or enteropathies in Terriers [4–7]. Nevertheless, the impact of dog size or breed on digestive parameters remains poorly described despite its full interest in canine nutrition and health.

This review paper provides for the first time an exhaustive survey of the literature on the impact of body size on dog's digestive physiology, in the entire gut from mouth to colon and feces, by gathering digestive anatomy, physicochemical parameters and gut microbiota variations. Relevant studies were identified, and information extracted regarding involved dogs (i.e. number of dogs, age, weight, breed, sex, reproduction state, living environment), nutrition (i.e. food type, feeding frequency, food's principal components) and analysis methods. Only *in vivo* studies on healthy adult dogs, fed with dry food or ingesting water were included. Here, canine body sizes were classified into three groups: "small" under 10 kg, "medium" between 10-30 kg and "large" up to 30 kg according to usual practice of main petfood suppliers. Then, the selected data were analyzed according to dog sizes and clarified through graphical representations to highlight a potential size effect on digestive parameters.

General observations of canine digestion and associated organs

External morphological differences observed between extreme dog sizes such as Chihuahua and Saint-Bernard obviously reveal internal anatomical modifications. The canine mature digestive tract length can represent 2.8 % to 7 % of the total body weight (BW), in a 60 kg and a 5 kg dog, respectively [8]. Since gastrointestinal tract (GIT) absolute length (in centimeters) is a reflect of dog height at the shoulder with a 6:1 ratio [9], it leads to the question: how does the size of dog impact digestive anatomy? Canine digestive anatomy is adapted to their facultative carnivorous diet (i.e. high-protein and high-fat diet) with a short and simple digestive tract. Digestion starts in the mouth with mastication process, helped by saliva. After swallowing, food boluses are transported through the esophagus into the stomach which is a J-shaped organ of glandular type, characterized by three anatomical compartments (i.e. fundus, corps and antrum) leading to the pylorus sphincter [10]. Canine gastric mucosal cells secrete hydrochloric acid (HCl), pepsin and lipase, which makes stomach essential in protein and lipid digestion. Canine stomach has a high dilatation capacity, varying from a maximal volume of 0.5 L for small dogs to 8 L in large dogs, which corresponds to the extreme quantity of food that a dog can ingest [10]. Digestion continues along the small intestine which is distributed as 10 % length for duodenum, 85 % for jejunum and 5 % for ileum [10,11]. Small intestine length measured *post mortem* is positively correlated (Pearson correlation of 0.672) to canine BW (from 240 cm for a 5 kg to 640 cm for a 33 kg dog), as well as small intestine width (weaker correlation, $R^2 = 0.36$) [11]. Canine small intestine, together with peripheral organs such as pancreas and liver, have a key role in canine digestion process. Pancreas produces pancreatic juice delivered into duodenum and associated with protein, carbohydrate and lipid digestion. Liver, coupled with gallbladder, has a central role in lipid digestion through bile acid (BA) production and induction of increased intestinal peristalsis [12]. Small intestine is also a central player in nutrient absorption, allowed by the presence of microvilli at the surface of enterocytes. When measuring intestinal wall thickness at different levels of the GIT (descending duodenum, proximal and distal jejunum, proximal and distal ileum), higher values were observed for male dogs compared to female (except for distal ileum) but no correlation was found with dog sizes whatever the intestinal compartment [13]. Regarding small intestinal villus length, an old study from 1978 showed no correlation between dog weight and mucosal dimensions [14]. In adult dogs from various sizes, duodenal villus length was 722 ± 170 µm [15]. Jejunal villi were longer in small dogs like Pomeranian and Fox Terrier (900 µm) than in medium ones such as Newfoundland (500 µm) [16]. Lastly, ileal villus length was measured in medium size Greyhound female and values around 796-823 µm were found [17]. Canine large intestine measures around 20-80 cm with 2-3 cm diameter in medium dogs [10]. The three parts of the canine colon (i.e. ascending, transverse and descending) are not so

well defined when compared to humans, with the particularity to be non-sacculated and devoid of sigmoid colon [10]. Ascending colon represents in medium size dog 20% of the colon length, while transverse and descending correspond to 30 % and 50 %, respectively. The two first parts are used for transport, electrolyte and water modification as well as for bacterial fermentation and storage areas, while descending colon mainly functions as conduit ending with rectum. Canine large intestine is involved in water and electrolyte absorption but also degradation of residual nutrients thanks to the fermentation activity of resident microorganisms called gut microbiota. Large intestine total length appears to vary according to dog's BW, from 32 cm for Miniature Poodles to 99 cm for Great Danes [18]. Volume and surface are also increased from Miniature Poodle to Great Dane (volume of 92 *versus* 2106 cm^3, surface of 191 *versus* 1612 cm^2). As the large intestine length increases with BW, the same positive relation is observed for absorption surface with a higher number of villi in large compared to small dogs [18]. Colonic crypts length was around 500-600 µm but without correlation with dog size [16]. To conclude, scarce anatomy data (only five publications) evidenced morphological differences depending on dog's BW (mainly related to the colonic compartment), even if important parameters have not been evaluated such as gastric wall thickness, intestinal microvilli characteristics (i.e. length or number) or peripheral organs anatomy and functions. Variations in digestive anatomy can obviously affect physicochemical parameters such as pH, digestive secretions and transit time, and consequently gut microbiota.

Methods of literature research

Our literature search was performed using *PubMed* (https://pubmed.ncbi.nlm.nih.gov) and *Google Scholar* (https://scholar.google.fr) with the key words "dog" OR "canine" AND "stomach", "small intestine", "intestine", "duodenum", "jejunum", "ileum", "ileal", "colonic", "large intestine", "rectum", "feces", AND "anatomy", "digestion", "pH", "enzyme", "digestive secretion", "digestibility", "permeability", "absorption", "microbiota", "bile acids", "transit time", "fatty acids", "fermentation", "gas", "mucus" in all available years. The online database search was last performed in January 2022 on titles, abstracts and key words including original articles, reviews, thesis, and books. Relevant studies were identified after consultation of the main text, figures, and supplementary materials. Information regarding involved dogs (i.e. number of dogs, age, weight, breed, sex, reproduction state, living environment), diet (i.e. type of food, feeding frequency, composition of food), health (i.e. healthy dogs only) and analysis methods were collected. Only *in vivo* studies on adult dogs, fed with dry food or ingesting water were included in the literature survey.

We found a total of 163 studies, including 87 providing information on a single dog size, with only small dogs involved in 7 publications, only medium dogs in 71 and only large dogs in 9 (**Figure S1**). The three dog sizes (i.e. small, medium and large dogs) were compared together in 8 additional studies. In the remaining 68 studies, 45 integrated dogs without specifying their characteristics and other 22 included different sizes of dogs but didn't discriminate them in their analysis (both classed in the "unclassified" group). Concerning publication date, 40 studies were performed over 30 years, 76 studies have been done between 5 and 30 years ago and 47 were performed in the last 5 years. Only 10 studies were directly targeting the influence of dog size on canine digestive physiology.

Impact of body size on digestive physicochemical parameters

Gastrointestinal pH

Gastrointestinal pH changes along the dog digestive tract (**Fig. 1**, **Table S1**). Mean salivary pH of medium dogs is around 7.3-7.8 and quickly decreases by 0.5 point with a stimulation using a piece of solid sugar on the tongue [19–21]. In the stomach, the arrival of food bolus stimulates HCl production. This compartment shows the lowest pH value along the GIT, allowing dogs to partially digest bones [22] and putrescent meat and largely depends on feed status. However, due to the paucity of data, it remains difficult to know how BW affects gastric, small intestinal and colonic pH (**Fig. 1**, **Table S1**). To date, gastric pH has not been assessed in small and large dogs [23–26]. Regarding medium dogs under fasted conditions, mean gastric pH of Beagles is around 1.5 (range 0.9-2.5), punctuated by occasional pH spikes with high frequency changes due to inter-individual variability [27]. Those values measured in laboratory animals are in accordance with pH found in mixed-breed owner dogs [28]. Small intestinal pH increases to value close to the neutrality because of the buffering capacity of pancreatic juice enriched in bicarbonate ions and bile [10]. It also increases from the proximal to the distal parts, from 6.5 to 8 in medium size dogs [29]. To date, there is no available study that investigates the influence of the dog size on duodenal and ileal pH [30]. The few studies investigating the canine jejunal pH measured a mean pH of 6.8 and 6.0 for medium and large dogs,

respectively [31,32]. Only few studies investigated colonic pH using colonic cannula or wireless capsules, and once new, most of them do not discriminate dogs in terms of BW. Colonic pH is more acidic than the small intestine one, with mean values of 5-6.5 and 6.2, respectively for medium and large dogs, whereas there is no data concerning small dogs [29,33–35]. Most of the time, colonic pH is estimated using faeces and there is no information on how pH varies depending on colonic sections. The average canine faecal pH values are in accordance with colonic pH, mainly around 6.4-6.6, as observed in **Fig. 1**. For small dog group, three studies used faeces of 43 dogs and pH values vary weakly from 6.4 to 6.8 [36–38]. There are also plenty of data on the faecal pH of medium (more than 121 dogs) and large (18 dogs) size dogs, with a pH range of 6-6.9 and 5.6-6.5, respectively [39–42]. This is an accordance with some studies reporting that colonic and faecal pH of large dogs are more acidic than that of other size dogs fed with the same diet [18,43].

Digestive secretion

Enzymes. First digestion step occurs in the oral cavity with salivary enzymes (**Table S2**). Numerous recent studies measured amylase activity in saliva of healthy dogs [44–49]. Mean amylase activity varies from 26.5 to 37.3 UI/L of saliva in medium dogs according to literature (**Table S2).** One study involves 75 dogs from 8 to 42 kg (52 mixed breeds and 23 pure breeds) and measured 35.9 ± 41 UI/L amylase in saliva but results weren't discussed regarding dog sizes [48]. Lactate dehydrogenase and adenosine deaminase activities were also quantified in saliva, without classification with canine BW [45,48,50]. Gastric mucosa secretes gastric juice containing proteolytic (pepsin, chymosin) and lipolytic (lipase) enzymes [20,51]. In laboratory Beagles, gastric juice volume output increases with meal viscosity, from a total of 37.2 mL secreted for a low viscosity to 190 mL for a high viscosity meal [52]. Pancreatic juice, discharged in canine duodenum, has an alkaline pH (7.4-8.3). It contains amylase (2013 U/kg BW), lipase (9.8-33.3 mL 0.05 N NaOH/mL -no longer used unit of measure), phospholipases, cholesterases, proteases (old value of 407.5-2440 mg tyrosin/mL -no longer used unit of measure) and nucleases, without further detailed information [12,53]. Digestive secretions were mainly studied before 2000s, but values were not discriminated depending on dog sizes, and no study focuses on small and large dogs. However, enzymatic activities may vary according to the different diet composition (i.e. protein, lipid, fiber contents) adapted to each dog size.

Bile salts. Bile is produced by liver, partially stored in gallbladder then discharged to duodenum during postprandial phase, allowing stimulation of intestinal motility, intestinal lipids saponification and vitamins A, D, E and K absorption. In liver, primary BA such as cholic acid (CA) and chenodeoxycholic acid (CDCA) are synthesized from cholesterol and conjugated to taurine or glycine [54]. Studies evaluating bile production in healthy dogs never discriminate dog sizes. Bile production was only evaluated in medium dogs and was found to be 29 mL/kg/24 h [55]. Once reached gallbladder, bile is up to 10 fold more concentrated than in liver with a total concentration around 50 (40-90) mmol/L [10,54,56,57]. Here, it contains up to 15 different BA but the three majors count for 99% of total pool, with 72.8% taurocholic acid, 20.3% taurodeoxycholic acid and 6.2% taurochenodeoxycholic acid [58]. In the small intestine, BA are deconjugated by gut microbiota and converted into secondary BA. 95% of BA are reabsorbed in ileum, return into liver and the 5% remaining fraction crosses colon [56]. Faecal BA concentrations were measured in three recent studies involving all dog sizes but curiously without BW distinction (**Fig. 2A, Table S2**). Authors found coherent results with concentrations ranged from 5.8 to 7.5 µg of total BA per mg of dry faeces [59–61]. Another recent study evaluated faecal BA concentrations in 24 healthy dogs [62]. After data retreatment (classification in size groups), small, medium and large dogs present respectively 5.1, 4.7 and 3.4 µg/mg of total BA per mg of dry faeces. This suggests a decrease in faecal BA concentrations with BW increase. Further analysis from 8 studies (**Fig. 2B**) indicates that relative percentages of faecal secondary BA (BA II: 84.9%) are higher than primary BA (BA I: 15.5%). Moreover, proportions of primary BA such as CA and CDCA seem to be inversely correlated to canine BW whereas the contrary is observed for secondary BA (only one study) (**Fig. 2C**). These results suggest that the microbiota activity, and notably the BA recycling, differs from small to large breed sizes.

Mucins. Mucins are produced by goblet cells all along the dog GIT [10]. Mucus thickness has been evaluated only in gastric compartment and stomach presents a mucosa covering mucin-layer of 576 µm and 425 µm, respectively in the antrum and fundus [10,63,64]. This mucin-layer allows protection of the epithelium against acidic pH of stomach and withstands bone fragments [65]. Influence of dog size on mucin secretion and mucin-layer thickness whatever the digestive compartment has never been assessed.

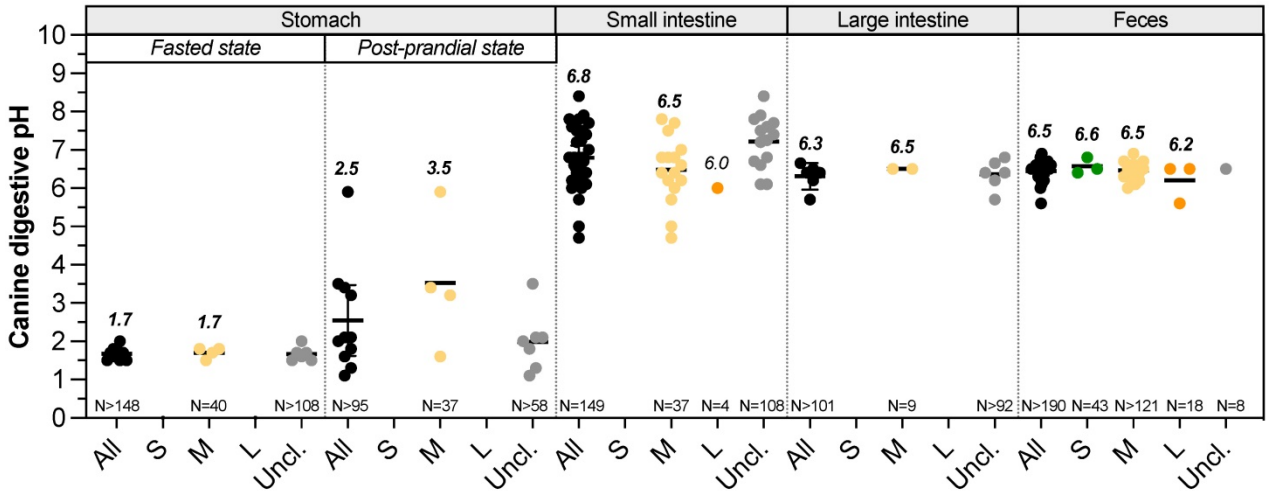

Figure 1. Impact of dog sizes on pH values in all digestive compartments. Results from studies measuring in dog's pH values in the stomach (under fasted or fed conditions), small intestine, large intestine and faeces are presented. Small dogs are plotted in green, medium dogs in yellow, large dogs in orange and unclassified dogs in grey. Raw data were pooled in "all" group (in black). Calculated median values are in italic bold, values for a single point in italic. Black bars represent 95% confidence intervals. The number of dogs involved in studies is indicated as "N="

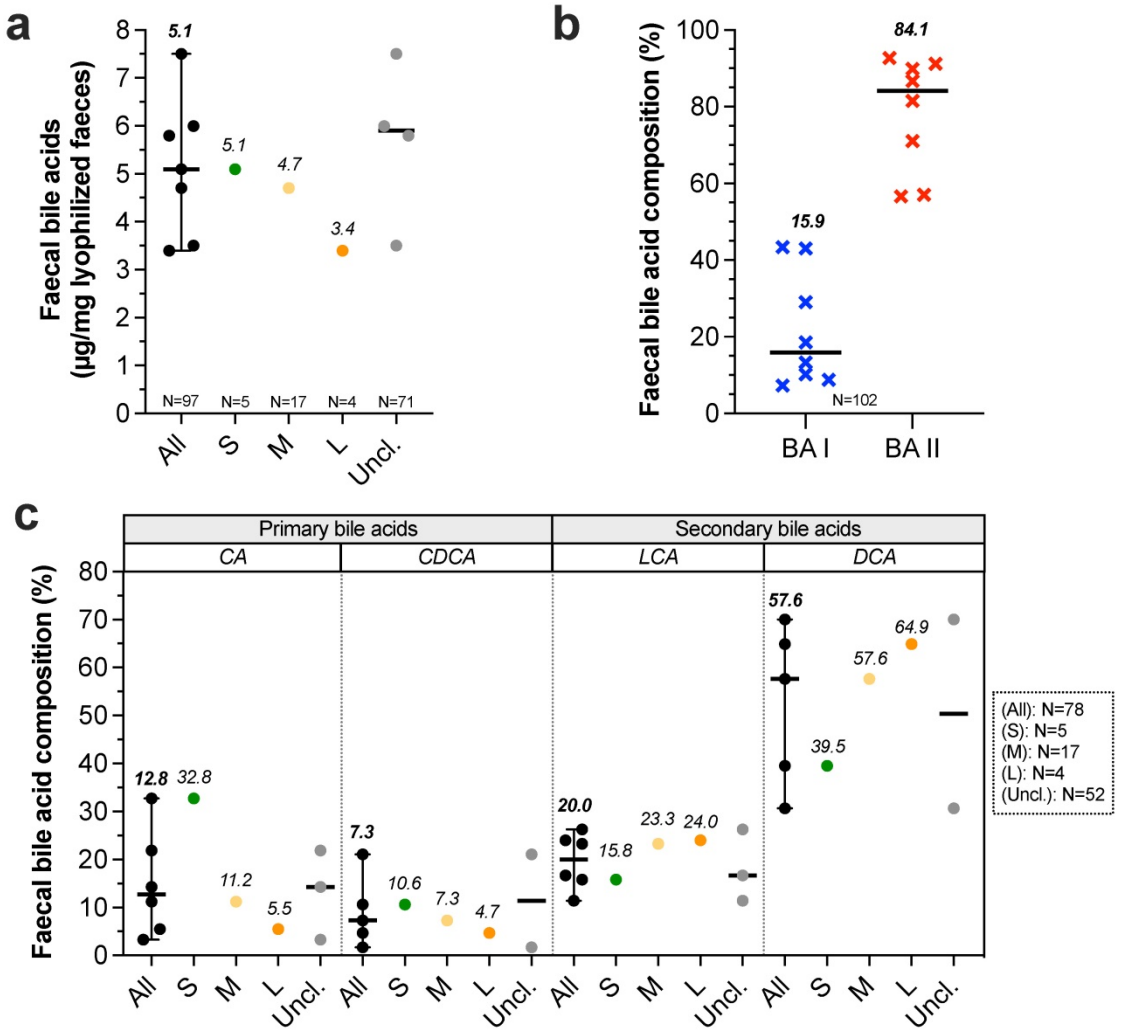

Figure 2. Impact of dog sizes on faecal bile acids. Results from studies in dog faeces quantifying total bile acids (BA) are represented in (a), further separated into primary (blue crosses) and secondary BA (red crosses) in (b). Detailed composition in cholic acid (CA), chenodeoxycholic acid (CDCA), lithocholic acid (LCA) and deoxycholic acid (DCA) is shown in (c). The same caption as used in **Fig. 1** was applied

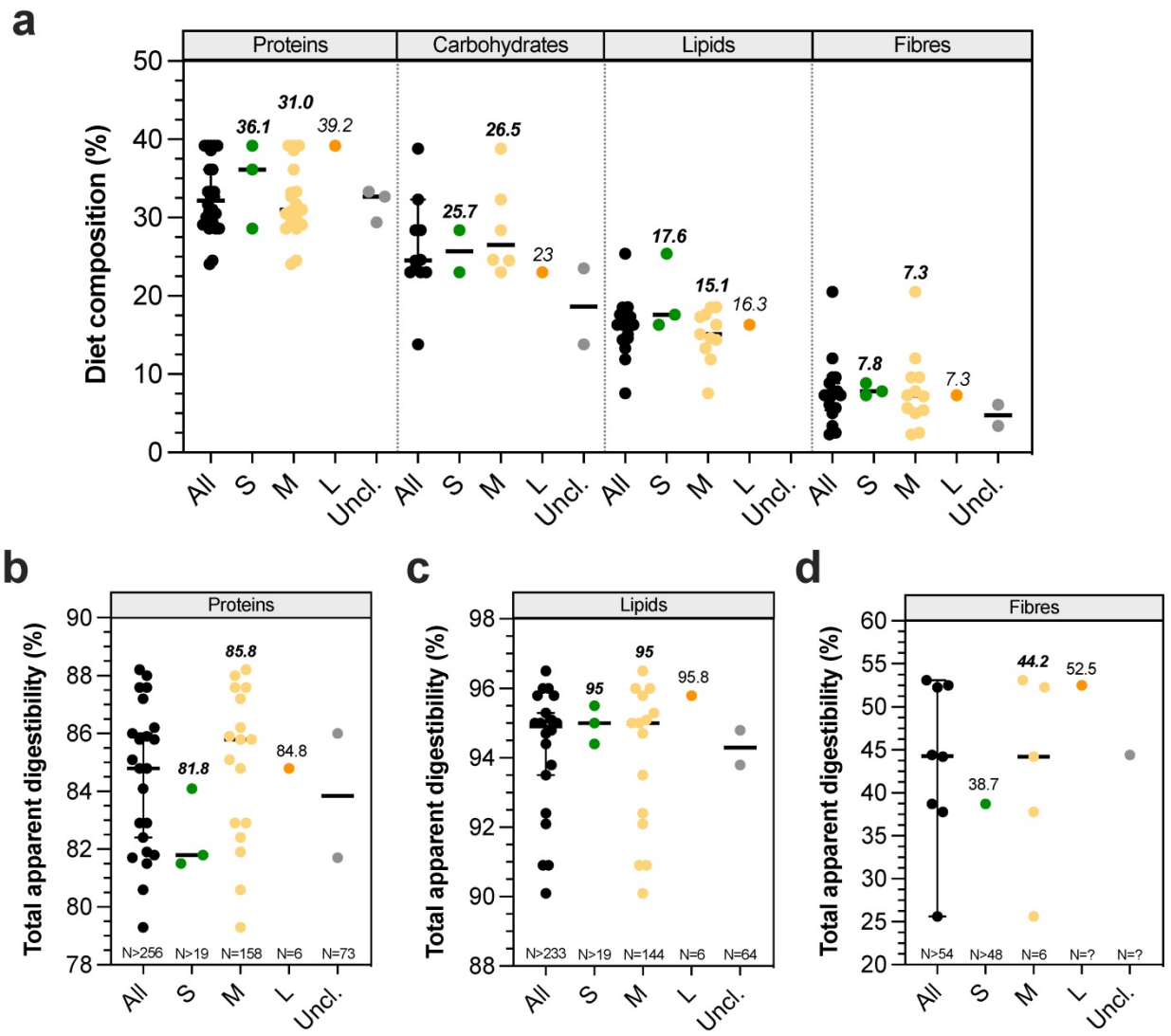

Figure 3. Diet composition and impact of dog sizes on total apparent digestibility. Nutritional composition of dry food diet used in canine studies is represented in (a). Results from studies investigating in dogs' total digestibility of proteins, lipids and fibres are presented in (b), (c) and (d), respectively. The same caption as used in **Fig. 1** was applied

Nutrient digestibility

Digestibility defines the degree to which organic matter is digested by an animal. Its measure provides a qualitative and quantitative indicator of food's quality, i.e. the more digestible a food is, the higher the proportion of absorbed nutrients will be. **Figure 3A** gives an overview of canine dry food composition in dogs according to BW. Digestibility performances can be evaluated in dogs by measuring ileal or total (in faeces) apparent digestibility of a tested diet, and standardized digestibility could be obtained by deducing endogen products such as enzymes or metabolites delivered from intestinal cell desquamation. As previously observed for physicochemical parameters, digestibility studies are mainly focused on medium dogs and there are only two publications on small [66,67] and one on large dogs [66] (**Table S3**). Due to their invasive nature, only 4 studies have been performed with ileal cannula (to measure ileal digestibility), including 3 on medium dogs [68–71]. Lipid digestibility seems to be almost complete at the ileum level (i.e. 89.3-96.5%), with only around 3-5% increased digestibility when evaluating total digestibility in faecal samples. Ileal protein digestibility appears to be lower (51.3-76.2%), with higher variations certainly related to protein quality which largely influences this parameter [67,72–74]. Surprisingly, the only study investigating total dietary fibre digestibility found an ileal digestibility of 17.8%, while according to their definition fibres are only degraded in the large intestine [68]. Given the lack of data, it is impossible to conclude on a possible effect of dog BW on ileal nutrient digestibility. Total apparent protein (82-88%) and lipid (95-95.8%) digestibilities appear to be equal between different

dog sizes, whatever the initial proportion of dietary proteins or lipids (**Fig. 3B-C**). In contrast, total apparent dietary fibre digestibility (**Fig. 3D**) appears to be higher in large than in small and medium dogs (52.5 ± 4% for Great Dane *versus* 39 ± 7.4% for Miniature poodle, and 26-38% for medium dogs) [42,75,76]. Indeed, it seems that fibre digestibility would be quite similar between small and medium dogs, while it would be improved in large dogs. In addition, faecal apparent digestibility of dry matter, organic matter and gross energy appears to be significantly higher for large compared to small dogs [66]. All in all, those results mean that the colonic fermentation seems to be more important in large than in medium and small breed size dogs.

Intestinal absorption

Permeability. During digestion process, food is broken down into small soluble compounds (amino acids, fatty acids, monosaccharides, minerals and vitamins), able to be absorbed mainly through the villi-covered wall of the small intestine. Nutrient passage through the epithelial wall is modulated by intestinal permeability, which is the property of epithelium to allow some molecules to be absorbed passively or actively through mucosa while avoiding the passage of microorganisms and macromolecules. Lactulose to L-rhamnose or lactulose to sucralose urinary ratios could be used to monitor changes in canine small and large intestine permeability, respectively [77]. A higher lactulose to L-rhamnose ratio is associated with a leakier small intestine, while a lower lactulose to L-rhamnose ratio indicates a higher colonic permeability. Using these methods, Weber *et al.* [78] observed an increased intestinal permeability in Giant Schnauzer and Great Danes (large dogs; lactulose to L-rhamnose ratio: 0.31) compared to small dogs (0.16), and Hernot *et al.* [77] found a higher colonic permeability in large dogs (lactulose to sucralose ratio: 0.35) than in small ones (0.51). Those differences could be related to modifications associated with dog size in intestinal area, pore size, frequency of tight junctions, differences in tightness of tight junctions or accessibility of luminal content to intestinal crypts [79]. Of note, breed differences were particularly noticed with a higher colonic permeability in Great Danes, as previously described [80,81]. An increased permeability could affect both nutrient, metabolite and electrolyte absorption but also microorganism's translocation. This may explain the weaker digestive tolerance of resistant-starch and higher digestive sensibility of large dogs compared to small ones, as discussed by Goudez et al. [82].

Passive absorption. Water, electrolytes and vitamins are absorbed through passive mechanisms in the small and large intestinal lumen. In healthy dogs, around 90% fluids crossing the colon are reabsorbed by mucosa [20,83]. Meyer *et al.* [81] demonstrated that total faecal water increases with dog BW, but the percentage of free faecal water decreases. This is of high interest because an increase in free faecal water content is associated with a higher colonic water content that can in turn influence *in vivo* drug dissolution, in the case of poorly soluble drugs for which dissolution continues in the large intestine [43]. Whereas small dogs tend to have drier stools, a tendency of poorer faecal consistency and higher water content is observed in larger dogs. Potassium and bicarbonate ions are secreted into the colonic lumen, whereas sodium and chloride ions are passively absorbed from luminal contents [83]. Uptake of sodium ions creates an hypertonic environment next to crypts, generating an electro-chemical gradient across colonic mucosa which drives water uptake from luminal contents by osmosis [83]. Based on observation that large digestibility variations are observed within the same breed and between different breeds, Zentek and Meyer [80] compared mineral digestibility of four food types in Great Danes and Beagles. There was no breed difference for calcium, magnesium and phosphorous absorption (**Table S3**), while net colonic sodium absorption tended to be 9-23% lower in Great Danes compared to Beagles. These data were further supported by Weber *et al.* [36] describing an increase in sodium faecal content with an increase in BW (2.1 ± 0.7 g/kg DM in Miniature Poodle *versus* 6.1 ± 1.3 g/kg DM in Great Dane), traducing a lower sodium absorption by large dogs. Moreover, a reduction of colonic absorption of sodium has been particularly observed in Beagle, Labrador Retriever, Springer Spaniel and Münsterländer, suggesting a breed sensitivity [18]. Besides, Neri *et al.* [84] reported a significantly greater faecal potassium concentration in large compared to smaller dogs. Independently of dog sizes, 90% vitamin D, 80-90% vitamin A, 40-90% vitamin K and 35-50% vitamin E are absorbed by passive absorption in the proximal small intestine [20].

Active absorption. Active absorption processes in the small intestine implicate co-transporters (e.g. glucose or sodium-dependent transports) and concerns monosaccharides from carbohydrate degradation and peptides from protein degradation. Thus, 95% of monosaccharides are absorbed in the duodenum and proximal jejunum [20], and 30% of amino acids and 70% of tripeptides are absorbed and assimilated in the proximal jejunum [12]. Regarding lipids, 80% of fatty acids and monoglycerides are

absorbed in form of micelles in the small intestine and resulting in chylomicrons that passed into the intestinal lymphatic capillary of villus by endocytosis. There is no available information on the influence of dog size on nutrient absorption. Moreover, the overall active transport capacity of small intestine has been assessed by examining urinary excretion ratio of D-xylose to 3-O-methyl-D-glucose [78]. Non-significantly different ratios of 0.57, 0.58 and 0.59 for small, medium and large dogs respectively have been reported, suggesting that small intestinal active transport is relatively consistent between sizes.

Mechanical digestion and gastrointestinal transit time

Motility. Canine gut motility was firstly evaluated using radiopaque markers, plastic beads or breath test. Recently, wireless motility capsule was developed to measure pressure, forces and gut contractions frequency. Using this method, Boscan *et al.* [85] observed in fed medium dogs a lower maximal amplitude contraction in the stomach compared to small intestine (52 mmHg *versus* 75 mmHg, respectively), coupled with higher gastric contraction frequency, with 3.7 contractions/min in the stomach *versus* 0.5 contraction/min in the small intestine. Another study involving dogs from different sizes observed similar tendency on maximal amplitude contraction (lower in stomach than in small intestine, with 0.2 *versus* 4.1 mmHg), but opposite results on frequency (0.8 in stomach *versus* 10.9 contractions/min in small intestine) [86]. Moreover, in this study, large intestinal contraction frequency seems to be similar to the gastric ones (0.6 contraction/min). Authors also calculated a motility index defined as the area under the pressure curve and the higher motility index was observed in small intestine (306.2 compared to 20 in stomach and 76.1 in colon). Using wireless motility capsule, Farmer *et al.* [87] found that motility indexes were higher in large intestine (199 mmHg*second/min) compared to small intestine (134 mmHg*second/min) and stomach (55 mmHg*second/min) with a similar maximum of 3.7 contractions/min in gastric compartment [88]. Lastly, no study has investigated how dog BW or size influences gut peristalsis.

Transit time. There is no available data on the duration of oral phase in dogs, but they are well known to quickly swallow their whole food. Data on gastric emptying time (GET), small intestinal transit time (SITT), orocaecal transit time (OCTT), large intestinal transit time (LITT) and total transit time (TTT) can be found in the literature with homogeneous definition between studies (**Fig. 4**, **Table S4**). Three different studies evaluate the impact of dog size on GET fed animals. Weber *et al.* [75] showed no significant difference in half-gastric emptying time between four breeds dogs (i.e. Miniature Poodle, Standard Schnauzer, Giant Schnauzer and Great Danes) using radiopaque markers ingested with food (T_{50} = 6.4-7.8 h). Without specifying any values, Bourreau *et al.* [89] concluded on a longer GET in large compared to small breeds after ingestion of a dry food meal using breath test method. Contrarily, Boillat *et al.* [4] described a shorter GET in large compared to medium breeds (range 6.8-15 h), using wireless motility capsule immediately administered after a dry food meal. Thus, there is apparently no relationship between BW and GET not only in fed, but also in fasted animals (**Fig. 4**). Besides, a liquid meal conduced to a shorter GET compared to meat, with 90% emptying in 0.4 h and 50% in 1-3 h, respectively (unknown dog size and method) [90]. This suggests that canine gastric emptying is influenced by food consistency [91]. There is also no consensus on the effect of dog size on SITT. Oswald *et al.* [43] and Weber *et al.* [8] found no influence of breed or BW, while Boillat *et al.* [4] measured a shorter SITT in largest dogs, ranging 1.6-3.7 h without linking transit time and dog size [4,8,43]. OCTT was evaluated in dogs using very different methods. Some studies used sulfasalazine (converted into sulfapyridine in plasma) but do not employ the same threshold to define OCTT, i.e. either 50% conversion or first appearance in plasma [75,92], whereas more recent studies used wireless motility capsule. As a consequence, extremely variable results of OCTT are provided, from 2.2-2.8 h with sulfapyridine [75,92] to 20.7 h with capsule [93]. Whatever the method used, these authors conclude to an absence of correlation between OCTT and BW. Studies of Boillat *et al.* [4] and Warrit *et al.* [94] assessed LITT in dogs from several breeds and various BW using wireless motility capsule. Both works conclude on the absence of correlation between LITT and BW (**Fig. 4**), with $T_{1/2}$ ranged 7.1-42.9 h [4] and 25.0 h (1.1-49.1 h) [86]. However, using plastic beads, researches revealed a longer LITT in large dogs (29.3 h for great Dane) than in small dogs (9.1 h for Miniature Poodle) and a significant positive correlation between LITT and BW, but also between LITT and shoulder height was demonstrated [92]. In this study, LITT accounts for 39% of mean TTT for small breed dogs and 70% for large ones, which means that longer transit times observed in large dogs could be related to a longer LITT. Lastly, TTT showed a clear positive correlation with BW, as highlighted in **Fig. 4** [18]. When gathering the data obtained in all the available studies, TTT ranged from 22.9-31 h (calculated median 24 h) in small dogs, 19.1-55 h

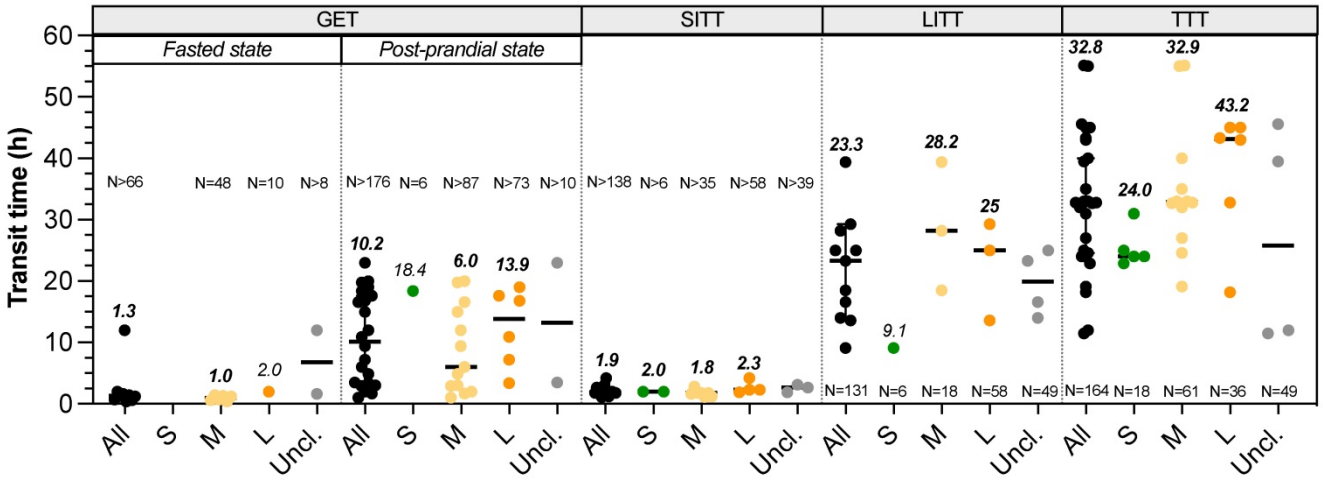

Figure 4. Impact of dog sizes on gastrointestinal transit time. Results from studies in dogs evaluating gastric emptying time (GET) under fasted or fed status, small intestinal transit time (SITT), large intestinal transit time (LITT) and total transit time (TTT) are represented. The same caption as used in **Fig. 1** was applied

(median 32.9 h) in medium dogs and 18.2-45 h (median 43.2 h) in large dogs. Especially, using plastic beads in small and large breeds, TTT observed was 22.9 h in Miniature Poodle and 43.3 h in Great Dane, whilst giant Schnauzer showed an even higher TTT of 55 h [95]. This result was explained by the authors through a high stress sensitivity of giant Schnauzer that could influence their transit time in refraining their defecation, emphasizing a breed effect in addition to body size influence.

Impact of body size on microbial parameters

Gut microbiota composition

Longitudinal variations. In dogs like in other mammals, microorganisms colonize the entire GIT from mouth to rectum. All along GIT, there are longitudinal variations in gut microbiota composition due to changes in pH, substrate concentrations (including oxygen and nutrient availability) and transit time [64,96,97]. Gut microbiota has been weakly described in dogs (compared to humans) and most of available studies have been performed since 2003 (for detailed information see **Table S5**). Canine oral microbiota present similar number (around 350 bacterial taxa from 148 genera) but significantly different populations compared to the human ones [98] and is mainly colonized by *Proteobacteria* (45%), *Bacteroidetes* (25%) and *Firmicutes* (19%). Most abundant species are *Porphyromonas cangingivalis* and *Porphyromonas gulae* [99,100]. Regarding the other digestive compartments, studies have been mostly performed on faeces to avoid invasive procedures. Stomach is the less colonized compartment with 10^4 to 10^5 colony forming units (CFU) per gram of content in medium dogs, mainly composed by *Proteobacteria* (**Fig. 5A**) including *Helicobacter spp.* that are potential pathogenic strains [31,96,101]. Small intestine contains 10^5 to 10^7 CFU/g of content [31,101]. Duodenum (**Fig. 5A**) is colonized by *Firmicutes* (calculated median 47%), *Proteobacteria* (27%), *Bacteroidetes* (9%), *Fusobacteria* (3%) and *Actinobacteria* (1%), whereas jejunum is characterized by a higher abundance in *Proteobacteria* (37%), *Actinobacteria* (11%) and *Fusobacteria* (10%), together with lower percentages of *Firmicutes* (33%) and *Bacteroidetes* (7%) [28,102,103]. Ileum (**Fig. 5A**) is dominated by 31% *Fusobacteria*, 24% *Firmicutes*, 23% *Bacteroidetes* and 22% *Proteobacteria* [104]. These abundances should be considered with caution as they have been found in a single study performed in 6 medium dogs. As for other mammals, large intestine is the most colonized part of the GIT, with up to 10^9 to 10^{11} CFU/g of content [96]. According to a unique publication using 16S Illumina sequencing to investigate microbiota composition from 6 healthy Hound dogs [104], colonic digesta is dominated by 37% *Firmicutes*, 33% *Bacteroidetes*, 29% *Fusobacteria* and 1% *Proteobacteria* including *E. coli*-like organisms (**Fig. 5A**). It's interesting to highlight that majority of taxa colonizing the colon are also found in canine faeces [105] which seems to be rather different from the human situation where a significant number of mucus-adherent bacteria from the colon are not found in faeces [105]. No study has investigated dog size effect on gut microbiota composition elsewhere than in stools, and the main variations in faeces are presented in **Figure 5B** and **5C**. Whatever dog sizes, faecal microbiota of healthy dogs is dominated by three main bacterial phyla: *Firmicutes*, *Bacteroidetes* and *Fusobacteria* [105]. Bacteria from *Actinobacteria* and *Proteobacteria* phyla are also found in canine faeces but in a lesser proportion. Of interest, a variable relative abundance of *Bacteroidetes* was reported and was

inversely correlated to *Fusobacteria* relative abundance indicating they might occupy the same ecological niches [106]. *Fusobacteria* and *Proteobacteria* seem to be more abundant in dogs than in other omnivorous, probably related to diet changes [107]. Unlike in human where *Fusobacterium* is frequently associated with diseases, in dogs this genus is related to non-stressful conditions and is therefore probably a marker of an healthy state, especially because its abundance increases when dogs have access to the outside [43]. In small dogs faeces (**Fig. 5B**), average *Firmicutes* proportions vary widely from 30 to 80%, followed by 13-28% *Bacteroidetes*, while a lower abundance of *Proteobacteria* (1-15%), *Fusobacteria* (1-16%) and *Actinobacteria* (1-3%) was detected [108–110]. Medium dogs display similar value ranges of *Firmicutes* (15-98%), *Bacteroidetes* (0.1-34%), *Proteobacteria* (0.1-27%) and *Actinobacteria* (1%), but a larger proportion of *Fusobacteria* (0.1-40%) compared to small dogs [108,111]. Only one study investigated faecal microbiota composition in 8 large dogs and quantified 71% *Firmicutes*, 22% *Bacteroidetes*, 5% *Fusobacteria,* and 1% *Actinobacteria*, with interestingly a much lower abundance of *Proteobacteria* (1%) than in small and medium dogs [40]. In few studies, canine faecal diversity was followed with Shannon index and calculated medians seem to be higher in medium dogs (4.8, four studies) compared to small (3.5, five studies) and large dogs (2.9, a single study) (**Fig. 5C**). In addition to Bacteria (representing 98%), canine faecal microbiota also contains 1.1% Archaea, 0.4% Fungi and 0.4% viruses, mainly bacteriophages [112,113]. Fungal part of the faecal microbiota is composed by 97.9% *Ascomycota* and 1% *Basidiomycota* [114]. Even if methanogen Archaea have been detected in healthy dogs faeces, there is no information on their methanogen potential [114].

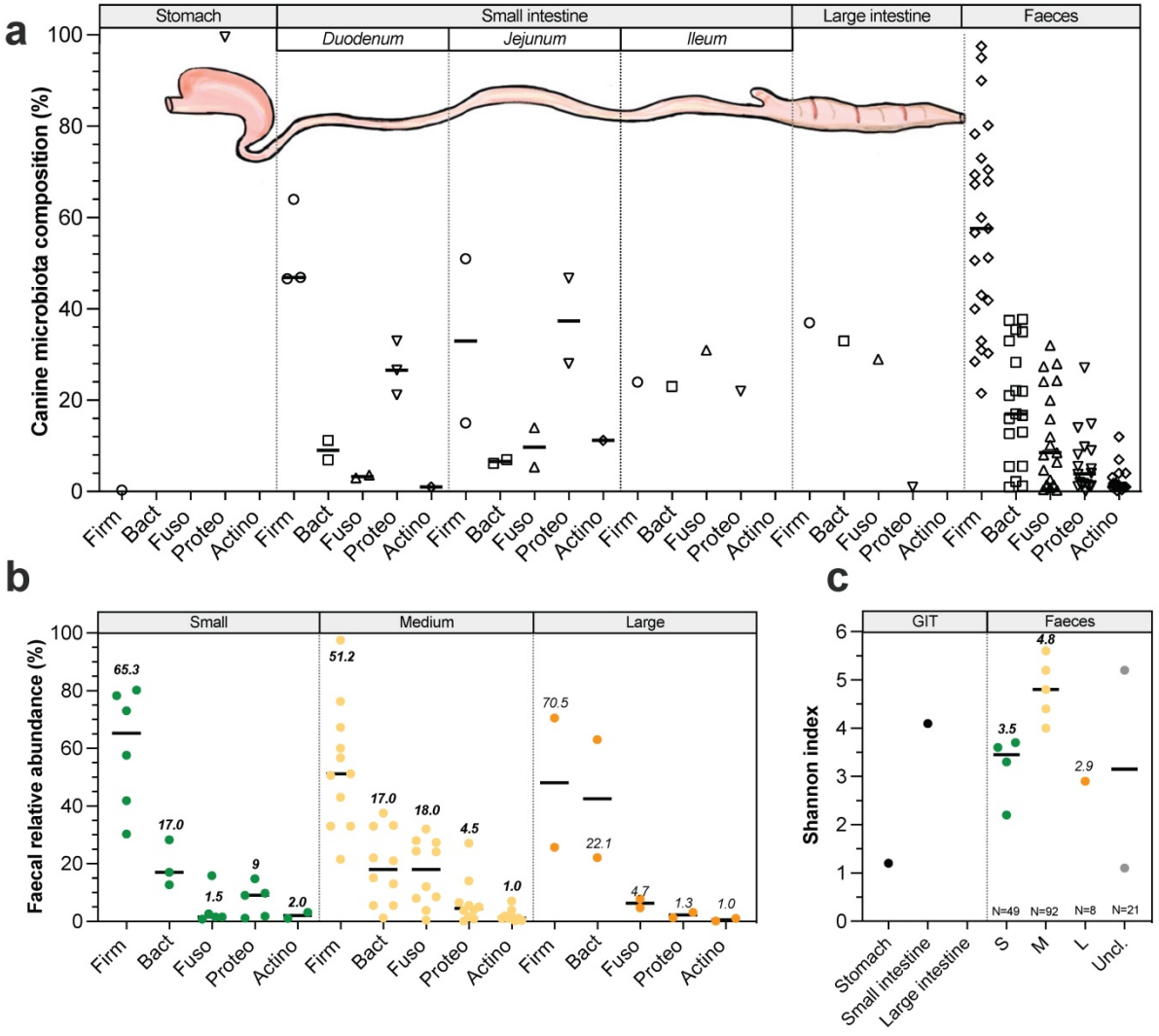

Figure 5. Variations in gut microbiota composition along the canine digestive tract and impact of dog sizes. Main bacteria populations found in the different compartments of the dog gastrointestinal tract are represented in (a). Bacteria counts are expressed in colony forming units (CFU) per gram of digestive content. Results from studies exploring by 16S rRNA Illumina sequencing canine microbiota composition (regardless of dog size) in the different digestive compartments are presented in (b). Influence of dog sizes on faecal microbiota composition at the phylum level is shown in (c) and corresponding Shannon index in (d). Canine main phyla are *Firmicutes* (Firm), *Bacteroidetes* (Bact), *Fusobacteria* (Fuso), *Proteobacteria* (Proteo) and *Actinobacteria* (Actino). The same caption as used in **Fig. 1** was applied

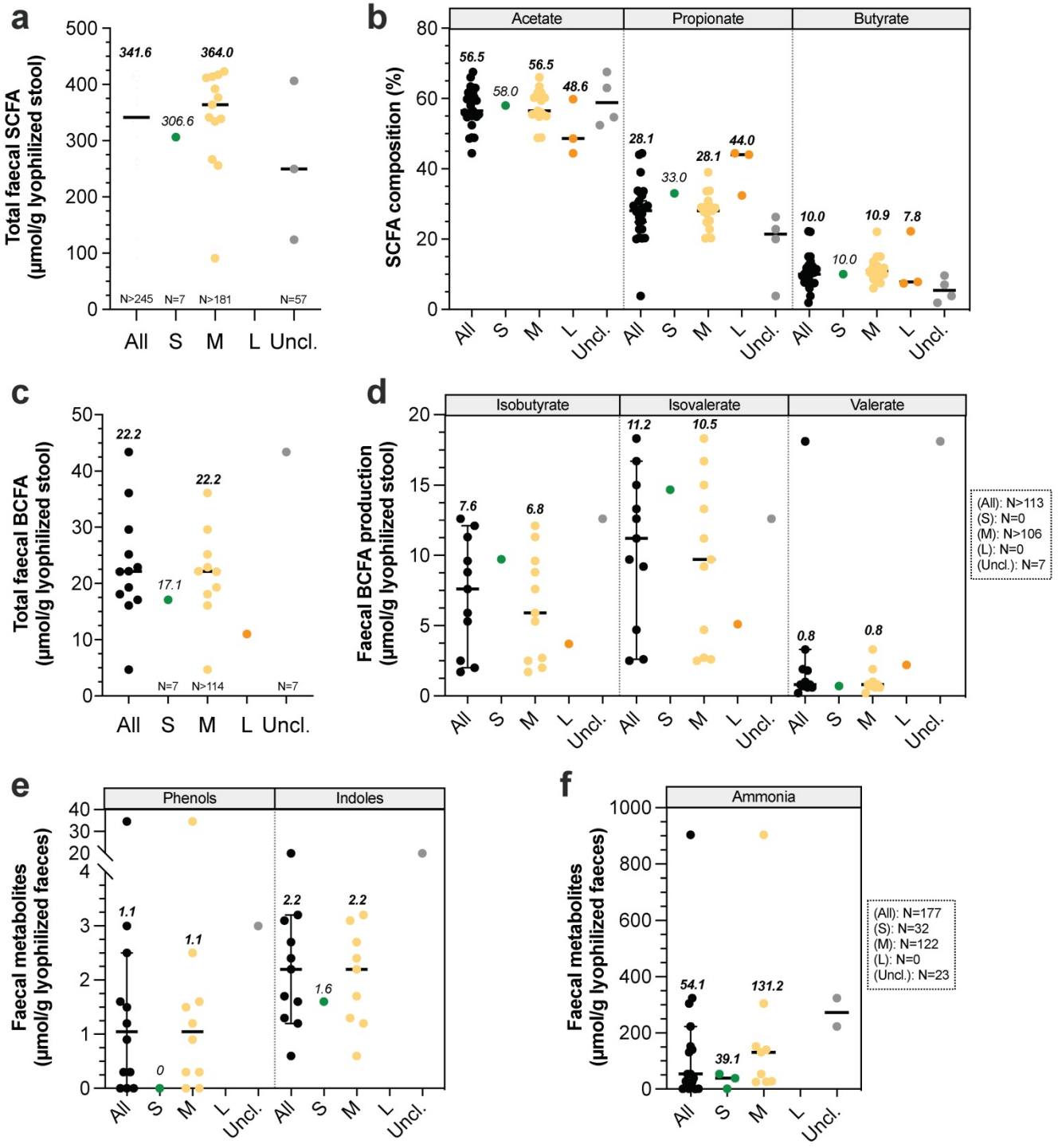

Figure 6. Impact of dog sizes on faecal microbial products production. Results from studies in dogs measuring total faecal major short-chain fatty acids (SCFA, i.e. acetate, propionate and butyrate) are presented in (a) and detailed in (b). Similarly, influence of dog size on major branched-chain fatty acids production (BCFA, i.e. isobutyrate, isovalerate and valerate) is shown in (c) and detailed in (d). Effect of dog size on other microbial metabolites are presented in (e) for phenols and indoles and (f) for ammonia. The same caption as used in **Fig. 1** was applied

Radial variations. In addition to longitudinal variations, there are also radial changes in gut microbial composition that starts to be described in human [115] but are still in infancy in dogs. Indeed, the entire gut epithelium is covered by a mucus layer that offers an alternative source of host-derived nutrients. This mucus is colonized by a specific mucus-adherent microbiota (namely mucosal microbiota) and seems to play a key role in host homeostasis [116]. Of note, there is a lack of studies on the canine mucosal microbiota. Only two studies investigated the mucosa-associated bacteria on the outer mucus layer in the colon of healthy dogs, using targeted FISH approach [117,118]. Analysis of colonic

biopsy samples from healthy Boxers revealed that bacteria appear to be restricted to the outer mucus layer, as no bacteria was detected within the mucosa [117]. In addition, Cassmann *et al.* [118] demonstrated that free ileal and colonic mucus of healthy young dogs (< 2 years old) was mainly colonized by *Bacteroidetes spp*. and *Eubacteria,* while *Eubacteria* represented the major bacteria attached to adherent mucus. Authors reported that there were almost no bacteria attached to surface epithelium or contained within mucosa. Of interest, *Akkermansia muciniphila*, a well-known mucin-degrading bacteria in humans, inversely correlated to obesity, was not yet identified in canine faeces [119].

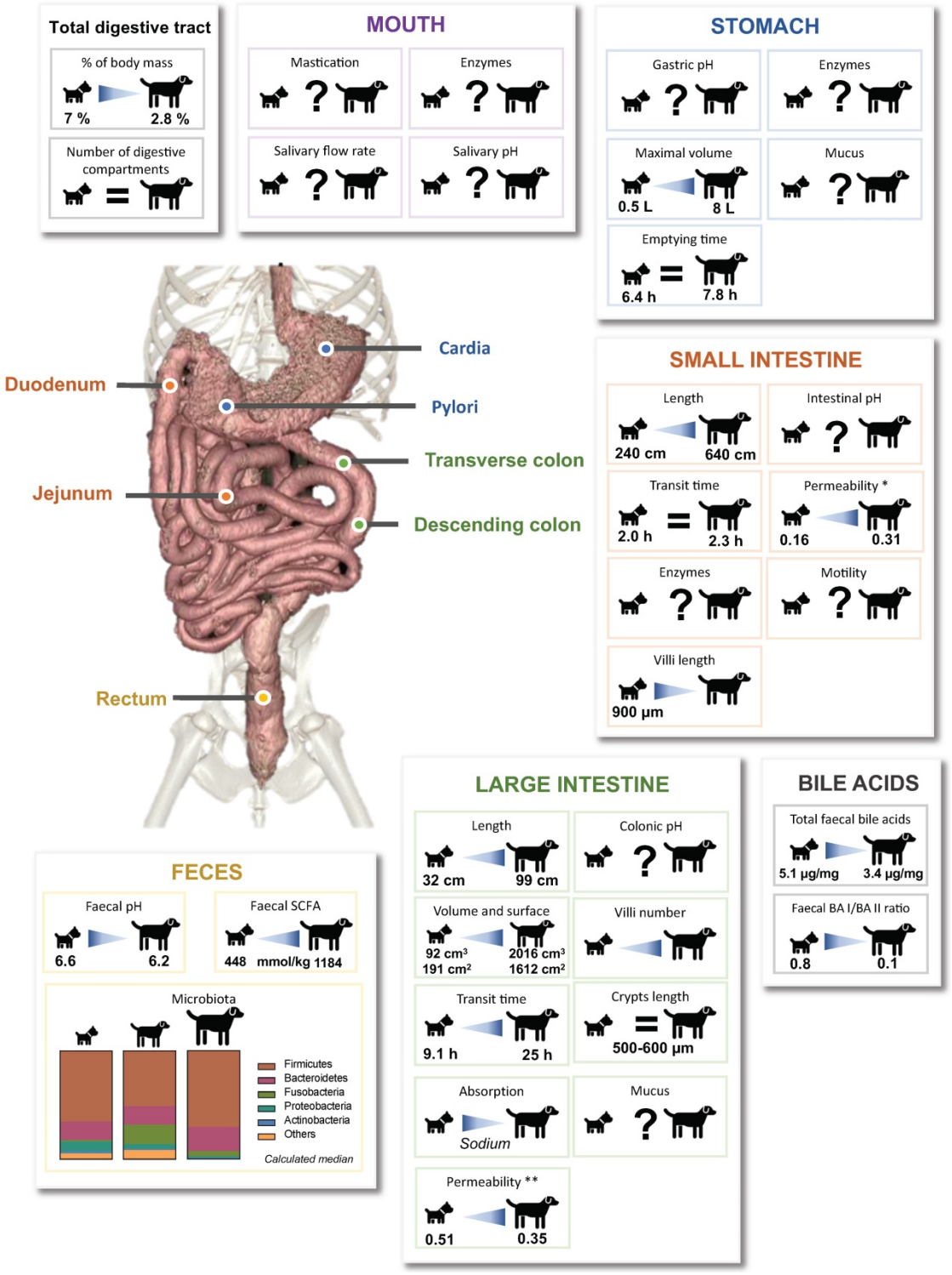

Figure 7. Overview of the impact of dog sizes on digestive physiology and faecal microbiota composition and activity. Key parameters of the oral, gastric, intestinal and colonic compartments from the canine digestive tract are summarized. Specified values were obtained from reports comparing in a same study the results obtained for small and large dogs. Lack of data are represented by "?", BA: bile acid, SCFA: short chain fatty acids. *: Lactulose/L-rhamnose ratio, **: Lactulose/sucralose ratio

Gut microbiota metabolic activities and functions

Gut microbiota is known to play a key role in host homeostasis and health maintenance, as it is implicated in many nutritional (e.g. vitamin synthesis, fibre degradation), immunological (immune system maturation) and physiological processes (e.g. vascularization, epithelium integrity, "barrier" effect against pathogens and lipid digestion via the metabolism of primary BA into secondary BA) [20,120]. At a functional level, whatever the type of food, identified gene content of microbiome from medium dogs was not modified and was associated with the metabolism of carbohydrates (12.5-13%), proteins (8.1-9.1%), DNA (7.1-7.4%), cell wall and capsule (7-7.6%), amino acids and derivatives (6.8-6.9%), cofactors, vitamins, prosthetic groups and pigments (5.7-6%) and bacterial virulence (6.2-7.2%) [112]. These results underline that all microbiota functions are far to be already discovered, as proved by the remaining 42.8% non-affiliated genes. Guard and Suchodolski [121] have studied faeces from 8 healthy dogs (2.7 to 31.8 kg) and observed high inter-variability microbiota composition between animals, while bacteria's functions were very consistent. Thus, even if gut microbiota composition highly vary between dogs, the functional potential seems to be unchanged whatever dog sizes [20]. Gut microbiota metabolic activity leads to gas and short-chain fatty acid (SCFA) production from soluble fibres. SCFAs stimulate intestinal motility and can be further used as an energy source for colonocytes, liver and brain. The three main SCFAs are acetate, propionate and butyrate, with faecal relative percentages of 60:25:15 [122]. Non-digested protein from diet and endogen proteins are also metabolized by gut microbiota, leading to the production of branched chain fatty-acids (BCFA), ammonia, indoles and phenols [18]. Canine faecal protein degradation products are associated with deleterious effects, such as poor faecal quality, inflammation and kidney diseases in dogs and colorectal cancer in humans [123,124]. Canine SCFA production was only evaluated in faecal samples (**Fig. 6A-B, Table S6**). Values were mainly obtained in medium dogs (especially Beagles) and are widely variable due to many differences in design study (e.g. type of food, food composition in carbohydrates, methods, type of units). However, in a study performed by Weber *et al.* [36] , the authors compared SCFA production between small, medium and large dogs and demonstrated that total SCFA concentration in stool significantly increased with BW, with 448 ± 67, 894 ± 80 and 1184 ± 259 mmol/kg of lyophilized faeces for small, medium and large dogs respectively. This is consistent with a longer LITT in large breed dogs that may promote microbial fermentation. Large quantity of organic acids produced could thus exceeds colonic mucosa absorption capacity, thereby leading to an accumulation in lumen, a decrease of colonic pH and an increased faecal excretion [18]. Similarly, total BCFAs were measured only in faecal samples, and mainly in medium dogs (**Fig. 6C**, **Table S6)**. BCFA concentrations seem to be lower in small dogs (a unique value of 17.1 µmol/g) compared to medium ones (calculated median of 22.2 µmol/g). Moreover, BCFA composition was only studied in medium dogs, with a calculated median concentration of 6.8 µmol/g isobutyrate, 10.5 µmol/g isovalerate and 0.8 µmol/g valerate (**Fig. 6D**). Phenols, indoles and ammonia concentrations were also poorly studied in small and medium dogs and to our knowledge never measured in large dogs (**Fig. 6E-F**). Based on our calculated medians, it appears that these products are found in higher concentrations in medium than in small dogs. Lastly, to our knowledge there is no data on gas production in dogs and the two studies on gas composition focused on malodorous compounds such as hydrogen sulphide [125,126].

Discussion and general conclusion

In an original way, this review gives an overview of available literature concerning the effect of dog sizes (i.e. "small", "medium" and "large" sizes) on digestive anatomy and associated physicochemical and microbial parameters, illustrating data with both synthetic graphs (**Fig. 1 to Fig. 6**) and exhaustive tabs (**Table S1 to S6**). Even if our conclusions may be hampered by the paucity and old age of many data, as well as the huge variability between experimental protocols (diet composition, measurement methods and data analysis processes) and animals (live or dead, anesthetized or not, companion or laboratory animals, environment), we evidenced clear effects of dog's BW on gastrointestinal physiology, mainly in relation with the colonic compartment (**Fig. 7**). Large intestine length, area and volume clearly increase with dog size. This seems to be associated with a higher colonic transit time that can affect nutrient and water absorption, gut microbiota composition and activity, as well as faecal moisture. Thus, sodium and potassium absorption are lower in larger dogs resulting in a higher concentration in faecal samples. Large dogs are also characterized by a higher intestinal permeability that can induce a backflow of absorbed electrolytes into the colonic lumen, translated into a luminal retention of electrolytes and water [18]. Besides, a longer colonic residence time in large dogs should promote microbial fermentations

and especially a higher fibre degradation by resident bacteria. This higher fermentation capacity results in a stronger production of SCFAs leading to a diminution in faecal pH, and to a potential disturbance of water absorption due to the high osmotic power of SCFAs [36]. Together with an increased colonic permeability, excessive SCFAs production would induce water retention in the colon, associated with higher faecal water content and loose watery stools frequently observed in large dogs [43,127]. In addition, faecal concentrations of microbial degradation products from proteins (phenol, indole, ammonium and BCFAs) seem to be positively associated with dog BW, which again may be explained by a longer transit time. Moreover, our data analysis suggests an increase in *Fusobacteria* according to BW (observed between small and medium dogs), which can be related to an increase in protein metabolites [65,124]. As certain bacteria are fully involved in BA deconjugation, changes in microbiota composition depending on dog's BW can also be linked to modifications in BA concentrations, inversely correlated with BW.

Further studies would be necessary to enhance available data on physicochemical parameters, especially in the upper GIT, but also on gut microbiota that remains very poorly described in each digestive compartment and not described at all in the mucus layer. Lastly, our bibliographic review revealed the large predominance of some breeds (i.e. Miniature Poodle, Beagle, Standard and Giant Schnauzer and Great Dane) and breeds showing well-known specific digestive particularities (like German Shepherd) or specific energy needs (like Husky, Great Danes or Terriers) [80]. It would be therefore of high interest to further analyze current data by considering not only the effect of body size but also that of breeds. Taken together, all the specificities raised in large dog digestive physiology may be correlated to their high sensitivity to diet and digestive diseases [18]. Finally, all these data concerning the effect of dog size on their digestive physiology can be helpful for the development of new food or veterinary products at the individual level, in accordance with a personalization step intended by petfood and pharma companies. In full accordance with the 3R rules (aiming to reduce animal experiments), such *in vivo* data also provide key information necessary to develop and validate *in vitro* gut models adapted to each dog sizes for in-depth mechanistic studies on dog digestive physiology [128].

Abbreviations

BA: bile acids; BCFA: branched-chain fatty acids; BW: body weight; CA: cholic acid; CDCA: chenodeoxycholic acid; CFU: colony forming units; DCA: deoxycholic acid; GET: gastric emptying time; HCl: hydrochloric acid; LCA: lithocholic acid; LITT: large intestine transit time; OCTT: orocaecal transit time; SCFA: short-chain fatty acids; SITT: small intestine transit time; TTT: total transit time.

Supplementary Material

Supplementary tables.
https://www.ijbs.com/v18p5086s1.pdf

Author contributions

SBD, EA and DH had the idea to make a literature review on this topic and designed the review. CD performed the literature survey, data analysis and figures design. SBD and CD wrote the first draft of the manuscript. All authors critically revised and approved the manuscript.

Competing Interests

The authors have declared that no competing interest exists.

References

1. Botigué LR, Song S, Scheu A, et al. Ancient European dog genomes reveal continuity since the Early Neolithic. Nat Commun. 2017; 8: 16082.
2. Axelsson E, Ratnakumar A, Arendt M-L, et al. The genomic signature of dog domestication reveals adaptation to a starch-rich diet. Nature. 2013; 495: 360–4.
3. Grandjean D, Haymann F. Encyclopédie du chien Royal Canin. 2010.
4. Boillat CS, Gaschen FP, Hosgood GL. Assessment of the relationship between body weight and gastrointestinal transit times measured by use of a wireless motility capsule system in dogs. Am J Vet Res. 2010; 71: 898–902.
5. German AJ, Helps CR, Hall EJ, Day MJ. Cytokine mRNA expression in mucosal biopsies from German shepherd dogs with small intestinal enteropathies. Dig Dis Sci. 2000; 45: 7–17.
6. Osto M, Lutz TA. Translational value of animal models of obesity-Focus on dogs and cats. Eur J Pharmacol. 2015; 759: 240–52.
7. Raffan E, Dennis RJ, O'Donovan CJ, et al. A Deletion in the Canine POMC Gene Is Associated with Weight and Appetite in Obesity-Prone Labrador Retriever Dogs. Cell Metab. 2016; 23: 893–900.
8. Weber M. Influence of size on the dog's digestive function. Bul de l'Ac Vét de France. 2006; 327.
9. Morris JG, Rogers GR. Comparative aspects of nutrition and metabolism of dogs and cats. In: Nutrition of the dog and cat. Cambridge University Press. Cambridge; 1989: 35–66.
10. Kararli TT. Comparison of the gastrointestinal anatomy, physiology, and biochemistry of humans and commonly used laboratory animals. Biopharm Drug Dispos. 1995; 16: 351–80.
11. López Albors O, Rojo D, Sarriá R, Soria F, Pérez Cuadrado E, Latorre R. Morphometry of the canine intestine with reference to the use of double balloon endoscopy. Vet J. 2011; 190: 113–8.
12. Robin A. Les enterpathies excudatives chez le chien: actualités, diagnostiques et analyse retrospective de series de cas cliniques. [Lyon]: Université Claude Bernard; 2007.
13. Sarriá R, Latorre R, Henroteaux M, et al. Morphometric study of the layers of the canine small intestine at five sampling sites. Vet J. 2012; 192: 498–502.
14. Hart IR, Kidder DE. The quantitative assessment of normal canine small intestinal mucosa. Res Vet Sci. 1978; 25: 157–62.
15. Washabau RJ, Day MJ, Willard MD, et al. Endoscopic, biopsy, and histopathologic guidelines for the evaluation of gastrointestinal inflammation in companion animals. J Vet Intern Med. 2010; 24: 10–26.
16. Baum B, Meneses F, Kleinschmidt S, Nolte I, Hewicker-Trautwein M. Age-related histomorphologic changes in the canine gastrointestinal

tract: a histologic and immunohistologic study. World J Gastroenterol. 2007; 13: 152–7.
17. Feldman EJ, Dowling RH, McNaughton J, Peters TJ. Effects of oral versus intravenous nutrition on intestinal adaptation after small bowel resection in the dog. Gastroenterology. 1976; 70: 712–9.
18. Weber MP, Biourge VC, Nguyen PG. Digestive sensitivity varies according to size of dogs: a review. J Anim Physiol Anim Nutr (Berl). 2017; 101: 1–9.
19. Smeets-Peeters M, Watson T, Minekus M, Havenaar R. A review of the physiology of the canine digestive tract related to the development of in vitro systems. Nutrition Research Reviews. 1998; 11: 45–69.
20. Durand A. Entéropathies exsudatives chez le chien: proposition d'une stratégie thérapeutique diététique et médiacale. Université Claude Bernard; 2010.
21. Larmas M, Scheinin A. Studies on dog saliva. I. Some physico-chemical characteristics. Acta Odontol Scand. 1971; 29: 205–14.
22. de Godoy MRC, Vermillion R, Bauer LL, et al. In vitro disappearance characteristics of selected categories of commercially available dog treats. J Nutr Sci. 2014; 3: e47.
23. Lui CY, Amidon GL, Berardi RR, Fleisher D, Youngberg C, Dressman JB. Comparison of gastrointestinal pH in dogs and humans: implications on the use of the beagle dog as a model for oral absorption in humans. J Pharm Sci. 1986; 75: 271–4.
24. Yamada I, Haga K. Measurement of gastric pH during digestion of a solid meal in dogs. Chem Pharm Bull. 1990; 38: 1755–6.
25. Akimoto M, Nagahata N, Furuya A, Fukushima K, Higuchi S, Suwa T. Gastric pH profiles of beagle dogs and their use as an alternative to human testing. Eur J Pharm Biopharm. 2000; 49: 99–102.
26. Sagawa K, Li F, Liese R, Sutton SC. Fed and fasted gastric pH and gastric residence time in conscious beagle dogs. Journal of Pharmaceutical Sciences. 2009; 98: 2494–500.
27. Mahar KM, Portelli S, Coatney R, Chen EP. Gastric pH and Gastric Residence Time in Fasted and Fed Conscious Beagle Dogs using the Bravo® pH System. Journal of Pharmaceutical Sciences. 2012; 101: 2439–48.
28. Garcia-Mazcorro JF, Dowd SE, Poulsen J, Steiner JM, Suchodolski JS. Abundance and short-term temporal variability of fecal microbiota in healthy dogs. Microbiologyopen. 2012; 1: 340–7.
29. Koziolek M, Grimm M, Bollmann T, et al. Characterization of the GI transit conditions in Beagle dogs with a telemetric motility capsule. Eur J Pharm Biopharm. 2019; 136: 221–30.
30. Martinez M. Applying the biopharmaceutics classification system to veterinary pharmaceutical products Part II. Physiological considerations. Advanced Drug Delivery Reviews. 2002; 54: 825–50.
31. Mentula S, Harmoinen J, Heikkilä M, et al. Comparison between cultured small-intestinal and fecal microbiotas in beagle dogs. Appl Environ Microbiol. 2005; 71: 4169–75.
32. Kalantzi L, Persson E, Polentarutti B, et al. Canine Intestinal Contents vs. Simulated Media for the Assessment of Solubility of Two Weak Bases in the Human Small Intestinal Contents. Pharm Res. 2006; 23: 1373–81.
33. Smith HW. Observations on the flora of the alimentary tract of animals and factors affecting its composition. J Pathol. 1965; 89: 95–122.
34. Lidbury JA, Suchodolski JS, Ivanek R, Steiner JM. Assessment of the Variation Associated with Repeated Measurement of Gastrointestinal Transit Times and Assessment of the Effect of Oral Ranitidine on Gastrointestinal Transit Times Using a Wireless Motility Capsule System in Dogs. Veterinary Medicine International. 2012; 2012: 1–8.
35. Warrit K, Boscan P, Ferguson LE, et al. Minimally invasive wireless motility capsule to study canine gastrointestinal motility and pH. The Veterinary Journal. 2017; 227: 36–41.
36. Weber MP, Hernot D, Nguyen PG, Biourge VC, Dumon HJ. Effect of size on electrolyte apparent absorption rates and fermentative activity in dogs. J Anim Physiol Anim Nutr (Berl). 2004; 88: 356–65.
37. Beloshapka AN, de Godoy MRC, Detweiler KB, et al. Apparent total tract macronutrient digestibility, fecal characteristics, and fecal fermentative end-product concentrations of healthy adult dogs fed bioprocessed soy protein. J Anim Sci. 2016; 94: 3826–34.
38. Igarashi H, Ohno K, Matsuki N, et al. Analysis of fecal short chain fatty acid concentration in miniature dachshunds with inflammatory colorectal polyps. J Vet Med Sci. 2017; 79: 1727–34.
39. Cutrignelli MI, Bovera F, Tudisco R, et al. In vitro fermentation characteristics of different carbohydrate sources in two dog breeds (German shepherd and Neapolitan mastiff). J Anim Physiol Anim Nutr. 2009; 93: 305–12.
40. Sandri M, Dal Monego S, Conte G, Sgorlon S, Stefanon B. Raw meat-based diet influences faecal microbiome and end products of fermentation in healthy dogs. BMC Veterinary Research [Internet]. 2016 [cited 21 October 2019]; 13. Available at: http://bmcvetres.biomedcentral.com/articles/10.1186/s12917-017-0981-z
41. Eisenhauer L, Vahjen W, Dadi T, Kohn B, Zentek J. Effects of Brewer's spent grain and carrot pomace on digestibility, fecal microbiota, and fecal and urinary metabolites in dogs fed low- or high-protein diets1. J Anim Sci. 2019; 97: 4124–33.
42. Nogueira JPDS, He F, Mangian HF, Oba PM, De Godoy MRC. Dietary supplementation of a fiber-prebiotic and saccharin-eugenol blend in extruded diets fed to dogs. J Anim Sci. 2019; 97: 4519–31.
43. Oswald H, Sharkey M, Pade D, Martinez MN. Canine gastrointestinal physiology: Breeds variations that can influence drug absorption. European Journal of Pharmaceutics and Biopharmaceutics. 2015; 97: 192–203.
44. Contreras-Aguilar MD, Tecles F, Martínez-Subiela S, Escribano D, Bernal LJ, Cerón JJ. Detection and measurement of alpha-amylase in canine saliva and changes after an experimentally induced sympathetic activation. BMC Vet Res. 2017; 13: 266.
45. Iacopetti I, Perazzi A, Badon T, Bedin S, Contiero B, Ricci R. Salivary pH, calcium, phosphorus and selected enzymes in healthy dogs: a pilot study. BMC Vet Res. 2017; 13: 330.
46. Sanguansermsri P, Jenkinson HF, Thanasak J, et al. Comparative proteomic study of dog and human saliva. PLoS ONE. 2018; 13: e0208317.
47. Tecles F, Escribano D, Contreras-Aguilar MD, et al. Evaluation of adenosine deaminase in saliva and serum, and salivary α-amylase, in canine pyometra at diagnosis and after ovariohysterectomy. The Veterinary Journal. 2018; 236: 102–10.
48. Ricci R, Perazzi A, Badon T, Bedin S, Iacopetti I. Effect of storage on long-term stability of salivary α-amylase, lysozyme, lactate dehydrogenase, calcium and phosphorus in dogs. Vet J. 2018; 242: 44–7.
49. Hong H-R, Oh Y-I, Kim YJ, Seo K-W. Salivary alpha-amylase as a stress biomarker in diseased dogs. J Vet Sci. 2019; 20: e46.
50. Lavy E, Goldberger D, Friedman M, Steinberg D. pH Values and Mineral Content of Saliva in Different Breeds of Dogs. Israel Journal of Veterinary Medicine. 2012; 67: 244–2448.
51. Aspinall V. Anatomy and Physiology of the Dog and Cat **8. The Digestive System**. Veterinary Nursing Journal. 2004; 19: 94–9.
52. Ehrlein H-J, Pröve J. Effect of viscosity of test meals on gastric emptying in dogs. Exp Physiol. 1982; 67: 419–25.
53. Kienzle E. Enzyme activity in pancreatic tissue, intestinal mucosa and chyme of dogs in relation to age and diet. Journal of Animal Physiology and Animal Nutrition. 1988; 276–88.
54. Kakimoto T, Kanemoto H, Fukushima K, Ohno K, Tsujimoto H. Effect of a high-fat–high-cholesterol diet on gallbladder bile acid composition and gallbladder motility in dogs. American Journal of Veterinary Research. 2017; 78: 1406–13.
55. Madrid JA, Salido GM, Mañas M, Martinez de Victoria E, Mataix FJ. Use of a bidirectional cannula to study biliary secretion in conscious dogs. Lab Anim. 1983; 17: 307–10.
56. Nagahara T, Ohno K, Kanemoto H, et al. Effect of prednisolone administration on gallbladder emptying rate and gallbladder bile composition in dogs. American Journal of Veterinary Research. 2018; 79: 1050–6.
57. Larcheveque S. Etat des connaissances sur la mucocèle biliaire chez le chien: étude bibliographique. Faculté de médecine de Créteil; 2019.
58. Washizu T, Ishida T, Washizu M, Tomoda I, Kaneko JJ. Changes in bile acid composition of serum and gallbladder bile in bile duct ligated dogs. J Vet Med Sci. 1994; 56: 299–303.
59. Schmidt M, Unterer S, Suchodolski JS, et al. The fecal microbiome and metabolome differ between dogs fed Bones and Raw Food (BARF) diets and dogs fed commercial diets. Loor JJ, Ed. PLoS ONE. 2018; 13: e0201279.
60. Blake AB, Guard BC, Honneffer JB, Lidbury JA, Steiner JM, Suchodolski JS. Altered microbiota, fecal lactate, and fecal bile acids in dogs with gastrointestinal disease. Staley C, Ed. PLoS ONE. 2019; 14: e0224454.
61. Manchester AC, Webb CB, Blake AB, et al. Long-term impact of tylosin on fecal microbiota and fecal bile acids of healthy dogs. J Vet Intern Med. 2019; 33: 2605–17.
62. Guard BC, Honneffer JB, Jergens AE, et al. Longitudinal assessment of microbial dysbiosis, fecal unconjugated bile acid concentrations, and disease activity in dogs with steroid-responsive chronic inflammatory enteropathy. Journal of Veterinary Internal Medicine. 2019; 33: 1295–305.
63. Bickel M, Kauffman GL. Gastric gel mucus thickness: effect of distention, 16,16-dimethyl prostaglandin e2, and carbenoxolone. Gastroenterology. 1981; 80: 770–5.
64. Etienne-Mesmin L, Chassaing B, Desvaux M, et al. Experimental models to study intestinal microbes-mucus interactions in health and disease. FEMS Microbiol Rev. 2019; 43: 457–89.
65. Moon CD, Young W, Maclean PH, Cookson AL, Bermingham EN. Metagenomic insights into the roles of Proteobacteria in the

gastrointestinal microbiomes of healthy dogs and cats. MicrobiologyOpen. 2018; 7: e00677.
66. Weber M, Martin L, Biourge V, Nguyen P, Dumon H. Influence of age and body size on the digestibility of a dry expanded diet in dogs. J Anim Physiol Anim Nutr (Berl). 2003; 87: 21–31.
67. Nery J, Biourge V, Tournier C, et al. Influence of dietary protein content and source on fecal quality, electrolyte concentrations, and osmolarity, and digestibility in dogs differing in body size1. Journal of Animal Science. 2010; 88: 159–69.
68. Bednar GE, Murray SM, Patil AR, Flickinger EA, Merchen NR, Fahey GC. Selected animal and plant protein sources affect nutrient digestibility and fecal characteristics of ileally cannulated dogs. Arch Tierernahr. 2000; 53: 127–40.
69. Flickinger EA, Schreijen EMWC, Patil AR, et al. Nutrient digestibilities, microbial populations, and protein catabolites as affected by fructan supplementation of dog diets. Journal of Animal Science. 2003; 81: 2008–18.
70. Propst EL, Flickinger EA, Bauer LL, Merchen NR, Fahey GC. A dose-response experiment evaluating the effects of oligofructose and inulin on nutrient digestibility, stool quality, and fecal protein catabolites in healthy adult dogs. J Anim Sci. 2003; 81: 3057–66.
71. Hendriks WH, Thomas DG, Bosch G, Fahey GC. Comparison of ileal and total tract nutrient digestibility of dry dog foods. J Anim Sci. 2013; 91: 3807–14.
72. Zentek J, Fricke S, Hewicker-Trautwein M, Ehinger B, Amtsberg G, Baums C. Dietary protein source and manufacturing processes affect macronutrient digestibility, fecal consistency, and presence of fecal Clostridium perfringens in adult dogs. J Nutr. 2004; 134: 2158S-2161S.
73. Pinna C, Vecchiato CG, Bolduan C, et al. Influence of dietary protein and fructooligosaccharides on fecal fermentative end-products, fecal bacterial populations and apparent total tract digestibility in dogs. BMC Vet Res [Internet]. 2018 [cited 7 November 2019]; 14. Available at: https://www.ncbi.nlm.nih.gov/pmc/articles/PMC5859515/
74. Carrière F, Laugier R, Barrowman JA, Douchet I, Priymenko N, Verger R. Gastric and pancreatic lipase levels during a test meal in dogs. Scand J Gastroenterol. 1993; 28: 443–54.
75. Weber MP, Stambouli F, Martin LJ, Dumon HJ, Biourge VC, Nguyen PG. Influence of age and body size on gastrointestinal transit time of radiopaque markers in healthy dogs. American Journal of Veterinary Research. 2002; 63: 677–82.
76. Detweiler KB, He F, Mangian HF, Davenport GM, de Godoy MRC. Effects of high inclusion of soybean hulls on apparent total tract macronutrient digestibility, fecal quality, and fecal fermentative end-product concentrations in extruded diets of adult dogs. J Anim Sci. 2019; 97: 1027–35.
77. Hernot DC, Nery J, Biourge VC, Martin LJ, Dumon HJ, Nguyen PG. Colonic permeability is higher in Great Danes compared with smaller breed-dogs. J Anim Physiol Anim Nutr (Berl). 2009; 93: 703–9.
78. Weber MP, Martin LJ, Dumon HJ, Biourge VC, Nguyen PG. Influence of age and body size on intestinal permeability and absorption in healthy dogs. Am J Vet Res. 2002; 63: 1323–8.
79. Bjarnason I, MacPherson A, Hollander D. Intestinal permeability: an overview. Gastroenterology. 1995; 108: 1566–81.
80. Zentek J, Meyer H. Normal handling of diets--are all dogs created equal? J Small Anim Pract. 1995; 36: 354–9.
81. Meyer H, Zentek J, Habernoll H, Maskell I. Digestibility and compatibility of mixed diets and faecal consistency in different breeds of dog. Zentralbl Veterinarmed A. 1999; 46: 155–65.
82. Goudez R, Weber M, Biourge V, Nguyen P. Influence of different levels and sources of resistant starch on faecal quality of dogs of various body sizes. Br J Nutr. 2011; 106 Suppl 1: S211-215.
83. Rolfe V. Colonic fluid and electrolyte transport in health and disease. Vet Clin North Am Small Anim Pract. 1999; 29: 577–88, viii.
84. Neri M, Phillips SF, Fich A, Haddad AC. Canine ileocolonic sphincter: flow, transit, and motility before and after sphincterotomy. Am J Physiol. 1991; 260: G284-289.
85. Boscan P, Cochran S, Monnet E, Webb C, Twedt D. Effect of prolonged general anesthesia with sevoflurane and laparoscopic surgery on gastric and small bowel propulsive motility and pH in dogs. Vet Anaesth Analg. 2013; 41: 73–81.
86. Warrit K, Boscan P, Ferguson LE, Bradley AM, Dowers KL, Twedt DC. Effect of hospitalization on gastrointestinal motility and pH in dogs. Journal of the American Veterinary Medical Association. 2017; 251: 65–70.
87. Farmer AD, Wegeberg A-ML, Brock B, et al. Regional gastrointestinal contractility parameters using the wireless motility capsule: inter-observer reproducibility and influence of age, gender and study country. Aliment Pharmacol Ther. 2018; 47: 391–400.
88. Farmer AD, Ruffle JK, Hobson AR. Linaclotide increases cecal pH, accelerates colonic transit, and increases colonic motility in irritable bowel syndrome with constipation. Neurogastroenterol Motil. 2019; 31: e13492.
89. Bourreau J, Hernot D, Bailhache E, et al. Gastric emptying rate is inversely related to body weight in dog breeds of different sizes. J Nutr. 2004; 134: 2039S-2041S.
90. Dressman JB. Comparison of canine and human gastrointestinal physiology. Pharmaceutical Research. 1986; 3: 123–31.
91. Ménard O, Famelart M-H, Deglaire A, et al. Gastric Emptying and Dynamic In Vitro Digestion of Drinkable Yogurts: Effect of Viscosity and Composition. Nutrients. 2018; 10.
92. Hernot DC, Dumon HJ, Biourge VC, Martin LJ, Nguyen PG. Evaluation of association between body size and large intestinal transit time in healthy dogs. Am J Vet Res. 2006; 67: 342–7.
93. Balsa IM, Culp WTN, Drobatz KJ, Johnson EG, Mayhew PD, Marks SL. Effect of Laparoscopic-assisted Gastropexy on Gastrointestinal Transit Time in Dogs. J Vet Intern Med. 2017; 31: 1680–5.
94. Warrit K, Boscan P, Ferguson LE, et al. Minimally invasive wireless motility capsule to study canine gastrointestinal motility and pH. The Veterinary Journal. 2017; 227: 36–41.
95. Hernot DC, Biourge VC, Martin LJ, Dumon HJ, Nguyen PG. Relationship between total transit time and faecal quality in adult dogs differing in body size. J Anim Physiol Anim Nutr. 2005; 89: 189–93.
96. Hooda S, Minamoto Y, Suchodolski JS, Swanson KS. Current state of knowledge: the canine gastrointestinal microbiome. Animal Health Research Reviews. 2012; 13: 78–88.
97. Friedman ES, Bittinger K, Esipova TV, et al. Microbes vs. chemistry in the origin of the anaerobic gut lumen. Proc Natl Acad Sci U S A. 2018; 115: 4170–5.
98. Dewhirst FE, Klein EA, Thompson EC, et al. Correction: The Canine Oral Microbiome. Ravel J, Ed. PLoS ONE [Internet]. 2012 [cited 23 May 2022]; 7. Available at: https://dx.plos.org/10.1371/annotation/c2287fc7-c976-4d78-a28f-1d4e024d568f
99. Bell JA, Kopper JJ, Turnbull JA, Barbu NI, Murphy AJ, Mansfield LS. Ecological Characterization of the Colonic Microbiota of Normal and Diarrheic Dogs. Interdisciplinary Perspectives on Infectious Diseases. 2008; 2008: 1–17.
100. Niemiec BA, Gawor J, Tang S, Prem A, Krumbeck JA. The bacteriome of the oral cavity in healthy dogs and dogs with periodontal disease. Am J Vet Res. 2021; 83: 50–8.
101. Benno Y, Nakao H, Uchida K, Mitsuoka T. Impact of the advances in age on the gastrointestinal microflora of beagle dogs. J Vet Med Sci. 1992; 54: 703–6.
102. Xenoulis PG, Palculict B, Allenspach K, Steiner JM, Van House AM, Suchodolski JS. Molecular-phylogenetic characterization of microbial communities imbalances in the small intestine of dogs with inflammatory bowel disease. FEMS Microbiol Ecol. 2008; 66: 579–89.
103. Suchodolski JS, Dowd SE, Westermarck E, et al. The effect of the macrolide antibiotic tylosin on microbial diversity in the canine small intestine as demonstrated by massive parallel 16S rRNA gene sequencing. BMC Microbiol. 2009; 9: 210.
104. Suchodolski JS, Camacho J, Steiner JM. Analysis of bacterial diversity in the canine duodenum, jejunum, ileum, and colon by comparative 16S rRNA gene analysis. FEMS Microbiol Ecol. 2008; 66: 567–78.
105. Pilla R, Suchodolski JS. The Role of the Canine Gut Microbiome and Metabolome in Health and Gastrointestinal Disease. Front Vet Sci. 2020; 6: 498.
106. Vázquez-Baeza Y, Hyde ER, Suchodolski JS, Knight R. Dog and human inflammatory bowel disease rely on overlapping yet distinct dysbiosis networks. Nat Microbiol. 2016; 1: 16177.
107. Simon M. L'anxiété chez le chien, les répercussions sur le microbiote intestinal: intérêt de l'utilisation des probiotiques dans la prise en charge thérapeutique. [Internet]. [Toulouse]: Ecole Nationale Vétérinaire de Toulouse; 2019. Available at: https://oatao.univ-toulouse.fr/25833/
108. Kim H, Rather IA, Kim H, et al. A Double-Blind, Placebo Controlled-Trial of a Probiotic Strain Lactobacillus sakei Probio-65 for the Prevention of Canine Atopic Dermatitis. J Microbiol Biotechnol. 2015; 25: 1966–9.
109. Omatsu T, Omura M, Katayama Y, et al. Molecular diversity of the faecal microbiota of Toy Poodles in Japan. J Vet Med Sci. 2018; 80: 749–54.
110. Reddy KE, Kim H-R, Jeong JY, et al. Impact of Breed on the Fecal Microbiome of Dogs under the Same Dietary Condition. Journal of Microbiology and Biotechnology. 2019; 29: 1947–56.
111. Algya KM, Cross T-WL, Leuck KN, et al. Apparent total-tract macronutrient digestibility, serum chemistry, urinalysis, and fecal characteristics, metabolites and microbiota of adult dogs fed extruded, mildly cooked, and raw diets1. Journal of Animal Science. 2018; 96: 3670–83.

112. Swanson KS, Dowd SE, Suchodolski JS, et al. Phylogenetic and gene-centric metagenomics of the canine intestinal microbiome reveals similarities with humans and mice. ISME J. 2011; 5: 639–49.
113. Suchodolski JS. Companion animals symposium: microbes and gastrointestinal health of dogs and cats. J Anim Sci. 2011; 89: 1520–30.
114. Deng P, Swanson KS. Gut microbiota of humans, dogs and cats: current knowledge and future opportunities and challenges. Br J Nutr. 2015; 113: S6–17.
115. Albenberg L, Esipova TV, Judge CP, et al. Correlation between intraluminal oxygen gradient and radial partitioning of intestinal microbiota. Gastroenterology. 2014; 147: 1055-1063.e8.
116. Etienne-Mesmin L, Chassaing B, Desvaux M, et al. Experimental models to study intestinal microbes-mucus interactions in health and disease. FEMS Microbiol Rev. 2019; 43: 457–89.
117. Simpson KW, Dogan B, Rishniw M, et al. Adherent and invasive Escherichia coli is associated with granulomatous colitis in boxer dogs. Infect Immun. 2006; 74: 4778–92.
118. Cassmann E, White R, Atherly T, et al. Alterations of the Ileal and Colonic Mucosal Microbiota in Canine Chronic Enteropathies. Isaacson RE, Ed. PLoS ONE. 2016; 11: e0147321.
119. Garcia-Mazcorro JF, Minamoto Y, Kawas JR, Suchodolski JS, de Vos WM. Akkermansia and Microbial Degradation of Mucus in Cats and Dogs: Implications to the Growing Worldwide Epidemic of Pet Obesity. Vet Sci. 2020; 7.
120. Andoh A. Physiological Role of Gut Microbiota for Maintaining Human Health. Digestion. 2016; 93: 176–81.
121. Guard BC, Suchodolski JS. HORSE SPECIES SYMPOSIUM: Canine intestinal microbiology and metagenomics: From phylogeny to function1. Journal of Animal Science. 2016; 94: 2247–61.
122. Mondo E, Marliani G, Accorsi PA, Cocchi M, Di Leone A. Role of gut microbiota in dog and cat's health and diseases. Open Vet J. 2019; 9: 253–8.
123. Hughes R, Magee EA, Bingham S. Protein degradation in the large intestine: relevance to colorectal cancer. Curr Issues Intest Microbiol. 2000; 1: 51–8.
124. Ephraim E, Cochrane C-Y, Jewell DE. Varying Protein Levels Influence Metabolomics and the Gut Microbiome in Healthy Adult Dogs. Toxins (Basel). 2020; 12.
125. Giffard CJ, Collins SB, Stoodley NC, Butterwick RF, Batt RM. Administration of charcoal, Yucca schidigera, and zinc acetate to reduce malodorous flatulence in dogs. J Am Vet Med Assoc. 2001; 218: 892–6.
126. Collins SB, Perez-Camargo G, Gettinby G, Butterwick RF, Batt RM, Giffard CJ. Development of a technique for the in vivo assessment of flatulence in dogs. Am J Vet Res. 2001; 62: 1014–9.
127. Zentek J, Hall EJ, German A, et al. Morphology and immunopathology of the small and large intestine in dogs with nonspecific dietary sensitivity. J Nutr. 2002; 132: 1652S-4S.
128. Deschamps C, Denis S, Humbert D, et al. In vitro models of the canine digestive tract as an alternative to in vivo assays: Advances and current challenges. ALTEX. 2022.

Appendix 4 – Original article in Microbiology Spectrum

ETIENNE-MESMIN, L., MESLIER, V., URIOT, O., FOURNIER, E., DESCHAMPS, C., DENIS, S., DAVID, A., JEGOU, S., MORABITO, C., QUINQUIS, B., THIRION, F., PLAZA OÑATE, F., LE CHATELIER, E., EHRLICH, S.D., BLANQUET-DIOT, S., *ET AL.* (**2023**) *In vitro* Modelling of Oral Microbial Invasion in the Human Colon. *Microbiology Spectrum*, e04344-22. https://doi.org/10.1128/spectrum.04344-22

AMERICAN SOCIETY FOR MICROBIOLOGY | Microbiology Spectrum

RESEARCH ARTICLE

In Vitro Modelling of Oral Microbial Invasion in the Human Colon

Lucie Etienne-Mesmin,[a] Victoria Meslier,[b] Ophélie Uriot,[a] Elora Fournier,[a] Charlotte Deschamps,[a] Sylvain Denis,[a] Aymeric David,[b] Sarah Jegou,[b] Christian Morabito,[b] Benoit Quinquis,[b] Florence Thirion,[b] Florian Plaza Oñate,[b] Emmanuelle Le Chatelier,[b] S. Dusko Ehrlich,[b] Stéphanie Blanquet-Diot,[a] Mathieu Almeida[b]

[a]UMR 454 UCA-INRAE Microbiologie Environnement DIgestif et Santé (MEDIS), Université Clermont Auvergne, Clermont-Ferrand, France
[b]Université Paris-Saclay, INRAE, MetaGenoPolis (MGP), Jouy-en-Josas, France

Lucie Etienne-Mesmin and Victoria Meslier contributed equally to this work. Author order was determined alphabetically.

ABSTRACT Recent advances in the human microbiome characterization have revealed significant oral microbial detection in stools of dysbiotic patients. However, little is known about the potential interactions of these invasive oral microorganisms with commensal intestinal microbiota and the host. In this proof-of-concept study, we proposed a new model of oral-to-gut invasion by the combined use of an *in vitro* model simulating both the physicochemical and microbial (lumen- and mucus-associated microbes) parameters of the human colon (M-ARCOL), a salivary enrichment protocol, and whole-metagenome shotgun sequencing. Oral invasion of the intestinal microbiota was simulated by injection of enriched saliva in the *in vitro* colon model inoculated with a fecal sample from the same healthy adult donor. The mucosal compartment of M-ARCOL was able to retain the highest species richness levels over time, while species richness levels decreased in the luminal compartment. This study also showed that oral microorganisms preferably colonized the mucosal microenvironment, suggesting potential oral-to-intestinal mucosal competitions. This new model of oral-to-gut invasion can provide useful mechanistic insights into the role of oral microbiome in various disease processes.

IMPORTANCE Here, we propose a new model of oral-to-gut invasion by the combined use of an *in vitro* model simulating both the physicochemical and microbial (lumen- and mucus-associated microbes) parameters of the human colon (M-ARCOL), a salivary enrichment protocol, and whole-metagenome shotgun sequencing. Our study revealed the importance of integrating the mucus compartment, which retained higher microbial richness during fermentation, showed the preference of oral microbial invaders for the mucosal resources, and indicated potential oral-to-intestinal mucosal competitions. It also underlined promising opportunities to further understand mechanisms of oral invasion into the human gut microbiome, define microbe-microbe and mucus-microbe interactions in a compartmentalized fashion, and help to better characterize the potential of oral microbial invasion and their persistence in the gut.

KEYWORDS oral microbial invasion, gut microbiota, mucus, M-ARCOL, metagenomics, oral microbiota

The human gastrointestinal (GI) tract harbors a vast and complex community including between 10 trillion and 100 trillion microbes dominated by bacteria, collectively referred to as the gut microbiota (1). The gut microbiota plays a major role in host physiology, with an involvement in energy extraction from food, vitamin synthesis, maturation of the immune system, and protection against invasion by enteric pathogens (2, 3). In the human body, oral and GI microbiomes represent the two largest microbial ecosystems (4, 5), and pioneering data from the Human Microbiome

Editor Diyan Li, Chengdu University

Address correspondence to Mathieu Almeida, mathieu.almeida@inrae.fr, or Stéphanie Blanquet-Diot, stephanie.blanquet@uca.fr.

The authors declare no conflict of interest.

Received 24 October 2022
Accepted 5 March 2023

Project demonstrated that they are taxonomically diverse, representing 26% and 29% of total bacteria from the human body, respectively (6).

Studies have shown that saliva contains approximately 10^7 to 10^9 bacteria per milliliter (7, 8), with a global diversity of approximately 700 species listed from the oral cavity of healthy subjects. These species are members of *Firmicutes*, *Proteobacteria*, *Bacteroidetes*, *Actinobacteria*, *Fusobacteria*, *Spirochaetes*, *Synergistetes*, and TM7 (5, 9). *Streptococcus* is the most abundant genus in the oral site, with *Haemophilus*, *Veillonella*, and *Prevotella* also prevalent (5, 10, 11). Countless studies have demonstrated that microbiota composition distinctively changes all along the GI tract due to differences in term of oxygenation, substrate availability, pH, and residence time between digestive compartments, therefore inducing microbial species niche preferences (12). The highest bacterial load (10^{11} to 10^{12} bacteria per g) and diversity are reached in the colon, where predominant phyla are *Bacteroidetes*, *Firmicutes*, *Actinobacteria*, and, to a lesser extent, *Proteobacteria* and *Verrucomicrobia* (13–16). It is now well established that each individual harbors a unique gut microbiota composed of an estimated 300 bacterial species detected per healthy individual on average (17–19).

Despite physical distance and chemical hurdles that keep apart the oral microbiome from the gut microbiome, cumulative evidence supports the notion that the oral microbiota is present in the overall gut microbial ecosystem. Li et al. demonstrated that transplantation of human saliva to gnotobiotic mice led to a distribution of oral genera throughout the GI tract, with *Fusobacterium*, *Haemophilus*, *Streptococcus*, and *Veillonella* being especially abundant in the gut of recipient mice (20). In humans, independent studies have demonstrated that some bacterial genera detected in the same healthy subject can overlap between oral and stool samples, confirming an extensive transmission of microbes through the GI tract (11, 21). Such a phenomenon of oral-gut transmission occurring under physiological conditions seems to be amplified in a pathological context. Orally derived microorganisms are particularly enriched in patients with altered gut microbiota (perturbation termed dysbiosis) and barrier disruption. In particular, Hu and colleagues showed that oral bacteria are enriched in the fecal microbiota of Crohn's disease patients (22), suggesting that the oral cavity might act as a reservoir of opportunistic pathogens with the ability to colonize the gut (23), even more important in such susceptible hosts. Likewise, a large fraction of species enriched in the fecal microbiota of patients with liver cirrhosis or after bariatric surgery are of oral origin (24, 25).

To date, the interconnections between oral and gut microbiota have not been fully elucidated and mechanisms associated with the gut colonization by oral bacteria are not clear. This can be explained by (i) the technical difficulties met when analyzing oral microbial samples with high-resolution shotgun metagenomic sequencing, due to the high proportions of retrieved host DNA, and (ii) the lack of relevant models. Clinical trials remain the gold standard approaches but are hampered by heavy regulatory, technical, and costly constraints. For evident ethical reasons, human gut microbiota studies are usually performed with fecal samples, making result interpretation difficult since direct access to the different segments of the GI tract—especially the colon—is limited. Animal models integrate host-microbe interactions, but translation to the human situation remains limited due to major differences of digestive physiology and the oral and gut microbiotas between most animal models and humans.

A relevant alternative in preclinical studies involves the use of an *in vitro* model simulating the human digestive environment. *In vitro* models permit accurate reproduction of the complexity and diversity of the *in vivo* microbial ecosystem (26–28) and were recently optimized to incorporate mucin beads leading to mucosal configuration of the models, i.e., mucosal simulator of the human intestinal microbial ecosystem (M-SHIME) and Mucosal ARtificial COLon (M-ARCOL) (13, 28–32). In the present study, we investigated oral-to-gut microbial invasion by using the M-ARCOL. Our main goal was to validate our experimental approach using shotgun metagenomic analysis of stools

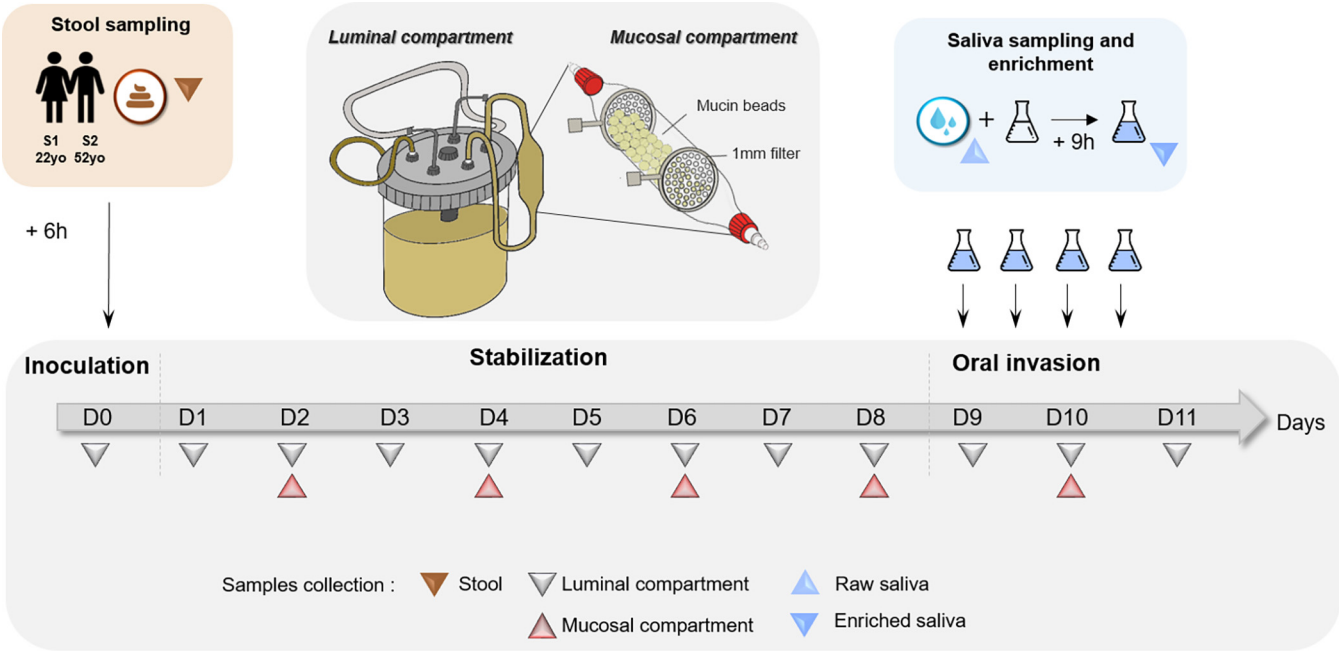

FIG 1 Experimental workflow for *in vitro* fermentation setup and oral invasion. Fresh stool samples from two healthy donors (S1 and S2) were used to inoculate two independent M-ARCOL bioreactors. Each fermentation was conducted for a total period of 11 days, including 24 h of batch amplification and 10 days of continuous fermentation. After an 8-day stabilization period, oral-to-gut invasion was simulated by injecting a 9-h enriched saliva from the same donor, twice a day and for 2 consecutive days (morning and late afternoon of days 9 and 10). Samples were collected from fresh stools (brown triangle), the luminal compartment of the bioreactor every day (gray triangle), and the mucosal compartment every 2 days (red triangle), as were raw saliva and enriched saliva samples (blue triangle) for each donor.

and saliva samples from healthy donors and to assess the effects of oral microbial invasion on the luminal and mucosal microenvironments in the simulated human colon.

RESULTS

Development of a novel experimental design for oral-to-gut invasion in M-ARCOL bioreactors. In this study, we developed an oral-to-gut invasion model using a one-stage fermentation system (M-ARCOL) setup to reproduce the main physicochemical parameters (pH, temperature, transit time, nutrient availability) found in the human colon (Fig. 1). M-ARCOL bioreactors, composed of two compartments used to mimic the luminal and mucosal microenvironments, were inoculated with fecal samples from two healthy adults. This study was conducted on fecal samples collected from two healthy donors, chosen to represent "extreme" conditions based on their sex, age, and nutritional habits: donor S1 is a methane producer female (age, 22 years; flexitarian-based (neo vegetarian) diet), while donor S2 is a non-methane producer male (age, 52 years; omnivorous diet). Gas analysis confirmed that anaerobic conditions were efficiently maintained in the bioreactors by the sole metabolic activity of the gut microbiota without gas flushing, which constitutes a main feature of the M-ARCOL model compared to other colonic *in vitro* models (see Fig. S1A and B in the supplemental material). Notably, methane production was detected for one of the donors, indicating the presence of methanogenic microorganisms. The three main short-chain fatty acids (SCFAs; acetate, butyrate, and propionate) were also measured in the luminal compartment with ratio similar to that found *in vivo* in the human colon, as previously validated (28) (Fig. S1B and C). To allow a combined oral invasion experiment and shotgun sequencing on human saliva samples, we generated enriched microbial saliva samples and inoculated them at days 9 and 10 in the luminal phase of M-ARCOL to evaluate oral-to-gut microbial invasion after gut microbial stabilization in the bioreactors (Fig. 1). DNA was extracted from all collected samples and subjected to shotgun metagenomic sequencing. All samples from fecal origins (raw stool and luminal and mucosal samples from the M-ARCOL) displayed high mapping rates onto the IGC2 gut gene

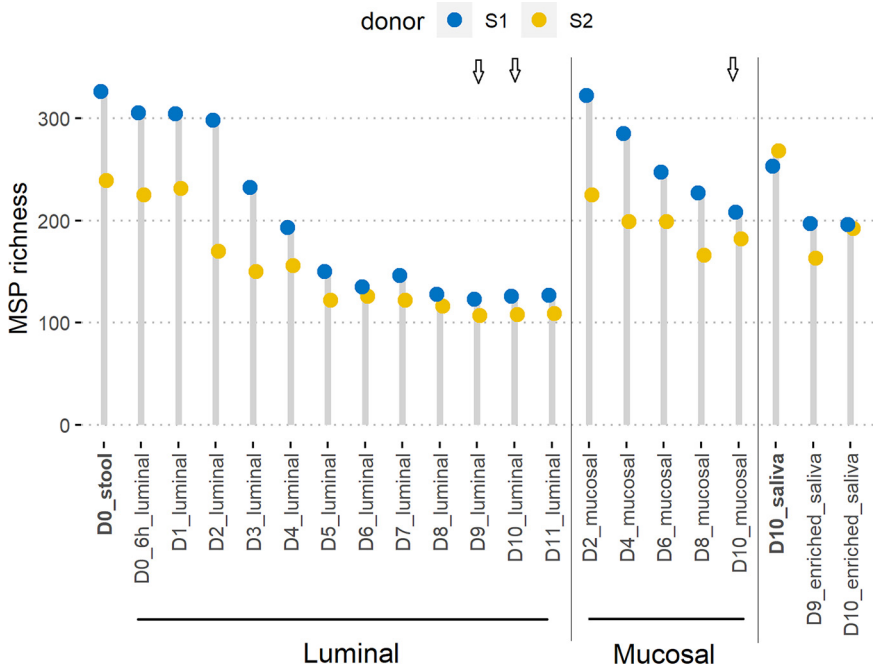

FIG 2 Dot chart for MSP richness dynamic over time. Metagenomic species pangenome (MSP) species richness was calculated as the number of detected MSP species in the corresponding sample for donors S1 and S2 on the merged MSP abundance table, for luminal and mucosal compartments of the M-ARCOL and for raw saliva and enriched-saliva samples. In bold are indicated initial raw stool and saliva samples. Times of fermentation in the colonic M-ARCOL model are indicated in days (D). Arrows indicate saliva injection into the bioreactors on days 9 and 10.

catalogue (median rates > 80%) but not onto the oral catalogue (median near 5%). Salivary samples displayed high mapping rates onto the oral microbial gene catalogue (median > 79%) and less than 40% mapping rates onto the gut microbial gene catalogue (Fig. S2 and Table S1). Profiles of atmospheric gases and luminal SCFAs were not modified by addition of enriched saliva (Fig. S1).

The mucosal microenvironment retained higher microbial richness during *in vitro* fermentation. We determined the metagenomic species pangenome (MSP) richness, defined as clusters of coabundant genes and representative of microbial species, over time and in the different compartments of the M-ARCOL (Fig. 2). For both donors, initial stool and raw saliva samples displayed the highest MSP species richness compared to the bioreactor samples. During *in vitro* fermentations, we observed a loss of richness in the luminal and mucosal compartments, until a stabilization at day 5 in the luminal compartment for both donors. Consistent with fecal MSP richness, donor S1 displayed a higher MSP richness during the first days of fermentation in the luminal and mucosal compartments than did donor S2 (delta of 87 and 15 MSP between donors S1 and S2 for stool and raw saliva, respectively). After MSP species richness equilibrium and until the end of the experiment, MSP richness levels were almost equivalent between the two donors in the luminal compartment (delta of 18 MSP at day 11), and individual microbial signature was maintained, as estimated from Bray-Curtis distance measures (Fig. S3). In the mucosal compartment, MSP richness was found to be systematically higher than the luminal one at each time point for both donors. The richness loss observed was thus lesser and slower all along the process. The MSP stool richness difference between the donors persisted longer (until at least day 8) in the mucosal compartment than in the luminal one (delta of 12 MSP in the luminal and 61 MSP in the mucosal compartment for donors S1 and S2 at day 8). The MSP species richnesses were found to be equivalent between donors S1 and S2 in raw saliva samples (delta of 15 MSP), and they decreased in enriched saliva of both donors at days 9 and 10 (delta of 4 MSP between donors S1 and S2 at day 10).

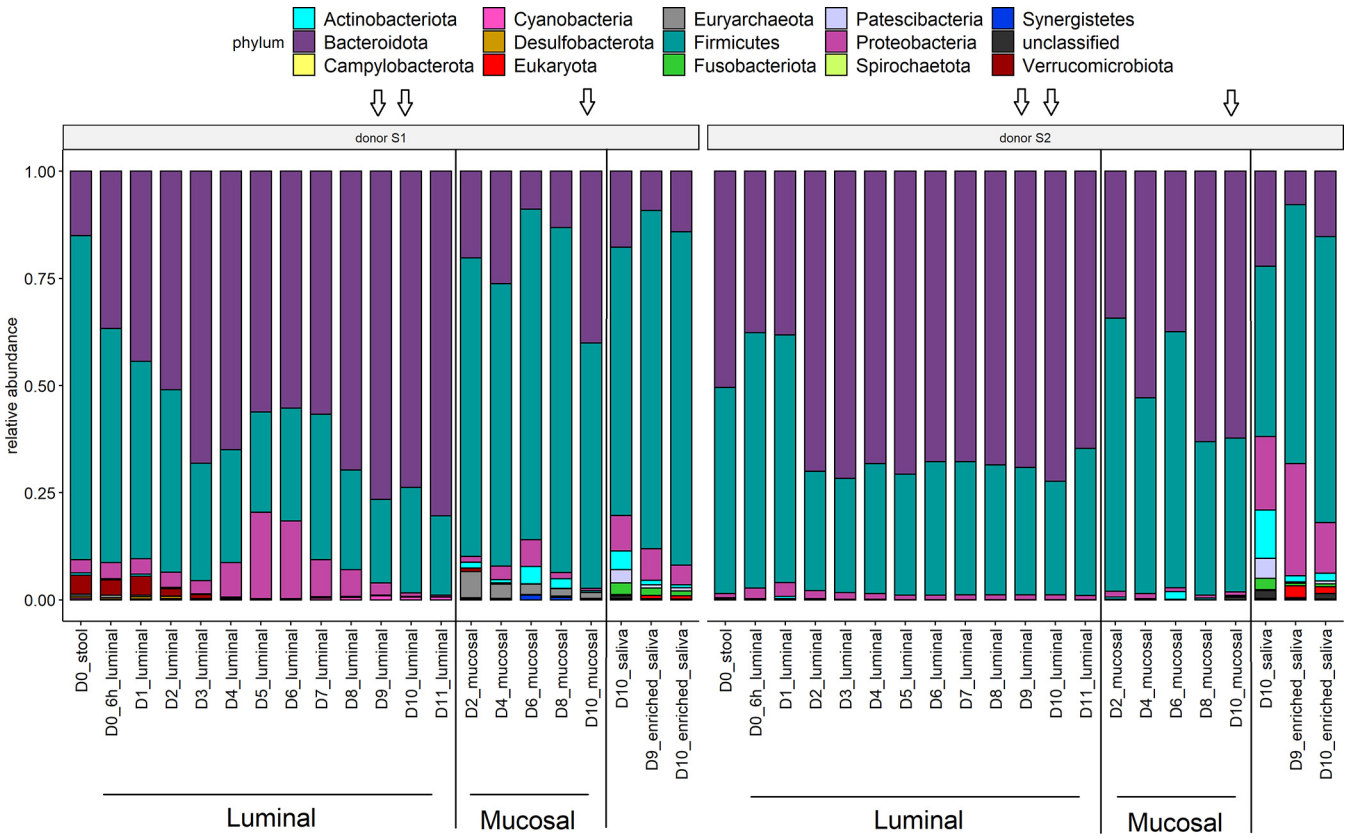

FIG 3 Phylum rank normalized composition per donor. MSP species abundance was normalized per sample by dividing its abundance by the sum of the MSP species abundances detected in the sample. Phylum rank composition was calculated as the sum of the normalized abundances of the corresponding MSP species. Donors (S1 or S2), M-ARCOL compartments (luminal and mucosal), and the days of fermentation are reported. Arrows indicate saliva injection into the bioreactors on days 9 and 10.

Differential microbial compositions between stool, salivary, luminal, and mucosal samples. Based on Bray-Curtis dissimilarity distance, the overall stool, luminal, and mucosal compositions appeared quite close for a given individual and contrasted between the two donors, which was also observed in the salivary microbiota (Fig. S3). Indeed, we found that samples clustered together by donor and sample type but also by time points. After the injection of saliva into the bioreactors on days 9 and 10, the luminal and mucosal samples collected were not distant from the same-donor fecal samples, suggesting that dominant microbial compositions were not drastically modified by the oral microbial administration. We also observed that raw saliva and enriched saliva clustered together for each donor, confirming their close microbial compositions.

We analyzed the composition of saliva, luminal, and mucosal microbial communities in the M-ARCOL at the phylum (Fig. 3) and family (Fig. S4) ranks. At the phylum rank, we found a dominance of *Firmicutes* and *Bacteroidetes* followed by *Proteobacteria*, with some differences between the two donors or between compartments. Main families included *Bacteroidaceae*, *Rikenellaceae*, and *Prevotellaceae* (*Bacteroidetes*) across samples and *Ruminococcaceae* and *Streptococcaceae* (*Firmicutes*) for fecal and oral samples, respectively. Stool of donor S1 was dominated by *Firmicutes* (0.75 relative abundance), and stool of donor S2 contained equivalent levels of *Bacteroidetes* and *Firmicutes* (0.5 and 0.47 relative abundances, respectively). While the ratio between *Firmicutes* and *Bacteroidetes* was modified in the luminal compartment over time, the primary ratio for these taxa observed in stool samples was globally maintained in mucosal samples, particularly for donor S2. An additional phylum was the *Verrucomicrobiota* phylum (including *Akkermansia muciniphila*), detected in the two donors in the luminal compartment but at higher levels in donor S1 (100 times more; maximum relative abundance of 0.04). The *Euryarchaeota*

phylum (*Methanobrevibacter smithii* species), detected exclusively in donor S1, consistent with methane detection in gas analyses (Fig. S1A), was found in low relative abundance in stool and the luminal compartment (relative abundance of $<$0.01) but was identified in higher levels in the mucosal samples already at day 2 (relative abundance between 0.01 and 0.06). Members of the *Actinobacteriota* phylum (mainly of the *Micrococcaceae*, *Bifidobacteriaceae*, and *Actinomycetaceae* families) were found in higher relative abundances in the mucosal and salivary samples (up to 0.02), were low in stool samples (below 0.01), and decreased for donor S1 after the oral-to-intestinal invasion. In salivary samples, ratios of *Firmicutes* to *Bacteroidetes* were found close to those observed in fecal samples for both donors, with additional phyla detected in these samples, such as higher levels of *Proteobacteria*, *Fusobacteria*, *Patescibacteria*, and *Actinobacteriota*. No major changes in raw or enriched saliva samples were found for either donor, as confirmed by Bray-Curtis dissimilarity analysis (Fig. S3).

A few oral microbial species are present in the luminal and mucosal compartments of the M-ARCOL before oral invasion. To evaluate the impact of the oral-to-gut invasion on the M-ARCOL microbial composition, we assigned the species to their preferred ecological niche, using their occurrence in raw stools or saliva samples, and three species types were defined as gut, oral, or not determined (ND; species that were either undetected in raw stool and raw saliva samples or detected in both stool and saliva samples before inoculation of the bioreactor at the initial time point [T0] [Table S2]). We then analyzed the niche distribution to assess the number of oral species before and after the invasion in the luminal and mucosal compartments (Fig. 4) and the relative abundance of each ecological niche (Fig. S5 and Table S3). Raw stools were exclusively dominated by gut-oriented MSP species and ND species, with no oral-oriented MSP species detected for either donor, and raw saliva was dominated exclusively by oral-oriented MSP species and ND species (Fig. 4, Fig. S5, and Table S3). Before oral-to-gut invasion, a dominance of oral-oriented species was observed in enriched saliva samples, yet four and seven ND MSP species were detected, respectively, in donors S1 and S2 (Fig. 4, Fig. S5, and Table S3).

Following stool inoculation of the bioreactor, luminal and mucosal compartments were largely dominated by gut MSP species, yet two oral MSP species were detected before simulated oral-to-gut invasion (Fig. 4 and Table S3). For donor S1, these oral MSP species were detected in luminal and mucosal samples (msp_0616 *Prevotella buccae* and msp_1193 *Dialister pneumosintes*), raising to up to a fourth of the relative abundance at day 8 in the luminal sample but remaining at low relative abundance (0.01) in the mucosal sample before oral-to-gut invasion. For donor S2, only one MSP species (msp_0616 *Prevotella buccae*) was detected in the luminal compartment (Fig. S5). Oral MSP species were nondominant, either by number or relative abundance, at day 8 in the mucosal compartment of the 2 donors before oral-to-gut invasion.

Preference of oral microbial invaders for the mucosal microenvironment. After the injection of enriched saliva in the system, we found only three oral MSP species in the luminal compartments of both donors at days 9 and 10 (msp_0616 *Prevotella buccae*, msp_0677c *Slackia exigua*, and msp_0884 *Veillonella atypica*) (Fig. 5); these low numbers persisted at day 11. In contrast, a much higher number (n = 28) was detected in the mucosal microenvironment of both donors, representing about 15% of the enriched saliva microbial diversity. Similar numbers of oral MSP species were found for donors S1 and S2 in the mucosal samples (17 and 20 oral MSP species, respectively), but their relative abundances differed between donors (relative abundances of 0.13 and 0.0043, respectively [Fig. S5]). These oral species invaders belonged to a limited number of taxa, with members of the genera *Veillonella*, *Streptococcus*, *Prevotella*, and *Haemophilus*, all common taxa of the oral microbiome (Fig. 5). Additional common taxa included *Porphyromonas*, *Neisseria* and *Rothia* genera. We also observed that the relative abundance of these 28 oral invaders in the mucosal microenvironment was not systematically related to their respective abundance in enriched saliva samples (rho Spearman, 0.21 and 0.88 for donors S1 and S2, respectively, between enriched

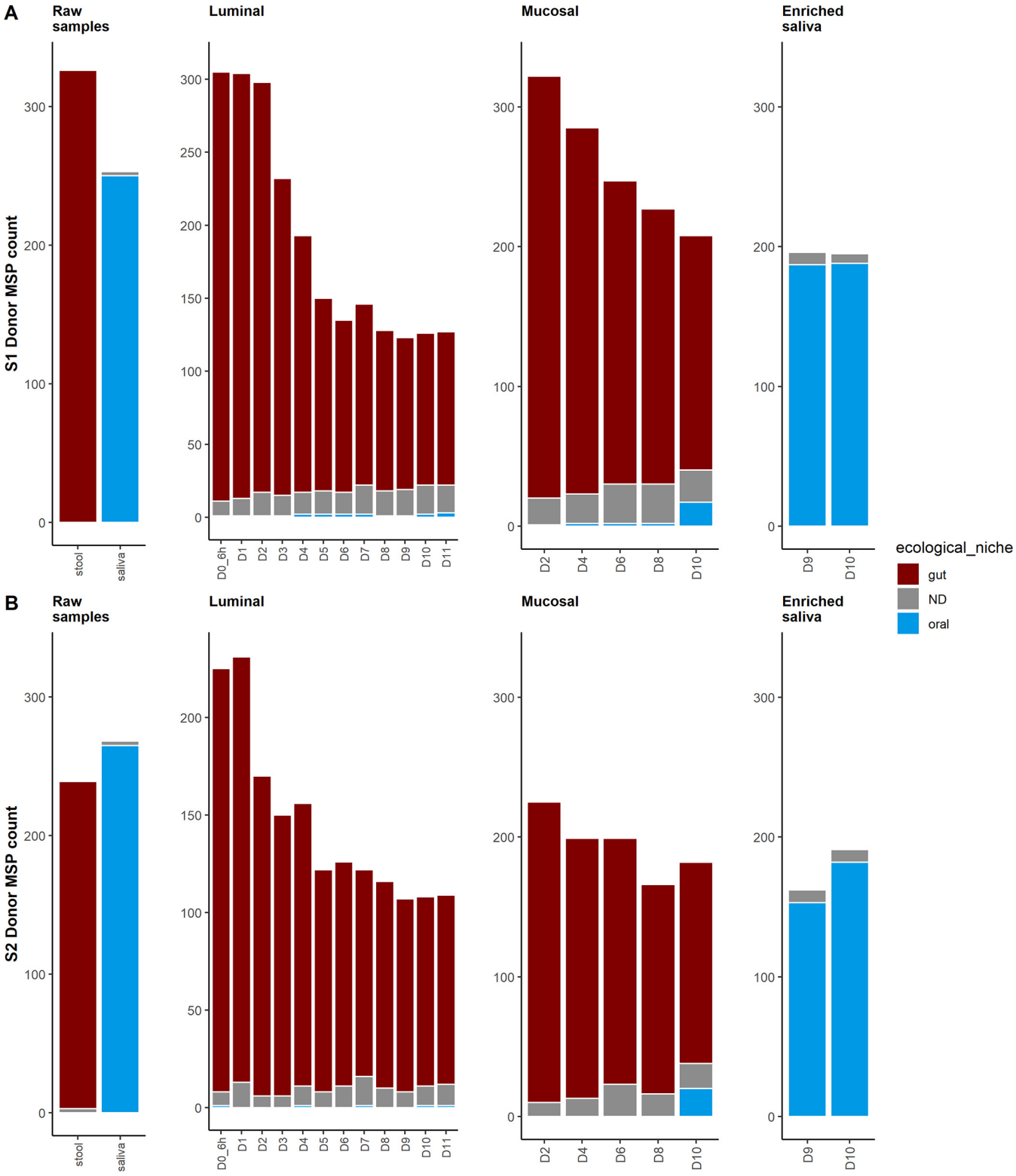

FIG 4 MSP species richness of oral-to-gut invasion using species ecological niche. MSP species richness was split by their corresponding ecological niche, namely, the dominant ecological ecosystem. (A) donor S1; (B) donor S2. Times of fermentation in the colonic M-ARCOL model are indicated in days.

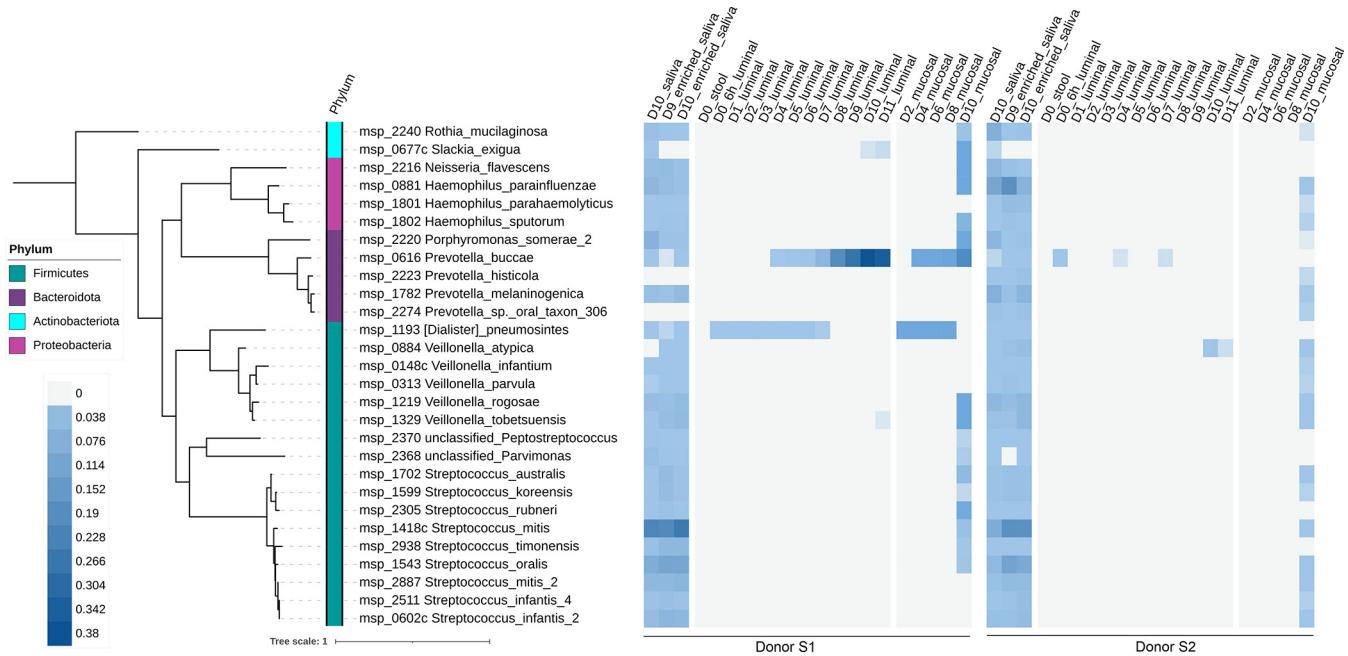

FIG 5 Phylogenetic tree for oral MSP species during oral-to-gut invasion. Shown is the phylogenetic tree for 28 oral MSP species detected in the initial stools and the luminal and mucosal samples from M-ARCOL, regardless of the raw and enriched saliva composition. The tree was generated using the 40 universal marker proteins from the oral MSP species extracted by the fetchMG software. For each of donors S1 and S2, a heat map for the oral MSP species normalized abundance is shown, with a color shade from gray (not detected) to dark blue (highly detected; maximum relative abundance = 0.38). Times of fermentation in the colonic M-ARCOL model are indicated in days.

saliva and mucosal at day 10; *P* values = 0.28 and $<$ 1.5e$-$9). At the end of the experiment (day 11), only three and one oral invader species were detected, respectively, for donors S1 and S2 in the luminal compartment (Fig. 5).

DISCUSSION

Here, we present a new model for oral-to-gut microbial invasion simulation using the M-ARCOL bioreactor and whole-metagenome sequencing, with the goal to provide a tool for a comprehensive understanding of the interactions of these two microbial ecosystems of the gastrointestinal tract. This experimental setup was motivated by the growing body of evidence for the oral microbial communities' impact on the gut microbiome composition and its potential effect on human health (22, 24, 33, 34). The new model consists of a colonic bioreactor inoculated with fecal samples from healthy adult donors, used to follow daily microbial changes for 11 days, combined with a simulated oral invasion by injecting enriched saliva on days 9 to 10. A shotgun metagenomics-based analysis was essential to achieve species-level resolution, to differentiate closely related species originating from the oral or gut ecosystem. This study also required a combined salivary and fecal *in silico* microbial exploration of two healthy donors with distinct fecal microbial compositions: *Firmicutes* dominance for donor S1 and *Bacteroidetes* dominance for donor S2. Since fecal microbiota interindividual variability is important, this pilot study was carried out on fecal samples collected from two healthy donors known to represent different conditions in terms of fecal microbial composition, methane-producing status, age (S1, 22 years; S2, 52 years), and dietary habits (S1, flexitarian (neo vegetarian) diet; S2, omnivorous diet). Lastly, we assessed the oral-to-gut microbial interactions using the mucosal configuration of the ARCOL *in vitro* gut model (28), providing a unique opportunity to independently investigate lumen- and mucosa-associated microbial communities, thanks to a distinct capture of the fine-scale regionalization of the human colon (28).

One key aspect of our investigation was to retrieve enough salivary material to perform both the oral injection into the bioreactor and the microbial DNA extraction for

shotgun metagenomic analysis. To circumvent a relatively small amount of saliva biomass, we performed a microbial saliva enrichment step prior to oral injection. While this enrichment reduced somewhat the oral microbial richness, a major part was retained (70%), with a composition close to that of the raw saliva, thus preserving the oral microbial signatures of the two donors. We also observed that the human DNA was still detected after saliva enrichment. We hypothesize that human DNA remained during enrichment by the formation of microbial aggregates seeding upon human salivary mucosa and associated host cells, as recently observed by Simon-Soro and colleagues (35). Interestingly, we found that, whatever the donor, the mucosal compartment of the M-ARCOL system enabled the subsistence of a higher microbial richness than the luminal one (28, 36, 37). This highlights the critical contribution of the mucosal setup in microbial dynamic analysis based on colonic *in vitro* models and supports the underestimated role of the mucus in many physiological and pathological processes involving the gut microbiome (38–40).

Using the microbial species ecological niche predisposition (gut or oral), we explored the number and amount of oral microbial species in the luminal and mucosal compartments of the M-ARCOL before and after simulated oral invasion. As expected, variations of oral microbial species after invasion were detected, indicating that the protocol design was successful in emulating the two microbial ecosystems. While the two donors displayed different raw oral and fecal microbial compositions, it was observed that oral invasion mostly occurred in the mucosal compartment and was limited in the luminal one for both donors. This suggests invasive oral species preference for the intestinal mucosal resources and that abundance of oral invaders alone, but likely the species-specific phenotypes, permitted bacteria to invade the mucosa. Interestingly, the oral invaders were all members of common salivary microbiota, as part of the healthy oral core microbiome (41–44). These results suggest that some oral species might possess functions to utilize MUC-2 proteins from the gut (45). We also observed for donor S1 a significant increase and resilience of several oral species prior to the simulated oral invasion, indicating that subabundant oral species present in stool samples could surge when appropriate conditions occurred, such as a decrease in gut microbial richness (19, 46).

The main objectives of the current study were to test the feasibility of the experimental approach to simulate oral microbial invasion in the intestinal compartment and the efficiency of the saliva enrichment. Our study demonstrates promising opportunities to (i) further understand mechanisms of oral microbial invasion of the human gut microbiome (5, 47), (ii) define microbe-microbe interactions in a compartmentalized fashion (luminal versus mucosal), and (iii) eventually help to clarify the potential impact of oral invasion on human health (20, 48). Future developments could include the implementation of an upper *in vitro* human digestive tract by coupling the M-ARCOL bioreactor with the TIM-1 stomach and small intestinal digester (30, 49, 50). This would allow the combined determination of oral microbiota survival and oral-to-intestinal microbial interactions. Moreover, it would be needed to study the invasion of oral microbes in the *in vitro* M-ARCOL model for a longer period to shed new light on long-term invasion outcomes. Several studies have shown that orally derived bacteria can colonize and persist better within the gut under diseased conditions (5, 23, 24, 33). Colon *in vitro* gut models, including the M-ARCOL, can be advantageously adapted to mimic pathological situations associated with gut microbial dysbiosis, such as obesity (51, 52), irritable bowel syndrome (53), and inflammatory bowel disease (54, 55). This can be performed by inoculating them with fecal samples from patients but also adapting all the nutritional and physicochemical parameters to the diseased situations (28, 50). Understanding the correlation of the oral-gut microbiome axis in pathogenesis confers an advantage for precise diagnosis and effective treatment via targeted microbial strategies such as probiotics or fecal microbiota transplantation. In order to get closer to the *in vivo* situation by integrating host-microbiota interactions, further studies will be needed coupling *in vitro* colon models to intestinal epithelial cells or

immune cells, intestinal organoids, or bioengineered human gut-on-chip devices such as HuMiX, Intestine-Chip, and Colon-Chip systems (31, 50).

MATERIALS AND METHODS

Sample collection for bioreactor inoculation and oral invasion. Donors (S1 and S2) were selected according to their sex (one female and one male), their age (23 and 52 years old), their dietary habits (one eating a flexitarian-based (neo vegetarian) diet and one consuming a omnivorous diet), and their methane status (one methane producer and one non-methane producer). The selected donors had no history of antibiotic treatment or drug or probiotic consumption for 3 months prior to sample collection. This study was a noninterventional study with no additions to usual clinical care. Fecal samples were prepared anaerobically as previously described (28), within 6 h after defecation. Saliva was collected from the same donor; each donor abstained from food and drink intake for 2 h prior to sample collection. Saliva was collected twice a day (morning and afternoon) by passive drool collection (no spitting and no blowing). Briefly, after allowing saliva to pool at the bottom of the mouth, the head was tilted forward, enabling a passive flow collected (10 mL) in a sterile container.

Fermentation in M-ARCOL. The Mucosal ARtificial COLon (M-ARCOL) is a one-stage fermentation system, used under continuous conditions, which simulates the physicochemical conditions encountered in the human colon as well as the lumen- and mucus-associated human intestinal microbial ecosystem (Applikon, Schiedam, The Netherlands) (28). It consists of pH-controlled, stirred, airtight glass vessels kept under anaerobic conditions maintained by the sole activity of resident microbiota, one vessel (300 mL) mimicking the lumen-associated microbiota and a second vessel containing mucin-alginate beads to mimic the mucus-associated microbiota (28). The vessels were operated with an initial sparging with O_2-free N_2 gas and then inoculated with fecal material from donors S1 and S2, respectively. This dynamic *in vitro* model was set up to reproduce conditions of a healthy human adult colon with a fixed temperature of 37°C, a controlled constant pH of 6.3, a stirring speed at 400 rpm, a mean retention time of 24 h, and a redox potential (Eh) of −200 mV. A sterile nutritive medium containing various sources of carbohydrates, proteins, lipids, minerals, and vitamins was sequentially introduced into the bioreactor as described previously (28, 56).

Gas and Short Chain Fatty Acids (SCFA) analysis. Analysis of O_2, CO_2, CH_4, and H_2 produced during the fermentation process in the atmospheric phase of the bioreactors was performed daily to ascertain that anaerobic conditions and gas composition were verified (Fig. S1). Gas composition was analyzed using an HP 6890 gas chromatograph (Agilent Technologies, USA) coupled with a Thermal Conductivity Detector (TCD) detector (Agilent Technologies). The three major SCFAs (acetate, butyrate, and propionate) were quantified in colonic samples from the luminal phase by high-performance liquid chromatography (HPLC) (Elite LaChrom, Merck Hitachi, USA) coupled with a Diode Array Detector (DAD) diode as described previously (28).

Mucin beads and mucin compartment. Type II mucin from porcine stomach (Sigma-Aldrich, USA) and sodium alginate (Sigma-Aldrich, USA) were diluted in sterile distilled water at concentrations of 5% and 2%, respectively. To produce mucin beads, the mucin-alginate solution was dropped into a 0.2 M solution of sterile $CaCl_2$ under agitation using a peristaltic pump. Mucin-alginate beads were introduced in the airtight glass compartment (total area of beads, 556 cm^2) connected to the main bioreactor, allowing a continuous flow of the luminal medium and ensuring the contact of the resident luminal microbiota with the mucin beads. The mucin bead compartment was kept at 37°C through the experiment using a hot water bath. Mucin-alginate beads were replaced every 48 h with fresh sterile ones under a constant flow of CO_2 to retain anaerobiosis.

Experimental design and sampling. Following fecal inoculation of the bioreactor, fermentation was conducted for a total duration of 11 days. On days 9 and 10, 10 mL of enriched saliva was introduced into the bioreactor twice a day (morning and late afternoon) after an enrichment of 9 h. A saliva washout was realized on day 11 without the injection of enriched saliva samples. For saliva enrichment, 10 mL of freshly collected saliva was resuspended in 15 mL of colonic nutritive medium (37°C, anaerobically, 100 rpm) (28) to favor multiplication of oral bacteria and enrich the microbial fraction over the human fraction in the saliva samples. Circulating medium from the bioreactor vessel, referred to as luminal microbiota, was collected daily. Medium circulating in the mucin bead compartment, referred to as mucosal microbiota, was collected every 2 days. The remaining enriched saliva samples (~5 mL) were collected for each donor (referred to as enriched saliva) to characterize enriched saliva. On day 10, a saliva sampling was performed for each donor without enrichment (referred to as raw saliva).

DNA extraction procedures. Prior to extraction, all samples were handled in the laboratory following International Human Microbiome Standards (IHMS) standard operating procedure (SOP) 004 (http://www.human-microbiome.org/) and stored at −80°C. Fecal and luminal samples were aliquoted into 200 mg and DNA extraction was performed following IHMS SOP P7 V2, which is adapted for low-microbial-biomass samples. A specific DNA preparation to remove human-related DNA was performed on saliva and enriched saliva as follow: 200 μL of saliva was centrifuged for 10 min at 10,000 $\times$ *g* for 4 min before adding 190 mL of sterile Milli-Q water to the pellet. After 5 min of incubation at room temperature, 10 μL of propidium monoazide (Clinisciences, Nanterre, France) was added to the tube to a final concentration of 10 μM. After 5 min of incubation at room temperature, samples were kept on ice and were exposed to halogen light for 25 min. Samples were stored at −80°C until extraction following IHMS SOP P7 V2. For mucosal samples, the same preparatory procedure was performed followed by DNA extraction using the IHMS SOP 06 V2 protocol, which is adapted to high-microbial-biomass samples. DNA was quantified using Qubit fluorometric

quantitation (Thermo Fisher Scientific, USA) and qualified using DNA size profiling on a fragment analyzer (Agilent Technologies, USA).

High-throughput sequencing. For each sample, 1 μg of high-molecular-weight DNA (>10 kbp) was used to build the library. DNA was sheared into 150-bp fragments using an ultrasonicator (Covaris, Woburn, MA), and DNA fragment library construction was performed using the Ion Plus fragment library and Ion Xpress barcode adapters kit (Thermo Fisher Scientific, USA), as previously described (57). We used an Ion Proton sequencer and Ion GeneStudio S5 prime sequencer to sequence the libraries (Thermo Fisher Scientific, USA), with a minimum of 20 million 150-bp high-quality reads generated per library for luminal, mucosal, and enriched saliva samples.

Read mapping. An average of 23.7 million $\pm$ 4.5 million reads was produced. We performed quality filtering using AlienTrimmer software to discard low-quality reads. Remaining human-related reads (0.02% for stools and luminal and mucosal samples and 61% for saliva and enriched saliva, on average) were removed using Bowtie2 (58), with at least 90% identity with human genome reference GRCh38 (GenBank assembly accession number GCA_000001405.15). Resulting high-quality reads were mapped onto the 10.4 million gut IGC2 (Integrated Gene Catalogue) catalogue of the human microbiome (59) and onto the 8.4 million oral catalogue (60) using METEOR software (https://forgemia.inra.fr/metagenopolis/meteor/-/tree/master/meteor-pipeline). Mapping was performed using a threshold of 90% for identity to the reference gene catalogue with Bowtie2 in a two-step procedure using a downsizing level of 12 million reads per sample, as described by Meslier et al. (61).

MSP species determination and ecological niche definition. The metagenomic species pangenome (MSP) was used to identify and quantify microbial species associated with the 10.4 million human gut genes on one hand (62) and the 8.4 million human oral genes on the other hand (60). MSP species are clusters of coabundant genes (minimum cluster size > 100 genes) used as a proxy for microbial species (63, 64). MSP abundances were estimated as the mean abundance of their 100 marker genes in both gut and oral catalogues, as far as at least 10% of these genes were detected (abundance strictly positive). From the independent gut and oral abundance tables, we computed a single abundance table by filtering overlapping MSP species between the two tables. MSP species ecological niche was determined by evaluating MSP detection in stools and raw saliva samples from the two donors. We assigned each MSP to gut and oral ecological niches when strict occurrence was found in either gut or saliva and not determined (ND) for MSP species that were either undetected in raw stool and raw saliva samples or detected in both stool and saliva samples before inoculation of the bioreactor at the initial time point (T0) (Table S2). MSP species richness was determined by counting the number of MSP species detected in the corresponding sample on the merged abundance table.

Computational analysis. All further steps were performed using R 3.5.0 (https://www.r-project.org). Data were processed and visualized using R packages *dplyr*, *stringr*, *tidyverse*, *ggpubr*, and *pheatmap*.

Ethics declarations. This study was a noninterventional study with no additions to usual clinical care. The donors provided written consent for the analysis and publication of the findings for their oral and fecal samples in the specific context of this study. This noninterventional study did not require approval from an ethics committee according to the French public health law (Code de la santé publique article L 1121-1.1).

Data availability. All sequencing data have been deposited at the European Nucleotide Archive database under the study accession PRJEB52431. Associated metadata are provided in Table S1.

SUPPLEMENTAL MATERIAL

Supplemental material is available online only.

SUPPLEMENTAL FILE 1, XLSX file, 0.02 MB.

SUPPLEMENTAL FILE 2, XLSX file, 0.1 MB.

SUPPLEMENTAL FILE 3, XLSX file, 0.02 MB.

SUPPLEMENTAL FILE 4, PDF file, 0.7 MB.

ACKNOWLEDGMENTS

This work was supported by the European FP7 Marie Skłodowska-Curie actions AgreenSkillsPlus PCOFUND-GA-2013-609398 grant to M.A. Additional funding was from Metagenopolis grant ANR-11-DPBS-0001 and from the SCUSI OBFIBRE program from Auvergne Rhône Alpes Region to MEDIS.

Oral invasion experiment design, M.A. and S.D.E.; M-ARCOL experiment design, S.B.-D. and L.E.-M.; bioreactor monitoring and sampling, L.E.-M., O.U., C.D., E.F., and S.D.; DNA extraction, A.D., S.J., and C.M.; metagenomic sequencing, B.Q.; metagenomic data preprocessing, V.M. and F.T.; oral microbial catalogue providers, F.P.O. and E.L.C.; data analysis and figures, V.M. and M.A.; data interpretation, V.M., M.A., L.E.-M., and S.B.-D.; writing, V.M., L.E.-M., M.A., and S.B.-D.; review and editing, V.M., L.E.-M., M.A., and S.B.-D.; resources, M.A. and S.B.-D.

We declare no conflicts of interest.

REFERENCES

1. Qin J, Li R, Raes J, Arumugam M, Burgdorf KS, Manichanh C, Nielsen T, Pons N, Levenez F, Yamada T, Mende DR, Li J, Xu J, Li S, Li D, Cao J, Wang B, Liang H, Zheng H, Xie Y, Tap J, Lepage P, Bertalan M, Batto J-M, Hansen T, Le Paslier D, Linneberg A, Nielsen HB, Pelletier E, Renault P, Sicheritz-Ponten T, Turner K, Zhu H, Yu C, Li S, Jian M, Zhou Y, Li Y, Zhang X, Li S, Qin N, Yang H, Wang J, Brunak S, Doré J, Guarner F, Kristiansen K, Pedersen O, Parkhill J, Weissenbach J, MetaHIT Consortium, Bork P, Ehrlich SD, Wang J. 2010. A human gut microbial gene catalogue established by metagenomic sequencing. Nature 464:59–65. https://doi.org/10.1038/nature08821.
2. Fan Y, Pedersen O. 2021. Gut microbiota in human metabolic health and disease. Nat Rev Microbiol 19:55–71. https://doi.org/10.1038/s41579-020-0433-9.
3. Lynch SV, Pedersen O. 2016. The human intestinal microbiome in health and disease. N Engl J Med 375:2369–2379. https://doi.org/10.1056/NEJMra1600266.
4. Peterson J, Garges S, Giovanni M, McInnes P, Wang L, Schloss JA, Bonazzi V, McEwen JE, Wetterstrand KA, Deal C, Baker CC, Di Francesco V, Howcroft TK, Karp RW, Lunsford RD, Wellington CR, Belachew T, Wright M, Giblin C, David H, Mills M, Salomon R, Mullins C, Akolkar B, Begg L, Davis C, Grandison L, Humble M, Khalsa J, Little AR, Peavy H, Pontzer C, Portnoy M, Sayre MH, Starke-Reed P, Zakhari S, Read J, Watson B, Guyer M. NIH HMP Working Group. 2009. The NIH Human Microbiome Project. Genome Res 19:2317–2323. https://doi.org/10.1101/gr.096651.109.
5. Park S-Y, Hwang B-O, Lim M, Ok S-H, Lee S-K, Chun K-S, Park K-K, Hu Y, Chung W-Y, Song N-Y. 2021. Oral-gut microbiome axis in gastrointestinal disease and cancer. Cancers (Basel) 13:2124. https://doi.org/10.3390/cancers13092124.
6. Human Microbiome Project Consortium. 2012. Structure, function and diversity of the healthy human microbiome. Nature 486:207–214. https://doi.org/10.1038/nature11234.
7. Dawes C. 2008. Salivary flow patterns and the health of hard and soft oral tissues. J Am Dent Assoc 139(Suppl):18S–24S. https://doi.org/10.14219/jada.archive.2008.0351.
8. Sedghi L, DiMassa V, Harrington A, Lynch SV, Kapila YL. 2021. The oral microbiome: role of key organisms and complex networks in oral health and disease. Periodontol 2000 87:107–131. https://doi.org/10.1111/prd.12393.
9. Dewhirst FE, Chen T, Izard J, Paster BJ, Tanner ACR, Yu W-H, Lakshmanan A, Wade WG. 2010. The human oral microbiome. J Bacteriol 192:5002–5017. https://doi.org/10.1128/JB.00542-10.
10. Zhao H, Chu M, Huang Z, Yang X, Ran S, Hu B, Zhang C, Liang J. 2017. Variations in oral microbiota associated with oral cancer. Sci Rep 7:11773. https://doi.org/10.1038/s41598-017-11779-9.
11. Segata N, Haake SK, Mannon P, Lemon KP, Waldron L, Gevers D, Huttenhower C, Izard J. 2012. Composition of the adult digestive tract bacterial microbiome based on seven mouth surfaces, tonsils, throat and stool samples. Genome Biol 13:R42. https://doi.org/10.1186/gb-2012-13-6-r42.
12. Roberts JA. 1996. Tropism in bacterial infections: urinary tract infections. J Urol 156:1552–1559. https://doi.org/10.1016/S0022-5347(01)65446-6.
13. Pereira FC, Berry D. 2017. Microbial nutrient niches in the gut. Environ Microbiol 19:1366–1378. https://doi.org/10.1111/1462-2920.13659.
14. Vuik FER, Dicksved J, Lam SY, Fuhler GM, Laan LJW, Winkel A, Konstantinov SR, Spaander MCW, Peppelenbosch MP, Engstrand L, Kuipers EJ. 2019. Composition of the mucosa-associated microbiota along the entire gastrointestinal tract of human individuals. United European Gastroenterol J 7:897–907. https://doi.org/10.1177/2050640619852255.
15. Wu GD, Chen J, Hoffmann C, Bittinger K, Chen Y-Y, Keilbaugh SA, Bewtra M, Knights D, Walters WA, Knight R, Sinha R, Gilroy E, Gupta K, Baldassano R, Nessel L, Li H, Bushman FD, Lewis JD. 2011. Linking long-term dietary patterns with gut microbial enterotypes. Science 334:105–108. https://doi.org/10.1126/science.1208344.
16. Arumugam M, Raes J, Pelletier E, Le Paslier D, Yamada T, Mende DR, Fernandes GR, Tap J, Bruls T, Batto J-M, Bertalan M, Borruel N, Casellas F, Fernandez L, Gautier L, Hansen T, Hattori M, Hayashi T, Kleerebezem M, Kurokawa K, Leclerc M, Levenez F, Manichanh C, Nielsen HB, Nielsen T, Pons N, Poulain J, Qin J, Sicheritz-Ponten T, Tims S, Torrents D, Ugarte E, Zoetendal EG, Wang J, Guarner F, Pedersen O, de Vos WM, Brunak S, Doré J, Antolín M, Artiguenave F, Blottiere HM, Almeida M, Brechot C, Cara C, Chervaux C, Cultrone A, Delorme C, Denariaz G, Dervyn R. MetaHIT Consortium, et al. 2011. Enterotypes of the human gut microbiome. Nature 473:174–180. https://doi.org/10.1038/nature09944.
17. Almeida A, Mitchell AL, Boland M, Forster SC, Gloor GB, Tarkowska A, Lawley TD, Finn RD. 2019. A new genomic blueprint of the human gut microbiota. Nature 568:499–504. https://doi.org/10.1038/s41586-019-0965-1.
18. Lloyd-Price J, Abu-Ali G, Huttenhower C. 2016. The healthy human microbiome. Genome Med 8:51. https://doi.org/10.1186/s13073-016-0307-y.
19. Le Chatelier E, Nielsen T, Qin J, Prifti E, Hildebrand F, Falony G, Almeida M, Arumugam M, Batto J-M, Kennedy S, Leonard P, Li J, Burgdorf K, Grarup N, Jørgensen T, Brandslund I, Nielsen HB, Juncker AS, Bertalan M, Levenez F, Pons N, Rasmussen S, Sunagawa S, Tap J, Tims S, Zoetendal EG, Brunak S, Clément K, Doré J, Kleerebezem M, Kristiansen K, Renault P, Sicheritz-Ponten T, de Vos WM, Zucker J-D, Raes J, Hansen T, MetaHIT consortium, Bork P, Wang J, Ehrlich SD, Pedersen O. 2013. Richness of human gut microbiome correlates with metabolic markers. Nature 500:541–546. https://doi.org/10.1038/nature12506.
20. Li B, Ge Y, Cheng L, Zeng B, Yu J, Peng X, Zhao J, Li W, Ren B, Li M, Wei H, Zhou X. 2019. Oral bacteria colonize and compete with gut microbiota in gnotobiotic mice. Int J Oral Sci 11:10. https://doi.org/10.1038/s41368-018-0043-9.
21. Schmidt TS, Hayward MR, Coelho LP, Li SS, Costea PI, Voigt AY, Wirbel J, Maistrenko OM, Alves RJ, Bergsten E, de Beaufort C, Sobhani I, Heintz-Buschart A, Sunagawa S, Zeller G, Wilmes P, Bork P. 2019. Extensive transmission of microbes along the gastrointestinal tract. Elife 8:e42693. https://doi.org/10.7554/eLife.42693.
22. Hu S, Png E, Gowans M, Ong DEH, de Sessions PF, Song J, Nagarajan N. 2021. Ectopic gut colonization: a metagenomic study of the oral and gut microbiome in Crohn's disease. Gut Pathog 13:13. https://doi.org/10.1186/s13099-021-00409-5.
23. Read E, Curtis MA, Neves JF. 2021. The role of oral bacteria in inflammatory bowel disease. Nat Rev Gastroenterol Hepatol 18:731–742. https://doi.org/10.1038/s41575-021-00488-4.
24. Qin N, Yang F, Li A, Prifti E, Chen Y, Shao L, Guo J, Le Chatelier E, Yao J, Wu L, Zhou J, Ni S, Liu L, Pons N, Batto JM, Kennedy SP, Leonard P, Yuan C, Ding W, Chen Y, Hu X, Zheng B, Qian G, Xu W, Ehrlich SD, Zheng S, Li L. 2014. Alterations of the human gut microbiome in liver cirrhosis. Nature 513:59–64. https://doi.org/10.1038/nature13568.
25. Farin W, Oñate FP, Plassais J, Bonny C, Beglinger C, Woelnerhanssen B, Nocca D, Magoules F, Le Chatelier E, Pons N, Cervino ACL, Ehrlich SD. 2020. Impact of laparoscopic Roux-en-Y gastric bypass and sleeve gastrectomy on gut microbiota: a metagenomic comparative analysis. Surg Obes Relat Dis 16:852–862. https://doi.org/10.1016/j.soard.2020.03.014.
26. Van den Abbeele P, Grootaert C, Marzorati M, Possemiers S, Verstraete W, Gérard P, Rabot S, Bruneau A, El Aidy S, Derrien M, Zoetendal E, Kleerebezem M, Smidt H, Van de Wiele T. 2010. Microbial community development in a dynamic gut model is reproducible, colon region specific, and selective for Bacteroidetes and Clostridium cluster IX. Appl Environ Microbiol 76:5237–5246. https://doi.org/10.1128/AEM.00759-10.
27. Zihler Berner A, Fuentes S, Dostal A, Payne AN, Vazquez Gutierrez P, Chassard C, Grattepanche F, de Vos WM, Lacroix C. 2013. Novel polyfermentor intestinal model (PolyFermS) for controlled ecological studies: validation and effect of pH. PLoS One 8:e77772. https://doi.org/10.1371/journal.pone.0077772.
28. Deschamps C, Fournier E, Uriot O, Lajoie F, Verdier C, Comtet-Marre S, Thomas M, Kapel N, Cherbuy C, Alric M, Almeida M, Etienne-Mesmin L, Blanquet-Diot S. 2020. Comparative methods for fecal sample storage to preserve gut microbial structure and function in an in vitro model of the human colon. Appl Microbiol Biotechnol 104:10233–10247. https://doi.org/10.1007/s00253-020-10959-4.
29. Daniel N, Lécuyer E, Chassaing B. 2021. Host/microbiota interactions in health and diseases—time for mucosal microbiology! Mucosal Immunol 14:1006–1016. https://doi.org/10.1038/s41385-021-00383-w.
30. Etienne-Mesmin L, Chassaing B, Desvaux M, De Paepe K, Gresse R, Sauvaitre T, Forano E, de Wiele TV, Schüller S, Juge N, Blanquet-Diot S. 2019. Experimental models to study intestinal microbes-mucus interactions in health and disease. FEMS Microbiol Rev 43:457–489. https://doi.org/10.1093/femsre/fuz013.
31. Sauvaitre T, Etienne-Mesmin L, Sivignon A, Mosoni P, Courtin CM, Van de Wiele T, Blanquet-Diot S. 2021. Tripartite relationship between gut microbiota, intestinal mucus and dietary fibers: towards preventive strategies against enteric infections. FEMS Microbiol Rev 45:fuaa052. https://doi.org/10.1093/femsre/fuaa052.
32. Van den Abbeele P, Roos S, Eeckhaut V, MacKenzie DA, Derde M, Verstraete W, Marzorati M, Possemiers S, Vanhoecke B, Van Immerseel F, Van de Wiele T. 2012. Incorporating a mucosal environment in a dynamic gut model results in a more representative colonization by lactobacilli. Microb Biotechnol 5:106–115. https://doi.org/10.1111/j.1751-7915.2011.00308.x.
33. Flemer B, Warren RD, Barrett MP, Cisek K, Das A, Jeffery IB, Hurley E, O'Riordain M, Shanahan F, O'Toole PW. 2018. The oral microbiota in

colorectal cancer is distinctive and predictive. Gut 67:1454–1463. https://doi.org/10.1136/gutjnl-2017-314814.
34. Fan X, Alekseyenko AV, Wu J, Peters BA, Jacobs EJ, Gapstur SM, Purdue MP, Abnet CC, Stolzenberg-Solomon R, Miller G, Ravel J, Hayes RB, Ahn J. 2018. Human oral microbiome and prospective risk for pancreatic cancer: a population-based nested case-control study. Gut 67:120–127. https://doi.org/10.1136/gutjnl-2016-312580.
35. Simon-Soro A, Ren Z, Krom BP, Hoogenkamp MA, Cabello-Yeves PJ, Daniel SG, Bittinger K, Tomas I, Koo H, Mira A. 2022. Polymicrobial aggregates in human saliva build the oral biofilm. mBio 13:e00131-22. https://doi.org/10.1128/mbio.00131-22.
36. Duncan K, Carey-Ewend K, Vaishnava S. 2021. Spatial analysis of gut microbiome reveals a distinct ecological niche associated with the mucus layer. Gut Microbes 13:1874815. https://doi.org/10.1080/19490976.2021.1874815.
37. Li H, Limenitakis JP, Fuhrer T, Geuking MB, Lawson MA, Wyss M, Brugiroux S, Keller I, Macpherson JA, Rupp S, Stolp B, Stein JV, Stecher B, Sauer U, McCoy KD, Macpherson AJ. 2015. The outer mucus layer hosts a distinct intestinal microbial niche. Nat Commun 6:8292. https://doi.org/10.1038/ncomms9292.
38. Corfield AP. 2018. The interaction of the gut microbiota with the mucus barrier in health and disease in human. Microorganisms 6:78. https://doi.org/10.3390/microorganisms6030078.
39. Grondin JA, Kwon YH, Far PM, Haq S, Khan WI. 2020. Mucins in intestinal mucosal defense and inflammation: learning from clinical and experimental studies. Front Immunol 11:2054. https://doi.org/10.3389/fimmu.2020.02054.
40. Paone P, Cani PD. 2020. Mucus barrier, mucins and gut microbiota: the expected slimy partners? Gut 69:2232–2243. https://doi.org/10.1136/gutjnl-2020-322260.
41. Zaura E, Keijser BJF, Huse SM, Crielaard W. 2009. Defining the healthy "core microbiome" of oral microbial communities. BMC Microbiol 9:259. https://doi.org/10.1186/1471-2180-9-259.
42. Liu G, Tang CM, Exley RM. 2015. Non-pathogenic Neisseria: members of an abundant, multi-habitat, diverse genus. Microbiology (Reading) 161:1297–1312. https://doi.org/10.1099/mic.0.000086.
43. van der Hoeven JS, van den Kieboom CW, Camp PJ. 1990. Utilization of mucin by oral Streptococcus species. Antonie Van Leeuwenhoek 57:165–172. https://doi.org/10.1007/BF00403951.
44. Derrien M, van Passel MW, van de Bovenkamp JH, Schipper RG, de Vos WM, Dekker J. 2010. Mucin-bacterial interactions in the human oral cavity and digestive tract. Gut Microbes 1:254–268. https://doi.org/10.4161/gmic.1.4.12778.
45. Kasprzak A, Adamek A. 2019. Mucins: the old, the new and the promising factors in hepatobiliary carcinogenesis. Int J Mol Sci 20:1288. https://doi.org/10.3390/ijms20061288.
46. Solé C, Guilly S, Da Silva K, Llopis M, Le-Chatelier E, Huelin P, Carol M, Moreira R, Fabrellas N, De Prada G, Napoleone L, Graupera I, Pose E, Juanola A, Borruel N, Berland M, Toapanta D, Casellas F, Guarner F, Doré J, Solà E, Ehrlich SD, Ginès P. 2021. Alterations in gut microbiome in cirrhosis as assessed by quantitative metagenomics: relationship with acute-on-chronic liver failure and prognosis. Gastroenterology 160:206–218.e13. https://doi.org/10.1053/j.gastro.2020.08.054.
47. Kitamoto S, Nagao-Kitamoto H, Jiao Y, Gillilland MG, Hayashi A, Imai J, Sugihara K, Miyoshi M, Brazil JC, Kuffa P, Hill BD, Rizvi SM, Wen F, Bishu S, Inohara N, Eaton KA, Nusrat A, Lei YL, Giannobile WV, Kamada N. 2020. The intermucosal connection between the mouth and gut in commensal pathobiont-driven colitis. Cell 182:447–462.e14. https://doi.org/10.1016/j.cell.2020.05.048.
48. Khor B, Snow M, Herrman E, Ray N, Mansukhani K, Patel KA, Said-Al-Naief N, Maier T, Machida CA. 2021. Interconnections between the oral and gut microbiomes: reversal of microbial dysbiosis and the balance between systemic health and disease. Microorganisms 9:496. https://doi.org/10.3390/microorganisms9030496.
49. Roussel C, De Paepe K, Galia W, de Bodt J, Chalancon S, Denis S, Leriche F, Vandekerkove P, Ballet N, Blanquet-Diot S, Van de Wiele T. 2021. Multi-targeted properties of the probiotic saccharomyces cerevisiae CNCM I-3856 against enterotoxigenic Escherichia coli (ETEC) H10407 pathogenesis across human gut models. Gut Microbes 13:1953246. https://doi.org/10.1080/19490976.2021.1953246.
50. Fournier E, Etienne-Mesmin L, Grootaert C, Jelsbak L, Syberg K, Blanquet-Diot S, Mercier-Bonin M. 2021. Microplastics in the human digestive environment: a focus on the potential and challenges facing in vitro gut model development. J Hazard Mater 415:125632. https://doi.org/10.1016/j.jhazmat.2021.125632.
51. Uriot O, Deschamps C, Brun M, Pouget M, Alric M, Chaudemanche C, Boirie Y, Etienne-Mesmin L, Blanquet-Diot S. 2022. Development and validation of an in vitro colonic model of gut microbiota dysbiosis associated to obesity. International Congress on Food Digestion, May 2022, Cork, Ireland.
52. Aguirre M, Bussolo de Souza C, Venema K. 2016. The gut microbiota from lean and obese subjects contribute differently to the fermentation of arabinogalactan and inulin. PLoS One 11:e0159236. https://doi.org/10.1371/journal.pone.0159236.
53. Uriot O, Fournier E, Lajoie F, Kerchove N, Scanzy J, Denis S, Alric M, Etienne-Mesmin L, Blanquet-Diot S. 2021. Development of an in vitro model of dysbiotic colonic conditions of IBS-D patients. 12. International Symposium on Gut Microbiology, INRAE, Rowett Institute UK, Oct 2021, En ligne, France.
54. Vermeiren J, den Abbeele P, Laukens D, Vigsnaes LK, Vos M, Boon N, Wiele T. 2012. Decreased colonization of fecal Clostridium coccoides/Eubacterium rectale species from ulcerative colitis patients in an in vitro dynamic gut model with mucin environment. FEMS Microbiol Ecol 79:685–696. https://doi.org/10.1111/j.1574-6941.2011.01252.x.
55. Van den Abbeele P, Marzorati M, Derde M, De Weirdt R, Joan V, Possemiers S, Van de Wiele T. 2016. Arabinoxylans, inulin and Lactobacillus reuteri 1063 repress the adherent-invasive Escherichia coli from mucus in a mucosa-comprising gut model. NPJ Biofilms Microbiomes 2:16016. https://doi.org/10.1038/npjbiofilms.2016.16.
56. Thévenot J, Cordonnier C, Rougeron A, Le Goff O, Nguyen HTT, Denis S, Alric M, Livrelli V, Blanquet-Diot S. 2015. Enterohemorrhagic Escherichia coli infection has donor-dependent effect on human gut microbiota and may be antagonized by probiotic yeast during interaction with Peyer's patches. Appl Microbiol Biotechnol 99:9097–9110. https://doi.org/10.1007/s00253-015-6704-0.
57. Meslier V, Quinquis B, Da Silva K, Plaza Oñate F, Pons N, Roume H, Podar M, Almeida M. 2022. Benchmarking second and third-generation sequencing platforms for microbial metagenomics. Sci Data 9:694. https://doi.org/10.1038/s41597-022-01762-z.
58. Langmead B, Salzberg SL. 2012. Fast gapped-read alignment with Bowtie 2. Nat Methods 9:357–359. https://doi.org/10.1038/nmeth.1923.
59. Wen C, Zheng Z, Shao T, Liu L, Xie Z, Le Chatelier E, He Z, Zhong W, Fan Y, Zhang L, Li H, Wu C, Hu C, Xu Q, Zhou J, Cai S, Wang D, Huang Y, Breban M, Qin N, Ehrlich SD. 2017. Quantitative metagenomics reveals unique gut microbiome biomarkers in ankylosing spondylitis. Genome Biol 18:142. https://doi.org/10.1186/s13059-017-1271-6.
60. Le Chatelier E, Almeida M, Plaza Oñate F, Pons N, Gauthier F, Ghozlane A, Ehrlich SD, Witherden E, Gomez-Cabrero D. 2021. A catalog of genes and species of the human oral microbiota. https://entrepot.recherche.data.gouv.fr/dataset.xhtml?persistentId=doi:10.15454/WQ4UTV.
61. Meslier V, Laiola M, Roager HM, De Filippis F, Roume H, Quinquis B, Giacco R, Mennella I, Ferracane R, Pons N, Pasolli E, Rivellese A, Dragsted LO, Vitaglione P, Ehrlich SD, Ercolini D. 2020. Mediterranean diet intervention in overweight and obese subjects lowers plasma cholesterol and causes changes in the gut microbiome and metabolome independently of energy intake. Gut 69:1258–1268. https://doi.org/10.1136/gutjnl-2019-320438.
62. Plaza Onate F, Pons N, Gauthier F, Almeida M, Ehrlich SD, Le Chatelier E. 2021. Updated metagenomic species pan-genomes (MSPs) of the human gastrointestinal microbiota. https://entrepot.recherche.data.gouv.fr/dataset.xhtml?persistentId=doi:10.15454/FLANUP.
63. Plaza Oñate F, Le Chatelier E, Almeida M, Cervino ACL, Gauthier F, Magoulès F, Ehrlich SD, Pichaud M. 2019. MSPminer: abundance-based reconstitution of microbial pan-genomes from shotgun metagenomic data. Bioinformatics 35:1544–1552. https://doi.org/10.1093/bioinformatics/bty830.
64. Nielsen HB, Almeida M, Juncker AS, Rasmussen S, Li J, Sunagawa S, Plichta DR, Gautier L, Pedersen AG, Le Chatelier E, Pelletier E, Bonde I, Nielsen T, Manichanh C, Arumugam M, Batto J-M, Quintanilha Dos Santos MB, Blom N, Borruel N, Burgdorf KS, Boumezbeur F, Casellas F, Doré J, Dworzynski P, Guarner F, Hansen T, Hildebrand F, Kaas RS, Kennedy S, Kristiansen K, Kultima JR, Léonard P, Levenez F, Lund O, Moumen B, Le Paslier D, Pons N, Pedersen O, Prifti E, Qin J, Raes J, Sørensen S, Tap J, Tims S, Ussery DW, Yamada T, MetaHIT Consortium, Renault P, Sicheritz-Ponten T, Bork P, Wang J, Brunak S, Ehrlich SD. 2014. Identification and assembly of genomes and genetic elements in complex metagenomic samples without using reference genomes. Nat Biotechnol 32:822–828. https://doi.org/10.1038/nbt.2939.

Appendix 5 – Original article in Microbiome

URIOT, O.[#], DESCHAMPS, C. [#], ETIENNE-MESMIN, L., BRUN, M., POUGET, M., CHALANCON, S., DURIF, C., CHAUDEMANCHE, C., ALRIC, M., BOIRIE, Y., BLANQUET-DIOT, S. Towards a mechanistic understanding of reciprocal interactions between microbiome and the colonic environment in obesity.

[#] co-first authors

Under review in *Microbiome*, **2023**

Colonic physicochemical parameters drive gut microbiota dysbiosis in obesity

Ophélie Uriot[1,§], Charlotte Deschamps[1,§], Lucie Etienne-Mesmin[1], Morgane Brun[1], Mélanie Pouget[2], Sandrine Chalancon[1], Claude Durif[1], Cyril Chaudemanche[3], Monique Alric[1], Yves Boirie[2,4] and Stéphanie Blanquet-Diot[1]

[§] co-first authors

[1] UMR 454 MEDIS, Microbiologie Environnement Digestif et Santé, Université Clermont Auvergne – INRAe, Clermont-Ferrand, France

[2] Service de Nutrition Clinique, Centre Hospitalo-Universitaire, Clermont-Ferrand, France

[3] General Mills France, Boulogne-Billancourt, France

[4] UMR 1019 INRAe, Unité de Nutrition Humaine, Université Clermont Auvergne, Clermont-Ferrand, France

Corresponding author:

Stéphanie Blanquet-Diot: stephanie.blanquet@uca.fr

Abstract

Background: Obesity has reached epidemic proportions worldwide with a heavy burden on individual health and society. Altered gut microbiota is acknowledged as a key factor in disease pathogenesis. However, ecosystem-level mechanistic understanding of gut microbiome's role is still required. Here, we performed dietary surveys and analysed 250 papers to set-up based on human *in vivo* data a new *in vitro* colonic model reproducing obese-specific nutritional, physicochemical and lumen vs mucus-associated microbial parameters.

Results: In a unique set-up, we cross-compared data on microbial structure and activities during fermentations performed with healthy (n=4) or obese (n=5) stools, run under healthy or newly designed obese parameters. Interestingly, applying obese parameters on healthy stools resulted in a significant decrease in microbial α-diversity and healthy-marker populations (e.g. *Akkermanciaceae*, *Rikenellaceae* and *Archaea*), associated to a tendency to produce more short chain fatty acids and associated energy, in full accordance with *in vivo* data. Reversely, applying healthy parameters on obese stools led to gut microbiota resilience.

Conclusions: These results show the importance of nutritional and physicochemical environment in shaping colonic bacterial and archaeal populations in obesity. This new validated model will provide a useful platform in preclinical trials to perform mechanistic studies on gut microbiome and evaluate food and pharma strategies aiming to restore microbiota eubiosis in a personalized way.

Keywords

Obesity, gut microbiota, dysbiosis, *in vitro* gut model, M-ARCOL, mucus, short chain fatty acid, bacteria, methanogenic *Archaea*

Main

Over the last decades, obesity has become a major public health concern with epidemic proportions. According to the World Health Organization (WHO), over 650 million adults are obese and the worldwide prevalence of obesity nearly tripled between 1975 and 2016 [1]. Obesity is defined in adults as an abnormal or excessive fat accumulation that may impair health and diagnosed with a body mass index (BMI) over 30 kg/m². This complex and multifactorial disease is due to an imbalance between energy intake (high fat and high sugar diet) and expenditure, and associated with many complications such as type II diabetes, cardiovascular disease or cancer [2]. Currently available evidence suggests that gut microbiota alterations could contribute to the pathogenesis of obesity or aggravation of the disease. A large number of studies based on human faecal stool analysis has demonstrated dysbiosis signatures of gut microbiota, characterized by a loss of microbial markers such as *Akkermansia muciniphila, Rikenellaceae* and methanogenic *Archaea*, but a rise in other populations like *Prevotella, Veillonella* or *Proteobacteria* [3,4]. Gut microbiota can improve energy extraction from diet by converting food carbohydrates into short-chain fatty acid (SCFA), but also increases intestinal permeability to bacterial lipopolysaccharides (LPS) in response to high-fat diet consumption, exacerbating low-grade inflammation and insulin resistance [5,6]. Faecal transplantation studies in germfree mice have provided decisive insights into the potential causative role of the gut microbiota in the development of obesity [7], but

our understanding of the interrelationships between gut microbes and disease remains mostly descriptive to date.

Although clinical studies remain the gold standard approach, *in vitro* human gut models present an unmatched opportunity to perform studies frequently challenged in humans or animals owing to ethical, technical or regulatory concerns [8,9]. Compared to rodent models, they advantageously simulate human physiologically relevant diet, physicochemical digestive parameters and microbiota, and can provide mechanistic insights into microbe-microbe interactions at the gut ecosystem level [10,11]. Up to now, most *in vitro* models integrating gut microbiome have been set-up to reproduce digestive conditions from healthy adult individuals [8,12,13]. Only two studies have reported the use of complex *in vitro* gut models under obese conditions, namely the TNO gastrointestinal model (TIM-2) and the simulator of the human intestinal microbial ecosystem (SHIME) [14,15]. Both systems had been inoculated with stools from obese patients, but the authors did not report any adaptation of nutritional or physicochemical parameters of the models to the specific colonic environment of obese subjects, although such factors are well known to shape gut microbiota. In addition, none of these models was validated by *in vitro*/*in vivo* comparisons.

Here, we developed and validated a new *in vitro* model that mimics the colon microbiome from obese individuals, taking into account all physiologically relevant parameters known in literature. This was performed using the dynamic Mucosal Artificial Colon (M-ARCOL) system which shows the unique feature to reproduce the lumen and mucus-associated microbiota under microbe's self-maintained anaerobiosis. Then, we exploited the full potential of this new model by cross-comparing gut microbiota structure and activity when fermentations were performed under healthy or obese conditions, with stools collected from either obese patients or healthy volunteers. This allowed to gather useful mechanistic insights into the bidirectional relationship between gut microbes and the human colonic environment under realistic obese conditions.

Results and discussion

Set-up of the new *in vitro* colon model of obesity

In the context of the "obesity epidemic" and reduction of animal experiments to the profit of *in vitro* alternative assays, we first developed a new *in vitro* model simulating the colonic ecosystem of obese patients. This system was adapted from the one-stage M-ARCOL model, which, once inoculated with faecal microbiota from a human individual, reproduces the main microbial, nutritional and physicochemical parameters of the human colon [16]. An in-depth literature review was performed on more than 250 articles to retain the 15 most relevant to set-up the model. The search strategy was constructed around the following criteria: human adults between 18 and 60 years, BMI > 40 kg/m^2, no bariatric surgery, no drug treatment (including antibiotics) nor probiotic or prebiotic supplementation, comparison between healthy and obese parameters under strict similar experimental conditions, colonic data prioritized over faecal ones whenever possible. In addition, food surveys from obese patients fitting our criteria were obtained from the Clinical Nutrition department of a university hospital (CHU Gabriel Montpied, Clermont-Ferrand, France). **Fig. 1a** summarizes the main parameters that were adapted under obese conditions. The first parameter adapted was the composition of the nutritive medium

which is regularly supplied to the bioreactor to simulate the composition of ileal effluents. Since no data was found in the literature on the composition of ileal effluents in obese patients, we calculated the amount of lipids, carbohydrates, fibres and salt based on clinical dietary surveys, digestibility indexes and faecal concentrations found in the literature [17,18]. Then, from healthy to obese parameters, lipids were increased by 6-fold (with 50 % butter and 50 % palm oil) and salt by 1.2-fold, while fibres were divided by 4 and replaced by starch products to reach the same total carbohydrate amount. Lastly, we increased in the nutritive medium the primary (BAI) to secondary bile acid (BAII) ratio (60/40 in obese *versus* 15/85 in healthy situation), without changing total bile acid concentrations, according to data from obese stools [19,20]. This allowed to reproduce *in vitro* the bile acid reabsorption deficiency associated with their overproduction in obese patients. Integrating bile acids modification associated with obesity is particularly relevant since those molecules have the ability to control and shape gut microbiota populations [21,22]. Secondly, colonic pH was decreased by 0.3 according to data collected from obese faecal samples where a modest acidification was observed and related to an increase in SCFA concentration [23,24]. Finally, regarding colonic transit time, available data fluctuated depending on diet, analytical methods used, and most studies did not compare obese versus healthy data. As a part of the selected publications demonstrated accelerated transit time in obese [25] while others observed no change [26,27], we decided to keep the same retention time than that previously applied under healthy situation (namely 24 hours).

Figure 1. Experimental design in M-ARCOL and donor stool characterization. a-b) Nine stools were collected from four healthy adult volunteers (H1, H2, H3 and H4) and five obese patients (O1, O2, O3, O4 and O5). Two bioreactors were inoculated with each stool and ran in parallel for twelve days, one set-up with healthy parameters, the other with obese ones, as described in the table. Samples were regularly collected from luminal and mucosal compartments of the model and from its atmospheric phase. Each stool was characterized by the c) proportion of the three main short chain fatty acids (acetate, propionate and butyrate), d-e) bacterial and archaeal microbiota abundances as determined by metabarcoding analysis, f) amounts of selected bacterial populations as quantified by qPCR and g) microbial diversity illustrated by the observed ASVs, Shannon and Simpson indexes (unpaired t-test).

a.

	Healthy parameters	Obese parameters
pH	6.3	6.0
Temperature	37°C	37°C
Retention time	24 h	24 h
Ileal effluents composition	Adapted from[16]	Adapted from[16] ↘ fibers ↗ starch ↗ lipids ↗ salt ↗ BAI / BAII ratio

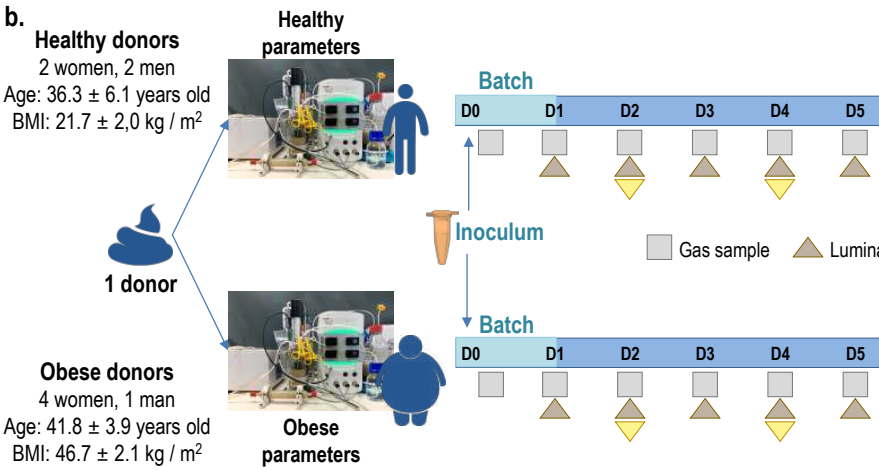

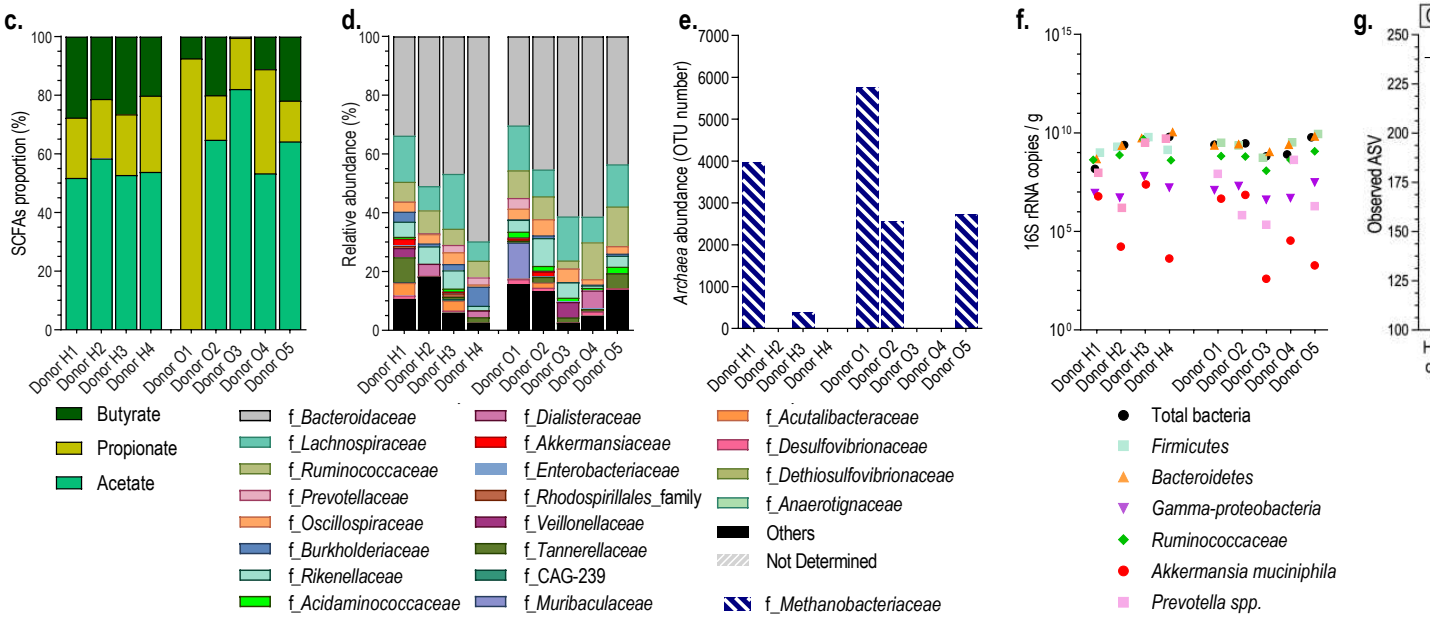

Figure 1. Experimental design in M-ARCOL and donor stool characterization.

Microbiota stabilization and shift from faecal to colonic profiles

M-ARCOL was then used to run colonic fermentations when implemented with healthy or obese parameters (as described above), and inoculated with either healthy stools (2 men, 2 women) or obese stools (1 man, 4 women) in separate runs (**Fig. 1**). By collecting samples every day both in the luminal and mucosal compartments of M-ARCOL and in its atmospheric phase, we followed gut microbiota composition and metabolic activities. M-ARCOL fermentation required a certain adaptation time before a microbiome with an obese or healthy phenotype is being established. Individual gas (**Suppl. Fig. 1**) and SCFA (**Suppl. Fig. 2**) profiles indicated that stabilization was reached after 3-4 days and 5-6 days with healthy and obese parameters, respectively. Stabilization of microbiota composition was longer, especially at the lower taxonomic levels (**Suppl. Fig. 3** to **5**). Nevertheless, redundancy analysis (RDA) of microbiota β-diversity confirmed an absence of time effect from days 8 to 11 on microbial profiles at the ASV level (**Suppl. Fig. 6**). This stabilization phase allows the microbial population to adapt following the transition from the *in vivo* to *in vitro* environment, with a decrease in microbial richness and evenness compared to the initial stools (**Fig. 1g** and **Fig. 2a**), as previously reported [16,28]. Of interest, this loss of bacterial diversity was less pronounced in the mucosal compartment of M-ARCOL (**Fig. 2a**). Simulation of this mucosal environment provided additional functional niches which allow to maintain in the bioreactor rare taxa from stool samples. Faecal microbiota stabilization in a colonic-like environment also led to clear shift in microbial profiles (**Fig. 1c** to **1f**, **Fig. 2b**, **Fig. 3**), with an enrichment in bacteria from Bacteroidetes and Proteobacteria phyla (**Suppl. Fig. 3**), according to human *in vivo* data [29,30]. The mucosal compartment also harbours a unique composition (**Fig. 2b**), with a clear enrichment in Firmicutes (**Suppl. Fig. 3**) containing specific species from *Clostridium* or *Roseburia* genera able to adhere to mucins or bacteria using substrates *via* cross feeding with mucin-degrading microbes [31]. The mucosal compartment is also colonized with a lower level of bacteria (7-8 Log_{10} 16S rDNA copies/g, **Fig. 3h**) compared to the luminal compartment (10 Log_{10} 16S rDNA copies/g, **Fig. 3d**), as reported *in vivo* [32].

Obese colonic parameters are sufficient to induce obesity-related dysbiosis

Carefully selected obesity parameters -diet, bile salt profiles, colonic pH and retention time- were implemented into M-ARCOL to investigate their impact on the microbiome from healthy donors (H1 to H4, **Fig. 1**). A clear shift in microbial profiles was observed with lower abundances of *Akkermansiaceae, Rikenellaceae*, *Ruminococcaceae* and *Christensenellaceae* but increase levels of *Prevotellaceae* and *Veillonellaceae* (**Fig. 3**). *Akkermansiaceae* disappeared from the luminal (**Fig. 3a**) and mucosal (**Fig. 3e**) compartments of M-ARCOL with obese parameters in donors H1, H3 and H4, leading respectively to significant 30- (**Fig. 3b**) and 9- (**Fig. 3f**) log_2 fold change decrease based on differential analysis, respectively. This drop was also confirmed by qPCR quantification of *A. muciniphila* with a significant 3-log_{10} decrease induced by the shift from healthy to obese conditions (**Fig. 3d** and **3h**). Remarkably, most of the changes observed *in vitro* are in line with alterations observed in stool samples from obese patients (**Table 1**), especially regarding the disappearance of healthy-related population markers such as *Akkermansiaceae, Rikenellaceae*, *Ruminococcaceae* and *Christensenellaceae* [33–39].

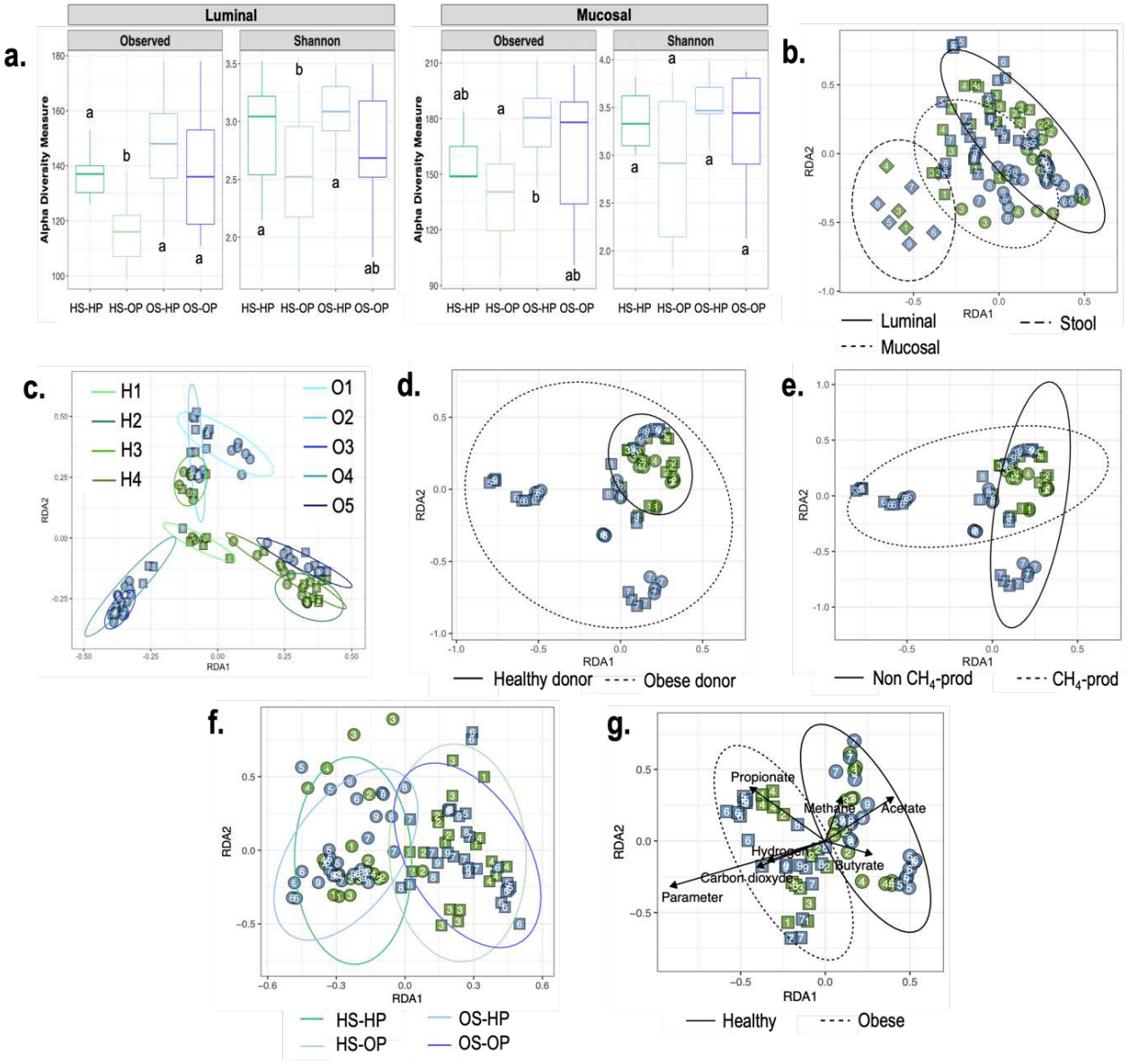

Figure 2: α and β-diversity of microbial communities during M-ARCOL experiments. Diversity indexes were calculated from ASV table and only the results of the last four days of fermentation are presented. **a**) α-diversity was illustrated by the observed ASVs and Shannon Index; significant statistical differences are indicated by different letters (P<0.05). **b** to **h**) RDA two-dimension plot visualizations reported the bacterial community β-diversity, excluding the donor variable (**d** to **h**) or not (**b-c**). For luminal samples only, corresponding SCFAs and gas data were added as environmental variables and RDA was recalculated accordingly (**h**). Variables associated statistical ellipses were added at 95% confidence interval to distinguish colonic microenvironments (**b**), stool donors (**c**), type of donors (**d**), methane status (**e**) and colonic parameters (**f-h**). *HS: healthy donors (in green); OS: obese donors (in blue); HP: healthy parameters (round shape); OP: obese parameters (square shape); initial stool (diamond shape).*

These changes, and particularly those of *Akkermansiaceae*, can be connected to the nutritional conditions associated with low fibers, high-fat or high-salt diets, as shown in mice [40–47] or humans [18]. The only population that varied in M-ARCOL inversely from human *in vivo* data [35,37,48] is *Enterobacteriaceae,* maybe due by its low abundance. Changes induced by obese conditions were associated to a significant decrease in α-diversity in the luminal compartment (**Fig. 2a**) and led to a clear sample clustering according to the parameters applied (i.e., healthy or obese) (**Fig. 2f** and **2g**). Once again, this loss of microbial diversity has already been widely described in obese adults [34,49–51] and is fully in agreement with the definition of gut microbiota dysbiosis [52]. In an original approach, we also investigated in the M-ARCOL a non-bacterial population, namely the archaeal community and especially methanogenic *Archaea*, which displays an inverse relationship with obesity. A previous study in mice [53] suggested that H_2 transfer between bacterial and archaeal species might be an important mechanism for increasing energy uptake in obesity, while others showed an inverse relationship between *Archaea* abundance in human stools and BMI [23,34,39,54–56]. In all the CH_4-producer healthy donors from our study, we found that applying obese parameters during fermentation led to a disappearance of methanogenic *Archaea*, strongly correlated with a decrease in CH_4 production (**Fig. 3c** and **3g**, **Fig. 4b, Suppl. Fig. 1**), in agreement with the second hypothesis. Other changes in metabolic profiles were also associated with obese conditions, such as an increase in CO_2 relative abundance (significant in non-CH_4 producers), mainly associated to carbohydrate fermentation, and a tendency to produce greater levels of gas, total SCFA and associated energy (**Fig. 4**). This is in line with human data showing higher SCFA concentrations in obese stools [23,57–60] and can be related (even if the models are clearly different) to the work from Turnbaugh *et al.* [61] who evidenced in mice that the obese microbiome had an increased capacity to harvest energy from the diet. This rise in SCFA concentration was not related to any change in the proportions of the three main SCFA, as already observed in human stools [23,57–60]. Lastly, pathway predictions were performed with Tax4Fun2 R-package [62] based on our metabarcoding data (**Fig. 5** and **Suppl. Fig. 7**). We showed that application of obese parameters was associated with an increase in amino acid and carbohydrate metabolisms, but with no change in fatty acid metabolism (**Fig. 5**). Interestingly, biotin metabolism was significantly ($P<0.0001$) decreased under obese condition. This *in vitro* result can be remarkably linked to pioneer data obtained by Belda *et al.* [63] who showed in a large cohort of obese patients that severe obesity was associated with an absolute deficiency in bacterial biotin producers and transporters. The authors also demonstrated that obese patients had altered serum and tissue biotin status in the host. When comparing healthy stool/obese parameters with obese stool/obese parameters, even if we can observe slight population differences -but not in *Akkermansiaceae*- (**Fig. 3b** and **3f**), data clearly clustered depending on parameters and not according to stool origin, as seen in β-diversity (**Fig. 2f** and **2g**) and Tax4Fun2 (**Fig. 5**) analysis. Taken all together, these results indicate that obese-related gut microbial dysbiosis can be obtained *in vitro* from healthy stools only by changing the dietary and physicochemical parameters. This suggests that obese stools are not essential when developing an *in vitro* obese colonic model.

Figure 3: Cross-compared effect of obese *versus* healthy stools and colonic parameters on bacterial and archaeal populations in the M-ARCOL. M-ARCOL was inoculated with stools collected from four healthy volunteers (H1, H2, H3 and H4) and five obese patients (O1, O2, O3, O4 and O5). Lumen (a to d) and mucus-associated (e to h) microbiota compositions were determined during fermentation. Data represents only the four endpoints of the experiment, i.e. during the stabilization period. (a-e) Bacterial and (c-g) *Archaea* methanogens abundances as determined by 16S rRNA gene amplicon sequencing. (b-f) Differential analysis performed with three different methods (DeSeq2, Metacoder and MetagenomeSeq R-analysis). Presented families are differentially more abundant in at least one method. (d-h) qPCR quantification of selected bacterial populations. Results are expressed as mean 16S rDNA copies /g ± standard error of the mean (SEM) and significant statistical differences base on ANOVA are indicated by different letters ($P < 0.05$).

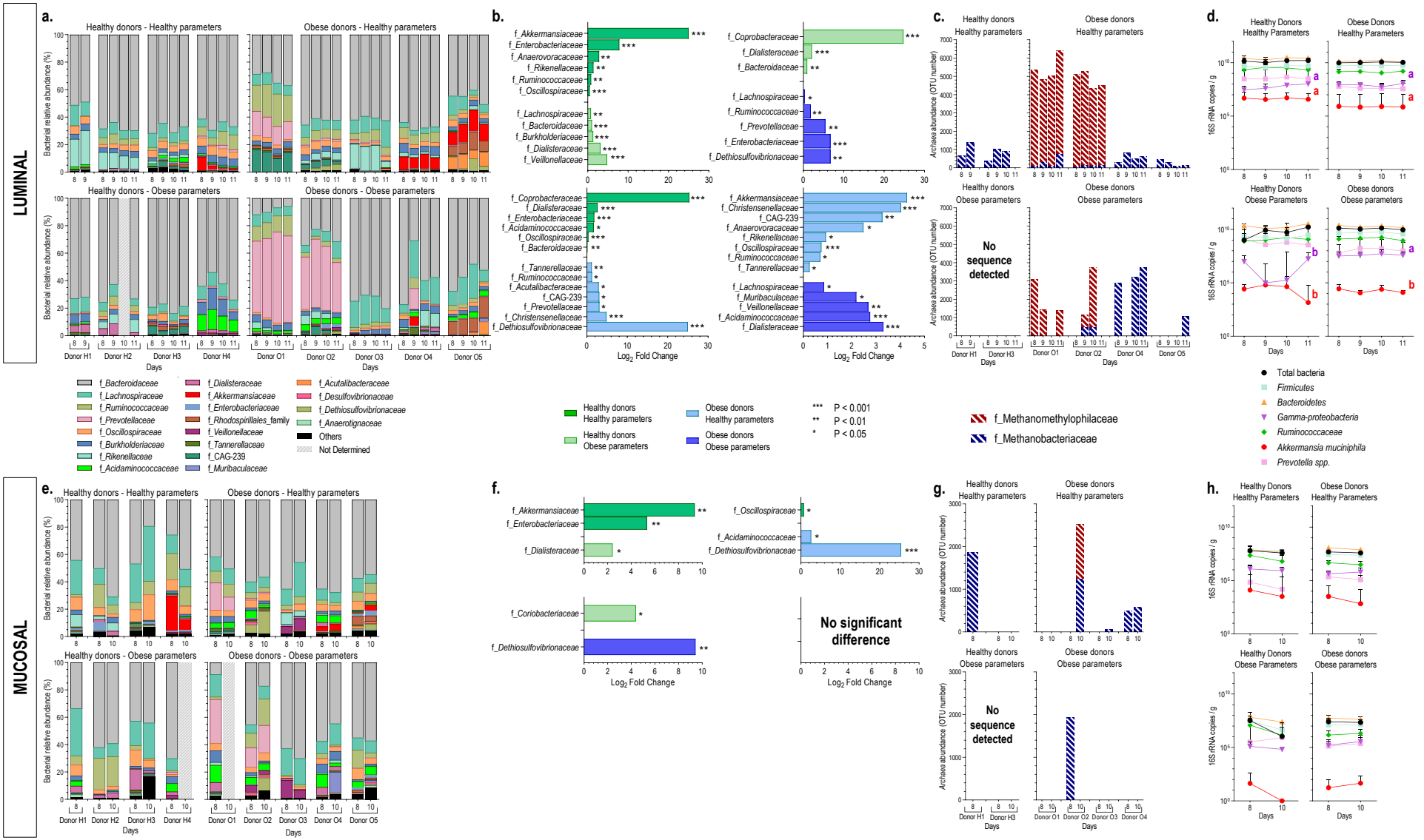

Figure 3: Cross-compared effect of obese *versus* healthy stools and colonic parameters on bacterial and archaeal populations in the M-ARCOL

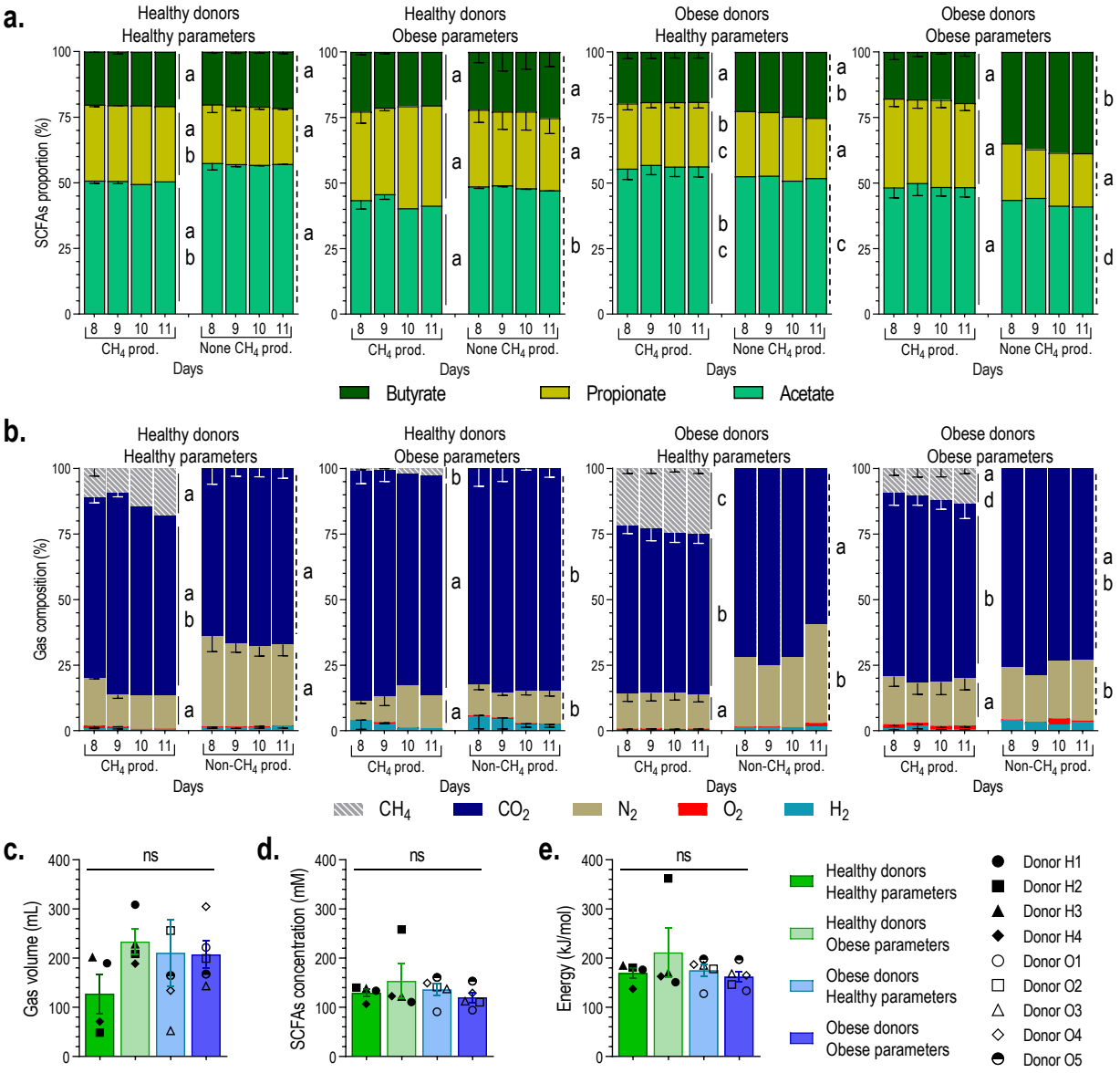

Figure 4: Cross-compared effect of obese *versus* healthy stools and colonic parameters on gut microbiota activities in the M-ARCOL. M-ARCOL was inoculated with the stools from four healthy volunteers (H1, H2, H3 and H4) and five obese patients (O1, O2, O3, O4 and O5). Microbiota activity was followed by gas and short chain fatty acid (SFCA) measurements during fermentation. Data represents only the four endpoints of the experiment, i.e. during the stabilization period. a) Proportion of the three main SCFAs (acetate, propionate and butyrate) in the luminal compartment and according to methane status of the donors (methane and non-methane producing donors). b) Gas composition of the atmospheric phase, in methane and non-methane producing donors. c) Daily amount of gas volume produced. d-e) Daily concentration of SCFAs in the luminal compartment and associated energy production. Results were expressed as means ± standard error of the mean (SEM). Significant statistical differences based on ANOVA are indicated by different letters ($P < 0.05$). *CH_4: methane, CO_2: carbon dioxide, H_2: dihydrogen, N_2: dinitrogen, O_2: dioxygen.*

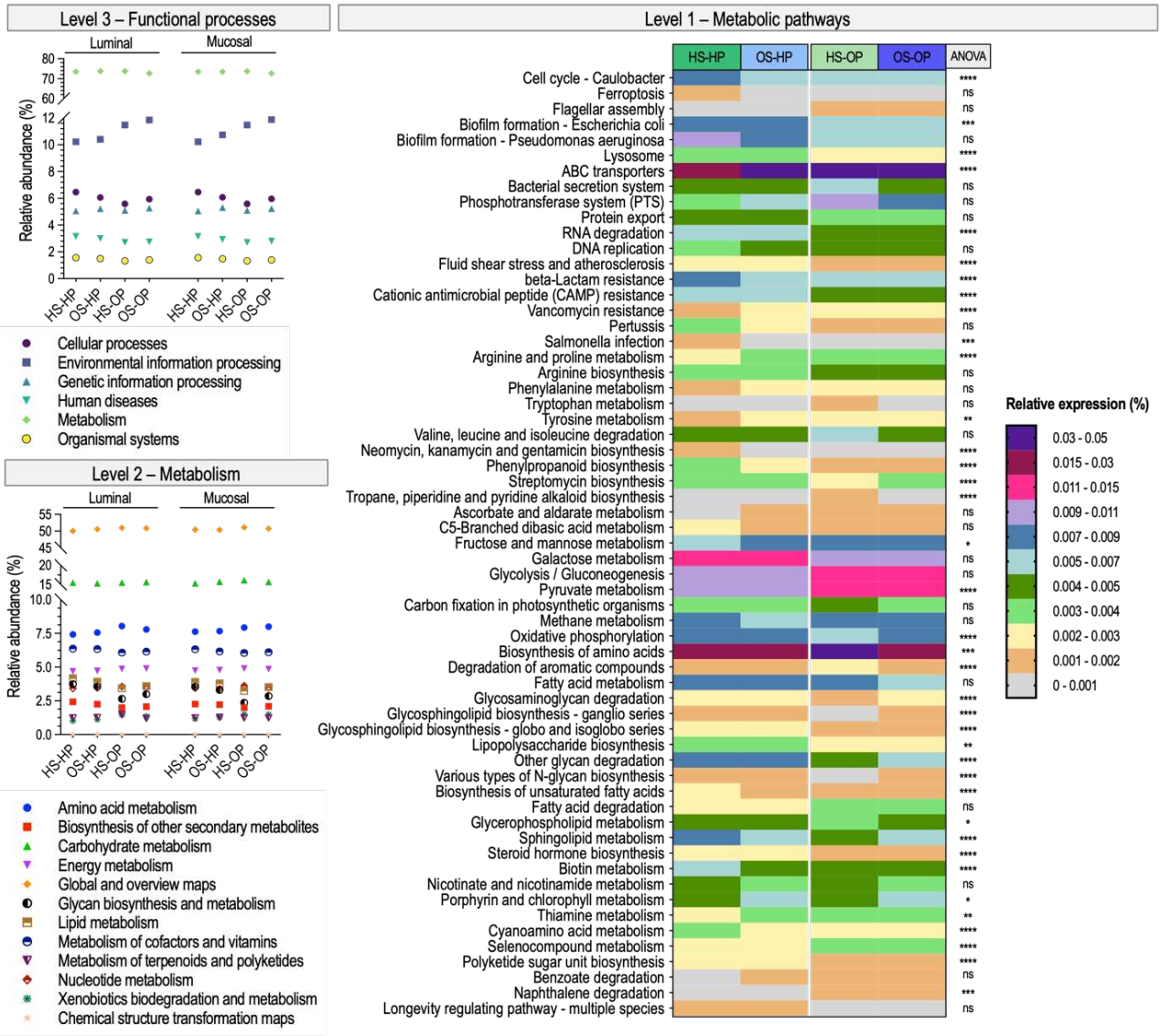

Figure 5. Metabolic pathways as predicted by Tax4fun2. Functional pathways were predicted using Tax4fun2 R-package with ASV table made from sequencing data matched against KEGG pathway database. Predicted functions were classified in three levels (functional processes, metabolism, and metabolic pathways). Data represent only the four endpoints of the experiments, i.e. during the stabilization period; and luminal and mucosal data were pooled. *HS: healthy donors; OS: obese donors; HP: healthy parameters; OP: obese parameters.*

Table 1= Shifts in microbiota composition and metabolic activities: *in vitro-in vivo* data comparisons

		***In vitro* data - BMI < 30**																**Obese microbiota *in vivo* data**					
		Luminal								**Mucosal**									**Less abundant**		**More abundant**		**No difference**	
	Microbial populations	**Obese *vs* Healthy parameters** H1	H2	H3	H4	**Healthy *vs* Obese parameters** O1	O2	O3	O4	O5	**Obese *vs* Healthy parameters** H1	H2	H3	H4	**Healthy *vs* Obese parameters** O1	O2	O3	O4	O5	***In vivo* data relevance**	**Human**	**Mice**	**Human**	**Mice**	**Human**	**Mice**
Microbiota composition	*Archaea*	↘	-	↘	-	↗	↗	-	↘	~	↘	-	-	-	-	↗	-	↗	↗	★★	**6/9** [23,54–56,64,65]		2/9 [53,66]		1/9 [57]	
	p_Verrucomicrobia	↘	-	↘	↘	~	-	-	↗	↗	-	-	↘	↘	↗	-	-	↗	↗	★★★	**2/8** [53,67]	**5/8** [40,42,44,45,47]			1/8 [68]	
	f_Akkermansiaceae	↘	-	↘	↘	~	-	-	↗	↗	-	-	↘	↘	↗	-	-	↗	↗	★★★	**1/3** [33]	**2/3** [40,41]				
	g_Akkermansia	↘	-	↘	↘	~	-	-	↗	↗	-	-	↘	↘	↗	-	-	↗	↗	★★★	**4/10** [54,64,69,70]	**6/10** [40–43,71,72]				
	p_Bacteroidetes	↗	↘	↗	↗	↘	↘	↘	~	↘	↘	↘	↗	↗	~	↗	↘	↘	~	★★	**10/24** [54–56,66,68,69,73–76]	**6/24** [42–45,47,77]	3/24 [23,33,51]	2/24 [40,78]	3/24 [38,49,53]	
	f_Bacteroidaceae	↗	↘	↗	↗	↗	↗	↘	~	↘	↘	↘	↗	↗	↗	↗	↘	~	~	★★		**2/3** [44,45]			1/3 [35]	
	g_Bacteroides	↘	↘	↘	~	↗	↗	↘	↗	↘	↘	↘	↘	↘	↗	↗	↘	~	~	★	**3/10** [35,49,75]	**2/10** [40,45]	1/10 [51]	1/10 [44]	3/10 [23,38,54]	
	f_Prevotellaceae	-	-	-	↗	↘	↘	↗	↘	-	-	-	-	↗	↘	↘	↗	-	-	★★★			**2/2** [35,53]			
	f_Rikenellaceae	↘	↘	↘	↘	↘	~	↗	↘	↗	↘	↘	↘	↘	↘	~	↗	↘	↗	★★★	**3/8** [35–37]	**4/8** [43–45,78]		1/8 [79]		
	f_Muribaculaceae	↗	-	-	-	↗	-	-	↘	↘	↗	-	-	-	↗	-	-	↘	↘	★★★		**2/2** [40,78]				
	f_Tannerellaceae	↗	↘	↘	↗	↗	↘	~	↘	↗	↘	↘	↗	↘	↗	↗	↘	~	↗	★		**1/1** [78]				
	f_Barnesiellaceae	↘	-	↗	↗	-	-	-	↗	↘	~	-	↗	~	~	-	-	~	↗	★	**2/4** [35,68]		1/4 [49]		1/4 [68]	
	p_Firmicutes	~	~	↘	↗	~	~	↘	↘	↘	↗	~	↗	↗	↘	↘	↘	↘	↘	★★	3/21 [23,38,54]	2/21 [40,78]	**7/21** [49,51,68,69,73,75,76]	**6/21** [42–45,47,77]	3/21 [55,56,66]	
	f_Ruminococcaceae	↘	↘	↘	↘	↗	↗	↗	↗	↘	↗	↗	↘	↘	↗	↘	↗	↘	↘	★★★	**4/9** [35,37,38,64]	**3/9** [40,78,79]		1/9 [45]		1/9 [44]
	f_Lachnospiraceae	~	↘	↘	↗	↘	↘	↘	↘	↘	↗	↘	~	↘	~	~	↘	↘	~	★★		1/8 [78]	**2/8** [64,68]	**3/8** [40,44,45]	2/8 [35,68]	
	f_Christensenellaceae	-	-	-	-	↗	↗	↗	↗	↗	↗	↘	↘	-	↗	↘	-	↗	↗	★★★	**3/3** [37,64,65]					
	f_Veillonellaceae	-	-	-	↗	-	↘	↘	-	-	-	-	-	↗	-	↘	↘	-	-	★★★			**2/2** [35,37]			

f_Clostridiaceae	-	↘	~	-	-	-	~	~	-	-	↘	~	-	-	-	~	~	-	★	1/4 [37]		**1/4** [68]	**1/4** [44]	1/4 [68]	
p_Proteobacteria	↗	↘	↗	↗	↗	~	↘	↗	↘	↘	↘	↗	↗	↘	~	↗	↘	~	★★		1/11 [40]	**5/11** [38,42,48,51,68]	**1/11** [45]	2/11 [49,54]	2/11 [43,44]
f_Rhodospirillales	↘	-	↗	-	↗	↗	-	-	↘	↘	-	↗	-	↗	-	-	-	↗	★				**1/1** [44]		
f_Enterobacteriaceae	↘	↘	-	↘	~	↘	↗	↗	↘	↘	↘	↘	↘	↗	↗	↗	↗	↗	★★			**2/3** [37,48]		**1/3** [35]	
p_Actinobacteria	↘	-	↗	-	↘	-	↘	↘	↘	↗	↘	↗	↗	↘	↘	↗	↘	↘	★		1/11 [45]	**3/11** [54,68,80]	**2/11** [40,42]	**3/11** [49,75,76]	**2/11** [43,44]

		***In vitro* data - BMI < 30**									**Obese microbiota *in vivo* data**			
		Obese *vs* healthy				Healthy *vs* obese					*In vivo* data relevance	Less abundant	More abundant	No difference
	SCFA concentrations	H1	H2	H3	H4	O1	O2	O3	O4	O5				
Microbiota activity	**Total**	↘	↗	~	↗	~	↗	↗	~	~	★★★		**4/5** [23,24,57,59]	1/5 [58]
	Acetate	↘	↗	↘	~	~	↗	↗	↗	↗	★★		**4/6** [24,57–59]	2/6 [23,59]
	Propionate	~	↗	~	↗	↘	↘	↗	~	↘	★★		**3/5** [5,8,38]	2/5 [24,58]
	Butyrate	~	↗	~	~	↗	↗	↘	~	~	★		**3/6** [24,58,59]	**3/6** [23,58,59]
	SCFA proportions (calculated from)													
	Acetate	~	↘	↘	~	~	↗	↗	~	~	★★	1/6 [59]	1/6 [58]	**4/6** [23,24,57,59]
	Propionate	~	~	↗	↗	↘	↘	↗	↘	↘	★★★	1/5 [58]		**4/5** [23,24,57,59]
	Butyrate	~	↗	~	~	~	~	↘	~	~	★★	1/6 [58]	1/6 [59]	**4/6** [23,24,57,59]

Inclusive parameters for obese *in vivo* data were BMI > 30 kg/m2, no drug, no probiotic or prebiotic treatments nor bariatric surgery, and comparison with healthy volunteers in the same study. Green box: *in vitro* data obtained in M-ARCOL are in line with *in vivo* data in human from literature; orange: no clear conclusion due to lack of consensus for *in vivo* data; red: *in vitro* and *in vivo* data are contradictory. ↗: >15% more abundant; ↘: >15% less abundant; ~: no difference. Ratio: proportion of the total number of articles in each category (less abundant/more abundant/no difference); Bold ratio: consensus for *in vivo* data, ★★★: more than 75 % of the *in vivo* studies from bibliography are in accordance; ★★: between 50 % and 75 % of the *in vivo* studies from bibliography are in accordance; ★: less than 50 % of the *in vivo* studies from bibliography are in accordance or only one article was found.

Healthy colonic parameters restore gut microbial eubiosis

In a reverse way, the next step of our study aimed to evaluate the impact of healthy *versus* obese parameters when fermenters were inoculated with stools from obese patients (**Fig. 1**, 5 donors O1 to O5). All the healthy microbial marker populations, i.e. *Akkermansiaceae, Rikenellaceae*, *Ruminococcaceae* and *Christensenellaceae* [33–39], which disappeared when applying obese parameters on healthy stools remarkably resumed ($P<0.05$) in the luminal phase when healthy parameters were implemented on obese stools (**Fig. 3a** and **3b**). Inversely, *Lachnospiraceae*, *Prevotellaceae* and *Veillonellaceae*, found in higher abundances in obese stools [34,35,37,40,44,45,68], are decreasing upon implementation of healthy reactor parameters (**Fig. 3a** and **3b**). Similar tendencies were observed in the mucosal phase for some donors, but significance was not observed using DESeq2 differential analysis (**Fig. 3e** and **3f**). As previously described in the reverse experiments, results obtained for *Akkermansiaceae* were really striking with the highest 4.3-fold change increase ($P<0.001$) in the luminal phase (**Fig. 3b**). These results were even more strengthened by qPCR quantification of *A. muciniphila* showing a significant 2-Log_{10} rise in both luminal and mucosal environments (**Fig. 3d** and **3h**). Applying healthy parameters also tended to restore bacterial α-diversity in the luminal but not in the mucosal phase (**Fig. 2a**). This trend can be certainly linked to an increase in fibre content in the nutritive medium, which displays an undeniable positive correlation with gut microbiota diversity [81]. Regarding methanogenic *Archaea*, reversibility was less obvious as evidenced with higher raw abundance of *Methanomethylophylaceae* in the luminal phase with healthy parameters in donors O1 and O2, but lower amount of *Methanobacteriaceae* in donors O2, O4 and O5 (**Fig. 3c**). *Methanomethylophylaceae* that was indisputably in very low abundance in obese stools, but not in healthy ones (**Fig. 1e**) seemed to be well adapted to *in vitro* fermentation conditions under healthy parameters in donors O1 and O2. The two well-known *Archaea M. smithii* and *M. stadtmanae* are affiliated with *Methanobacteriaceae,* but scarce data are available on *Methanomethylophylaceae*. However, remarkably, a very recent study detected this *Archaea* family in faecal samples from obese subjects [82]. Of note also, in donors O1 and O2, the higher prevalence in *Methanomethylophylaceae* under healthy condition could be related to a decrease in *Prevotellaceae* (**Fig. 3a** and **3c**). A strong relationship between these two populations has already been suggested [83], although their putative synergistic role in obesity is not in agreement with our results [53]. Still, related CH_4 production was significantly higher under healthy *versus* obese parameters, showing again microbiota reversibility (**Fig. 4b**). This was the most important modification regarding gut metabolites since total gas and SCFA production were unchanged whatever the parameters applied with obese stools (**Fig. 4**). β-diversity analysis (**Fig. 2f** and **2g**) and Tax4Fun2 pathway predictions (**Fig. 5**) also confirmed that obese stools/healthy parameters largely clustered together with healthy stools/healthy parameters. Our results associated with the shift from obese to healthy parameters when conducting *in vitro* assays can be correlated with *in vivo* data from obese patients subjected to restrictive diet (e.g. calories, fat or carbohydrate restriction). In particular, *Akkermansiaceae, Christensenellaceae* and *Rikenellaceae (Alistipes)* are increasing while *Prevotella* and *Veillonellaceae* decreased in stools from obese patients following low-calorie diet [84–86]. All together, these data suggest that the M-ARCOL model can capture microbiota restoration and health-promoting effects of balanced diets.

M-ARCOL retains individual features of human gut microbiota

In humans, it is well acknowledged that microbial composition of faecal samples is largely individual-dependent [30,87]. In particular, only part of the population hosts methanogenic *Archaea* and is methane producer. Here, RDA pointed out that donor origin was the predominant explanatory variable for dissimilarities in terms of gut microbiota composition (**Fig. 2c**). This is of particular importance since it demonstrates that the *in vivo* inter-individual variability in donor stool microbiota composition and function was maintained in the M-ARCOL model (**Fig. 2c** to **2e**). Differences between donor stools in marker populations related to obesity (e.g., *Akkermansiaceae*, methanogenic *Archaea*, *Rikenellaceae*, *Christensenellaceae*) was maintained in the *in vitro* gut model (**Fig. 1d** to **1f**, **Suppl. Fig. 4, 5** and **8**). Inter-individual variability related to microbial composition also correlated with donor-dependent variations in terms of SCFA and gas production (**Fig. 1c**, **Suppl. Fig. 1** and **2**). Especially, the presence of methanogenic *Archaea* populations in stools and fermentation medium was strongly correlated with CH_4 production in M-ARCOL (**Fig. 1e**, **Fig. 3c** and **3g**, **Fig. 4b**, and **Suppl. Fig. 1**). This strengthens the relevance of the strategy based on the use of a single faecal sample per experiment compared to pooling stools, since gut microbiota itself is a major driver of inter-individual variability [88].

***In vitro* obese model for personalized medication and nutrition**

In line with 3R European rules strongly encouraging the development of alternative *in vitro* methods to reduce as much as possible animal experiments [89], we developed an innovative *in vitro* model of the obese colon. Taken all together, our results showed that the new system accurately reproduces the structure and metabolic activity of obese gut microbiota, catching the main fine-scale perturbations associated with the disease. To our knowledge, this model is the first one where specific physicochemical parameters of the obese colon have been set-up (in addition to inoculation with obese stools [14,15,90]) and relevant *in vitro*/*in vivo* comparisons have been performed. In an original way, we also distinguished mucus from lumen-associated microbiota in M-ARCOL, which is obviously an added value to follow shifts in mucin-degrader populations such as *Akkermansiaceae*. For the first time, we also cross-compared the results obtained with healthy *versus* obese parameters and healthy *versus* obese stools. This original experimental set-up led us to conclude that inoculation with obese stools may not be required for the obese model, which can simplify regulatory approaches. This also emphasizes that physicochemical and nutritional parameters of the colonic environment are key factors to shape gut microbiota [91]. As exemplified in the present study, this model can be a useful platform to increase our understanding of the interrelationships between gut microbes and obesity, moving toward mechanistic studies in the absence of the host. In a next future, this model can be advantageously used to test various nutritional or pharmaceutical (e.g. dietary ingredients with lower obesogenic effects, prebiotic, probiotic, drug or faecal microbiota transplantation) approaches in a context of obesity, with the objective aim to identify innovative strategies able to restore gut microbial eubiosis. Of great interest, as aforementioned, this *in vitro* model is able to capture fine-scale gut microbiota inter-individuality, allowing the possibility to shift toward the identification and the better understanding of responders *versus* non-responders to a given pharmaceutic treatment or dietary intervention [92]. In particular, the effect of any treatment could be linked (or

not) to the individual diversity of microbiota, since *in vivo* data in human have already shown that the effect of restrictive diet in obese is strongly correlated to their faecal microbial diversity before regimen [93]. Ultimately, in preclinical phases, the obese colon model could be an essential tool to develop personalized interventions taking into consideration gut microbiota. In addition, in combination with host cell cultures and gut-on-chip models, the model can be used for a better understanding the etiopathology of obesity and subsequent secondary pathologies.

Methods

Stool sampling and treatment

Fresh stool samples were collected anaerobically from four healthy adults (2 women and 2 men, 36.3 ± 6.1 years old, BMI = 21.7 ± 2.0 kg/m^2) and five obese adults (4 women and 1 man, 41.8 ± 3.9 years old, BMI = 46.7 ± 2.1 kg/m^2). The exclusion criteria for both groups included the use of antibiotic or pre- and probiotic treatments in the 2 months prior to the beginning of the study, and bariatric surgery for obese patients. Stools were frozen at -80°C within 6 hours following defecation without cryoprotectants [16]. For each donor, a 10 % inoculum (w/v) suspension was prepared under strict anaerobic conditions (COY Laboratory Products Inc, Grass Lake, MI, USA) by mixing faeces in 30 mM sodium phosphate buffer (pH 6.5) supplemented with 1.9 mM cysteine. The resulting suspension was filtered through a 500-µm sieve in a sterile bottle.

M-ARCOL system

M-ARCOL is a one-stage fermentation system (**Fig. 1b**) used under continuous conditions which simulates, based on *in vivo* data, the main physicochemical (pH, body temperature, retention time, composition of ileal effluents used as a nutritive medium) and microbial (lumen and mucus-associated microbiota) conditions found in the human colon [16,94]. At the beginning of experiments, each airtight glass vessel containing 200 mL of nutritive medium was set under anaerobiosis by flushing with O_2-free N_2 gas before adding the faecal suspension (100 mL). Anaerobiosis was maintained during the total course of the fermentation by the sole activity of the resident microbiota and through ensuring the system airtightness [8,16]. Overproduced gases were collected daily in a sampling bag connected to the condenser. Bioreactors were kept at body temperature using an incorporated panel heater. Colonic pH and redox potential were constantly recorded (Applikon, Delft, The Netherlands) and pH was adjusted with an automatic addition of 2 M NaOH. The nutritive medium containing various sources of carbohydrates, proteins, lipids, minerals, and vitamins was continuously introduced into the bioreactor, while the fermentation medium was automatically withdrawn, ensuring the appropriate mean retention time. Colonic mucosal environment was reproduced through by-passing the fermentation medium from the main vessel towards an airtight removable compartment maintained at body temperature and containing an average surface of 556 cm^2 mucin-alginate beads [16,95]. Mucin beads were obtained by dropwise gelation of a 5 % mucin (Mucin from porcine stomach type II, Sigma-Aldrich, Saint-Louis, Missouri, USA) and 2 % sodium alginate (Sigma-Aldrich, Saint-Louis, Missouri, USA) solution inside 0.2 M $CaCl_2$ [16,95].

Experimental design

Each stool was used to inoculate two fermenters ran in parallel, one set-up with healthy parameters and the other with obese ones, based on *in vivo* data in humans (**Fig. 1a** and **1b**). After a 24h-batch fermentation allowing microbiota amplification, bioreactors were run under continuous conditions during 10 additional days (**Suppl. Fig. 9**). Samples were daily collected from the main vessel (termed luminal compartment) and centrifugated (18,000 g, 15 min, 4°C). Pellets were kept at -80°C for downstream luminal gut microbiota analysis and supernatant were collected and stored at -20°C for further SCFA measurement. Atmospheric phase was also sampled every day to check anaerobic condition and determine gas composition. Total volume of overproduced gases was measured daily. Every two days, mucin beads were collected from external vessel (termed mucosal compartment) and renewed by fresh ones under a constant CO_2-flow to maintain anaerobiosis. Beads were washed thrice in sterile Phosphate Buffer Saline (PBS) and stored at -80°C before mucosal microbiota analysis.

DNA extraction

Genomic DNA was extracted from luminal and mucosal samples using the QIAamp Fast DNA Stool Mini Kit® (Qiagen, Hilden, Germany). Samples were incubated 10 min at 37°C with 2 mL of 55 mM citrate buffer, then vortexed 3 min at full speed [96]. After centrifugation (8000 g, 1 min, 20°C), pellets were subjected to mechanical disruption using a bead beater (5 min, 20 beat/sec) with 300 mg of sterile glass beads (diameter ranging from 0.1 to 0.6 mm) and 1 mL of InhibitEX buffer from Qiagen kit. Then, DNA was extracted following manufacturer's instructions. DNA integrity was verified by agarose gel electrophoresis and quality checked by A260/280 absorbance using the NanoDropTM 2000 (Thermo Scientific, Wilmington, DE, USA). DNA quantity was measured with the Qubit dsDNA Broad Range Assay Kit® (Invitrogen, Carlsbad, USA) on a Qubit 3.0 Fluorometer® (Invitrogen, Carlsbad, USA). DNAs were stored at -20°C prior to quantitative PCR analysis and 16S Illumina sequencing.

Quantitative PCR

Total bacteria, *Firmicutes*, *Bacteroidetes*, *γ-proteobacteria*, *Ruminococcaceae*, *Prevotellaceae*, and *A. muciniphila* were quantified by qPCR. Primers and hybridization temperatures are listed in **Supplemental Table 1**. qPCR analysis was performed on a Biorad CFX96TM Real-Time System (Bio-Rad Laboratories, Hercules, USA) using Takyon Low ROX SYBR 2X MasterMix blue dTTP kit (Eurogentec, Liège, Belgium). Each reaction was run in duplicate in a final volume of 10 µL prepared as previously described in Deschamps *et al.* [16]. The amplification conditions consisted in 1 cycle at 95°C for 5 min, followed by 40 cycles of 95°C for 30 s, annealing temperatures (**Supplemental Table 1**) for 30 s and 72°C for 30 s. A melting step was added to ensure primer specificity. Standard curves were generated from 10-fold dilutions of bacterial DNA (isolated from reference strains) and allowed the calculation of DNA concentrations from extracted samples.

Gut microbiota composition by 16S Metabarcoding

The bacterial V3-V4 region of 16S ribosomal DNA (rDNA) and the archaeal 16S rDNA were amplified with primers described in **Supplemental Table 1**. Amplicons were generated using a Fluidigm Access Array followed by high-throughput sequencing on an Illumina MiSeq system (Illumina, USA) performed at the Carver Biotechnology Center of the University of Illinois (Urbana, USA). Bioinformatics analysis was performed by

GeT-Biopuces platform (INSA/TBI, Toulouse, France) using R software version 4.1.1 (2021-08-10) and rANOMALY package (version 0.0.0.9000) [97,98]. Demultiplexed raw sequence data were quality filtered and denoising process was performed using DADA2 R-package [99]. Reads with N bases or low phred quality score (under 2) were eliminated and reads under 100 pb length were removed. Decontamination steps were carried out to filter out sequences corresponding to PhiX DNA used as a spike-in control for MiSeq runs and chimeric sequences were filtered out. Taxonomic affiliation of the sequences was performed with rANOMALY package based on DECIPHER package [100]. SILVA 138 release [101] and GTDB_bac120_arc122 [102] were used and results were merged. To improve completeness of taxonomic affiliation, BLAST [103] alignments were carried out (98 % identity and coverage) on representative sequences of unassigned amplicon sequence variants (ASVs) or assigned with incomplete taxonomy. A phylogenetic tree was reconstructed based on ASVs representative sequences using DECIPHER package [104]. Alpha-diversity indices were calculated using the diversity_alpha_fun function from rANOMALY package. Beta-diversity were estimated using VEGAN R-package [105] from the complete ASV table. The across-sample microbiota diversity was described using RDA based on Bray-Curtis dissimilarities. Environmental factor's impact on dissimilarities among groups was evaluated using PERMANOVA permutation tests (999 permutations).

Tax4fun2 metabolic predictions

Computational predictions of the functional capabilities using data from 16S rDNA sequencing was performed using Tax4fun2 R-tool [62] based on the KEGG (Kyoto Encyclopedia of Genes and Genomes) database [106]. Briefly, Tax4Fun2 transforms ASV picked up against the Ref99NR database into taxonomic profiles of KEGG organisms and normalize these predictions by the 16S rDNA copy number.

Gas analysis by gas chromatography

The proportion of O_2, N_2, CO_2, CH_4, and H_2 in the atmospheric phase of M-ARCOL was determined using a 490 Micro-gas chromatograph (Agilent Technologies, Santa Clara, CA, USA) prepared with Molecular Sieve 5A column and PoraPlot U column coupled with thermal conductivity detector TCD detectors. Argon was used as the carrier gas. Calibration curves are made from four gas: (i) ambient air (78 % N_2, 21 % O_2 and 0.04 % CO_2), (ii) mixture A (5 % CO_2, 5 % H_2 and 90 % N_2), (iii) mixture B (20 % CO_2 and 80 % H_2), and mixture C (19.9 % CO_2, 19.9 % CH_4, 20 % H_2 and 40 % N_2). Results were expressed as relative percentages.

Short Chain Fatty Acids (SCFAs) analysis

The three main SCFA (acetate, propionate and butyrate) concentrations were determined on luminal samples using High Pressure Liquid Chromatography (Elite LaChrom, HITACHI, San Jose, CA, USA) coupled with a diode-array detector. The HPLC column (Concise Separations, San Jose, CA, USA) was maintained at 50°C. A mobile phase composed of sulfuric acid 0.04M was used at a flow rate of 0.6 mL/min to separate the different SCFAs. Data were analyzed by the EZChrom Elite software at 205 nm. SCFA concentrations (expressed in mM or relative percentages) were calculated from standard curves established with known concentrations of acetate, propionate and butyrate (0, 10, 25 and 40 mM) [8]. Total energy produced (kJ/mol) was calculated using the following value for acetate (874.2 kJ/mol), butyrate (2183.5 kJ/mol) and propionate (1527.3 kJ/mol) [15].

Statistical analysis

Results were expressed as means ± SEM (n = 4 or 5). Statistical analyses were processed using either GraphPad Prism software version 9.3.1 (GraphPad Software, San Diego, CA) or R studio. Data normal distribution was verified by combining Anderson-Darling, D'Agostino & Pearson, Shapiro-Wilk and Kolmogorov-Smirnov tests and homoscedasticity was checked using the Fisher test. Then, appropriate statistical analysis was applied (either two-way ANOVA, t-test, Mann-Whitney or Welch's tests). A Tukey's multiple comparisons test was applied after ANOVA if necessary. Beta-diversity was evaluated by Principal Coordinates Analysis (PCoA) and Non-metric multidimensional scaling (NMDS) prior to RDA performed using VEGAN package [105]. Differential analyses (DESeq2, metagenomeSeq, metacoder) were performed using rANOMALY package [97,98]. A Permutational Multivariate Analysis of Variance (PERMANOVA) were performed with ADONIS (999 permutations) with non-parametric tests. Differences were considered statistically significant when $P < 0.05$.

Ethics approval and consent to participate

Informed consent was obtained from all subjects involved in the study. Consent for faecal collection was obtained under registration number 2017-69 (OBESAR study, University Hospital Gabriel Montpied, Clermont-Ferrand).

Consent for publication

Not applicable.

Availability of data and materials

The 16S RNA gene amplicon sequencing data have been deposited and is publicly available on the NCBI Sequence Read Archive database with accession number PRJNA826426.

Competing interests

S.B.-D. is advising NexBiome as a science officer. C.C. is employee of General Mills. The other authors declare that the research was conducted in the absence of any commercial or financial relationships that could be considered as a potential conflict of interest.

Funding

This study was performed in the frame of the PSPC RESTORBIOME (2019-2023) and SCUSI-Région Auvergne-Rhône-Alpes project (2019-2021). This project was supported by the Program Investissement Avenir operated by BpiFrance, General Mills/Yoplait and Greencell industrial partners, Clermont Auvergne Metropole and Région Auvergne Rhône Alpes.

Author contributions

SBD and OU contributed to the conceptual design of this project and provided the study design with contributions from LEM, MP, YB, MA and CC. MP and YB enrolled the patients and obtained the informed consent. OU, CDe, MB, SC and CDu performed the experiments. OU, CDe, MB and CDu performed data analysis. OU, CDe and MB provided data visualizations. OU, CDe and SBD wrote the manuscript and revised the manuscript with contributions from YB and LEM. SBD supervised the project. SBD, MA and CC performed the project administration and funding acquisition. All authors have read and agreed to the published version of the manuscript.

Acknowledgements

We thank all the partners from RESTORBIOME and SCUSI projects for fruitful scientific discussions and the anonymous donors for their participation in the study. We would like also to thank Etienne Rifa from GeT-Biopuces Platform (Toulouse, France) for assistance with Illumina sequencing analysis.

References

1. Obesity and overweight [Internet]. [cited 2021 Oct 13]. Available from: https://www.who.int/news-room/fact-sheets/detail/obesity-and-overweight

2. Hruby A, Hu FB. The Epidemiology of Obesity: A Big Picture. Pharmacoeconomics. 2015;33:673–89.

3. Crovesy L, Masterson D, Rosado EL. Profile of the gut microbiota of adults with obesity: a systematic review. Eur J Clin Nutr. 2020;

4. Castaner O, Goday A, Park Y-M, Lee S-H, Magkos F, Shiow S-ATE, *et al.* The Gut Microbiome Profile in Obesity: A Systematic Review. Int J Endocrinol. 2018;2018:4095789.

5. Blaut M. Gut microbiota and energy balance: role in obesity. Proc Nutr Soc. 2015;74:227–34.

6. Aoun A, Darwish F, Hamod N. The Influence of the Gut Microbiome on Obesity in Adults and the Role of Probiotics, Prebiotics, and Synbiotics for Weight Loss. Prev Nutr Food Sci. 2020;25:113–23.

7. Ridaura VK, Faith JJ, Rey FE, Cheng J, Duncan AE, Kau AL, *et al.* Gut microbiota from twins discordant for obesity modulate metabolism in mice. Science. 2013;341:1241214.

8. Verdier C, Denis S, Gasc C, Boucinha L, Uriot O, Delmas D, *et al.* An Oral FMT Capsule as Efficient as an Enema for Microbiota Reconstruction Following Disruption by Antibiotics, as Assessed in an *In vitro* Human Gut Model. Microorganisms. 2021;9:358.

9. Hartung T. Thoughts on limitations of animal models. Parkinsonism Relat Disord. 2008;14 Suppl 2:S81-83.

10. Payne AN, Zihler A, Chassard C, Lacroix C. Advances and perspectives in *in vitro* human gut fermentation modeling. Trends Biotechnol. 2012;30:17–25.

11. Guerra A, Etienne-Mesmin L, Livrelli V, Denis S, Blanquet-Diot S, Alric M. Relevance and challenges in modeling human gastric and small intestinal digestion. Trends in Biotechnology. 2012;30:591–600.

12. Bell L, Whyte A, Duysburgh C, Marzorati M, Van den Abbeele P, Le Cozannet R, *et al.* A randomized, placebo-controlled trial investigating the acute and chronic benefits of American Ginseng (Cereboost®) on mood and cognition in healthy young adults, including *in vitro* investigation of gut microbiota changes as a possible mechanism of action. Eur J Nutr. 2022;61:413–28.

13. Isenring J, Geirnaert A, Hall AR, Jans C, Lacroix C, Stevens MJA. *In vitro* Gut Modeling as a Tool for Adaptive Evolutionary Engineering of Lactiplantibacillus plantarum. mSystems. 2021;6:e01085-20.

14. Mazier W, Le Corf K, Martinez C, Tudela H, Kissi D, Kropp C, *et al.* A New Strain of Christensenella minuta as a Potential Biotherapy for Obesity and Associated Metabolic Diseases. Cells. 2021;10:823.

15. Bussolo de Souza C, Roeselers G, Troost F, Jonkers D, Koenen ME, Venema K. Prebiotic effects of cassava bagasse in TNO's *in vitro* model of the colon in lean versus obese microbiota. Journal of Functional Foods. 2014;11:210–20.

16. Deschamps C, Fournier E, Uriot O, Lajoie F, Verdier C, Comtet-Marre S, *et al.* Comparative methods for fecal sample storage to preserve gut microbial structure and function in an *in vitro* model of the human colon. Appl Microbiol Biotechnol. 2020;104:10233–47.

17. Moreland AM, Santa Ana CA, Asplin JR, Kuhn JA, Holmes RP, Cole JA, *et al.* Steatorrhea and Hyperoxaluria in Severely Obese Patients Before and After Roux-en-Y Gastric Bypass. Gastroenterology. 2017;152:1055-1067.e3.

18. Seck EH, Senghor B, Merhej V, Bachar D, Cadoret F, Robert C, *et al.* Salt in stools is associated with obesity, gut halophilic microbiota and Akkermansia muciniphila depletion in humans. International Journal of Obesity. Nature Publishing Group; 2019;43:862–71.

19. Faloon WW, Rubulis A, Knipp J, Sherman CD, Flood MS. Fecal fat, bile acid, and sterol excretion abd biliary lipid changes in jejunoileostomy patients. Am J Clin Nutr. 1977;30:21–31.

20. Mok HY, Grundy SM. Cholesterol and bile acid absorption during bile acid therapy in obese subjects undergoing weight reduction. Gastroenterology. 1980;78:62–7.

21. Ridlon JM, Kang DJ, Hylemon PB, Bajaj JS. Bile Acids and the Gut Microbiome. Curr Opin Gastroenterol. 2014;30:332–8.

22. van Best N, Rolle-Kampczyk U, Schaap FG, Basic M, Olde Damink SWM, Bleich A, *et al.* Bile acids drive the newborn's gut microbiota maturation. Nat Commun. Nature Publishing Group; 2020;11:3692.

23. Schwiertz A, Taras D, Schäfer K, Beijer S, Bos NA, Donus C, *et al.* Microbiota and SCFA in lean and overweight healthy subjects. Obesity (Silver Spring). 2010;18:190–5.

24. Rahat-Rozenbloom S, Fernandes J, Gloor GB, Wolever TMS. Evidence for greater production of colonic short-chain fatty acids in overweight than lean humans. Int J Obes (Lond). 2014;38:1525–31.

25. Delgado-Aros S, Camilleri M, Garcia MA, Burton D, Busciglio I. High body mass alters colonic sensory-motor function and transit in humans. Am J Physiol Gastrointest Liver Physiol. 2008;295:G382-388.

26. Bouchoucha M, Potier M, Arinei G, Catheline JM, Fournier JL, Cohen R, *et al.* Variation du transit colique chez les patients obèses morbides après pose d'un ballon intragastrique. Gastroentérologie Clinique et Biologique. 2009;33:A39.

27. Wisén O, Johansson C. Gastrointestinal function in obesity: motility, secretion, and absorption following a liquid test meal. Metabolism. 1992;41:390–5.

28. Van den Abbeele P, Grootaert C, Marzorati M, Possemiers S, Verstraete W, Gérard P, *et al.* Microbial community development in a dynamic gut model is reproducible, colon region specific, and selective for Bacteroidetes and Clostridium cluster IX. Appl Environ Microbiol. 2010;76:5237–46.

29. Stearns JC, Lynch MDJ, Senadheera DB, Tenenbaum HC, Goldberg MB, Cvitkovitch DG, *et al.* Bacterial biogeography of the human digestive tract. Sci Rep. 2011;1:170.

30. Jiao L, Kourkoumpetis T, Hutchinson D, Ajami NJ, Hoffman K, White DL, *et al.* Spatial Characteristics of Colonic Mucosa-Associated Gut Microbiota in Humans. Microb Ecol. 2021;

31. Van den Abbeele P, Belzer C, Goossens M, Kleerebezem M, De Vos WM, Thas O, *et al.* Butyrate-producing Clostridium cluster XIVa species specifically colonize mucins in an *in vitro* gut model. ISME J. 2013;7:949–61.

32. De Weirdt R, Van de Wiele T. Micromanagement in the gut: microenvironmental factors govern colon mucosal biofilm structure and functionality. NPJ Biofilms Microbiomes. 2015;1:15026.

33. Yassour M, Lim MY, Yun HS, Tickle TL, Sung J, Song Y-M, *et al.* Sub-clinical detection of gut microbial biomarkers of obesity and type 2 diabetes. Genome Med [Internet]. 2016 [cited 2020 May 7];8. Available from: https://www.ncbi.nlm.nih.gov/pmc/articles/PMC4756455/

34. de la Cuesta-Zuluaga J, Corrales-Agudelo V, Carmona JA, Abad JM, Escobar JS. Body size phenotypes comprehensively assess cardiometabolic risk and refine the association between obesity and gut microbiota. Int J Obes (Lond). 2018;42:424–32.

35. Koo SH, Chu CW, Khoo JJC, Cheong M, Soon GH, Ho EXP, *et al.* A pilot study to examine the association between human gut microbiota and the host's central obesity. JGH Open. 2019;3:480–7.

36. Lv Y, Qin X, Jia H, Chen S, Sun W, Wang X. The association between gut microbiota composition and BMI in Chinese male college students, as analysed by next-generation sequencing. British Journal of Nutrition. Cambridge University Press; 2019;122:986–95.

37. Peters BA, Shapiro JA, Church TR, Miller G, Trinh-Shevrin C, Yuen E, *et al.* A taxonomic signature of obesity in a large study of American adults. Sci Rep. 2018;8:9749.

38. Gao R, Zhu C, Li H, Yin M, Pan C, Huang L, *et al.* Dysbiosis Signatures of Gut Microbiota Along the Sequence from Healthy, Young Patients to Those with Overweight and Obesity. Obesity (Silver Spring). 2018;26:351–61.

39. Goodrich JK, Davenport ER, Beaumont M, Jackson MA, Knight R, Ober C, *et al.* Genetic determinants of the gut microbiome in UK Twins. Cell Host Microbe. 2016;19:731–43.

40. Cao W, Chin Y, Chen X, Mi Y, Xue C, Wang Y, *et al.* The role of gut microbiota in the resistance to obesity in mice fed a high fat diet. International Journal of Food Sciences and Nutrition. 2019;0:1–11.

41. Everard A, Belzer C, Geurts L, Ouwerkerk JP, Druart C, Bindels LB, *et al.* Cross-talk between Akkermansia muciniphila and intestinal epithelium controls diet-induced obesity. PNAS. National Academy of Sciences; 2013;110:9066–71.

42. Yang Y, Zhong Z, Wang B, Xia X, Yao W, Huang L, *et al.* Early-life high-fat diet-induced obesity programs hippocampal development and cognitive functions via regulation of gut commensal Akkermansia muciniphila. Neuropsychopharmacol. 2019;44:2054–64.

43. Alard J, Lehrter V, Rhimi M, Mangin I, Peucelle V, Abraham A-L, *et al.* Beneficial metabolic effects of selected probiotics on diet-induced obesity and insulin resistance in mice are associated with improvement of dysbiotic gut microbiota. Environmental Microbiology. John Wiley & Sons, Ltd; 2016;18:1484–97.

44. Clarke SF, Murphy EF, O'Sullivan O, Ross RP, O'Toole PW, Shanahan F, *et al.* Targeting the Microbiota to Address Diet-Induced Obesity: A Time Dependent Challenge. PLoS One [Internet]. 2013 [cited 2020 May 28];8. Available from: https://www.ncbi.nlm.nih.gov/pmc/articles/PMC3676335/

45. Nagpal R, Mishra SP, Yadav H. Unique Gut Microbiome Signatures Depict Diet-Versus Genetically Induced Obesity in Mice. Int J Mol Sci. 2020;21:E3434.

46. Wang B, Kong Q, Li X, Zhao J, Zhang H, Chen W, *et al.* A High-Fat Diet Increases Gut Microbiota Biodiversity and Energy Expenditure Due to Nutrient Difference. Nutrients. 2020;12:E3197.

47. Cheng DM, Roopchand DE, Poulev A, Kuhn P, Armas I, Johnson WD, *et al.* High phenolics Rutgers Scarlet Lettuce improves glucose metabolism in high fat diet-induced obese mice. Mol Nutr Food Res. 2016;60:2367–78.

48. Betrapally NS, Gillevet PM, Bajaj JS. Changes in the Intestinal Microbiome and Alcoholic- and Non-alcoholic Liver Diseases—Causes or Effects? Gastroenterology. 2016;150:1745-1755.e3.

49. Andoh A, Nishida A, Takahashi K, Inatomi O, Imaeda H, Bamba S, *et al.* Comparison of the gut microbial community between obese and lean peoples using 16S gene sequencing in a Japanese population. J Clin Biochem Nutr. 2016;59:65–70.

50. Stanislawski MA, Frank DN, Borengasser SJ, Ostendorf DM, Ir D, Jambal P, *et al.* The Gut Microbiota during a Behavioral Weight Loss Intervention. Nutrients. 2021;13:3248.

51. Yasir M, Angelakis E, Bibi F, Azhar EI, Bachar D, Lagier J-C, *et al.* Comparison of the gut microbiota of people in France and Saudi Arabia. Nutr Diabetes. 2015;5:e153.

52. Wilkins AT, Reimer RA. Obesity, Early Life Gut Microbiota, and Antibiotics. Microorganisms. 2021;9:413.

53. Zhang H, DiBaise JK, Zuccolo A, Kudrna D, Braidotti M, Yu Y, *et al.* Human gut microbiota in obesity and after gastric bypass. Proc Natl Acad Sci U S A. 2009;106:2365–70.

54. Jinatham V, Kullawong N, Kespechara K, Gentekaki E, Popluechai S. Comparison of Gut Microbiota between Lean and Obese Adult Thai Individuals. Microbiology and Biotechnology Letters. 2018;46:277–87.

55. Million M, Angelakis E, Maraninchi M, Henry M, Giorgi R, Valero R, *et al.* Correlation between body mass index and gut concentrations of Lactobacillus reuteri, Bifidobacterium animalis, Methanobrevibacter smithii and Escherichia coli. Int J Obes (Lond). 2013;37:1460–6.

56. Million M, Maraninchi M, Henry M, Armougom F, Richet H, Carrieri P, *et al.* Obesity-associated gut microbiota is enriched in Lactobacillus reuteri and depleted in Bifidobacterium animalis and Methanobrevibacter smithii. Int J Obes (Lond). 2012;36:817–25.

57. Fernandes J, Su W, Rahat-Rozenbloom S, Wolever TMS, Comelli EM. Adiposity, gut microbiota and faecal short chain fatty acids are linked in adult humans. Nutr Diabetes. 2014;4:e121.

58. Fernández-Navarro T, Salazar N, Gutiérrez-Díaz I, de los Reyes-Gavilán CG, Gueimonde M, González S. Different Intestinal Microbial Profile in Over-Weight and Obese Subjects Consuming a Diet with Low Content of Fiber and Antioxidants. Nutrients. 2017;9:551.

59. Dugas LR, Bernabé BP, Priyadarshini M, Fei N, Park SJ, Brown L, *et al.* Decreased microbial co-occurrence network stability and SCFA receptor level correlates with obesity in African-origin women. Sci Rep. 2018;8:17135.

60. Rahat-Rozenbloom S, Fernandes J, Gloor GB, Wolever TMS. Evidence for greater production of colonic short-chain fatty acids in overweight than lean humans. Int J Obes (Lond). 2014;38:1525–31.

61. Turnbaugh PJ, Ley RE, Mahowald MA, Magrini V, Mardis ER, Gordon JI. An obesity-associated gut microbiome with increased capacity for energy harvest. Nature. Nature Publishing Group; 2006;444:1027–31.

62. Wemheuer F, Taylor JA, Daniel R, Johnston E, Meinicke P, Thomas T, *et al.* Tax4Fun2: prediction of habitat-specific functional profiles and functional redundancy based on 16S rRNA gene sequences. Environ Microbiome. 2020;15:11.

63. Belda E, Voland L, Tremaroli V, Falony G, Adriouch S, Assmann KE, *et al.* Impairment of gut microbial biotin metabolism and host biotin status in severe obesity: effect of biotin and prebiotic supplementation on improved metabolism. Gut. 2022;gutjnl-2021-325753.

64. de la Cuesta-Zuluaga J, Corrales-Agudelo V, Carmona JA, Abad JM, Escobar JS. Body size phenotypes comprehensively assess cardiometabolic risk and refine the association between obesity and gut microbiota. Int J Obes (Lond). 2018;42:424–32.

65. Goodrich JK, Davenport ER, Beaumont M, Jackson MA, Knight R, Ober C, *et al.* Genetic determinants of the gut microbiome in UK Twins. Cell Host Microbe. 2016;19:731–43.

66. Armougom F, Henry M, Vialettes B, Raccah D, Raoult D. Monitoring bacterial community of human gut microbiota reveals an increase in Lactobacillus in obese patients and Methanogens in anorexic patients. PLoS One. 2009;4:e7125.

67. Duranti S, Ferrario C, van Sinderen D, Ventura M, Turroni F. Obesity and microbiota: an example of an intricate relationship. Genes Nutr. 2017;12:18.

68. Del Chierico F, Abbatini F, Russo A, Quagliariello A, Reddel S, Capoccia D, *et al.* Gut Microbiota Markers in Obese Adolescent and Adult Patients: Age-Dependent Differential Patterns. Front Microbiol [Internet]. 2018 [cited 2020 May 13];9. Available from: https://www.ncbi.nlm.nih.gov/pmc/articles/PMC5996250/

69. Ettehad Marvasti F, Moshiri A, Taghavi MS, Riazi S, Taati M, Sadati SF, *et al.* The First Report of Differences in Gut Microbiota Composition between Obese and Normal Weight Iranian Subjects. Iran Biomed J. 2020;24:148–54.

70. Dao MC, Everard A, Aron-Wisnewsky J, Sokolovska N, Prifti E, Verger EO, *et al.* Akkermansia muciniphila and improved metabolic health during a dietary intervention in obesity: relationship with gut microbiome richness and ecology. Gut. BMJ Publishing Group; 2016;65:426–36.

71. Rodriguez J, Hiel S, Neyrinck AM, Roy TL, Pötgens SA, Leyrolle Q, *et al.* Discovery of the gut microbial signature driving the efficacy of prebiotic intervention in obese patients. Gut [Internet]. BMJ Publishing Group; 2020 [cited 2020 May 12]; Available from: https://gut.bmj.com/content/early/2020/02/10/gutjnl-2019-319726

72. Wei M, Huang F, Zhao L, Zhang Y, Yang W, Wang S, *et al.* A dysregulated bile acid-gut microbiota axis contributes to obesity susceptibility. EBioMedicine. 2020;55:102766.

73. Verdam FJ, Fuentes S, de Jonge C, Zoetendal EG, Erbil R, Greve JW, *et al.* Human intestinal microbiota composition is associated with local and systemic inflammation in obesity. Obesity (Silver Spring). 2013;21:E607-615.

74. Dominianni C, Sinha R, Goedert JJ, Pei Z, Yang L, Hayes RB, *et al.* Sex, body mass index, and dietary fiber intake influence the human gut microbiome. PLoS ONE. 2015;10:e0124599.

75. Kasai C, Sugimoto K, Moritani I, Tanaka J, Oya Y, Inoue H, *et al.* Comparison of the gut microbiota composition between obese and non-obese individuals in a Japanese population, as analyzed by terminal restriction fragment length polymorphism and next-generation sequencing. BMC Gastroenterol. 2015;15:100.

76. Koliada A, Syzenko G, Moseiko V, Budovska L, Puchkov K, Perederiy V, *et al.* Association between body mass index and Firmicutes/Bacteroidetes ratio in an adult Ukrainian population. BMC Microbiol. 2017;17:120.

77. Ley RE, Turnbaugh PJ, Klein S, Gordon JI. Microbial ecology: human gut microbes associated with obesity. Nature. 2006;444:1022–3.

78. Wang J-H, Shin NR, Lim S-K, Im U, Song E-J, Nam Y-D, *et al.* Diet Control More Intensively Disturbs Gut Microbiota Than Genetic Background in Wild Type and ob/ob Mice. Front Microbiol [Internet]. 2019 [cited 2020 May 12];10. Available from: https://www.frontiersin.org/articles/10.3389/fmicb.2019.01292/full

79. Daniel H, Gholami AM, Berry D, Desmarchelier C, Hahne H, Loh G, *et al.* High-fat diet alters gut microbiota physiology in mice. ISME J. 2014;8:295–308.

80. Turnbaugh PJ, Hamady M, Yatsunenko T, Cantarel BL, Duncan A, Ley RE, *et al.* A core gut microbiome in obese and lean twins. Nature. 2009;457:480–4.

81. Menni C, Jackson MA, Pallister T, Steves CJ, Spector TD, Valdes AM. Gut microbiome diversity and high-fibre intake are related to lower long-term weight gain. Int J Obes (Lond). 2017;41:1099–105.

82. Chibani CM, Mahnert A, Borrel G, Almeida A, Werner A, Brugère J-F, *et al.* A catalogue of 1,167 genomes from the human gut archaeome. Nat Microbiol. 2022;7:48–61.

83. Aguilar-Marin SB, Betancur-Murillo CL, Isaza GA, Mesa H, Jovel J. Lower methane emissions were associated with higher abundance of ruminal Prevotella in a cohort of Colombian buffalos. BMC Microbiology. 2020;20:364.

84. Dong TS, Luu K, Lagishetty V, Sedighian F, Woo S-L, Dreskin BW, *et al.* The Intestinal Microbiome Predicts Weight Loss on a Calorie-Restricted Diet and Is Associated With Improved Hepatic Steatosis. Front Nutr. 2021;8:718661.

85. Louis S, Tappu R-M, Damms-Machado A, Huson DH, Bischoff SC. Characterization of the Gut Microbial Community of Obese Patients Following a Weight-Loss Intervention Using Whole Metagenome Shotgun Sequencing. PLoS One. 2016;11:e0149564.

86. Cuevas-Sierra A, Romo-Hualde A, Aranaz P, Goni L, Cuervo M, Martínez JA, *et al.* Diet- and sex-related changes of gut microbiota composition and functional profiles after 4 months of weight loss intervention. Eur J Nutr. 2021;60:3279–301.

87. Eckburg PB, Bik EM, Bernstein CN, Purdom E, Dethlefsen L, Sargent M, *et al.* Diversity of the human intestinal microbial flora. Science. 2005;308:1635–8.

88. Aguirre M, Ramiro-Garcia J, Koenen ME, Venema K. To pool or not to pool? Impact of the use of individual and pooled fecal samples for *in vitro* fermentation studies. J Microbiol Methods. 2014;107:1–7.

89. EMA. Regulatory acceptance of 3R (replacement, reduction, refinement) testing approaches [Internet]. European Medicines Agency. 2018 [cited 2022 Apr 16]. Available from: https://www.ema.europa.eu/en/regulatory-acceptance-3r-replacement-reduction-refinement-testing-approaches

90. Garzarella EU, Navajas-Porras B, Pérez-Burillo S, Ullah H, Esposito C, Santarcangelo C, *et al.* Evaluating the effects of a standardized polyphenol mixture extracted from poplar-type propolis on healthy and diseased human gut microbiota. Biomed Pharmacother. 2022;148:112759.

91. Zihler Berner A, Fuentes S, Dostal A, Payne An, Vazquez Gutierrez P, Chassard C, *et al.* Novel Polyfermentor intestinal model (PolyFermS) for controlled ecological studies: validation and effect of pH. PloS one [Internet]. PLoS One; 2013 [cited 2022 Apr 16];8. Available from: https://pubmed.ncbi.nlm.nih.gov/24204958/

92. Cani PD, Van Hul M. Gut microbiota and obesity: causally linked? Expert Rev Gastroenterol Hepatol. 2020;14:401–3.

93. Bel Lassen P, Belda E, Prifti E, Dao MC, Specque F, Henegar C, *et al.* Protein supplementation during an energy-restricted diet induces visceral fat loss and gut microbiota amino acid metabolism activation: a randomized trial. Sci Rep. 2021;11:15620.

94. Thévenot J, Etienne-Mesmin L, Denis S, Chalancon S, Alric M, Livrelli V, *et al.* Enterohemorrhagic Escherichia coli O157:H7 survival in an *in vitro* model of the human large intestine and interactions with probiotic yeasts and resident microbiota. Appl Environ Microbiol. 2013;79:1058–64.

95. Gresse R, Chaucheyras-Durand F, Denis S, Beaumont M, Van de Wiele T, Forano E, *et al.* Weaning-associated feed deprivation stress causes microbiota disruptions in a novel mucin-containing *in vitro* model of the piglet colon (MPigut-IVM). J Anim Sci Biotechnol. 2021;12:75.

96. Capone SH, Dufresne M, Rechel M, Fleury M-J, Salsac A-V, Paullier P, *et al.* Impact of alginate composition: from bead mechanical properties to encapsulated HepG2/C3A cell activities for *in vivo* implantation. PLoS One. 2013;8:e62032.

97. Theil S, Rifa E. rANOMALY: AmplicoN wOrkflow for Microbial community AnaLYsis. F1000Res. 2021;10:7.

98. Rifa E, Theil S. ExploreMetabar: v1.0.1, https://forgemia.inra.fr/umrf/exploremetabar. [Internet]. Zenodo; 2021 [cited 2022 Apr 19]. Available from: https://zenodo.org/record/5245195

99. Callahan BJ, McMurdie PJ, Rosen MJ, Han AW, Johnson AJA, Holmes SP. DADA2: High-resolution sample inference from Illumina amplicon data. Nat Methods. 2016;13:581–3.

100. Murali A, Bhargava A, Wright ES. IDTAXA: a novel approach for accurate taxonomic classification of microbiome sequences. Microbiome. 2018;6:140.

101. Quast C, Pruesse E, Yilmaz P, Gerken J, Schweer T, Yarza P, *et al.* The SILVA ribosomal RNA gene database project: improved data processing and web-based tools. Nucleic Acids Res. 2013;41:D590-596.

102. Parks DH, Chuvochina M, Rinke C, Mussig AJ, Chaumeil P-A, Hugenholtz P. GTDB: an ongoing census of bacterial and archaeal diversity through a phylogenetically consistent, rank normalized and complete genome-based taxonomy. Nucleic Acids Res. 2022;50:D785–94.

103. Altschul SF, Gish W, Miller W, Myers EW, Lipman DJ. Basic local alignment search tool. J Mol Biol. 1990;215:403–10.

104. Schliep K, Potts AJ, Morrison DA, Grimm GW. Intertwining phylogenetic trees and networks. Methods in Ecology and Evolution. 2017;8:1212–20.

105. Oksanen J, Blanchet FG, Friendly M, Kindt R, Legendre P, McGlinn D, *et al.* vegan: Community Ecology Package. R package version 2.5-5, 2019. 2019.

106. Kanehisa M, Goto S. KEGG: kyoto encyclopedia of genes and genomes. Nucleic Acids Res. 2000;28:27–30.

107. Yu Y, Lee C, Kim J, Hwang S. Group-specific primer and probe sets to detect methanogenic communities using quantitative real-time polymerase chain reaction. Biotechnol Bioeng. 2005;89:670–9.

108. Bacchetti De Gregoris T, Aldred N, Clare AS, Burgess JG. Improvement of phylum- and class-specific primers for real-time PCR quantification of bacterial taxa. J Microbiol Methods. 2011;86:351–6.

109. Garcia-Mazcorro JF, Suchodolski JS, Jones KR, Clark-Price SC, Dowd SE, Minamoto Y, *et al.* Effect of the proton pump inhibitor omeprazole on the gastrointestinal bacterial microbiota of healthy dogs. FEMS Microbiol Ecol. 2012;80:624–36.

110. Klindworth A, Pruesse E, Schweer T, Peplies J, Quast C, Horn M, *et al.* Evaluation of general 16S ribosomal RNA gene PCR primers for classical and next-generation sequencing-based diversity studies. Nucleic Acids Res. 2013;41:e1.

111. Takai K, Horikoshi K. Rapid detection and quantification of members of the archaeal community by quantitative PCR using fluorogenic probes. Appl Environ Microbiol. 2000;66:5066–72.

Supplemental Table 1. Primers used for quantitative PCR analysis and 16Sr RNA sequencing

Primer name	Sequence 5'-3'	Target	Annealing temperature (°C)	Reference
qPCR primers				
BAC338R	ACTCCTACGGGAGGCAG	Total bacteria	58	[107]
BAC516F	GTATTACCGCGGCTGCTG			
789cfbF	CRAACAGGATTAGATACCCT	*Bacteroidetes*	61	[108]
cfb976R	GGTAAGGTTCCTCGCGTAT			
928F-Firm	TGAAACTYAAAGGAATTGACG	*Firmicutes*	61	[108]
1040FirmR	ACCATGCACCACCTGTC			
1080γF	TCGTCAGCTCGTGTYGTGA	*γ-proteobacteria*	56	[54]
γ1202R	CGTAAGGGCCATGATG			
RumiF	ACTGAGAGGTTGAACGGCCA	*Ruminococcaceae*	59	[109]
RumiR	CCTTTACACCCAGTAAWTCCGGA			
Prov-F1	GCCGCGGTAATACGGAAGG	*Prevotellaceae*	61	[54]
Prov-R1	CTAATCCTGTTYGATACCCGCAC			
AkMf1	CAGCACGTGAAGGTGGGGAC	*A. muciniphila*	61	[54]
AkMR1	CCTTGCGGTTGGCTTCAGAT			
Sequencing primers				
V3_F357_N	CCTACGGGNGGCWGCAG	*Bacteria*		[110]
V4_R805	GACTACHVGGGTATCTAATCC			
Arch349F	GYGCASCAGKCGMGAAW	*Archaea*		(Takai & Horikoshi, 2000)
Arch806R	GGACTACVSGGGTATCTAAT			

Supplementary data

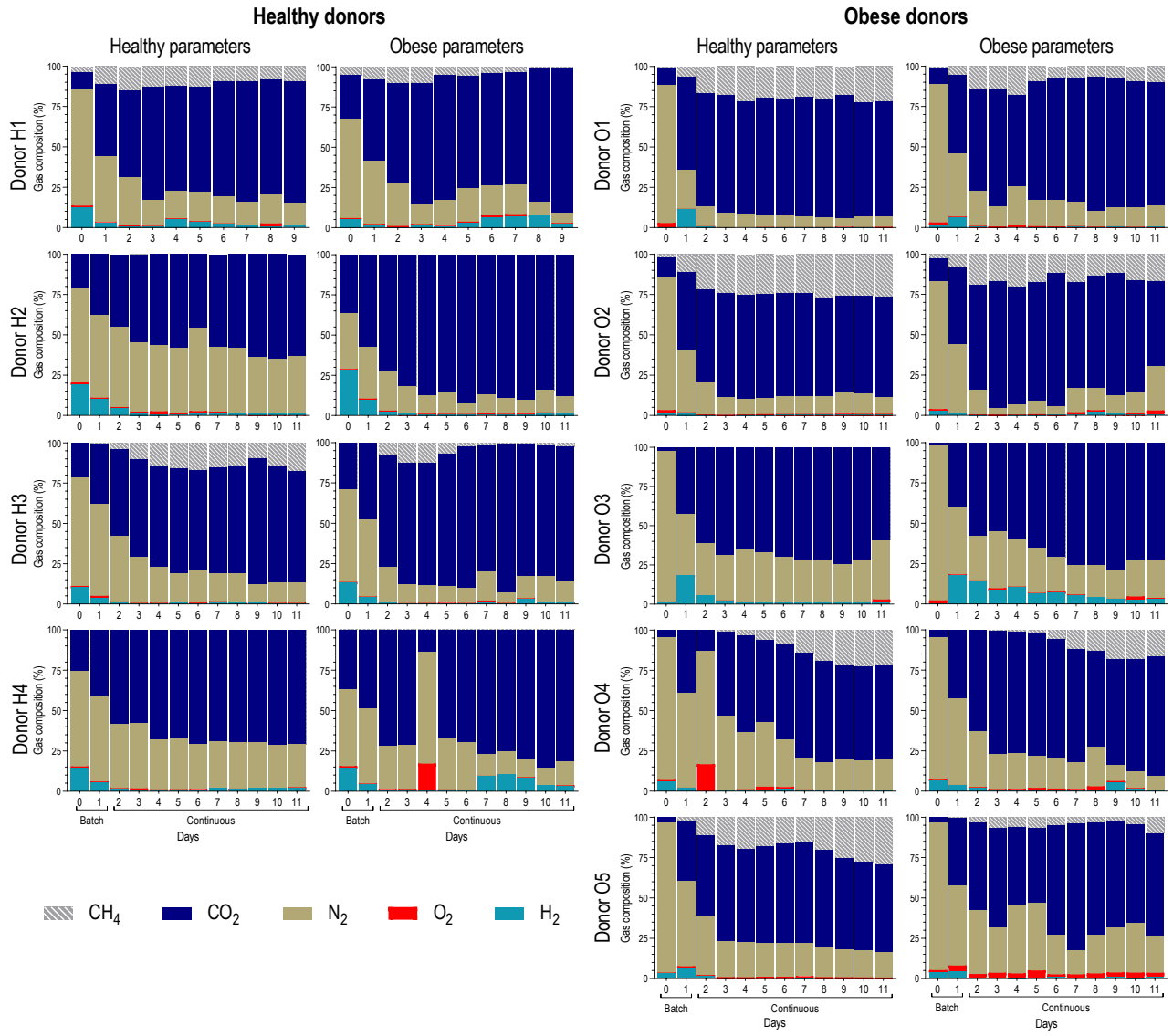

Suppl. Fig.1: Effect of stools origin and M-ARCOL parameters (obese versus healthy) on individual gas composition. Gas composition of the atmospheric phase of M-ARCOL was determined daily by gas chromatography. Results are expressed as relative percentages throughout fermentations for each donor. Healthy donors: H1, H2, H3 and H4. Obese donors: O1, O2, O3, O4 and O5. *CH_4: methane, CO_2: carbon dioxide, H_2: dihydrogen, N_2: dinitrogen, O_2: dioxygen.*

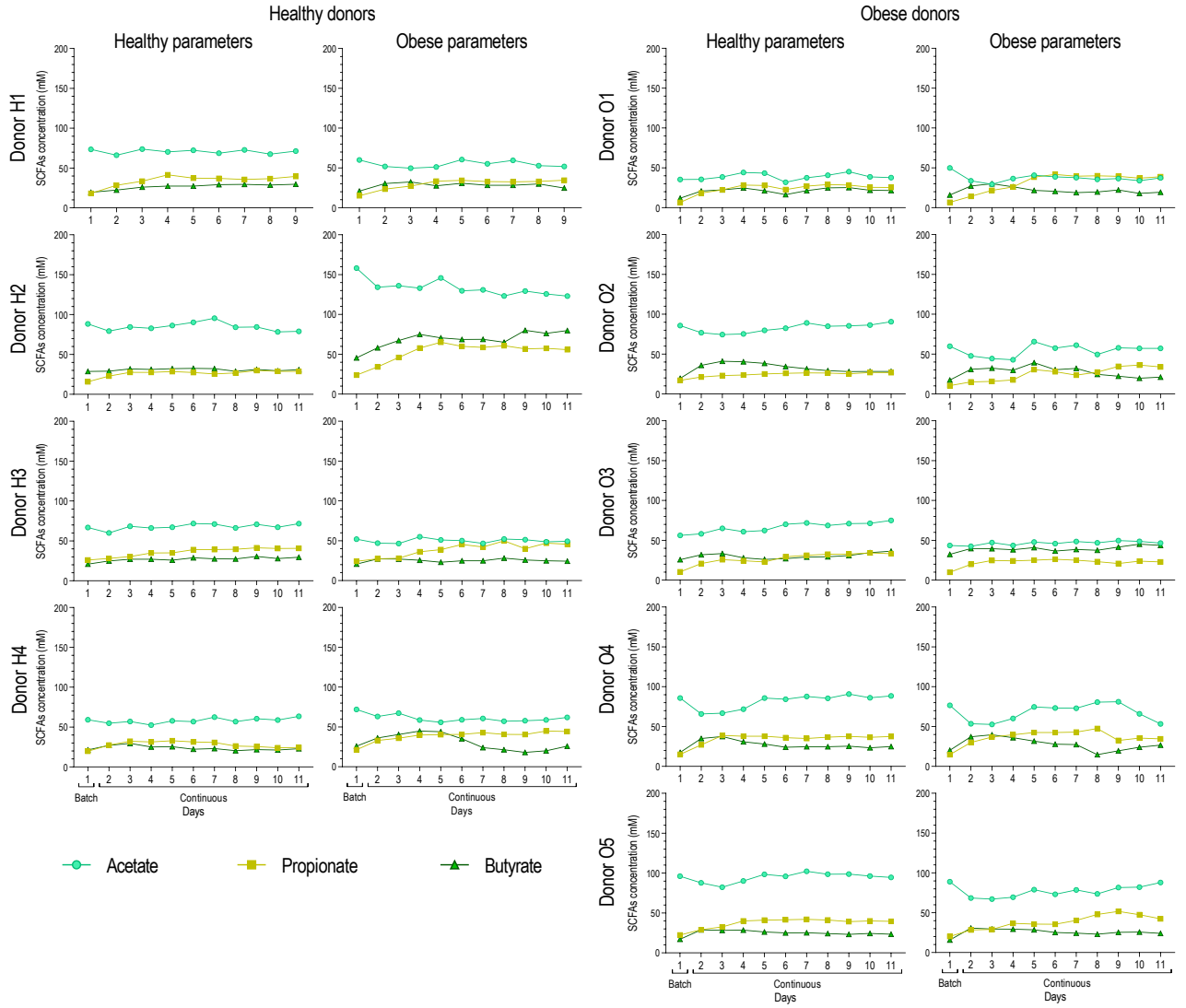

Suppl. Fig.2: Effect of stools origin and M-ARCOL parameters (obese versus healthy) on individual short chain fatty acid composition. Main short chain fatty acids (acetate, propionate and butyrate) were measured by liquid chromatography in the luminal compartment of M-ARCOL. Results are expressed as mmol throughout the total duration of fermentation for each individual donor. *Healthy donors: H1, H2, H3 and H4. Obese donors: O1, O2, O3, O4 and O5.*

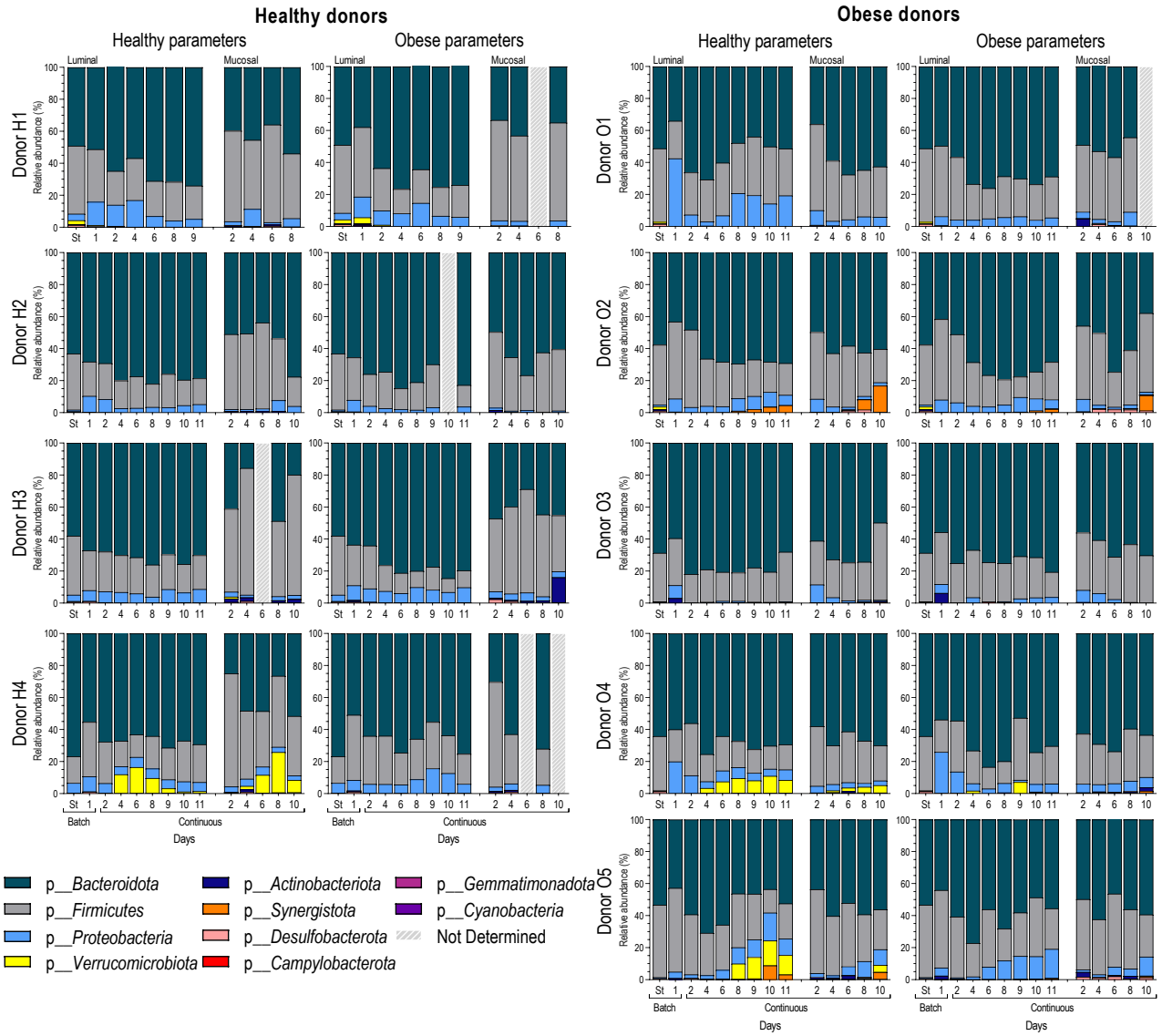

Suppl. Fig.3: Individual bacterial composition at the phylum level. For each donor and M-ARCOL parameters (obese and healthy), the composition of the lumen and mucus-associated microbiota was determined by 16S rRNA gene amplicon sequencing. Results are expressed as relative abundance at the phylum level throughout the total duration of the fermentation for each individual donor. *Healthy donors: H1, H2, H3 and H4. Obese donors: O1, O2, O3, O4 and O5. Not determined: sequencing trouble.*

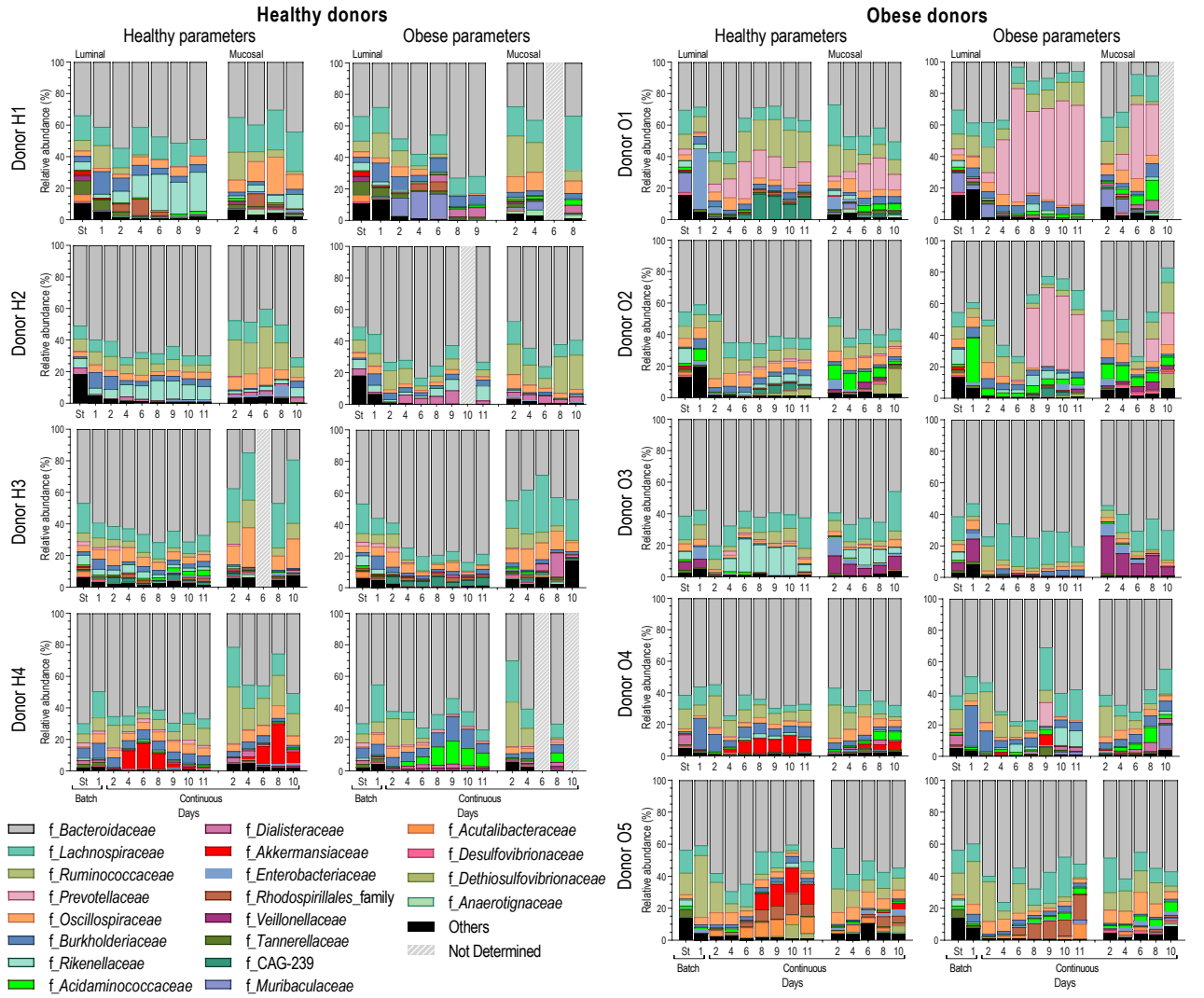

Suppl. Fig.4: Individual bacterial composition at the family level. For each donor and M-ARCOL parameters (obese and healthy), the composition of the lumen and mucus-associated microbiota was determined by 16S rRNA gene amplicon sequencing. Results are expressed as relative abundance at the family level throughout the total duration of the fermentation for each individual donor. *Healthy donors: H1, H2, H3 and H4. Obese donors: O1, O2, O3, O4 and O5. Not determined: sequencing trouble.*

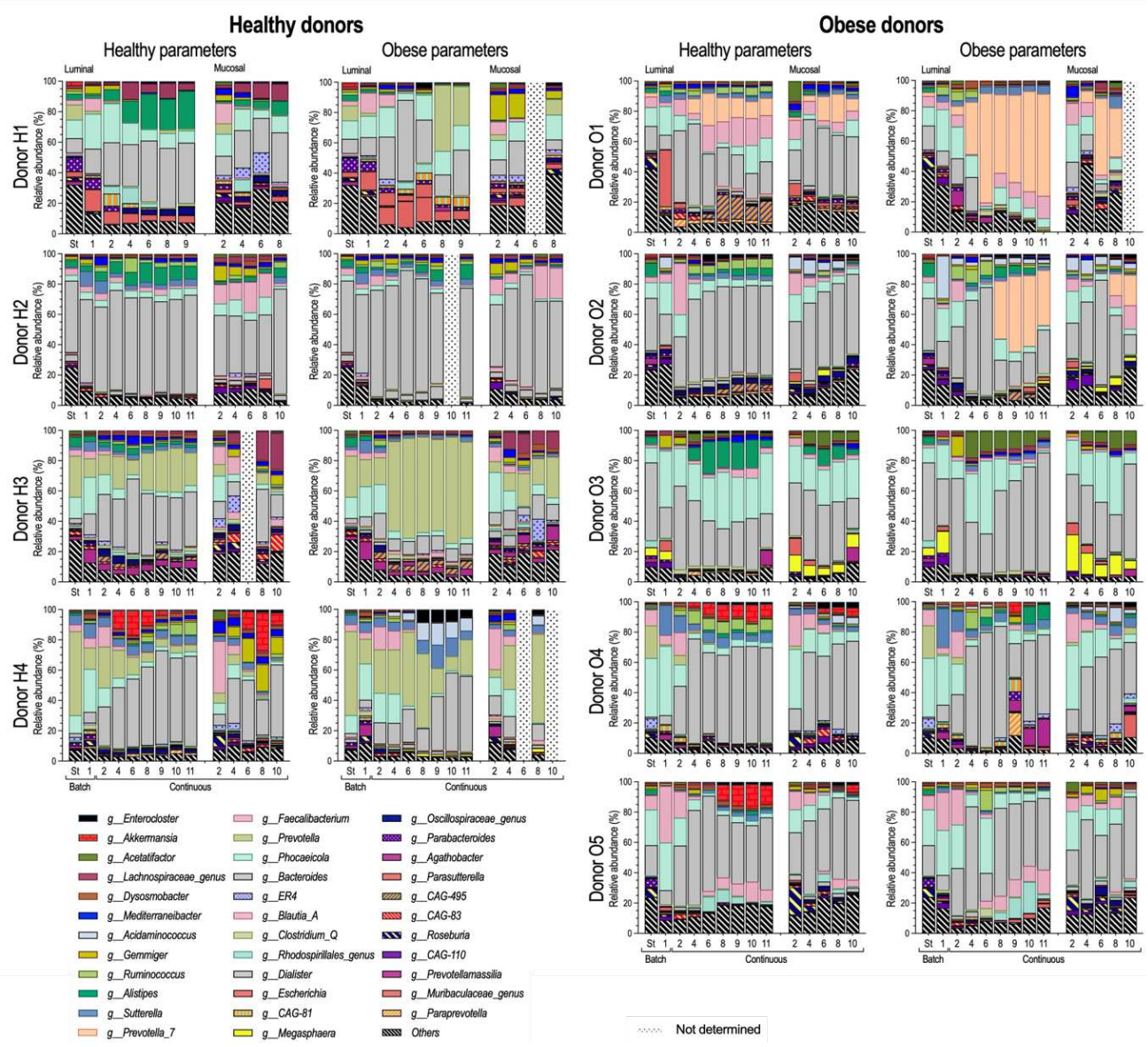

Suppl. Fig.5: Individual bacterial composition at the genus level. For each donor and M-ARCOL parameters (obese and healthy), the composition of the lumen and mucus-associated microbiota was determined by 16S rRNA gene amplicon sequencing. Results are expressed as relative abundance at the genus level throughout the total duration of the fermentation for each individual donor. *Healthy donors: H1, H2, H3 and H4. Obese donors: O1, O2, O3, O4 and O5. Not determined: sequencing trouble.*

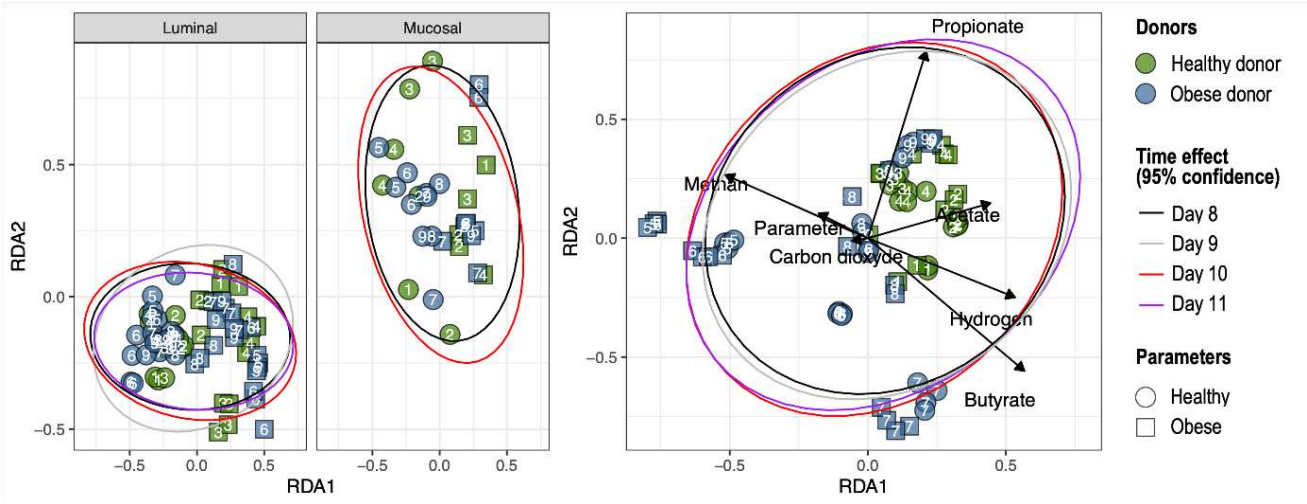

Suppl. Fig.6: Impact of fermentation time on bacterial β-diversity RDA two dimension-plot investigated bacterial community β-diversity at the ASV level (excluding donor variable) for all donors when applying healthy or obese parameters (4 healthy and 5 obese donors). Data represents only the last four days of fermentation (from day 8 to day 11). Numbers inside the symbols represent donor's number. Both luminal and mucosal samples were compared in graph a) whereas graph b) integrated environmental variables (i.e. SCFA and gas) for luminal samples only. Statistical ellipses were calculated based on 95% confidence interval to highlight variable's effect.

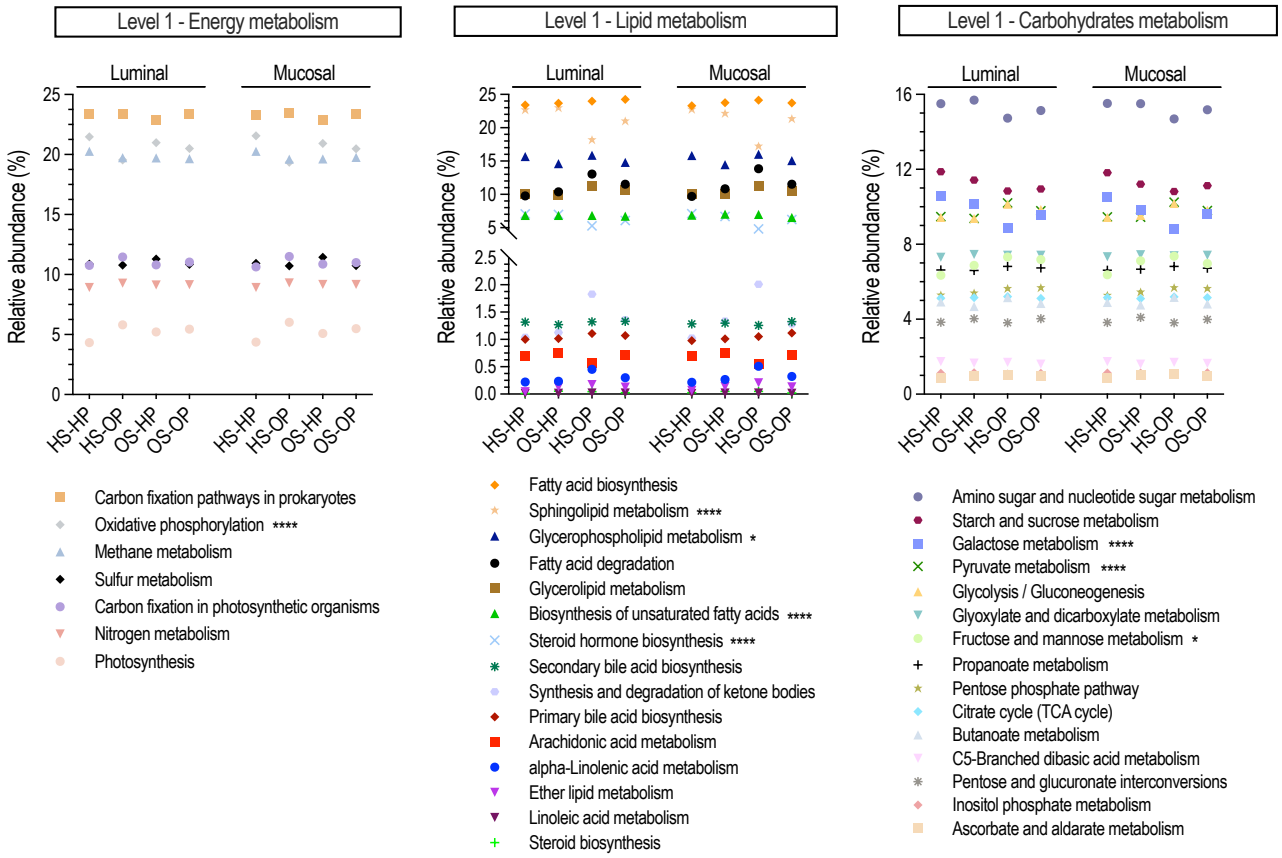

Suppl. Fig.7. Metabolism pathways predicted by Tax4fun2. Metabolic pathways were predicted using Tax4fun software from 16S rDNA sequencing data obtained the last four days of fermentation (Day 8 to Day 11) matched against KEGG pathway database. Data from energy, lipid and carbohydrates metabolism are presented. HS: healthy donors; OS: obese donors; HP: healthy parameters; OP: obese parameters. Statistical differences based on ANOVA are shown: **** $P < 0.0001$; * $P < 0.05$.

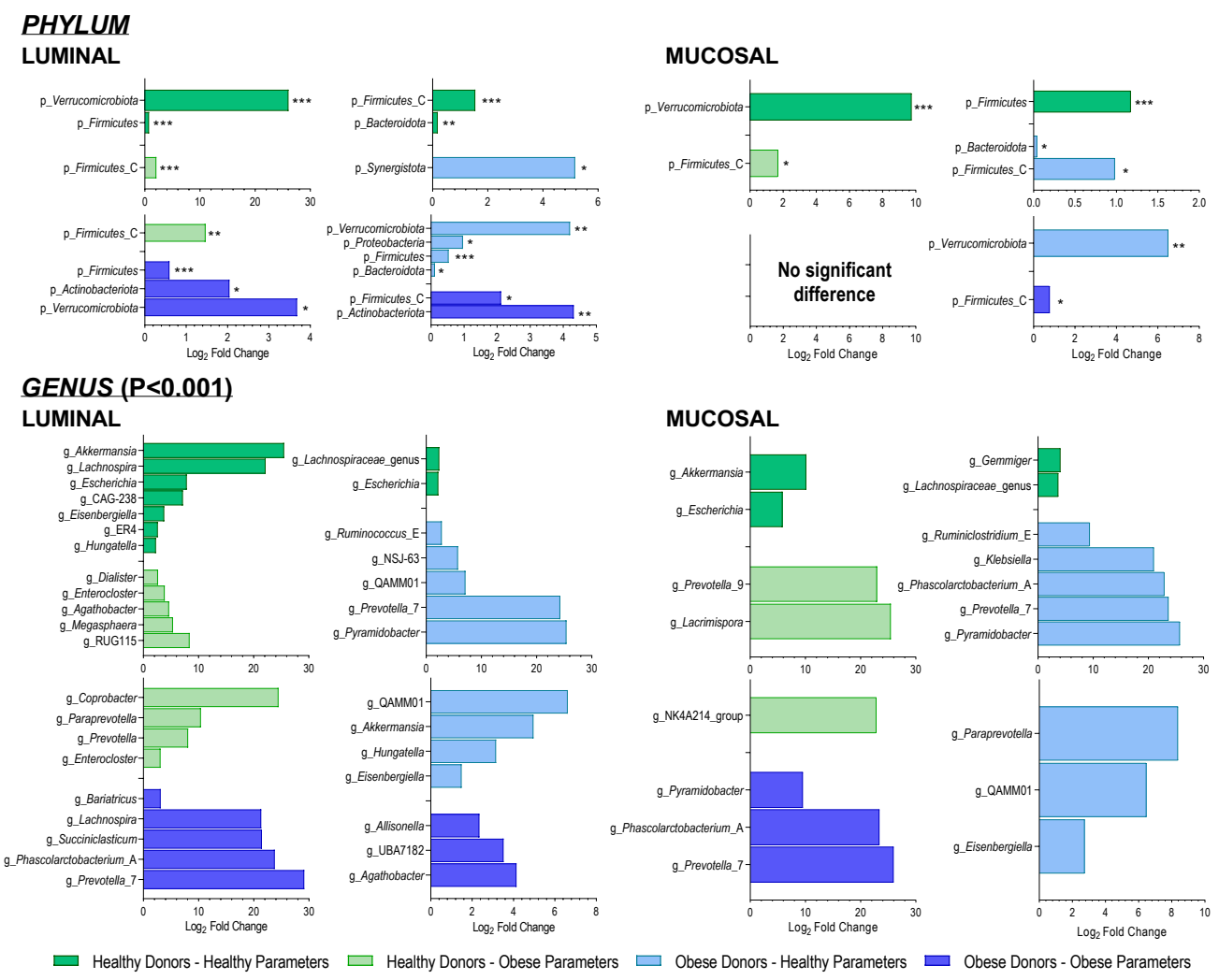

Suppl. Fig.8: Differential analysis of bacterial populations at the phylum and genus levels. Bacterial differential analysis was performed from 16S rDNA data obtained for the lumen (left) and mucus (right)-associated microbiota, both at the phylum and genus levels. Results obtained during the last four days of fermentation are shown (Day 8 to Day 11). Differential analysis performed with three different methods (DeSeq2, Metacoder and MetagenomeSeq R-analysis). Presented families are differentially more abundant in at least one method: P < 0.001; **: P < 0.01 and *: P < 0.05.

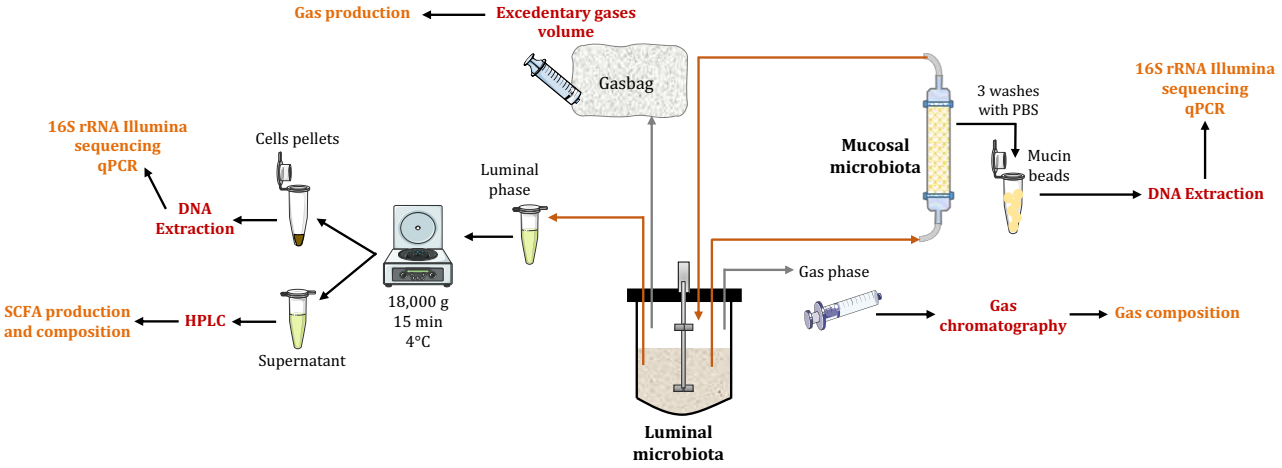

Suppl. Fig.9. Overview of sample collection, treatment, and analysis during M-ARCOL experiments. Every day, luminal medium from M-ARCOL was collected and centrifuged. Pellets were kept for DNA extraction (qPCR and 16S rRNA Illumina sequencing) while supernatants were used for SCFA analysis. The atmospheric phase was also collected to determine gas composition and total gas production. Every two days, mucin beads contained in the external glass compartment were collected and washed with PBS before DNA extraction.

Appendix 6 – Poster communication

DESCHAMPS, C., HUMBERT, D., PRIYMENKO, N., DENIS, S., APPER, E. & BLANQUET-DIOT, S. Colonic physicochemical parameters from different dog's sizes reshape canine microbiota activity and structure in an *in vitro* gut model. *12th International Symposium on Gut Microbiology*, virtual, October 13-15th, **2021**

Colonic physicochemical parameters from different dog's sizes reshape canine microbiota activity in an *in vitro* gut model

DESCHAMPS Charlotte[1,2], HUMBERT Delphine[3], PRIYMENKO Nathalie[4], DENIS Sylvain[1], APPER Emmanuelle[2], BLANQUET-DIOT Stéphanie[1]

[1] UMR 454 MEDIS UCA/INRAe, Clermont-Ferrand, France; [2] Lallemand Animal Nutrition, Toulouse, France; [3] Dômes Pharma, Pont-du-Château, France; [4] École Nationale Vétérinaire de Toulouse, Toulouse, France.

INTRODUCTION

Digestion and gut microbiota are key parameters in canine health, with a great impact of body weight on several digestive parameters, such as changes in colonic pH, transit time and permeability.

In a context of 3Rs rules aiming to reduce *in vivo* experiments, we adapted the M-ARCOL (Mucosal Artificial Colon), first developed to simulate the human colon compartment, to dog digestive conditions, integrating variations associated to the three dog's sizes (i.e. small under 10 kg, medium from 10 to 30 kg and large dogs over 30 kg).

In this context, the aim of this study was to investigate how colonic physicochemical parameters can reshape canine microbiota activity and structure in the new *in vitro* model called CANIN'ARCOL.

MATERIAL AND METHODS

For each experiment, 3 bioreactors were inoculated with a stool from a medium size dog and run in parallel, when set-up with parameters corresponding to the three size conditions (*i.e.* small, medium and large dog size). Two biological replicates were performed using faeces from two medium dogs.

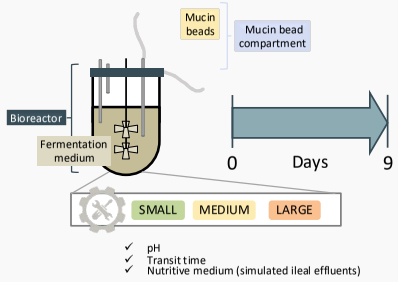

CONTACT
Charlotte Deschamps
PhD student
charlotte.deschamps@etu.uca.fr

RESULTS

Canine microbiota activity

- Average daily gas production increased significantly with dog size
- Carbon dioxide (CO_2) relative percentages significantly increased between the three size groups while the opposite was found for dinitrogen (N_2)
- Higher oxygen (O_2) and methane (CH_4) percentages were observed in the small dog group
- Total short-chain fatty acids (SCFA) production also increased with body size
- Around 60% acetate for each dog size but propionate relative percentages decreased with body weight (from 27% to 15% from small to large) associated to an increase in butyrate (13% to 27%).

➔ Similar observations (for gas and SCFA) to that reported *in vivo* in dogs by Mondo *et al.* (2019) and Beloshapka *et al.* (2014, 2016)

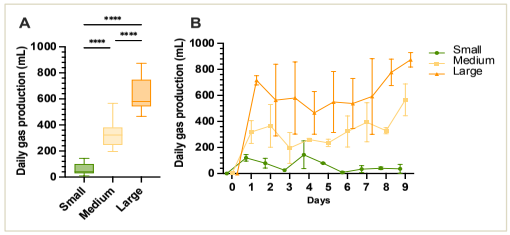

Gas production. Mean daily gas production (A) and gas produced during fermentations (B) (n=2).

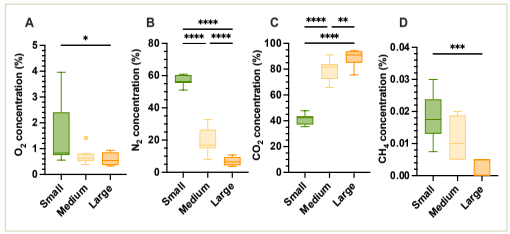

Gas composition (GC). Mean gas concentrations in O_2 (A), N_2 (B), CO_2 (C) and CH_4 (D) (n=2).

Canine microbiota structure

- Mean total bacteria concentrations of 9.9, 9.2 and 9.7 Log_{10} copies/g respectively for small, medium and large dog conditions in luminal samples (non significant differences)
- Mucosal samples less concentrated in total bacteria than luminal ones with 6.4, 7.0 and 6.4 Log_{10} copies/g respectively (also not significant between dog sizes).

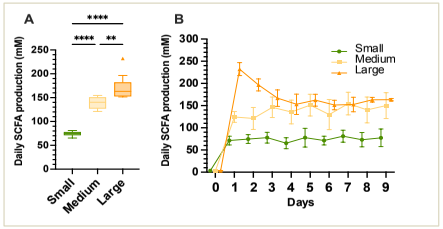

SCFA production (HPLC). Mean daily total SCFA production (A) and SCFA produced during fermentations (B) (n=2).

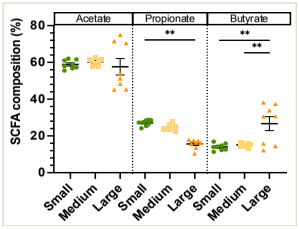

SCFA composition (HPLC). SCFA composition in acetate, propionate and butyrate (n=2).

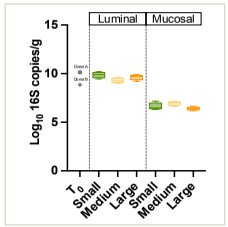

Total bacteria quantification (qPCR). Samples from luminal and mucosal environments were analysed to determine total bacteria levels (n=2).

CONCLUSION

Our study suggests that physicochemical parameters applied to the M-ARCOL colon model (i.e. pH, transit time and composition of the nutritive medium) are sufficient to shift canine microbiota metabolic activities toward *in vivo* profiles found in three dog's sizes (small, medium and large dogs), even if the bioreactors were only inoculated with faecal samples from medium dogs.

As gas and SCFA are main end-products resulting from fiber fermentation by gut microbiota, our results indicate a higher fermentative activity in large *versus* small bioreactors, in accordance to *in vivo* data in small *versus* large dogs.

Similar total bacteria abundance was observed between the three dog sizes *in vitro*, but these results can not be challenged with *in vivo* data, especially for mucus-associated microbiota. To go further, characterization of microbial profiles at different taxonomic levels using 16S Metabarcoding is ongoing.

This study is the first step in the development and validation of *in vitro* colon canine models adapted to three dog's sizes, that can provide a useful tool in food and pharma to assess the impact of nutrients, probiotics and/or drugs on canine microbiota structure and functions.

Appendix 7 – Poster communication

DESCHAMPS, C., DENIS, S., HUMBERT, D., CHALANCON, S., ACHARD, C., APPER, E. & BLANQUET-DIOT, S. Colonic physicochemical parameters from different dog's sizes reshape canine microbiota activity and structure *in vitro*. *4th Ghent Gut Inflammation Group Meeting, Ghent, Belgium, February 8-10th,* ***2023***

Colonic physicochemical parameters associated to different dog sizes reshape canine microbiota structure and function *in vitro*

Deschamps Charlotte[1,2], Denis Sylvain[1], Humbert Delphine[3], Chalancon Sandrine[1], Achard Caroline[2], Apper Emmanuelle[2], Blanquet-Diot Stéphanie[1]

1- Université Clermont Auvergne, UMR 454 MEDIS UCA-INRAE, Clermont-Ferrand, France
2- Lallemand Animal Nutrition, Blagnac, France 3- Dômes Pharma, Pont-du-Château, France

INTRODUCTION

Canine digestion is a complex and regionalized process playing a key role in maintaining dog health. Decades of breeding selection have led to variations in dog's size associated to changes in digestive physiology, markedly in the **large intestine**. In particular, an important impact of **body weight** on several digestive parameters can be observed such as modifications of the **colonic pH, transit time and permeability**.

In the context of 3Rs rules, the aim of this study was to evaluate, using the **CANIM-ARCOL** (Canine Mucosal Artificial Colon), how physicochemical and nutritional conditions specific to different dog's sizes can shape lumen and mucus-associated microbiota *in vitro*.

MATERIAL & METHODS

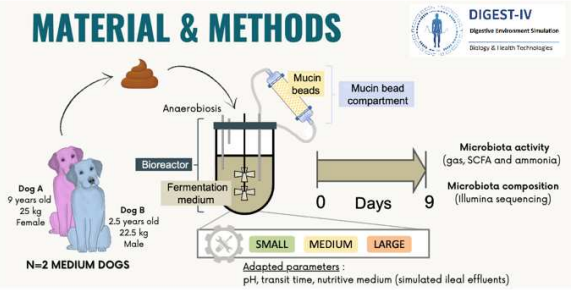

RESULTS — Microbiota composition

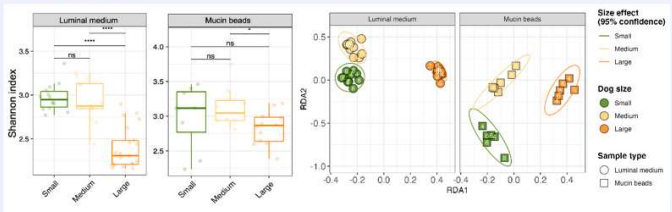

Diversity. Shannon index (left) and redundancy analysis (RDA) without donor effect for luminal medium and mucin beads. Only days 2 to 9 were kept for the analysis. Numbers indicates sampling days. *Anova one-way: * p<0.05, **** p<0.0001.*

- **Shannon index** decreases with dog size in both luminal and mucosal environments
- **RDA analysis** reveals that both colonic environments and size impact significantly (p<0.001) microbiota composition at ASV level

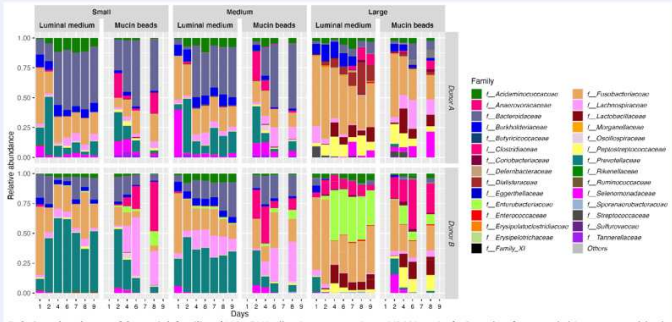

Relative abundance of bacterial families (16S rRNA Illumina sequencing - V3-V4 region). Samples from each bioreactor and both luminal medium and mucin beads were analyzed for donor A (top) and B (bottom).

- Regarding **families**, microbial signatures of each dog were maintained (higher relative abundance of *Acidaminococcaceae* and *Selenomonadaceae* for donor A and higher *Clostridiaceae*, *Lachnospiraceae* and *Enterobacteriaceae* for donor B)
- Close profiles between small and medium conditions
- In large condition, increase in *Fusobacteriaceae*, *Lactobacillaceae* and *Peptostreptococcaceae* relative abundances compared to small and medium ones

VALIDATION

→ Shannon Index decreases with dog size as observed *in vivo* on feces (Deschamps *et al.* 2022)

→ Appropriate adequacy between families observed in vivo and in vitro regarding dog size effect

→ Results on mucosal microbiota cannot be challenged with *in vivo* data since there is no available literature

→ From small to large dog sizes, opposite trends for *Prevotellaceae*

Families	Observed in fecal samples (literature)				Observed in bioreactors				*Similar tendency in vivo and in vitro*
	Small[a]	Medium[b]	Large[c]	Size effect	Small	Medium	Large	Size effect	
Bacteroidaceae	Yes	Yes	Yes	↘	Yes	Yes	Yes	↘	=
Fusobacteriaceae	Yes	Yes	Yes	↭	Yes	Yes	Yes	↭	=
Lachnospiraceae	Yes	Yes	Yes	↘	Yes	Yes	Yes	↭	±
Clostridiaceae	Yes	Yes	Yes	↭	Yes	Yes	Yes	↗	±
Enterobacteriaceae	Yes	Yes	Yes	↭	Yes	Yes	Yes	↗	±
Sutterellaceae	ND	ND	Yes	ND	No	No	No	ND	ND
Peptostreptococcaceae	Yes	Yes	Yes	↭	Yes	Yes	Yes	↭	=
Prevotellaceae	Yes	Yes	Yes	↗	Yes	Yes	Yes	↘	≠
Ruminococcaceae	Yes	Yes	Yes	↭	Yes	Yes	No	↘	±
Acidaminococcaceae	ND	ND	Yes	↭	Yes	Yes	Yes	↭	=
Veillonellaceae	ND	Yes	Yes	↭	No	No	No	ND	ND
Erysipelotrichaceae	ND	Yes	Yes	↭	Yes	Yes	No	↭	=

a. Kim *et al.* (2017), Omatsu *et al.* (2018) and You and Kim (2021); b. Nogueira *et al.* (2019), Kubinyi *et al.* (2020), Garcia-Mazcorro *et al.* (2021) and Paßlack *et al.* (2021); c. Sandri *et al.* (2016) and Hullar *et al.* (2018); *ND: not detected*

Microbiota activity

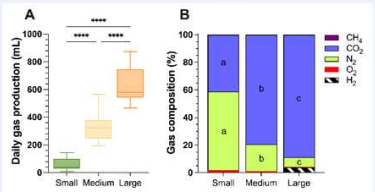

Gas production. Mean daily production (A), and mean gas composition (B) calculated on days 2 to 9. *Anova one-way: **** p<0.0001. Letters indicates significant differences (p<0.05).*

- **Daily gas production** significantly increases with dog size
- Significant differences between the three sizes for CO2 and N2 relative percentages

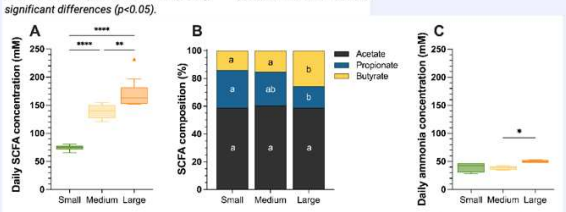

SCFA and ammonia concentrations. Mean daily short-chain fatty acids concentrations (A), composition (B) and daily ammonia concentrations (C) calculated on days 2 to 9. *Anova one-way: * p<0.05, ** p<0.01, **** p<0.0001.*

- **Short-chain fatty acids (SCFA) concentrations** increase significantly with size
- Proportions of propionate and butyrate significantly different in large condition compared to small and medium ones
- Propionate relative percentages decrease with body weight associated to an increase in butyrate
- **Ammonia** levels in large condition were significantly higher than in medium one

VALIDATION

→ No data on colonic gas production but similar impact of dog size on fecal SCFA reported by Weber *et al.* (2004), Mondo *et al.* (2019) and Beloshapka *et al.* (2014, 2016)

→ Deschamps *et al.* 2022 reported an increase of fecal ammonia from small to medium dogs (no data in large dogs)

→ Fermentation activity increases with dog size

DISCUSSION

Our study suggests that nutritional (composition of the nutritive medium) and physicochemical (pH and transit time) parameters applied to the **CANIM-ARCOL** model are sufficient to shift canine microbiota structure and functions toward *in vivo* profiles associated to **three dog's sizes** (small, medium and large dogs), despite the bioreactors were only inoculated with faecal samples from **medium dogs**.

The newly developed model is a promising tool for food and pharmaceutical studies to assess the impact of nutrients, pre, pro, sym, and postbiotics or antibiotherapy on canine microbiota structure and functions. To further integrate host interactions, the model can be coupled in a next future with canine intestinal cells or organoïds.

Charlotte DESCHAMPS
PhD student
charlotte.deschampsseetu.uca.fr

Stéphanie BLANQUET-DIOT
Co-director of UMR MEDIS
Scientific manager of the DIGEST-IV platform
stephanie.blanquetuca.fr

4TH GHENT GUT INFLAMMATION GROUP MEETING

Charlotte DESCHAMPS – Impact of body weight and antibiotic disturbance on canine gut microbiota: *in vitro* simulation and restoration strategies

This PhD will be defended on June 30th, 2023

Different dog sizes are associated with variations in digestive physiology, mainly related to the large intestine and its resident microorganisms. This gut microbiota plays a key role in animal health, supporting nutritional, immunological and physiological processes. Nevertheless, diseases or antibiotherapy can disturb microbial equilibrium and induce a perturbated state called dysbiosis. To restore microbiota eubiosis, new restorations strategies have been developed such as pre-, pro- or postbiotics. However, very few studies have evaluated their effects on gut microbiota in the context of antibiotherapy. This joint PhD between the Microbiology, Digestive Environment and Health unit from Université Clermont Auvergne and the two compagnies Lallemand Animal Nutrition and Dômes Pharma, aimed to investigate the impact of body weight and antibiotic disturbance on canine colonic microbiota, as well as the potential of microbial restoration strategies, using *in vitro* gut models.

This thesis started by evaluating the impact of different methods for faecal sample storage (48-h freezing -80°C, 48-h -80°C with glycerol or lyophilization with maltodextrin/trehalose) on the kinetics of microbiota colonization and metabolic activities in the Mucosal Artificial Colon (M-ARCOL). Compared to fresh stools, inoculating with raw frozen stool without cryoprotectant was the best option among those tested. Second, thanks to a large literature review, the M-ARCOL model was adapted to reproduce the main nutritional, physicochemical and microbial parameters specific from small, medium and large size conditions in a new model called Canine M-ARCOL (CANIM-ARCOL), further validated through *in vitro-in vivo* comparisons. This adaptation allowed to reproduce *in vitro* the increase in *Bacteroidota* and *Firmicutes* abundances and higher main short-chain fatty acid (SCFA) concentrations observed *in vivo*. Then, we used the CANIM-ARCOL to perform a mechanistic study, which revealed that nutritional and physicochemical parameters are enough to shape microbiota activity according to dog size, but faecal inoculum was necessary to reproduce size-related microbiota composition. The next step was to adapt the CANIM-ARCOL to diseased situation, focusing on antibiotic-induced dysbiosis. In accordance with *in vivo* data, antibiotherapy induced an increase in *Enterobacteriaceae*, *Streptococcaceae* and *Lactobacillaceae* relative abundances while alpha-diversity and SCFA production decreased. Similar but lower effects were observed in mucus-associated microbiota. Lastly, we evaluated the effect of the live probiotic yeast *Saccharomyces boulardii* CNCM I-1079 and the heat-inactivated bacteria *Lactobacillus helveticus* HA-122 on microbiota resistance during antibiotic treatment and resilience afterwards. Of interest, both microbial strategies decreased the *Enterobacteriaceae* bloom during antibiotherapy and allowed, in the first two days, a quicker recovery of microbiota composition and activity, in both the luminal and mucosal compartments.

This PhD work provided pioneering and significant insights into the impact of dog size and antibiotherapy on canine colonic luminal and mucus-associated microbiota composition and activity, filling gaps in knowledge in these fields. This work also contributed to a better understanding of microbiota resilience in response to antibiotic disturbance. In a near future, in accordance with the European 3R's rules aiming to reduce at a maximum animal experiments, our *in vitro* approaches could be used for mechanistic studies on the interactions between nutrients, feed additives or veterinary products and canine colonic microbiota. Such experiments could be performed under healthy but also disturbed gut microbial situations (including obesity, inflammatory bowel diseases or chronic enteropathies), always considering interindividual variabilities to move towards personalized nutrition and medicine.

Keywords: Dog, digestive physiology, gut microbiota, size, *in vitro* gut models, faecal sample storage, dysbiosis, antibiotherapy, restoration strategies.

UMR **MEDIS** 454, Microbiologie Environnement Digestif et Santé, Université Clermont Auvergne et INRAE, **Lallemand Animal Nutrition**, Blagnac & **Dômes Pharma**, Pont-du-Château